NOTE TO USERS

ULTRA-HIGH RESOLUTION SEDIMENT ANALYSIS AND DIATOM PALEOECOLOGY FROM EFFINGHAM INLET, BRITISH COLUMBIA, CANADA: IMPLICATIONS FOR LATE HOLOCENE ENVIRONMENTAL CHANGE

Alice S. Chang

B.Sc. (Honours), University of British Columbia, 1995
M.Sc., University of British Columbia, 1997

A THESIS SUBMITTED IN PARTIAL FULFILLMENT OF THE REQUIREMENTS
FOR THE DEGREE OF DOCTOR OF PHILOSOPHY

in

THE FACULTY OF GRADUATE STUDIES AND RESEARCH
(Department of Earth Sciences)

CARLETON UNIVERSITY
OTTAWA-CARLETON GEOSCIENCE CENTRE

January 2004

Your file Votre référence
ISBN: 0-612-89885-7
Our file Notre référence
ISBN: 0-612-89885-7

ABSTRACT

Late Holocene laminated sediments from Effingham Inlet, a small anoxic fjord on the southwest coast of Vancouver Island, Canada, were analyzed at ultra-high resolution (subannual to annual) time scales in order to detect short-term environmental shifts from modern times to 5500 yr BP. Four topics were examined in detail. 1) Nature of laminae. A core dating from ~600–5500 yr BP was examined using 52 thin sections from ten ~60-year long sediment slabs. The sediments consist of alternating diatom-rich and silt-rich laminae, where a diatom/silt couplet represents one year of deposition. A distinct seasonal succession of diatoms was determined. 2) Modern-day sediments. Fifty-five sediment trap samples taken over a 16-month period from 1999–2000 were compared to environmental records. A seasonal diatom succession was determined where *Skeletonema costatum*, *Thalassioisira* spp., *Minidiscus chilensis* and *Chaetoceros* spp. resting spores were common during spring and summer. Benthic taxa and terrigenous debris were common in autumn and winter. Detrended canonical correspondence analysis (DCCA) identified daylength, sea surface temperature (SST), precipitation, and wind stress as important variables. 3) Late 20th century sediments. Forty-two samples from a freeze core spanning from 1947–1993 were examined for diatom abundance and sedimentation patterns and compared with environmental data. Diatom abundance and the environment were influenced by the 1976–1977 climate regime shift from cooler to warmer conditions. DCCA indicated that SST, sea surface salinity and the Aleutian Low Pressure Index were important variables. Cyclostratigraphy revealed that sedimentation patterns and total diatom abundance had significant 2–5 year El Niño cycles and ~11-year sunspot cycles, suggesting that solar forcing on time scales other than the annual cycle were

important for influencing primary productivity. 4) Mid-Holocene sediments. Diatoms from 67 samples were examined from a 15-cm long sediment slab encompassing at least 62 years of deposition and dated at ca. 4450 yr BP. Sedimentary couplets show a thinning-upward pattern. Laminae in thicker couplets are abundant in *S. costatum*. Benthic species dominate the thinner, siltier couplets. This sequence indicates a shift from strong coastal upwelling to weakened upwelling and increased rainfall washing benthic diatoms and silt into the inlet. Cyclostratigraphy detected the 2–5 year El Niño cycle, and a 9–15 year cycle which may correspond to the sunspot cycle. This research illustrates how laminated sediments can be used as an ultra-high resolution paleoenvironmental archive, and how past environmental conditions and diatom assemblages have changed throughout the late Holocene in coastal British Columbia.

ACKNOWLEDGMENTS

I could not have completed this work without the support and guidance from many people and institutes. I would like to thank all those who have been involved throughout the research.

First, I thank my thesis supervisor, Dr. Tim Patterson, for introducing me to the Effingham Inlet project. I am grateful for his continued support for my work and exposing me to endless research possibilities. Thanks for enlightening me on a small corner of British Columbia that, before this project, I did not know existed. It is a beautiful part of Canada that I would like to revisit.

Second, I am most grateful to Murray Hay (Ph.D. candidate, Université Laval, Quebec, Canada). Murray taught me everything I ever needed to know about diatoms, how to study them, and what to do with them. Without his patient guidance I would still be at the point of existence where I was certain that there were *only* two kinds of diatoms: round ones and long ones. I am deeply indebted to him and am greatly appreciative of his continuing support.

Third, I thank all those at the Pacific Geoscience Centre and the Institute of Ocean Sciences in Sidney, BC, for taking care of me, allowing me to use their facilities on numerous occasions, and sharing their data and ideas. Dr. Richard E. Thomson, Kim Conway, Dr. Audrey Dallimore, Roy Hourston, Cindy Wright, Dr. Brenda Burd, Doug Yelland, and Mary O'Brien have been extremely kind and generous, and I have learned so much from them. Captain Frost and the crew of the Canadian Coast Guard Ship *John P. Tully* were superb and professional during my 1-week cruise to Effingham Inlet. They made my first ever research cruise enjoyable, even when I was feeling green.

Many people were instrumental in providing me with technical expertise on this project. I am deeply indebted to Dr. Miriam (Mimi) Bertram (University of Washington, Seattle) for orchestrating the sediment trap studies, providing me with the samples, discussing them with me, and reviewing that part of my thesis; Dr. Andreas Prokoph (SpeedStat, Ottawa) for performing computerized cyclostratigraphy of my freeze core and piston core slabs; Dr. Bassam Ghaleb (GEOTOP, University of Quebec, Montreal) for providing cesium and lead analyses of freeze core sediments; Dr. Roelf Beukens (IsoTrace Radiocarbon Laboratory, University of Toronto) for performing the radiocarbon dating of piston core samples; Roger McNeely (Geological Survey of Canada, Ottawa) for x-raying the freeze core and piston core slabs; Paul Hamilton (Canadian Museum of Nature, Gatineau) for giving me tips on how to freeze dry sediments, Malcolm Bilz (Canadian Conservation Institute, Ottawa) for freeze drying the sediments and giving me a wonderful tour of the Conservation Institute; Dr. Arun Kumar (Carleton University) for helping to identify dinoflagellate cysts in my samples and for discussing all aspects of life; Dr. Reinhard Pienitz (Université Laval) and Dr. Michel Poulin (Canadian Museum of Nature) for additional help with diatom taxonomy; Lewis Ling (Carleton University) for guidance on the scanning electron microscope; Drs. Tom Pedersen (University of Victoria, BC), Steve Calvert and John Crusius (University of British Columbia, Vancouver) for providing the freeze corer for the cruise and explaining how the apparatus works; Dr. Brian Menounos (Simon Fraser University, Burnaby, BC) for showing me how to resin-impregnate sediments; Mike Jackson (Carleton University) for polishing thin sections; and David Robinson (Climate Services, Vancouver office, Environment Canada) for providing instrumental environmental data. With respect to

statistical analyses, I am very grateful to Dr. Irene Gregory-Eaves (University of Ottawa) for helping me iron out the wrinkles in using CANOCO and what it all means; and to Drs. Susan E. Wilson (Ottawa), Melissa R. McQuoid (Göteborg Universitet, Sweden) and Sonja Hausmann (Université Laval) for helping to interpret sediment trap and environmental data and answering questions about statistical analysis of the diatoms. Finally, I thank Patrick Lyons, Leslie Taylor-Rogers and Davin Carter (Carleton University) for converting x-ray negatives into positive images, creating excellent websites showcasing the research, backing up my files, fixing my computer, and everything else hardware related. I give special thanks to Pat for saving my little Macintosh from annihilation on more than one occasion.

I am grateful for discussions on a variety of topics with Dr. Helen Roe (Queen's University of Belfast, Northern Ireland); Trecia Schell (Ph.D. graduate, Dalhousie University, Halifax); Drs. Dave and Kumiko Azetsu-Scott (Halifax, Nova Scotia); and Dr. Fred Michel and Bob Boudreau (Carleton University). I am extremely grateful to my colleague Dr. Lisa White (San Francisco State University) who first made me aware of this project; and to my colleague Dr. Kurt Grimm (University of British Columbia), who has stood by my side throughout the entire project; thanks for allowing me to borrow your cookie cutters, too! Thanks go to the staff from Carleton University's Science and Technology Centre for professionally fashioning cookie cutters and x-ray accessories from my hand-drawn plans. I am greatly appreciative to all those who responded on the Diatom List-Server to my various queries concerning anything diatom-related.

I thank my thesis examining committee, Dr. John Smol (Queen's University, Kingston), Dr. Andreas Prokoph, Dr. James Cheetham (Carleton University, Biology)

and Dr. George Dix (Carleton University, Earth Sciences), for doing a thorough reading of my thesis and providing constructive comments. Ms. Sheila Thayer, Dr. Sharon Carr and Dr. Richard Taylor (Carleton University) provided administrative and student support to me.

This project was made possible by generous financial support from a Natural Sciences and Engineering Research Council of Canada strategic grant and a grant from the Canadian Foundation for Climate and Atmospheric Sciences provided to Dr. Patterson. The Geological Society of America Student Research Grant Program, the Ontario Graduate Scholarship Program (Ontario Ministry of Training, Colleges and Universities, Canada), the Cushman Foundation for Foraminiferal Research Student Award Program (USA), and the Geological Association of Canada-Mineralogical Association of Canada scholarship program provided generous funding to me.

Finally, I would like to thank my parents, Paul and Rosemary Chang, who were at first apprehensive of my studying geology, but then were unconditionally supportive. In a statement they submitted to my high school that was read at my graduation, they said, "We hope one day Alice will study rocks and bugs." How right they were.

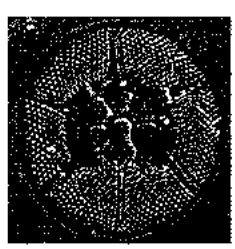

Asteromphalus sp.

TABLE OF CONTENTS

LIST OF TABLES

TABLE 7.2. Summary statistics for the first four axes of a detrended canonical correspondence analysis (DCCA) performed on species-environment data from Slab 8, using freeze core TUL99B04 DCCA as a template.

LIST OF FIGURES

FIGURE 7.3. Relative abundance data (%) for major diatom taxa, benthic diatoms, CRS and silicoflagellates from Slab 8, core TUL99B03.

FIGURE 7.4. Absolute abundance data ($\times 10^6$ valves/g) for major diatom taxa, benthic diatoms, CRS and silicoflagellates from Slab 8, core TUL99B03.

FIGURE 7.5. Relative abundance data (%) for selected major diatom taxa from Slab 8, core TUL99B03.

FIGURE 7.6. Absolute abundance data ($\times 10^6$ valves/g) for selected major diatom taxa from Slab 8, core TUL99B03.

FIGURE 7.7. Final detrended canonical correspondence analysis (DCCA) ordination diagram of species-environment relations for Slab 8, core TUL99B03, using the DCCA ordination from freeze core TUL99B04 as a template.

FIGURE 7.8. Wavelet scalograms for Slab 8, core TUL99B03.

FIGURE 7.9. Fish scale abundance and cyclostratigraphy of interval 873–910 cm from core TUL99B03.

LIST OF APPENDICES

LIST OF COMMON ABBREVIATIONS

AL	Aleutian Low
ALPI	Aleutian Low Pressure Index
APS	sea surface salinity (Amphitrite Point)
APT	sea surface temperature (Amphitrite Point)
BSEM	backscattered electron microscopy
cal yr BP	calibrated radiocarbon years before present
CBP	precipitation (Cape Beale)
cm/yr	centimeters per year
CRS	*Chaetoceros* resting spores
DCA	detrended correspondence analysis
DCCA	detrended canonical correspondence analysis
DL	daylength
ENSO	El Niño-Southern Oscillation
IOS	Institute of Ocean Sciences
ka	thousands of years ago
LM	light microscopy
Ma	millions of years ago
mab	metres above bottom
MBT	sea surface temperature (Meteorological Buoy 46206)
MB300V	along shore wind (300° true) velocity (Meteorological Buoy 46206)
MB30V	cross shore wind (30° true) velocity (Meteorological Buoy 46206)
MB300U	along shore wind (300° true) stress (Meteorological Buoy 46206)
MB30U	cross shore wind (30° true) stress (Meteorological Buoy 46206)
mm/yr	millimeters per year
NPH	North Pacific High
NSERC	Natural Sciences and Engineering Research Council of Canada
PCA	principal components analysis
PDO	Pacific Decadal Oscillation
PGC	Pacific Geoscience Centre
PPT	precipitation
SEM	secondary electron microscopy
SOI	Southern Oscillation Index
SSS	sea surface salinity
SST	sea surface temperature
yr BP	years before present

CHAPTER 1

INTRODUCTION

PUPRPOSE OF STUDY

Late Holocene laminated sediments from Effingham Inlet, Vancouver Island, were described and analyzed with the goal of finding relationships among diatom assemblages, the sediment record, and ocean-atmosphere variability, in order to interpret environmental change. To achieve this goal, several research objectives were proposed, with the results from each objective acting as a stepping stone before the next objective could be undertaken. The first and most important objective was to determine the composition and origin of the laminae by using thin sections. The second objective was to understand present-day diatom communities in the inlet from sediment trap and freeze core samples, and relate this to past assemblages determined from sediment cores. The third objective was to use cyclostratigraphy to detect short-term cycles in ocean-atmosphere variability as signals recorded in diatom assemblages and sedimentation patterns. Using diatom assemblages and their ecology, along with historical climate records, past environmental conditions can be reconstructed. Because the focus of this dissertation is on ultra-high resolution (i.e., subannual to annual) sedimentology and diatom paleoecology, detecting and determining short-term (annual to decadal) environmental shifts and cycles along coastal British Columbia, and for the northeast Pacific Ocean in general, is of particular interest. With global climate change and their effects on the environment and human populations becoming of ever-increasing concern,

finely laminated sediments and their paleoenvironmental record must be studied to their full potential.

STRATEGIC FISHERIES PROJECT

This Ph.D. dissertation is a contribution to a multidisciplinary Natural Science and Engineering Research Council of Canada (NSERC) strategic grant project entitled "Long-term Variability in Pelagic Fish Abundance and Oceanographic Conditions on the British Columbia Shelf: Implications for Strategic Fisheries Planning". My supervisor Dr. R. T. Patterson is Principal Investigator for this project. Support for this project was provided by the Herring Conservation and Research Society of British Columbia (HCRS), and the Department of Fisheries and Oceans (DFO).

The objective of the NSERC project is to provide an understanding of the natural periodicity of ocean-atmosphere variability and ecosystems of the northern Pacific, from the late Holocene to present day, by examining the sediment record. Reaching far beyond the approximate 100-year instrument record, the sediments yield crucial information about paleoceanographic and paleoclimatic trends that are currently unavailable. The results from this study can be used as a predictive tool for the conservation and optimal harvesting of Pacific fish stocks along the Canadian west coast.

The well being of coastal fishing industries is of constant concern because fisheries directly affect people, communities and the economy. The highly publicized Atlantic cod fishery collapse in 1995, the disputes over Pacific salmon in 1999, and the eventual shut down of the Atlantic cod fishery in 2003, demonstrate the increasing need

to understand why fish stocks fluctuate, and that fishery collapses may not result solely from overfishing. Naturally occurring climate cycles, such as the El Niño-Southern Oscillation or the Pacific Decadal Oscillation, influence atmospheric and oceanic circulation on a Pacific basin-wide scale, and affect the population abundances of fish over time (Lange et al., 1990; Baumgartner et al., 1994; Chavez et al., 2003). The effect of overfishing may act only as an imprint on these large-scale natural cycles (cf. Aebischer et al., 1990). This is why it is important for researchers to be able to differentiate natural variability in fish stock abundances from anthropogenic influences.

Several researchers and students from numerous government facilities and universities across North America are involved in this NSERC strategic project. The backgrounds of the researchers are diverse, with expertise in sedimentology, oceanography, vertebrate paleontology (fish remains, with special attention to fish scales), micropaleontology (diatoms, foraminifera, dinoflagellates), and geochemistry. My role in the multidisciplinary project is to provide a better understanding of sedimentary processes and diatom paleoecology at an ultra-high temporal resolution, in order to determine rapid shifts in ocean-atmosphere variability and productivity that can be overlooked in a low-resolution study. In this dissertation, I will present my data in concert with data gathered from my collaborators, so that a more complete picture of late Holocene sedimentation and paleoproductivity can be illustrated. This dissertation, however, will not directly address the relationship between diatom and fish productivity, as this task was undertaken by my colleague Murray Hay (Université Laval).

WHY LAMINATED SEDIMENTS AND DIATOMS?

Laminated sediments are common in coastal upwelling environments along productive eastern boundary oceanic currents. These sediments are formed in anoxic conditions when there is a seasonally heterogeneous sediment supply and a lack of physical or biological reworking (Grimm et al., 1996). Laminated hemipelagic sediments represent a unique paleoenvironmental archive useful for interpreting depositional, oceanographic and climatic conditions over a continuous interval of time. Because laminated sediments are deposited at annual and subannual time scales, a record of environmental change can be compiled at a high temporal resolution. With recent popular and scientific interest on global climate change, the study of laminated sediments has become more important than ever.

Diatoms (class Bacillariophyceae) are ideal for paleoproductivity and paleoenvironment studies because they are sensitive to changes in their environment, and because their productivity in the surface waters is thought to be correlated to the abundance of their remains accumulated in the sediments. Unique diatom assemblages can reflect changes in upwelling strength, water temperature, salinity and solar irradiance levels. For example, certain diatom taxa, such as *Chaetoceros* and *Skeletonema*, proliferate or "bloom" in response to increased nutrient levels brought about by upwelling pulses (Pitcher, 1990; cf. Grimm et al., 1996). The presence of a conspicuous diatomaceous lamina, representative of a bloom species, in the sediment record can be interpreted as a signature of a strong upwelling event. This information in turn can help to infer oceanographic conditions at the time of formation.

Diatoms can be used to link ocean-atmosphere relationships to the recruitment success of coastal fish stocks (Ryther, 1969; Barber and Chavez, 1983; Cury and Roy, 1989; Ware and Thomson, 1991). Favorable conditions, such as intensified wind strength, cooling of sea surface temperatures and the subsequent shallowing of the thermocline, bring nutrients closer to the sea surface for diatoms to utilize (McFarlane and Beamish, 1992). Zooplankton, such as the copepods that graze on diatoms, benefit from the increased diatom biomass, and fish that feed on the copepods also benefit. Some fish species and juvenile fish may feed directly on large colonies of diatoms (Ryther, 1969). A reverse in conditions favorable for diatoms has been observed to cause dramatic decreases in fish stocks (cf. Aebischer et al., 1990). Thus, the survival of fish stocks is dependent on coastal upwelling and the health of the diatom community.

STRUCTURE OF DISSERTATION

Due to the multidisciplinary nature of the NSERC strategic project, certain tasks normally performed by a single individual in a more classic thesis study have, instead, been distributed amongst other members of the research group. Efforts have been made to integrate the methods and results of the other researchers' work into this dissertation when applicable. Research already published by various colleagues, and work that is still in progress, is cited.

This dissertation is divided into several parts. The following two chapters (Background, and Methodology) provide information that is pertinent throughout the entire dissertation. This was done to reduce repetition in each chapter. Chapters 4, 5, 6

and 7 describe methods specific to analyses performed in each study, and provide the main results of this study. I begin in Chapter 4 with the discussion of high-magnification studies of laminated fabrics with the use of thin sections and backscattered electron microscopy. This chapter will help the reader with understanding the nature of the laminated sediments in Effingham Inlet. This mainly semi-quantitative chapter describes older sediments from a piston core and forms a baseline for subsequent chapters. In Chapter 5, I present results from sediment trap studies. This quantitative study describes phytoplankton dynamics from the most recent sedimentation. In Chapter 6, I present quantitative results from a freeze core that recorded sedimentation from the last half of the 20th century. To elucidate environmental change during this time span, the results are compared to the sediment trap results from Chapter 5. Finally, in Chapter 7, I return to the piston core samples to discuss results from quantitative analyses performed on a discrete package of sediments, and make comparisons to the younger sediments from the freeze core and sediment trap samples. Chapter 8 is intended to tie all of the main conclusions together and to discuss future research plans with respect to Effingham Inlet and the environmental studies along the British Columbia coast.

COLLABORATIONS WITH CO-AUTHORS

The main results chapters will be formatted into manuscripts to be published in journals. A manuscript based on the findings in Chapter 4 has been published in the December 2003 issue of *Palaios* (Chang, et al., 2003; v. 18, n. 6). This paper is co-authored by R. Timothy Patterson and Roger McNeely. The findings in Chapter 5 will be

submitted to *Marine Ecology Progress Series*, and will be co-authored by Miriam Bertram, Richard E. Thomson and R.T. Patterson. Results from Chapter 6 will be divided into two separate research papers based on diatom ecology and cyclostratigraphy. The first paper will be co-authored by Murray B. Hay and R.T. Patterson, and the second paper will be co-authored by Andreas Prokoph and R.T. Patterson. A manuscript based on the findings in Chapter 7 will be submitted as a research paper with co-authors R.T. Patterson and A. Prokoph.

CHAPTER 2

BACKGROUND

INTRODUCTION

The purpose of this chapter is to familiarize the reader with the regional and local environments of the study area, as well as basic concepts of diatom ecology. Although much is known about the regional geology, climate and oceanography of the southwest coast of Vancouver Island, there is recent information regarding the physical aspects of Effingham Inlet and the oceanographic regime specific to this area.

BEDROCK GEOLOGY

Much of British Columbia is composed of allochthonous terranes. These terranes, which comprise the Canadian Cordillera, consist of relict island arcs, oceanic plateaus, and continental margin fragments (Tipper et al., 1981). The terranes were accreted onto the North American craton in Mesozoic and Cenozoic times during oblique convergence of the Pacific Ocean plate and the North American plate (Silver and Smith, 1983; Coney et al., 1980; Chamberlain and Lambert, 1985). There are five major geologic belts, each with a distinct tectonic history and assemblage of rocks (Tipper et al., 1981). From east to west, these belts are: the Foreland Belt, the Omineca Belt, the Intermontane Belt, the Coast Belt and the Insular Belt.

The Insular Belt includes Vancouver Island, the Queen Charlotte Islands, the northwest corner of British Columbia, and the southwest corner of the Yukon Territory.

The part of the Insular Belt that includes Vancouver Island is known specifically as Wrangellia. Based on the fossil and magnetic evidence of the rocks, it is believed that the Insular Belt and was formed far to the south and traveled northward to accrete to the North American continent. Accretion of the Insular Belt probably occurred at ~100 Ma. During this collision, the rocks were compressed and uplifted to form the mountain ranges that extend throughout much of Vancouver Island.

The geology of Vancouver Island consists mainly of late Proterozoic to mid-Cretaceous volcanic and sedimentary rocks which formed in island-arc or oceanic plateau settings, Carboniferous to Permian fossiliferous limestones, mid-Cretaceous and younger clastics eroded from uplifting Coast Belt deposits, Paleozoic to Tertiary granitic intrusions, and Late Jurassic to Holocene accretionary complexes (Clague, 1989a; Yorath and Naismith, 1995 and references therein).

PLEISTOCENE GLACIATION

The landscape and surficial deposits seen in Vancouver Island today are a direct result of the latest glaciation event, locally known as the Fraser Glaciation (regionally called the Wisconsinan Glaciation), and post-glacial processes. Fraser Glaciation began ~29 ka, as climate became cooler and wetter (Alley and Chatwin, 1979). Advancing glaciers filled valleys in coastal mountains and carved out fjords along the coasts, and covered large areas of the continental shelf. In some places, the ice reached the edge of the continental shelf and calved into deeper waters (Luternauer and Murray, 1983).

Glaciomarine sediments were deposited onto the seafloor in front of temperate tidewater glaciers (Clague, 1989b). These sediments originated from glacial outwash from meltwater streams, supraglacial debris directly from the ice, and by the melting of icebergs (e.g., dropstones). The most common type of glacial marine sediment is massive to stratified mud, consisting mostly of < 5% gravel-size material, although some muds can contain a high gravel content (Clague, 1989b).

Maximum advance of the Fraser Glaciation occurred at 15 ka. After this time, the climate began to warm and the ice sheet deteriorated rapidly. Ice retreated from the periphery and lowland areas first, followed by retreat in mountainous areas by 12 ka (Clague, 1981, 1983). By ~10 ka, the glaciers had retreated to their present elevations and positions.

The glaciers left behind a distinctive landscape along the western coasts of both Vancouver Island and mainland British Columbia. These coastlines are highly indented with long and narrow fjords, many of which are bordered by steep and rocky slopes (Yorath and Naismith, 1995). The fjords have flat bottoms due to the infilling of sediment, and have water depths of as great as 755 m (Pickard, 1961). Major fjords also tend to be situated perpendicular to the coastline.

HOLOCENE CLIMATE HISTORY

Knowledge of the Holocene climate history of south coastal British Columbia is based mainly on studies of plant microfossils, such as pollen and spores (see Heusser, 1983; Mathewes 1985; Hebda, 1983; Pellat et al., 2001), and neoglaciation (see Ryder

and Thomson, 1986, and references therein). Hebda (1995) has compiled a comprehensive report of Holocene climate on Vancouver Island interpreted from the pollen record. The data were taken from thirteen sites on Vancouver Island, including one at the mouth of Effingham Inlet in Barkley Sound. Pellatt et al. (2001) have compiled a study of Holocene climate zones for the area surrounding Saanich Inlet because the vegetation history around the inlet is slightly different than that on the British Columbia mainland.

Shore and beach pines (*Pinus contorta*) dominated the coastal region prior to 13000 yr BP (calibrated radiocarbon years) when the climate was cooler and drier than today following the end of the last glacial maximum (Hebda, 1983). In the vicinity of Saanich Inlet, the interval from 11450–8300 yr BP was warmer and drier than today, as interpreted from the presence of fir (*Pseudotsuga*), pine, alder (*Alnus*), and grass (Poaceae) pollen (Hebda, 1995; Pellatt et al., 2001). Similar conditions were reported for Vancouver Island in general during from 10000–7500 yr BP (Hebda, 1995). A warm period with mild winters persisted from 8300–7040 yr BP, with a transitional mid-Holocene climate from 7040–5750 yr BP (Pellatt et al., 2001). For Vancouver Island in general, the interval from 7500–4000 yr BP was slightly warmer than today, perhaps by about 1 °C mean annual temperature, although precipitation may have been similar to modern conditions (Hebda, 1995). This warm interval is known as the Holocene Hypsithermal. During the hypsithermal, the south coastal forest was dominated by oak (*Quercus*), fir, alder and western hemlock (*Tsuga heterophylla*) (Heusser, 1983; Mathewes, 1985). This interval was followed by slightly wetter and cooler conditions

from 4000–2000 yr BP during which oak declined (Hebda, 1985). Pellatt et al. (2001) report that climate after 5750 yr BP around Saanich Inlet became cooler and wetter with the expansion of cedar (Cupressaceae), western hemlock and spruce (*Picea*). Modern conditions were reached by 2000 yr BP, with south coastal forests dominated by western red cedar (*Thuja plicata*) and western hemlock (Hebda, 1995; Mathewes, 1985).

Glaciers grew and expanded from the middle to late Holocene during a period referred to as Neoglaciation (Porter and Denton, 1967). Glacier expansion in the southern Coast Mountains of British Columbia occurred around 6000–5000 yr BP during the transition from the warm Holocene Hypsithermal event to cooler and wetter conditions (Lowden and Blake, 1968, 1975). In many parts of the Canadian Cordillera, glaciers expanded to their maximum extent from 3300–1900 yr BP (Porter and Denton, 1967; Ryder and Thomson, 1986). This interval coincides with the cooler and wetter conditions derived from pollen studies in southern Vancouver Island. Maximum glacier advances in the southern Coast Mountains of British Columbia occurred at Tiedemann Glacier (2300 yr BP) and at Gilbert Glacier (1900 yr BP) (Ryder and Thomson, 1986). Late Neoglacial advances took place during the Little Ice Age (AD 1350–1800) during which the Tiedemann Glacier and glaciers worldwide expanded (Ryder and Thomson, 1986). The pollen and neoglacial records suggest that climate varied greatly throughout the Holocene since the end of the last glacial maximum.

CLIMATE AND OCEANOGRAPHY TODAY

Coastal Climate

The coastal climate of southwest Vancouver Island is cool-temperate; the air is very moist and precipitation can be up to 250 cm annually (see Ryder, 1989 and references therein). Winters are relatively cool and rainy, and the coastal region is affected by a succession of frontal systems associated with cyclonic storms. Although the majority of snow falls at higher elevations, small amounts of snow occasionally fall at sea level (Ryder, 1989). Air temperatures are mild, ranging from 1 °C to 5 °C. Summers are relatively warmer and drier, and the coastal region is influenced by large anticyclonic systems. Coastal air temperatures can reach up to 20 °C.

Currents

The dominant surface currents seaward of the continental slope of North America are the northward-flowing Alaska Current and the southward-flowing California Current (Thomson, 1981). Vancouver Island is situated at the bifurcation of these two currents, although offshore circulation is likely dominated by the Alaska Current (Thomson et al., 1989). The surface currents are seasonally variable over the continental slope off Vancouver Island in response to the prevailing wind direction. In the winter, the Northeast Pacific Coastal Current flows northwestward in response to winds associated with the counterclockwise circulation of the Aleutian Low (AL) atmospheric pressure system (Thomson, 1981; Thomson and Gower, 1998). In the summer, the shelf-break current flows southeastward in response to winds associated with the clockwise

circulation of the North Pacific High (NPH) pressure system (Thomson and Gower, 1998) (Figure 2.1A).

The California Undercurrent also exerts a major influence off the southwest coast of Vancouver Island. The northwestward flowing current is situated at an intermediate depth (below 200 m) along the Vancouver Island continental shelf (Reed and Halpern, 1976; Hickey, 1979 in Thomson et al., 1989). The nutrient-rich California Undercurrent plays an important role in summer upwelling-induced phytoplankton success (Freeland and Denman, 1982).

Upwelling

Generally, coastal upwelling occurs when winds force surface waters to be pushed offshore. The "void" left by the shifted surface waters is subsequently replaced by relatively colder and nutrient-rich, upwelled deeper water. The results of this coastal upwelling include cool summers, high primary productivity, and an increase in fish populations feeding on the plankton. The Vancouver Island coast belongs to an upwelling domain, the Coastal Upwelling Domain, that extends down to southern California. Within this domain, mean sea surface temperatures can be as much as 5 °C lower, and salinities 0.1-0.3‰ higher, than immediately adjacent waters offshore (Thomson, 1981).

Wind-induced annual upwelling along the west coast of Vancouver Island is most prevalent from May through August (Figure 2.1B). The upwelling extends seaward of the shelf break, with subsequent transport of deeper (> 150 m) oxygenated and nutrient-rich

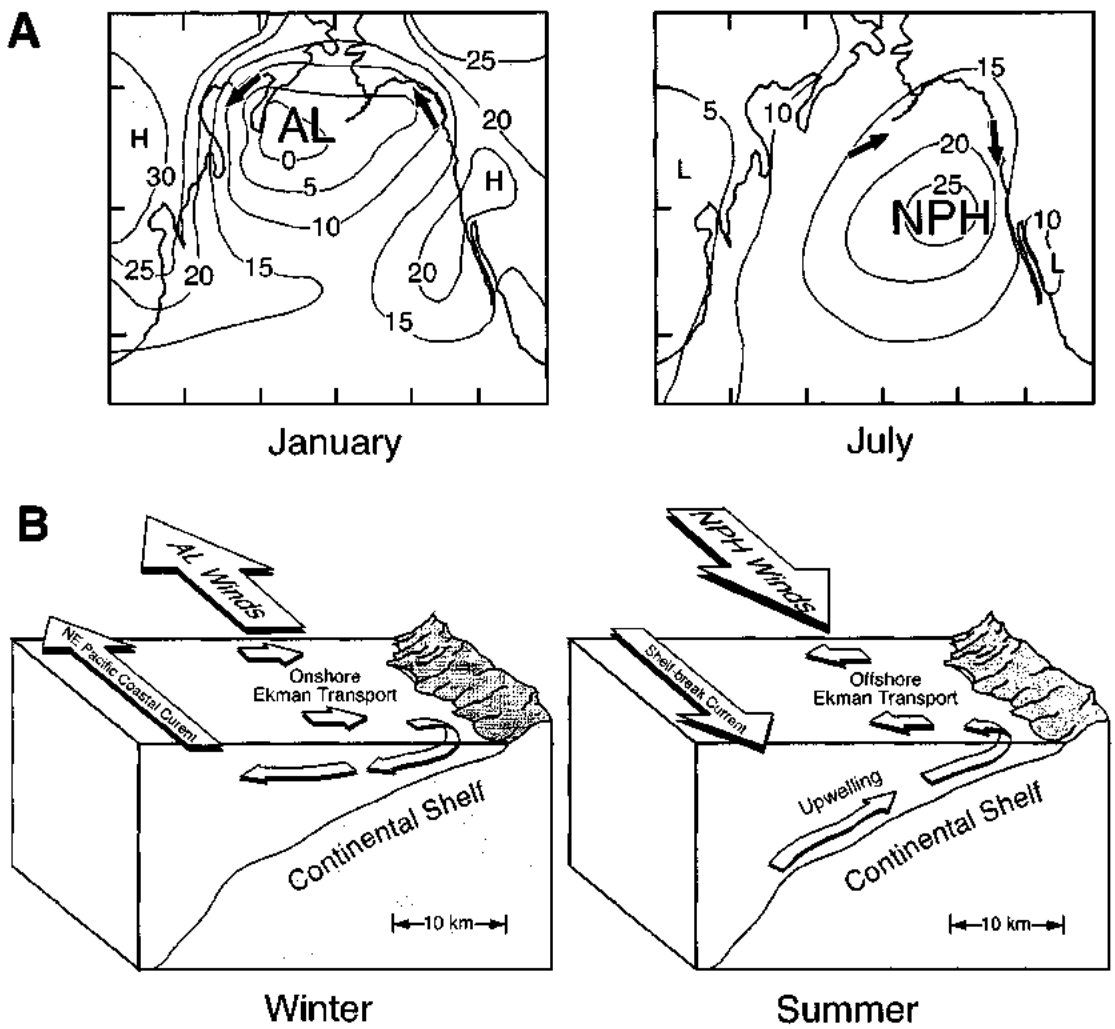

FIGURE 2.1. Seasonal atmospheric gyres and upwelling off western Canada. **A.** Mean air pressure at sea level during winter and summer from 1951 to 1970. During the winter, when the land is cooler relative to the ocean, a large-scale counter-clockwise low pressure system (Aleutian Low, AL) develops. During the summer, when the land is warmer than the ocean, a large-scale clockwise high-pressuere system (North Pacific High, NPH) migrates from the south and dissipates the AL. Arrows indicate prevailing wind direction. Values + 10,000 divided by10 gives pressure in millibars. Modified from Favorite et al. (1976). **B.** Wind-induced coastal upwelling over the Vancouver Island continental shelf. Ekman-induced upwelling occurs mainly during the spring and summer when northerly winds related to the NPH pressure system cause offshore movement of the surface waters. During the winter, southerly winds related to the AL pressure system cause onshore movement of the surface waters and subsequent downwelling. Modified from Thomson (1981).

slope waters onto the outer shelf (Thomson et al., 1989). The upwelled waters then move shoreward where they can lead to a marked increase in phytoplankton production in the adjoining coastal inlets. The seasonal upwelling is initiated in response to a seaward, wind-forced Ekman transport in the surface layer and coincides with the southeastward-flowing shelf-break current. This summer flow structure is, in turn, driven by clockwise circulating winds associated with the North Pacific High atmospheric pressure system (Thomson and Gower, 1998).

El Niño-Southern Oscillation

The normal pattern of seasonal upwelling off Vancouver Island can be interrupted in some years by cyclical climatic or oceanic events, such as particularly strong El Niño-Southern Oscillation (ENSO) events in the equatorial Pacific Ocean. The ENSO phenomenon is a cyclical disturbance to the equatorial ocean dynamics, occurring on average every 2 to 7 years. During an El Niño event, upwelling along eastern boundary regions weakens, leading to anomalously warm, low-nutrient waters, and reduced phytoplankton and fish populations (Barber and Chavez, 1983; Wilkerson et al., 1987; Lange et al., 2000). Anti-El Niño, or La Niña, events generally follow El Niños whereby anomalously cooler waters move across the equatorial Pacific Ocean. During strong El Niño events, which occur on average every 10 to 25 years, the effects are propagated poleward through the atmosphere (as teleconnections) or along the coastal ocean (as an oceanic wave guide) where they can impact mid-latitude oceanic regions (Subbotina et al., 2001; R. Thomson, personal communication, 2003).

Pacific Decadal Oscillation

The Pacific Decadal Oscillation (PDO) operates in a similar manner to El Niño except on much longer time scales. Sea surface temperatures in the Pacific Ocean have been found to cycle in two periodicities: 15–25 years and 50–70 years (Minobe, 1997, 1999). Based on 20th century sardine (warm water) and anchovy (cool water) records from the eastern Pacific Ocean, there were two cool PDO phases from about 1900–1925 and 1950–1975 and two warm PDO phases from about 1925–1950 and 1975 to the mid-1990s (Chavez et al., 2003). During the cool phase at mid-latitude northeastern Pacific localities, the Aleutian Low is weak, sea surface temperature is lower, the thermocline is shallow, nutrient levels and primary productivity are higher, and salinity and precipitation are higher. During the warm phase, the Aleutian Low is stronger, temperature is higher, the thermocline is depressed, nutrient levels and productivity are lower, and salinity and precipitation are lower (figure 3 from Chavez et al., 2003). Hence, the PDO has a direct influence on the relative seasonal importance of the NPH and AL and directly affects coastal upwelling (Mantua et al., 1997; Ware and Thomson, 2000).

PREVIOUS AND CONCURRENT WORK

Spatial and temporal distribution of modern and fossil microplankton communities have been well documented from the inner, more protected waters of coastal British Columbia (e.g., Sancetta, 1989a, b; Sancetta, 1990; McQuoid and Hobson, 1997, 2001). These studies include sites from Saanich Inlet, the Strait of Georgia, and inlets on the British Columbia mainland. Studies in open coastal or oceanic British

Columbia, namely over the Vancouver Island shelf and in Barkley Sound, have been far more limited (e.g., Denman et al., 1981; Mackas and Sefton, 1982; Taylor and Haigh, 1996). Before the current strategic fisheries project began, research in Effingham Inlet was lacking.

Work in Effingham Inlet began with a reconnaissance cruise in 1995. Effingham Inlet was chosen as a target site for studying the variability of pelagic fish populations because the inlet is silled and has anoxic bottom waters capable of preserving finely laminated sediments. These laminated sediments are ideal for extrapolating paleoclimatic and paleoceanographic signals important for fisheries studies. Also important is that Effingham Inlet sediments contain records of fish scale deposition of several economic Pacific fish species (e.g., hake, herring, anchovy, salmon and sardine) (Holmgren, 2001; Patterson et al., 2002). During a second reconnaissance cruise in 1997, small piston cores (6 cm diameter, 9 m length) were taken, and various oceanographic parameters were studied, including salinity, temperature, and dissolved oxygen (Patterson et al., 2000). The results provided further affirmation that Effingham Inlet was a prime site for paleoceanographic, paleoclimate and fisheries studies. Following these results, full-scale coring, sediment trap deployment and oceanographic surveys were carried out in 1999 and 2000 for the NSERC strategic fisheries project. Most recently, in May 2002, a 40-m long, ~12,000-year sediment record was obtained in the inlet during the International Marine Past Global Changes (IMAGES) coring program for climate change studies (T.F. Pedersen, personal communication, 2002).

To date, a few studies have been completed on the sediments in Effingham Inlet.

These works include studies of foraminifera and oxygen levels (Patterson et al., 2000), description of bulk sedimentology (Dallimore, 2001), a discussion of fish abundance variability (Holmgren, 2001), a compilation atlas of fish scales (Patterson et al., 2002), dinoflagellate assemblages (Kumar and Patterson, 2002), and surface distributions of diatoms (Hay et al., 2003).

EFFINGHAM INLET

Effingham Inlet is located on the southwest coast of Vancouver Island, and opens to the Pacific Ocean via Barkley Sound (Figure 2.2). The mountains surrounding the inlet are steep and forested, range in elevation from 700–1200 m, and consist of Mesozoic volcanic rocks (Figure 2.3). The shoreline is steep and rocky, except for some areas where the inlet waters meet tidal marshes. The inlet measures 17 km in length, has an average width of 1 km, and contains two bedrock sills and two basins. The outer basin sill, situated near the mouth of the inlet, is 65 m deep and separates the outer basin from Barkley Sound. The inner basin sill is 40 m deep and separates the outer basin from the inner basin. The larger outer basin has a maximum depth of 210 m, and the smaller inner basin has a maximum depth of 120 m (Figure 2.4). The physical characteristics of the inlet waters and sediments are briefly discussed below.

Discharge

Inlets on the British Columbia mainland experience a summer maximum river runoff from June to September. In contrast, inlets on the west coast of Vancouver Island

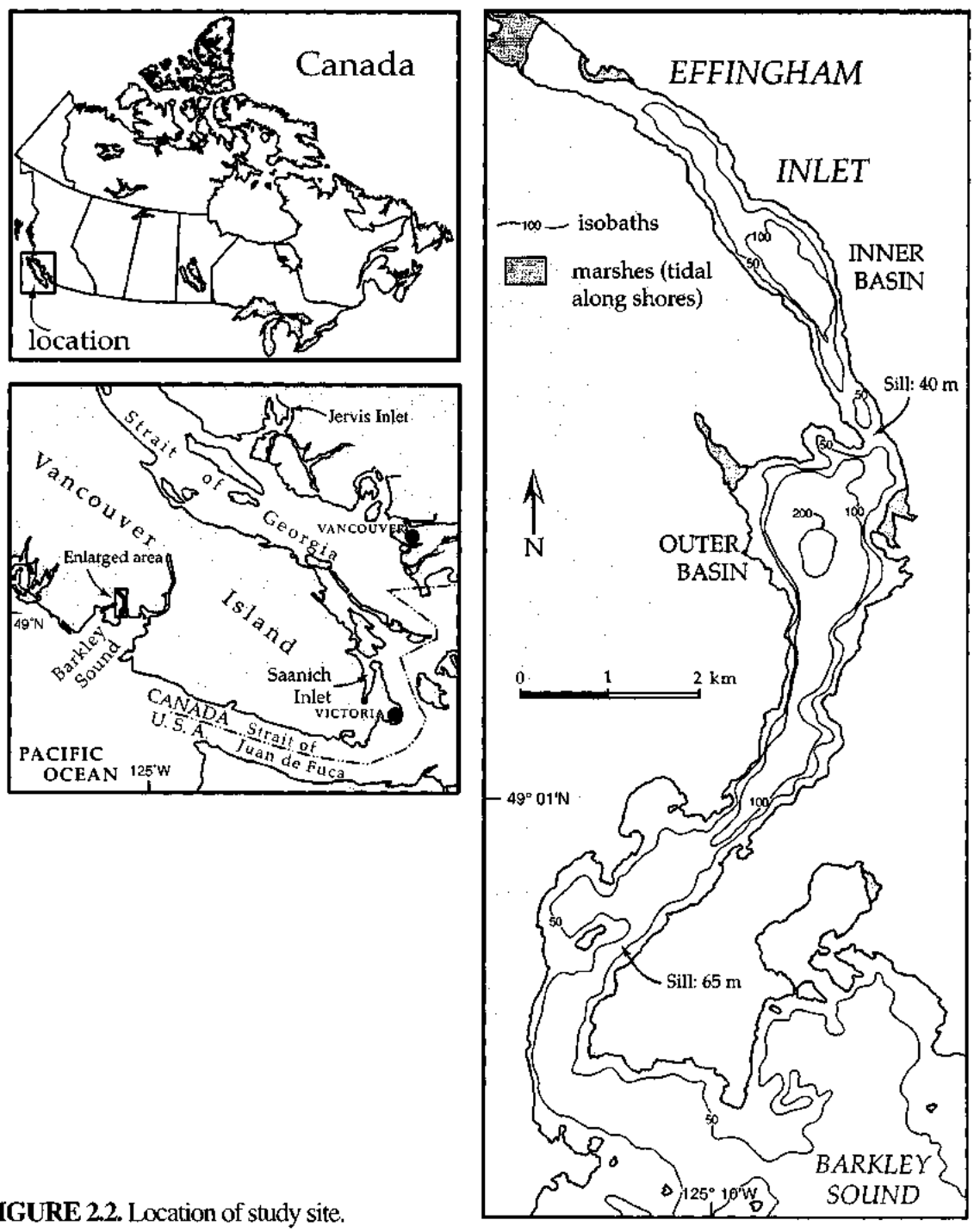

FIGURE 2.2. Location of study site.

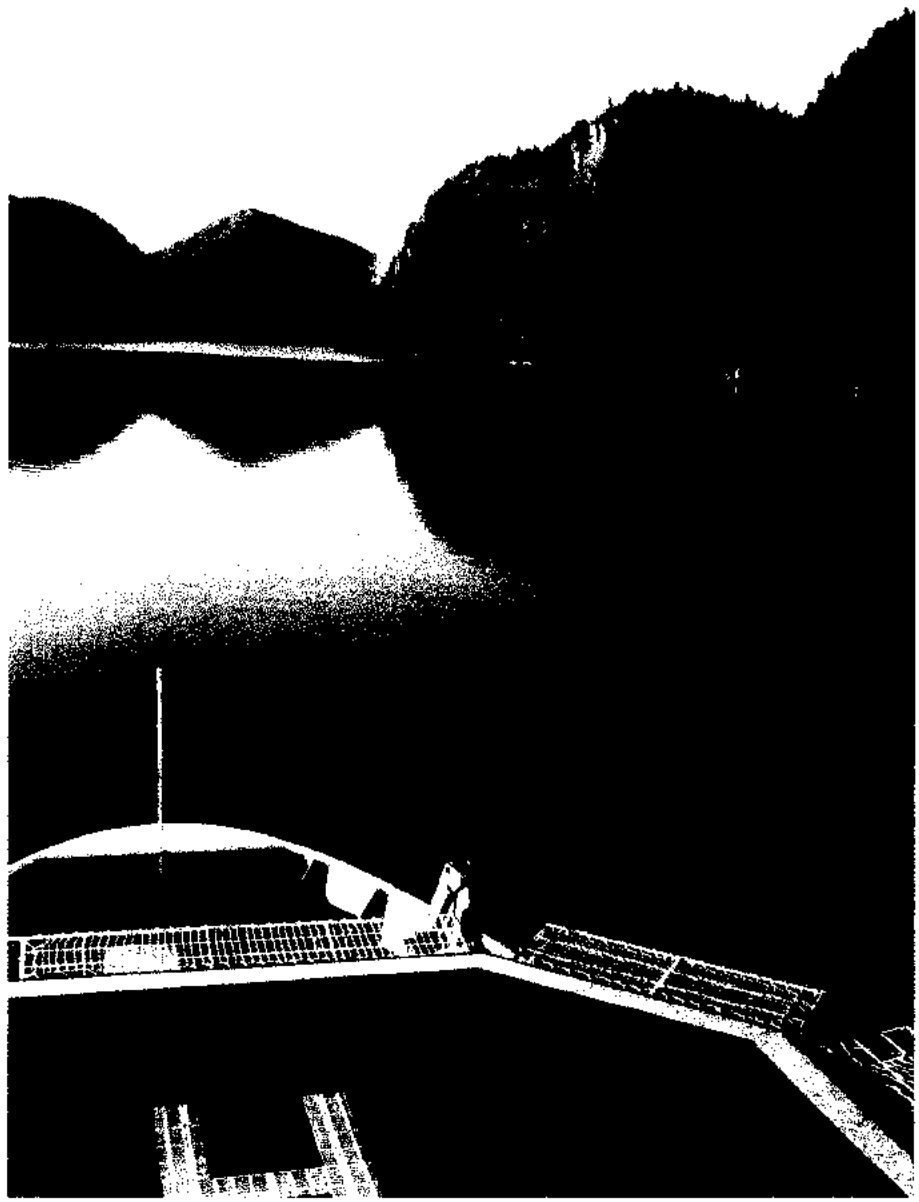

FIGURE 2.3. Effingham Inlet and steep mountains; a view looking west over the bow of the CCGS *John P. Tully*.

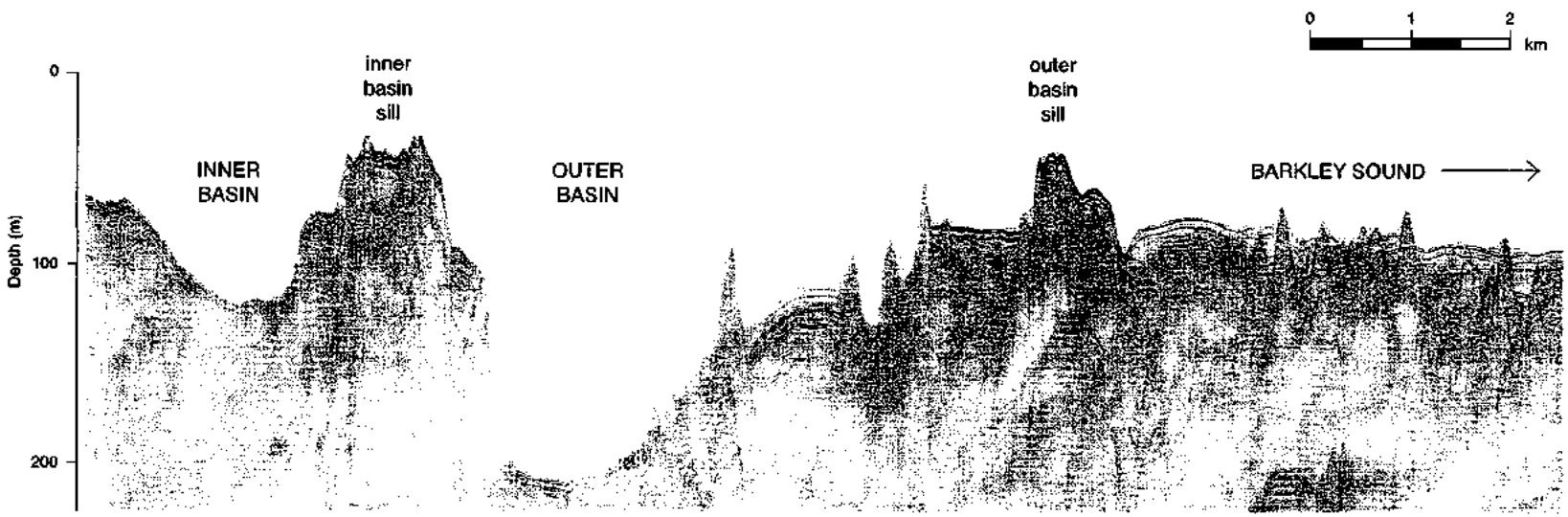

FIGURE 2.4. Seismic profile of Effingham Inlet generated from a 3.5 kHz airgun seismic traverse. Vertical exaggeration ~50 x.

experience minimum summer runoff in August or September (Pickard, 1963). Like most inlets on Vancouver Island, Effingham Inlet is classified as a low-runoff fjord (Pickard, 1963). Effingham River, which enters at the head of the inlet, has a low mean discharge of 6 to 8 m^3/s between December and June, and a maximum mean monthly discharge of 14 m^3/s (Stronach et al., 1993). Coeur d'Alene Creek, which enters at the outer basin, has an estimated mean discharge of 2 m^3/s throughout the year, with a November maximum of 4 m^3/s (Stronach et al., 1993). Peak discharge in Effingham Inlet occurs during the winter months when precipitation is at a maximum. A combination of low discharge and small spring snowmelt produces weak estuarine circulation during the summer months.

Salinity

Bottom salinity reported at the outer basin sill is ~32‰ (Patterson et al., 2000). Within the outer basin, salinity increases gradually with depth until reaching a constant reading at a depth of 130 m; from here to the bottom of the basin, the salinity stays constant at 32.8‰. At the inner basin sill, bottom salinity is 30.9 to 31.2‰ (Figure 2.5A). In the inner basin, salinity gradually increases from the surface to a depth of about 70 m. From this depth to the deepest part of the inner basin, salinity is a constant 32.5 ‰ (Patterson et al., 2000). Salinity at the head of the inlet is low (25‰) in the upper water column, but increases rapidly at depth to 32.5‰. The salinities at the bottom of each basin are higher than those measured at sill depth. This leads to stagnant, low-oxygen water at the bottom of the basins (Tully, 1949; Syvitski and Shaw, 1996).

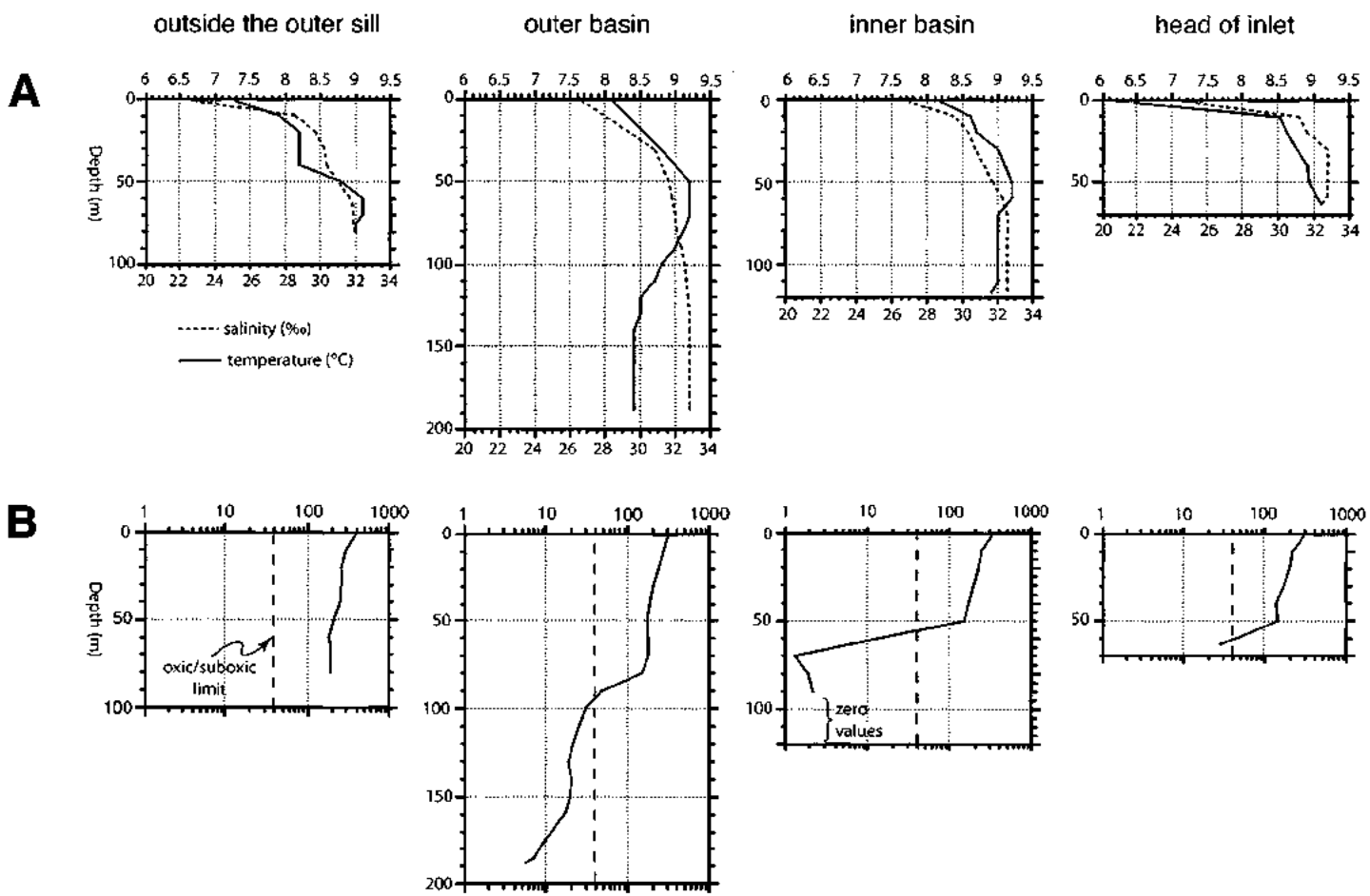

FIGURE 2.5. Water property profiles for Effingham Inlet. **A.** Salinity (bottom axis) and temperature (top axis). **B.** Dissolved oxygen (μM of O_2 per kg of seawater). From Patterson et al. (2000); reprinted by permission.

Temperature

Water temperature outside the outer sill begins at 7.7 °C and increases stepwise until reaching a maximum of about 9.0 °C at a depth of 60 m. This is also the depth at which salinity reaches a constant maximum of 32‰. In the outer basin, water temperature increases from 8.1 °C at the surface to a maximum of 9.2 °C at 50 m (Figure 2.5A). The water temperature beneath this depth decreases and reaches a constant of 8.4 °C at 140 m. Water temperature in the inner basin increases incrementally from 8.2 °C at the surface to a maximum of 9.2 °C at 60 m and then decreases to 9.0 °C from 70 m to the bottom of the basin. At the head of the inlet, temperature increases rapidly in the upper 10 m of the water column from 6.5 to 8.5 °C. From the 10 m mark to the bottom, the temperature increases gradually to 9.2 °C (Patterson et al., 2000).

Oxygen

The combination of salinity-induced stratification and high organic productivity leads to the development of an oxygen minimum zone within each basin. The oxygenation level classification index of Kaiho (1994) is used in the following discussion. In the outer basin, the dissolved oxygen content from the surface to a depth of about 70–80 m is low oxic (> 100 μM/kg). Oxygen levels decrease to suboxic conditions (40 μM/kg) at a depth of 90–100 m (Patterson et al., 2000). At the bottom of the basin, the water is suboxic to dysoxic with dissolved oxygen concentrations of < 40 μM/kg (Figure 2.5B).

In the inner basin, surface waters are well oxygenated until a depth of about 50 m. Dissolved oxygen levels decrease rapidly below this depth. At a depth of 60 m, the oxygen concentration essentially reaches a value of zero or near zero (Patterson et al. 2000). Both the outer and the inner basins show characteristic stratification with a well-oxygenated upper mixed layer, a transitional suboxic layer, and a well-developed oxygen minimum zone at depth.

Circulation

Most fjords exhibit typical estuarine circulation, with an upper "wedge" of freshwater, generated by riverine input flowing toward the ocean, and a lower saline layer flowing into the fjord at depth. In highly stratified estuary fjords with shallow sills and weak freshwater input however, the inflow of saline water at depth can be interrupted and the bottom waters become stagnant (Tully, 1949; Syvitski and Shaw, 1996).

Salinity and oxygen profiles indicate that Effingham Inlet experiences well-developed estuarine-type stratification and circulation for most of the time. However, with the bottom water salinity of the outer basin higher than that at the outer sill, it may be inferred that higher salinity and denser seawater occasionally breaches the sill and spills into the outer basin. Such seawater incursions presumably occur during the winter, under the influence of strong northerly winds at the time of Arctic outbreak conditions (Patterson et al., 2000), or early in the annual spring upwelling season during a rare combination of weak tidal currents in the inlet, significant rainfall, and strong (> 10 m/s) northeasterly winds (Thomson, 1981; Griffin and Leblond, 1990). The influxed seawater

has the effect of periodically oxygenating the bottom waters of the inlet. Such an oxygenation event was witnessed in January 1999, and again in June 1999, with normal anoxia returning within a few months (Figures 2.6, 2.7).

Density profiles show that the waters in Effingham Inlet are well stratified for the most part of the year from 1999 to 2000, attesting to the low discharge and weak circulation within the inlet (Figure 2.7). The surface waters are well stratified during January 1999 and this surface layer becomes thinner and less stratified during the spring and summer months when surface mixing occurs. Stratified conditions become re-established in the later summer to autumn.

General Sedimentology

The sediments on the bottom of the inner and outer basins of Effingham Inlet consist primarily of clay- to coarse sand-size sediments. There are two main sediment facies in the inlet: laminated sediments and nonlaminated sediments. Laminated sediments consist of millimetre-scale laminae that were preserved due to the anoxic bottom waters and lack of bioturbation. Alternating brown and olive green laminae comprise a sedimentary couplet. As the focus of this dissertation, laminated sediments will be discussed in depth in subsequent chapters.

Nonlaminated sediments include massive beds, graded beds and sand beds. Massive beds, containing muds and silts, are intercalated with the laminated sediments and occur at irregular stratigraphic intervals. These beds are commonly less than 10 cm thick and are dark olive grey to black in colour. In hand sample, massive beds have a

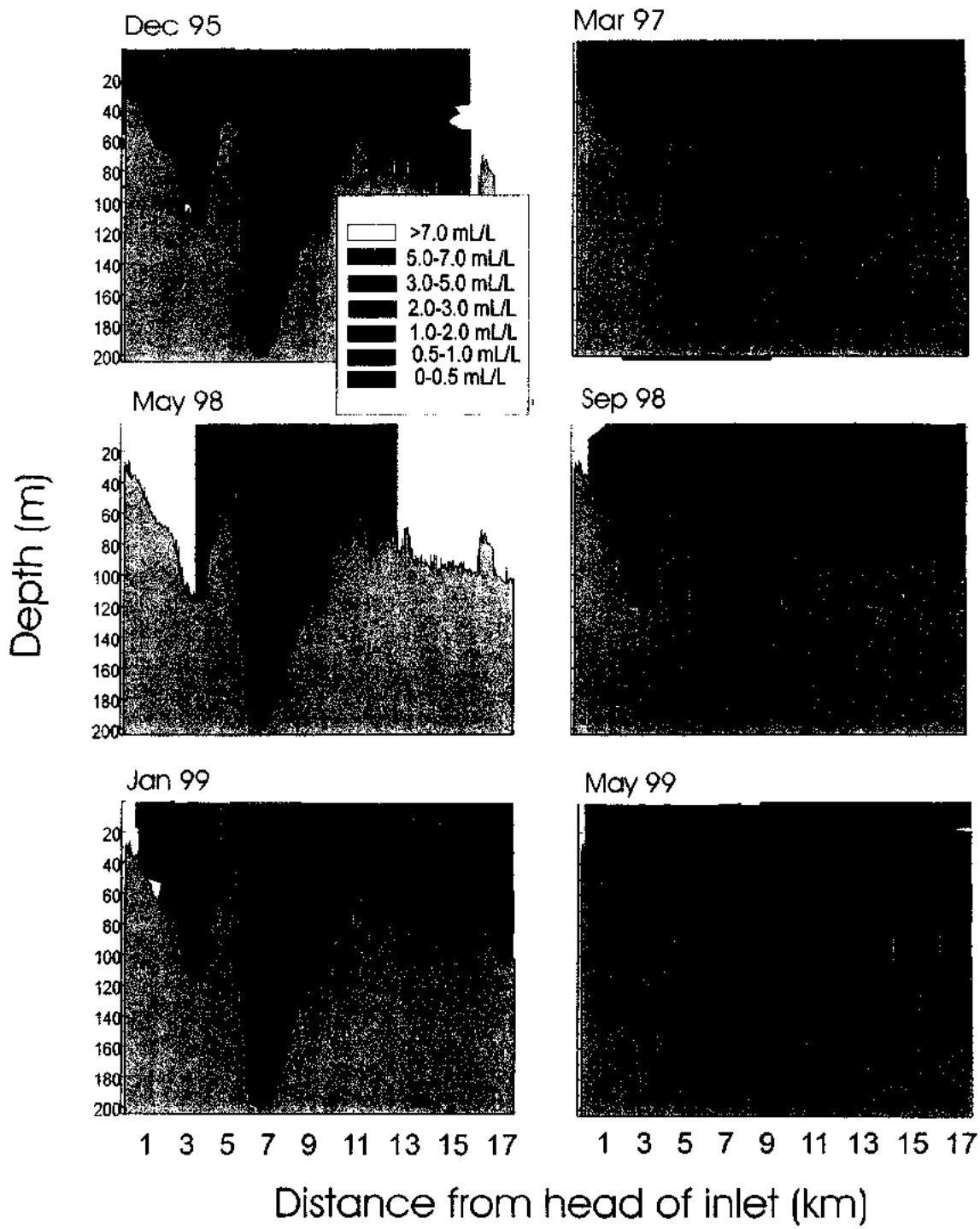

FIGURE 2.6. Seasonal oxygen level profiles in Effingham Inlet from December 1995–July 2000 (courtesy of B. Burd; reprinted by permission).

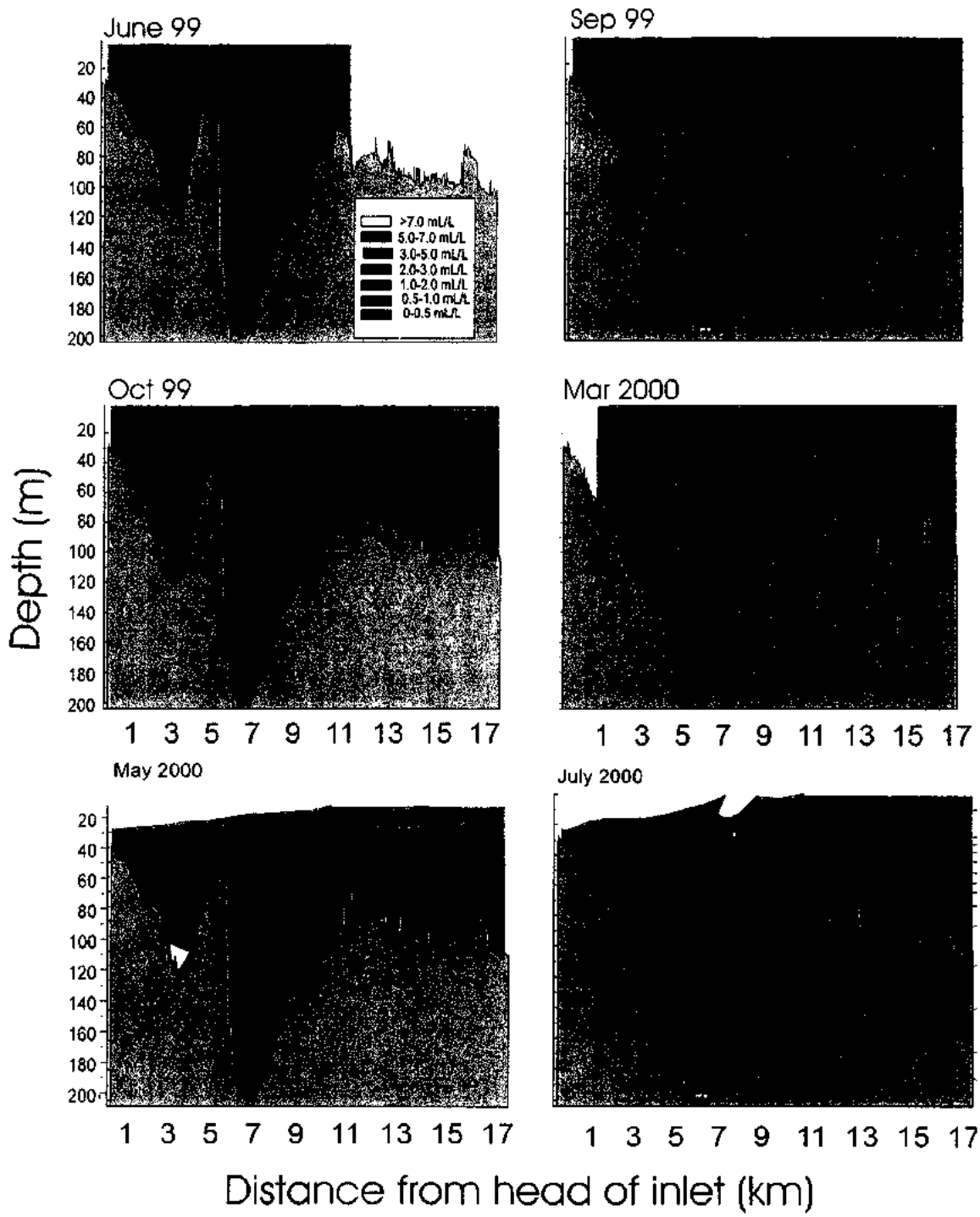

FIGURE 2.6. (continued)

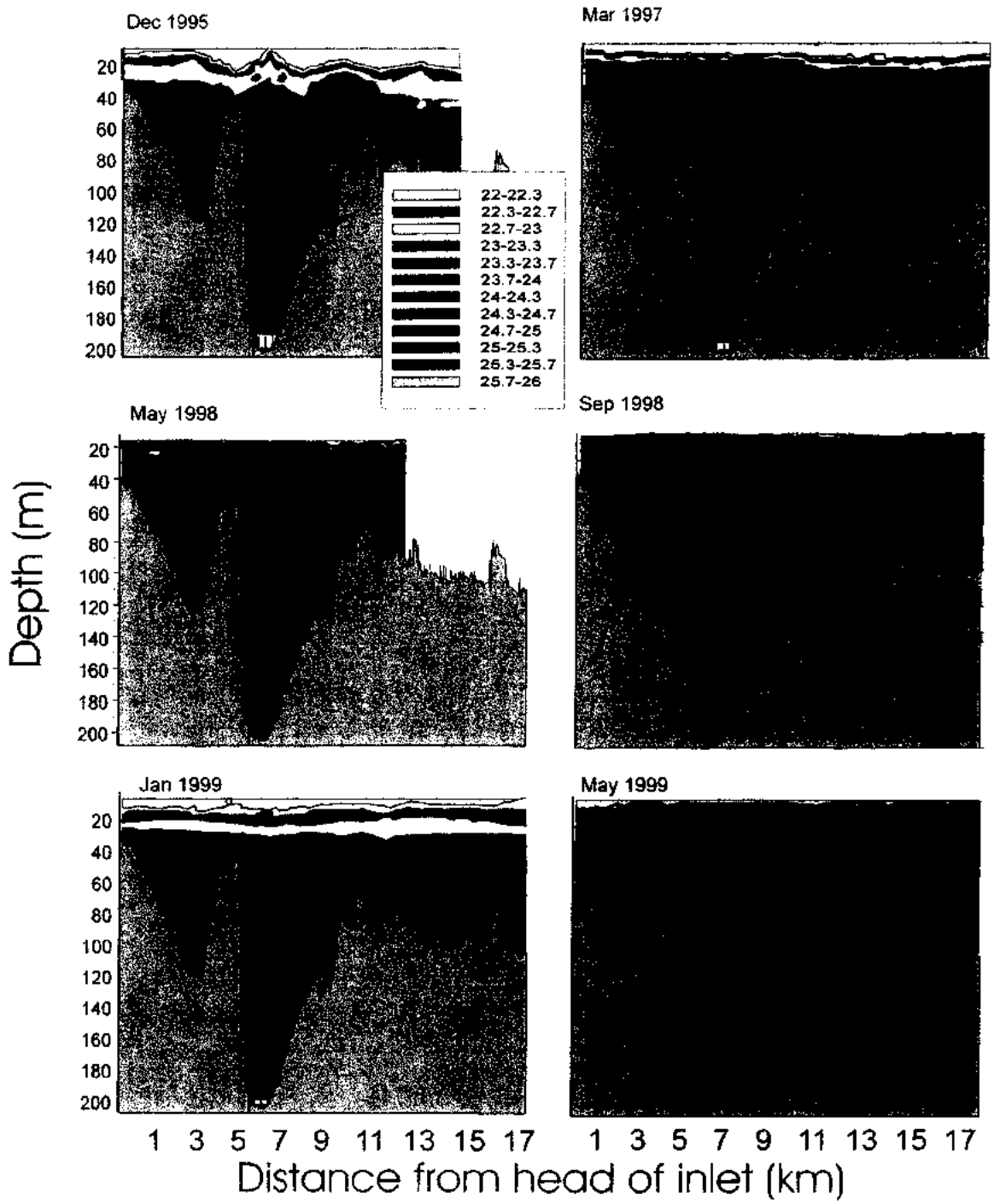

FIGURE 2.7. Seasonal water density profiles in Effingham Inlet from December 1995–July 2000 (courtesy of B. Burd; reprinted by permission).

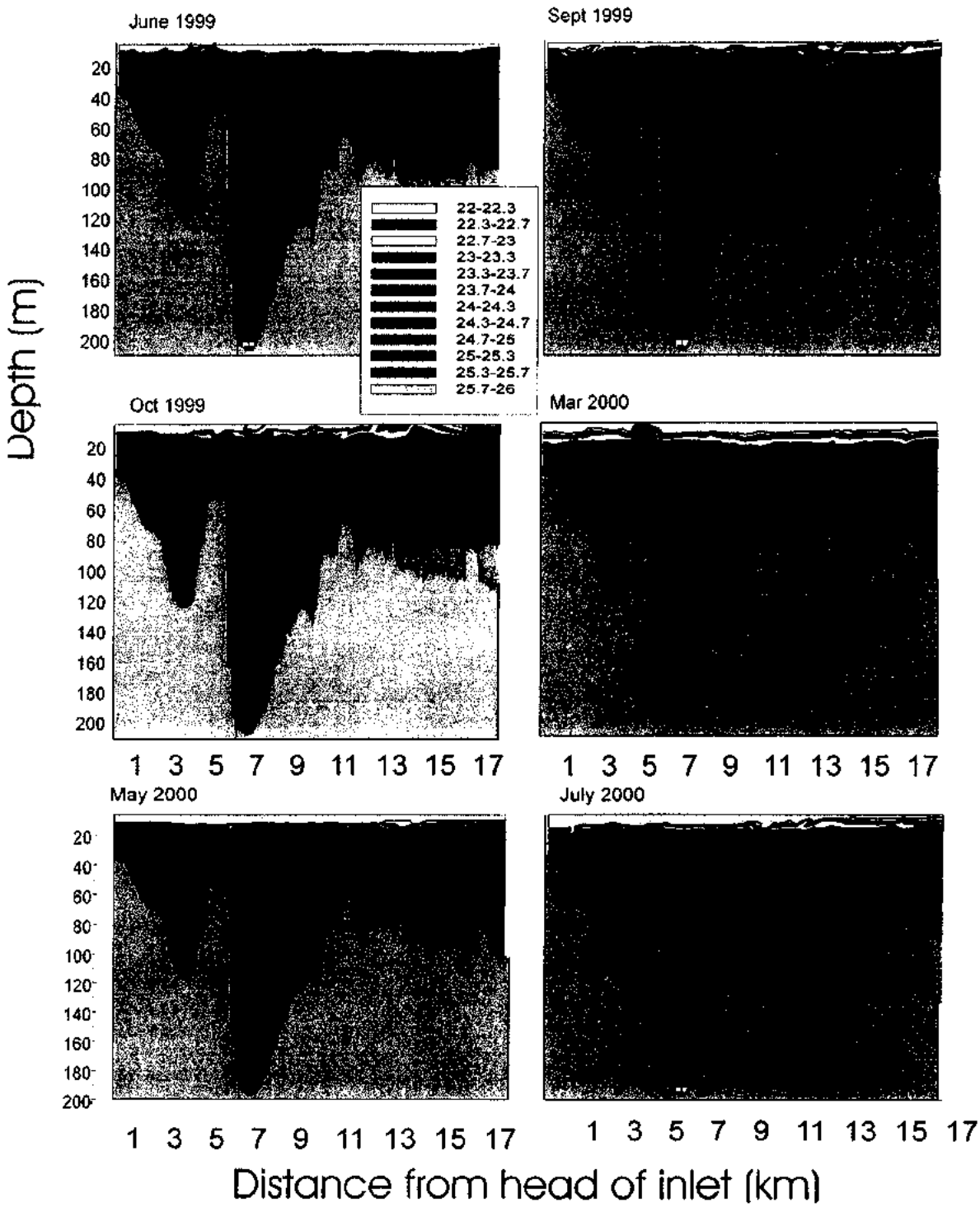

FIGURE 2.7. (continued)

homogenous texture. A subtle fining upwards grading is seen only in x-rays (Dallimore, 2001) or in thin section analysis (Chapter 4). The formation of these beds has been attributed to oxygenation of the bottom waters of the inlet. During oxygenation events, it is hypothesized that sediment at the sediment-water interface can be resuspended by bottom-hugging currents; in addition, oxygenation of the waters can allow for entry of bioturbating macrobenthos. Resuspension and bioturbation can lead to the homogenization of sedimentary laminae (Dallimore, 2001). However, no evidence of bioturbation has been observed in or below massive beds (cf. Chang and Grimm, 1999).

Graded beds are also found intercalated with laminated sediments and occur at irregular stratigraphic intervals. These beds are also usually less than 10 cm in thickness and have a dark olive grey to black colour. The beds have a sharp basal contact and a distinct fining upward grading that is visible in both the hand sample and x-rays. Coarse material, such as coarse sand, shell fragments and plant debris are commonly found at the base. Common at the top of the bed is a 1 to 2 cm thick light grey mud layer. The formation of graded beds is attributable to deposition from gravity flows such as turbidity currents. The initiation of gravity flows can have several triggers, from seismic activity to gravitational forces acting on oversteepened slopes to loss of sediment strength (Blais-Stevens et al., 1997; Middleton and Hampton, 1976, Keller, 1983).

Sand beds are rare in Effingham Inlet. They can be up to several centimeters thick and represent the coarsest sediments found in the inlet (Dallimore, 2001).

Laminated sediments are more continuous and well defined in the inner basin and contain more plant and wood fragments than the sediments from the outer basin. The

outer basin sediments consist of more massive beds and the laminae are not as well defined as those in the inner basin. Laminated intervals are usually no thicker than 20 cm in both basins.

DIATOM BIOLOGY AND ECOLOGY

A brief biological description of diatoms is provided here. Readers who are interested may refer to Werner (1977) and Round et al. (1990) for more detailed discussions of diatom biology, morphology and ecology.

Biology and Morphology

Diatoms (class Bacillariophyceae) are photosynthesizing, unicellular golden-brown algae that build an intricate shell composed of amorphous silica. As the most abundant of the phytoplankton groups in the ocean, diatoms comprise 20–25% of the net primary production per year. Diatoms can proliferate in great numbers during favorable environmental conditions, and are capable of covering large expanses of the ocean surface and removing nutrients and CO_2 from the photic zone (Smetacek et al., 1992; Frost, 1996).

The basic morphology of the diatom shell, or frustule, consists of an upper half (epivalve), a lower half (hypovalve), and encompassing girdle bands (cingula). The nucleus, cytoplasm, organelles and various chloroplasts are housed within the frustule. There are several basic shapes of diatoms by which classification is made, although the two common forms are centric diatoms and pennate diatoms. Centric diatoms have a

geometry that is symmetrical about a central point and are often round or polygonal in shape. Pennate diatoms have a biradial symmetry and are often elongated in shape.

The surface of the frustule is highly ornamented, and the pattern of the ornamentation, along with the general shape of the diatom, distinguishes the genus and species. Traditional taxonomic identification of fossil material involves light microscopy in which parameters such as cell diameter and the pattern of ornamentation are used. The development and use of secondary electron microscopy in the last 40 years has permitted the high magnification imagery of fine structural details not visible with light microscopy. This advent has led to the reclassification of some species and even some genera of diatoms.

Marine diatoms can reproduce asexually or sexually. Asexual reproduction involves mitotic cell division and the phenomenon of cell-size reduction (known as the MacDonald-Pfitzer rule; see Crawford, 1980 and references therein). This reproductive method is commonly found in centric diatoms. Once a population reaches a critical minimum size of approximately 30% of the original cell diameter, and cell size reduction can no longer be maintained, sexual reproduction occurs (Lewis, 1984). Sexual reproduction involves auxosporulation, where the sperm fertilizes the egg. After auxosporulation is complete, the new diatom will be restored to its original maximum size.

Some centric species have a two-stage life cycle involving a vegetative, reproductive stage, as described above, and a dormant resting stage when heavily silicified resting spores are developed. The functions of the resting spore are to: 1) act as

a long-term strategy to keep the species alive during adverse conditions during which the normal cell cannot survive; 2) provide a short-term escape from temporary conditions such as nutrient deficiency, and then germinating once conditions improve; and 3) act as a dispersal device for seeding new territory by traveling great distances in the guts of fish and copepods (French and Hargraves, 1980).

Many diatoms experience expedited rates of cell division and reproduction during a certain time of year. This is the annual spring or summer bloom. Blooming is an important and vital method for centric diatoms to prolong the population. The release of eggs and sperm at this time optimizes the chances of fertilization and production of zygotes (Crawford, 1995). The formation of a bloom is induced by a combination of environmental conditions in addition to an abundance of cells in the right size range for reproduction (Jewson, 1992). The development of the spring bloom is dependent on changes in nutrient levels, intensity of light penetrating the water column, and depth of wind mixing. Important nutrients are nitrate, silicate and phosphate, which are brought to surface waters by coastal upwelling and/or terrigenous runoff. Dimensions of the blooms range from small isolated patches to blankets that cover up to 20,000 km^2 (Smetacek et al., 1992). Blooms can grow rapidly, reaching peak cell numbers of up to 10,000 cells/L within days (Clemons and Miller, 1984), and can last up to a week before terminating with the exhaustion of nutrients (Barlow, 1984).

After the termination of the bloom, diatoms, both senescent and living, sink out from the surface waters. Some species form resting spores at this time and wait for resuspension to the surface waters once conditions improve. Mass sinking of live cells

and resting spores from the nutrient-depleted surface waters can be beneficial; some species have a better chance of survival at depth where the water is slightly colder and the nutrient levels are higher (Smetacek, 1985). Sinking can also prevent cells from being grazed by herbivorous zooplankton (Smetacek, 1985). To expedite sinking, many diatoms form aggregates or flocs by secreting sticky transparent gels that bind together cells and detrital grains (Smetacek, 1985; Alldredge and Gotschalk, 1989; Grimm et al., 1997). These flocs may have a sinking rate of 100 m per day or more. The rate of sinking determines which species are able to inoculate the bloom for the following season. Waite et al. (1992) suggest that low sinking rates may be advantageous for inoculum survival and the subsequent bloom of a species. Diatoms that are dead or sink too deeply are deposited to the seafloor and are incorporated into the sediments.

Ecology

Margalef (1958) first recognized that planktonic diatom species appear in a distinct three-stage succession during the annual cycle. This succession is found in many coastal temperate and subarctic regions, from the fjords of British Columbia (Sancetta, 1989a) to Alaskan waters (Waite et al., 1992) to the fjords of Norway (Braarud et al., 1974). The pattern of seasonal succession reflects the geographical distribution of the diatoms and their seed populations. Species that occur early in the succession are common in eutrophic coastal and estuarine waters, whereas species that appear later are common in oligotrophic waters (Guillard and Kilham, 1977). Species successions are most rapid and pronounced in mid- to high-latitutes and are least pronounced in tropical

regions (a relation to the strength of seasons). Guillard and Kilham (1977) have modified the three-stage succession first introduced by Margalef (1958).

Stage I begins with the introduction of nutrients to the photic zone via upwelling, strong mixing, or terrigenous runoff. Diatoms that bloom during this time are small and have high rates of vegetative reproduction. Guillard and Kilham (1977) divide this stage into two parts. Stage Ia represents the early bloom, while water temperatures are relatively cool (1 to 5 °C). The typical assemblage includes *Chaetoceros debilis* and small species of the genera *Thalassiosira*. Stage Ib represents the later bloom, as water temperatures increase. *Skeletonema costatum* and various *Chaetoceros* species (*C. affinis, C. compressus, C. radians, C. socialis*) are common at this time. Population densities can reach up to 10^7 cells/L. Stage I is typical of turbulent, mixed water conditions.

During Stage II, larger species of *Chaetoceros* and *Chaetoceros* species that have stiff bristles and form long chains appear, along with a high diversity of other genera such as *Bacteriastrum, Nitzschia* and *Rhizosolenia*. Population densities are generally lower than those found during Stage I, reaching up to 10^5 cells/L.

In Stage III, only diatoms capable of growing in low-nutrient waters persist. Both large and small diatoms are present, and dinoflagellates are introduced at this time. Diatoms characteristic of this stage include *Rhizosolenia alata, R. hebetata, Mastogloia rostrata* and some *Chaetoceros* species. Population densities are often lower than 10^4 cells/L. Most of the diatoms that proliferated in Stage II form resting spores and settle rapidly out of the photic zone as nutrients are exhausted. Stage III is typical of stratified conditions.

Other Microfossils

Silicoflagellates (class Chrysophyceae) are photosynthesizing and heterotrophic golden algae with a single flagellum and a siliceous skeleton. These planktonic algae have two life stages: the skeleton-bearing stage, which is preserved in the sediments, and the uninucleate naked stage. Dinoflagellates (division Pyrrhophyta) are photosynthesizing and heterotrophic protists with two dissimilar flagella and an organic test. Dinoflagellates have a two-stage life cycle: the free-swimming stage and the cyst stage. The cysts, which are composed of a durable organic compound called sporopollenin, are preserved in the sediments. Both silicoflagellates and dinoflagellates are discussed throughout this dissertation, but a detailed discussion of their biology and morphology is not treated here. Readers who are interested may refer to Lipps (1993) for a general discussion of these and other microfossil groups, and Tomas (1997) for a discussion of marine diatoms and dinoflagellates.

CHAPTER 3

METHODOLOGY

INTRODUCTION

Field materials and methodology are described in this chapter, as are preliminary laboratory procedures performed by me and other researchers before my samples were processed further at Carleton University for sediment and diatom analysis. Methods and materials specific to a certain type of analysis are described in subsequent chapters.

FIELD METHODS AND MATERIALS

I participated in a research cruise (IOS cruise #9940) to Effingham Inlet from 23–28 October 1999 aboard the Canadian Coast Guard Ship *John P. Tully* (Figure 3.1A). Before departure, the ship was specially fitted with a temporary A-frame and cable winch and was mounted on the starboard aft to facilitate the deployment of coring devices. The shipboard scientific and technical staff handled the logistics of the coring activity. The deployment and recovery of various coring devices used during this cruise are described below, as is sediment trap deployment and recovery performed on a prior research cruise.

Piston Core Recovery

Piston cores were taken to obtain a long sediment record. The outer and inner basins were first seismically profiled with a 3.5 kHz air gun to locate piston coring sites where sediment packages seemed relatively gas free in the top few meters (Figure 2.4).

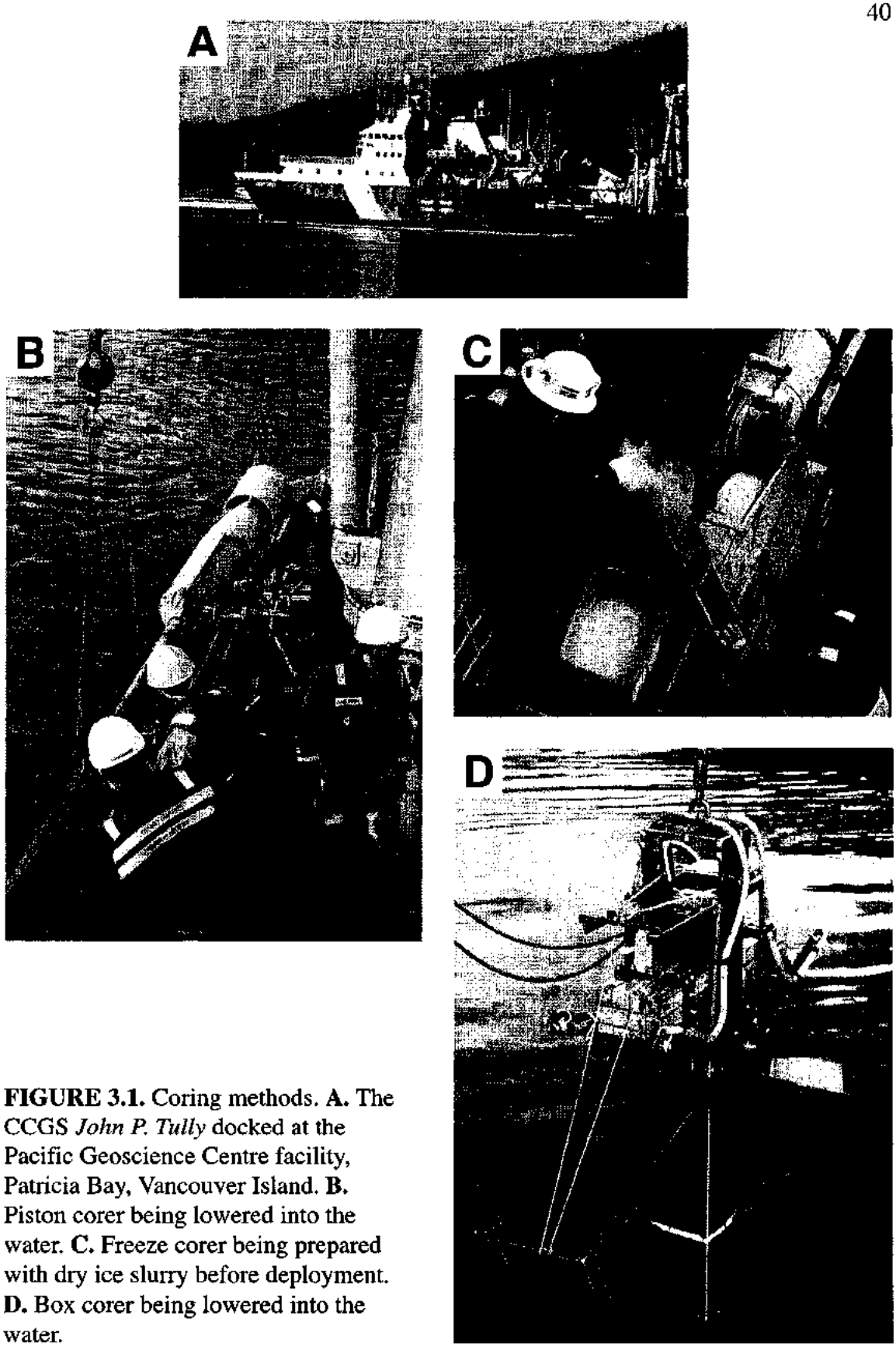

FIGURE 3.1. Coring methods. **A.** The CCGS *John P. Tully* docked at the Pacific Geoscience Centre facility, Patricia Bay, Vancouver Island. **B.** Piston corer being lowered into the water. **C.** Freeze corer being prepared with dry ice slurry before deployment. **D.** Box corer being lowered into the water.

It was also imperative to find locations away from the steep underwater walls of the basins to minimize the incidence of slumped and disturbed sediments.

For each core, a plastic core liner was inserted into the 12-m long, 11-cm diameter metal core barrel before the entire apparatus was deployed (Figure 3.1B). The corer was then lowered to within a few metres of the inlet floor until a trip mechanism was activated, allowing the corer to penetrate the sediments. Coring was mostly successful, except for a few minor complications involving the unintended overpenetration of the sediment-water interface. This interface is essentially a water-saturated "colloidal soup" of unconsolidated sediments (Kim Conway, personal communication, 1999) that presented no resistance to the free-falling piston corer. The coring device was stopped only when the end of the tether was reached. Five piston cores, each 10 cm in diameter and ~11 m in length, were collected. Four cores were taken from the inner basin within 500 m of each other in order to provide enough material for fish scales analyses. One piston core was recovered from the outer basin (Figure 3.2, Table 3.1).

After each piston core was recovered, it was raised back on board and laid down horizontally on a rack to facilitate sectioning. The plastic liner containing the sediments was extruded from the metal barrel and sectioned into eight ~1.5-m long sections. The ends were capped with plastic core caps and sealed with electrical tape. The sediments were quite gas-rich, as evidenced from the immediate expansion of the sediments once the plastic liner was cut and the pressure released. In some instances, pieces of core up to 20 cm in length at the ends of the sections were blown off by the expanding gas and disoriented before the caps could be fitted. These pieces were collected in plastic bags,

SAMPLING SITES

Inner Basin
- Site 1:
  - TUL 99 B01 (Freeze Core 1)
  - TUL 99 B02 (Box Core 1)
  - TUL 99 B03 (Piston Core 1)
- Site 2:
  - TUL 99 B04 (Freeze Core 2)
  - TUL 99 B05 (Box Core 2)
  - TUL 99 B06 (Piston Core 2)
  - TUL 99 B13 (Piston Core 5)
- Site 3:
  - TUL 99 B07 (Freeze Core 3)
  - TUL 99 B08 (Box Core 3)
  - TUL 99 B09 (Piston Core 3)

Outer Basin
- Site 4:
  - TUL 99 B10 (Freeze Core 4)
- Site 5:
  - TUL 99 B11 (Piston Core 4)
- Site 6:
  - TUL 99 B12 (Freeze Core 5)

Sediment Traps
- Site A: CTC3
- Site B: CTC11

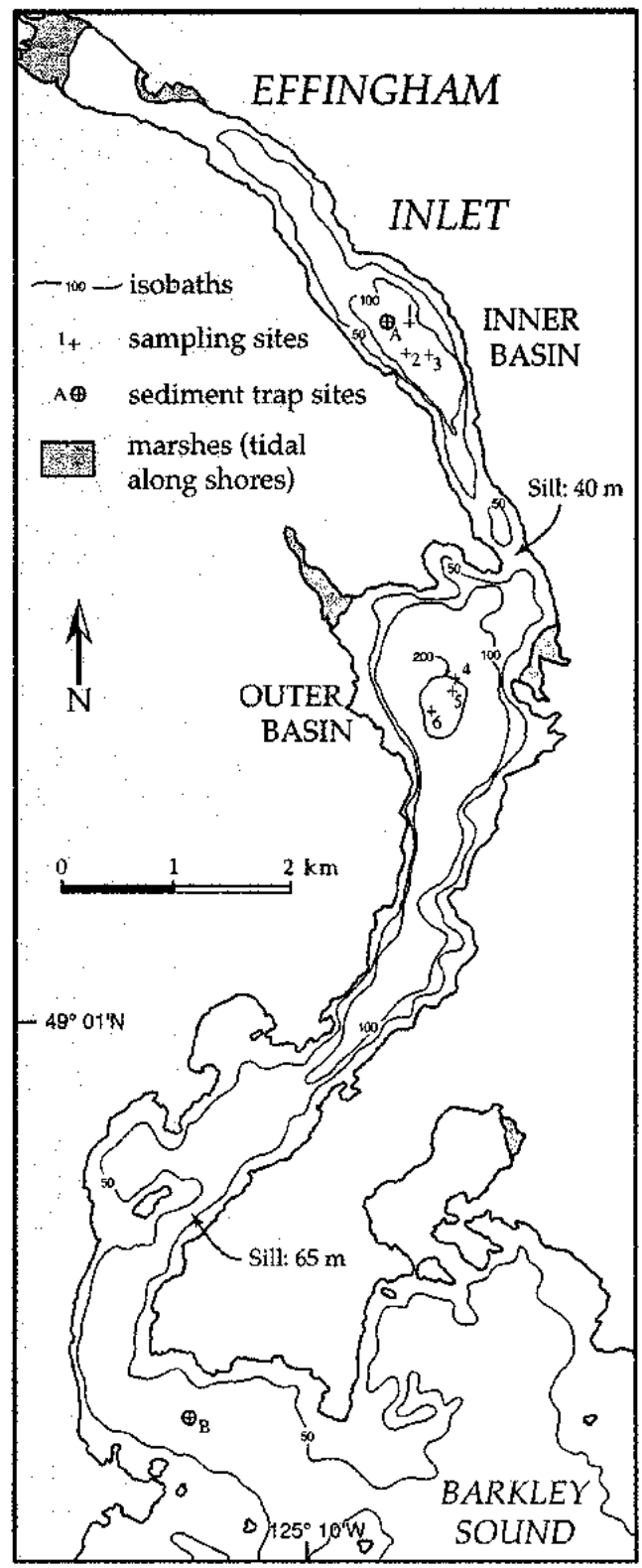

FIGURE 3.2. Sampling locations for cores and sediment traps.

TABLE 3.1. Core locations, depths of recovery and lengths

A. Inner Basin

Core	Type	Latitude (N)	Longitude (W)	Water Depth (m)	Length (cm)
TUL99B01	freeze	49° 04.269'	125° 09.399'	119	129
TUL99B02	box	49° 04.277'	125° 09.334'	118	124
TUL99B03	piston	49° 04.275'	125° 09.359'	120	1140
TUL99B04	freeze	49° 04.218'	125° 09.429'	120	124
TUL99B05	box	49° 04.266'	125° 09.417'	120	104
TUL99B06	piston	49° 04.188'	125° 09.337'	121	1151
TUL99B07	freeze	49° 04.145'	125° 09.337'	121	129
TUL99B08	box	49° 04.145'	125° 09.279'	122	109
TUL99B09	piston	49° 04.145'	125° 09.279'	122	1122
TUL99B13	piston	49° 04.173'	125° 09.401'	122	1092

B. Outer Basin

Core	Type	Latitude (N)	Longitude (W)	Water Depth (m)	Length (cm)
TUL99B10	freeze	49° 02.042'	125° 09.043'	205	90
TUL99B11	piston	49° 02.632'	125° 09.023'	205	1016
TUL99B12	freeze	49° 02.632'	125° 09.023'	205	70

labeled and catalogued. Small holes were drilled into the plastic core liners to aid in gas release and to allow for drainage of excess water from the sediments. Once the core sections were secured, they were stored upright in an on-board cooler at 4 °C.

Freeze Core Recovery

Freeze cores were recovered in the same areas as the piston cores. The freeze corer is used to retrieve the uppermost sediment layers (the sediment-water interface) with minimal disturbance because the sediments and their water content are frozen onto the surface of the corer.

The freeze coring device used during the cruise was designed by Dr. John Crusius (Department of Earth and Ocean Sciences, University of British Columbia) based on existing designs (e.g., Hughen et al., 1996). Measuring ~3 m long by 10 cm^2, the corer is a rectangular aluminum box which tapers to a wedge at the bottom. The aluminum is insolated with incompressible syntactic foam on three sides of the box, with one side of aluminum exposed to allow sediments to adhere to the exterior (J. Crusius, written communication, 2001). At the top of the box is a cryogenic temperature check valve from which CO_2 from dry ice is allowed to escape. Prior to deployment, the box was filled with a slurry of crushed dry ice and isopropyl alcohol (Figure 3.1C). Lead weights were added to the corer to provide upright stability and to allow the corer to penetrate the sediments. The corer was lowered into the water and into the sediments, taking care not to have the corer enter the sediments at an angle. The corer was allowed to sit in the sediment for twenty to thirty minutes as the sediments froze to the supercooled surface of

the corer. After the sediments were sufficiently frozen to the surface of the corer, it was carefully brought back on board the ship. Five freeze cores were collected, with three from the inner basin and two from the outer basin (Figure 3.2, Table 3.1).

The laminae in the freeze cores were clearly visible as the cores were brought on deck. After a few minutes a frosty rind had developed and the laminae were no longer visible. The corer was laid down horizontally and the sediment was permitted to fully freeze over. The sediment was then sectioned diagonally with a handsaw into ~1-m lengths for easier handling and storage. The pieces were carefully pried off the frozen corer surface and placed on plywood boards, wrapped in plastic film and heavy-duty aluminum foil, and then stored horizontally in an on-board chest freezer for the duration of the cruise.

Box Core Recovery

Box cores were also taken in the same areas as the piston cores. The box core is intended to recover unfrozen sediments from the sediment-water interface. The coring device consists of a metal box about 2 m by 400 cm^2, with spring-loaded doors on the bottom (Figure 3.1D). The box is lowered into the sediments and the spring-loaded doors are triggered, holding the sediment in. Three box cores were recovered from the inner basin (Figure 3.2, Table 3.1).

The sediments from box coring were brought up on deck and were left in the device standing upright for the duration of the cruise. I collected two surface samples (3

scoops each with a tablespoon) from box cores TUL99B05 and TUL99B08 in sealed plastic bags and stored them in a refrigerator throughout the duration of the cruise.

Sediment trap recovery

The logistics of the sediment trap project were planned and coordinated by Dr. Miriam Bertram (Pacific Marine Environmental Laboratory, Seattle, Washington; currently at the University of Washington, Seattle). Technical aspects of sediment trap moorings, deployment and recovery were handled by the Institute of Ocean Sciences (principally Dr. Rick Thomson, Dr. Brenda Burd, Mary O'Brien and Doug Yelland). A sediment trap consists of a collection cone open to the water column, and an array of collection cylinders timed to open beneath the cone at programmed intervals. Moorings equipped with two types of particle traps and Aanderaa RCM4 Savonious rotor current meters were deployed in May 1999 by the CCGS *Tully* inside the inner basin and at the mouth of the inlet (Figure 3.2). Baker traps have a collection area of 0.03 m^2 and OSU traps have a collection area of 0.49 m^2. A Baker trap was placed approximately 40 metres above the bottom of the inlet (mab) and an OSU trap was placed approximately 30 mab at a water depth of 116 m in the inner basin, and a water depth of 80 m at the inlet mouth. The current meters were placed at 38.35 mab at both sites.

Each trap consists of 14 sequential sample collection cylinders timed to rotate every 8 to 15 days, depending on the trap type and anticipated length of mooring deployment (Table 3.2). The collection time intervals varied in length to allow for enough material to be collected in each cylinder (M. Bertram, personal communication,

TABLE 3.2. Collection times (days) for Baker and OSU traps from May 1999 to September 2000. Data courtesy of M. Bertram.

	May 1999		Sept. 1999		May 2000	
	Baker	OSU	Baker	OSU	Baker	OSU
Inner Basin	13.25	8.86	22	15	13.75	9.82
Mouth	13.25	×	22	×	13.75	9.82

×: loss of data due to mechanical failure

2003). Each collection cylinder was mechanically sealed from the surroundings except during the programmed interval when opened to the water above by rotation of the collection cone. Cylinder solutions were composed of filtered seawater (GFF and/or 0.2 μm Nuclepore^{TM}), poisoned with sodium azide (4 g/L NaN_3) to prevent bacterial decomposition yet minimize solubilization of metals, and NaCl (3 g/L) to prevent mixing between ambient and cylinder seawater (M. Bertram, personal communication, 2002). Glass rods were included in the cylinders to minimize dissolution of diatom frustules. All cylinders and glass rods were soap and acid washed, and rinsed with deionized water prior to use. The moorings and traps at each site were replaced approximately every 6 months, for a total deployment of 18 months. Mechanical failures in the OSU trap deployed at the mouth of the inlet resulted in the loss of samples during the first 12 months of the experiment.

The Baker traps were deployed for their reliability and cleanliness (less contamination potential) for geochemical analyses. The OSU traps provided larger samples that could be used for various microfossil analyses.

LABORATORY METHODS

Laboratory procedures for the cores were carried out at the Pacific Geoscience Centre (PGC) in Sidney, British Columbia, in the week after the October cruise. The PGC is a sector of the Geological Survey of Canada and occupies research and docking facilities along with the Department of Fisheries and Oceans and the Institute of Ocean

Sciences. The CCGS *Tully* and other Coast Guard vessels are also docked at these facilities.

The piston cores were transferred upright to the laboratory for processing while the freeze cores were stored away in a chest freezer at the PGC. The box cores were stored upright in a former helicopter hangar on the PGC premises. Sediment trap samples were sent to the Pacific Marine Environmental Laboratory in Seattle, Washington, to be processed by Dr. Miriam Bertram.

Piston Cores

The lower 5 sections (sections 4 to 8) of each piston core were processed first because they had been sufficiently dewatered. These sections were split lengthwise in half using a small power saw to cut through the plastic liner, and fishing line to splice the sediments, to produce a working half and an archive half. The halves were then wrapped in plastic film and stored flat in plastic D-tubes with a wet sponge to maintain moisture. The upper three sections (sections 1 to 3) still contained excess water and were stored upright in a walk-in cool room for two months to allow further dewatering. All eight sections of each core were then described in detail and photographed by my colleague Audrey Dallimore who was stationed at the PGC for the duration of her doctoral studies. After descriptions were completed, the cores were stored horizontally in their D-tubes on racks in the hangar. The year-round ambient temperature within the hangar remains below 10 °C.

I returned to the PGC in December 1999 to photograph and subsample the piston cores. The drier sections of the cores were slightly dessicated, as small cracks that were present when the core was first split were now larger. However, the continuous handling and movement of the cores by various co-workers may also have created these cracks. After visual inspection of the cores and consultation with Dr. Dallimore, I decided to focus on core TUL99B03 (from the inner basin) because it recovered the highest percentage of visibly distinct laminae of all the cores.

Sediment slabs were extracted from piston core TUL99B03 using a sediment slab extraction device nicknamed the "cookie cutter" (Figure 3.3). The original cookie cutter was described in Schimmelmann et al. (1990) and subsequently modified (Grimm et al, 1996). With the aid of the Science and Technology Centre at Carleton University, a copy of the Grimm cutters was made where I added minor modifications to the design to further improve sediment recovery. The cutters were made in lengths of 20 cm and 15 cm.

The construction and concept of the cookie cutters is simple, yet very effective for the extraction of wet, unconsolidated sediment slabs of a constant thickness. The cookie cutters consist of a rectangular metal sheath, in which the sediment is extracted, and an acrylic plunger for extruding the sediment from the sheath. When the metal sheath is pressed into the sediment, the moist sediment adheres to the metal surface and allows for the extraction of the slab. The cutters produce slabs of 1 cm thickness and a breadth of 3 cm, which is ideal for x-radiography.

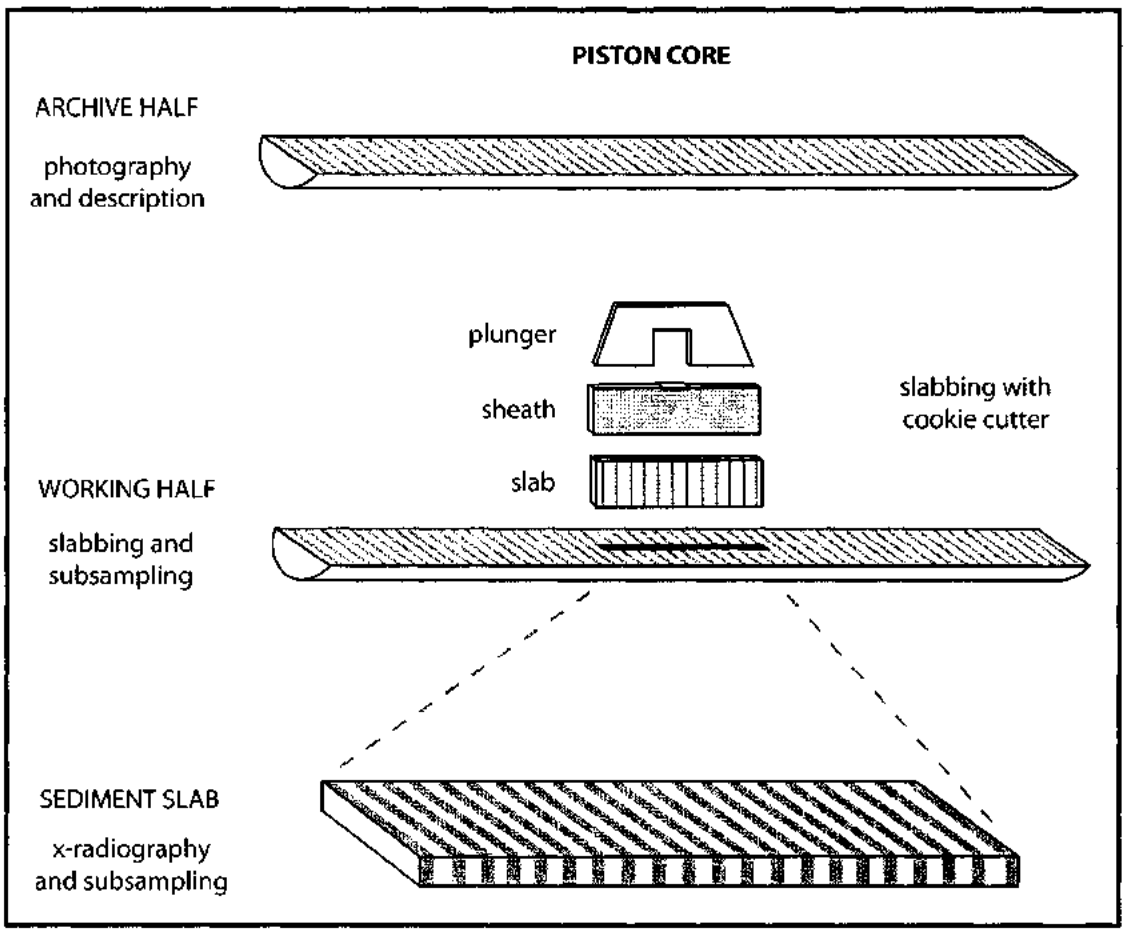

FIGURE 3.3. Schematic diagram showing methodology of piston core processing and sediment slab extraction with a cookie cutter slabbing device. No scale is intended.

Locations for sediment slabbing were selected based on the quality of the preservation of laminae in order to ensure an ultra-high resolution examination of a variety of representative laminated sequences throughout the core. Ten slabs were extracted from intervals containing well-preserved laminae (see Chapter 4). The slabs were wrapped in household plastic wrap, placed in a cardboard liner for stability, and wrapped in aluminum foil. The slabs were kept refrigerated and transported in a cooler to Carleton University. The slabs would eventually be used for x-radiography, ultrta-high resolution sedimentary analyses, and quantitative diatom analyses and cyclostratigraphy (Chapters 4 and 7).

Freeze Cores

The cores were stored at –15 ˚C at the PGC until they were to be analyzed. Dr. Dallimore described the cores one month after the October cruise. The surface of the sediments had already oxidized into a black color by this time and the laminae were not visible (Dallimore, 2001).

After descriptions were completed, the cores were rewrapped and stored into a chest freezer. The freezer and its contents were then transported in by truck from the PGC to Carleton University. Core TUL99B04 was chosen for detailed diatom analysis because of its well-laminated character (Chapter 6).

Box Core Samples

Sediments from the box cores were not used for this study and remained in storage in the hangar at the PGC. Only the three small surface samples I took were analyzed for ^{210}Pb in order to determine the age of the sediment/water interface. This was done to provide a correlation between the box and freeze cores. However, the box core surface samples could not be correlated with the tops of the freeze cores and were not used for any subsequent analyses.

Sediment Trap Samples

Trap materials were collected from the cylinders by M. Bertram and M. O'Brien at the end of each collection interval. The samples were processed by Dr. Bertram at the Pacific Marine Environmental Laboratory. The samples were stored at 4 °C, and within 3 months of trap recovery, collection material was divided into 6 subsamples using an air driven precision plankton splitter (M. Bertram, personal communication, 2002). Samples for the determination of total dry mass were filtered onto preweighed 0.4 μm pore size Nuclepore™ membranes. Salts from the trap solutions were removed with pH-adjusted (8.0) deionized water (M. Bertram, written communication, 2002). The samples were then dried in a dessicator, and the total mass of each sample determined.

Samples from the Baker traps were retained by Dr. Bertram for geochemical analyses and will be briefly discussed in Chapter 5. OSU samples were distributed to various researchers for work on diatoms, dinoflagellates and foraminifera. The diatom work is detailed in Chapter 5.

SUMMARY

Materials used exclusively for this ultra-high resolution study were: 1) piston core TUL99B03 from the inner basin, 2) freeze core TUL99B04 from the inner basin, and 3) sediment traps CTC3 and CTC11 from the inner basin and mouth of the inlet, respectively. The main results from the study of these materials are detailed in the next four chapters.

CHAPTER 4

ULTRA-HIGH RESOLUTION SEDIMENT FABRIC ANALYSIS, WITH EMPHASIS ON SEASONAL VARIABILITY

ABSTRACT

Laminated diatomaceous sediments from the inner basin of Effingham Inlet are described and classified in this study. Analyses were made from ten 15-cm long sediment slabs, spanning the last 5500 years, and 52 thin sections from which 408 sedimentary couplets were identified. Microfossil analysis and radiocarbon dating of the sediments reveal that the laminae are annually deposited (i.e., varves), with couplets containing a terrigenous and diatomaceous lamina pair. Terrigenous laminae, averaging 0.56 mm in thickness, consist of silt, organic debris and robust diatoms, and are deposited during the winter months. Diatomaceous laminae, with a mean thickness of 1.85 mm, can be divided into three component laminae of differing compositions that reflect changing seasonal conditions during the spring, summer and autumn months. This seasonal succession is seen in 76% of the couplets examined, recurring year after year with variations in couplet thickness and species composition. Couplets lacking the succession may represent deposition during periods of low diatom production or years with weak seasonality (e.g., El Niño). Variability in couplet styles corroborates climate trends derived from pollen and neoglacial studies. Sediments older than 4000 yr BP (calibrated radiocarbon dates) contain couplets with a distinct annual succession, and are interpreted to have been deposited during conditions that were warmer than today. Sediments deposited between 2000 to 4000 yr BP also contain couplets with an annual succession, but the laminated

sediments are interrupted by brief nonlaminated sediments. The sediments were likely deposited during cooler and wetter conditions than today. Sediments younger than 2000 yr BP were deposited during modern conditions. This study illustrates the effective utility of an ultra high-resolution analysis of laminated sediment records, once proxy indicators are defined, and is important for understanding post-glacial climate evolution along the coast of British Columbia and throughout the northeast Pacific Ocean during the late Holocene.

INTRODUCTION

Before detailed research began in Effingham Inlet, there was only a basic knowledge of the composition of the sediments in the basins. From small piston cores taken in 1997, and by comparing these sediments with those from other anoxic basins, the sediments were known to contain couplets of alternating diatomaceous and terrigenous laminae. Beyond that, not much was known about the internal structure of these laminae or the conditions of their formation. The main objective of this chapter, therefore, is to explore the nature of the laminated sediments in Effingham Inlet.

In order to reconstruct past climate records, it is important to understand what the sediments are composed of and how they were formed. The finely laminated sediments from Effingham Inlet are ideal for such a paleoclimate study because they represent a high-resolution paleoenvironmental archive. Hence, three key tasks performed to accomplish the objective of this study were to: (1) determine a chronology for the sediments, (2) determine the composition and origin of individual couplets and laminae,

and (3) establish a broad-scale climate record based on chronology and sediment composition. The chronology of the core was determined using radiocarbon dating. The composition of the sediments was determined by examining the laminated fabric and diatom content at an ultra-high stratigraphic resolution over specific intervals of core. The sequence and composition of laminae could then be related to subtle changes in local climate and coastal ocean dynamics of the late Holocene, illustrating the utility of ultra high-resolution diatom stratigraphy to paleoenvironmental interpretations. The baseline data presented in this chapter will be used to interpret late Holocene paleoclimatic and paleoceanographic changes in the northeast Pacific Ocean. A comparison of the laminated sediments with modern sedimentary flux patterns (Chapter 5) will allow for an understanding of the timing and magnitude of flux events, and how these events relate to environmental conditions.

METHODS AND MATERIALS

Determination of Chronology

Shell and wood material were extracted from piston core TUL99B03 (inner basin, Figure 4.1) and other piston cores by Dr. Dallimore for accelerated mass spectrometry (AMS) radiocarbon dating (Dallimore, 2001). A single shell and wood pair collected from outer basin core TUL99B11 was used to determine the local marine reservoir correction factor, ΔR, for the Effingham Inlet sediments. The marine reservoir correction is used to correct for radiocarbon ages determined from marine and terrestrial sources due to slightly different ^{14}C compositions between the two sources. It must be noted,

Inner Basin

Site 1:
TUL99B03 (Piston Core 1)

Latitude: 49° 04.275' N
Longitude: 125° 09.359' W
Depth: 120 m

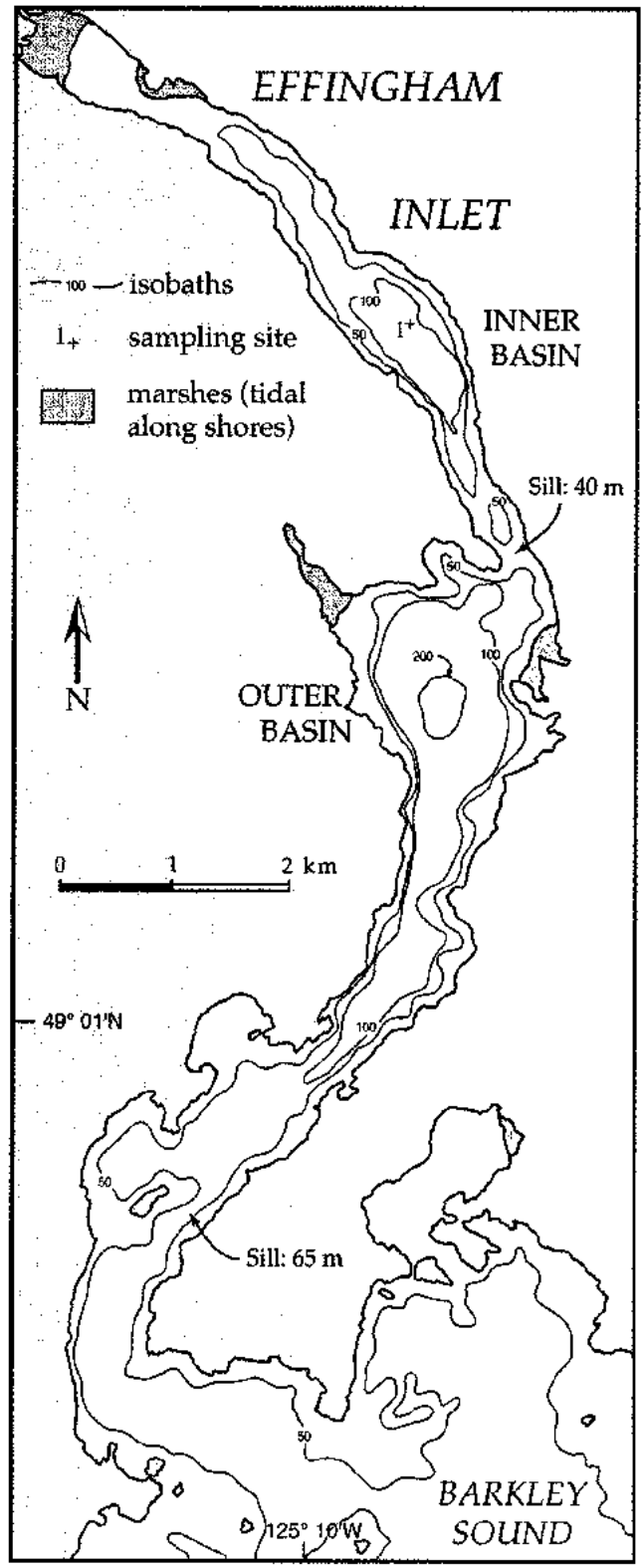

FIGURE 4.1. Location of piston core TUL99B03.

however, that the shell and wood pair were separated in the core by 41 cm. Dating of the material was performed by Dr. Roelf Beukens at the IsoTrace Radiocarbon Laboratory at the University of Toronto. The dates were calibrated by Dr. Beukens' calibration program C14CAL98 by comparison to the dendrochronologically derived INTCAL98 dataset for terrestrial material and the MARINE98 dataset for marine material (Stuiver et al., 1998a, b). A reservoir correction of 390 ± 25 yr (Stuiver and Braziunas, 1993) was used for the marine correction as this is the accepted factor for waters west of Vancouver Island.

X-radiography

X-radiography is a useful tool for elucidating differences in texture, density and composition of sedimentary components that are not readily visible in the hand sample. Saturation of the x-ray film is inversely proportional to the bulk density of the sediments. Laminae rich in diatoms are less dense due to the porous nature of diatom frustules. These laminae have a high x-ray transimissivity and appear as light shades in x-radiograph positive images. Terrigenous laminae are denser and will appear as dark shades in positive images.

X-radiography was performed at the Geological Survey of Canada (Ottawa) by Roger McNeely on a Faxitron Series 43805-N 110 kV X-ray system. This machine emits x-rays in a cone with a maximum exposure diameter of ~25 cm. At the center of the exposure area, x-rays are emitted almost vertically from the source to the target so images produced here will be sharp. Away from the center and toward the edge, the x-rays traveling from the source to the target are emitted at increasing angles from the vertical.

As a result of this parallax, the images are not as sharp because the incoming x-rays are passing through the sedimentary lamina obliquely. An x-ray source with a collimated, or more focused, cone would reduce this problem (Algeo et al., 1994).

Sediment slabs were removed from their foil and plastic wrappings prior to x-radiography to eliminate the appearance of "ghost" wrinkles that may appear if the slabs remained inside the wrap. X-rays were shot onto Agfa™ D7 and D4 strip film, with voltages ranging from 32 to 35 kVp, a constant current of 3.2 mA, and exposure times ranging from 90 to 165 seconds.

The x-radiograph negatives were scanned into a computer and converted into positive images using Adobe® Photoshop™ software. The positive images were used to describe the sedimentary fabrics, determine laminated sequences ideal for backscattered electron microscopy, and to choose sites for subsequent high-resolution diatom sampling (see Chapter 7). The preservation quality of laminae was assessed from the x-radiographs (Table 4.1).

Epoxy Impregnation

Epoxy impregnation of the unconsolidated sediments is required for the production of polished thin sections for use in microscopy. The impregnation technique is far superior to air drying or freezing the sediments that can distort fine sedimentary features (Lamoureux, 1994). Spurr™ low-viscosity epoxy resin was used for the impregnation. The low viscosity allows the epoxy to penetrate the fine pores and voids of the sediment and diatom frustules. The proportions of epoxy components required to

TABLE 4.1. Descriptive terminology for lamina quality, component abundance estimates, and microfossil preservation criteria

Quality*	
Distinct	lamina contacts sharp; thickness constant; high colour contrast between lamina types
Indistinct	lamina contacts diffuse or gradational; thickness uneven; low colour contrast between lamina types
Well-preserved	laminae distinct or indistinct; laterally continuous; no distortion
Poorly preserved	laminae distinct or indistinct; laminae are truncated, distorted or broken
Abundance†	
Abundant	≥50%
Common	25-50%
Occasional	5-25%
Rare	<5%
Absent	0%
Preservation§	
Excellent	specimens pristine; fine morphological features preserved; specimens not altered by physical or chemical dissolution
Good	lightly silicified and robust specimens present; minor alteration
Moderate	lightly silicified specimens present but altered; robust specimens dominate
Poor	lightly silicified specimens absent or rare and altered; robust specimens altered

* quality of laminae in hand sample and x-rays

† abundance of components per field of view per lamina in thin section

§ preservation of microfossils in microscope analyses

produce a hard, polishable resin are listed in Polysciences, Inc., Data Sheet #127 (Polysciences, 1995). The impregnation technique used in this study is similar to that described by Lamoureux (1994).

A 5-mm wide sediment strip was sliced perpendicular to laminae along the edge of each sediment slab and embedded with epoxy resin for the production of a continuous set of thin sections for each slab (Figure 4.2). The remainder of each slab was reserved for quantitative diatom analyses. The strips were produced by using a kitchen spatula that was pressed into the slab with a single downward motion to prevent smearing of laminae. The strips were carefully transferred onto a plastic artist's mesh (7-mesh, clear plastic canvas) and then placed in a 3.78 L heat resistant plastic food container with an air-tight lid. The mesh helps to improve the circulation of liquids underneath the sediment strips.

The water in the sediment first needed to be removed before the epoxy could be applied (Lamoureux, 1994). The epoxy will not set correctly and will become cloudy if water remains in the sediment. Water removal was accomplished with several acetone exchanges. The first five exchanges were carried out with laboratory grade acetone. The acetone was gently poured down a stirring rod at the corner of the container. The unexpected result of this was that the sediment strips readily floated off the mesh, with some of the strips breaking into several pieces. Any sections of sediment that became completely disoriented or were unusable were discarded. After reorienting any broken strips, the container lid was tightly closed and the acetone was allowed to sit for a minimum of five hours. The old acetone was then vacuumed out with a vacuum pump. Once the sediment strips became saturated with acetone, they no longer floated off the

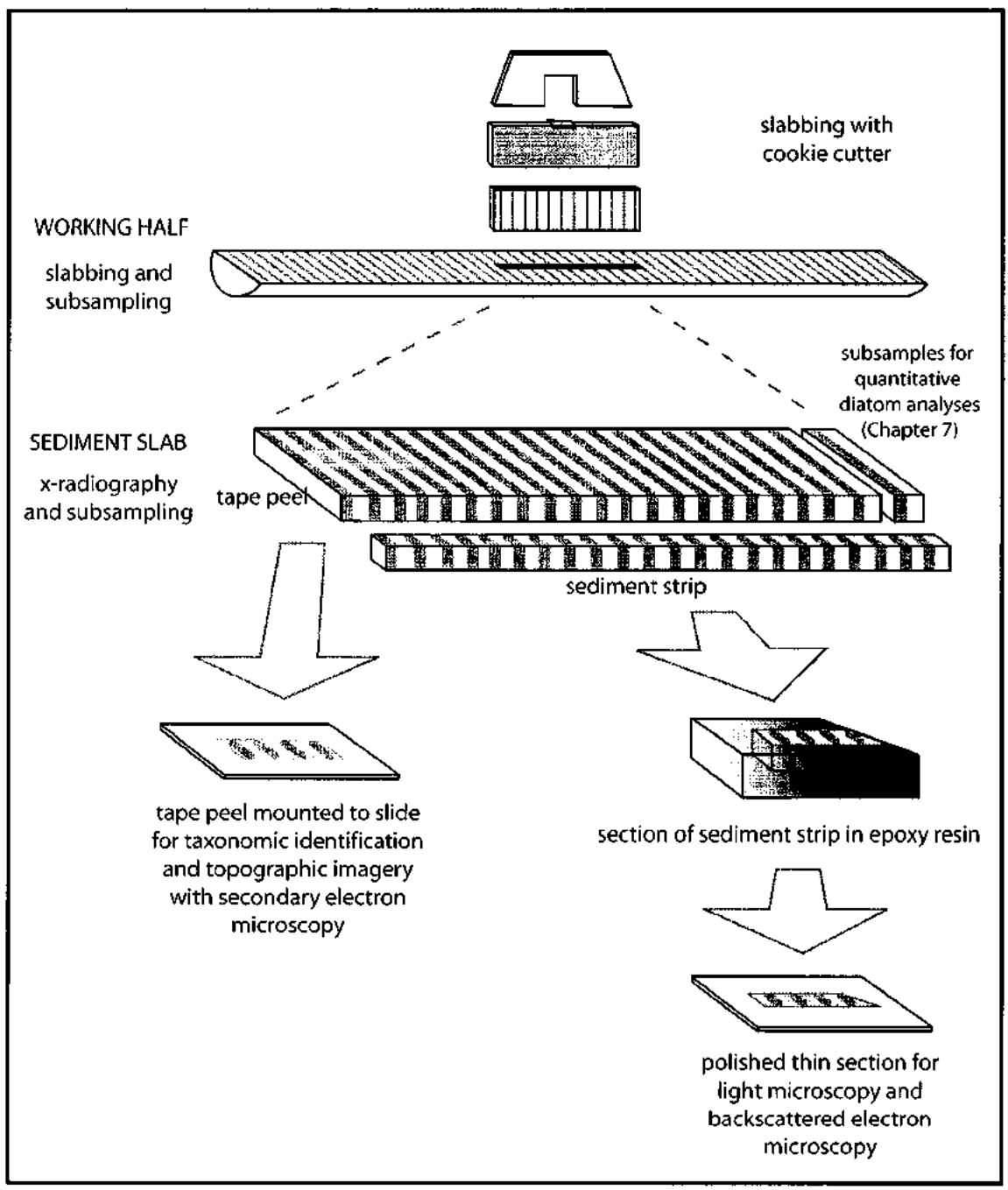

FIGURE 4.2. Schematic diagram showing methodology used for producing thin sections and tape peels from sediment slabs. No scale is intended.

mesh in subsequent exchanges. After the first five exchanges, reagent grade acetone was used for four additional exchanges. After the reagent grade acetone exchanges were completed, there were eight exchanges of epoxy resin. After the final epoxy exchange, the epoxy and sediments were cured in an oven at 50 °C for 48 hours. The cured epoxy-impregnated sediment was then sectioned diagonally into 3-cm long pieces with a high-powered bandsaw and highly polished into thin section slides using conventional techniques. Fifty-two slides were produced.

Light Microscopy

Each thin section was first photographed at a magnification of 12× with an Olympus SZH-10 stereo microscope and a digital microscope camera. The images served as a basemap for the subsequent description of laminae. Measurements of lamina thickness were also made from the photographs. The thin sections were then examined with a petrographic microscope at magnifications of up to 400×. Diatoms and other microfossils were identified to generic level and to species level when possible. The abundance of microfossils and other particles were semi-quantitatively assessed by visually estimating the percentage proportion of the microfossil or particle per field of view per lamina (Table 4.1). The percentage estimates and compositions were then used to classify laminae. Preservation status of microfossils was also assessed (Table 4.1).

Backscattered Electron Microscopy

The thin sections were prepared for backscattered electron microscopy (BSEM) with the application of a conductive carbon coating. BSEM was accomplished with a JEOL 6500 scanning electron microscope system in backscattered electron mode. BSEM produces cross-sectional images of sediments and allows for the high-magnification examination of submillimeter fabrics (Kemp 1990, Kemp and Baldauf 1993). Images are produced when the electron beam excites a target zone on the sample that emits electrons and allows for the evaluation of elemental difference. Objects such as mineral grains that have a high backscatter coefficient (related to the average atomic number of the target) will appear bright in the image, whereas objects with a low coefficient, such as the carbon-based epoxy, will appear dark. Therefore, backscattered images can be used as both a compositional and porosity index (Pike and Kemp 1996).

Secondary Electron Microscopy

Secondary electron microscopy (SEM) allows for the topographic imagery of sediments *in situ*, and is also useful for taxonomic identification. Several tape peels approximately 3 cm in length were produced by pressing double-sided adhesive tape to a glass slide, and then pressing the exposed adhesive surface to the sediment slab surface. The slide was allowed to air dry and was then coated with a gold-palladium mixture. SEM was accomplished with a JEOL 6500 scanning electron microscope system in secondary electron mode.

RESULTS

Chronology

Results from AMS radiocarbon dating pertinent to this study are reported in Table 4.2 (see Appendix A for results from all piston cores). Shell dates calibrated with $\Delta R = 390 \pm 25$ yr yielded ages that were -801 ± 23 yr too old for marine samples for the region (Dallimore, 2001). The ΔR for Effingham Inlet calculated from the shell and wood pair collected from outer basin core TUL99B11 was determined to be -120 ± 45 yr, which is different than the accepted value for this region. As a result, calibrated shell dates were not used in the determination of the sediment accumulation rate because a marine reservoir correction has not been definitively established for restricted fjords, such as Effingham Inlet, on the coast of British Columbia (R. Beukens, written communication, 2002). Additionally, the wood sampled at 97 cm depth in TUL99B03 was not used for determining the sediment accumulation rate because it has a wide rage of possible ages and is too young for its depth (Appendix A). This is because anthropogenic fossil fuel burning in the last 500 years has diluted the ^{14}C content in the atmosphere, making the remaining radiocarbon in very recent sediments difficult to match with the INTCAL98 dataset (Dallimore, 2001). The wood date at the bottom of the core TUL99B03 is suspect because it was collected in a massive interval, however, this wood date falls in line with the two wood dates collected in the middle of the core.

Using these three wood dates shows that ~5500 years of deposition were recovered in core TUL99B03 (Figure 4.3). A linear sediment accumulation rate of 2.25 mm/yr was calculated from the regression line drawn through the three calibrated wood

TABLE 4.2—Radiocarbon dates obtained from core TUL99B03 (after Dallimore, 2001). See Appendix A1 for details.

Sample Number	Lab Number	Depth in Core (cm)	Material Dated	Lithology	Radiocarbon Age (yr BP)	Correction 801 ± 23 yr BP*	Calibrated Age (cal yr BP)† ΔR = 390 ± 25 yr (–120 ± 45 yr)	Calibrated Calendar Dates§ ΔR = 390 ± 25 yr (–120 ± 45 yr)
RC03S101	TO-8671	97	wood	poorly laminated	160 ± 40		195 ± 150	AD 1655–1955
RC03S201	TO-8672	169	shell pair	poorly laminated	1770 ± 60	969 ± 83	970 ± 135 (1495 ± 160)	AD 895–1165 (AD 345–665)
RC03S301	TO-8673	286	twig	well laminated	2050 ± 70		1858 ± 62	BC 80–AD 205
RC03S501	TO-8674	553	twig	laminated	2830 ± 60		2980 ± 150	BC 1130–830
RC03S601	TO-8675	822	shell pieces	well laminated	3890 ± 80	3089 ± 103	3435 ± 185 (4085 ± 245)	BC 1620–1250 (BC 2330–1840)
RC03S701	TO-8676	937	wood	massive	4190 ± 80		4745 ± 175	BC 2920–2565

* correction applied to marine ages after calibrating with ΔR = 390 ± 25 yr; reported by Robinson and Thomson (1981)

† calibrated age after applying ΔR = 390 ± 25 yr (Stuiver and Braziunas, 1993) or ΔR = -120 ± 45 yr (determined from Effingham Inlet outer basin samples RC11S801A [shell, 2830 ± 30 yr BP] and RC11S801 [wood, 2570 ± 60 yr BP])

§ calibrated results are reported at the 2-sigma (95.5% confidence interval) range

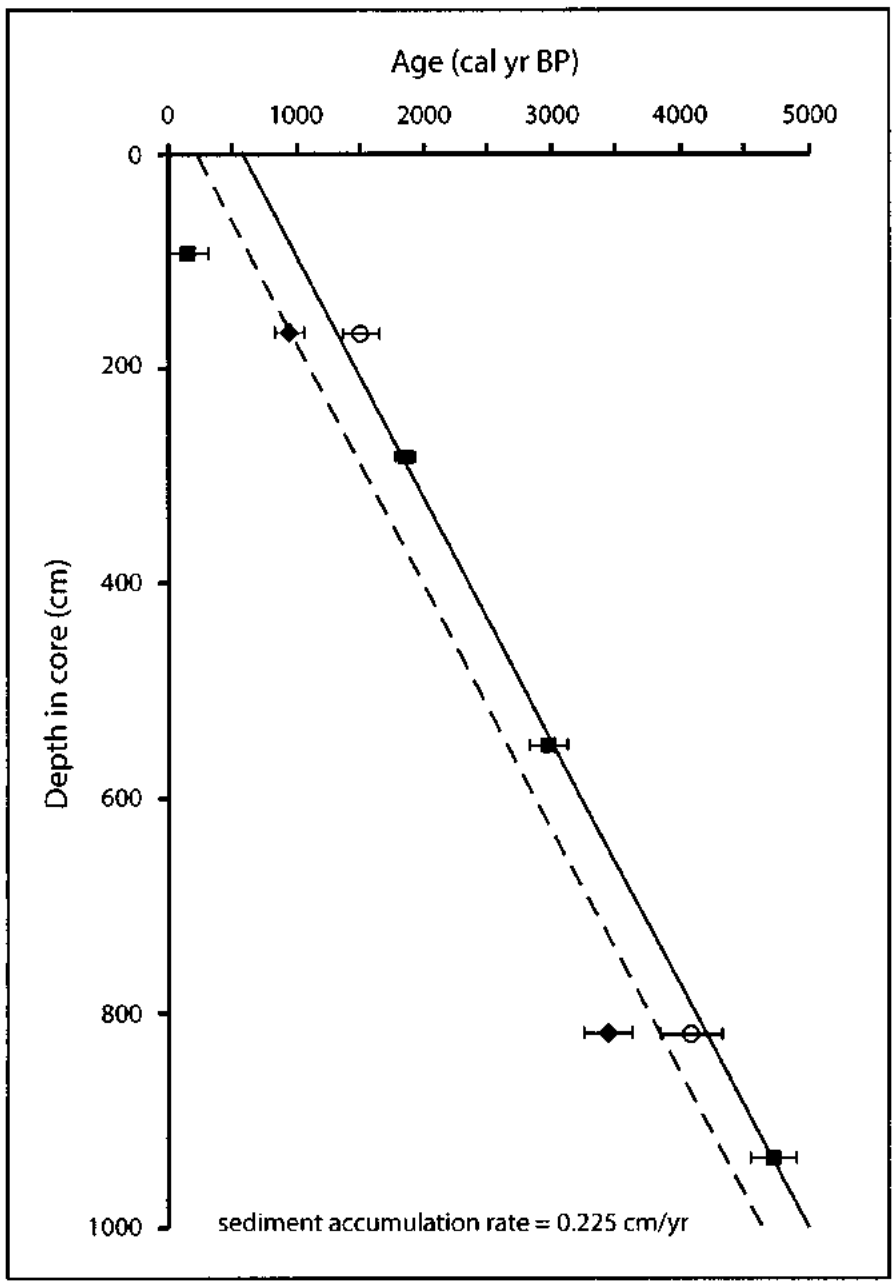

FIGURE 4.3. Age-depth diagram showing positions for wood/twig material (■), shell material (◆) calibrated using ΔR = 390 ± 25 yr, and the same shell material (○) calibrated using ΔR = −120 ± 45 yr. Regression line (solid line) is fitted to three wood dates; wood dated at 97 cm depth is suspect and therefore not included in regression line. Calibrated shell depths were not used to determine this regression line, but shell dates calibrated with ΔR = −120 ± 45 yr fit the regression line better than shell dates calibrated with ΔR = 390 ± 25 yr. Alternate regression line (dashed line) is fitted to all dates calibrated using ΔR = 390 ± 25 yr. Average linear sediment accumulation rate calculated from slope of each regression line is 2.25 mm/yr.

dates, and shows that the top ~600 yr (~1.4 m) of sediments were not recovered. The number of years not recovered is likely less than presented due to the less compacted nature of the sediment toward the sediment-water interface. Using an alternate trendline, involving all dates calibrated with $\Delta R = 390 \pm 25$ yr, yields the same sediment accumulation rate, but a different date for the top of the core (Figure 4.3). Moreover, the sediment accumulation rate varies depending on whether all calibrated dates are used in the calculation, only valid dates are used, and which ΔR for the shell dates was used. The sediment accumulation rate can be calculated as low as 1.90 mm/yr, or as high as 2.60 mm/yr (which is what Dallimore, 2001, reported when using all calibrated shell and wood dates, using $\Delta R = 390 \pm 25$ yr). A rate of 2.25 mm/yr also represents an average between these two extremes, and it is this rate, along with the top of the core at ~600 yr, that will be used for all subsequent discussion. The sediment accumulation rates were calculated based on the assumption that gravity flow deposits added and eroded sediments equally, and that down core compaction was negligible; hence, the sediment accumulation rate reported here represents an average rate.

Sediment Slab Descriptions

After a few months in refrigerated storage, Slabs 1 and 2 were still moist. These slabs were from the upper two sections of the piston core (Figure 4.4). Slabs 3 to 10, from the lower sections of the core, were drier and more cohesive. The slabs were lightly sprayed with distilled water to keep them from desiccating in the refrigerator. The distilled water also helped to temporarily enhance the appearance of the laminae.

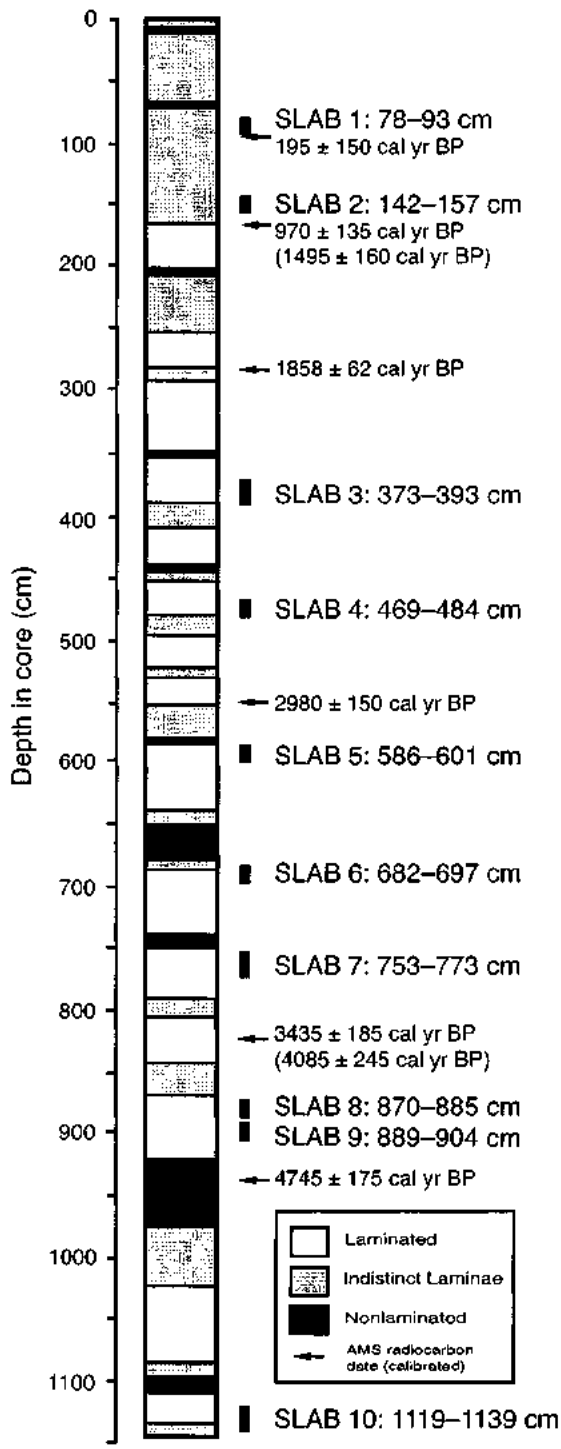

FIGURE 4.4. Stratigraphic column of core TUL99B03 depicting bulk sediment fabrics, positions of slabs and calibrated radiocarbon ages. Dates calibrated with $\Delta R = -120 \pm 45$ yr are in parentheses. Indistinct laminae include poorly laminated intervals intercalated with thin (≤ 3 cm) nonlaminated intervals, and nonlaminated intervals include massive beds, graded beds and sand beds. No horizontal scale is implied.

The laminae from Slab 1 are faint. The colours of the slab are mainly brown to dark brown (Figure 4.5A). The colour contrast between the olive-green laminae and the brown laminae is low, and it is difficult to discern the boundaries between the two lamina types. The laminae from Slab 2 are more distinct. Thick, olive green laminae up to 2 mm thick are visible (Figure 4.5B). Small pieces of plant material are also visible in the upper portion of the slab.

Laminae from slabs 3 to 10 are even more distinct (Figure 4.5C-J). The colour contrast of juxtaposed olive and brown laminae is high and sedimentary contacts are clear. Thick, green to olive green laminae up to 5 mm thick are found in several slabs, including slabs 3, 4, 8, 9, and 10. Slab 9 has the most conspicuous of the green laminae, with two couplets occurring side by side (Figure 4.5I). Lamina thickness in most slabs appears to be random, but Slab 8 shows a definite thinning upwards of couplets (Figure 4.5H). Sediment compaction appears to be negligible down core as the average lamina thickness of each slab is similar. In general, the green diatomaceous laminae appear to be thicker than the brown terrigenous laminae.

Thin, nonlaminated intervals, mostly measuring less than 3 cm in the sediment slabs, intercalate with the laminated intervals. These nonlaminated intervals consist of the massive ungraded beds and the graded beds described in Chapter 2. The nonlaminated beds have a brown colour that is the same as or lighter in shade than the terrigenous laminae. Plant debris has been found in some of the intervals. The debris consists of small twigs, fragments of blackened cedar fronds, and other unidentifiable organic matter. Examples of massive, ungraded intervals are found throughout slabs 3, 4, 7, 8,

and 10 (Figure 4.5). The upper and lower contacts of these intervals are sharp to gradational, and the contacts are conformable with the bedding plane. In gradational contacts, the laminae appear to diffuse into the massive interval from above and below. Examples of graded beds are found in slab 2 and 7 (Figure 4.5B, G). The lower contacts of graded intervals are usually sharp to erosive and the upper contacts are sharp to gradational. No examples of sand beds were described from the sediment slabs collected for this study.

Distorted laminae are not common in the slabs examined; this is a result of a sampling bias intended to reduce the occurrence of such laminae. Some distortion is visible in slabs 5, 6 and 7. The laminae are mostly intact and coherent, but have been folded or convoluted. The nature of the distorted laminae is more visible in the x-radiographs.

X-radiograph Descriptions

The x-radiograph positive images reveal sedimentary structures that are not readily visible in the sediment slabs. Distorted laminae and fining upwards sequences are easy to see, as are the differences between diatomaceous and terrigenous laminae. The diatomaceous laminae appear as bright bands because the x-rays are able to transmit through the porous diatom frustules. The purer diatom laminae yield brighter images. The dark bands are the terrigenous laminae that contain dense concentrations of silt and organic matter that are not x-ray transmissive. Laminae of an intermediate composition, and some nonlaminated intervals, appear as shades of grey.

FIGURE 4.5. Core photographs and correlative x-radiograph positive images of sediment slabs. Core photographs (left) show the surface expression of laminae from the working half of the piston core. X-radiographs (right) are of the sediment slabs which were extracted perpendicular to the working half surface. Hence some laminae do not match perfectly between the core photograph and x-radiograph. Single asterisks denote conspicuously thick *Skeletonema costatum* laminae; double asterisks denote conspicuously thick *Chaetoceros* resting spore laminae. Black dots indicate couplets with a high terrigenous content. Intervals labeled m represent massive intervals, g represents graded beds. Intervals labeled with capital letters represent thin section positions; gaps indicate where sediment was damaged during the epoxy embedding process. The black bar beside Slab 6 represents the interval where high-magnification imagery was taken (Figure 4.13). A magnified image of slide F from Slab 7 is show in Figure 4.12. Ruler for scale shows both centimeters (left side) and inches (right side).

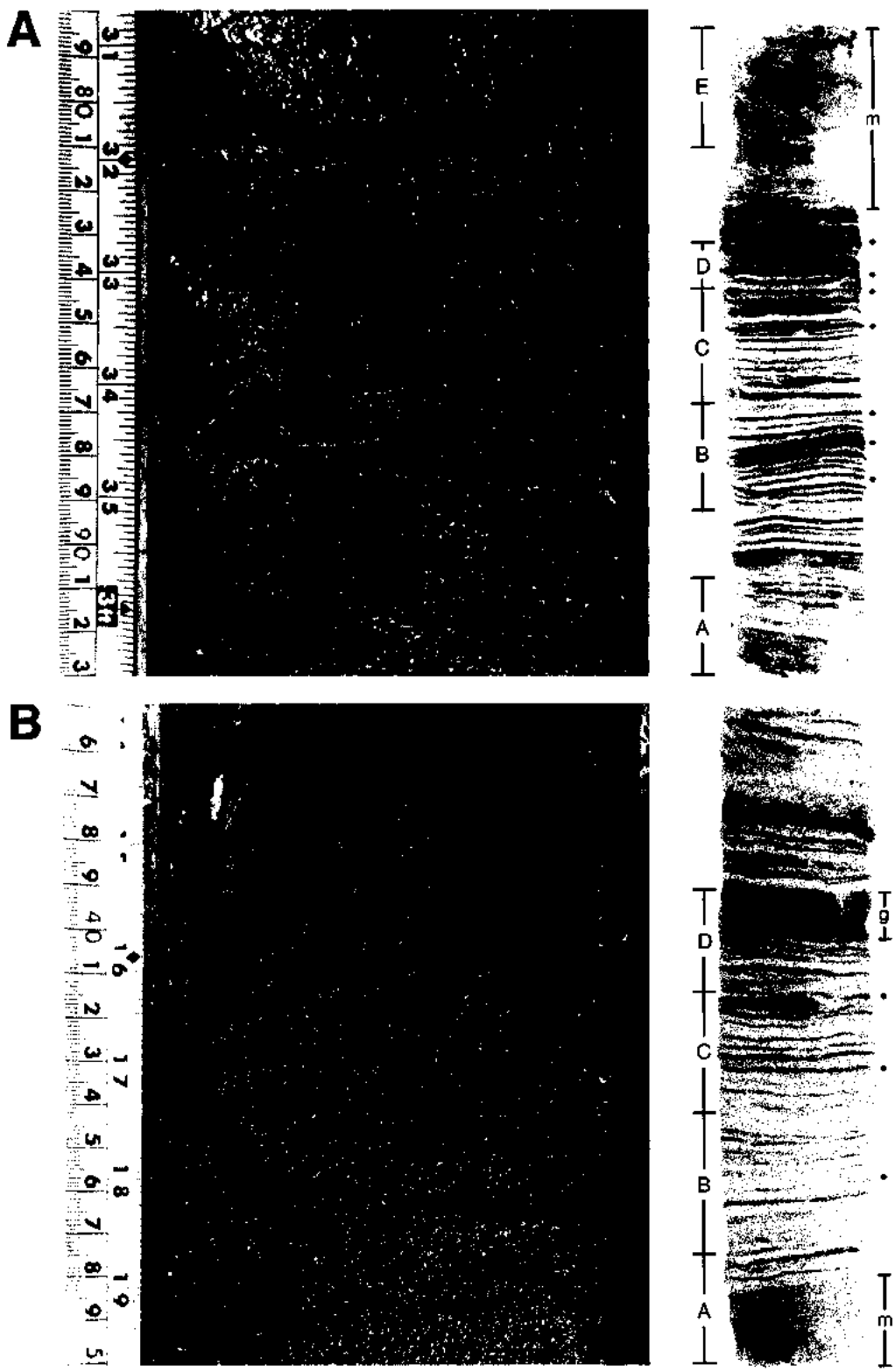

FIGURE 4.5 (continued). **A.** Slab 1 (78 - 93 cm). **B.** Slab 2 (142 - 157 cm).

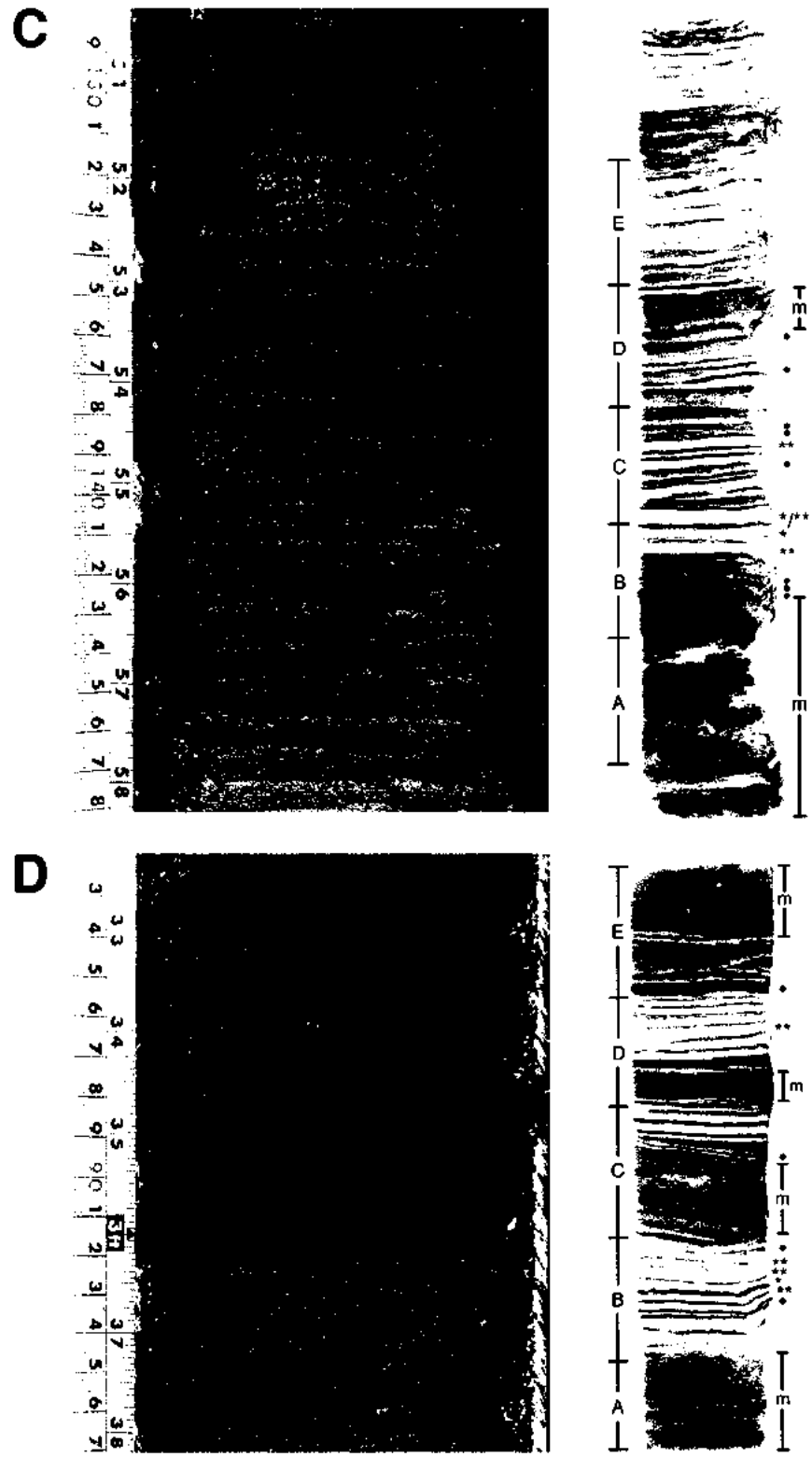

FIGURE 4.5 (continued). **C.** Slab 3 (373 - 393 cm). **D.** Slab 4 (469 - 484 cm).

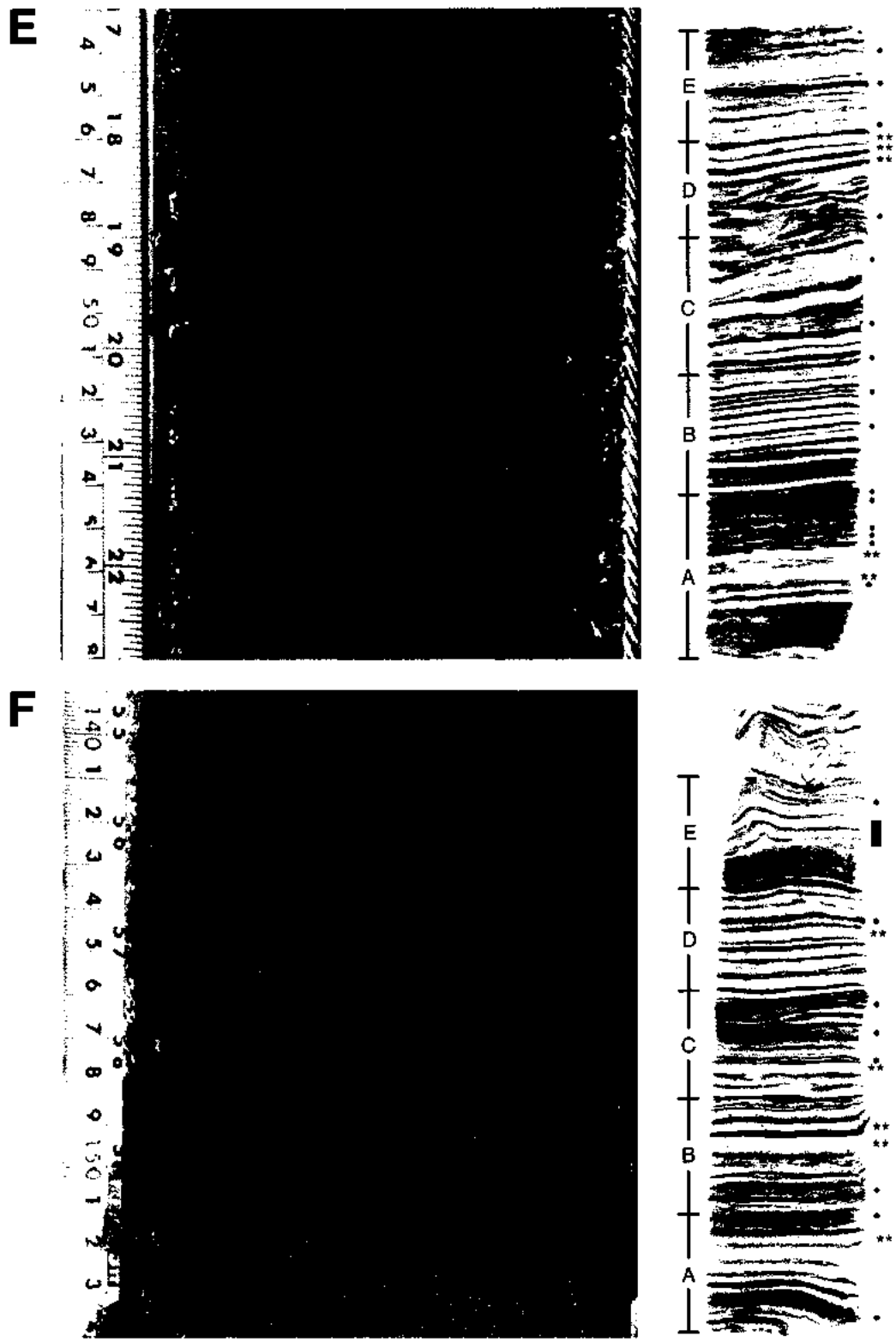

FIGURE 4.5 (continued). **E.** Slab 5 (586 - 601 cm). **F.** Slab 6 (682 - 697 cm).

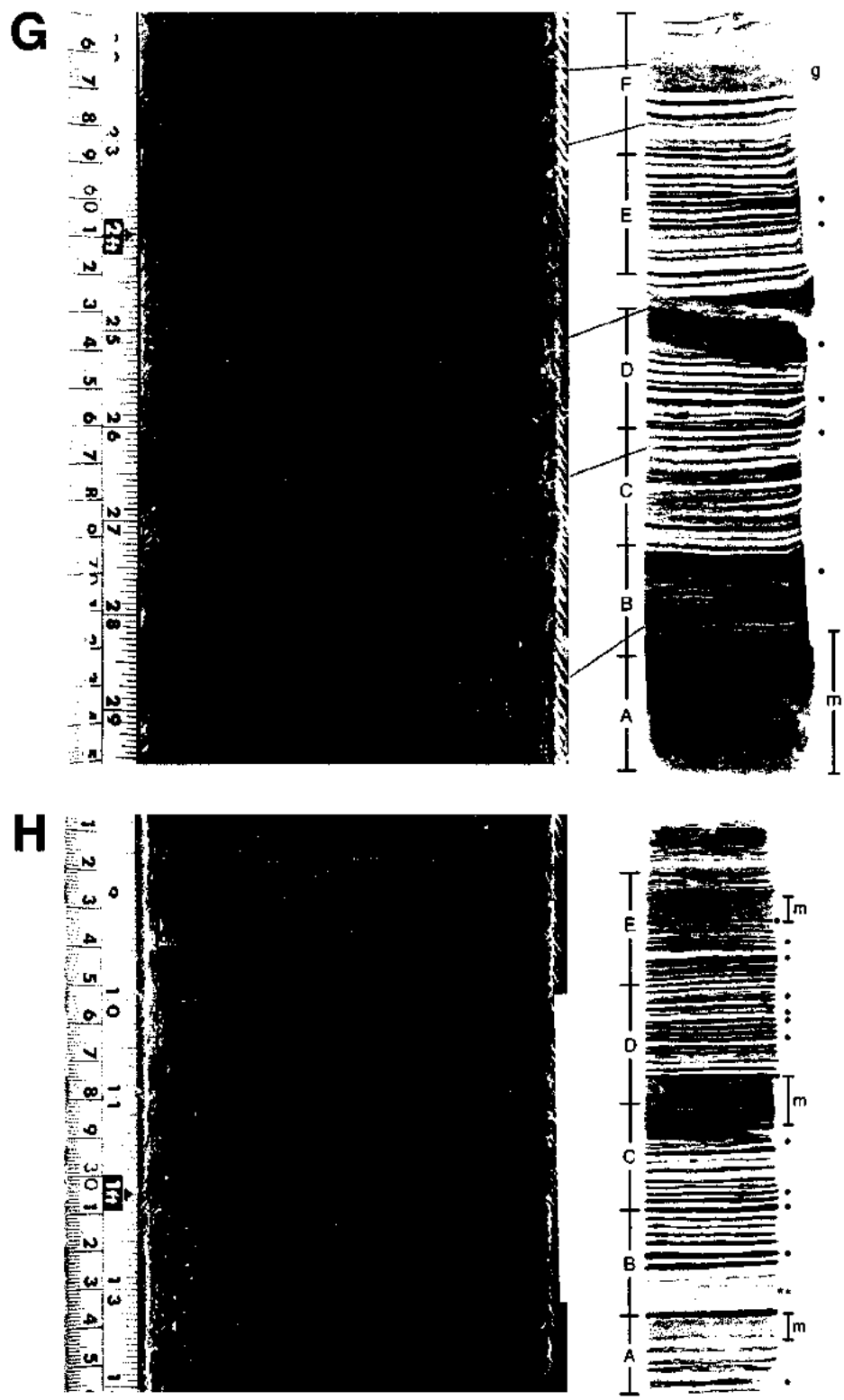

FIGURE 4.5 (continued). **G.** Slab 7 (753 - 773 cm). **H.** Slab 8 (870 - 885 cm).

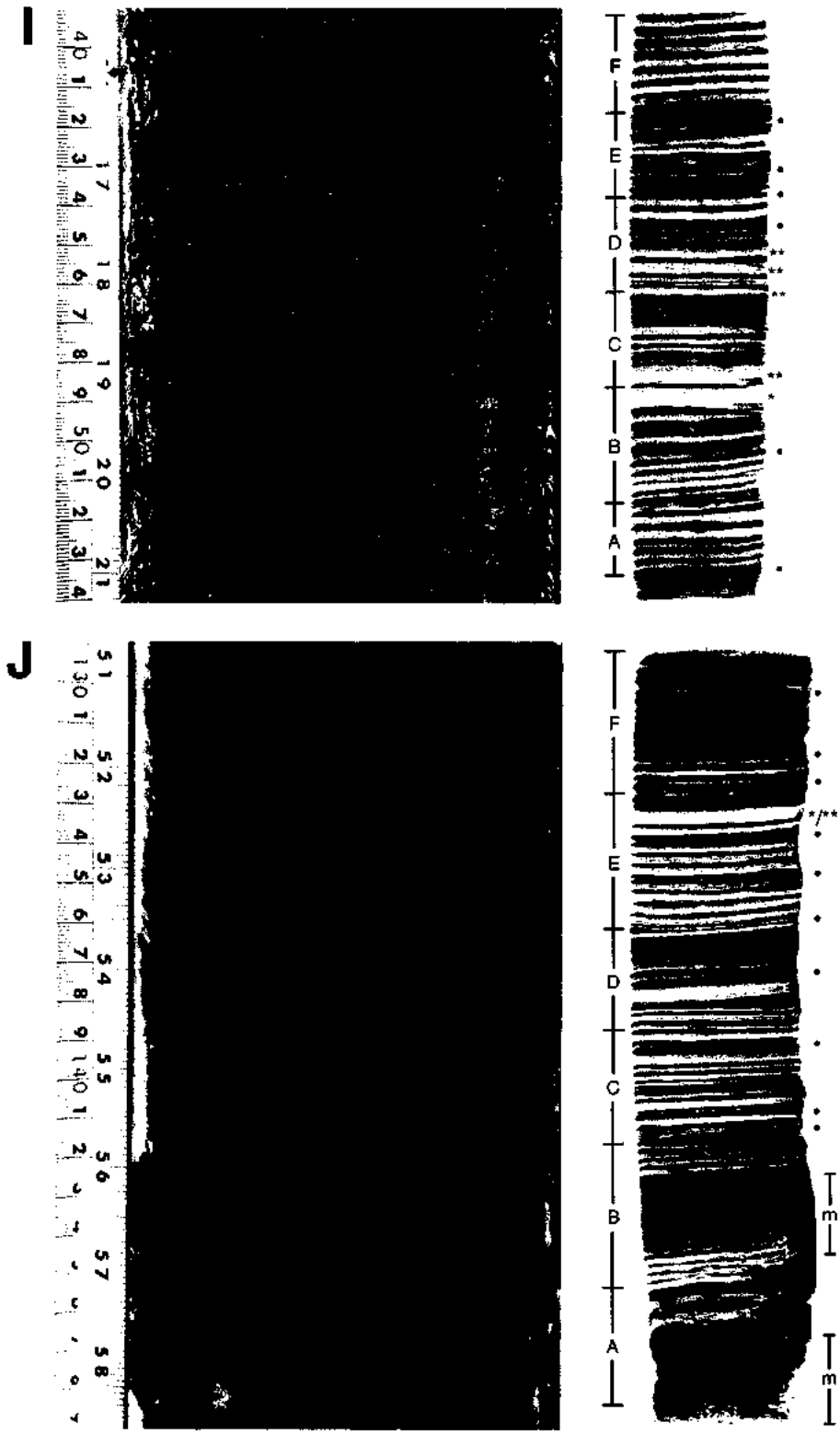

FIGURE 4.5 (continued). **I.** Slab 9 (889 - 904 cm). **J.** Slab 10 (1119 - 1139 cm).

A caveat must be presented before sedimentary interpretations can be made from the x-radiographs. Because the Faxitron Series 43805-N emits x-rays in an exposure cone, images produced near the center will be sharper than those produced at the edges. Thus, the upper or lower 2 cm of some slabs have laminae that are well defined in the core but blurry in the x-radiographs. In some instances, such as the top 2 cm of slabs 8 and 10, intervals that appear to be massive or poorly laminated in the x-radiographs are actually well laminated (Figure 4.5H, J). A comparison of the x-ray images with the core is important to keep in mind.

Slabs 1 and 2 are darker than images from other slabs due to the higher water content. The x-radiograph positive shows that Slab 1 is well laminated, despite the fact that the laminae are difficult to see in the core. The numerous thick, green laminae in Slab 3 appear as thick white bands (Figure 4.5C). It is clear in this image that the diatomaceous laminae are much thicker than the terrigenous laminae. The x-radiographs of slabs 4 to 10 show a high contrast between diatomaceous and terrigenous laminae. The sedimentary contacts also are sharper and better defined. These slabs also show that the diatomaceous laminae are generally thicker than the terrigenous laminae.

Lamina Description from Thin Sections

Fifty-two thin sections, containing 408 couplets, were examined from a total of 142.2 cm of sediment. Diatoms are the most common microfossil in the sediments. Other microfossils such as fish scale fragments, coccoliths, radiolaria, planktonic foraminifera, and benthic foraminifera were rarely observed. Terrigenous laminae have a mean

thickness of 0.56 mm (n = 405; range: 0.15–3.91 mm), and diatomaceous laminae have a mean thickness of 1.85 mm (n = 408; range: 0.20–5.67 mm) (Table 4.3 and Appendix B). The average thickness of a couplet, calculated from the thickness of all 813 laminae measured, is 2.41 mm; average couplet thickness calculated from each slab varies down the core. There are fewer terrigenous laminae as a result of their being cut off at the bottom of three thin sections. Diatomaceous laminae can be further divided into near-monospecific laminae, mixed-species laminae, and silty diatomaceous laminae (Figure 4.6). Each lamina type is described in detail below.

Terrigenous laminae

This type of lamina has a grainy texture and opaque brown color when observed with light microscopy (LM). With BSEM, images appear bright due to numerous dense mineral grains (Figure 4.7A, B). Quartz, pyroxene, clay minerals, wood fragments, and organic detritus are abundant. There is also a minor but consistent microfossil component. Diatoms include intact *Paralia sulcata* chains, *Coscinodiscus* spp., *Actinoptychus* spp., *Cyclotella* spp., *Cymbella* spp., *Diploneis* spp., and *Chaetoceros* resting spores. Fragments of diatom valves and cingula are common. Silicoflagellate species include the 6-spined *Dictyocha speculum* and the 4-spined *D. fibula*, with *D. speculum* being the more dominant form. An unidentified 8-spined silicoflagellate (*Octactis*?) was rarely observed. Silicoflagellates can occur as monospecific blebs and sublaminae. Preservation of the microfossils ranges from poor to good. The lower contact of terrigenous laminae is gradational whereas the upper contact is sharp.

TABLE 4.3. Thickness of terrigenous (T) and diatomaceous (D) laminae

Slab	Lamina Type	Number of Laminae	Average Thickness (mm) (s.d.)	Average Couplet Thickness (T+D) (mm) (s.d.)
1	T	24	0.73 (0.46)	2.25 (0.69)
	D	24	1.52 (0.67)	
2	T	24	0.52 (0.22)	2.35 (0.88)
	D	25	1.83 (0.78)	
3	T	28	0.70 (0.46)	2.95 (1.31)
	D	28	2.25 (1.42)	
4	T	25	0.55 (0.28)	2.43 (0.86)
	D	26	1.88 (0.70)	
5	T	52	0.60 (0.29)	2.36 (0.87)
	D	52	1.76 (0.88)	
6	T	45	0.69 (0.63)	2.65 (1.03)
	D	45	1.96 (0.97)	
7	T	53	0.56 (0.20)	2.41 (0.87)
	D	53	1.85 (0.80)	
8	T	56	0.42 (0.19)	1.82 (0.71)
	D	56	1.40 (0.70)	
9	T	43	0.48 (0.26)	2.93 (1.23)
	D	43	2.45 (1.02)	
10	T	55	0.52 (0.21)	2.31 (0.88)
	D	56	1.79 (0.84)	
Total	T	405	0.56 (0.35)	2.41 (0.95)
	D	408	1.85 (0.92)	

s.d. standard deviation

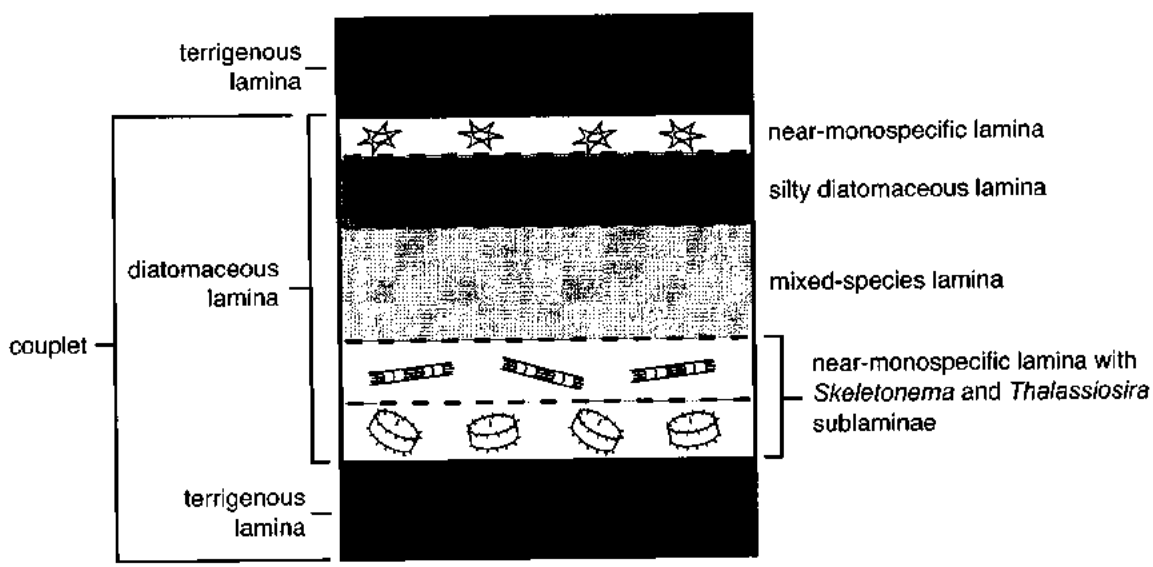

FIGURE 4.6. Schematic diagram depicting the terminology used to describe laminae in this study. No scale is intended.

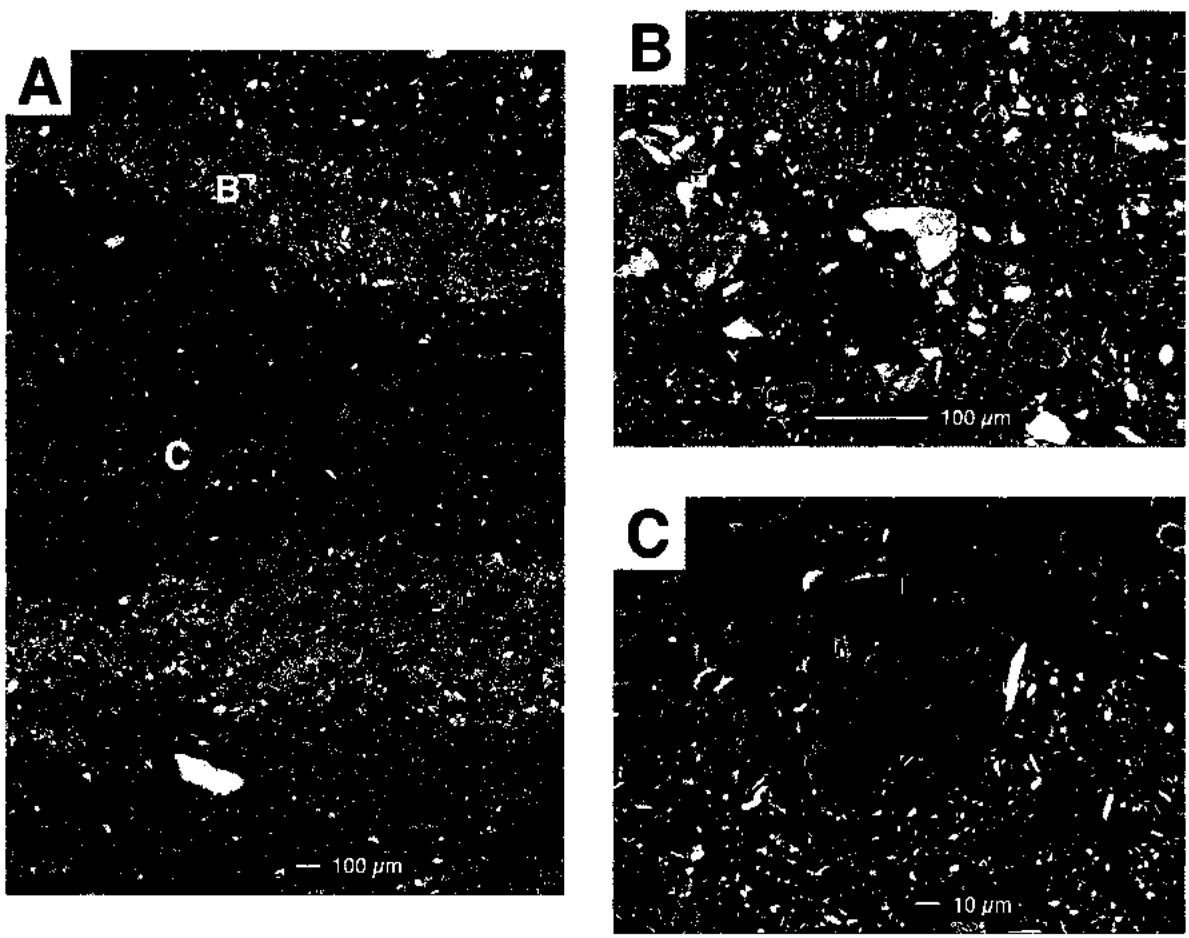

FIGURE 4.7. BSEM images of terrigenous and silty diatomaceous laminae. **A.** Photomicrograph showing two couplets. The brighter laminae are rich in mineral grains, and the darker laminae are rich in diatoms. Letters B and C indicate where higher magnification images were taken. **B.** Close-up view showing detail of terrigenous lamina. Silt grains and robust diatoms are visible. **C.** Close-up view showing detail of a silty diatomaceous lamina. This example is rich in finely fragmented diatoms.

Near-monospecific laminae

These laminae consist of clean, excellently preserved diatom frustules. Green particles can be seen inside some diatoms, particularly *Chaetoceros* resting spores (CRS). In BSEM, near-monospecific laminae appear dark due to numerous low-density, resin-filled diatom frustules. Silt and terrigenous organic detritus are rare to absent. No greater than three species (often from the same genus) occur per lamina, with one species dominating ≥50% of the assemblage (Figure 4.8). Dominant taxa include *Skeletonema costatum*, CRS, *Thalassiosira nordenskioeldii*, *T. pacifica*, *Thalassionema nitzschioides*, *Odontella longicruris*, and *Ditylum brightwell*, respectively. Less dominant taxa include *Asteromphalus* sp., *Coscinodiscus* sp., *Cyclotella* sp., *Odontella aurita*, and *Stephanopyxis turris*, respectively. There are also laminae consisting of only setae from *Chaetoceros* vegetative cells or diatom cingula. Laminae rich in CRS and *S. costatum* can be thick (5 mm) as in Slab 9. Colonial chains of *S. costatum* and *Chaetoceros* spp. are well preserved and can be up to 30 cells in length (Figure 4.9). Near-monospecific laminae have a sharp lower contact and a gradational to sharp upper contact. Of the 372 individual near-monospecific laminae and sublaminae examined in all of the couplets, 271 laminae (73%) lie directly above the terrigenous lamina.

Other features are blebs containing near-monospecific assemblages. The blebs measure from less than a millimeter in length to 2 mm, with the long axis oriented with the bedding plane. The blebs are found in both laminated and nonlaminated intervals but are more often seen in nonlaminated intervals. Blebs can contain a near-monospecific

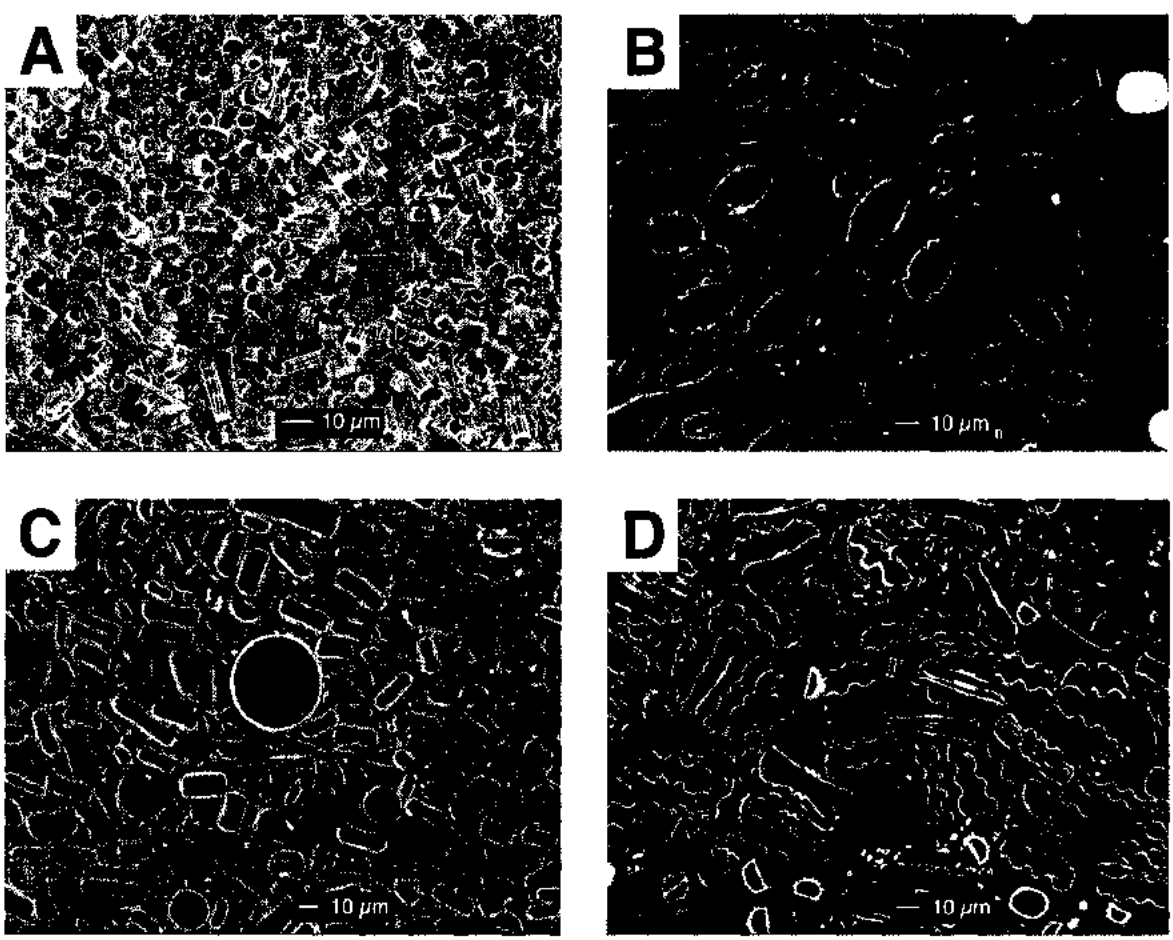

FIGURE 4.8. Scanning electron images of near-monospecific laminae. 4.8A was taken by SEM from a tape peel; 4.8B–D were taken by BSEM. **A.** Pristine *Skeletonema costatum* frustules. **B.** *Odontella aurita*. **C.** *Thalassiosira* sp. **D.** *Asteromphalus* sp.

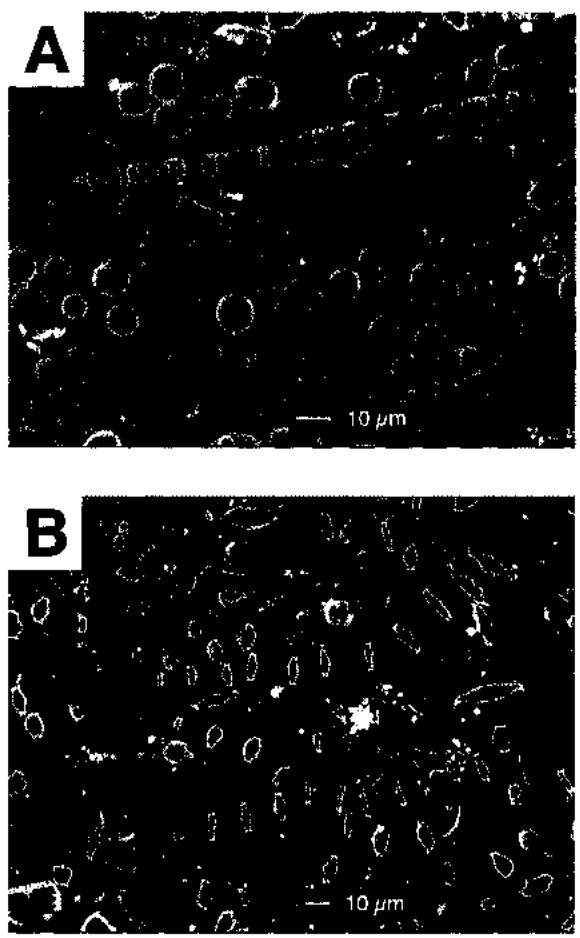

FIGURE 4.9. BSEM images of diatom chains. **A.** Monospecific *Skeletonema costatum*. Most chains are shown end-on; however, one chain is in cross section. **B.** *Chaetoceros* resting spores in residual vegetative chains. Lightly silicified vegetative cell frustules likely dissolved, leaving behind only robust spores in the sediments.

assemblage of any of the taxa mentioned above, including concentrations of setae and girdle bands, and the preservation state of frustules is excellent.

Mixed-species laminae

These laminae do not appear as clean as near-monospecific laminae when viewed in LM. In BSEM, the laminae still appear dark unless there is a silt or organic detritus component (Figure 4.10). The proportion of silt and organic detritus ranges from 10-20%. Finely fragmented diatom frustules, or diatom hash (Sancetta, 1989b), are also present. This lamina type can consist of at least three species (from different genera) with no particular species dominating the assemblage, or more than three species per lamina with one or two taxa slightly dominating the assemblage (i.e., 25-50%). Taxa include *Thalassiosira* spp., *Skeletonema costatum*, *Coscinodiscus* spp., *Actinocyclus* spp., *Asteromphalus* spp., *Thalassionema nitzschoides*, *Thalassiothrix* sp., *Odontella aurita*, *Ditylum brightwellii*, and CRS. Preservation of diatom frustules ranges from moderate to excellent. Both upper and lower contacts of this lamina type are gradational.

Silty diatomaceous laminae

These laminae have a composition that is intermediate between mixed-species laminae and terrigenous laminae. Silt and organic detritus are common (25-50%), but not as abundant as in terrigenous laminae (Figure 4.7C). The diatom component is mixed, containing taxa such as *Actinoptychus senarius*, *A. vulgaris*, *Ditylum brightwellii*, *Cyclotella* spp. (Figure 4.11A), CRS, and *Thalassionema nitzschioides*. Monospecific

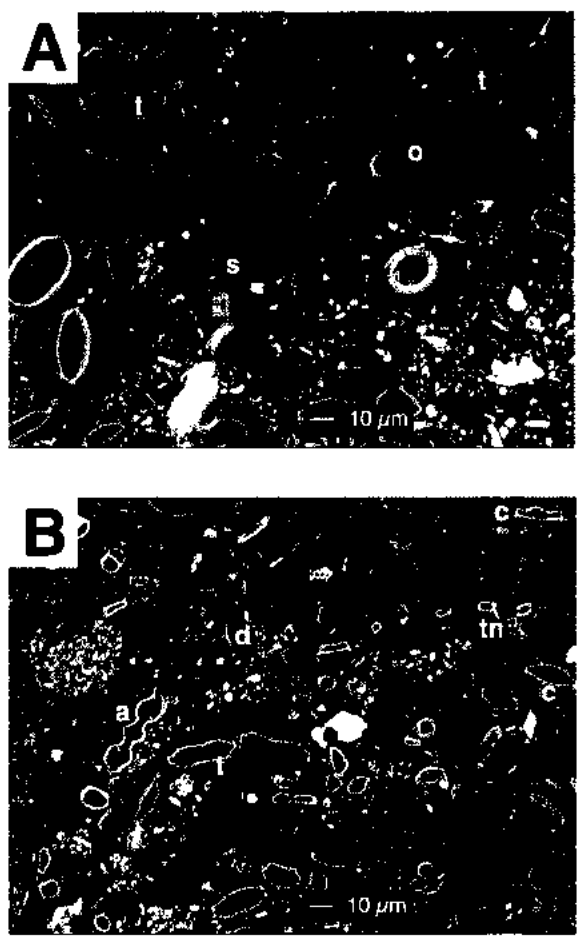

FIGURE 4.10. BSEM photomicrographs of mixed-species laminae. **A.** Identifiable diatoms include a chain of *Skeletonema costatum* (s), two connected frustules of *Odontella* sp. (o), and *Thalassiosira nordenskioeldii* (t). Diatom hash and silt grains are also present. **B.** Identifiable taxa include *T. nordenskioeldii* (t), square cross sections of *Thalassionema nitzschioides* (tn), *Asteromphalus* sp. (a), a *Ditylum brightwellii* spine (d), and various morphologies of *Chaetoceros* resting spores (c).

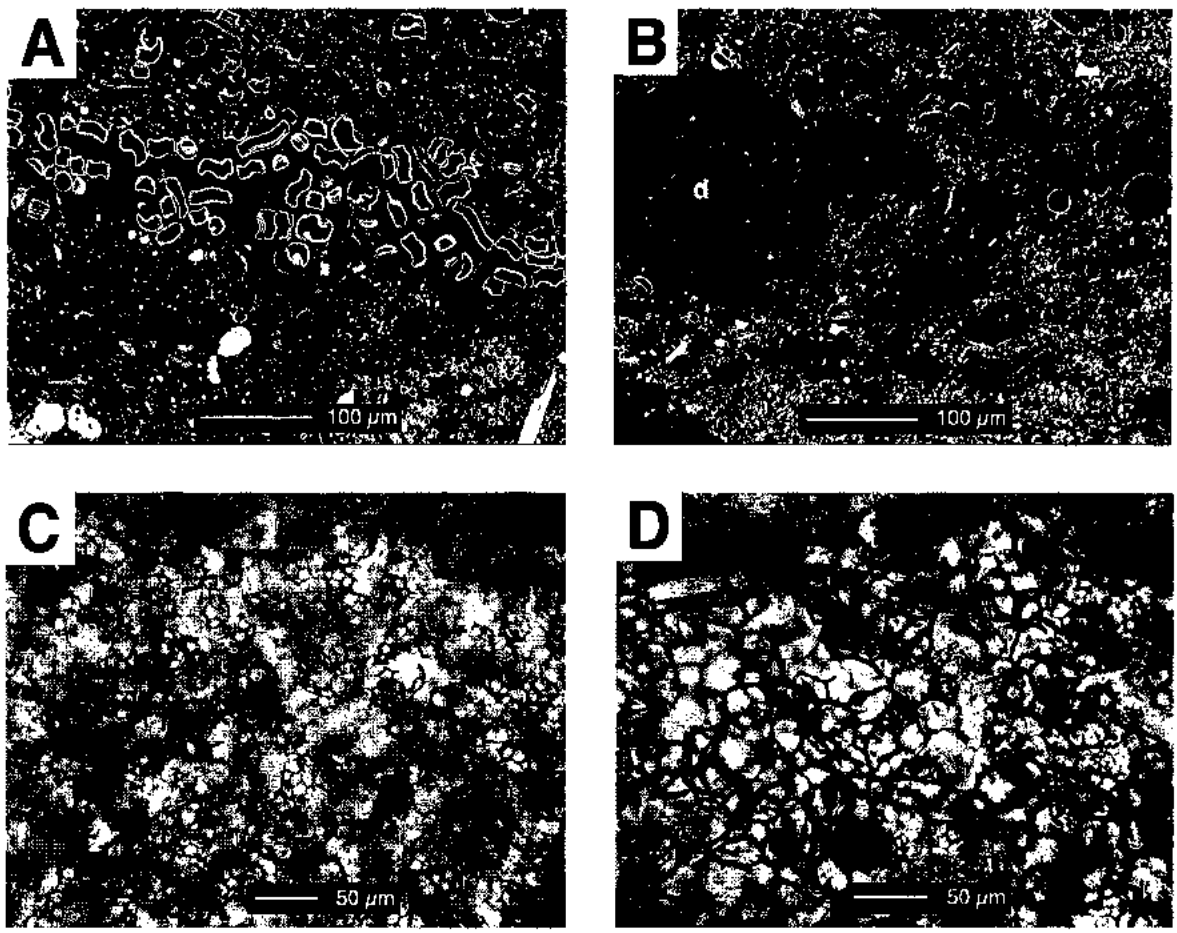

FIGURE 4.11. Examples of near-monospecific sublaminae and blebs from silty diatomaceous laminae. A and B were taken with BSEM; C and D were taken with LM. **A.** Sublamina of *Cyclotella* sp. within silty diatom hash. **B.** Bleb of *Operculodinium centrocarpum* dinoflagellate cysts (d) within diatom hash. **C.** Monospecific bleb of the silicoflagellate *Dictyocha speculum*. Similar blebs are found in terrigenous laminae. **D.** Near-monospecific bleb of the silicoflagellate *Dictyocha fibula* with a few *D. speculum* skeletons.

blebs and sublaminae of the dinoflagellate cyst *Operculodinium centrocarpum* only occur within silty diatomaceous laminae (Figure 4.11B). Silicoflagellate blebs and sublaminae are common (Figure 4.11C, D). Monospecific sublaminae, containing *Skeletonema costatum*, *Thalassionema nitzschioides*, *Ditylum brightwellii*, *Asteromphalus* sp., *Cyclotella* sp. or *Odontella aurita*, respectively, can occur within silty diatomaceous laminae. Preservation of the microfossils is poor to good, except in monospecific sublaminae where the preservation is moderate to excellent. There is also an occassional component of diatom hash. This hash gives rise to images of unclean diatoms in LM and intermediate brightness in BSEM. Both upper and lower contacts are gradational. In 67% of all couplets examined, this lamina type underlies terrigenous laminae. In the remaining couplets, the silty diatomaceous lamina is separated from the overlying terrignous laminae by a near-monospecific sublamina or a thin (0.2-0.5 mm) mixed-species lamina.

Depositional Succession of Laminae

Of the 408 couplets examined, 115 couplets (28%) contain the following 4-component sucession of laminae, from bottom to top: terrigenous, near-monospecific, mixed diatom, and silty diatomaceous laminae (Figure 4.12). Near-monospecific laminae lying sharply above terrigenous laminae consist of their own distinct succession of sublaminae, beginning with a *Thalassiosira* spp. sublamina, and followed by either *Skeletonema costatum* and/or sublaminae containing *Chaetoceros* vegetative chains and/or resting spores (Figure 4.13). In 56% of 4-component successions, the near-

FIGURE 4.12. LM thin-section image from the top of Slab 7 (see Figure 4.5G), showing examples of seasonal succession, and a 6-mm thick graded massive interval. **A.** Photomicrograph of the thin section. **B.** Couplet number and succession type. Single asterisk denotes a 4-component succession; double asterisk denotes a 3-component succession. **C.** Lamina type. **D.** Description of major components within each lamina, with the most abundant component listed first. Appendix D contains the complete set of thin section photomicrographs.

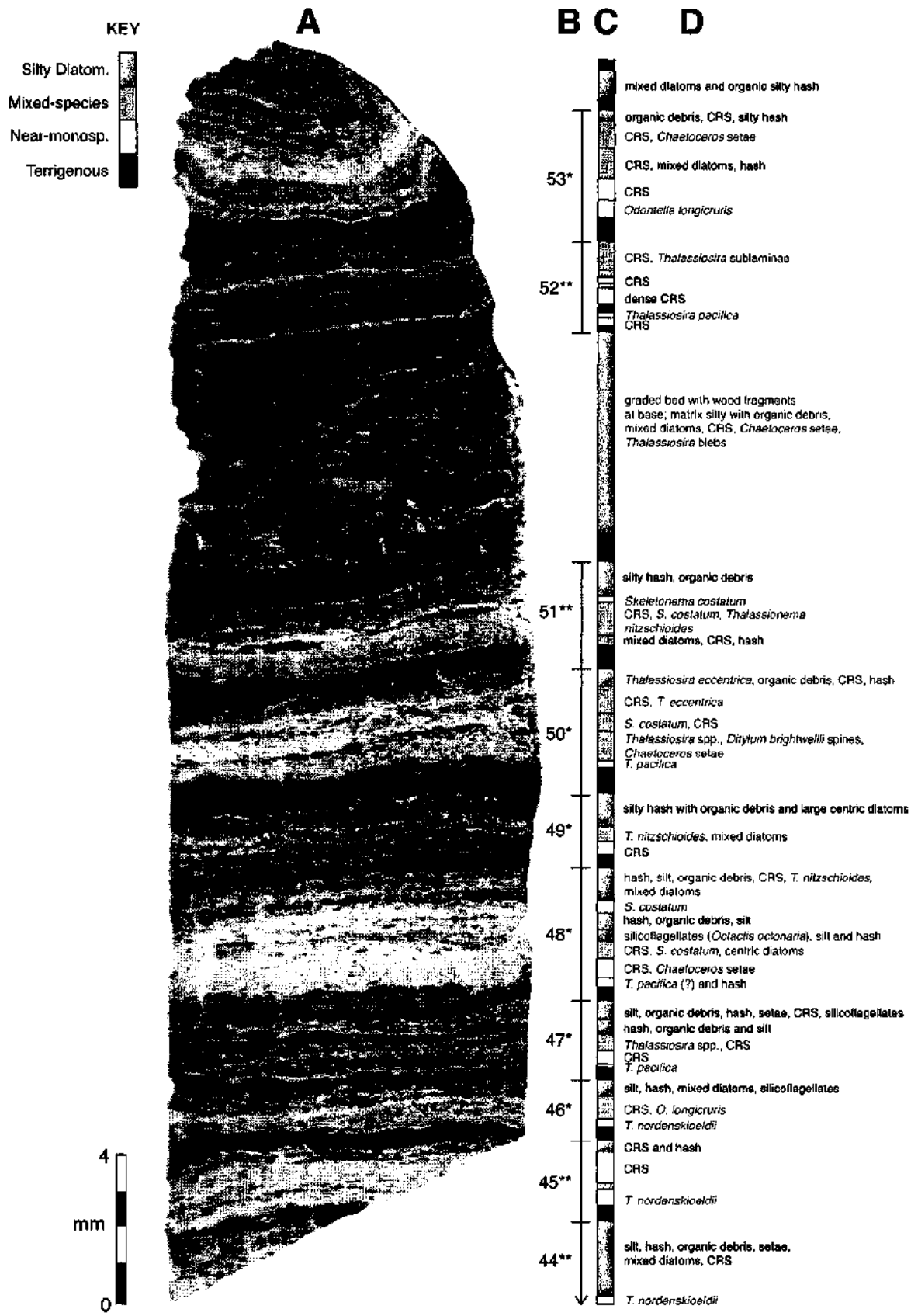
KEY
Silty Diatom.
Mixed-species
Near-monosp.
Terrigenous
A
B C D
mixed diatoms and organic silty hash
organic debris, CRS, silty hash
CRS, Chaetoceros setae
CRS, mixed diatoms, hash
53*
CRS
Odontella longicruris
CRS, Thalassiosira sublaminae
CRS
52**
dense CRS
Thalassiosira pacifica
CRS
graded bed with wood fragments
at base; matrix silty with organic debris,
mixed diatoms, CRS, Chaetoceros setae,
Thalassiosira blebs
silty hash, organic debris
Skeletonema costatum
CRS, S. costatum, Thalassionema
nitzschioides
51**
mixed diatoms, CRS, hash
Thalassiosira eccentrica, organic debris, CRS, hash
CRS, T. eccentrica
S. costatum, CRS
Thalassiosira spp., Ditylum brightwellii spines,
Chaetoceros setae
50*
T. pacifica
silty hash with organic debris and large centric diatoms
T. nitzschioides, mixed diatoms
49*
CRS
hash, silt, organic debris, CRS, T. nitzschioides,
mixed diatoms
S. costatum
hash, organic debris, silt
48*
silicoflagellates (Octactis octonaria), silt and hash
CRS, S. costatum, centric diatoms
CRS, Chaetoceros setae
T. pacifica (?) and hash
silt, organic debris, hash, setae, CRS, silicoflagellates
hash, organic debris and silt
47*
Thalassiosira spp., CRS
CRS
T. pacifica
silt, hash, mixed diatoms, silicoflagellates
46*
CRS, O. longicruris
T. nordenskioeldii
CRS and hash
45**
CRS
T. nordenskioeldii
silt, hash, organic debris, setae,
44**
mixed diatoms, CRS
T. nordenskioeldii
4
mm
0

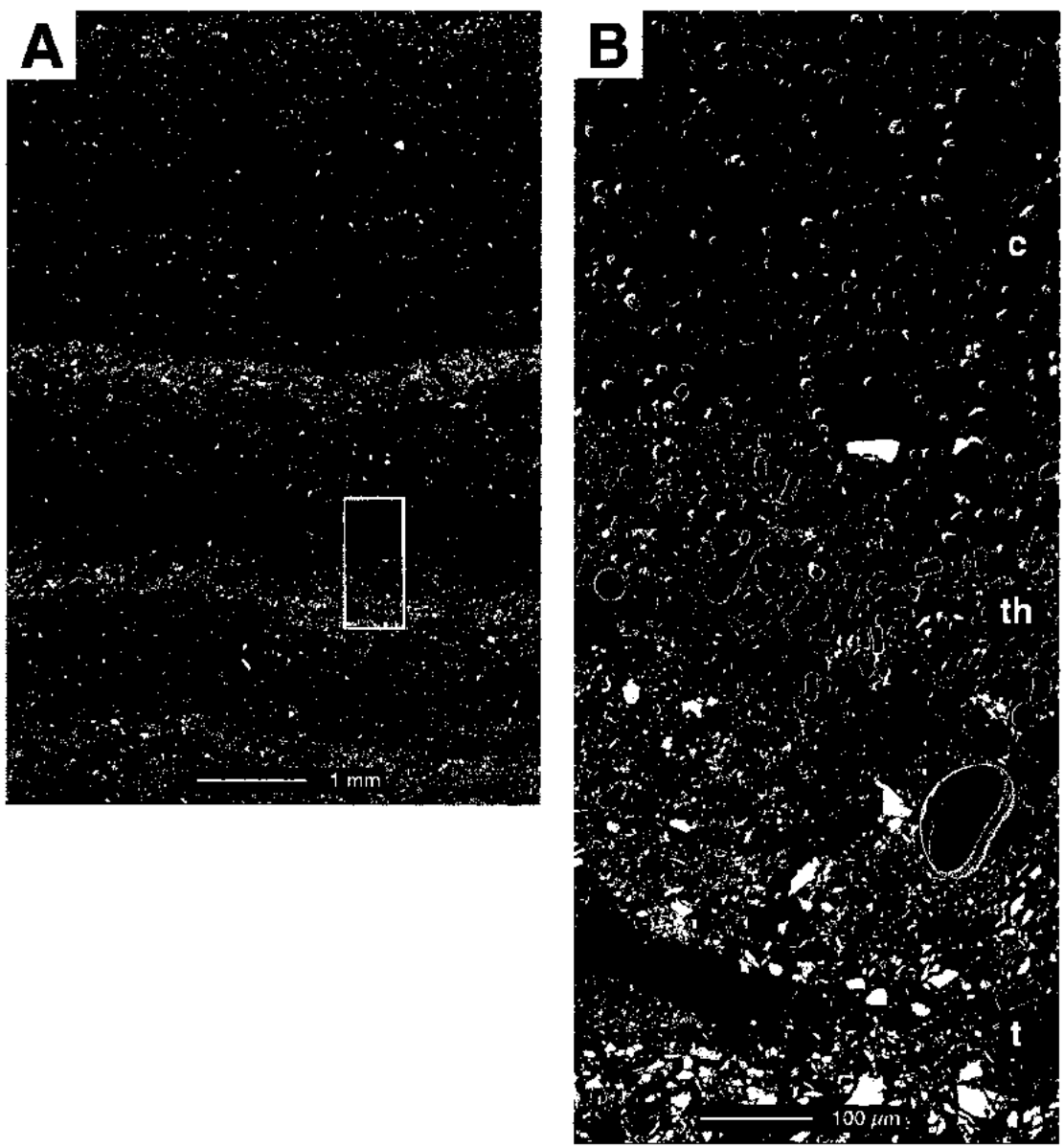

FIGURE 4.13. BSEM photomosaics of magnified area from Slab 6 (see Figure 4.5F). **A.** Low-magnification image showing three couplets. **B.** High-magnification image showing seasonal succession of a terrigenous lamina (t), a *Thalassiosira* sp. sublamina (th), and a sublamina enriched with *Chaetoceros* resting spores (c) with a minor component of *Thalassiosira nordenskioeldii*.

monospecific succession began with a *Thalassiosira* sp. sublamina, followed by *S. costatum* and/or CRS sublaminae. In 30% of 4-component successions, *S. costatum* or CRS sublaminae lay directly above the terrigenous lamina. In the remaining 14% of couplets, another taxon (e.g., *Odontella* sp., *Ditylum brightwellii*) comprised the near-monospecific laminae overlying the terrigenous lamina.

One hundred and ninety-five couplets (48%) contain the following 3-component succession, from bottom to top: terrigenous, mixed-species, and silty diatomaceous laminae; or terrigenous, near-monospecific, and mixed species or silty diatomaceous laminae (Figure 4.12). In the first scenario, one or two sublaminae from the *Thalassiosira-Skeletonema-Chaetoceros* sequence are present but either the mixed-species or silty diatomaceous lamina is absent. In this scenario, 41% of all 3-component couplets had a *Thalassiosira* sp. sublamina lying directly above the terrigenous lamina. Twenty-four percent of all 3-component couplets had either *S. costatum* or a CRS sublamina above the terrigenous lamina. The remaining 3-component successions had another taxon (e.g., *Coscinodiscus* sp., *Odontella longicruris*, *Ditylum brightwellii*) lying above the terrigenous lamina. In the second scenario, the discrete *Thalassiosira-Skeletonema-Chaetoceros* sequence is not present and is replaced by a mixed-species lamina with elevated abundances of *Thalassiosira*, *Skeletonema*, and/or *Chaetoceros* resting spores.

The remaining 98 couplets (~24%) contain only a 2-component succession of laminae, consisting of a terrigenous lamina and either a mixed diatom or silty diatomaceous lamina.

Downcore Variation

Slabs 6 to 10 from the lower part of the core (~3600 to ~5500 cal yr BP) contain more couplets with the 3-component lamina succession than slabs from the upper part of the core (~600 to ~3600 cal yr BP) (Figure 4.14, Appendix B2). The lower part of the core also has more visibly distinct laminae, as is seen from the slab x-rays. Two of the most abundant taxa in the sediments are *Chaetoceros* spp. resting spores and *Skeletonema costatum*. The thickness and occurrence of laminae containing these taxa change within a given slab and throughout the core (Figure 4.14E, F). In slabs 9 and 10, CRS laminae are common and *S. costatum* laminae are thicker than in any other slab.

DISCUSSION

Laminated sediments from Effingham Inlet consist of couplets with alternating terrigenous and diatomaceous laminae. The formation of these couplets and their constituent laminae results from the differing effects of biological production and sediment delivery into the basin. In the following discussion, the annual nature of the laminae is explained, along with the origin of each component lamina.

Determination of the Annual Nature of Laminae

Microfossil evidence shows that the laminated sediments were deposited according to a rhythmic cycle. The repetitive taxonomic succession of diatoms and other microfossils within the 3- and 4-component couplets, and even the sublamina succession of diatom species within a near-monospecific lamina, reveal that the sediments were

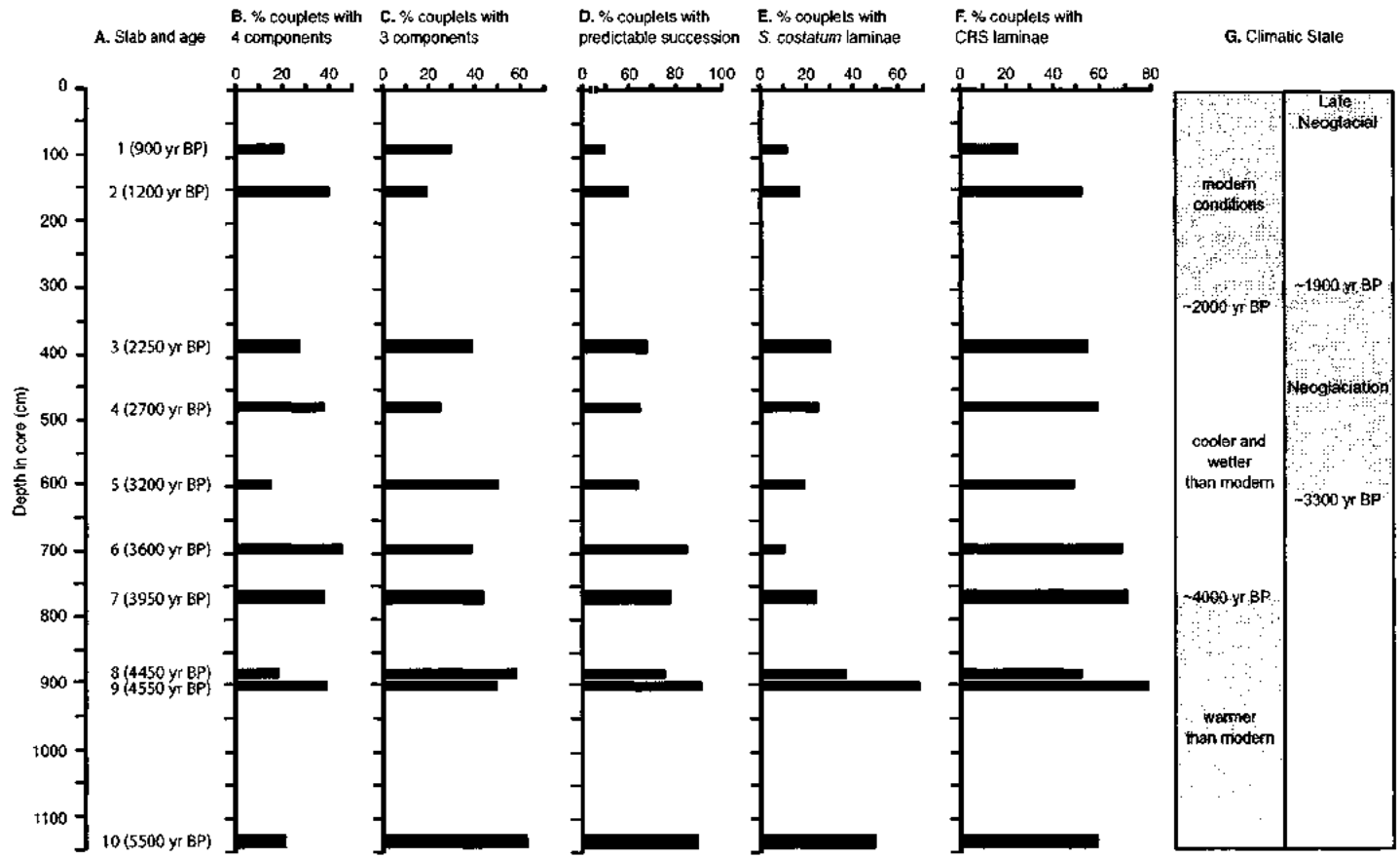

FIGURE 4.14. Downcore trends of couplet styles and lamina compositions. Climatic states from pollen studies after Hebda (1995); Neoglaciation studies from Ryder and Thomson (1986); see text for details. Ages of slabs based on chronology from Figure 4.3.

deposited annually because similar annual patterns are observed elsewhere in places such as Auke Bay in Alaska (Waite et al., 1992), the Skagerrak in the North Atlantic (Lange et al., 1992), and Saanich and Jervis inlets in British Columbia (Sancetta, 1989a; McQuoid and Hobson, 1997). The succession in Effingham Inlet also conforms to the three-stage annual diatom succession described by Margelef (1958) and Guillard and Kilham (1977).

The determination of couplet thickness, as measured from the thin section images, and the calculation of an average sediment accumulation rate from calibrated radiocarbon dates, supports the annual depositional time scale. If a sedimentary couplet represents one year of deposition, then a comparison between the mean couplet thickness of 2.41 mm (Table 4.3) and the annual sediment accumulation rate of 2.25 mm/yr, derived from radiocarbon dating (Figure 4.3), suggests that the couplets in Effingham Inlet are annually deposited. The mean couplet thickness (i.e., sediment accumulation rate) from most slabs falls within the 1.9-2.6 mm/yr range determined by radiocarbon dating (Dallimore, 2001).

Origin of Terrigenous Laminae

Terrigenous laminae in Effingham Inlet are mainly deposited during the late autumn and winter months when increased rainfall leads to increased runoff. Sources of terrigenous material delivery into the inner basin include the Effingham River, and a small, unnamed stream leading into the inner basin (Dallimore, 2001). Numerous ephemeral, precipitation-dependent waterfalls on the steep sides of the inlet probably transport a significant, yet ungauged, amount of freshwater input and detritus into the

basin. Such waterfalls were observed during the October 1999 cruise during a rainstorm (A. Chang, personal observation). The waterfalls continued for a few hours after the rainstorm ceased, and the surface of the inlet was noticeably covered with soil, twigs, and bark.

The assemblage of microfossils within terrigenous laminae contains species derived from environments outside the inlet or washed off from the margins of the inlet. The chain-forming diatom *Paralia sulcata* is often observed in terrigenous laminae. McQuoid and Hobson (1998) found *P. sulcata* in plankton records from Saanich Inlet during winter months. They suggest that *P. sulcata* can be easily sloughed off from the benthos or sandy substrates by increased storm activity during the winter, leading to the dispersal of seed populations. Cells then can be stirred into the plankton by winter runoff and storm waves (McQuoid and Hobson, 1998). Genera such as *Cymbella* and *Diploneis* include freshwater species that can enter the inlet during winter runoff from rivers. The presence of coastal neritic and benthic taxa, such as *Actinoptychus*, suggests that sediments have been reworked from the shelf and carried into the inlet (Pike and Kemp, 1996; McQuoid and Hobson, 1997). Silicoflagellates are common in terrigenous laminae. Sautter and Sancetta (1992) found that the maximum abundance of silicoflagellates in sediment traps from San Pedro Basin off the southern California Bight occurred during the winter, and attribute their presence to the intrusion of pelagic waters into the basin. Similar conditions may occur in Effingham Inlet.

Origin of Near-Monospecific Laminae

The occurrence of most near-monospecific laminae overlying terrigenous laminae can be attributed to the annual spring bloom. The spring bloom can be divided into several events, each a response to changing environmental conditions as the bloom progresses. The sharp contact between near-monospecific laminae and terrigenous laminae likely reflects the onset of the spring bloom in response to a probable combination of events, including increased sunlight and the infusion of nutrients into the surface waters via coastal upwelling (Margelef, 1958; Guillard and Kilham, 1977).

In 35% of all couplets examined, *Thalassiosira* species were the first taxa to appear in the Effingham Inlet spring bloom, followed by the appearance of *Skeletonema costatum* and/or different species of CRS. In Auke Bay, *Thalassiosira* species such as *T. aestivalis*, *T. nordenskioeldii*, and *T. gravida,* that can tolerate low water temperatures (1–5 °C), tend to initiate the bloom as soon as light levels increase in the early spring (Guillard and Kilham, 1977; Waite et al., 1992). *Skeletonema costatum* and *Chaetoceros* spp. then appear later in the spring as the water temperature rises and nitrate is consumed by *Thalassiosira* (Waite et al. 1992). In 20% of couplets examined, *S. costatum* or CRS were the first taxa to appear above the terrigenous lamina, perhaps indicating a spring bloom during temperatures above 5 °C. The appearance of *Thalassiosira* spp., *S. costatum*, and *Chaetoceros* spp. sublaminae in Effingham Inlet sediments is consistent with Stage I of the seasonal succession outlined by Margalef (1958) and Guillard and Kilham (1977) (Figure 4.15A).

FIGURE 4.15. Model showing the formation of different annual couplet successions. No scale is intended, however the proportion of each particle type symbolizes their relative abundance as seen in the thin sections (cf. Table 4.1). **A.** Four-component succession. This example shows Stage I with separate *Thalassiosira*, *Skeletonema*, and *Chaetceros* blooming events. **B.** Three-component succession, Scenario 1. A near-monospecific lamina occurs above the terrigenous lamina but either the mixed-species lamina or the silty diatomaceous lamina is absent. **C.** Three-component succession, Scenario 2. Stages I and II are mixed together, although there is an elevated occurrence of a spring bloom taxon, represented here by *Skeletonema*. **D.** Two-component succession exemplified by a thick terrigenous laminae and a silty diatomaceous laminae with increased silt and organic content.

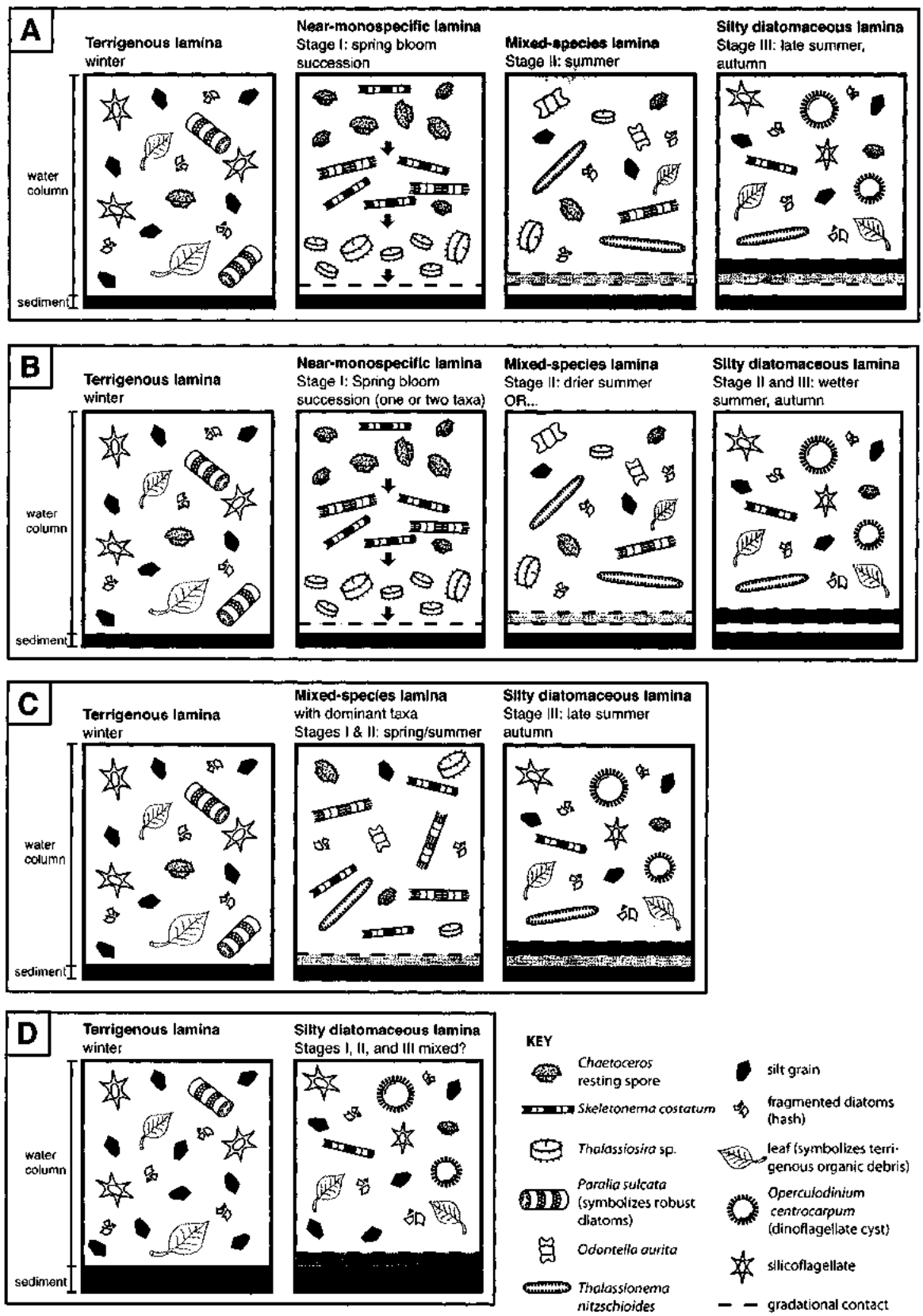
A
Terrigenous lamina
winter
Near-monospecific lamina
Stage I: spring bloom
succession
Mixed-species lamina
Stage II: summer
Silty diatomaceous lamina
Stage III: late summer,
autumn
water
column
sediment
B
Terrigenous lamina
winter
Near-monospecific lamina
Stage I: Spring bloom
succession (one or two taxa)
Mixed-species lamina
Stage II: drier summer
OR...
Silty diatomaceous lamina
Stage II and III: wetter
summer, autumn
water
column
sediment
C
Terrigenous lamina
winter
Mixed-species lamina
with dominant taxa
Stages I & II: spring/summer
Silty diatomaceous lamina
Stage III: late summer
autumn
water
column
sediment
D
Terrigenous lamina
winter
Silty diatomaceous lamina
Stages I, II, and III mixed?
water
column
sediment
KEY
Chaetoceros
resting spore
Skeletonema costatum
Thalassiosira sp.
Paralia sulcata
(symbolizes robust
diatoms)
Odontella aurita
Thalassionema
nitzschioides
silt grain
fragmented diatoms
(hash)
leaf (symbolizes terri-
genous organic debris)
Operculodinium
centrocarpum
(dinoflagellate cyst)
silicoflagellate
gradational contact

The excellent preservation of the frustules in near-monospecific laminae is attributable to three possible conditions: (1) diatom proliferation exceeded zooplankton grazing pressure in the water column, or grazing was absent (Smayda, 1973); (2) diatoms were rapidly exported from the photic zone via biologically mediated flocculation and self-sedimentation (Grimm et al., 1996, 1997), thereby bypassing grazing or dissolution in the water column (Silver and Alldredge, 1981; Alldredge and Gotschalk, 1989); and (3) dissolution after burial was minimal as is the case in Saanich inlet (see Nissembaum et al., 1972). Further *in situ* observations will be required to test which condition, or a combination of conditions, is at work in Effingham Inlet for near-monospecific laminae to be preserved.

The green particles found within some of the CRS may be chloroplasts with residual chlorophyll pigments. These pigments may be responsible for the olive green hue of the diatomaceous laminae. Intact chloroplasts or green particles have been observed in 4500 year-old freshwater diatoms (R. Hall, written communication, 2001), and even in 10000 year-old diatoms from lake sediments (R. Telford, written communication, 2001). The organic content of some of the diatoms may have never degraded in the dysoxic bottom waters of the inlet.

Near-monospecific sublaminae occurring above or within silty diatomaceous laminae may represent deposition from a late summer or autumn production event. Sancetta (1989a) found a distinct fall (September to October) assemblage in Saanich Inlet, consisting of *Thalassionema nitzschioides*, *Rhizosolenia* spp., *Skeletonema costatum*, and several species of *Chaetoceros*. Larger diatoms occurring at this time of

year are likely able to grow slowly under nutrient-poor, low-light conditions, or can regulate their buoyancy to acquire nutrients at depth (Guillard and Kilham, 1977; Kemp et al., 2000). These late summer and autumn laminae may represent deposition of what Kemp et al. (2000) call "fall dump" assemblages. Alternatively, periodic disturbances to the stratified waters (i.e., by storms or strong winds) can bring nutrients back to the surface and lead to diatom miniblooms (Harrison et al., 1983; Haigh et al., 1992).

Origin of Mixed-species Laminae

Mixed-species laminae contain a diverse assemblage of larger diatoms and CRS, and are consistent with Stage II of the seasonal succession described by Margalef (1958) and Guillard and Kilham (1977) (Figure 4.15). The species types and preservation status are characteristic of production and deposition during the late spring to summer months. Diatom hash may represent fragmentation as a function of zooplankton grazing as zooplankton populations catch up with the diatom bloom, or as a function of summer flora being more lightly silicified and susceptible to fragmentation (Sancetta, 1989a). Increased diatom fragmentation was also observed in Saanich Inlet during the summer months (Sancetta, 1989a). The gradational lower contact of this lamina type in Effingham Inlet may represent deposition reflecting the waning spring bloom and the gradual phasing in of a mixed, high diversity assemblage from the late spring to autumn seasons.

Origin of Silty Diatomaceous Laminae

The occurrence of oligotrophic, fall-dump species confirms that silty diatomaceous laminae were deposited after the main spring and summer blooms had waned. The presence of silicoflagellates and dinoflagellates in these laminae further suggests that production and deposition occured mainly from the late summer to the autumn. Silicoflagellates and dinoflagellates showed maximum abundances in sediment traps studies from Saanich Inlet (Sancetta, 1989a), Santa Barbara Basin (Lange et al., 1997), and Jervis Inlet (Sancetta, 1989a) during the late summer to early autumn.

The mixed assemblage of large diatoms, along with the appearance of silicoflagellates and dinoflagellates, is consistent with the description of Stage III of the seasonal succession (Margalef, 1958; Guillard and Kilham, 1977) (Figure 4.15). The gradational upper and lower contacts of silty diatomaceous laminae may represent the gradual increase of silt and organic debris, reflecting the increase in precipitation and terrigenous runoff into the basin during the autumn.

Variability in the Seasonal Succession

The thickness of a terrigenous lamina with respect to a diatomaceous lamina in a given couplet is a function of the amount of terrigenous material influx (which depends on the timing and intensity of rainfall), and the intensity of diatom production (which depends on the amount of sunlight, upwelling strength, and nutrient levels). Couplets exhibiting the recognizable 3- or 4-component seasonal succession are inferred to represent "normal" years of deposition or years with strong seasonality (Chang et al.,

1998). During these conditions, the majority of rainfall occurs during the autumn and winter, and the spring and summer are relatively dry during which diatom blooms occur.

Twenty-eight per cent of the couplets examined contain the well-defined 4-component succession, with at least one, two, or all three of the *Thalassiosira*, *Skeletonema* or CRS sublaminae present directly above the terrigenous lamina (Figure 4.15A). Preservation of the *Thalassiosira-Skeletonema-Chaetoceros* sequence may represent discrete blooms of each of these taxa, and stability of the water column near the sediment-water interface in order for the sublaminae to become preserved (i.e., no bottom-water currents or mixing).

Conversely, 48% of the couplets examined contain the 3-component succession. In scenario 1, a succession with only a silty diatomaceous lamina directly above the near-monospecific lamina may signify a wetter summer, and an absent silty diatomaceous lamina may signify a drier autumn (Figure 4.15B). In scenario 2, the presence of a mixed species lamina and a lack of a near-monospecific lamina may represent mixing of taxa in the water column, or be the result of monospecific sublaminae that were reworked or mixed at the sediment-water interface by bottom water currents (Figure 4.15C). Apart from these differences, the 3-component succession is otherwise similar to the 4-component succession in its record of seasonal flux of particles.

Couplets lacking the recognizable succession, i.e., 2-component couplets or 3-component couplets possessing anomalously thick (2-3 mm) terrigenous and silty diatomaceous laminae and thin (0.2 mm) near-monospecific laminae, may record "abnormal" years or years of weak seasonality (Figure 4.15D). In this situation, increased

rainfall during the spring and summer leads to an increased silt content in diatomaceous laminae. An analysis of the couplets from thin sections reveals that terrigenous-rich 2- and 3-component couplets occur on average every 3–20 years, although there can be a bundle of up to 3 successive couplets with abundant terrigenous debris (Figure 4.5). El Niño conditions may be responsible for the lowered diatom abundance and increased terrigenous debris in some of these couplets. During an El Niño year, upwelling and nutrient delivery into the inlet can be insufficient to result in a diatom bloom. Diatomaceous laminae may also be masked by elevated deposition of terrigenous material to the sediments (see Sancetta, 1996) as a consequence of higher rainfall that often accompanies major El Niño phenomenon in this region. The cyclicity of El Niño and other ocean-atmosphere phenomenon is the topic of continuing research which will include statistical and time-series analyses of a ~12000-year sediment record obtained in Effingham Inlet during the International Marine Past Global Changes (IMAGES) coring program in May 2002 (R. Thomson and T. Pedersen, personal communication, 2002).

PALEOENVIRONMENTAL INTERPRETATION

Downcore trends in the observed characteristics of slab lithologies and microfossil content (represented by laminae abundant with *Skeletonema costatum* and CRS; Figure 4.14) were compared to a record of local and regional climate change in Vancouver Island as interpreted from pollen (Hebda, 1995) and Neoglacial records (Ryder and Thomson, 1986). Although only the one piston core was examined, which in itself cannot be used to reconstruct paleoclimate across the region, an attempt was made

to see how the lamina styles relate to the pollen-derived climate record. The timing of climatic intervals listed below indicates approximate ages, as the transition from one climate state to another may have lasted for as much as 1500 to 2000 years (Mathewes and Heusser, 1981).

Slabs 6 to10 (~3600 to 5500 cal yr BP) contain the most couplets with the seasonal succession and laminae containing CRS and *S. costatum* (Figure 4.14). This evidence infers that sustained levels of nutrient supply to the coastal ocean and climatic conditions favorable to annual seasonal upwelling were present prior to ~3600 cal yr BP. In particular, slabs 8 to 10 (4400 to 5500 cal yr BP) contain the most distinctly laminated intervals in the entire core. Seasonality was apparently strong during this time and conditions favored the proliferation of fast-growing, spring bloom species. The inlet likely experienced consistently anoxic conditions during this interval, resulting in the distinctly laminated character of slabs 8 to10. The pollen record suggests that prior to ~4000 yr BP, climate conditions were warmer and drier than they are today (Hebda, 1995; Figure 4.14G), with the Holocene Hypsithermal event occurring at ~6000 ka.

In contrast, slabs 1 to 5 (~900 to ~3100 cal yr BP) have fewer couplets with the seasonal succession and a relatively low number of couplets containing CRS and *S. costatum* (Figure 4.14). This may indicate a slight decrease in primary production and hence decreased delivery of nutrients to the coastal ocean from recent times to ~3100 cal yr BP.

Nonlaminated intervals are common in slabs 3 to 7 (~2200 to ~4000 cal yr BP), indicating a departure during this time from the normally anoxic conditions that are

conducive to the preservation of laminated sediments. Results from continuing research show that on rare occasions, it is possible for the bottom waters of the inner basin to be briefly aerated by deeply upwelled and oxygenated waters (Dallimore, 2001). These bottom-hugging waters can enter the inlet either in the winter during Arctic outbreak conditions, or early in the annual spring upwelling season during a rare combination of weak tidal currents in the inlet, significant rainfall, and strong (> 10 m/s) northeasterly winds (Thomson, 1981; Griffin and Leblond, 1990). Therefore, the higher incidence of nonlaminated units in slabs 3 to 7 may indicate that precipitation was greater during this time. Indeed, wetter conditions are indicated by the pollen record from 2000–4000 yr BP for this region of Vancouver Island (Hebda, 1995). Additionally, this interval coincides with the mid-Neoglacial advance of the Tiedemann glacier (3300–1900 cal yr BP) in the Coast Mountains, with the advance a likely response to climate deterioration after the Holocene Hypsithermal (Ryder and Thomson, 1986). This interval also contains some of the thickest diatomaceous laminae found throughout the core (Table 4.3; Figure 4.5). These thick diatomaceous laminae occur in discrete packets of 7- to 10-year intervals and may represent isolated cycles of increased biological production.

The frequency at which couplets with a high terrigenous content occurs does not appear to flucutate greatly throughout the three time periods. If these couplets represent deposition during possible El Niño years, then further research is required in order to understand the timing of El Niño cycles during the late Holocene.

CONCLUSION

This study indicates that variations in the annual sequence of lamina components are proxies for changes in primary production and precipitation, factors which themselves are proxies for climate and nutrient supply to the coastal ocean, which in turn can be related to coastal ocean dynamics. The results show that the late Holocene climate varied substantially in southwest Vancouver Island. Primary production was highest and persistent anoxia of the bottom waters occurred prior to ~4000 yr BP, with cooler and wetter conditions than present occurring between ~2000 and 4000 yr BP, after which modern conditions were established.

A distinctive seasonal succession of diatom species observed in the sediments agrees well with observations made by Margalef (1958) and Guillard and Kilham (1977) for marine planktonic diatoms. This evidence, along with radiocarbon dating of the sediments, shows that the laminated sediments in Effingham Inlet are annual deposits. El Niño cycles may also be recorded in the sediment where silt-rich couplets occur every 3–20 years in the slabs examined.

The next step in continuing research in Effingham Inlet is being taken toward a full understanding of the annual diatom depositional cycle and diatom ecology, by comparing late Holocene sediments with modern sediment-trap data, weather records, and El Niño records for Effingham Inlet and the surrounding region. The determination of quantitative diatom abundances from each season will pinpoint the timing and strength of the production of various species and identify the modern environmental triggers for each event. This is important for modeling and reconstructing a continuous high-

resolution climate record for southwestern British Columbia and the northeast Pacific Ocean in general during the late Holocene.

CHAPTER 5

SEASONAL VARIABILITY IN DIATOM FLUX FROM A SEDIMENT TRAP STUDY (1999–2000)

ABSTRACT

Sediment traps were deployed in the inner basin and at the mouth of Effingham Inlet for a period of 16 months from 29 May 1999 to 28 September 2000 in order to understand modern phytoplankton dynamics in the inlet. Mass flux and species compositions and abundance were determined from the collected material and related to environmental data gathered from meteorological stations. Total mass flux was greater in the mouth of the inlet than in the inner basin throughout the entire collection period, and the absolute abundance of diatoms, *Chaetoceros* spp. resting spores and silicoflagellates were consistently higher in the mouth of the inlet. *Thalassiosira* spp., *Minidiscus chilensis*, *Skeletonema costatum* and *Chaetoceros* spp. resting spores formed the bulk of spring and summer blooms in the inner basin, whereas the mouth of the inlet experienced more oceanic influence, with higher abundances of *Rhizosolenia* spp. Taxa appearing in the inner basin are likely indigenous to the inlet as they are common throughout the collection interval and are found in the sediment record throughout the late Holocene. An exception is the appearance of *Fragilariopsis atlantica*, which comprised 40.7% of the diatom assemblage in the summer 1999 and then disappeared from the trap record. This diatom and other inconsistently appearing taxa may represent allochthonous species advected into the inlet. The first four axes of a detrended canonical correspondence analysis (DCCA) performed on 55 diatom taxa from the inner basin dataset explained

42% of the species variation, where 83% of the variation was explained by the chosen environmental variables. Daylength, sea surface temperature, precipitation and wind velocity were important variables for explaining the species variance. DCCA and diatom composition analyses indicate that the assemblages in the inner basin and mouth of the inlet represent different environments. The results presented here will be used as a future calibration set for reconstructing past environments and climates in southwestern British Columbia.

INTRODUCTION

Since Margelef (1958) first reported the occurrence of a predictable seasonal succession of diatoms in coastal waters, biological oceanographers have been interested in determining the relationships between various phytoplankton groups and the environmental factors influencing their growth and distribution. An understanding of how the environment affects diatoms and other phytoplankton in modern waters is essential for interpreting past environmental change. Collecting data on modern diatom fluxes and environmental variables is accomplished through the use of sediment traps and meteorological stations. Sediment traps have been deployed in a variety of productive coastal environments in order to study the seasonal changes in lithogenic flux, biological productivity, and the distribution of plankton, including diatoms, silicoflagellates, radiolaria, foraminifera and coccolithophores. Previously studied areas include the Panama Basin (Honjo, 1982); the Gulf of California (Thunnell et al., 1993); Santa Barbara Basin, California (Lange et al., 1997); Jervis, Sechelt, and Saanich inlets, British

Columbia (e.g., Timothy and Pond, 1997; Sancetta, 1989a, 1990); and Auke Bay, Alaska (Waite et al., 1992).

There are three main advantages for employing sediment traps. First, samples can be collected over time intervals ranging from days to months, enabling the highest possible sampling frequency and the construction of a high-resolution time series. The exact timing and absolute magnitude of subseasonal events, such as the bloom of a specific diatom species, can be resolved and related to instrumental environmental data. Second, sediment trap samples can be compared to the sediment record to verify whether or not the sediment record represents an accurate portrayal of phytoplankton communities occurring in the surface waters. It is important to know whether processes such as dissolution or physical fragmentation have altered the phytoplankton assemblage from the time of production in the surface waters to the time of deposition and burial. Third, samples collected from sediment traps document the modern phytoplankton community. Since real-time climate and oceanic variables are being recorded concomitantly, relationships between phytoplankton and the environment can be drawn. These modern dynamics can therefore be used as a point of comparison with fossil assemblages in order to determine past environmental conditions.

In this chapter, I describe the results of a 16-month long sediment trap study that took place in the inner basin and mouth of Effingham Inlet from 29 May 1999 to 28 September 2000. This study represents a first attempt at using sediment traps in a British Columbian inlet that opens directly to the Pacific Ocean. There are three objectives to this study: (1) to determine the temporal and spatial distribution of diatoms over the 16-

month collection period, (2) to relate the appearance of different diatom species to environmental variables, and (3) to relate these modern assemblages and the seasonal succession to what was observed in the sediment record.

METHODS AND MATERIALS

OSU and Baker sediment traps were deployed in the inner basin of Effingham Inlet and at the mouth of the inlet (Figure 5.1). Samples were processed and analyzed by Dr. Miriam Bertram (Pacific Marine Environmental Laboratory, Seattle, Washington) before aliquots were distributed to other researchers (Chapter 3). I worked exclusively on the OSU trap samples.

Handling of Samples for Micropaleontology

Figure 5.2 gives a summary of the processing techniques used for sediment trap samples. I received the first group of frozen samples (series CTC3A) from Dr. Bertram. Because these samples were to be shared for diatom, dinoflagellate and foraminifera analysis, I split each sample again using a wet plankton splitter of a design similar to that described in Scott and Hermelin (1993). Six equal portions of each sample were obtained. Two portions, one each for diatom and dinoflagellate work, were retained at Carleton University, and the remaining two-thirds of the sample were shipped to Dalhousie University for foraminifera analyses. The remaining sediment trap samples (series CTC3B, CTC3C, and CTC11C) contained samples already pre-split by Dr. Bertram for each microfossil component, and the diatom and dinoflagellate portions were shipped

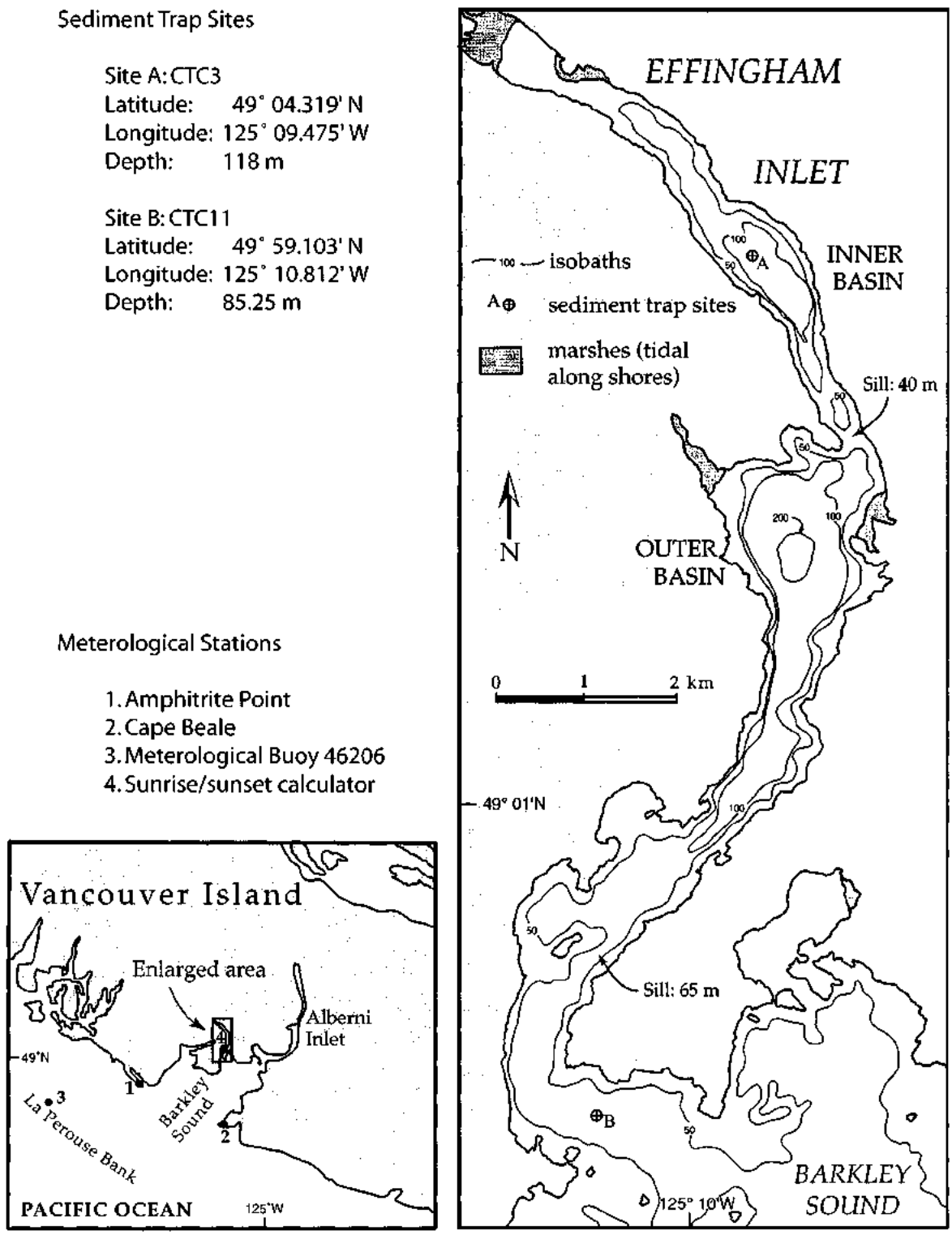

FIGURE 5.1. Location of sediment trap sites and meterological stations (inset, see Table 5.3 for details).

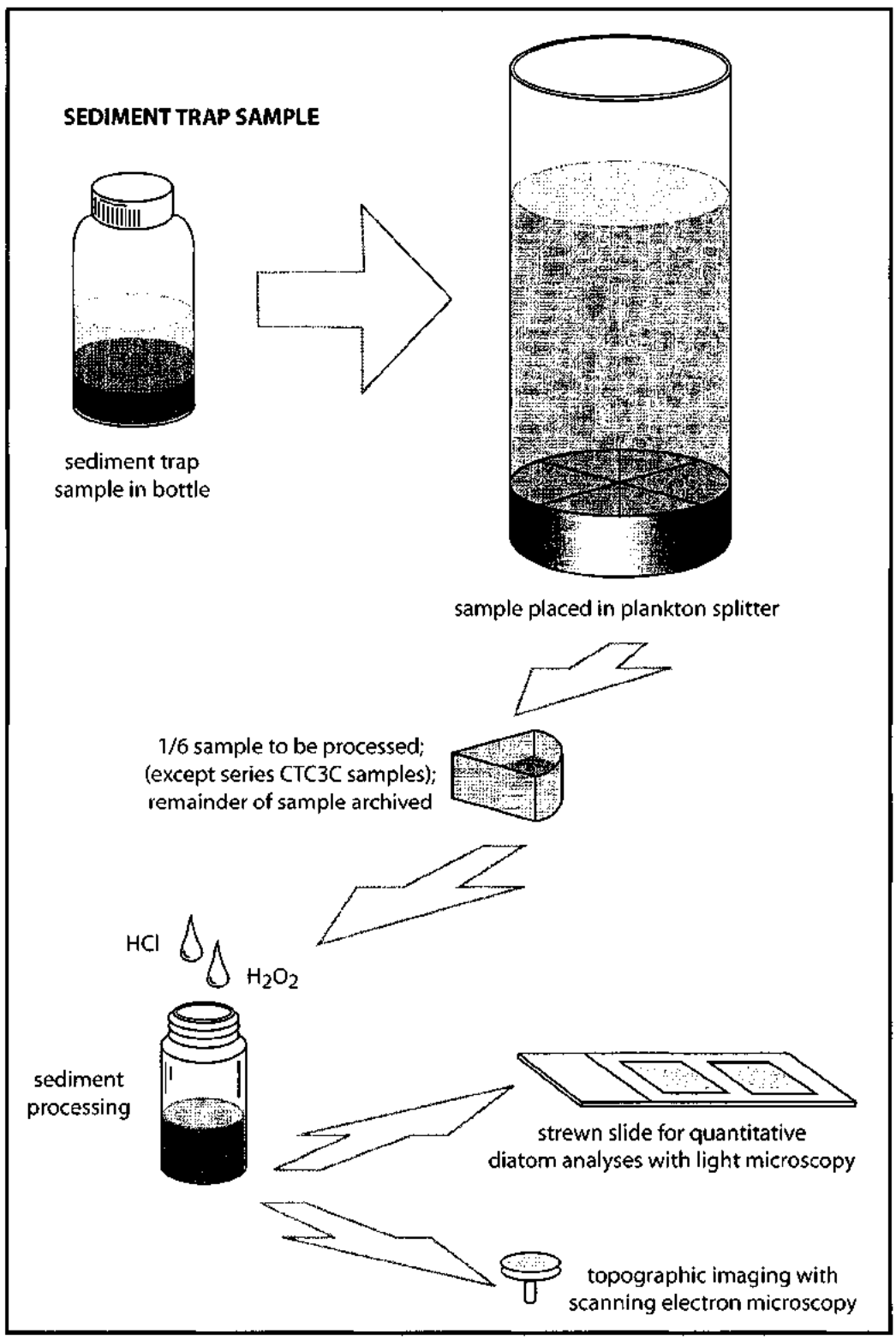

FIGURE 5.2. Schematic diagram showing processing of sediment trap samples. No scale is intended.

refrigerated to Carleton University. A total of 55 samples, with 41 from the inner basin and 14 from the mouth of the inlet, were analyzed for diatom content.

For diatom work, samples from series CTC3B, and CTC11C were large, so they were split again using the plankton splitter to obtain more manageable sample sizes (Table 5.1). Samples from series CTC3C were very small and therefore not split. All samples were kept refrigerated until used for slide processing. Estimated initial sediment weights for the split samples were calculated by Dr. Bertram from the total dry mass from each cylinder (Table 5.1). In this chapter, sample labels and opening dates are used interchangeably; refer to Table 5.1 for equivalent sample descriptors.

Sample Processing for Diatom Analyses

Sediment solutions of a manageable sample size were transferred into 20-mL glass scintillation vials for processing. Sediments were processed with 10% hydrochloric acid (HCl), to dissolve carbonate, and 30% hydrogen peroxide (H_2O_2), for the digestion of organic matter. The sediment showed no reaction to the HCl, indicating no carbonate. However, when the samples were heated at ~50 °C, there was some violent bubbling of the solution, which was the reaction of the organic matter with the H_2O_2. The samples were heated for about 40 minutes, and the reaction continued until organics were dissolved and the bubbling subsided. During this time, the sediment changed from a dark brown colour to tan or white where mainly silica remained. The vials were then removed from the heat and left undisturbed for an hour to cool and for remaining reactions to continue. After an hour, a 4 g/L solution of sodium polyphosphate [$(NaPO_3)_n$] was

TABLE 5.1. Sample labels, mass and descriptions (total dry mass data courtesy of M. Bertram)

Series/ Location	Sample	Date opened	Total dry mass per cylinder (g)	Estimated initial mass after split* (g)	Description
CTC3A	3A-1	5/29/99	2.49	0.12	sparse greenish brown mud
(inner	3A-2	6/6/99	3.68	0.13	sprarse greenish brown mud, black specks (plant material?)
basin)	3A-3	6/15/99	1.75	0.06	sparse flocculent greenish brown mud
	3A-4	6/24/99	0.70	0.02	sparse flocculent greenish brown mud
	3A-5	7/3/99	2.15	0.08	sparse greenish brown mud
	3A-6	7/12/99	10.48	0.37	flocculent brownish green mud
	3A-7	7/21/99	11.38	0.43	flocculent brown mud
	3A-8	7/30/99	3.61	0.13	flocculent brown mud
	3A-9	8/7/99	2.20	0.08	flocculent brown mud
	3A-10	8/16/99	1.65	0.06	flocculent brown mud
	3A-11	8/25/99	1.12	0.17	flocculent brown mud, plant material
	3A-12	9/3/99	0.38	0.07	sparse flocculent brown mud, plant material
	3A-13	9/12/99	0.34	0.01	sparse flocculent brown mud, plant material
	3A-14	9/21/99	n.s.	n.s.	
CTC3B	3B-1	10/11/99	3.79	0.10	cohesive thick brown mud, minor silt, plant material
(inner	3B-2	10/26/99	4.79	0.12	cohesive thick brown mud, minor silt, plant material
basin)	3B-3	11/11/99	6.69	0.18	cohesive thick brown mud, minor silt, plant material (moss?)
	3B-4	11/27/99	7.10	0.18	cohesive thick brown mud, minor silt, plant material
	3B-5	12/12/99	7.26	0.19	cohesive thick brown mud, minor silt, blackened twig
	3B-6	12/28/99	5.44	0.14	cohesive thick brown mud, minor silt, minor plant material
	3B-7	1/13/00	5.19	0.14	cohesive thick brown mud, minor silt, minor plant material
	3B-8	1/29/00	5.58	0.14	cohesive thick brown mud, minor silt, minor plant material
	3B-9	2/13/00	5.95	0.15	cohesive thick brown mud, minor silt, minor plant material
	3B-10	2/29/00	9.74	0.25	cohesive thick brown mud, minor silt, plant material
	3B-11	3/16/00	8.23	0.23	cohesive thick brown mud, minor silt, plant material
	3B-12	3/31/00	5.14	0.13	flocculent suspended greenish brown mud
	3B-13	4/16/00	5.04	0.12	flocculent greenish brown mud, 2 shrimp
	3B-14	5/2/00	14.29	0.29	flocculent greenish brown mud
CTC3C	3C-1	5/15/00	1.22	1.22	flocculent tan mud, minor plant material
(inner	3C-2	5/24/00	1.30	1.30	flocculent tan mud, minor plant material
basin)	3C-3	6/3/00	1.25	1.25	flocculent tan mud, minor plant material
	3C-4	6/13/00	4.38	4.38	flocculent greenish brown mud, minor plant material
	3C-5	6/23/00	2.94	2.94	flocculent greenish brown mud, minor plant material
	3C-6	7/3/00	2.45	2.45	flocculent greenish brown mud, minor plant material
	3C-7	7/12/00	0.05	0.05	trace of greenish brown mud, mainly green tinted water
	3C-8	7/22/00	0.04	0.04	trace of greenish brown mud, mainly green tinted water
	3C-9	8/1/00	0.04	0.04	trace of greenish brown mud, mainly green tinted water
	3C-10	8/11/00	0.05	0.05	trace of greenish brown mud, mainly green tinted water
	3C-11	8/21/00	0.06	0.06	trace of greenish brown mud, mainly green tinted water
	3C-12	8/31/00	0.07	0.07	trace of greenish brown mud, mainly green tinted water
	3C-13	9/9/00	0.09	0.09	trace of greenish brown mud, mainly green tinted water
	3C-14	9/19/00	0.08	0.08	trace of greenish brown mud, mainly green tinted water
CTC11C	11C-1	5/15/00	7.04	0.18	flocculent thick brown mud
(mouth)	11C-2	5/24/00	5.55	0.14	flocculent thick brown mud, conifer needle
	11C-3	6/3/00	12.40	0.30	flocculent thick greenish brown mud
	11C-4	6/13/00	17.82	0.46	flocculent thick greenish brown mud
	11C-5	6/23/00	7.56	0.20	flocculent thick greenish brown mud
	11C-6	7/3/00	7.60	0.19	flocculent greenish brown mud, minor silt
	11C-7	7/12/00	7.52	0.19	flocculent greenish brown mud
	11C-8	7/22/00	10.40	0.28	flocculent thick greenish brown mud
	11C-9	8/1/00	4.18	0.11	flocculent thick greenish brown mud
	11C-10	8/11/00	12.77	0.36	flocculent thick greenish brown mud
	11C-11	8/21/00	5.25	0.14	flocculent thick greenish brown mud, conifer needle
	11C-12	8/31/00	7.02	0.18	flocculent thick greenish brown mud
	11C-13	9/9/00	8.68	0.22	flocculent thick greenish brown mud
	11C-14	9/19/00	5.18	0.14	flocculent thick greenish brown mud

* samples from series CTC3C not split
n.s. = no sample

added to each sample to disperse clay minerals. The vials then sat for an additional 1.5 h after which the vials were topped up with distilled water and left undisturbed for 24 h. The supernatant from each vial was then decanted each day for five days to remove the HCl and H_2O_2. After each decantation, the vials were topped up with distilled water.

After each vial was fully decanted, a test slide was made to determine what dilution factor was appropriate for making a slide with the most optimal concentration of diatoms for counting and identification. An optimal concentration is where there are 3–5 intact diatom valves per field of view at 1000× magnification. Because the initial sediment concentrations of the samples were highly variable, a variety of dilutions had to be made (Table 5.2). Before the slurry was extracted for plating the cover slip, the scintillation vial was thoroughly shaken to ensure that heavy and light diatoms were well mixed. Using a calibrated micropipet, the appropriate amount of diatom slurry was extracted from the scinitillation vial and transferred to a plastic centrifuge tube. Two drops of HCl were added to the tube, and then distilled water was added to a total volume of 7.5 mL. The centrifuge tube was then thoroughly shaken, and 500 µL of diluted slurry was extracted with the calibrated micropipet. Plating was done by carefully extruding the diluted slurry onto a pre-cleaned 18 × 18 mm cover slip. A single drop in the center of the cover slip was put down first, followed by subsequent drops at the corners. The drops were then connected together until the entire surface of the cover slip was covered. This action is to ensure that large diatoms or a higher concentration of diatoms do not converge at the center of the cover slip (M. Hay, personal communication, 2000). Two different dilutions of each sample were made. The cover slips were shielded from dust

TABLE 5.2. Volumes (mL) of diatom slurry and distilled water per dilution

	Dilution				
	60×	30×	15×	5×	2.5×
Diatom Slurry	0.125	0.25	0.5	1.5	3.0
Distilled Water	7.375	7.25	7.0	6.0	4.5
Total Volume	7.500	7.50	7.5	7.5	7.5

and allowed to dry at room temperature without disturbance for 24–36 h. Once dry, the cover slips were inspected for quality. Where the slurry had seeped underneath the cover slip or the distribution of the dried diatom residue was not even, a new cover slip for that sample was plated. Interference patterns, created by minute vibrations or disturbance, were absent to minimal.

After the cover slips were completely dry, they were mounted to glass slides. Two drops of toluene-diluted Naphrax™ mountant (refractive index = 1.74) were put on a microscope slide. The cover slip was then carefully transferred to the glass slide and placed residue-side down onto the mountant. The slide was then heated until the mountant started bubbling, driving off the toluene. When the bubbling action stopped, the slide was removed from heat and placed on a flat board and allowed to cool and set for up to two weeks.

Microscopy

Identification and enumeration of diatoms and other microfossils was carried out at 1000× magnification with an Olympus BX-51 stereo light microscope equipped with a differential interference contrast filter. Diatom taxa were identified to the lowest taxonomic level (i.e., variety) when possible, although some varieties and forms were subsequently grouped together for statistical analyses. Identification was based mainly on the floras of Cupp (1943), Campeau et al. (1999), Cumming et al. (1995), Bérard-Therriault et al. (1999), and Witkowski et al. (2000). Some *Chaetoceros* spp. resting spores (CRS), such as *C. radicans*, *C. debilis*, and *C. vanheurckii*, were recognizable,

however a majority of spores could not be identified. As a result, CRS were grouped together as a genus, along with *Chaetoceros* spp. vegetative cells, which were found in low abundance and were often poorly preserved and therefore difficult to identify. Resting spores of the genera *Leptocylindrus* and *Stephanopyxis* occurred sporadically in low abundance and were not included in subsequent analyses. Silicoflagellates were identified to species level when possible.

Diatoms were counted as valves (one half of a frustule), as were CRS (one half of a spore), and silicoflagellates were counted as skeletons. At least 500 diatom valves were counted per sample for statistical validity (Patterson and Fishbein, 1989), except for sample 3A-13 where only 250 diatom valves were counted because the sample was very sparse. CRS and silicoflagellates were enumerated until the diatoms were fully counted. The counting of CRS will provide minimum values since one spore is not necessarily equal to one vegetative cell (cf. Hemphill-Haley and Fourtanier, 1995). At least 40 random fields of view were examined over at least half the area of the cover slip, except for samples 3C-3 to 3C-7 where diatoms were abundant, although an effort was made to randomly space out the fields of view as much as possible. Diatom counting procedures followed that of Laws (1983) and Schrader and Gersonde (1978). Preservation criteria for microfossils follow that in Table 4.1.

Selected samples were prepared for secondary electron microscopy by placing a drop of cleaned diatom slurry onto a stub and allowing the liquid to dry at room temperature (Hasle and Fryxell, 1970). The dried slurry was then coated with an Au-Pd mixture. However, the procedure proved to be unsuccessful and no images were

collected. The diatoms were obscured by a contiguous coating of unknown composition, and where diatoms were exposed, they were highly fractured. It appears that the contiguous coating was a chemical residue left over after the water in the slurry had evaporated.

Abundance, Flux and Diversity Calculations

The relative abundance of a diatom taxon represents its proportion relative to the total number of diatoms counted in a sample. Relative abundance was calculated with the equation

$$C_r = \frac{n_i}{N} 100\% \tag{5.1}$$

where C_r is the relative abundance of diatom taxon i expressed as a percentage, n_i is the number of diatom taxon i counted in the sample, and N is the total number of individuals counted in the sample. Relative abundance was calculated for every diatom taxon in every sample examined.

The absolute abundance (concentration) of diatoms, resting spores and silicoflagellates in each sample was calculated with the equation

$$C_a = \frac{Nadv_s}{fAwv_p} \tag{5.2}$$

where C_a is the estimated absolute abundance of valves or skeletons per gram of dry sediment; N is the total number of valves or skeletons counted on the slide; a is the area (3.24×10^8 μm^2) of the cover slip; d is the dilution factor of the slurry plated to the cover slip; v_s is the initial volume (mL) of slurry used from the scintillation vial; f is the number

of fields of view examined; A is the area (34636 μm^2) of the field of view at 1000× magnification; w is the initial weight (g) of sediment used; and v_p is the volume (mL) of slurry plated onto the cover slip (Appendix E2). The absolute abundance for total diatoms, resting spores and silicoflagellates was determined, as was the absolute abundance for individual taxa.

Absolute abundance values were converted to daily flux values so that samples from different times of the year could be compared without the effects of different collection time intervals or sediment masses. Flux was calculated with the equation

$$F = \frac{C_a m}{tc} \tag{5.3}$$

where F is the estimated flux of valves or skeletons per square meter per day, C_a is the absolute abundance of valves or skeletons per gram of sediment calculated from Equation 5.2, m is the total dry mass (g) of material collected in each sediment trap cylinder (Table 5.1), t is the number of days the cylinder was opened for, and c is the sediment trap collection area (0.49 m^2) (Appendix E2). Benthic diatom abundance and flux were extracted from the total diatom vegetative cell concentrations.

Specific diversity was calculated for diatoms using Margelef's (1958) formula

$$S.D.I. = \frac{S_i - 1}{\ln(N_i)} \tag{5.3}$$

where $S.D.I.$ stands for specific diversity index, a dimensionless value; S_i is the number of taxa in sample i; and N_i is the total number of valves counted in sample i. A high S.D.I. indicates that there are more species represented, or a high diversity of different species, in a particular sample.

Instrumental Data

Instrumental environmental data are used to determine what environmental variables are related to the appearance of certain diatom species throughout the trap collection period. Environmental variables available were daylength, sea surface temperature, sea surface salinity, precipitation, wind velocity, and wind stress (Table 5.3). Temperature, salinity and wind data were provided by Roy Hourston (Institute of Ocean Sciences); precipitation data were obtained as raw data files from Climate Services, Environment Canada; and daylength data were calculated from the Herzberg Institute of Astrophysics, National Research Council of Canada (HIA-NRC), website (www.hia-iha.nrc.cnrc.gc.ca/sunrise_e.html). Data were obtained from Amphitrite Point, Cape Beale, and Meteorological Buoy 46206 because these stations are relatively close to Effingham Inlet (Figure 5.1), and they also recorded the necessary data during the appropriate time interval. Additional data, such as water temperature, density and oxygen content, were collected periodically in Effingham Inlet by R. Thomson and B. Burd (Institute of Ocean Sciences) from 1995 to 2000 (see Figures 2.6, 2.7), but these data were not used in statistical analyses in this study. No *in situ* nutrient data was collected. Abbreviations for environmental variables in the following discussion are used as identifiers in subsequent statistical analyses.

Daylength (DL) governs the growing period of diatoms and other photosynthetic algae. Daylength data were obtained in lieu of data for solar irradiance and hours of bright sunshine because these data were not available for the study area or the time interval studied. Daylength was calculated for the coordinates of 49° 1.02'N and

TABLE 5.3. Environmental monitoring stations

Geographic Area	Station	Data Description	Location		Data Type*						
			Latitude (N)	Longitude (W)	SST	SSS	PPT	300V	30V	300U	30U	DL†
West Coast Vancovuer Is.	Amphitrite Point	Lighthouse	48° 55.3'	125° 32.3'	●	●						
West Coast Vancovuer Is.	Cape Beale	Lighthouse	48° 47.2'	125° 12.9'			●					
La Perouse Bank, B.C.	46206	Meteorological Buoy	48° 50.1'	125° 59.9'	●			●	●	●	●	
West Coast Vancovuer Is.		sunrise calculator	49° 1.02'	125° 10.02'								●

SST sea surface temperature
SSS sea surface salinity
PPT total precipitation (includes rain and snow)
300V alongshore (300 degrees true) wind velocity
30V cross shore (30 degrees true) wind velocity
300U alongshore (300 degrees true) wind stress
30U cross shore (30 degrees true) wind stress
DL daylength

* all data were obtained as daily means unless otherwise stated
† daylength data taken from midpoint of each collection interval

125° 10.02'W and included only sunrise to sunset times.

Sea surface temperature is useful for determining the seasonal distribution of diatoms. Sea surface salinity can delineate temporal and spatial patterns of freshwater, brackish and marine species, and gives an indication of the onset of water column stratification. Sea surface temperature data were obtained from Amphitrite Point (APT) and Meteorological Buoy 46206 (MBT). Sea surface salinity (APS) data were obtained from Amphitrite Point. Both datasets were obtained as daily values.

The amount of precipitation governs how much sediment enters the inlet after heavy rainfall, which in turn can affect the salinity and turbidity of the upper water column and the amount of benthic taxa washed into the inlet. Precipitation data were obtained from Cape Beale (CBP) as daily values. The amount of rainfall and snowfall were combined to represent a measure of total precipitation for a given day.

Wind velocity and wind stress profiles are useful proxies for determining the timing and strength of coastal upwelling and surface mixing. Wind data obtained from Meteorological Buoy 46206 as hourly values were low-pass filtered to obtain daily values (R. Hourston, written communication, 2002). Wind velocity is a vector, which means it has two scalar components, speed and direction. Wind stress is the square of the wind velocity multiplied by a drag coefficient and air density, and is a measure of the lateral force (drag) exerted on the water surface by the wind. Because wind stress is derived from the wind velocity, wind stress is more indicative of (and more closely related to) wind-driven upwelling and downwelling than wind velocities themselves (R. Thomson, written communication, 2002).

The wind velocity and stress components (northward and eastward) have been rotated to fit the orientation of the British Columbia coast line as this is most suitable when wind-driven upwelling and downwelling are of interest. For example, at Amphitrite Point along-shore winds are at 300° true, where a direction of 0° is northward and the direction angle increases positively in a clockwise direction (R. Hourston, written communication, 2002). When along-shore winds are positive values, they are blowing toward a west-northwest direction, and since net wind-driven oceanic transport is 90° to the right of the wind in the northern hemisphere (Figure 2.1), positive along-shore winds favor onshore oceanic flow and downwelling. Conversely, negative along-shore winds, blowing toward an east-southeast direction, favor upwelling. Cross-shore winds are measured at 30° from true north, and are at a right angle to the along-shore winds. Positive values mean that the winds are being pushed toward the land, signifying downwelling action of the surface water. Conversely, negative values indicate that winds are being blown off shore, signifying upwelling along the coast. Wind data used in this study include along-shore (300° true) wind velocity (MB300V), cross-shore (30° true) wind velocity (MB30V), along-shore (300° true) wind stress (MB300U) and cross-shore (30° true) wind stress (MB30U).

STATISTICAL ANALYSES

Species, samples, and environmental variables were correlated using the multivariate statistics program CANOCO version 4.0 (ter Braak and Smilauer, 1998). The program produces an ordination diagram that is a two-dimensional representation of

data plotted in multidimensional space. A majority of the variation in the data is explained by the first four axes of the ordination, so CANOCO provides information of data variance along these axes. Of the four axes, the first two axes usually explain the greatest proportion of the data so these axes are plotted on the ordination diagram. Species and samples are plotted as points, and environmental variables are plotted as vectors. Species and sample points are plotted at their relative optima (i.e., maximum value on a Gaussian distribution) for each environmental variable; by drawing a perpendicular line from the point to the vector, one can determine the relative environmental optima of each species or sample. The relative length and direction (sign) of the vectors indicates the relative importance of the environmental variable for predicting species composition. The most important variables are those with long vectors and are at a low angle with the axis the variable is most correlated with. The mean value of each environmental variable lies at the origin of the diagram. The vector points toward the high end of the environmental gradient. The vectors for each variable can be extended beyond the origin to explain species occurrences on the low end of the environmental gradient. The significance of the ordination is summarized by the eigenvalues where high eigenvalues indicate wide environmental gradients that explain much of the species variation. Readers who are interested in detailed mathematical explanations of gradient theory can refer to ter Braak and Prentice (1988), Birks (1995), and Jongman et al. (1995).

Data Screening

Before analyses could be performed, the data had to be screened for rare species, skewed environmental gradients, and sample outliers. Only samples from the inner basin trap were used because this dataset spanned the entire deployment period. Samples representing the partial record from the mouth of the inlet were plotted as supplemental (passive) samples in the final ordination diagram.

Species data

A total of 237 diatom taxa were identified from both the inner basin and the mouth of the inlet (Appendix E1). To reduce the number of rare taxa, the data were screened to include only taxa that appeared in at least three samples, and had a relative abundance of at least 1% in one sample. Although the taxa *Fragilariopsis* sp. (3A-7) and *Navicula* sp. (3C-1) fulfilled this requirement, they were eliminated because their identification was not certain (i.e., whether these taxa represented single species or a suite of very similar appearing species). As a result, 55 taxa remained (Table 5.4).

Environmental variables

Environmental data from meteorological stations listed in Table 5.3 were included in the multivariate analysis. Daily values were averaged over the same time intervals that the samples were collected. Daylength was not averaged over a period of time, but was calculated at a midpoint date for each sediment trap collection interval. The environmental variables were correlated using commercial statistical software to

TABLE 5.4. Diatom taxa occurring in at least three samples, and ≥ 1% in at least one sample (code numbers correspond to those in Figure 5.10C)

1 *Achnanthes minutissima* Kützing 1833
2 *Actinocyclus curvatulus* Janisch in A. Schmidt 1878
3 *Actinoptychus vulgaris* Schumann 1867
4 *Amphora* cf. *helenensis* Giffen 1973
5 *Bacteriastrum delicatulum* Cleve 1897
6 *Berkeleya rutilans* (Trentepohl) Grunow 1880
7 *Cocconies disculus* (Schumann) Cleve in Cleve and Jentzsch 1895
8 *Cocconeis neothumensis* Krammer 1991
9 *Cocconeis placentula* Ehrenberg 1838
10 *Cocconeis scutellum* Ehrenberg 1838
11 *Cocconeis stauroneiformis* (Rabenhorst) Okuno 1957
12 *Diatomella minuta* Hustedt in A. Schmidt, Atlas 1874
13 *Ditylum brightwellii* (West) Grunow in van Heurck 1883
14 *Eunotia* spp. Ehrenberg 1837
15 *Fragilaria* cf. *sopotensis* Witkowski and Lange-Bertalot 1993
16 *Fragilariopsis atlantica* Paasche 1961
17 *Fragilariopsis pseudonana* (Hasle) Hasle 1993
18 *Gomphonemenopsis lindae* Witkowski, Metzelin and Lange-Bertalot in Metzelin and Witkowski 1996
19 *Gomphonemopsis obscurum* (Krasske) Lange-Bertalot
20 *Hyalodiscus scoticus* (Kützing) Grunow 1879
21 *Melosira nummuloides* (Dillwyn) C.A. Agardh 1824
22 *Minidiscus chilensis* Rivera and Koch 1984
23 *Navicula gregaria* Donkin 1861
24 *Navicula perminuta* Grunow in Van Heurck 1880
25 *Nitzschia coarctata* Grunow in Cleve and Moller 1878
26 *Nitzschia frustulum* (Kützing) Grunow in Cleve and Grunow 1880
27 *Opephora* cf. *horstiana* Witkowski 1994
28 *Opephora mutabilis* (Grunow) Sabbe and Vyverman 1995
29 *Paralia sulcata* (Ehrenberg) Cleve 1873
30 *Planothidium delicatulum* (Kützing) Round and Bukhtiyarova 1996
31 *Planothidium* cf. *engelbrechtii* (Cholnoky) Round and Bukhtiyarova 1996
32 *Planothidium hauckianum* (Grunow) Round and Bukhtiyarova 1996
33 *Pleurosigma* spp. W. Smith 1852
34 *Pseudonitzschia multiseries* (Hasle) Hasle 1995
35 *Pseudonitzschia seriata* (Cleve) H. Peragallo in H. and M. Peragallo 1897-1908
36 *Rhizosolenia* spp. Brightwell 1858 (mainly *R. setigera* Brightwell 1858 processes)
37 *Skeletonema costatum* (Greville) Cleve 1878
38 *Skeletonema costatum* (Greville) Cleve 1878 (weak form)
39 *Tabularia fasciculata* (Agardh) Williams and Round 1986
40 *Thalassionema bacillare* (Heiden) Kolbe 1955

TABLE 5.4 (continued)

41	*Thalassionema nitzschioides* (Grunow) Mereschkowsky 1902
42	*Thalassionema pseudonitzschioides* (Schuette and Schrader) Hasle in Hasle and Syvertsen 1996
43	*Thalassiosira angulata* (Gregory) Hasle 1978
44	*Thalassiosira conferta* Hasle in Hasle and Fryxell 1977
45	*Thalassiosira decipiens* (Grunow) Jørgensen 1905
46	*Thalassiosira eccentrica* (Ehrenberg) Cleve 1904
47	*Thalassiosira* cf. *leptopus* (Grunow) Hasle and Fryxell 1977
48	*Thalassiosira minima* Gaarder 1951
49	*Thalassiosira nordenskioeldii* Cleve 1873
50	*Thalassiosira oestrupii* (Ostenfeld) Hasle 1972
51	*Thalassioisra pacifica* Gran and Angst 1931
52	*Thalassiosira rotula* Meunier 1910
53	*Thalassiosira tealata* Takano 1980
54	*Thalassiosira tenera* Proschkina-Lavrenko 1961
55	*Thalassiosira* sp. (cf. *T. tenera* but no marginal processes)

determine the relative significance of each variable in comparison to others. A two-tailed Pearson correlation was performed with Bonferroni adjustment, which reduces the incidence of artificially high significance that occurs when more than six variables are compared. All variables with a non-normal distribution were then transformed using the program Calibrate version 0.70 (Juggins, 1997). Variable CBP was square root transformed, and DL, APS, APT, MB30V, MB300U, and MB30U were log transformed. Variables MB300V and MBT did not require transformation because they had normal distribution.

Sample outliers

Samples were tested for statistical validity by performing principle components analysis (PCA) of environmental variables and detrended correspondence analysis (DCA) of species data (Hall and Smol, 1992). Samples that have sample scores derived from both PCA and DCA falling outside the 95% confidence limits are considered outliers. No outliers were detected in the dataset.

Ordination

DCA was first used to determine the length of the gradient represented by the main direction of variation within the species data. The gradient length was relatively short (1.8 standard deviation units) which represents a linear response model. This means that the species abundances appear to change linearly through short sections of the unimodal environmental gradient, or the samples collected covered only narrow sections

of environmental variation (ter Braak and Prentice, 1988). PCA was then performed but there was a pronounced arch effect (ter Braak, 1986), which signifies an approximately quadratic dependence between the scores of the first two axes and occurs whenever a relatively short gradient is dominated by a longer gradient (Gauch, 1982). Hence, detrended canonical correspondence analysis (DCCA) was used as the final ordination technique.

Before presenting the final ordination, strong "site-environmental influences" (i.e., an influence greater than 8×, which corresponds to a site or sample whose environmental measurement exceeds four standard deviation units from the mean; ter Braak and Smilauer, 1998) were determined to further eliminate anomalous samples or environmental variables. Using DCCA and a global permutation test with 1000 Monte Carlo permutations, two site-environmental pairs were identified with high collinearity: 3B-4 & MB30U, and 3B-6 & MB30U. Variable MB30U ($P = 0.259$) was removed instead of the samples because retaining a continuous set of samples representing diatom assemblages from distinct times during the collection period was more important than keeping the one variable. After MB30U was eliminated, a second DCCA was run and the output analyzed. Following this, variable APT was removed because it was highly correlated to MBT and had a relatively high variable inflation factor (9.3) compared to the other variables (1.4-3.2). APS was also removed because it was highly correlated to both DL and APT (Table 5.5). Additionally, after analyzing the inter-set correlations of environmental variables with the axes, variables MB300U and MB300V were removed

because they were significantly correlated with CBP. For the final ordination, only variables MBT, DL, CBP and MB30V remained.

RESULTS

Observed Environmental Variables

At a latitude of 49° N, there is a noticeable difference in daylength between the seasons. On the summer solstice (June 21), the daylength is 16.2 hours, whereas on the winter solstice (December 21), daylength is only 8.2 hours (Figure 5.3A).

The profiles of sea surface temperatures measured at Amphitrite Point and Meteorological Buoy 46206 are very similar (Table 5.5), except that the temperatures at Amphitrite Point are on average 1–2 degrees lower (Figure 5.3B). Only sea surface temperatures from Meteorological Buoy 46206 are discussed from here on. The temperature reflects the daylength cycle, although there is a 1.5-month lag in temperature (Figure 5.3B). Maximum temperatures occurred in the summer months from mid-July to mid-September, averaging 13.8 °C in 1999 and 13.5 °C in 2000 (n=67). Minimum temperatures occurred from January to March with an average of 8.6 °C (n=89).

The majority of precipitation occurred from October 1999 to April 2000, with a core interval from late October to mid December when precipitation averaged 21.4 mm per day (n=50). A maximum of 83.2 mm was recorded on 1 December 1999. The spring months were drier, averaging 6.1 mm per day (n=93). The summer months experienced even less precipitation but were punctuated by brief precipitation events lasting 1–3 days (Figure 5.3C).

TABLE 5.5. Matrix of sediment trap environmental variables using Pearson correlation and Bonferroni-adjusted significance. Refer to text for explanation of abbreviations.

	DL	APS	APT	CBP	MB300V	MB30V	MBT	MB300U	MB30U
DL	1.000								
APS	**0.708	1.000							
APT	**0.651	**0.687	1.000						
CBP	**-0.602	**-0.681	**-0.617	1.000					
MB300V	**-0.660	**-0.667	*-0.537	**0.627	1.000				
MB30V	-0.127	-0.327	-0.268	0.464	0.258	1.000			
MBT	**0.655	**0.709	**0.929	**-0.675	**-0.556	-0.247	1.000		
MB300U	**-0.606	**-0.611	*-0.494	**0.588	**0.965	0.283	-0.478	1.000	
MB30U	-0.453	*-0.498	-0.455	**0.609	0.412	**0.873	-0.442	0.447	1.000

** very significant ($P < 0.01$)

* significant ($P < 0.05$)

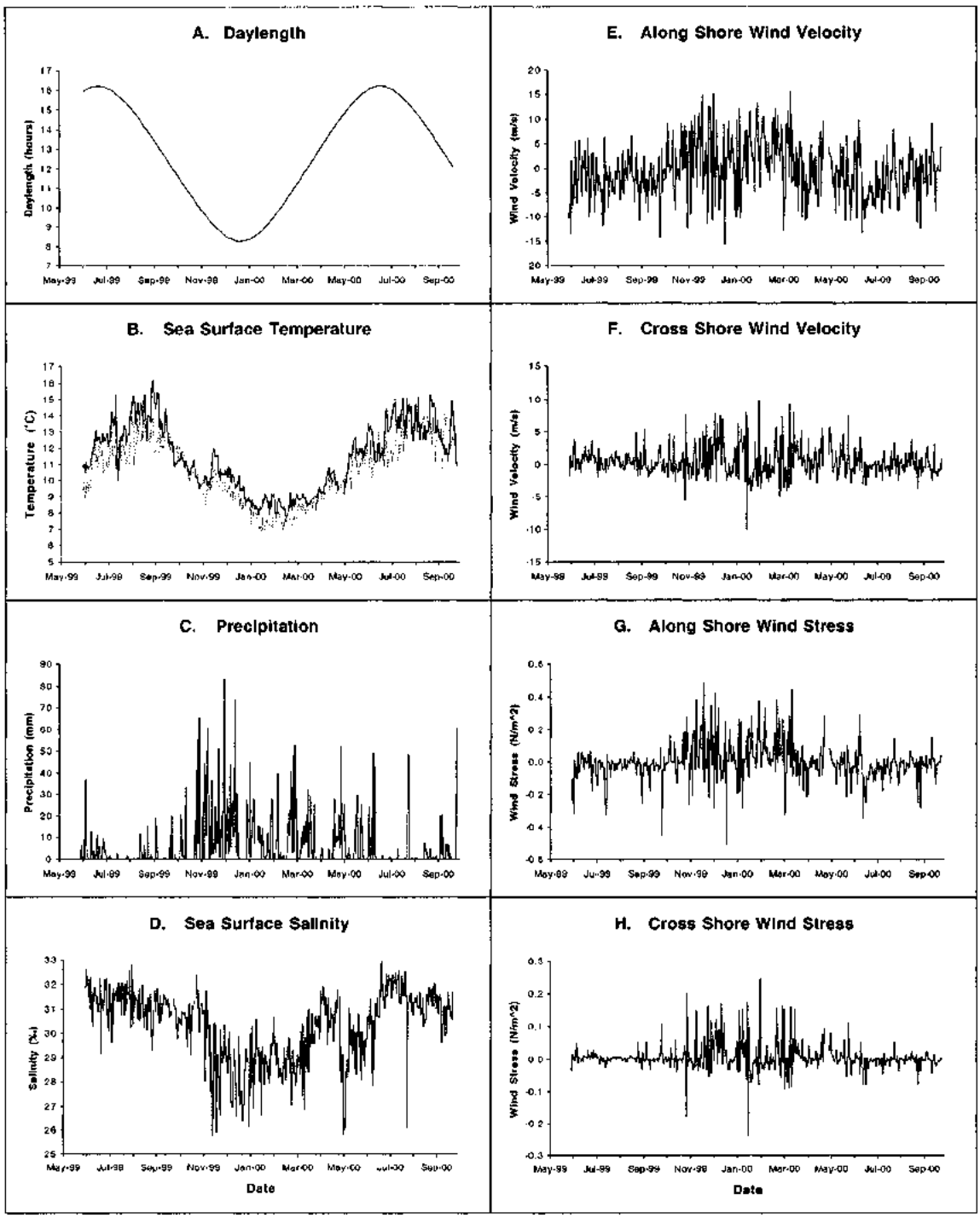

FIGURE 5.3. Profiles of daily environmental records from southwestern Vancouver Island from 29 May 1999 to 28 September 2000. Temperature profile is from Meteorological Buoy 46206 (black line) and Amphitrite Point (grey line). See text for details.

Sea surface salinity is inversely correlated with precipitation (Table 5.5, Figure 5.3C, D). The onset of heavy precipitation in late October 1999 resulted in a marked decrease in salinity at Amphitrite Point. Generally, salinity is lower in the autumn to early spring months, and increases in the spring and summer months when precipitation decreases and evaporation increases. A minimum salinity of 25.8‰ occurred in November 1999, and a maximum of 33.5‰ was reached in June 2000.

The wind velocity profiles are highly variable, but there is a general trend in downwelling and upwelling activity. In the along-shore profile, there is a core of strong (> 10 m/s), positive wind velocities (i.e., blowing towards WNW direction) from mid-October to mid-March, indicating downwelling during the autumn to winter months (Figure 5.3E). Cross-shore velocities are not as strong as along-shore winds, and the positive values extend into early June 2000 (Figure 5.3F). In the spring and summer, positive wind velocity values are lower and there are more negative value incursions (i.e., winds blowing towards ESE direction), indicating more upwelling during these months.

The wind stress profiles are less variable and the seasonal difference between upwelling and downwelling is more pronounced. There is greater variability in wind stress during the mid-October to mid-March period when most of the positive values and downwelling occur. Along-shore wind stress during the spring to summer months shows numerous negative value incursions indicative of upwelling-favourable wind stress (Figure 5.3G). Cross-shore wind stress is nearly negligible during the spring and summer months of both years observed (Figure 5.3H). Because wind stress is derived from wind velocities, these variables are highly correlated (Table 5.5).

Sediment Description

Sediments and supernatant were described from the sample bottles I received from Dr. Bertram. In general, the sediments from series CTC3A, CTC3B, CTC11C, and the first six samples of series CTC3C consist mainly of watery and sparse to thick and soupy, brown to olive green organic-rich mud (Table 5.1). The supernatant was clear to cloudy and ranged in colour from a brown to green tinge. Terrestrial plant debris, such as pieces of leaves, bark, twig, moss, conifer needles, and cedar fronds, were present in a few samples, as were green marine algal filaments. There were also small crustaceans present in some of the samples. Two 10-mm long, unidentified shrimp-like amphipods were found in sample 3B-13. Unidentified amphipods of varying sizes and colours were found in unprocessed samples from the spring and summer of both years at both sites (mainly from CTC3A and CTC11C) (M. Bertram, personal communication, 2002).

Flocculent greenish brown mud was present mainly in the spring and summer samples from both years at both sites, whereas thick, cohesive brown mud with a minor silt component was present mainly in the autumn to early spring samples. Sediment from the spring and summer samples maintained their coherence when the sample bottle was gently moved; the sediment was water-saturated and "fluffy", and the sediment-water interface gently undulated with the movement of the supernatant. However, when the sample bottle was swirled gently the sediment was easily disturbed and mm-size flocs of mud became suspended. Sediment from the autumn and winter samples were more "weighted down" with lithic particles; the sediment was not as water saturated and the

sediment-water interface did not undulate with movement. The cohesive brown mud required more agitation for the sediment to be churned into suspension.

Flux, Abundance and Specific Diversity

Figure 5.4A shows the total mass flux represented in each cylinder. There is a missing sample (what should have been sample 3A-14) due to mechanical failure at the opening date of 21 September 1999. The cylinder collected from 2–14 May 2000 (sample 3B-14) came up open during trap recovery and lead to an anomalously large sample (M. Bertram, personal communication, 2002). Data from this sample must therefore be interpreted with caution. The last 8 samples from series CTC3C (15 May to 28 September 2000) have a very low to almost non-existent mass flux (Table 5.1). The mean mass flux for all inner basin samples (n=41) is 0.62 $g/m^2/day$. For the period of time during which the two trap sites have overlapping samples (16 May 2000 to 28 September 2000, n=14), the mean mass flux is much greater in the mouth of the inlet (1.77 $g/m^2/day$) than in the inner basin flux (0.21 $g/m^2/day$).

In the inner basin, diatom vegetative cells (collectively called diatoms) comprise the greatest proportion of the siliceous phytoplankton assemblage, with a mean flux of 1.37×10^8 valves/m^2/day (n=41), followed by CRS (2.50×10^7 valves/m^2/day), and silicoflagellates (7.31×10^5 skeletons/m^2/day). In the mouth of the inlet, the ranking of phytoplankton is the same, with diatoms as the most abundant (4.74×10^8 valves/m^2/day, n=14), followed by CRS (7.86×10^7 valves/m^2/day) and silicoflagellates (5.28×10^6 skeletons/m^2/day). For the period of time during which the two trap sites have

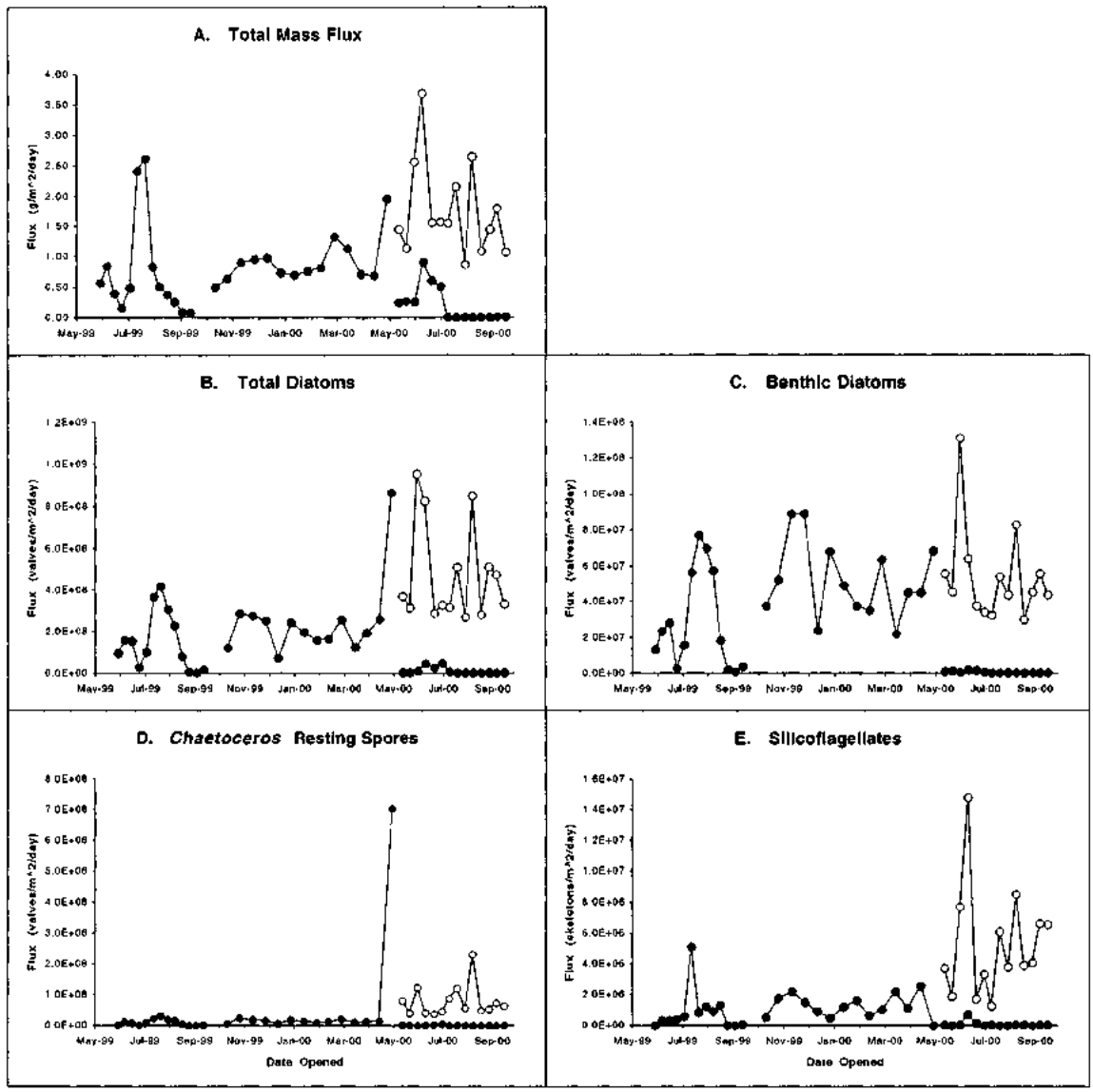

FIGURE 5.4. Flux profiles for total mass, total diatoms, benthic diatoms, CRS and silicoflagellates for the inner basin (●) and the mouth of the inlet (○). Each data point represents a single sample. Total mass flux profile after Bertram et al. (in preparation).

overlapping samples, the mouth of the inlet shows a greater flux of diatoms, CRS and silicoflagellates than the inner basin (Figure 5.4).

Because the phytoplankton fluxes were calculated using the total dry mass from each cylinder, phytoplankton flux profiles tend to resemble the total mass flux profile. In the inner basin, diatom flux maxima occurred from July to August 1999 (3.30×10^8 valves/m^2/d, n=4), and 2–14 May 2000 (8.60×10^8 valves/m^2/d, n=1). CRS flux reached a maximum from 2–14 May 2000 (7.04×10^8 valves/m^2/d), and was composed mainly of the species *C. debilis and C. socialis*. Benthic diatom flux was elevated mainly during the autumn and winter months, from October 1999 to February 2000 (5.67×10^7 valves/m^2/d, n=9), although there is a peak from July to August 1999 (6.54×10^7 valves/m^2/d, n=4). Silicoflagellate fluxes were also elevated during the same autumn to winter months (1.26×10^6 skeletons/m^2/d, n=9), although there is an isolated peak in flux (5.13×10^6 skeletons/m^2/d) on 12 July 1999 that corresponds to a peak in the total mass flux.

In the mouth of the inlet, the flux profiles for total diatoms, benthic diatoms, and silicoflagellates are similar, with maxima from 3–13 June 2000 and 11 August 2000. There is only a single CRS flux maximum of 2.29×10^8 valves/m^2/d for the sample collected from 11–20 August 2000.

A comparison between total mass flux and the absolute abundance of phytoplankton shows similarities and differences (Figure 5.5). In spring and summer 1999, the phytoplankton abundance and flux profiles are more or less similar, although some peaks are offset. For example, a total mass flux peak from 12 July–7 August corresponds to a total diatom abundance minimum at the same time (Figures 5.4B, 5.5A),

and during this time, these samples were enriched with terrigenous organic debris and mud (Table 5.1). The mass flux and phytoplankton abundance profiles are most similar for samples collected for series CTC3B (11 October 1999 to 14 May 2000). The total mass flux and phytoplankton abundance profiles from spring and summer 2000 show a clear inverse relationship. The first six samples of this series contain abundant mud and organic debris and incidentally the phytoplankton abundance is lower (Figures 5.4, 5.5). However, in the last eight samples, which contained trace amounts of mud and had near-negligible total mass fluxes, the phytoplankton abundance was higher. In fact, the total diatom abundance reaches an overall maximum of 7.07×10^8 valves/g for the sample collected from 12–21 July 2000 (Figures 5.4B, 5.5A). Although there was a lack of mud and debris to provide a noticeable total mass flux, the high absolute abundance suggests that the samples were not barren, and that the green tinted water contained a suspension that was likely composed almost entirely of phytoplankton remains (Table 5.1). Mean absolute abundance of phytoplankton in the mouth of the inlet is consistently higher than in the inner basin during overlapping time periods for total diatoms (mouth: 2.69×10^8 valves/g, inner basin: 1.53×10^8), benthic diatoms (mouth: 3.21×10^7, inner basin: 1.37×10^7), CRS (mouth: 4.51×10^7, inner basin 1.24×10^7), and silicoflagellates (mouth: 2.98×10^6, inner basin: 1.33×10^6) (Figure 5.5).

There appears to be an inverse relationship between total mass flux and phytoplankton abundance in the mouth of the inlet, although the pattern is not as pronounced as in the inner basin. For example, samples 11C-3 and 11C-4 (3-22 June) contained relatively abundant mud and a high total mass flux, and the diatom abundance

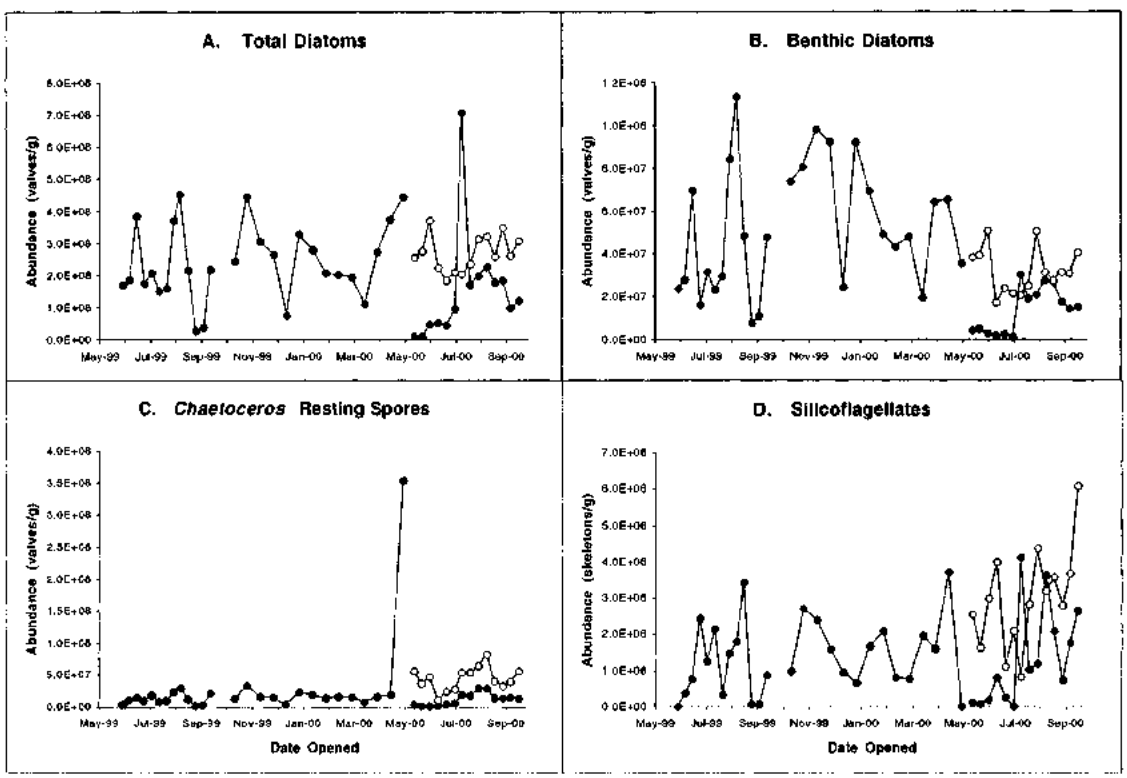

FIGURE 5.5. Absolute abundance per sample of total diatoms, benthic diatoms, *Chaetoceros* resting spores, and silicoflagellates for the inner basin (●) and the mouth of the inlet (○).

is low at this time (Figures 5.4A, 5.5A).

A total of 218 diatom taxa were identified in the inner basin, and 150 diatom taxa in the mouth of the inlet. The total number of diatom taxa at both sites may actually be higher since some of the diatoms were identified only to genus level (e.g., *Delphineis* spp., *Eunotia* spp., *Rhizosolenia* spp.), and *Chaetoceros* spp. were not included. In the inner basin, the specific diversity is greatest during the autumn and winter months (S.D.I. 11.43, n=11), and lower in the spring and summer months (S.D.I.=9.85, n=13, in 1999 and 7.81, n=17, in 2000) (Figure 5.6, Appendix E3). At the mouth of the basin, the mean diversity index is 8.33 (n=17) for the spring and summer of 2000.

Seasonal Variation of Species

Diatoms appear during specific times throughout the collection period: spring (May to mid June) 1999, summer (mid June to mid September) 1999, late summer to early autumn (mid September to November), autumn/winter (November to March), early spring (March to April), spring 2000, and summer 2000. Some diatoms peak in only one or two of these time intervals, while others are present all year round with no seasonal peak. Others still are present year-round but then increase in abundance during specific times of the year (Figures 5.7, 5.8, 5.9). In general, planktonic species and lightly silicified species occur during the spring and summer months, while benthic and more robust species occur during the autumn to winter months.

In spring 1999, the most abundant diatom species, in decreasing order of relative abundance, were *Fragilariopsis atlantica*, *Skeletonema costatum*, *Minidiscus chilensis*,

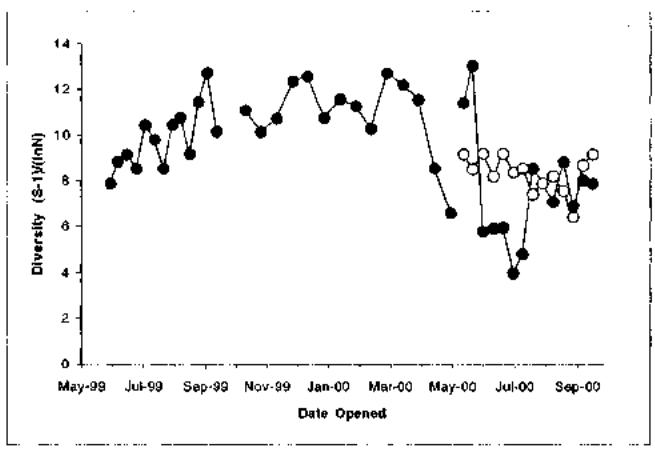

FIGURE 5.6. Specific diversity of diatoms in the inner basin (●) and in the mouth of the inlet (○).

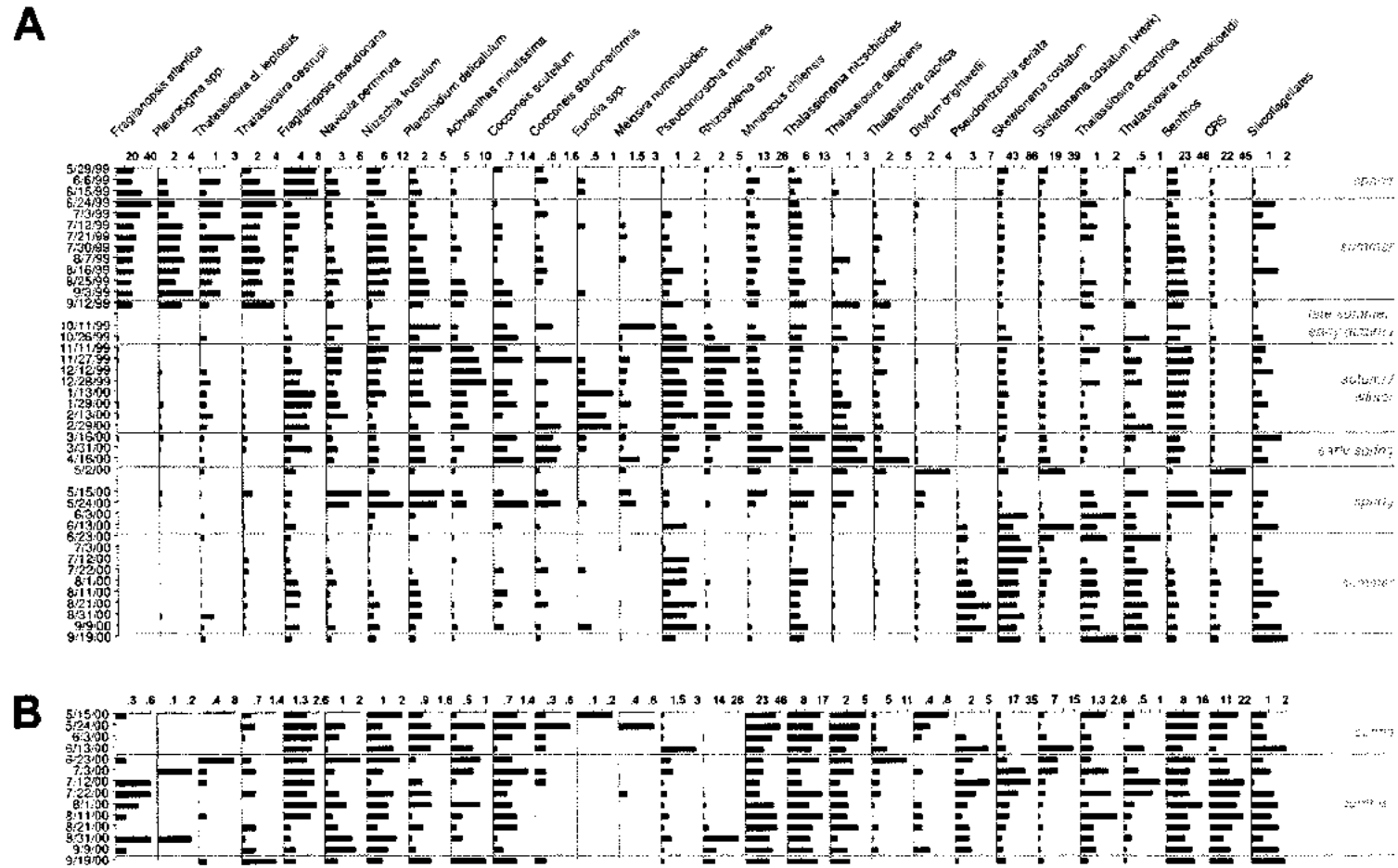

FIGURE 5.7. Relative abundance (%) of selected major diatom taxa, benthic diatoms, CRS and silicoflagellates from the inner basin (**A**) and the mouth of the inlet (**B**). Taxa are arranged so that seasonal patterns are evident. Note that x-axis values for each taxon are different. Y-axis values are sample opening dates (refer to Table 5.1 for equivalent sample labels). See Appendix E4 for data on all major taxa.

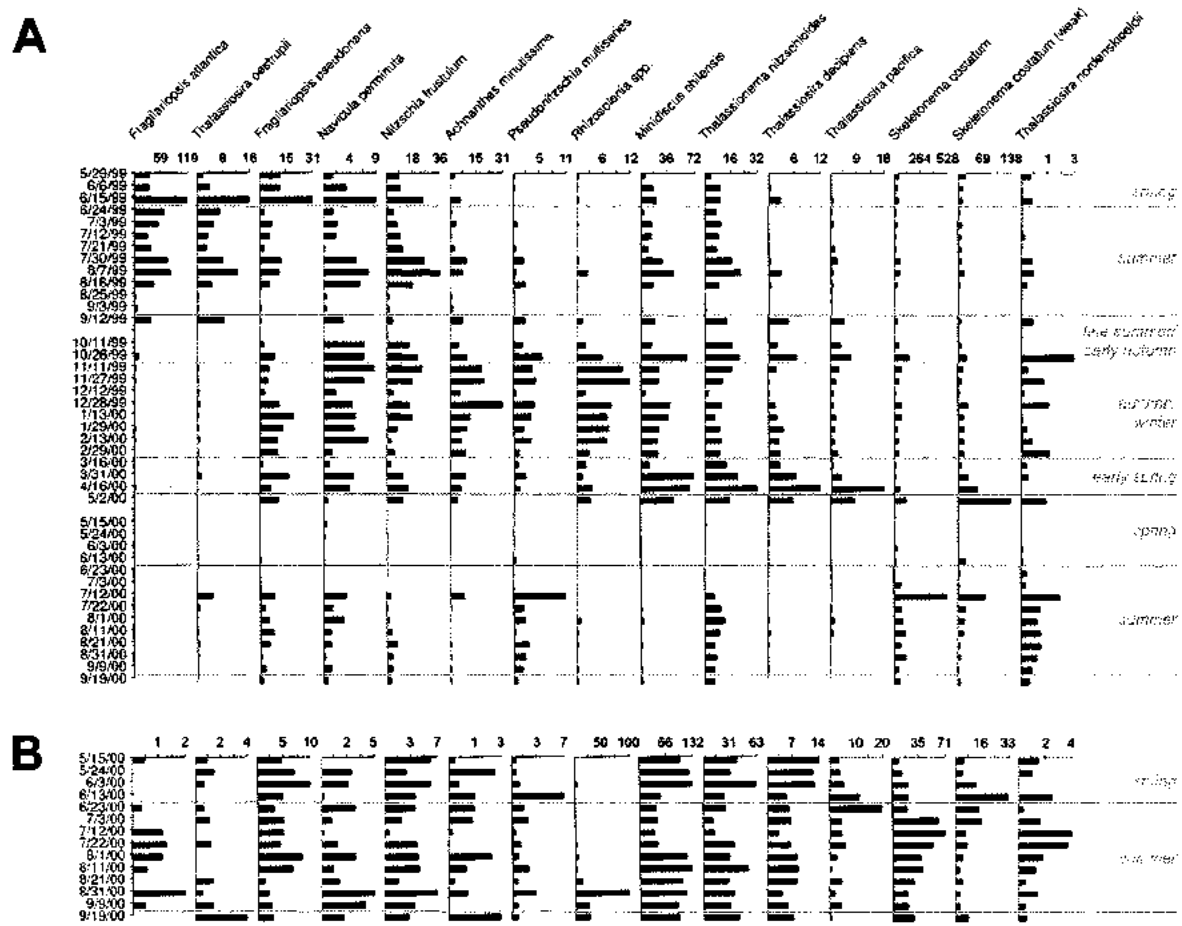

FIGURE 5.8. Absolute abundance ($\times 10^6$ valves/g of dry sediment) of selected major diatom taxa from the inner basin (**A**) and the mouth of the inlet (**B**). Taxa are arranged so that seasonal patterns are evident. Note that x-axis values for each taxon are different. Y-axis values are sample opening dates (refer to Table 5.1 for equivalent sample labels). See Appendix E5 for data on all major taxa.

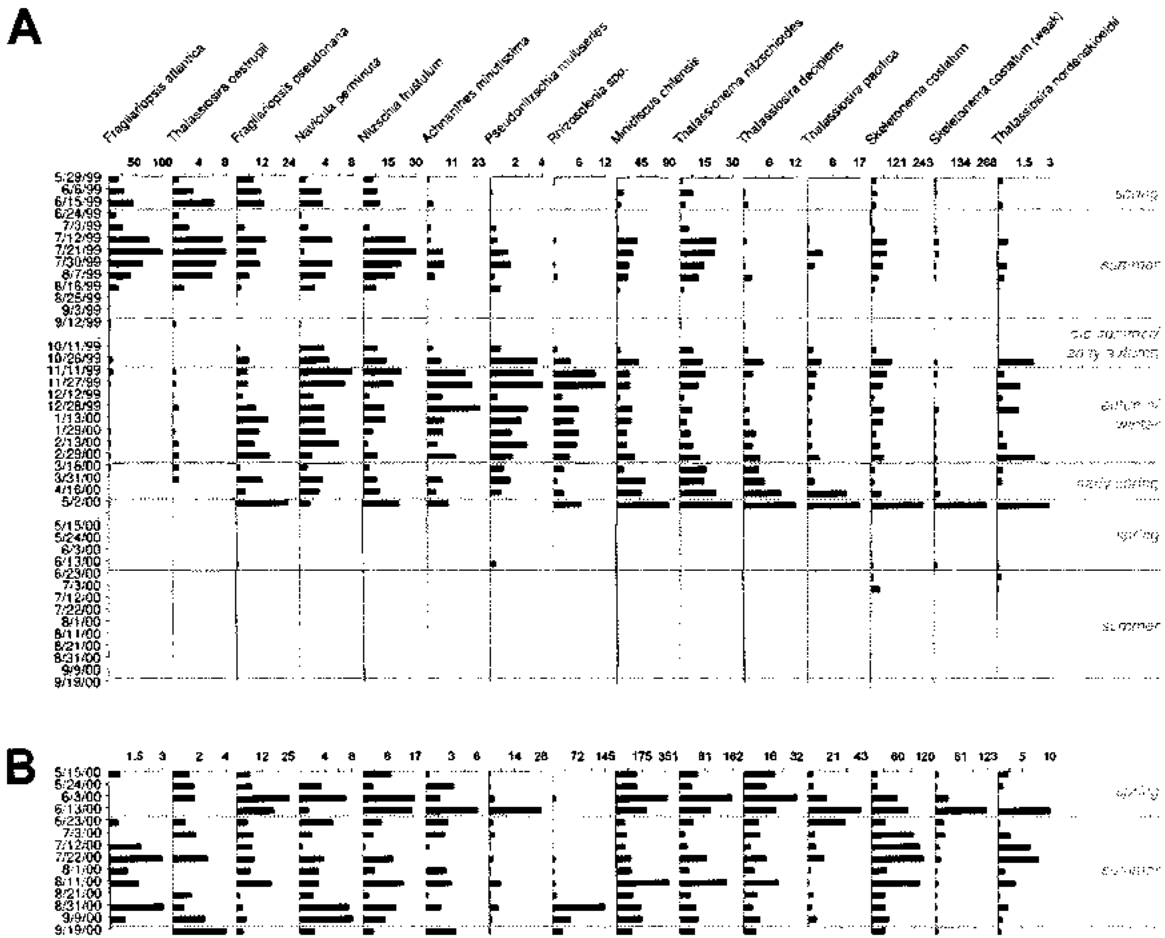

FIGURE 5.9. Flux data ($\times 10^6$ valves/m^2/day) for selected major diatom taxa from the inner basin (**A**) and the mouth of the inlet (**B**). Taxa are arranged so that seasonal patterns are evident. Note that x-axis values for each taxon are different. Y-axis values are sample opening dates (refer to Table 5.1 for equivalent sample labels). See Appendix E6 for data on all major taxa.

and *Fragiliariopsis pseudonana*. Two forms of *S. costatum*, the nominal and robust form, and a smaller and weakly silificied form, were found in all samples throughout the entire collection period. Benthic diatoms peaked at 18.1% of all diatoms counted at this time. CRS ranged from 2–6% of the combined diatom and CRS count. Silicoflagellates were almost non-existent at this time. Preservation of frustules was good.

In summer 1999, *Fragiliariopsis atlantica* was the most abundant taxon, reaching an overall maximum of 40.7%, followed by *S. costatum*, *M. chilensis*, *Nitzschia frustulum*, and *Thalassionema nitzschioides*. Less dominant taxa that appeared in summer 1999 and then all but disappeared from the record include *Actinoptychus vulgaris*, *Pleurosigma* spp., *Thalassiosira conferta*, *Thalassiosira* cf. *leptopus* and *T. oestrupii*. Benthic diatoms increased steadily in relative abundance throughout the summer and peaked at 29.1% near the end of the summer. CRS remained at constant levels between 5–7% throughout this time. Silicoflagellates reached a maximum of 1.6%. Microfossil preservation was moderate to good with minor fracturing of larger (> 25 μm) valves.

In the late summer and early autumn of 1999, dominant taxa were *F. atlantica*, *T. nitzschioides*, *Pleurosigma* spp., *Thalassioisra decipiens*, *T. oestrupii* and *Melosira nummuloides*. Less dominant taxa were *Paralia sulcata* and *Pseudonitzschia multiseries*. The relative abundance of benthic taxa increases slightly to 30.2% at this time. Microfossil preservation was moderate.

Several taxa had maxima in the autumn and winter months. These taxa were *Achnanthes minutissima*, *F. pseudonana*, *Rhizosolenia* spp. (mainly *R. setigera* processes), *Planothidium delicatulum*, *Pseudonitzschia multiseries*, and *Eunotia* spp.

Benthic diatoms reached a maximum during this time, comprising 35% of all diatoms counted. CRS remained constant throughout this time at 5–7%, and silicoflagellates reached a maximum of 1.2% abundance at this time. Microfossil preservation was moderate, although small taxa such as *P. delicatulum* and *F. pseudonana* had good preservation.

Taxa that appeared in early spring 2000 were *M. chilensis*, *T. nitzschioides*, *Thalassiosira pacifica*, and *T. decipiens*. Microfossil preservation was moderate to excellent.

In spring 2000, the dominant taxa included both forms of *S. costatum*, *M. chilensis*, *T. nitzschioides*, *Ditylum brightwellii*, and *A. minutissima*. CRS represented 44.7% of combined diatoms and CRS counted for the sample collected from 2–14 May, with the main species being *C. debilis* and *C. socialis*. There was an isolated peak of benthic diatoms that reached an overall maximum of 46.6% of all diatoms counted for the sample collected from 24 May–2 June. Microfossil preservation was good to excellent. In the mouth of the inlet, the diatom assemblage was dominated by *M. chilensis* (46.6%), followed by *T. nitzschioides*, both forms of *S. costatum*, *T. decipiens*, and *P. seriata*. Benthic diatoms accounted for ~15% of all diatoms counted, CRS comprised 18%, and silicoflagellates peaked at 2%. Microfossil preservation was moderate to good with minor fracturing and dissolution.

In summer 2000 in the inner basin, *S. costatum* (robust and weak forms) dominated the inner basin assemblage by reaching 92% of the diatom taxa counted for the sample collected from 3–11 July. The absolute abundance of *S. costatum* (robust

form) reached an overall maximum of 5.28×10^8 valves/g in the sample collected from 12–21 July. Other important taxa were *Pseudonitzschia seriata*, *P. multiseries T. nitzschioides*, *F. pseudonana*, *Thalassiosira eccentrica*, and *T. nordenskioeldii*. Benthic diatoms reached an abundance of 15.1%, and CRS were reduced to a constant 9–14%. Microfossil preservation was moderate to good. In the mouth of the inlet, dominant diatom taxa included *M. chilensis* (42.5%), both forms of *S. costatum*, *Rhizosolenia* spp. (mainly *R. setigera* processes), *T. nitzschioides*, and *T. pacifica*. Benthic diatoms reached 16.2%, and CRS reached 21.3% during this time. Microfossil preservation was moderate with minor fracturing of larger valves and lightly silicified taxa. Small diatoms such as *M. chilensis* had good preservation.

Species Assemblages and Environmental Variables

The first four DCCA axes explained 42% of the variance in the diatom data, and the environmental data explained 83% (axis 1) of this variation (Table 5.6). The first three axes are the most important, explaining 18.4% of the variance, because the data along these axes were constrained to the environmental variables. Axis 4 (23.6%) was less important because the data along this axis were not constrained to the environmental variables, resulting in a zero species-environmental value on this axis (Table 5.6). Axis 4 has a higher eigenvalue because the data are not constrained and therefore are explaining other variability present in the data.

Variables DL, APS, APT, CBP, MB300V, MB300U, MB30U and MBT are highly correlated with the first axis (Figure 5.10A). Variable MB30V is correlated with

TABLE 5.6. Summary of statistics for the first four axes of a detrended canonical correspondence analysis performed on species-environment data from the inner basin of Effingham Inlet

	Axis 1	Axis 2	Axis 3	Axis 4
Eigenvalues	0.107	0.060	0.017	0.236
Species-environment correlations	0.832	0.479	0.656	0.000

the second axis. Variables DL, APT, APS, and MBT are grouped together and point toward the left side of the diagram. This is sensible as these variables are positively correlated (Table 5.5; Figure 5.3A, B, D). Variables CBP, MB300V, MB300U and MB30U also form a group of positively correlated variables but this group points in the opposite direction because these variables are negatively correlated to the first group (Table 5.5). Hence, the left side of the DCCA ordination diagram shows a preference for longer daylength, higher sea surface temperatures and higher sea surface salinities, indicative of summer conditions, whereas the right side shows a preference for higher precipitation, and positive along-shore and cross-shore wind velocity and stress (i.e., downwelling activity) which is indicative of winter conditions.

The positions of the plotted samples and species on the final ordination diagram give a qualitative indication of their environmental optima. Samples from series CTC3A and most of the samples from series CTC3C (except for 3C-1, 2, and 13) are grouped on the left side of the diagram (Figure 5.10B). This is expected since these samples were collected during the spring and summer months. Samples from series CTC3B are grouped on the right side of the diagram because these samples were collected during the autumn and winter months. Samples 3B-1 and 3C-1, 2, and 13 fall closer to the center of the diagram because these samples were collected during seasonal transitions. Samples from series CTC11 (mouth of inlet) plot mainly on the far lower right side of the diagram even though these samples were taken in the spring and summer of 2000. This is likely because the species assemblages from the mouth of the inlet differ from the inner basin and therefore are not adequately represented on a plot derived for inner basin

FIGURE 5.10. DCCA ordination diagrams for sediment trap studies. **A.** Positions of environmental variables before data screening. Solid arrows represent active variables; dashed arrows indicate variables that were removed after screening. **B.** Sample distribution. Samples from series 11C were plotted passively. Numbers beside data points represent sample numbers from each series. Refer to Table 5.1 for opening dates of samples. **C.** Diatom distribution. See Table 5.4 for explanation of code numbers beside data points. Large numbers beside ellipses denote assemblage groups. See text for details.

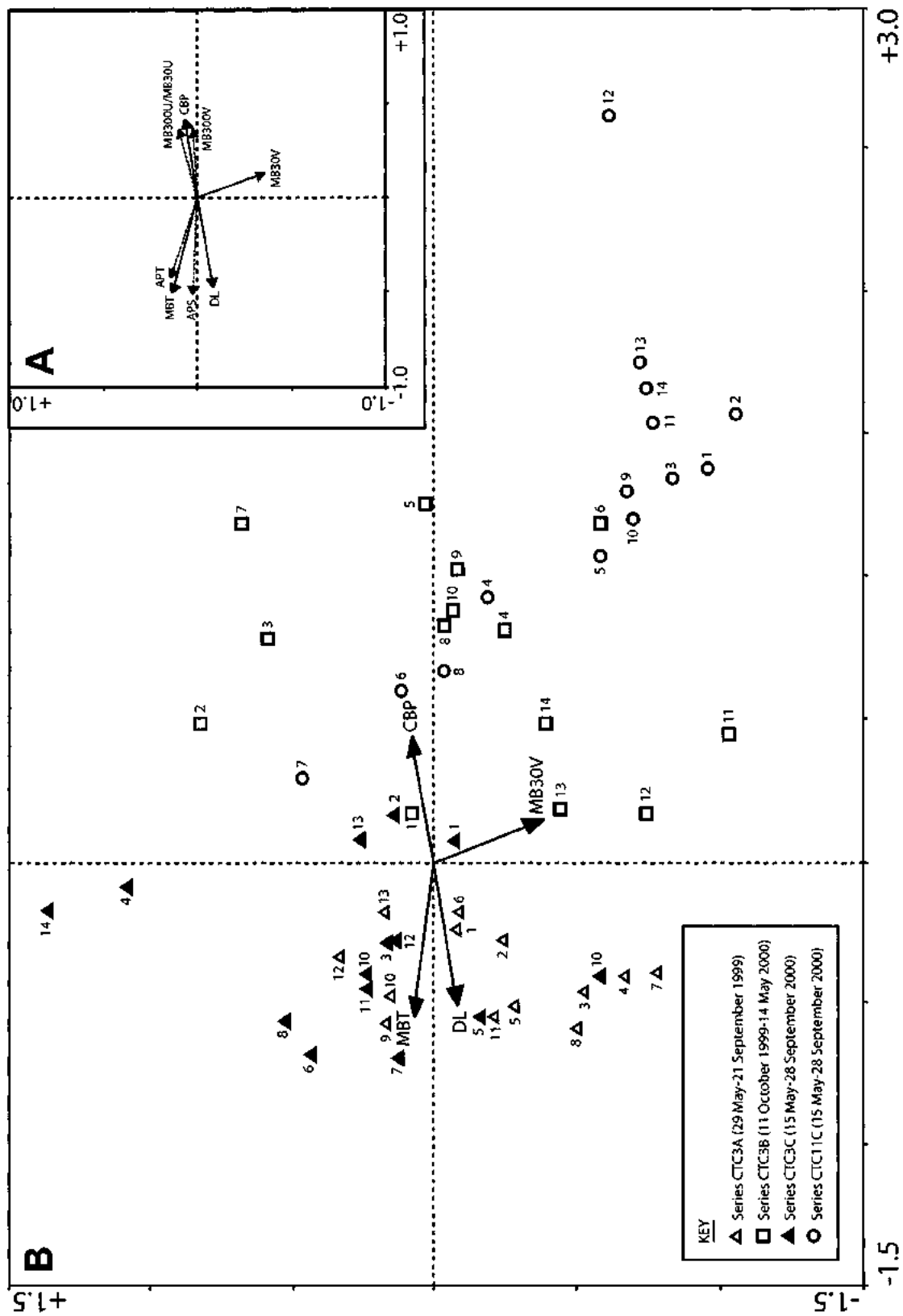
A
+1.0
-1.0
MB30OU/MB30U
CBP
MB30OV
MB30V
APT
MBT
APS
DL
B
+3.0
-1.5
+1.5
CBP
MB30V
MBT
DL
KEY
Series CTC3A (29 May-21 September 1999)
Series CTC3B (11 October 1999-14 May 2000)
Series CTC3C (15 May-28 September 2000)
Series CTC11C (15 May-28 September 2000)

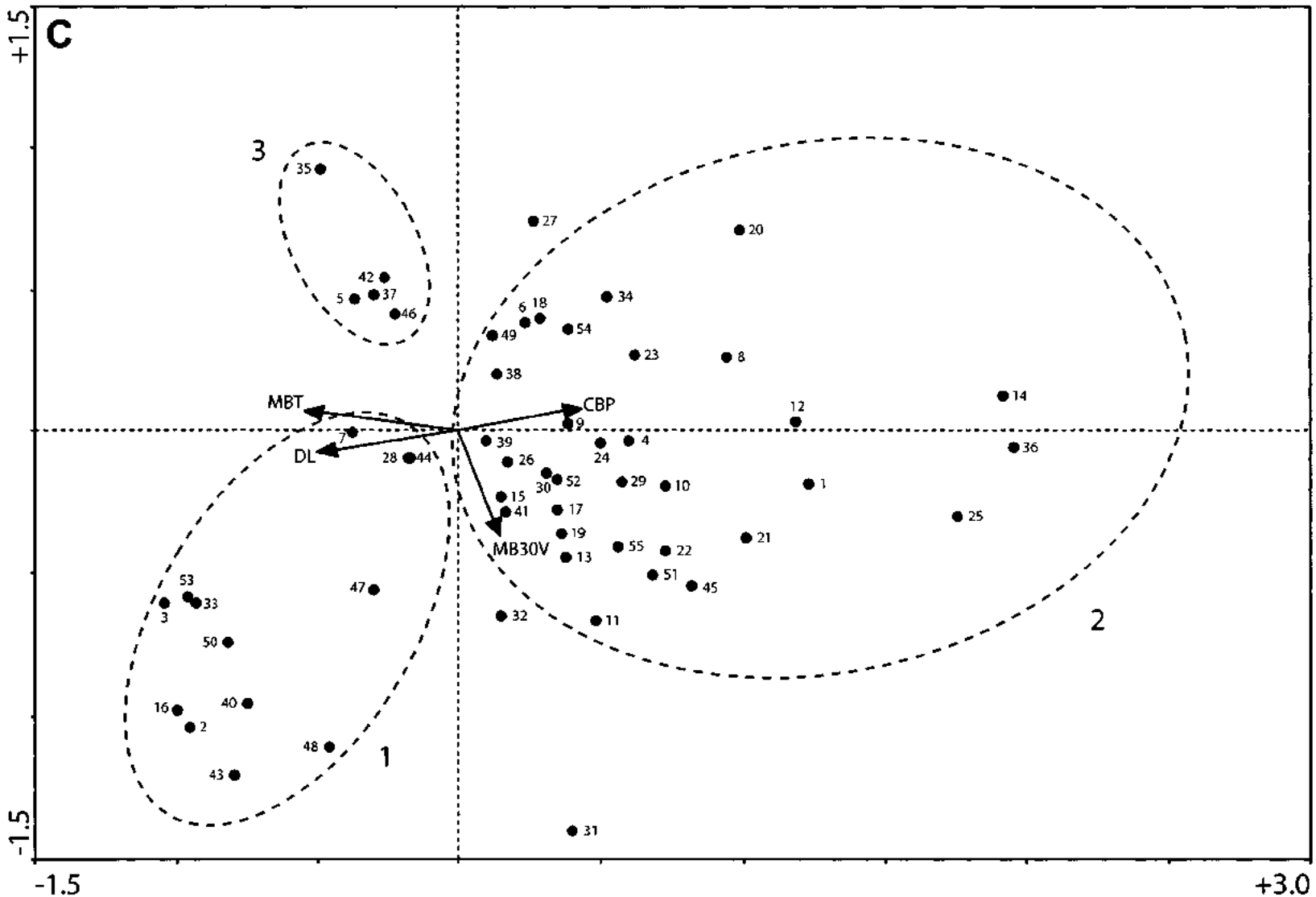
C
+1.5
-1.5
-1.5
+3.0
MBT
CBP
DL
MB30V
1
2
3
35
27
20
42
5
37
46
6
18
34
49
54
23
8
38
14
12
7
9
39
4
36
28
44
24
26
30
52
29
10
1
15
41
17
25
19
21
55
22
13
51
45
53
47
33
3
32
11
50
16
40
2
48
43
31

assemblages only.

There are three distinct groups of taxa on the ordination diagram (Figure 5.10C). Taxa in Group 1, such as *Fragilariopsis atlantica* (16), *Thalassiosira* cf. *leptopus* (47), *Thalassiosira oestrupii* (50) and *Thalassionema hacillare* (40), were abundant on relatively long days with warm temperatures and high salinities, low precipitation and strong upwelling. These taxa all had relative abundance maxima during the spring and summer of 1999 after which they became virtually absent from the inner basin sediment trap record (Figure 5.7). Taxa in Group 2, such as *Gomphonemenopsis obscurum* (19), *Minidiscus chilensis* (22), *Navicula gregaria* (23), *Paralia sulcata* (29), *Skeletonema costatum* (weak form, 38) and *Thalassiosira nordenskioeldii* (49), were abundant on relatively short days with cool water temperatures, strong positive along-shore and cross-shore winds (downwelling), and high precipitation. Incidentally, these taxa appeared mainly in the autumn, winter and early spring months during the collection period. Taxa in Group 3, which include *Bacteriastrum delicatulum* (5), *Pseudonitzschia seriata* (34), *Skeletonema costatum* (robust form, 37), *Thalassionema pseudonitzschia* (42) and *Thalassiosira eccentrica* (46), were abundant on moderately long days with moderate temperatures and salinities, low precipitation and good upwelling activity. These species mainly had relative abundance maxima during the early spring to summer months of the year 2000 (Figure 5.7). This group differs from Group 1 in that it favors relatively strong negative cross-shore wind velocities (indicative of upwelling). Taxa appearing near the origin of the ordination diagram occurred either sporadically or consistently throughout the year, or had multiple seasonal maxima (Figure 5.7, Figure 5.10C).

DISCUSSION

The appearance and abundance of diatoms and other microfossils in Effingham Inlet varies both temporally and spatially. A comparison of the sediment trap results to the thin section analyses in Chapter 4 indicates that the seasonal succession of diatoms is present, especially in the complete inner basin record. As with the thin sections, the most abundant diatoms in the sediments traps were *Skeletonema costatum*, *Thalassiosira* spp. and CRS. However, numerically important diatoms such as *Minidiscus chilensis* or *Achnanthes minutissima* were not detected in the thin sections not because they were absent, but because of the small size of these diatoms and because the thin sections were examined at 400× magnification. These small and lightly silicified diatoms do eventually become preserved in the sediments as they were subsequently noted in quantitative analyses of core samples (Chapters 6 and 7; see also Hay et al., 2003). Silicoflagellates did not appear to have an affinity for any time interval throughout the collection period, unlike in thin section analyses where silicoflagellates were associated with autumn and winter laminae. It is likely that not enough silicoflagellates were counted for trends to be detected.

Flux, Abundance and Preservation

Geochemical analyses from both Baker and OSU traps indicate that the organic matter content from the OSU traps is 2–4% more than in the Baker traps and that organic content in the OSU traps is coupled with the total mass flux (M. Bertram, personal commincation, 2003). One explanation for this is that the collection area of the OSU traps

is much larger than the Baker traps, permitting large organic objects such as leaves and twigs to enter the cylinders at any time of the year, adding to the total mass flux (M. Bertram, personal communication, 2003). Alternatively, the OSU traps were moored closer to the inlet bottom and may have recorded a signal of resuspended, organic-rich bottom sediments that the more shallow Baker traps did not experience (e.g., Dymond, 1984; Hedges et al., 1988), or that lateral advection of particles occurred (Deuser et al., 1988; Sancetta, 1990). However, $\delta^{13}C$ and $\delta^{15}N$ analyses from the OSU traps indicate separate seasonal groups of organic matter compositions, indicating that resuspension of bottom sediments is not a controlling factor of organic matter in the traps throughout the collection period (M. Bertram, personal communication, 2003). Resuspension of bottom sediments may still have occured intermittently throughout the year, or during extraordinary oceanographic events.

The large sample collected from 2–14 May 2000 (3B-14) may be an anomaly because the cylinder came up open upon recovery. Because the mechanical trigger for closing the cylinder failed, the open cylinder collected additional material as it came up through the water column during recovery. The timing of the mechanical failure is unfortunate because it is uncertain as to whether the dramatic increases in *Skeletonema costatum* and CRS are due to actual blooms that would normally occur at this time in the spring (Taylor and Haigh, 1996), or due to the open cylinder being dragged up through the water column. Judging from the flux and absolute abundance estimates of other samples, it is likely that the large *S. costatum* and *Chaetoceros* peaks do not represent real maxima because the flux and absolute abundance immediately before and after the

peak are relatively low. This being said, an actual peak may still have existed from 2–14 May 2000 but the true magnitude is not known. The near-monospecific nature of this sample (low S.D.I.) suggests that a bloom did take place during this time. Additionally, the Baker trap indicated a mid-April peak in total mass flux and biogenic silica, indicating that a mid-April to early May spring bloom most likely took place (Bertram et al., in preparation).

The mouth of the inlet experienced a higher total mass flux and greater mean absolute abundance of phytoplankton than the inner basin from the late spring to summer of 2000 when the two traps had concurrent samples. At the mouth of the inlet, the collected material consisted mainly of flocculent greenish brown mud, which contributed to the high total mass and phytoplankton fluxes, whereas in the inner basin there were trace amounts of sediment and mainly greenish coloured water, which contributed to the low total mass flux but high phytoplankton flux. Timothy and Soon (2001) found that primary production in Saanich and Jervis inlets was 1.4 times greater at sampling locations in the mouths of both inlets than in more landward locations. The authors attribute the increase in flux to the presence of biological fronts, where surface waters are enriched with nutrients immediately outside the inlet mouths due to upwelling into Juan de Fuca and Haro straits. For primary production to occur in Effingham Inlet, it is not difficult to imagine a biological front developing within Barkley Sound or immediately outside the sound during upwelling of nutrient rich waters over the Vancouver Island shelf break (Chapter 2). Unlike in mainland inlets, where summer stratification sets in and diatom production falls, persistent offshore upwelling and onshore advection into

Barkley Sound throughout the summer leads to an extended diatom growing season (Ikeda and Emery, 1984; Taylor and Haigh, 1996). As a result, the shelf zone is characterized throughout the summer by high levels of dissolved nutrients and phytoplankton production (Denman et al., 1981). Therefore it is not surprising that the mouth of the inlet experiences more production than the inner basin. Additionally, the inner basin is more restricted and probably experiences less penetration of nutrient-rich surface waters, and the quiescent nature of the inner basin leads to the formation of stratified waters during the summer. Lateral transport of sediments, resuspension of bottom sediments (Sancetta, 1989b), or the interaction between bottom topography and currents within the more open mouth of the inlet may also contribute additional material to the sediment trap at the mouth of the inlet. The higher sediment accumulation rate, derived from core material, in the outer basin record (~5.5 mm/yr) versus the inner basin rate (~2.2 mm/yr) attests to the higher flux of material in more seaward locations (Chapter 4; Dallimore, 2001).

Diatoms within the sediment record (i.e., surface and core samples) are found to be more abundant in the inner basin than in the outer basin or in the seaward side of the outer sill (M. Hay, unpublished core data; Hay et al., 2003, figure 2). Several physio-chemical processes may be affecting the diatoms from the time they are sinking through the water column to the time they are incorporated and preserved in the sediments. The different environments and oceanographic regimes of the inner basin and the mouth of the inlet have a direct influence on the preservation potential of the diatoms, and even the types of diatoms in the assemblage will affect the overall abundance. For example, the

assemblage in the mouth of the inlet contains more lightly silicified taxa, such as *Thalassiosira nordenskioeldii*, *Minidiscus chilensis* and the weak form of *Skeletonema costatum* than concurrent samples from the inner basin. However, these taxa are highly susceptible to dissolution, and the effects of dissolution were observed more often on *T. nordenskioeldii* valves from the mouth of the inlet. Hay et al. (2003) found that diatom assemblages in stations seaward from the inner basin were similarly affected by dissolution. In addition, the outer basin and the mouth of the inlet experience more frequent oxygen turnovers of the water column, by intrusion of oxygenated waters along the inlet bottom, as is evident from the poorly laminated fabric of the sediment when compared to the laminae from the inner basin (Dallimore, 2001). Oxygenation of the bottom waters leads to increased bioturbation of the sediments by benthic organisms, resulting in mechanical breakage of lightly silicified diatoms (McMinn, 1995). This in turn can lead to a greater proportion of diatoms being destroyed within the sediment column in the mouth of the inlet, and the subsequent observed decrease in absolute abundance in the core material. Hence, persistent anoxia and the quiescent waters of the inner basin lead to the better preservation of lightly silicified diatoms and a relative increase in overall absolute abundance once the diatoms are incorporated into the sediments. The preservation potential and abundance of diatoms within sediments is discussed further in Chapters 6 and 7.

Changes in preservation status of diatoms throughout the collection period were too subtle to discern any seasonal trends with respect to zooplankton grazing. The presence of unidentified amphipods found in spring and summer samples from both trap

sites suggests that grazing likely took place in the upper water column. A variety of zooplankton species have been found to cluster geographically and temporally with increased phytoplankton abundances over La Perouse Bank in summertime studies (Mackas and Sefton, 1982). It is possible that zooplankton communities can migrate into Effingham Inlet to graze, perhaps more so in the accessible inlet mouth than in the restricted inner basin. Further sampling would be required to delineate the timing and grazing activities of zooplankton and which species are present inside the inlet.

Temporal Variations in Diatom Assemblages

The diatom taxa listed in Table 5.4 are similar to those found in other British Columbia fjords. The seasonal succession of taxa in Effingham Inlet is similar to that in BC fjords and other temperate coastal waters such as the Skagerrak (Lange et al., 1992) and Narragansett Bay (Karentz and Smayda, 1984) where the *Thalassiosira-Chaetoceros-Skeletonema* sequence dominates the spring and summer blooms.

The only taxon that seems atypical of BC fjords is *Fragilariopsis atlantica*. The appearance of *F. atlantica* in Effingham Inlet in summer 1999 is unexpected because of its dominant abundance (40.7%) and because it is not mentioned in any of the literature for British Columbia fjords. This diatom is present in the sediments only in low abundance (< 2%; Chapters 6 and 7; M. Hay, unpublished data), suggesting that *F. atlantica* is not a taxon that appears regularly in this region. Other diatoms that appeared mainly in summer 1999 samples were *Pleurosigma* spp., *Thalassiosira* cf. *leptosus* and *Thalassiosira oestrupii*, but did not reappear in summer 2000. The appearance of these

diatoms, along with *F. atlantica*, may be related to the June 1999 oxygenation event that affected the entire inlet (Chapter 2; A. Dallimore and M. Bertram, personal communication, 2002). During June 1999, there was significant rainfall (up to 36 mm) and strong enough northerly winds (5–13 m/s) to favor upwelling and breaching of the sills (Figure 5.3). The intrusion of nutrient-rich, oxygenated upwelled waters may have introduced these taxa to the inlet from outside sources, or may have set up conditions within the inlet conducive to the growth of these taxa. The elevated abundance of benthic diatoms in summer 1999 in the inner basin may also be a result of the June 1999 oxygenation event and associated meteorological conditions. Benthics may have been washed into the basin via the increased precipititation during this time, or may have been resuspended from bottom sediments as the bottom-hugging oxygenated waters entered the inlet. Even so, the current meters did not detect any measurable current in the inlet throughout the collection period, or any increase in bottom water velocity during the oxygenation event (M. Bertram, personal communication, 2002).

The late summer and early fall 1999 assemblage in the inner basin is not dominated by any blooms and the diversity is relatively high (Figure 5.6, Appendix E3). This assemblage, containing a mixture of large and small diatoms of various species is typical of Stage III conditions described by Margelef (1958) and Guillard and Kilham (1977), and signifies stratified water conditions. Density profiles show the upper surface waters over the inner basin becoming stratified in September and October 1999 (Figure 2.7).

Approximately 35% of the diatoms counted in the autumn and winter assemblages in the inner basin were benthic such as the brackish water taxa *Achnanthes minutissima* and *Planothidium* spp., and the marine benthic taxa *Cocconeis scutellum* and *Cocconeis stauroneiformis*. According to environmental records, sea surface temperature dipped by 1 °C at the end of October and beginning of November, accompanied by increased positive wind velocity, wind stress, and precipitation (Figure 5.3). This onset of winter storm activity and increased precipitation can dislodge benthic taxa from shallow substrates and subsequently wash them into the center of the inner basin by runoff. Additionally, riverine runoff through tidal marshes at the head of the inlet during increased precipitation can wash in freshwater and brackish taxa into the inner basin during the autumn and winter. These conditions indicate that benthic input during the autumn and winter months came from above the sediment traps, and not as a result of resuspended bottom sediments.

Taxa such as *Rhizosolenia* spp. and *Pseudonitzschia multiseries* had abundance maxima during the autumn and winter and likely represent pelagic intrusions from outside the inlet (Mackas and Sefton, 1982; Sancetta, 1989a; Taylor and Haigh, 1996). However, these authors describe the abundance of these taxa occurring mainly during the late summer or autumn in Saanich Inlet and Barkley Sound.

Early spring production began in mid March 2000 with the elevated abundance of species such as *Thalassiosira decipiens*, *T. pacifica*, *Skeletonema costatum*, *Thalassionema nitzschioides* and *Minidiscus chilensis*. Sea surface temperatures at this time were 8–9 °C. This assemblage is typical of Stage Ia described by Guillard and

Kilham (1977) with the exception of the occurrence of *T. nitzschioides*. In Saanich Inlet, *M. chilensis*, along with *T. nordenskioeldii* or *T. pacifica*, were major constituents of the March-April spring bloom (Sancetta, 1989a).

The spring bloom in Effingham Inlet appeared to truly take off at the end of April 2000 to the beginning of May 2000, when water temperatures were 9–10 ˚C and the absolute abundance of total *S. costatum* and CRS increased dramatically (Figures 5.8, 5.9). Again, these data must be interpreted with caution because the sample in which this dramatic increase takes place came up open (sample 3B-14). However, if both abundance and flux data are disregarded, and only the relative abundance data are examined (Figure 5.7), *S. costatum* and CRS still have dramatic increases at the beginning of May and the assemblage resembles Stage Ib of the seasonal succession. If the assemblage represents the true proportions of the diatoms at the time, even if the cylinder was dragged up through the water column during recovery, then the observations in Effingham Inlet corroborates the findings of Taylor and Haigh (1996) who found that the spring bloom of diatoms in Barkley Sound began in May and consisted mainly of *S. costatum*.

The relative abundance profile (Figure 5.7) shows additional increased spring abundance in the last two weeks of May, with elevated benthic abundance. This relative increase in benthic taxa in the inner basin may be attributable to a late-April to early May precipitation event—and a subsequent decrease in sea surface salinity about a week afterward (Figure 5.3)—which could have washed in benthic taxa from the margins of the inlet.

The summer 2000 inner basin assemblage was characterized by a secondary bloom from 12–21 July and was dominated by the robust form of *S. costatum*. Secondary blooms have been observed in Saanich Inlet in the summer and autumn and are attributable to a breakdown in summer stratification where new nutrients are introduced to the surface waters via mixing and light levels are still high enough to promote primary production (Sancetta, 1989a; Takahashi et al., 1977). Indeed, discrete near-monospecific laminae containing bloom species such as *S. costatum* were found situated between mixed species laminae and silty diatomaceous laminae from thin sections, indicating that a similar breakdown in stratification can occur in the inner basin of Effingham Inlet (Chapter 4). Harrison et al. (1983) and Haigh et al. (1992) found that summer blooms can be initiated in the Strait of Georgia after the primary spring bloom has waned from the exhaustion of nutrients, providing that some trigger, such as wind or storms, disturbs the stratification and permits nutrients to come to the surface. The environmental profiles show that in mid-July 2000 there was a 2–3 day pulse of precipitation and moderate wind velocities (7–10 m/s) that may have been enough to mix the surface waters (Figure 5.3). The diatom assemblage at this time resembles Stage II of the seasonal succession.

Spatial Variations in Diatom Assemblages

The sediment trap records for the inner basin and the mouth of the inlet overlap in spring and summer 2000. During this time, the diatom assemblages for both sites differ substantially, with the samples at the mouth of the inlet recording predominantly oceanic assemblages with the higher relative abundance of *T. nitzschioides*, *Pseudonitzschia*

multiseries and *Rhizosolenia* spp. For example, *Rhizosolenia* spp. feature prominently (28% relative abundance) at the end of the summer in the mouth of the inlet. It is highly likely that *Rhizosolenia* spp. was advected into the inlet at this time. Taylor and Haigh (1996) found that persistent offshore upwelling coupled with advection onshore created conditions favorable for increase abundances of *Rhizosolenia* spp. and other diatoms during the summer in Barkley Sound. The persistent occurrence of CRS, *Thalassionema nitzschioides*, *Minidiscus chilensis*, and *Thalassiosira decipiens* throughout spring and summer 2000 in the mouth of the inlet may be explained in the same manner. Conversely, there may also be a resident seed population of these diatoms in the mouth of the inlet, where persistent upwelling and nutrient delivery can lead to prolonged diatom blooms throughout the summer.

The consistently higher relative abundance of benthic diatoms in the mouth of the inlet at the end of summer 2000 is puzzling, since there are no marshes or freshwater sources flowing into this part of the inlet. It is highly likely that this increase in benthic species does not represent *in situ* production. Lateral advection of sediment and benthic species living on the outer sill into the mouth of the inlet may be the source of increased benthic diatoms content (cf. Sancetta, 1989a). In surface sediment studies of Effingham Inlet, the relative abundance of benthic diatoms was found to increase at sampling stations atop the inner sill and on stations seaward of the outer sill (Hay et al., 2003).

Environmental Influence on Species Assemblages

From DCCA ordination, daylength, sea surface temperature and precipitation play a major role in determining the placement of the taxa since most of the taxa are correlated with the first axis. The taxa appearing in Group 2 of the ordination represent an autumn to early spring assemblage (Figure 5.10C). Although some of these taxa may not be cool-water taxa *per se* or represent *in situ* production, there are freshwater, brackish water, and benthic taxa that could have been washed into the inner basin from rivers or off the sides of the inlet during the more frequent occurrence of storms during the autumn and winter, and snowmelt during the early spring (cf. Sancetta and Calvert, 1988). The appearance of pelagic oceanic taxa, such as *Rhizosolenia* spp., and *Pseudonitzschia multiseries* may represent the advection of these colder water taxa from offshore sites into the inlet as mentioned before. Finally, *Thalassiosira* spp., such as *T. nordenskioedii*, are known to have an affinity for cool-water (1–5 °C) conditions (Guillard and Kilham, 1977; Waite et al., 1992).

The taxa in groups 1 and 3 of the ordination occur during the spring and summer when upwelling brings nutrients into the inlet and wind-induced mixing of the surface waters lead to the breakdown of stratification. Sea surface temperatures were higher (~9–15 °C, Figure 5.3), and diatoms such as *Skeletonema costatum* proliferated. *S. costatum* appears to prefer semi-enclosed waters and warmer (10–15 °C) temperatures, and are not prevalent in oceanic environments (Smayda, 1957; Sancetta, 1989a). These reasons may explain why *S. costatum* is such a dominant species in a restricted fjord such as Effingham Inlet. The separation between taxa in groups 1 and 3 may be explained by

the June 1999 oxygenation event, where the taxa in Group 1 represent an anomalous assemblage. Hence, the assemblage in Group 3 may reflect a normal spring/summer assemblage.

Provenance of Diatoms

It is highly likely that diatoms such as *Thalassiosira pacifica, T. decipiens, T. nordenskioeldii, S. costatum, Thalassionema nitzschioides, Paralia sulcata* and some species of CRS are indigenous to Effingham Inlet because of their constant occurrence during the entire sampling interval. In addition, these taxa were observed year after year in laminae from thin section analyses (Chapter 4), and in core material throughout the late Holocene. This indicates that there is a resident seeding population of these and perhaps many other taxa within the inlet (Hjort and Gran, 1900; Sancetta, 1989a). The reason that any of these taxa could not be allochthonous is because the probability of the same taxa being introduced from outside the inlet at the same time of year each year is remote (Sancetta, 1989a).

Taylor and Haigh (1992) and Mackas and Sefton (1982) indicate that diatoms such as *Chaetoceros debilis, C. radicans*, and *Pseudonitzschia multiseries* can be advected from cooler offshore waters into Barkley Sound during the summer, although these taxa do not necessarily appear year after year. *Fragilariopsis atlantica* and other taxa found exclusively in summer 1999 are likely allochthonous for similar reasons or because they were influenced by the June 1999 oxygenation event. Other allochthonous

taxa include any freshwater and brackish water taxa that were washed into the inlet from rivers and marshes, respectively.

CONCLUSION

A seasonal succession of diatoms was preserved in the sediment trap record and is similar to the succession observed in thin section analyses from Chapter 4. The results from this study indicate that daylength, sea surface temperature and precipitation are important for explaining the observed variation of diatom species inside Effingham Inlet. The analysis of phytoplankton compositions from both trap sites also shows that it is important to compare the results from mass flux, relative abundance and absolute abundance in order to interpret discrepancies in the records and to delineate what kind of material is contributing to the flux.

The assemblage of diatoms determined from the sediment traps from 1999 to 2000 may represent "normal" conditions since this time interval did not cover an El Niño year. However, the sampling interval does come at the very end of the 1997–1998 ENSO cycle, so it is not known exactly how the diatoms and other phytoplankton may have been affected. It is therefore imperative that further sediment trap work be carried out in Effingham Inlet in the near future for a time period spanning up to 5 years, where collection intervals can be as much as 1 month apart. Baseline conditions can then be established from these data.

Another aspect of a more fully involved sediment trap study would be to collect *in situ* nutrient data and environmental variables unique to each sediment trap site. By doing

this, multivariate analyses can be carried out on the separate traps instead of using a general meteorological database that spans a large area. For example, if there was a precipitation event occurring at Amphitrite Point, it is not known how much precipitation was falling over the inner basin or the mouth of the inlet. Hence, interpretations of diatom occurrences in the inner basin based on distal meteorological records are not as accurate as they can be. And, because the inner basin and the mouth of the inlet differ in environmental response, as was evident from the diatom compositions and DCCA, a thorough analysis of each site is required to understand how localized oceanography and climate variations affect the diatom populations. Only then can a more precise picture of climate variability can be reconstructed for the region.

CHAPTER 6

A 46-YEAR RECORD OF DIATOM ECOLOGY AND CYCLOSTRATIGRAPHY FROM RECENT SEDIMENTS, AD 1947–1993

ABSTRACT

Laminated sediments were analyzed for diatom content and sedimentation patterns in order to determine productivity and climate cycles in the northeast Pacific over the last half of the twentieth century. Quantitative analyses were performed on a 32-cm section, spanning from AD 1947–1993, of a freeze core recovered from the sediment-water interface in the inner basin of Effingham Inlet. The mean diatom abundance from 42 samples was 3.40×10^8 valves/g of dry sediment. Major taxa include *Skeletonema costatum* (robust and weakly silicified forms), *Thalassiosira* spp., *Thalassionema nitzschioides*, and *Minidiscus chilensis*. The mean *Chaetoceros* resting spores abundance was 5.09×10^7 valves/g of dry sediment. The first four axes of a detrended canonical correspondence analysis (DCCA) based on 50 dominant taxa explained 27.7% of variance in the diatom data, where 55% of this variance was explained by environmental data along the first axis. Sea surface temperature and salinity and Aleutian Low Pressure anomalies were important environmental factors for explaining the species variance. Morlet wavelet analysis of sediment grey scale values and total diatom abundance revealed significant and stationary ~2.5–6 year cycles, which correlate with known El Niño-Southern Oscillation cycles, and ~10–12 year cycles, which correlate with known sunspot cycles. The diatom records and cyclostratigraphy both show that a significant environmental change occurred in the mid 1970s, and is likely related to the well-

documented 1976–1977 "regime shift" from cooler to warmer conditions described from around the north Pacific Ocean. These results indicate that diatom productivity is not only affected by short- and long-term ocean-atmosphere cycles, but is also significantly affected by solar forcing and its effects on long-term climate.

INTRODUCTION

Diatoms and other microfossils recovered from hemipelagic sediments in the last century can be compared with historical instrumental environment data in order to understand the response of phytoplankton communities to environmental changes during modern times. Understanding how diatoms respond during modern environmental conditions is essential for reconstructing past environmental conditions, for comparisons to be drawn between the past and present, and for trajectories to be drawn for the future. Well-preserved laminated sediments in the inner basin of Effingham Inlet provide just such an opportunity to look into environmental change during the recent past.

Climate in the northeast Pacific Ocean is affected by numerous short and long-term cyclical events. El Niño and La Niña episodes, along with warm and cool phases of the Pacific Decadal Oscillation (PDO), are interdependent events that can influence ocean productivity from sub-decadal to multidecadal time scales. To understand modern climate variability, unconsolidated sediments near the sediment-water interface must be collected. These sediments can record recent fluctuations in climate and productivity for the past 100 years or so during which an instrumental environmental record exists. To capture these unconsolidated sediments, a freeze coring device was used (Wright 1980,

Shapiro, 1958) by which sediments are frozen *in situ* to the corer and distortion of the laminae during the coring process is minimal (Hughen et al., 1996).

In the last two chapters, I demonstrated that the laminated sediments in Effingham Inlet are annual in nature and that specific diatoms appear during certain times of the year in response to environmental triggers. In this chapter, a freeze core (TUL99B04) from the inner basin of Effingham Inlet is described and analyzed, with focus on a 32-cm long laminated section deposited during the latter half of the 20th century. The objectives for this study are to: 1) determine a precise chronology for the sediments, 2) quantify diatoms and other microfossils and relate their abundance and appearance to historical environmental variables, and 3) define cycles in depositional patterns and diatom stratigraphies using cyclostratigraphy, and to compare the cycles with observed historical environmental data.

METHODS AND MATERIALS

When each of the five freeze cores were recovered from Effingham Inlet and brought on board the CCGS *Tully*, core TUL99B04 was the only one to display well-preserved laminae. Each core was slabbed and x-rayed, and from the x-ray positive images and surface expression of the cores, it was decided that TUL99B04 from the inner basin (Figure 6.1) be analyzed in detail because this core contained the greatest proportion of well-preserved laminae. The methods used to analyze this core are explained below, and Figure 6.2 summarizes the procedures used.

Inner Basin

Site 2:
TUL99B04 (Freeze Core 2)

Latitude: 49° 04.218' N
Longitude: 125° 09.429' W
Depth: 120 m

Meteorological Stations:

1. Amphitrite Point
2. Bamfield

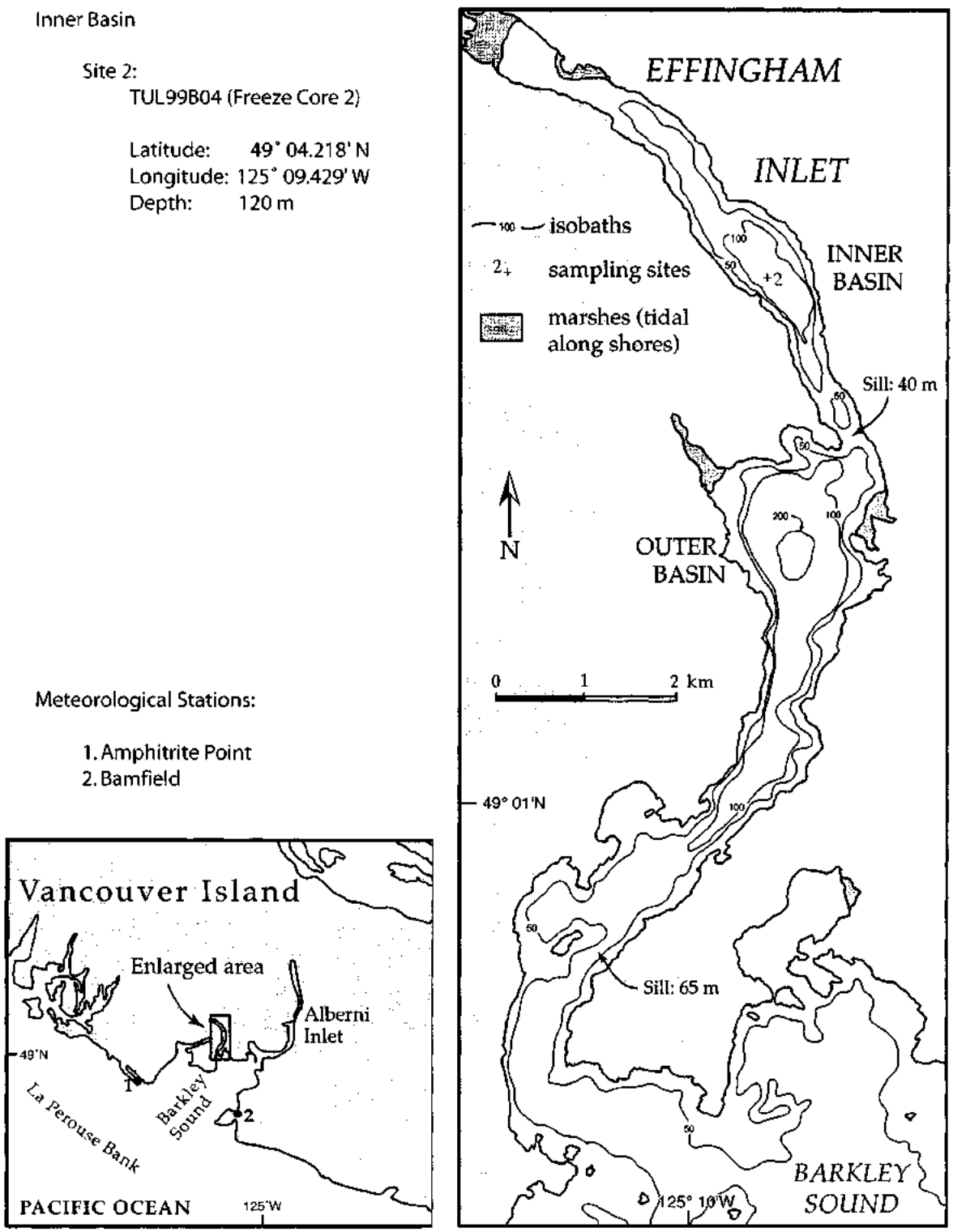

FIGURE 6.1. Location of freeze core TUL99B04 and meteorological stations.

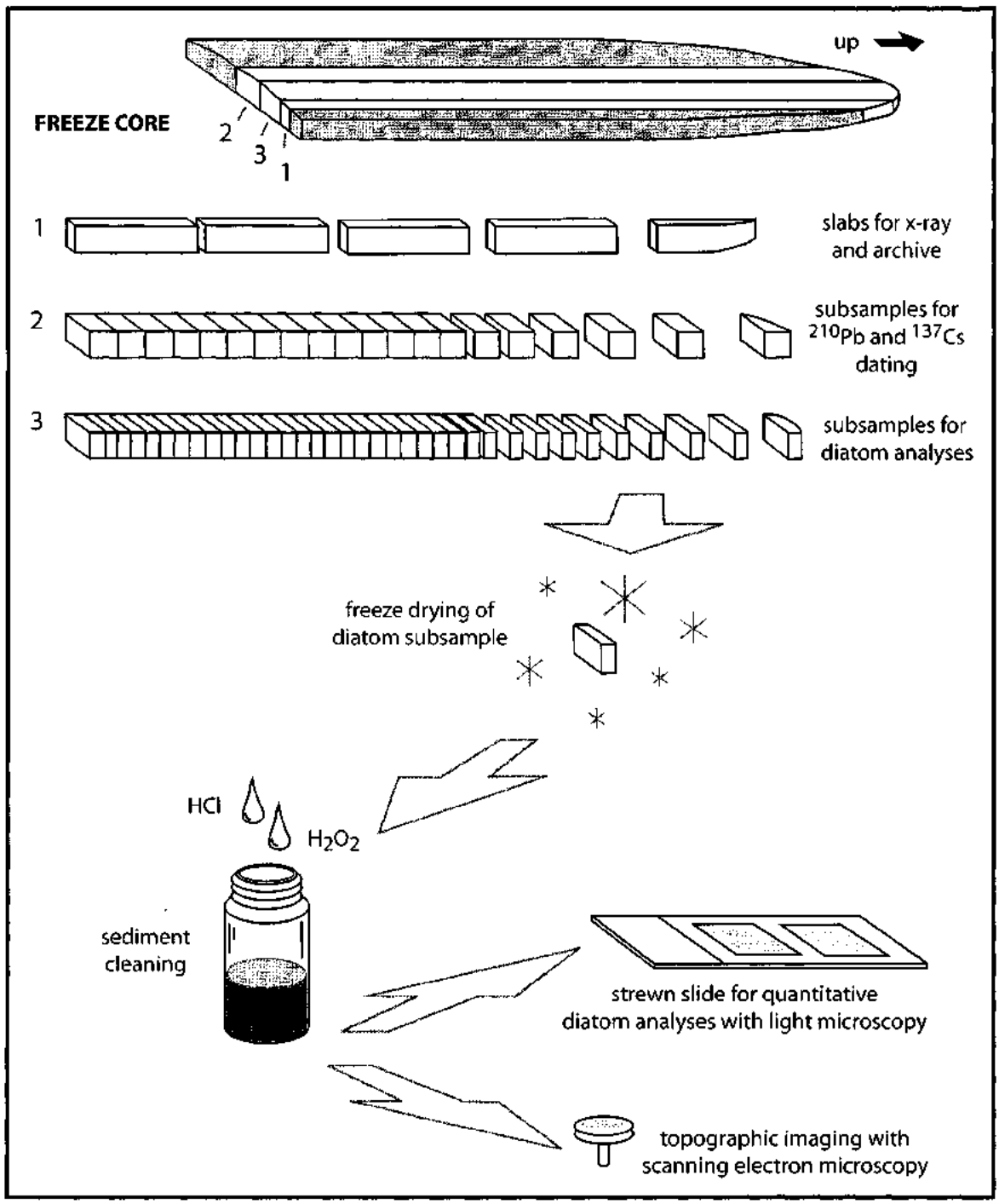

FIGURE 6.2. Schematic diagram showing the subsampling and processing of freeze core sediments. No scale is intended.

All sawing and sampling took place in a walk-in freezer to maintain core integrity and prevent cross-contamination of samples that can result from melting if sampling took place at room temperature. The maximum length of the core TUL99B04 (123 cm) was measured down the middle of the core. Because the core was irregularly shaped (as were the other freeze cores), where the edges of the core were shorter than the middle, it was decided that all analyses take advantage of the longest part of the sediment record. Thus, to reach the center of the core, the edges of the core were cut away with a bandsaw, perpendicular to the bedding plane. Murray Hay (Université Laval) assisted me with the sawing, and since this was our first attempt at cutting a frozen core, there were a few mistakes resulting in some broken and unusable core. After the problems were rectified, and our cutting technique improved, all other freeze cores were slabbed.

Slabs for x-radiography were produced by sawing 1- to 1.5-cm thick pieces perpendicular to laminae, down the middle of the core (Figure 6.2). The frozen sediment occasionally broke along bedding planes during the sawing process. Slabs that remained intact but were too long (e.g., 20–30 cm) were spliced diagonally to laminae into pieces 10–15 cm long that were more easily handled. Slabs were wrapped in plastic film and aluminum foil for storage.

X-radiography

X-radiography was performed to determine internal sedimentary structures not visible to the naked eye. The frozen slabs were transported in a cooler filled with dry ice to the Geological Survey of Canada (Ottawa) where x-radiography was performed by

Roger McNeely on a Faxitron Series 43805-N X-ray system. The slabs were removed from the aluminum foil, and the plastic wrap partially removed prior to x-raying to reduce the incidence of "ghost" wrinkles appearing on the x-ray image. Because these were the first slabs to be x-rayed (i.e., before the cookie cutter slabs from Chapter 4 were x-rayed), a series of tests was performed on several slabs using a variety of film types, voltages, currents and exposure times to determine the best results. Agfa™ D7 film produced results with the best contrast, and the slabs were x-rays while still frozen. Voltages ranging from 27–35 kVp, currents from 3.1–3.2 mA, and exposure times from 45–167 s were used. The range in settings took into account the varying thickness, composition and water content of each individual slab. The x-ray negatives were then scanned into a computer and converted into positive images with Adobe Photoshop™ software.

Analysis of the x-radiograph images from all of the freeze cores confirmed that core TUL99B04 from the inner basin provided the most intact and continuous record of sedimentary laminae for dating and diatom work.

Determination of Chronology

Chronology of the sediments was determined using three methods: varve counting, ^{137}Cs analysis and ^{210}Pb analysis. With the aid of the x-radiograph positive images, couplets were first assigned a year value starting from a known age. Beneath the 32-cm long laminated section was a massive interval that was found in correlative sediments throughout Effingham Inlet (Dallimore, 2001). A similar deposit was found in

nearby Saanich Inlet (Blais-Stevens et al., 1997). This massive interval is a slump deposit likely produced during the 8 June 1946, M 7.6 earthquake centered in central Vancouver Island (Rogers, 1980). Therefore, the first couplet (defined in Chapter 4 as a terrigenous lamina overlain by a diatomaceous lamina) above the 1946 slump layer was assigned a year value of 1947.

Cesium-137 is ideal for dating young sediments, especially sediments deposited during the time of nuclear testing from the 1940s to 1964, after which above ground testing was banned. Lead-210, ideal for dating sediments up to 150 years old, provides an independent assessment of sediment ages and is useful for corroborating dates obtained by ^{137}Cs dating.

During the coring process, sediments touching the freeze corer surface were slightly sheared as the corer was lowered into the sediment column. The sheared part of the laminae, which extended approximately 7 mm into the 3-cm thickness of the core, was sawed off to prevent time-averaging contamination. Samples were taken at 1 cm intervals parallel to laminae. A minimum of 10 g (wet, 1 g dry) of sediment was obtained for both the ^{137}Cs analysis and ^{210}Pb analyses (the latter analysis requires only 5 g of wet sediment or 0.5 g dry). Only one sample from each horizon was required because the non-invasive ^{137}Cs analysis would be performed before the destructive ^{210}Pb analysis. A total of 29 samples were taken. The samples were dried in an oven for 7 h at 70 °C until fully dessicated and then ground to a powder. The samples were then shipped to GEOTOP Laboratories (University of Quebec at Montreal) and analyzed by Dr. Bassam Ghaleb, and the results presented in Appendix F1. A peak in the ^{137}Cs disintegration

profile signifies the 1963–1964 peak of atmospheric nuclear testing. Results from ^{210}Pb analyses were converted into calendar years using the constant flux-constant sedimentation model. This model postulates that where there is a constant input of detrital material, there will also be a constant accumulation rate of ^{210}Pb to the bottom where each sediment layer will have the same initial ^{210}Pb concentration (Sorgente et al., 1999). Assuming that no migration of ^{210}Pb has occurred in the sediment column, the ^{210}Pb concentration will decline exponentially with cumulative dry mass of sediment. Because sediment density measurements derived from organic matter content determined by loss on ignition were not undertaken for my samples, an average dry density of 2.275 g/cm^3 from correlative box core EFBC9703-2 (M. Hay, unpublished data) was used for the ^{210}Pb dating calculation (Appendix F2).

Sample Processing for Diatom Analyses

As with sampling for ^{137}Cs and ^{210}Pb, the sheared side of the core was cut off prior to sampling to reduce the incidence of contamination across years. An attempt was made to sample annual couplets from the frozen core using a hacksaw blade, although several difficulties arose. First, although sampling positions were aided by x-radiographs, the couplets were difficult to see since the surface of the core had oxidized and the laminae were no longer visible. Second, the laminae were not perpendicular to the core surface (i.e., the laminae were at an angle), so care had to be taken to cut the couplets at the same angle along the bedding plane. Third, the couplets were much thinner (mean thickness 0.6 cm) than those found in Saanich Inlet (up to 2 cm thick; McQuoid and

Hobson, 1997) and the thickness varied from one couplet to the next, making the placement of cuts difficult. Fourth, sampling took place before the results from the ^{137}Cs and ^{210}Pb dates were obtained. As soon as the results from the ^{137}Cs and ^{210}Pb analyses were available and converted in calendar years, each diatom sample was assigned a time interval based on the geochemical dates and the x-radiograph varve counts. In the end, most of the samples represented individual annual couplets, however, some samples represented half-year to two-year time intervals (Appendix G2).

The samples were then freeze dried to remove the moisture content of the sediments for storage and slide processing. Freeze drying was performed by Malcolm Bilz at the Canadian Conservation Institute in Ottawa. After freeze drying, the samples kept their original shape, but when slight pressure was added with a metal spatula, the sediments readily fell apart. The dried sediments were carefully disaggregated to aid in the sediment digestion process, but care was taken not to powder or crush the sediments as this action can destroy diatom frustules.

To process the sediment, 0.4 grams of disaggregated sample was weighed out to four decimal places and placed in a 20-mL glass scintillation vial. Sediment digestion and slide processing then followed the same procedure as detailed in Chapter 5. The only difference between the two procedures is that because the initial weight was known and constant for the freeze core samples, I was able to keep the dilution factors for each slide constant as well. Dilution factors of 5 and 15× were used for all slides.

Microscopy

Microscope techniques follow those detailed in Chapter 5. However, as the freeze core samples were the first set that I enumerated, I did not resolve *Chaetoceros* resting spores (CRS) to species level. At least 40 fields of view were counted, except for three samples (B04-27, 35, and 36) where diatoms were more abundant. The slides were counted 3 times to ensure statistical accuracy. The relative and absolute abundance of microfossils were calculated using equations 5.1 and 5.2.

Instrumental Data

Data available for the southwestern Vancouver Island region between 1947 and 1993 were sea surface temperature (SST), sea surface salinity (SSS), precipitation (PPT), and the Aleutian Low Pressure Index (ALPI). Sea surface temperature and salinity data were obtained from Amphitrite Point as monthly values from the Institute of Ocean Sciences, Ocean Sciences and Productivity website (www-sci.pac.dfo-mpo.gc.ca/osap/data/SearchTools/Searchlighthouse_e.htm). Precipitation data were obtained as daily values from Climate Services, Environment Canada. Two datasets were compiled to complete the precipitation record: one from Bamfield (1 January 1947 to 30 September 1956) and one from Bamfield East (7 August 1959 to 31 December 1992). ALPI data were obtained from a Department of Fisheries and Oceans (Canada) website (www.pac.dfo-mpo.gc.ca/sci/sa-mfpd/downloads/alpi.txt) and is described in Beamish and Bouillon (1993) and Beamish et al. (1997). ALPI measures the relative intensity of the Aleutian Low Pressure system over a given area of the north Pacific Ocean (from

December through March, representing an average over one "year") and is expressed as an anomaly from the 1950–1997 mean. A positive index indicates a strong, or intensified, Aleutian Low, and a negative index indicates a weak low-pressure system. Subsequently, ALPI can be used as a proxy for winter storminess in the north Pacific.

Additional environmental parameters that were compared to the diatom dataset in cyclostratigraphic analysis, but not used in multivariate analysis, were the Southern Oscillation Index (SOI) and the sunspot cycle. SOI is a measure of the air pressure difference between the western and eastern tropical Pacific Ocean during El Niño and La Niña events, and is expressed as an anomaly from the 1951–1980 mean. Measurements are made from Darwin, Australia, and Tahiti, and averaged over 6 months from October to March. A negative SOI indicates that air pressures are below normal at Tahiti and above normal at Darwin. Moderately negative SOI values coincide with anomalously warm water temperatures typical of El Niño conditions. Alternatively, positive SOI values correspond with cool water temperatures indicative of La Niña conditions. Data were obtained from the Western Regional Climate Center website (www.wrcc.dri.edu/enso/ensodef.html; see also Redmond and Koch, 1991), although the original data from that study were obtained from the NOAA Climate Prediction Center (Redmond and Koch, 1991).

The sunspot cycle is quantified by the number of sunspots visible on the sun's disk for given interval of time. The number of sunspots cycles approximately every 11 years, ranging from near zero to 250 sunspots observed per month. The number of sunspots can alter the amount of solar output and the amount of solar irradiation received

by the earth. Changes in solar output alone cannot directly account for temperature fluctuations on earth; hence, an amplification mechanism is required. The premise behind the mechanism is that an increase in solar activity results not only in enhanced thermal energy flux, but also an increase in solar wind that attenuates the galactic cosmic ray flux (CRF) reaching earth (Shaviv and Veizer, 2003). Cosmic ray activity indicators (e.g. ^{10}Be, ^{14}C) in earth's atmosphere show that the amount of CRF reaching the earth affects low-altitude cloud cover, albedo and subsequently climate (Marsh and Svensmark, 2000; Todd and Kniveton, 2001; Carslaw et al., 2002). The sequence of events is postulated to be: more sunspots, more solar flares, brighter sun, enhanced thermal flux and solar wind, muted CRF, less low-level clouds, less albedo, warmer climate (Shaviv and Veizer, 2003). Decreased sunspot activity results in an opposite effect. Data for sunspot number used in this study were obtained from the NASA Marshall Space Flight Center solar physics website (science.msfc.nasa.gov/ssl/pad/solar/sunspots.htm).

STATISTICAL ANALYSES

Data Screening

Data were screened and analyzed in a manner similar to that described in Chapter 5. A total of 252 diatom taxa were identified from the freeze core samples (Appendix G1). To reduce the number of rare taxa, the data were screened to include only taxa that appeared in at least three samples, and had a relative abundance of at least 1% in one sample. As a result, 50 taxa remained (Table 6.1). Environmental variables SST, SSS, PPT and ALPI were included in multivariate analyses. Data for temperature, salinity and

TABLE 6.1. Diatom taxa occurring in at least three samples, and ≥1% in at least one sample (code numbers correspond to those in Figure 6.10C)

1	*Achnanthes minutissima* Kützing 1833
2	*Amphora acutiuscula* Kützing 1844
3	*Amphora copulata* (Kützing) Schoeman & Archibald 1986
4	*Asteromphalus sarcophagus* Wallich 1860
5	*Bacteriastrum delicatulum* Cleve 1897
6	*Berkeleya rutilans* (Trentepohl) Grunow 1880
7	*Cocconies disculus* (Schumann) Cleve in Cleve and Jentzsch 1895
8	*Cocconeis placentula* Ehrenberg 1838
9	*Cocconeis scutellum* Ehrenberg 1838
10	*Cocconeis stauroneiformis* (Rabenhorst) Okuno 1957
11	*Cyclotella choctawhatcheeana* Prasad 1990
12	*Cyclotella striata* (Kützing) Grunow 1880
13	*Ditylum brightwellii* (West) Grunow in van Heurck 1883
14	*Fragilaria capucina* Desmazieres 1825 complex
15	*Fragilaria investiens* (W. Smith) Cleve-Euler
16	*Fragilaria* cf. *soptonensis* Witkowski and Lange-Bertalot 1993
17	*Fragilariopsis cylindriformis* (Hasle in Hasle & Booth) Hasle
18	*Fragilariopsis pseudonana* (Hasle) Hasle 1993
19	*Gomphonemenopsis lindae* Witkowski, Metzelin and Lange-Bertalot in Metzelin and Witkowski 1996
20	*Gomphonemopsis obscurum* (Krasske) Lange-Bertalot
21	*Melosira nummuloides* (Dillwyn) C.A. Agardh 1824
22	*Minidiscus chilensis* Rivera and Koch 1984
23	*Navicula perminuta* Grunow in Van Heurck 1880
24	*Nitzschia frustulum* (Kützing) Grunow in Cleve and Grunow 1880
25	*Nitzschia perminuta* (Grunow) M. Peragallo 1903
26	*Odontella longicruris* (Greville) Hoban 1983
27	*Opephora mutabilis* (Grunow) Sabbe and Vyverman
28	*Paralia sulcata* (Ehrenberg) Cleve 1873
29	*Planothidium delicatulum* (Kützing) Round and Bukhtiyarova 1996
30	*Pseudonitzschia multiseries* (Hasle) Hasle 1995
31	*Rhizosolenia* spp. Brightwell 1858 (mainly *R. setigera* Brightwell 1858 processes)
32	*Skeletonema costatum* (Greville) Cleve 1878
33	*Skeletonema costatum* (Greville) Cleve 1878 (weak form)
34	*Tabellaria flocculosa* (Roth) Kützing 1844
35	*Tabularia fasciculata* (Agardh) Williams and Round 1986
36	*Thalassionema bacillare* (Heiden) Kolbe 1955
37	*Thalassionema nitzschioides* (Grunow) Mereschkowsky 1902
38	*Thalassionema pseudonitzschioides* (Schuette and Schrader) Hasle in Hasle and Syvertsen 1996
39	*Thalassiosira bioculata* (Grunow) Ostenfeld 1903
40	*Thalassiosira decipiens* (Grunow) Jørgensen 1905

TABLE 6.1 (continued)

41	*Thalassiosira eccentrica* (Ehrenberg) Cleve 1904
42	*Thalassiosira gravida* Cleve
43	*Thalassiosira kushirensis* Takano 1985
44	*Thalassiosira* cf. *leptopus* (Grunow) Hasle and Fryxell 1977
45	*Thalassiosira nordenskioeldii* Cleve 1873
46	*Thalassiosira oestrupii* (Ostenfeld) Hasle 1972
47	*Thalassioisra pacifica* Gran and Angst 1931
48	*Thalassiosira punctigera* (Castracane) Hasle 1983
49	*Thalassiosira tenera* Proschkina-Lavrenko 1961
50	*Thalassiosira* sp. (cf. *T. tenera* but no marginal processes)

precipitation were averaged over the same time intervals represented by the samples (Appendix G2). ALPI values were assigned to annual and subannual samples of the closest corresponding year. For samples representing multiple years, a mean ALPI value for that time interval was used. These environmental variables were then correlated using commercial statistical software (2-tailed Pearson correlation with Bonferroni adjustment) to determine the significance of each variable. All variables were also analyzed with Calibrate version 0.70 (Juggins, 1997) to determine the distribution of the data and to normalize skewed distributions. Variables SSS and ALPI were log transformed, while PPT was square root transformed. Variable SST needed no transformation because it had a normal, though slightly left-skewed, distribution. Samples were tested for statistical validity (95% confidence limit) by performing principle components analysis (PCA) of environmental variables and detrended correspondence analysis (DCA) of species data (Hall and Smol, 1992). No outlying samples were identified.

Ordination

CANOCO version 4.0 (ter Braak and Smilauer, 1998) was used for ordination of samples, species and environmental variables. DCA was first used to determine the length of the gradient represented by the main direction of variation within the species data. The gradient length was relatively short (1.9 standard deviation units) which represents a linear response model. PCA was then performed but there was a slight arch effect (ter Braak, 1986). Hence, as with the sediment trap analyses, a detrended canonical correspondence analysis (DCCA) was used as the final ordination technique.

DCCA was performed using a global permutation test with 1000 Monte Carlo permutations to identify multicollinearity in samples and environmental variables. Initially, ALPI and SST were closely positioned on the ordination diagram, and PPT was situated opposite from SSS, which was to be expected. Although there were no strong "site-environmental influences", variable PPT did show collinearity with samples B04-34 and B04-37, and continued collinearity with other samples when these initial two samples were removed. PPT was removed and the ordination reanalyzed. As a result, ALPI moved away from the SST vector and took the place of PPT on the ordination diagram (Figure 6.10).

CYCLOSTRATIGRAPHY AND WAVELET ANALYSIS

Continuous wavelet transform, or wavelet analysis, is a cyclostratigraphic method for analyzing time series data by transforming information from the depth- or time-domain into the spectral domain using short filtering functions called "wavelets" (Prokoph and Patterson, in press). Wavelet analysis was initially used as a filtering and data compression method in the 1980s (e.g., Morlet et al., 1982) and has since been widely applied in geophysics (e.g., Grossman and Morlet, 1984). Because time series data from a sedimentary core, for example, inherently contains information on both a uniform depth scale and a non-uniform time scale, wavelet analysis converts the data into an equidistant time scale so that stationary and non-stationary cycles can be detected (Prokoph and Patterson, in press). If the sediment accumulation rate is known for the core, or the time interval for the deposition of individual beds is known (in this case,

couplets are annual), then cycles can be defined providing that couplet sedimentation is truly being influenced by external (allocyclic) forces, such as the changing of seasons. Cyclical and quasi-cyclical oceanographic and climate oscillations embedded within sedimentary signals can then be extrapolated and visually displayed in a wavelet scalogram. Traditional spectral analysis may be able to display the frequencies of cycles on a graph, but such a diagram does not give a visual representation of where in the core these cycles occur. Wavelet analysis and the resulting scalogram have the benefit of visually displaying the position of cycles through time along the length of the core, and give an idea of how shorter-length cycles are embedded within longer cycles through time. However, spectral analysis is able to provide estimates of the "power" (signal variance per unit frequency band) and confidence levels of the cycle as a function of frequency (Davis, 1986).

Continuous wavelet transform, spectral and cross spectral analyses were performed on the x-radiographs and quantitative diatom counts of freeze core TUL99B04 by Dr. Andreas Prokoph (University of Ottawa). Grey scale values, sediment accumulation rate and cycle periodicities were determined from a computerized line scan of 256 shades of grey on the x-ray positive images of the laminated interval. In wavelet analysis, the computer uses a linear algorithm to determine the amplitude, phase and "power" of short wavelength cycles (i.e., annual cycles), and then progressively determines longer wavelength cycles based on the shorter cycles. Periodicities were also identified from total diatom abundance and compared to cycles derived from the sediment grey values. A brief explanation of image processing and wavelet analysis is

given in Appendix I, although readers who are interested in a detailed discussion of the methods and application of wavelet analysis for cyclostratigraphy can refer to Prokoph and Patterson (in press). Spectral analysis was applied using a Fast Fourier transform on equidistant diatom and sediment data. Cross spectral analysis was used to identify the bandwidth dependent correlation between diatom and sediment data, because it is possible that these datasets may not be correlated on long time scales, but are correlated on short time scales (Patterson et al., in review B).

RESULTS

Historical Instrumental Environment Record

Sea surface temperature increases progressively and ALPI becomes more intense (positive) from 1947–1992 (Figure 6.3B, E). At the same time, sea surface salinity and the amount of precipitation decrease slightly (Figure 6.3C, D). A major change in the ocean-atmosphere system occurred in the winter of 1976–1977 when the Aleutian Low intensified and sea surface temperatures in the eastern Pacific increased (e.g., Chavez et al, 2003; Venrick et al., 1987). The effects of this large-scale "regime shift" are visible in the local temperature data and regional ALPI profile. The average temperature from 1977–1992 was 10.8 °C, compared with an average temperature of 10.3 °C from an equivalent 16 years prior, representing a 0.5 °C increase. Likewise, ALPI averages –0.6 $km^2 \times 10^6$ from 1961-1976, and 1.5 $km^2 \times 10^6$ from 1977-1992, indicating increased storminess in more recent times. A correlation matrix of these variables shows that temperature and ALPI are significantly correlated with each other (Table 6.2),

FIGURE 6.3. Diatom abundance profile compared with annually averaged environmental variables from 1947–1992 inclusive. Diatom abundance is displayed in the time domain (compare with Figure 6.4D); numbers next to profile represent sample labels. Temperature and salinity profiles derived from Amphitrite Point data. Precipitation profile derived from Bamfield data. Aleutian Low Pressure Index (ALPI) data from Department of Fisheries and Oceans (Canada) website (www.pac.dfo-mpo.gc.ca/sci/sa/downloads/alpi.txt); see Beamish et al. (1997). Southern Oscillation Index (SOI) data from Western Regional Climate Center website (www.wrcc.dri.edu/enso/ensodef.html); see Redmond and Koch (1991). Number of sunspots data from the NASA Marshall Space Flight Center solar physics website (science.msfc.nasa.gov/ssl/pad/solar/sunspots.htm). Climate phases after Chavez et al. (2003); see discussion for explanation.

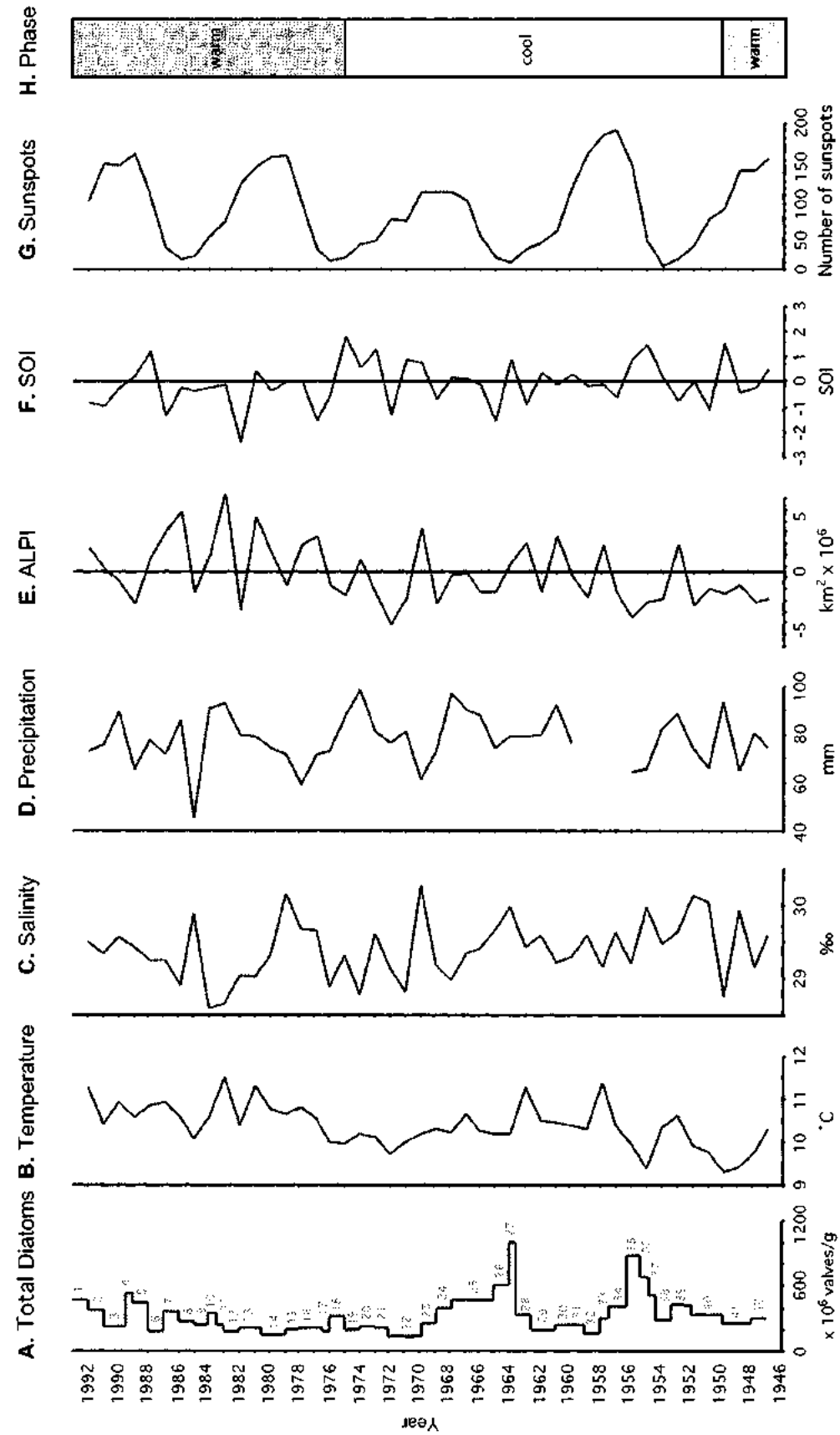
A. Total Diatoms
B. Temperature
C. Salinity
D. Precipitation
E. ALPI
F. SOI
G. Sunspots
H. Phase
warm
cool
warm
x 10⁶ valves/g
°C
‰
mm
km² x 10⁶
SOI
Number of sunspots
Year

TABLE 6.2. Pearson correlation matrix and Bonferroni-adjusted significance of annually averaged environmental variables (1947–1992 inclusive). Refer to text for explanation of abbreviations.

	SST	PPT	SSS	ALPI
SST	1.000			
PPT	0.012	1.000		
SSS	0.191	**-0.577	1.000	
ALPI	**0.517	0.305	-0.366	1.000

** very significant ($P < 0.01$)

while precipitation and salinity are significantly but negatively correlated with each other. During the study interval, negative SOI anomalies (El Niño type conditions) have occurred 14 times with varying intensity (Figure 6.3F) (Quinn et al., 1987). According to historical records, strong El Niño events occurred in 1957–1958, 1972–1973, and 1982–1983 (Quinn et al., 1987). SOI appears to become more negative from 1947–1993, with more frequent and intense El Niño events from 1972–1993. Approximately 5 sunspot cycles occurred during the study interval, with maxima in 1947, 1957, 1968, 1979 and 1990 (Figure 6.3G).

Chronology

Dating by varve counting starting at the year 1947 above the earthquake slump layer reveals that the youngest complete couplet represents the year 1992 (Figure 6.4A). The couplet for 1993 is incomplete and was not included in subsequent analyses or interpretations. The years 1963 and 1964 were counted at a depth of 22-23 cm (Figure 6.4E). The ^{137}Cs profile corroborated this age as a prominent peak, signifying peak radioactive fallout from atmospheric nuclear testing at this time, was found at a depth of 22.5 cm. The ^{210}Pb profile represents a typical exponential decay curve for younger sediments (Figure 6.4F). Using the constant flux-constant sedimentation model (Sorgente et al., 1999), analysis from ^{210}Pb content further confirms the position of the 1963 level (Appendix F2). These three lines of evidence, along with the sediment descriptions from Chapter 4, show that the laminated sediments in Effingham Inlet are indeed annually

deposited, and that 46 years of deposition were recovered by freeze core TUL99B04. A sediment accumulation rate of 6.7 mm/yr was calculated from the ^{210}Pb chronology.

Laminated Sediment Description

As with the sediments from inner basin core TUL99B03, sediments from the freeze core consist mainly of clay to silt size particles of biogenic and lithogenic origin. The difference in bulk density and sediment texture between the laminated interval and the 1946 massive interval is clearly visible in the x-radiographs (Figure 6.5). The laminated interval is relatively lighter in colour because of the presence of porous diatomaceous laminae. The darkness of the massive intervals indicates a mixture of numerous dense mineral grains, organic debris, and diatom remains.

The mean thickness of the couplets increases toward the top of the sediment column (Figure 6.4B). The couplets are thinner from 1947–1970, averaging 6.0 mm (Appendix F3). From 1970 to approximately 1984, the couplets average 6.3 mm in thickness. The uppermost couplets from 1984–1992 average 10.2 mm and are indistinct. This progressive increase in thickness toward the top does not signify increasing sedimentation near the end of the 20th century, but likely signifies a change in sediment compaction by dewatering. The older couplets have experienced more compaction from the weight of the overlying younger sediments, which have experienced little to no compaction near the sediment-water interface. A sediment accumulation rate of 6.9 mm/yr is calculated if all couplets are taken into consideration. This rate is comparable to the rate derived from ^{210}Pb dating. However, if only the compacted couplets from

FIGURE 6.4. Chronology, bulk sediment composition and diatom abundance from the laminated interval, freeze core TUL99B04. **A.** Year value assigned to couplets by varve counting, and adjusted with results from ^{137}Cs and ^{210}Pb dating. A year is defined by the placement of the label beside the terrigenous lamina of each couplet. Because the laminae are at an angle, the position of the year label for each couplet corresponds to the couplet expression along left edge of the x-ray image. **B.** X-radiograph positive image of sediments. Lighter coloured layers are diatomaceous laminae. Darker coloured layers are terrigenous laminae. **C.** Labels for quantitative diatom sampling. The position of the sample labels corresponds to the couplet expression along left edge of the x-ray image **D.** Absolute diatom abundance per sample. **E.** Decay profile of ^{137}Cs with a prominent peak at 1963 and 1964. **F.** Decay profile of ^{210}Pb showing exponential decrease in disintegrations towards depth. Dashed portion of decay profiles indicate extrapolation of the curve where there is no data (see Appendix F1 and F2 for data).

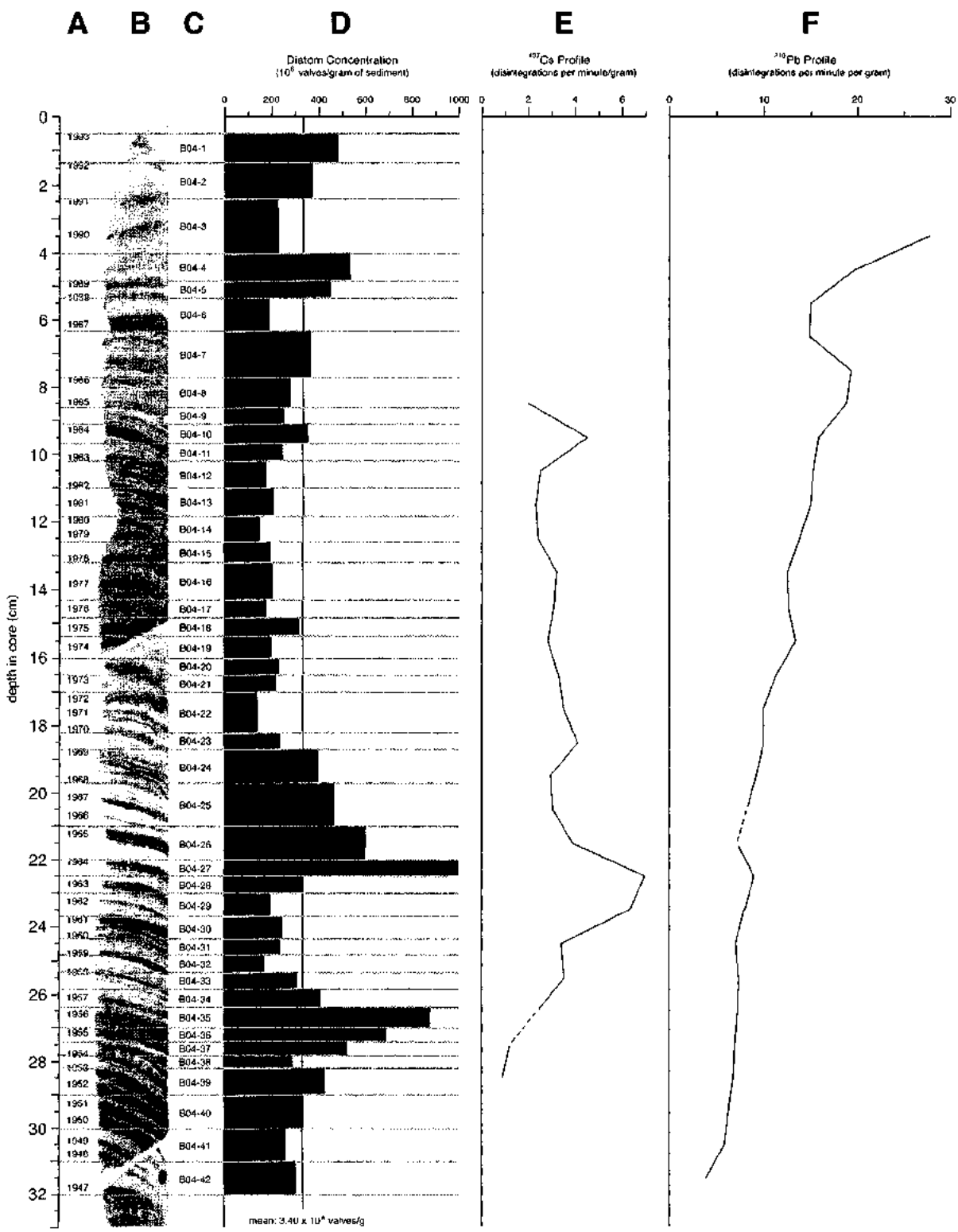
A
B
C
D
E
F
Diatom Concentration
(10^6 valves/gram of sediment)
0
200
400
600
800
1000
137Cs Profile
(disintegrations per minute/gram)
0
2
4
6
210Pb Profile
(disintegrations per minute per gram)
0
10
20
30
depth in core (cm)
0
2
4
6
8
10
12
14
16
18
20
22
24
26
28
30
32
1993
1992
1991
1990
1989
1988
1987
1986
1985
1984
1983
1982
1981
1980
1979
1978
1977
1976
1975
1974
1973
1972
1971
1970
1969
1968
1967
1966
1965
1964
1963
1962
1961
1960
1959
1958
1957
1956
1955
1954
1953
1952
1951
1950
1949
1948
1947
B04-1
B04-2
B04-3
B04-4
B04-5
B04-6
B04-7
B04-8
B04-9
B04-10
B04-11
B04-12
B04-13
B04-14
B04-15
B04-16
B04-17
B04-18
B04-19
B04-20
B04-21
B04-22
B04-23
B04-24
B04-25
B04-26
B04-27
B04-28
B04-29
B04-30
B04-31
B04-32
B04-33
B04-34
B04-35
B04-36
B04-37
B04-38
B04-39
B04-40
B04-41
B04-42
mean: 3.40 x 10^6 valves/g

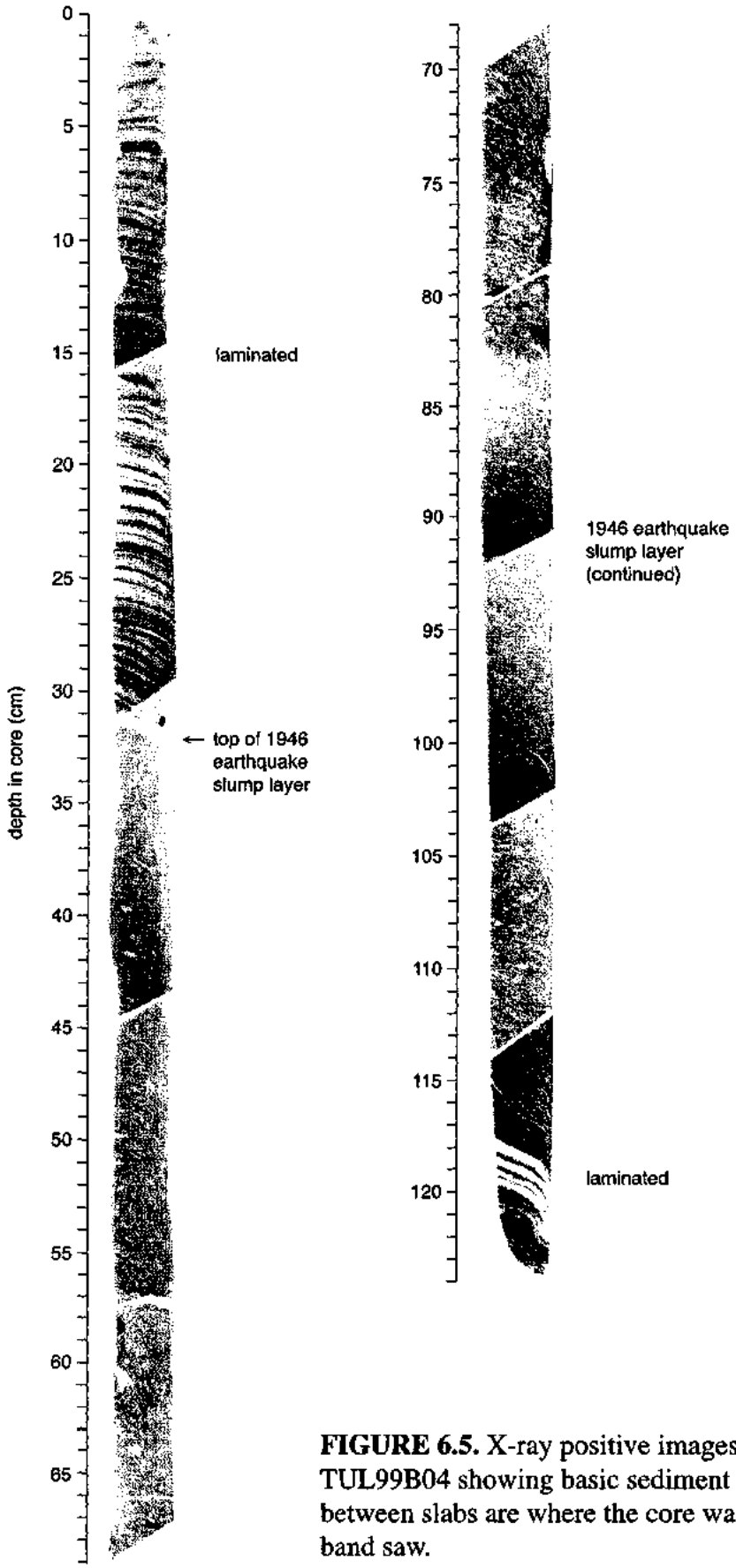

FIGURE 6.5. X-ray positive images of freeze core TUL99B04 showing basic sediment textures. Gaps between slabs are where the core was spliced by a band saw.

1947–1985 are included, then the sediment accumulation rate is reduced to 6.1 mm/yr.

Couplets dating from the end of 1993 to 1999 were not preserved on the freeze corer probably due to disturbance of the colloidal sediment-water interface during the coring process. At the bottom of the core, beneath the 1946 massive interval, is a 2-cm thick laminated interval. These laminae were not analyzed to see if they are varves. The brightness of these laminae in the x-radiograph suggests that the laminae contain almost pure diatom remains.

Diatom Abundance and Assemblages

The mean diatom abundance counted from the 42 samples is estimated at 3.40×10^8 valves/g (Figure 6.4D; Appendix G2). Diatom abundance is highest in 1956 (B04-35; 8.80×10^8 valves/g) and 1964 (sample B04-27; 1.01×10^9 valves/g), and is lowest from 1970-1972 (B04-22; 1.38×10^8 valves/g), with a recovery of diatom populations in the 1980s. The mean *Chaetoceros* resting spore (CRS) abundance is estimated at 5.09×10^7 valves/g. Highest CRS abundance occurs in 1984 (B04-9; 3.13×10^8 valves/g) and the lowest occurs in 1978 (B04-15; 5.35×10^6 valves/g) (Figures 6.6, 6.7). Silicoflagellates were not major components of the microfossil composition, with a mean abundance of 2.72×10^6 skeletons/g.

The coastal marine planktonic diatom *Skeletonema costatum* (nominal or robust form) constitutes the bulk of the diatoms counted, with a maximum relative abundance of 71.6% and absolute abundance of 6.30×10^8 valves/g for sample B04-35. Other dominant diatoms, all of which have concentrations greater than 1×10^8 valves/g are, in order of

decreasing abundance, *Thalassionema nitzschioides*, *Thalassiosira kushirensis* (limited occurrence in only 2 samples), the weakly silicified form of *Skeletonema costatum*, and *Minidiscus chilensis* (Figures 6.8, 6.9).

Several taxa have noticeable trends. The brackish water diatom *Cyclotella chochtawhatcheeana* has its greatest abundance at the bottom of the laminated section. The abundance of this diatom then decreases until none are observed after ~1980. *C. chochtawhatcheeana* was observed in sediment trap samples but in low amounts (Appendix E1). Other brackish water taxa, such as *Cocconeis scutellum*, *Gomphonemopsis obscurum*, *Navicula perminuta* and *Planothidium delicatulum*, also decrease in absolute abundance throughout the study interval, although *Ditylum brightwellii* appears to increase in abundance (Figures 6.8, 6.9). *Pseudonitzschia multiseries* and *Thalassiosira* cf. *leptopus* occur in low abundance prior to ~1984 and then increase in abundance in recent years. These diatoms, however, are abundant down core (Chapter 7), signifying that they are not new arrivals to Effingham Inlet in the late 20th century. In the freeze core, *Thalassionema nitzschioides* reached peak abundance in 1968/1969 (sample B04-24; 1.98×10^8 valves/g). *Thalassiosira kushirensis* also reaches peak abundance in 1963/1964 (B04-27; 1.87×10^8 valves/g) but is virtually absent above and below this horizon.

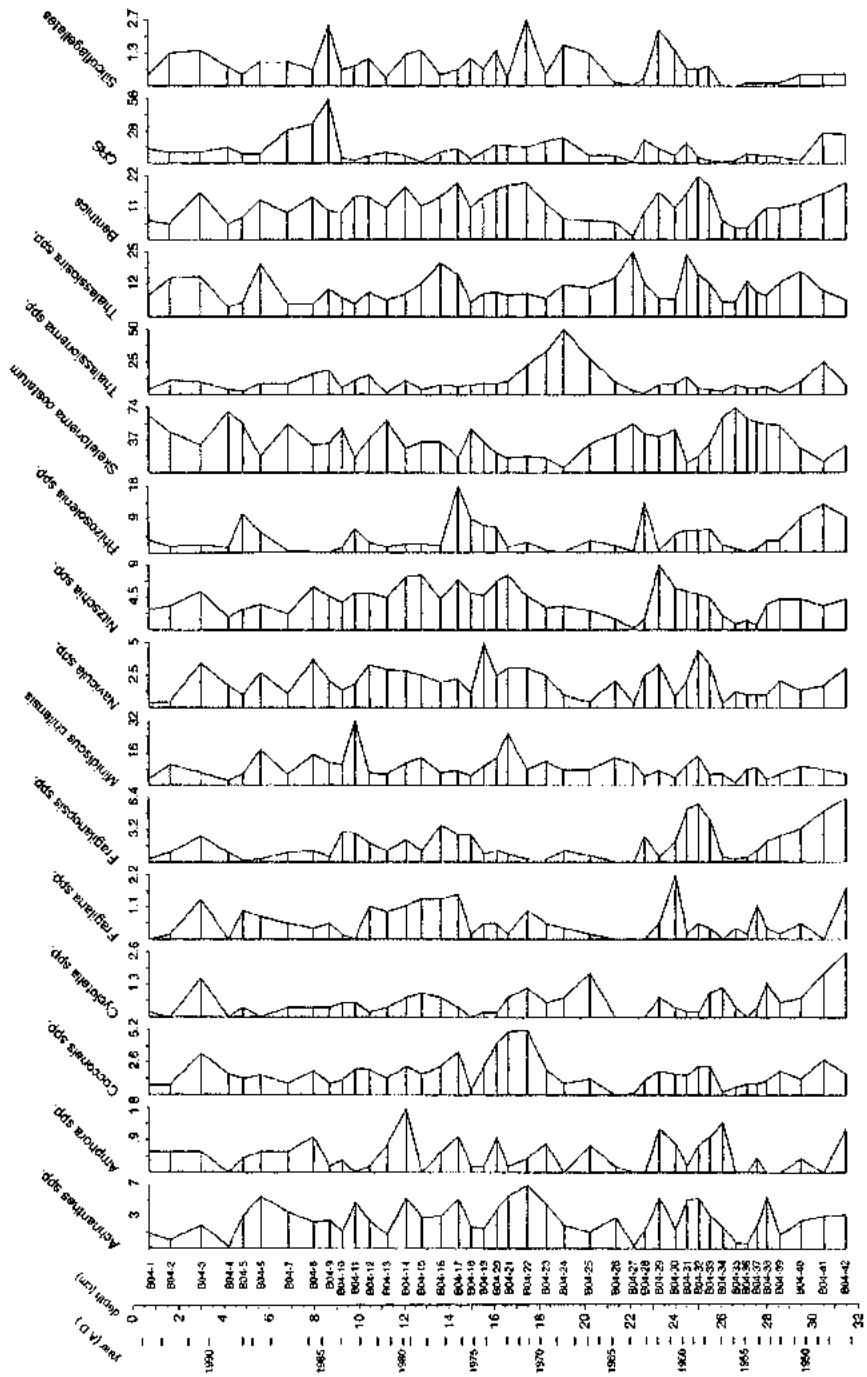

FIGURE 6.6. Relative abundance data (%) for major diatom taxa, total benthic diatoms, CRS and silicoflagellates from freeze core TUL99B04.

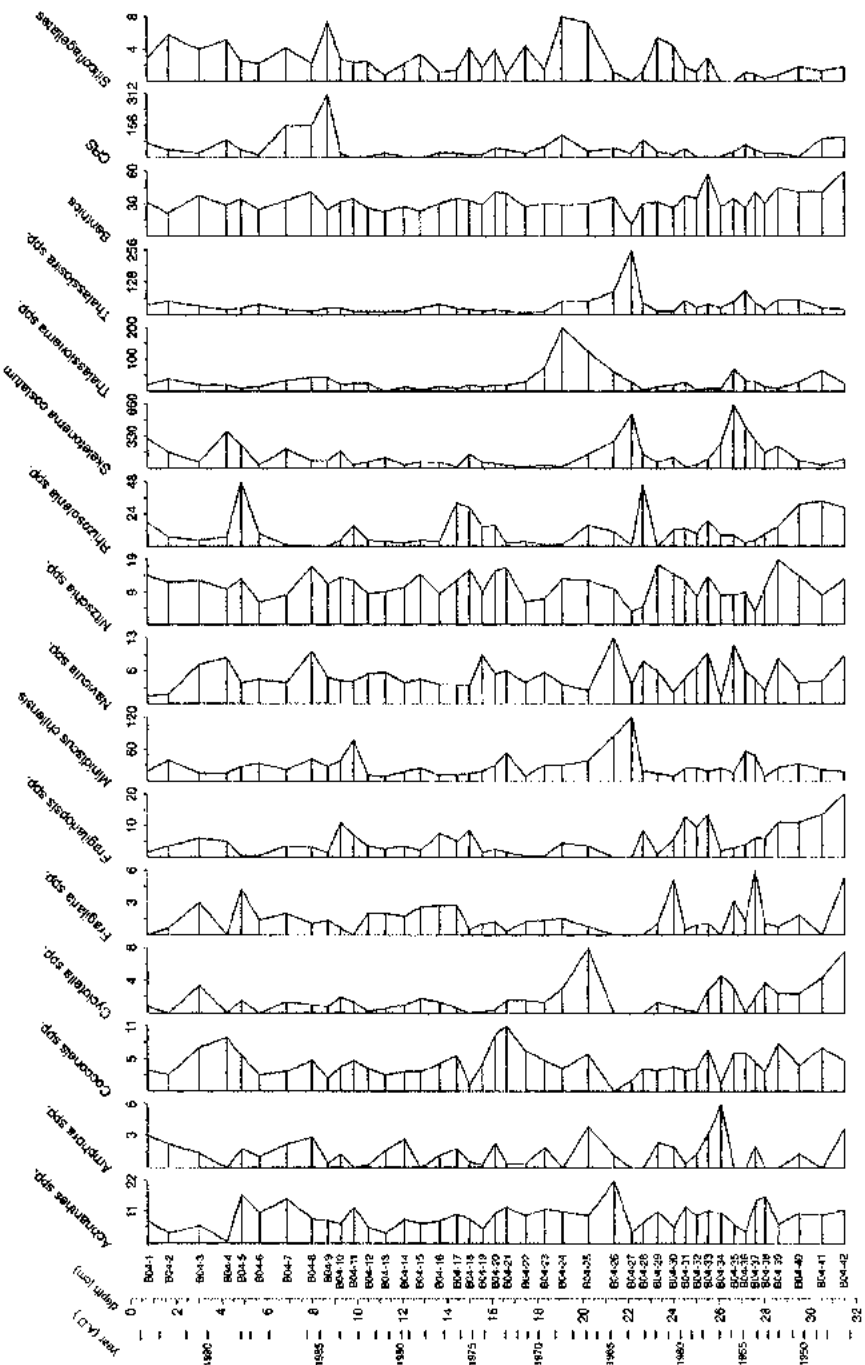

FIGURE 6.7. Absolute abundance data ($\times 10^6$ valves/g) for major diatom taxa, total benthic diatoms, CRS and silicoflagellates from freeze core TUL99B04.

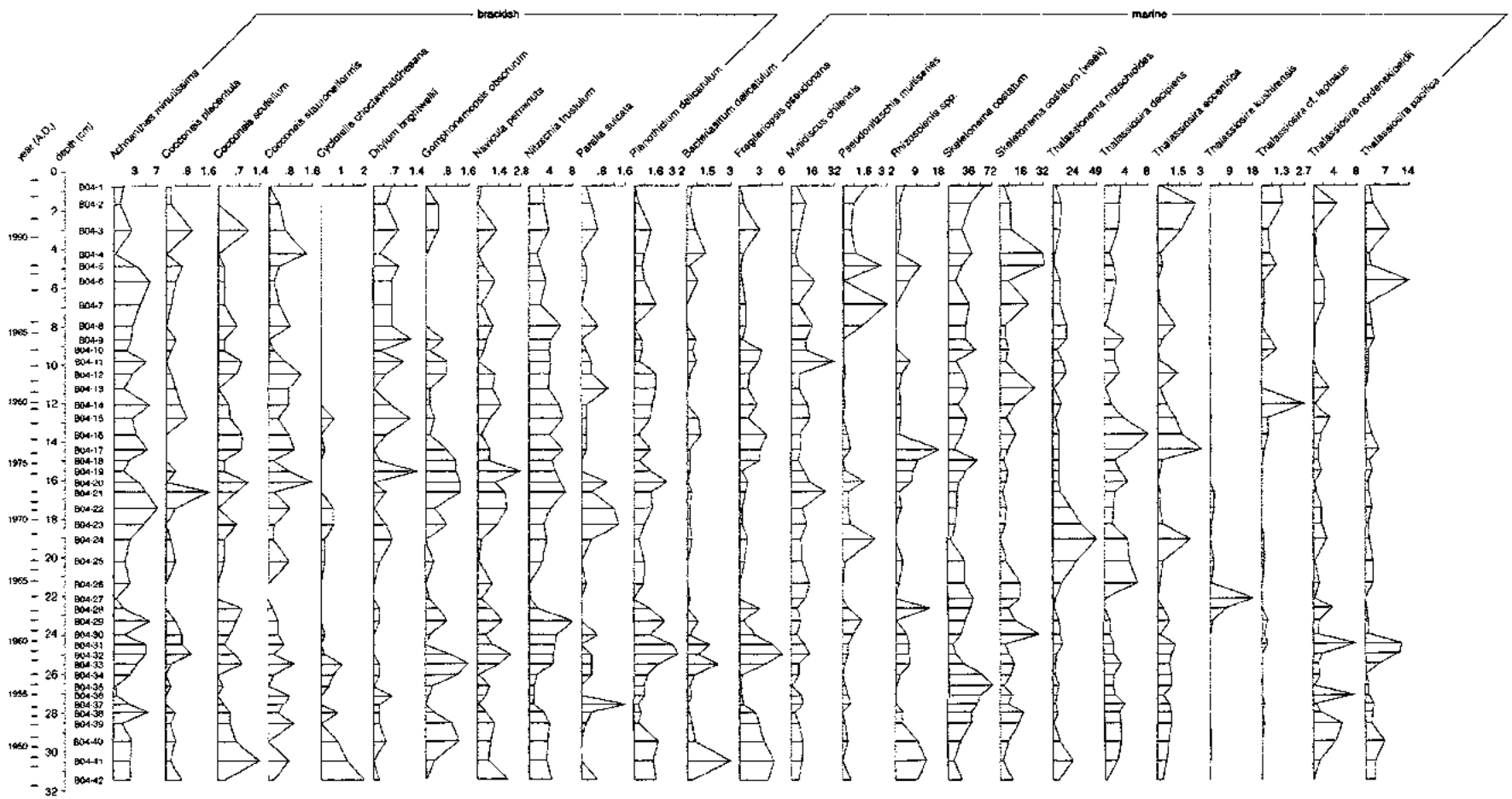

FIGURE 6.8. Relative abundance data (%) for selected major diatom taxa from freeze core TUL99B04. Data for other major taxa are presented in Appendix G3.

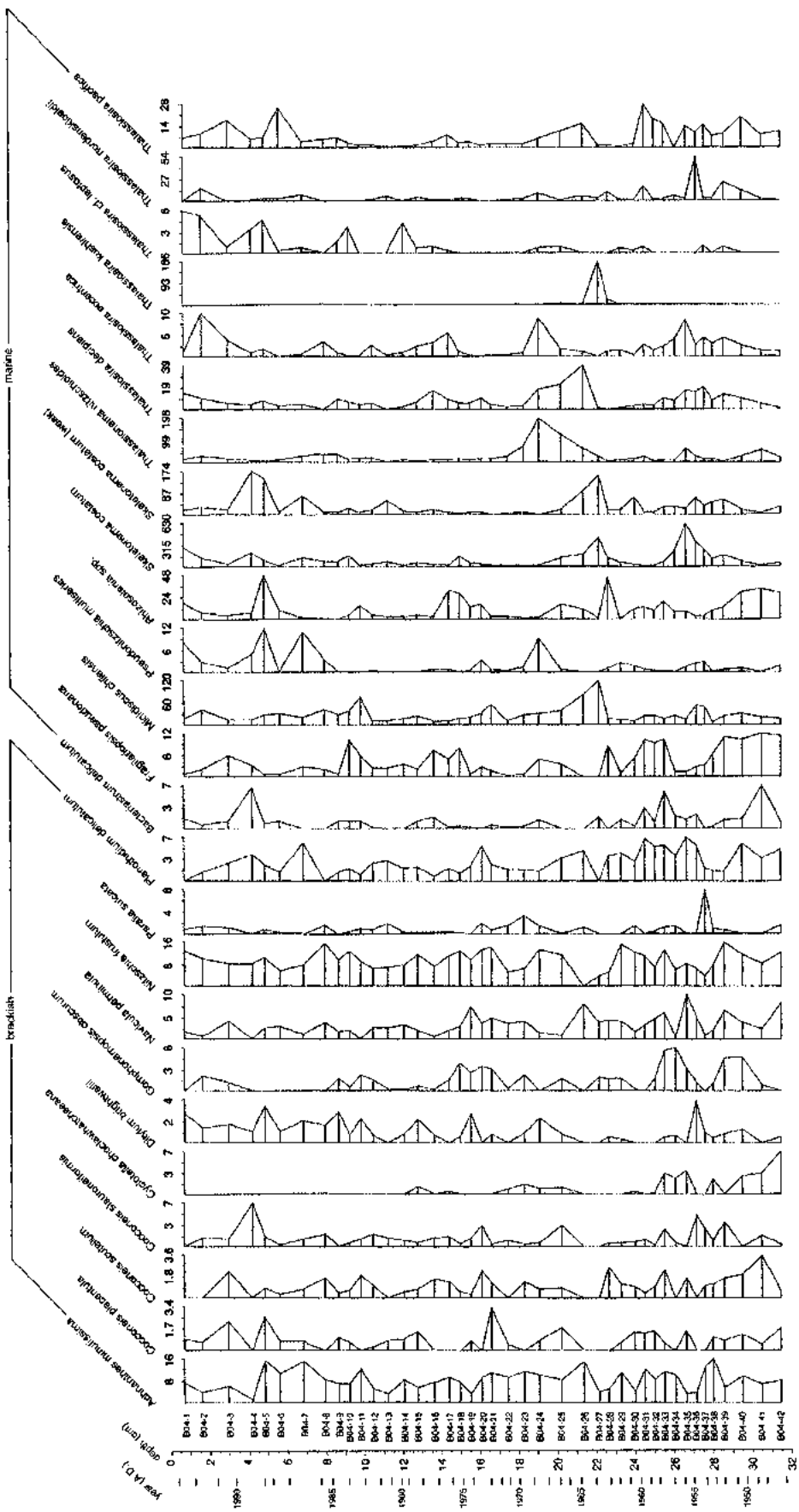

FIGURE 6.9. Absolute abundance data ($\times 10^6$ valves/g) for selected major diatom taxa from freeze core TUL99B04. Data for other major taxa are presented in Appendix G4.

Species Assemblages and Environmental Variables

The first four axes of the final DCCA ordination explained 27.7% of variance in the diatom data, and the environmental data explained 54.8% of this variation along the axis 1 (Table 6.3). The first two axes are the most important, although only explaining 4.2% of the variance, because the data along these axes were constrained to the environmental variables. Axes 3 and 4 (23.5%) were less important because the data along these axes were not constrained to the environmental variables, resulting in a zero species-environmental value on these axes (Table 6.3). These axes have higher eigenvalues because the data are not constrained and therefore are explaining other variability present in the data.

In the original ordination, when all four environmental variables were used, variables PPT and SST were correlated with axis 1, while SSS and ALPI were correlated with axis 2 (Figure 6.10A). After PPT was removed from the ordination, the configuration of the environmental vectors and species and sample points changed by inverting along axis 1. SST is now more strongly correlated with axis 1, while SSS and ALPI are strongly correlated with axis 2 (Figure 6.10B, C).

The positions of the plotted samples and species on the final ordination diagram give a qualitative indication of their environmental optima. Most of the samples fall toward the origin of the diagram, indicating that many samples have similar environmental optima. Additionally, because many of the samples are annually time-averaged, extreme environmental signals have been smoothed out. A general trend shows that samples from the lower portion of the core, namely samples B04-20 to 42, plot on

TABLE 6.3. Summary of statistics for the first four axes of a detrended canonical correspondence analysis performed on species-environment data from 1947–1992 (inclusive)

	Axis 1	Axis 2	Axis 3	Axis 4
Eigenvalues	0.027	0.015	0.158	0.077
Species-environment correlations	0.548	0.524	0.000	0.000

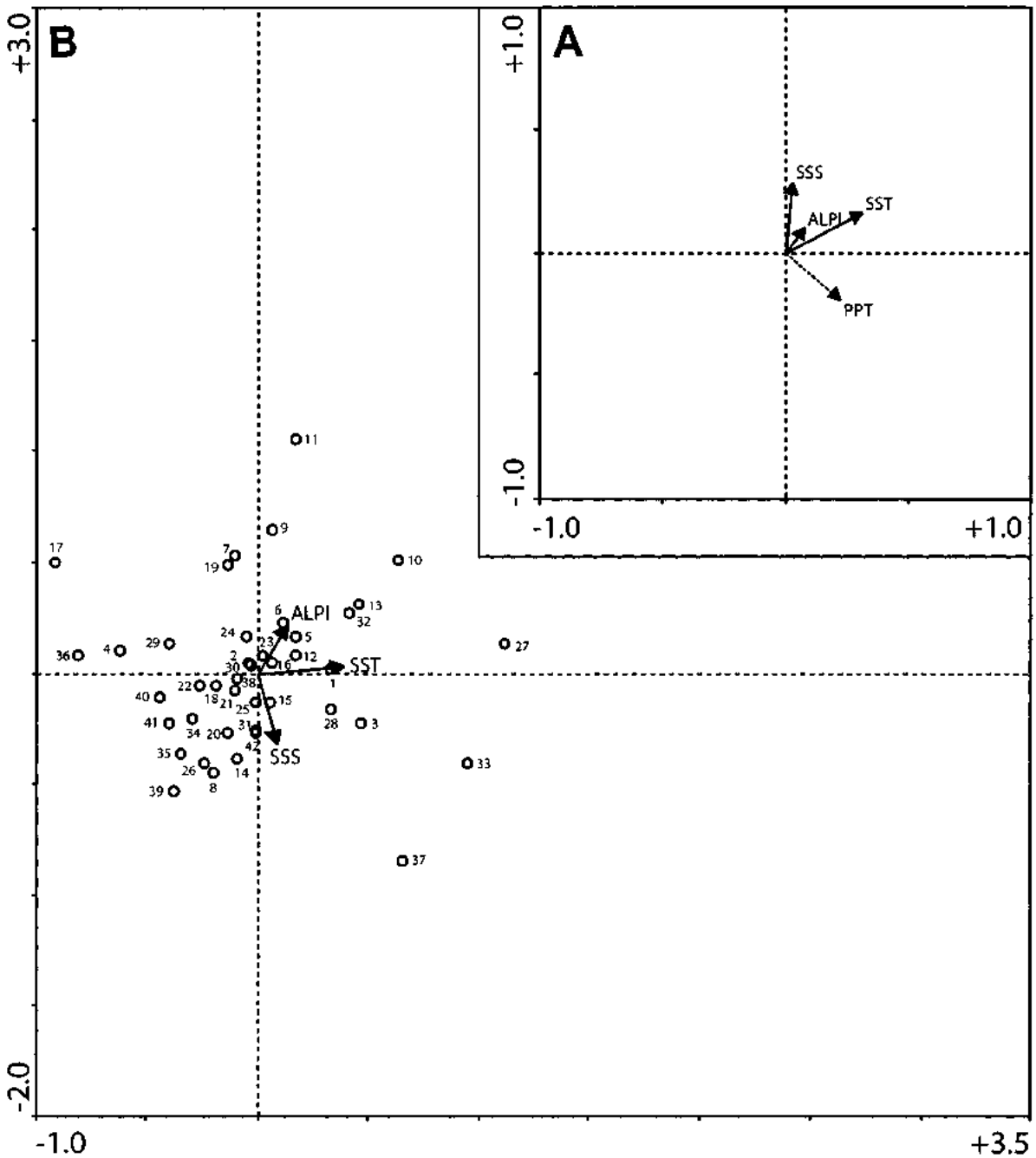

FIGURE 6.10. Detrended canonical correspondence analysis (DCCA) diagrams for 42 samples from freeze core TUL99B04. **A.** Positions of environmental vectors before the removal of PPT. **B.** Positions of sample points and environmental vectors after the removal of PPT.

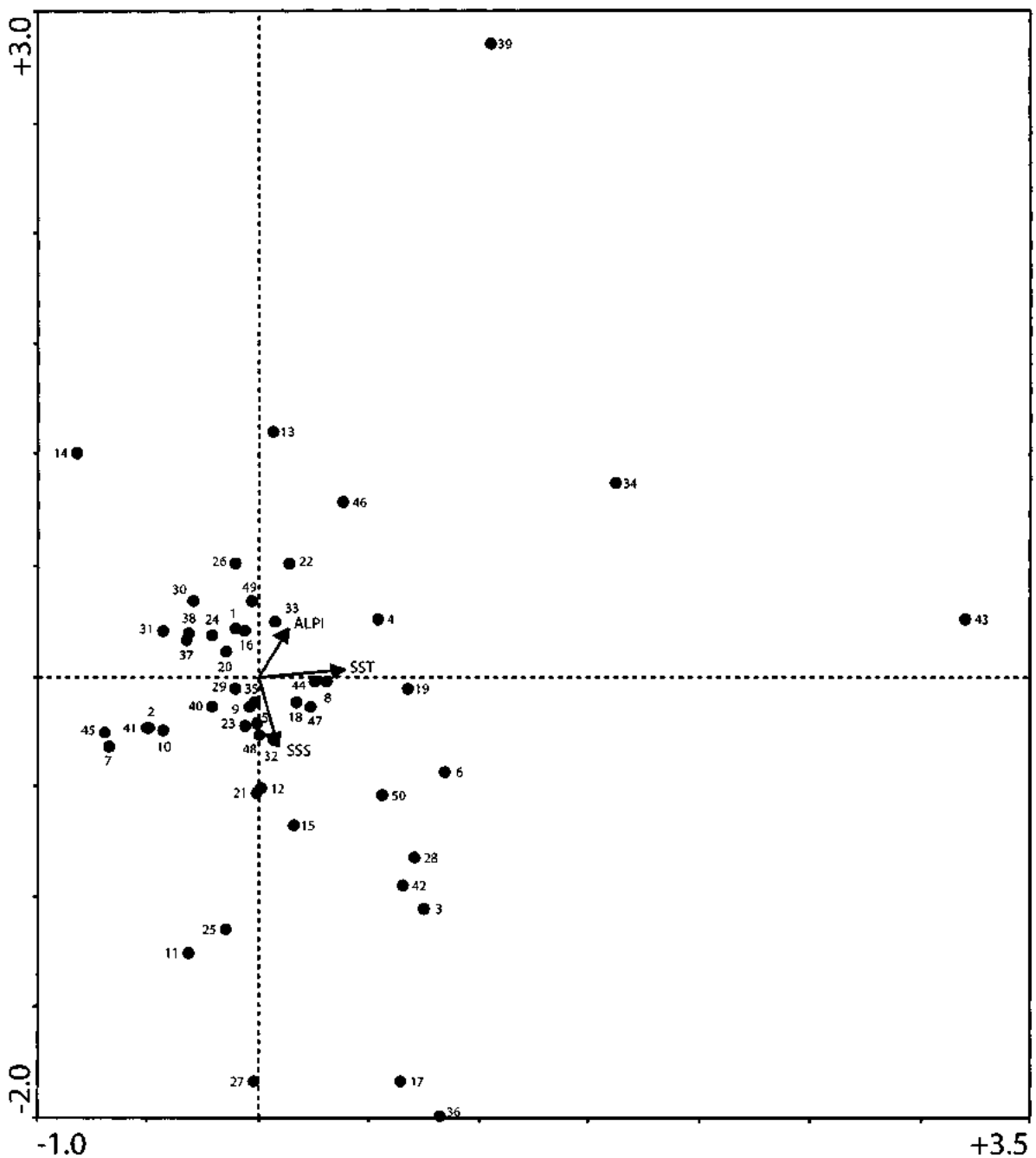

FIGURE 6.10 (continued). **C.** Positions of major diatom taxa from freeze core TUL99B04. Code numbers corresponding to taxa names listed in Table 6.1.

the low side of the temperature vector, and samples from the upper portion of the core plot on the relatively higher end of the temperature vector, following the temperature profile (Figure 6.3B). Samples B04-4, 10, 11, 17, 27, 33, 36 and 37 lie farther away from the origin of the diagram because these samples only covered a portion of the year. The species represented by these samples, and their environmental optima, are only representative of a couple of seasons and therefore show more extreme positions on the ordination diagram. Of these samples, B04-4, 11 and 17 sampled the winter and spring seasons (lower half of the couplets), and the positions of the samples lie toward the lower end of the temperature vector. Samples B04-10, 27 and 33 were taken from the summer and autumn seasons (upper half of the couplet), and the sample points lie on the right side of the ordination diagram. Sample B04-36 sampled the autumn to spring seasons, and therefore lies on the left side of the diagram, while sample 37 sampled the winter to summer seasons.

Diatom taxa are distributed mainly along the second axis of the ordination. By drawing perpedicular lines from the species points to the environmental vectors, the environmental optima of these taxa can be illustrated (Figure 6.10C). For instance, taxa such as *Thalassionema bacillare* (36), *Opephora mutabilis* (27), *Cyclotella chochtawhatcheeana* (11), *Nitzschia perminuta* (25), *Amphora copulata* (3), *Thalassiosira gravida* (42), *Paralia sulcata* (28), *Melosira nummuloides* (21), *Fragilaria investiens* (15) and *Cyclotella striata* (12) had optima on the high side of salinity. *Thalassiosira kushirensis* (43), *Tabellaria flocculosa* (34), *Gomphonemopsis lindae* (19) and *Asteromphalus sarcophagus* (4) had high temperature optima. Other diatoms, such as

Thalassiosira bioculata (39), *Ditylum brightwellii* (13), *Fragilaria capucina* (14), *Thalassiosira oestrupii* (46), and *Odontella longicruris* (26) appeared when ALPI was high (strong Aleutian Low). Diatoms such as *Tabularia fasciculata* (35), *Thalassionema nitzschioides* (37), *Skeletonema costatum* (32, 33), *Bacteriastrum delicatula* (5), and *Planothidium delicatulum* (29) are situated at the center of the ordination, with no particular environmental affinity.

The total abundance of diatoms appears to follow the sea surface temperature profile (Figure 6.3), with generally increased productivity from 1947–1958 and 1964–1970. Low productivity occurs from 1970–1972 with a gradual increase toward 1992. Low diatom abundance appears to coincide with lowered sea surface salinity and precipitation, and with episodes of negative ALPI, or a weakened low-pressure system (except in 1956). Low diatom abundance also occurs during episodes of negative SOI, or El Niño events (Figure 6.4). There is no visual correlation between diatom abundance and sunspot numbers.

Cyclostratigraphy

Using wavelet analysis, significant cycles have been detected in both the sediment grey value and absolute diatom abundance. Wavelet analysis of sediment grey value reveals annual cycles of 0.3 to ~1.5 cm thickness, giving a mean sediment accumulation rate of 0.61 cm/yr (Figure 6.11D). This is identical to the rate calculated using physical measurements of couplet thickness when only compacted couplets are considered, and is similar to the rate derived from ^{210}Pb dating, indicating that all three methods have

FIGURE 6.11. Wavelet scalograms for freeze core TUL99B04. Horizontal axis at the bottom represents the depth scale, vertical axes on scalograms represent the logarithmic scaled wavelength (or period); orange and yellow colours mark high wavelet coefficients (high spectral power or amplitude), and blue colour marks low wavelet coefficients (low spectral power or absent amplitude) at specific wavelengths at specific locations. Raw data are provided in Appendices G5 and G6. **A.** Three most pronounced (strongest local wavelet coefficients) wavelengths in diatom abundance. Dotted line denotes the 11-year cycle. **B.** Scalogram of diatom abundance in the time domain. **C.** Scalogram of diatom abundance in the depth domain. **D.** Scalogram of x-ray sediment grey value in the depth domain. **E.** Absolute abundance of diatoms plotted against depth, as in Figure 6.4B. **F.** X-radiograph positive image as from Figure 6.4A.

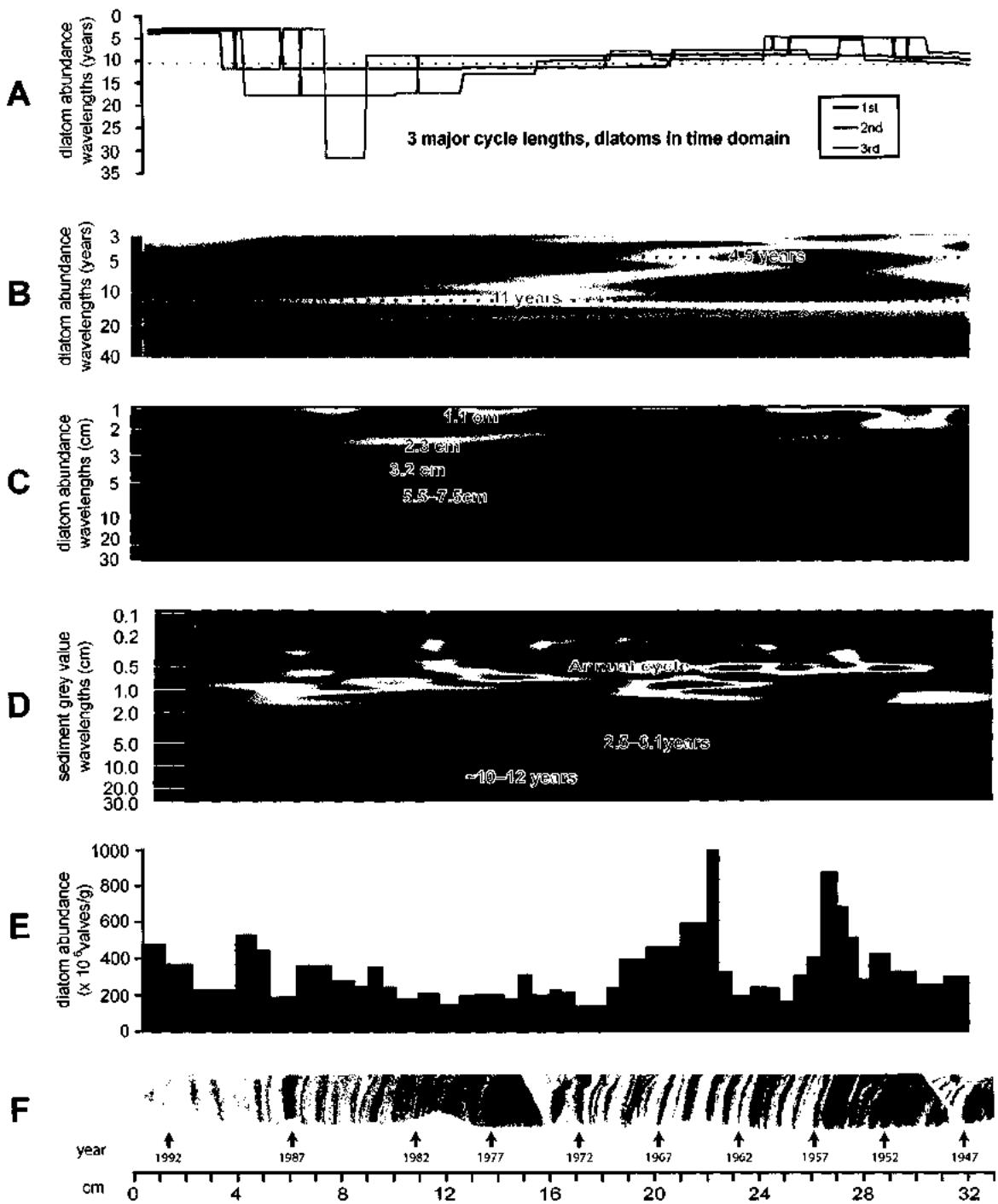
A
diatom abundance wavelengths (years)
0
5
10
15
20
25
30
35
3 major cycle lengths, diatoms in time domain
1st
2nd
3rd
B
diatom abundance wavelengths (years)
3
5
10
20
40
4-5 years
11 years
C
diatom abundance wavelengths (cm)
1
2
3
5
10
20
30
1.1 cm
2.3 cm
3.2 cm
5.5–7.5cm
D
sediment grey value wavelengths (cm)
0.1
0.2
0.5
1.0
2.0
5.0
10.0
20.0
30.0
Annual cycle
2.5–3.1years
~10–12 years
E
diatom abundance (x 10⁶valves/g)
1000
800
600
400
200
0
F
year
1992
1987
1982
1977
1972
1967
1962
1957
1952
1947
cm
0
4
8
12
16
20
24
28
32

detected the annual cycle. According to this rate, there are also significant and stationary ~10–12 year cycles (~12–15 cm), and weaker ~2.5–6 year cycles (4.8–8 cm) in sediment grey value (Figure 6.11D).

In diatom abundance, significant cycles occur at 1.1 cm, 2.3 cm, 3.2 cm and 5.5–7.5 cm in the depth domain, and 3 years, 4.5 years, and 9–11 years in the time domain (Figure 6.11A, B, C). There are also longer wavelength cycles at 17 years and 31 years of diatoms in the time domain (Figure 6.11A) but these cycles are of weaker strength and less confidence can be assigned to them. These long cycles may also be anomalous or unrepresentative of the diatoms quantified because the measured section was only 32 cm long and covered only 46 years.

When diatom abundance and sediment grey value are transformed into the time domain and compared with historical records of sunspot activity and El Niño occurrences, some trends are visible. Maximum amplitudes of the 10–12 year cyclicity in sediment x-ray grey values correspond to three of the five cycles of maximum sunspot number from 1947–1993 (Figure 6.12A, B). However, there is no visual relationship between grey values, sediment accumulation rate and sunspot number. El Niño years of climatic importance for British Columbia do not appear to show good correspondence with sediment accumulation rates (Figure 6.12 D). Maximum diatom abundance does not appear to coincide with sunspot activity (Figure 6.12A, C), but periods of low diatom abundance generally coincide with El Niño events. The 1958 El Niño correlates with maximum sunspot activity while the strong 1983 El Niño corresponds with a sunspot low. Consequently, a direct or slightly phase-shifted relationship between El Niño and

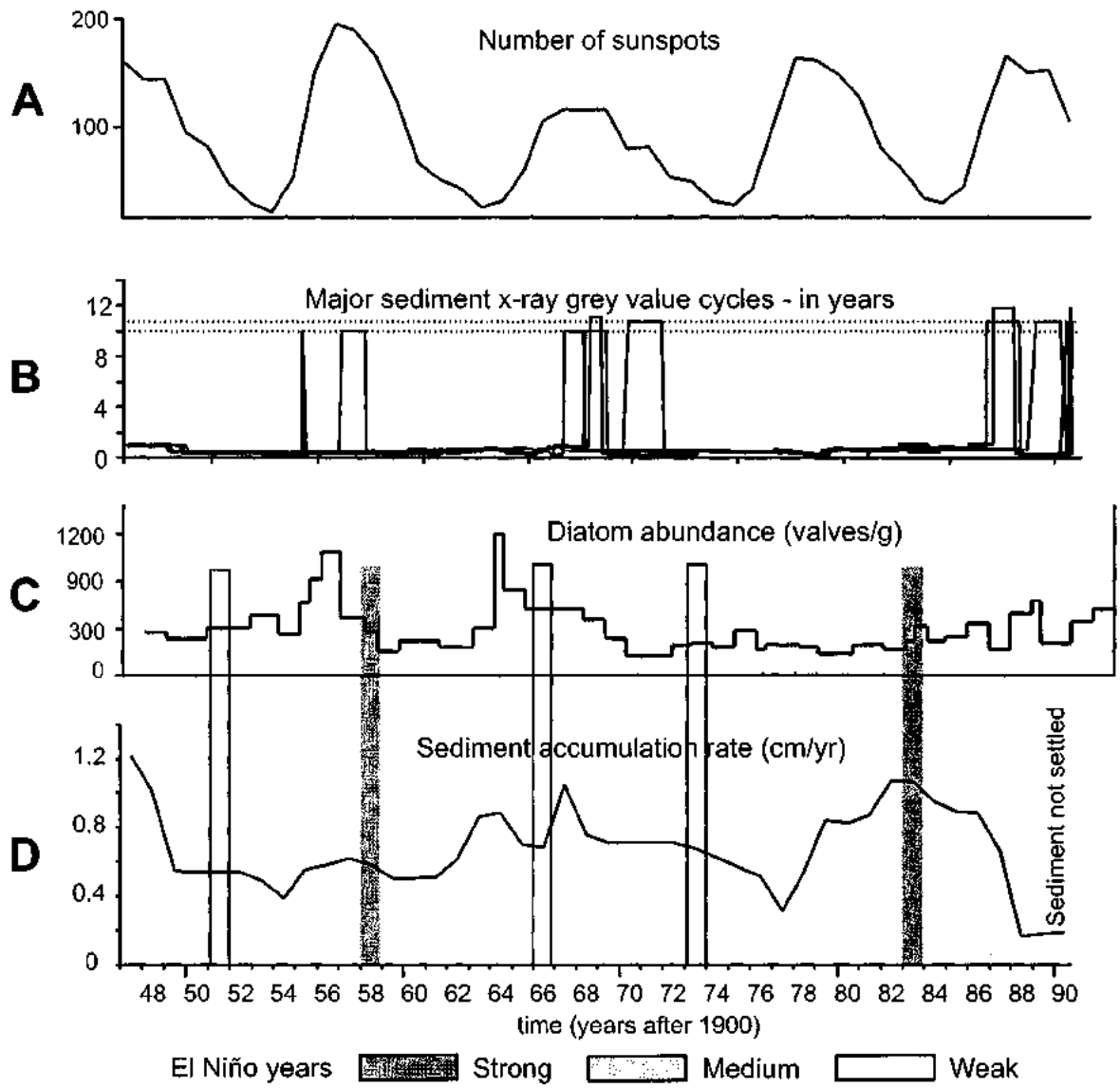

FIGURE 6.12. Diatom and sediment data transformed into the time domain with comparisons to sunspot activity and El Niño events. Raw data are provided in Appendices G5 and G6. **A.** Sunspot numbers as from Figure 6.3G. **B.** Major sediment grey values (in years). **C.** Diatom abundance (in millions of valves/g). **D.** Sediment accumulation rate (cm/yr) based on scans from x-radiograph positive images.

the 11-year sunspot cycle is not evident from this record.

Spectral analysis extracts the frequencies at which significant cycles occur. Sediment grey values show significant periodicities at 5.5, 11 and 22 years while diatom abundance has significant cycles at 4.9, 11 and 31 years (Figure 6.13A). Using cross-spectral analysis to compare the diatom abundance and sediment grey value shows correlations not visible in the linear comparison between the two components from Figure 6.12. In cross spectral analysis, maximum diatom abundance is shown to occur 2–3 years earlier (positive phase) than mean annual sediment grey value at the 5.5 year waveband (Figure 6.13B). At the 11-year waveband, maximum diatom abundance occurs 1–2 years later than mean annual sediment gray value.

DISCUSSION

Diatom Preservation and Comparison with Sediment Trap Material

A comparison between the absolute abundance of diatoms from sediment trap material with diatoms in the sediment record reveals that only a few percent of the diatoms in the water column are preserved in the sediments. If the diatom concentrations from each sediment trap sample spanning one year (e.g., from 29 May 1999 to 24 May 2000) were summed, then the number of valves theoretically reaching the sediments would be ~6.53×10^9 valves/g for one year of deposition (Appendix E2). The mean diatom concentration, however, from the 42 freeze core samples representing more or less annual deposition, is 3.40×10^8 valves/g per year (Appendix G2). This accounts for an average of only ~5% of the annual production falling through the water column being

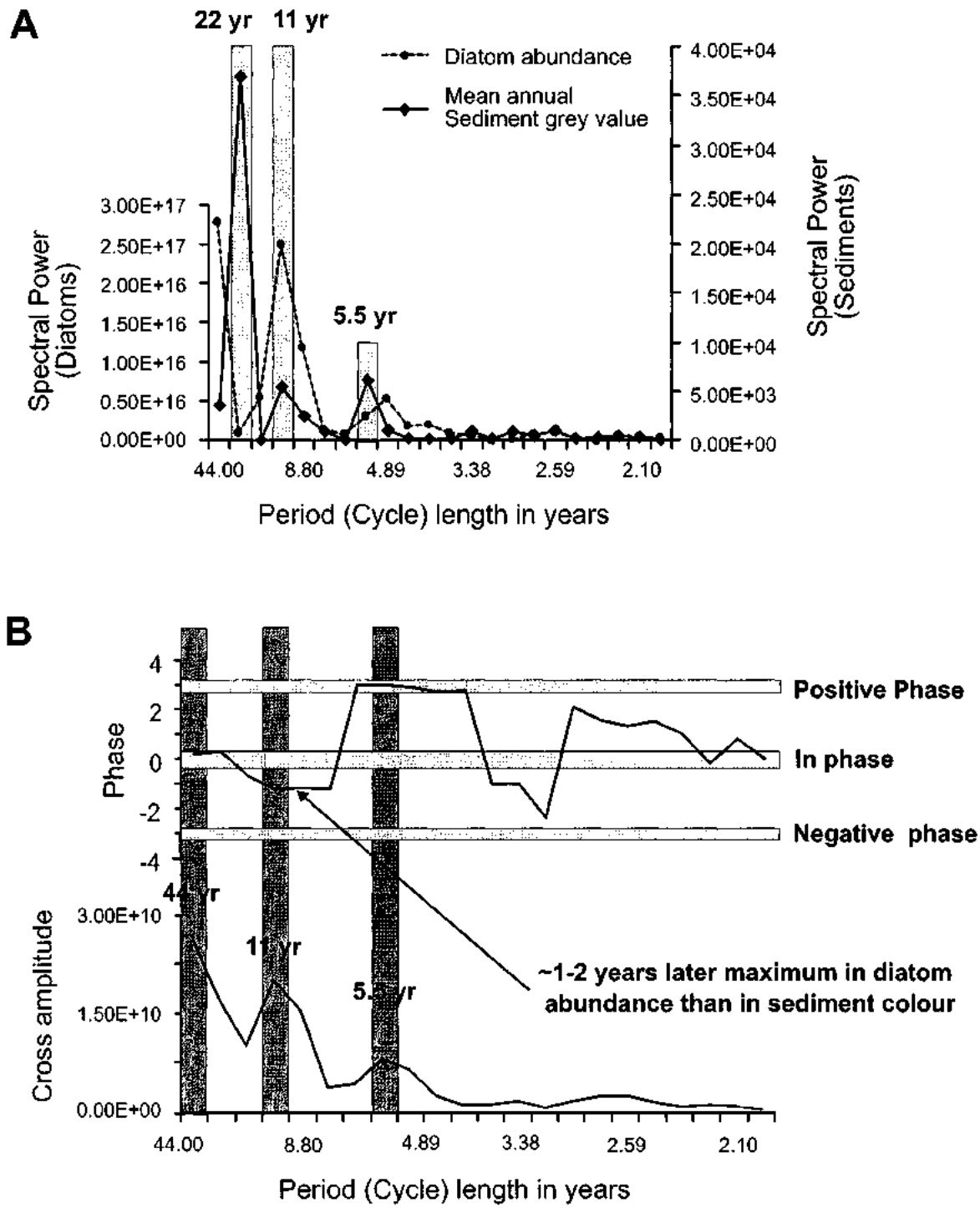

FIGURE 6.13. Spectral (**A**) and cross spectral (**B**) analysis of diatom abundance and sediment grey value cycle frequencies.

preserved in the sediments. Takahashi (1986) found that diatoms at Station Papa show no significant dissolution through the water column from material collected at depths of 1000 and 3800 m. He suggests that the good preservation of diatoms at the deeper trap is attributable to rapid export of the diatoms from shallow waters to deeper waters via mucus protection of the frustules (cf. Alldredge and Gotschalk, 1989). However, once the diatoms are incorporated in the sediments, Takahashi (1986) found that absolute abundance was substantially reduced, with only 1.95% of sinking diatoms found in surface sediments. Dissolution and preferential preservation were the main selecting factors determining which taxa were found in the sediments.

It is difficult to understand why certain diatom taxa are preferentially preserved while others are not. It is known that lightly silicified diatoms such as *Chaetoceros* vegetative cells are susceptible to dissolution and fracturing and are therefore rarely found in the sediments. However, other lightly silicified diatoms such as *Skeletonema costatum* represent the most abundant diatoms in both sediment trap and freeze core samples, whereas various *Thalassiosira* species (e.g., *T. nordenskioeldii, T. pacifica*) actually increased in relative abundance in the sediments. This is most likely due to the relative decrease in the abundance of other taxa. The occurrence of other diatoms, such as the moderately silicified *Fragilaiopsis atlantica*, which had a relative abundance of up to 41% in the sediment trap samples but < 2% in freeze core samples, may be completely unrelated to dissolution effects and may actually reflect the spatial or temporal distribution of such diatom species. Similarily, *Achnanthes minutissima* reaches up to 9% in sediment trap samples, but only ranges from 1-2% in freeze core samples. Still other

diatoms, such as the lightly silicified brackish water pelagic species *Cyclotella choctawhatcheeana*, which showed a gradual disappearance through time in the freeze core samples, appear to reflect changing environmental conditions, instead of dissolution, affecting the abundance of such species. Alternatively, because percentage data are susceptible to the relative changes of a species within a sample, percentages can be subjective depending on how the abundance of a dominant taxon changes (Takahashi, 1987). Indeed, a more detailed and rigorous study of the effects of dissolution and preservation between diatoms in the water column and in the sediments is required, as well as how lightly silicified and robust species react to dissolution and burial within the sediments (cf. Roelofs, 1983).

Interannual Variability of Diatom Assemblages from 1947–1992

The absolute abundance of total diatoms appears to follow the sea surface temperature profile from Amphitrite Point (Figure 6.3A,B). Instrumental records from around the Pacific Ocean indicate that large-scale multidecadal temperature cycles have occurred throughout the 20th century. These 20–70 year cycles, or the Pacific Decadal Oscillation (PDO), are poorly understood and appear to arise from global-scale teleconnections (Mann et al., 1995; Ware and Thomson, 2000). The effects of the 1950–1975 cool PDO phase and the 1975–1992 warm PDO phase are visible on the environment profiles from the vicinity of Effingham Inlet (Figure 6.3B-F, H). The diatom abundance profile at Effingham Inlet reflects the general productivity trends dictated by the cool and warm PDO regimes.

Some diatom species in Effingham Inlet appear to be responding to the environmental regime shift of the mid-1970s. Several brackish water species appear to decrease in abundance throughout the study interval. The most dramatic decrease occurs in *Cyclotella choctawhatcheeana*, which disappears after ~1980. This taxon may experience extreme environmental sensitivity where the general decrease in surface salinity in the mid-1970s onward caused the demise of this diatom in the inlet. A shift back to the cool regime after the mid-1990s likely caused a reintroduction of *C. choctawhatcheeana* and its appearance in recent sediment trap samples. The increase in abundance of species such as *Pseudonitzschia multiseries* and *Thalassiosira* cf. *leptopus* after the regime shift may signify that these species are partial to the broad environmental conditions represented during the warm phase. The isolated abundance peaks seen in the profiles of *Thalassionema nitzschioides* (~1968/1969) and *Thalassiosira kushirensis* (~1963/1964) are difficult to explain, but may represent an isolated influx of these species into the inlet from oceanic sources, or favorable environmental conditions supporting the proliferation of these species due to the cool regime of the PDO.

Apical spines (processes) from the oceanic diatom *Rhizosolenia* are present in the sediments from 1947–1992 (Figure 6.6), and are also present in sediment trap samples (Figure 5.7). *Rhizosolenia* spp., however, are absent from sediments further down in the sediment record, as is evident from the thin section record (Chapter 4) and annual sampling from a sediment slab dated ca. 4450 yBP (Chapter 7). McQuoid and Hobson (1997) found that *Rhizosolenia* spp. appeared suddenly ca. 1940 in Saanich Inlet freeze cores dated 1900–1991. It is unfortunate that the Effingham Inlet freeze core laminated

records are truncated by the 1946 earthquake massive interval. It has been postulated that *Rhizosolenia* spp. are a recent arrival in British Columbia waters, and were either carried into the area via the ballast waters of transport ships (Hallegraeff and Bolch, 1992), or imported with aquaculture species (Quayle, 1988). Both aquaculture and ship travel increased during the 1930s and 1940s in British Columbia (McQuoid and Hobson, 1997). To that end, the disappearance of *C. choctawhatcheeana* from the inlet, which delineates a natural environmental change in the region, and the appearance of *Rhizosolenia* spp., which delineates anthropogenic influence, can be used as marker species for correlating other sediments of similar age in the southern Vancouver Island region.

Diatom Assemblages and Environmental Variables

Based on the species variability in each sample, the position of the sample points plotted on the DCCA ordination diagram reflect the environmental conditions present during each sampling interval (Figure 6.10B) and matches well with the profiles of total diatom abundance and environmental variables (Figure 6.3). During the 1950–1975 cool PDO phase, many samples occurring at this time plotted on the low side of the temperature vector, with the exceptions of samples B04-28 and 33. Meanwhile, samples representing only partial years (B04-33, 37) plotted at higher temperature ranges because these samples only covered the spring and summer months. Likewise, during the 1975–1992 warm PDO phase, samples occurring at this time plotted on the higher side of the temperature vector, except for samples covering the colder seasons of partial years (e.g., B04-4, 17). Other relationships between samples and environmental variables are

also displayed on the ordination. For example, sample B04-11 is plotted high on the ALPI vector. Although this sample only covered a portion of the year, it coincided with a particularly strong positive ALPI anomaly (Figure 6.3). Sample B04-9, which covers one year of deposition, also plots relatively high on the ALPI vector. This sample also shows low salinity and moderate temperature affinities of the warm phase (compare Figures 6.3 and 6.10). Sample B04-39 shows a high affinity for salinity, but coincides with a negative ALPI and low temperatures of the cool PDO phase. These results show that DCCA is a useful tool for portraying the environmental affinities of samples derived from different times in the last 50 years, and also for differentiating samples covering one year or multiple years of deposition from samples covering only a partial year.

Species distribution on the ordination diagram reflects environmental data provided for 1947-1992 (Figure 6.10C). For instance, many species plotted on the high end of the salinity vector are marine and brackish water taxa, such as *C. choctawhatcheeana*, *Cyclotella striata*, *Fragilariopsis cylindriformis*, *Nitzschia perminuta*, *Opephora mutabilis*, *Melosira nummuloides* and *Paralia sulcata*. Species plotted at the high end of the temperature vector represent a variety of ecologies. *Asteromphalus sarcophagus* is usually a warm-water taxon, but also has distributions in temperate regions (Simonsen, 1974). Other diatoms are not as well correlated with temperature. The environmental affinities of *Gomphonemopsis lindae* are not well known, but this diatom prefers brackish waters. *Tabularia flocculosa*, a planktonic freshwater diatom, was described as found mainly in deep lakes in British Columbia (Cumming et al, 1995). *Thalassiosira bioculata* and *Thalassiosira kushirensis* have

affinities for moderate water temperatures (9-13 °C) and salinities (23-26‰) (Bérard-Therriault et al., 1999). *T. flocculosa*, *T. bioculata* and *T. kushirensis* show extreme positions on the high end of the temperature vector because each of these taxa has its relative maximum abundance in samples taken from a partial year. *T. flocculosa* and *T. bioculata* had maxima in sample B04-10 and *T. kushirensis* had a maximum in sample B04-27 (Appendix G3). *Thalassioisra gravida* is a cold water diatom (3 °C, Syvertsen, 1977) but plots on the high end of temperature. This diatom was rare throughout the sampling interval and had maximum relative abundance in sample B04-26 (Figure 6.10B; Appendix G3). The appearance of diatom taxa plotted on the high end of the ALPI vector is not as easy to explain. The intensity of the Aleutian Low increased at the same time SST increased after the mid-1970s. A few taxa represent warm- to temperate-water affinities; these include *Odontella longicruris*, *A. sarcophagus* and *Thalassionema pseudonitzschioides*. Many species are also oceanic, such as *Thalssionema nitzschioides*, *Rhizosolenia* spp. and *Pseudonitzschia multiseries*, which may have entered the inlet via pelagic water intrusions during increased storm activity. The appearance of other taxa, such as the dominant species *Minidiscus chilensis* and *Skeletonema costatum* (weak form), may benefit from increased storm activity disrupting stratification and bringing additional nutrients to the surface waters for extended production from early spring to late autumn (Haigh et al., 1992). It is interesting to see that freshwater and benthic taxa are underrepresented in this assemblage at high ALPI values because increased storm activity and subsequent runoff should lead to increased delivery of such taxa into the inlet as was seen in autumn and winter sediment trap samples. *Achnanthes minutissima*, a

benthic brackish water species, does plot on the positive end of the ALPI vector but is also not far from the origin of the diagram. Perhaps dissolution upon burial and reduction in abundance has muted the environmental signal of this and other similar taxa. Species plotted near the center of the ordination most likely represent cosmopolitan distributions and ecologies and are able to tolerate a wide range of environmental conditions, or represent taxa that have affinities for average temperature, salinity and winter storminess.

Cyclostratigraphy and Long-term Environmental Implications

Morlet wavelet analysis and spectral analysis have revealed prominent cyclicity displayed in both the sedimentary grey values (from x-radiographs) and total diatom abundance. The most pronounced cycles in the time domain are the annual cycle, the 2.5–6 year cycle and the 10–12 year cycle. The 2.5–6 year cycles correlate with known ENSO cyclicity whereas the 10–12 year cycles correlate with known sunspot cyclicity. These results have significant implications, suggesting that diatom productivity, and the resulting sedimentation pattern, are affected not only by large-scale ocean-atmosphere perturbations, but also by solar forcing on scales other than the annual cycle. The response of the diatoms to the sunspot cycle further supports recent findings that solar activity indirectly affects cloud formation and climate, solar irradiance received by the earth's surface and hence phytoplankton productivity and sedimentation patterns over long (millennial) time scales (Patterson et al., in review A; Patterson et al., in review B).

There are several lines of evidence that support the effect of ENSO on north Pacific and British Columbia waters. Tabata (1989) found that the most common periods

for interannual variability are 2.5 and 6–7 years in the northeast Pacific Ocean, based on long-term studies of ocean properties. Haigh et al. (1992) reported that there was a 7-year toxicity cycle for dinoflagellates in coastal British Columbia and attributes the cyclicity to ENSO. McQuoid and Hobson (1997) saw that *Skeletonema costatum* had a ~4-year cycle in abundance in Saanich Inlet in which high numbers of this taxon occurred between warm cycles of ENSO. In Effingham Inlet, the abundance of *S. costatum* dictates the total diatom abundance profile that is also ascribed to ENSO cyclicity.

Long-term fluctuations in ENSO have been attributed to modulation by solar cycles (Anderson, 1990; see review in Kemp, 1995). For example, decadal to millennial cycles of oxygen minimum zone intensity along the California margin, as described from bioturbated versus well-preserved laminated sediments, were attributed to solar cycles affecting longer-term alternations of El Niño and La Niña (Anderson et al., 1990). Sardine and anchovy populations over the last 2000 years in the California Current system show 50- to 60-year cycles (Baumgartner and Ferreira-Bartrina, 1993). Similar cycles were found in fish scale records from Effingham Inlet (Patterson et al., in review B). Pisias (1978) found that upwelling in the Santa Barbara Basin over the last 8000 years, as indicated by radiolaria, were correlated with the sunspot cycle, as determined from ^{14}C records.

According to the x-ray image and wavelet scalograms (Figure 6.11), the annual cycle of sedimentation is continuous and persistent throughout the late 20th century, only to be interrupted by the 1946 earthquake debris flow deposit. Based on total diatom abundance, the ENSO cycle, which is not as easily detected on the x-ray image, was

detected by wavelet analysis and appears to be most prominent from 1947 to the mid-1960s (red and orange colours) and then less prominent from the mid-1960s to the mid-1970s and again from the mid 1980s to the early 1990s (green colours). The least prominent cyclicity of ENSO took place from the mid 1970s to the mid 1980s (blue colours). ENSO cyclicity on the sediment grey value scalogram shows similar results where the cyclicity is prominent from 1947 to the mid 1970s.

The sunspot cycle is most prominent from 1947 to the early 1980s (red to yellow colours) and remains relatively strong throughout the length of the core, as indicated by both the diatom abundance and sediment grey value scalograms. Spectral and cross spectral analyses both reveal that the major periodicities center around the 11-year sunspot cycle and multiples of this cycle, suggesting again that solar activity exerts a major force on climate and phytoplankton productivity.

Both the ENSO and sunspot cycles are prominent from 1947 to the mid 1970s, suggesting that perhaps these cycles are related to the cool PDO regime, or that the ENSO cycles and the cool regime are regulated by sunspot activity combined with other environmental factors that are yet to be determined.

CONCLUSION

The late 20th century laminated record from Effingham Inlet indicates that diatom assemblages and sedimentation patterns are influenced by ocean-atmosphere fluctuations and long-term solar activity. The 1976–1977 temperature regime shift had a subtle effect on the coastal British Columbia environment and this shift is evident in the diatom

abundances and species compositions. Other than the 1946 earthquake layer, the continuously laminated record from 1947 to 1993 indicates that the bottom waters of the inner basin have been mainly anoxic during that interval to preclude bioturbation of the sediments by macrobenthos. Only intermittent dysoxia and suboxia have permitted low-oxygen tolerant benthic foraminifera to colonize the substrate (Patterson et al., 2000), although they do not cause enough bioturbation to homogenize the laminae. A longer record sampling below the 1946 earthquake layer is required to see what sedimentation patterns and cycles exist from the early 20th century and into the 19th century while there are still historical instrument records to refer to. Box core EFBC9703-2 from the inner basin does extend below the earthquake layer and is currently being analyzed by my colleague Murray Hay. The top of this core, however, only reaches to ~1983. In addition to this, freeze cores taken from the outer basin (TUL99B10 and TUL99B12) need to be examined in order to see differences in diatom composition and sedimentation along the length of the inlet. From these records, climate and environmental variability in the northeast Pacific Ocean can be assessed during modern industrialized times.

CHAPTER 7

HIGH-RESOLUTION DIATOM STRATIGRAPHY AND PALEOECOLOGY FROM A 62-YEAR, MID-HOLOCENE SEDIMENT RECORD

ABSTRACT

Diatom paleoecology and environmental interpretations were assessed from a 15-cm long sediment slab, which spanned at least 62 years, and was deposited approximately 4450 cal yr BP. The slab (Slab 8, core TUL99B03, depth 870-885 cm) shows a unique sedimentation pattern with thick diatom-rich couplets at the bottom, and thinner silt-rich couplets at the top. Annual-scale subsampling showed that the abundance of coastal marine diatoms, namely the weakly silicified form of *Skeletonema costatum*, decreased over the 62-year period, while benthic and brackish water diatoms, such as *Planothidium delicatulum*, increased with the concomitant increase in silt. The increase in such benthic species and silt is interpreted to represent progressively increasing precipitation over time. Samples plotted passively using detrended canonical correspondence analyses from a 20th century freeze core (TUL99B04) as a template show that the thicker couplets are associated with a strong Aleutian Low (AL) and high sea surface temperature (SST), and thinner couplets are associated with a weak AL and lower SST. The general environmental trend is indicative of the cool phase of the Pacific Decadal Oscillation. Cyclostratigraphic analyses based on sedimentation patterns and total diatom abundance reveal that significant cycles were detected at 2–5 year and 9–15 year intervals. These cycles may represent El Niño-Southern Oscillation and sunspot cycles, respectively, suggesting that large-scale ocean-atmosphere fluctuations and solar forcing had

significant influences on primary productivity and sedimentation patterns at ~4500 yr BP. The findings in this study show that significant environmental change can occur in a few decades, and can provide a basis for the study of modern climate change.

INTRODUCTION

In the previous three chapters, the composition and origins of laminae and sublaminae were described from piston core samples, modern-day biogenic flux was quantified from sediment traps, and recent sedimentation and diatom ecology was assessed from a 46-year long freeze core record. In this chapter, I return to the piston core sediment slabs to reanalyze the diatom content of the laminae at annual scale and relate sedimentation patterns and diatom abundances to ocean-atmosphere cycles based on evidence from the previous studies, as well as from cyclostratigraphic analysis.

For both the sediment trap and freeze core study, historical instrumental records were available for interpreting the occurrence of diatom species and assemblages. In this study, Slab 8 (depth in core 870-885 cm) was dated at approximately 4450 cal yr BP, so there is no historical record for comparison. In this situation, it would be ideal to produce a statistical model, or transfer function, based on known modern environmental variables and diatom compositions to infer past environmental conditions from the diatom assemblages in the sediment record. These transfer functions would be rigorously tested for precision through bootstrapping and jackknifing techniques, providing that the original model is well constructed, and that modern environmental and diatom data are accurate.

For the sediment trap and freeze core work, environmental data were gathered from several sites that were up to 50 km away from the inlet (Figure 5.1). Hence, the environmental data are explaining the appearance of certain diatom assemblages only by proxy, and do not represent actual *in situ* conditions at the time of biological production in the surface waters. Additionally, the gradient lengths in detrended correspondence analysis were short, indicating that either sampling did not cover the entire environmental gradient, or that the environmental data were not entirely suitable to explain the observed species. In this chapter, therefore, a transfer function is not constructed to infer past environmental conditions. Instead, the objectives of this study are to 1) explain interannual environmental variability based on sedimentation patterns and diatom ecologies, 2) use multivariate analysis from freeze core TUL99B04 as a template to interpret environmental conditions from ~4450 yr BP, and 3) define ocean-atmosphere cycles in sedimentation patterns and diatom abundance using cyclostratigraphy techniques.

METHODS AND MATERIALS

Slab 8 from piston core TUL99B03 was chosen for the high-resolution stratigraphic study (Figures 4.1, 4.4, 4.5H). The reasons for focusing on this slab are that the slab contains well-preserved laminae and the couplets also show a unique thinning upwards sequence. The sediments in this slab were also deposited during a climate state different from the sediments from the sediment traps and freeze core, and comparisons can be drawn between the two climate states.

Sample Processing for Diatom Analyses

After taking samples for thin section production, the remainder of Slab 8 had been kept refrigerated and wrapped in plastic wrap and aluminum foil for 23 months until it was ready to be processed. Throughout this time, the slab was periodically inspected to ensure that desiccation or distortion of the sediments had not occurred. Preservation of the slab throughout this time was remarkably good, and the slab was periodically sprayed with distilled water to maintain sediment moisture. When the slab was ready for subsampling, it was removed from its protective wrapping and sampled at an annual scale, i.e., the slab was subsampled as couplets (Figure 7.1). Working with a magnifying glass, a scalpel was used to separate the couplets, with care taken to minimize contamination between samples. As explained in Chapter 4, couplets are defined as one brown terrigenous lamina overlain by an olive green diatomaceous lamina. Thin (~1 cm) nonlaminated intervals were also sampled separately, as were indistinct couplets immediately below one of the intervals. The subsamples were then freeze dried and processed into microscope slides using the same procedures described in Chapters 5 and 6. Dilution factors of 5 and 15× were used for each slide.

Microscopy

Microscope techniques follow the procedures described in Chapter 5. At least 30 fields of view were counted for all of the slides, except for three (S8-18, 36, and 50) where diatoms were more abundant. The relative and absolute abundance of microfossils were calculated using equations 5.1 and 5.2.

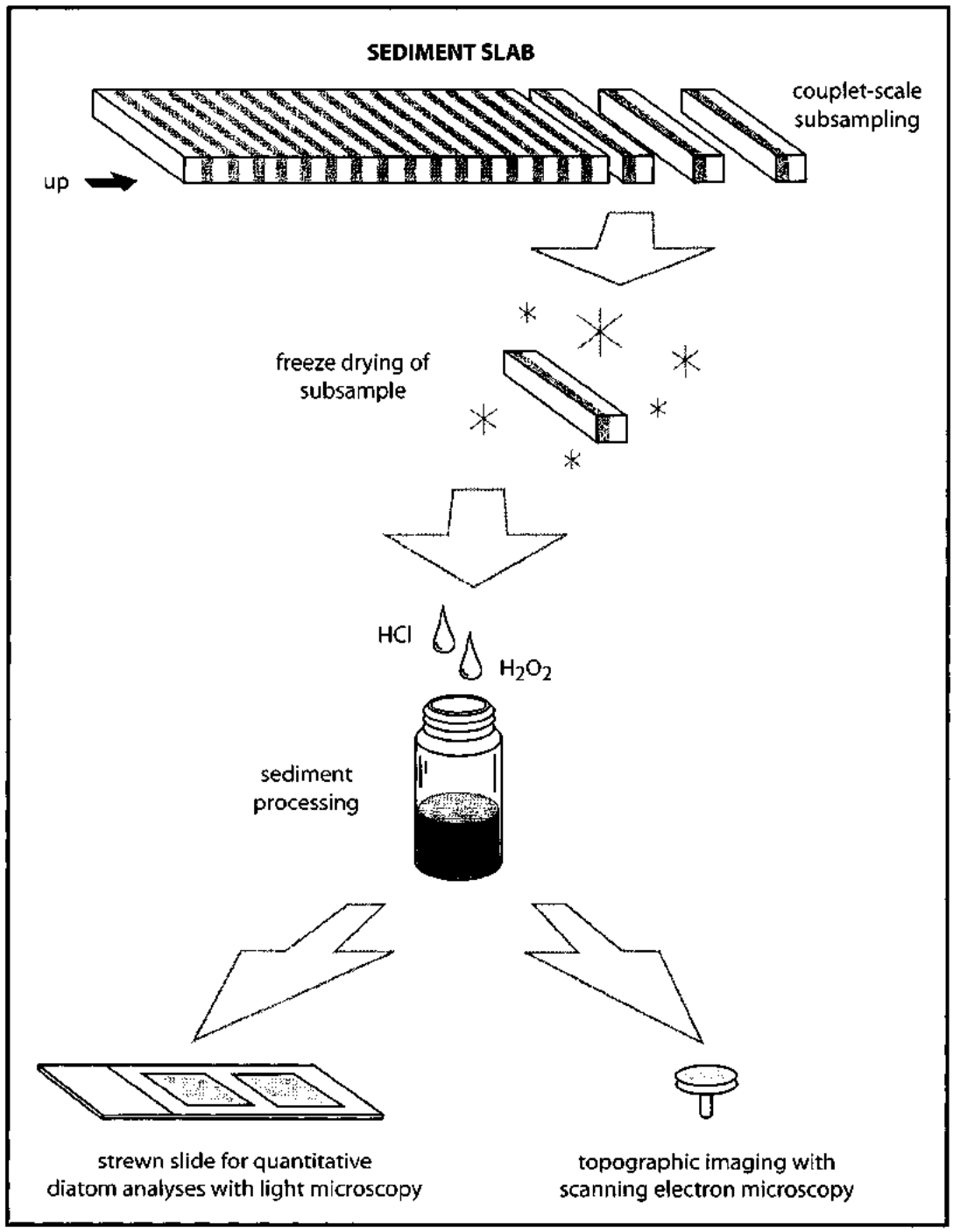

FIGURE 7.1. Schematic diagram showing the processing of subsamples from a sediment slab. No scale is intended.

STATISTICAL ANALYSES

Data Screening

Data were screened and analyzed in a manner similar to that described in Chapter 5. A total of 226 diatom taxa were identified from the sediment slab (not including resting spores). To reduce the number of rare taxa, the data were screened to include only taxa that appeared in at least three samples, and had a relative abundance of at least 1% in one sample. As a result, 64 taxa remained (Table 7.1).

Ordination

The final detrended canonical correspondence analysis (DCCA) plot from freeze core TUL99B04 was used as a template for plotting the species variance from Slab 8. In order to do this, an assumption must be made that environmental conditions from the late 20th century can be used to explain environmental conditions at ~4450 cal yr BP (i.e., that environmental conditions during these two time intervals were similar). It is known, however, that conditions at ~4450 yr BP were slightly warmer than during modern times, and that diatom productivity has been steadily decreasing over the last 5000 years (Figure 4.14; Hay and Pienitz, submitted). With no other basis for comparison, however, I still chose to compare Slab 8 and freeze core TUL99B04, if not for similarities in environmental conditions, then for the known difference.

Only taxa that were found in common to both freeze core and sediment slab sample sets were used. As a result, only 35 taxa were used in the ordination (Table 7.1). Samples for Slab 8 were given neutral (zero) readings for environmental variables that

TABLE 7.1. Diatom taxa occurring in at least three samples and ≥1% in at least one sample. Abbreviations correspond to taxa appearing in final DCCA plot (see Figure 7.7B)

	Achnanthes kriegeri Krasske 1943
	Achnanthes lemmermannii Hustedt 1933
A.min	*Achnanthes minutissima* Kützing 1833
	Achnanthidium biasolettianum (Grunow in Cleve and Grunow) Round & Bukhtiyarova 1996
	Actinocyclus curvatulus Janisch in A. Schmidt 1878
	Actinoptychus vulgaris Schumann 1867
	Amphora acutiuscula Kützing 1844
	Amphora copulata (Kützing) Schoeman & Archibald 1986
	Asteromphalus heptactis (Brébisson) Ralfs in Pritchard 1861
B.del	*Bacteriastrum delicatulum* Cleve 1897
	Cocconeis costata Gregory 1885
C.scu	*Cocconeis scutellum* Ehrenberg 1838
C.cho	*Cyclotella choctawhatcheeana* Prasad 1990
C.str	*Cyclotella striata* (Kützing) Grunow 1880
	Cyclotella sp. (S8-6)
	Diatomella minuta Hustedt in A. Schmidt, Atlas 1874
D.bri	*Ditylum brightwellii* (West) Grunow in van Heurck 1883
	Eunotia spp. Ehrenberg 1837
F.inv	*Fragilaria investiens* (W. Smith) Cleve-Euler
	Fragilaria pinnata Ehrenberg 1843
F.sop	*Fragilaria* cf. *soptonensis* Witkowski and Lange-Bertalot 1993
	Fragilariopsis atlantica Paasche 1961
F.cyl	*Fragilariopsis cylindriformis* (Hasle in Hasle & Booth) Hasle
F.pse	*Fragilariopsis pseudonana* (Hasle) Hasle 1993
G.lin	*Gomphonemenopsis lindae* Witkowski, Metzelin and Lange-Bertalot in Metzelin and Witkowski 1996
G.obs	*Gomphonemopsis obscurum* (Krasske) Lange-Bertalot
	Grammatophora angulosa Ehrenberg
	Grammatophora oceanica Ehrenberg 1841
M.num	*Melosira nummuloides* (Dillwyn) C.A. Agardh 1824
M.chi	*Minidiscus chilensis* Rivera and Koch 1984
	Navicula gregaria Donkin 1861
N.per	*Navicula perminuta* Grunow in Van Heurck 1880
	Nitzschia fonticola Grunow in Cleve & Möller 1879
N.fru	*Nitzschia frustulum* (Kützing) Grunow in Cleve and Grunow 1880
O.lon	*Odontella longicruris* (Greville) Hoban 1983
	Opephora cf. *horstiana* Witkowski 1994
	Opephora marina (Gregory) Petit 1888
	Opephora minuta (Cleve-Euler) Witkowski, Lange-Bertalot & Metzeltin 2000
O.mut	*Opephora mutabilis* (Grunow) Sabbe and Vyverman
P.sul	*Paralia sulcata* (Ehrenberg) Cleve 1873
P.del	*Planothidium delicatulum* (Kützing) Round and Bukhtiyarova 1996
	Planothidium hauckianum (Grunow) Round & Buktiyarova 1996
P.mul	*Pseudonitzschia multiseries* (Hasle) Hasle 1995

TABLE 7.1. (continued)

	Pseudonitzschia seriata (Cleve) H. Peragallo in H. and M. Peragallo 1897-1908
S.cos	*Skeletonema costatum* (Greville) Cleve 1878
S.cosw	*Skeletonema costatum* (Greville) Cleve 1878 (weak form)
T.flo	*Tabellaria flocculosa* (Roth) Kützing 1844
T.fas	*Tabularia fasciculata* (Agardh) Williams and Round 1986
T.bac	*Thalassionema bacillare* (Heiden) Kolbe 1955
T.nit	*Thalassionema nitzschioides* (Grunow) Mereschkowsky 1902
T.pse	*Thalassionema pseudonitzschioides* (Schuette and Schrader) Hasle in Hasle and Syvertsen 1996
	Thalassiosira binata Fryxell
	Thalassiosira conferta Hasle in Hasle and Fryxell 1977
T.dec	*Thalassiosira decipiens* (Grunow) Jørgensen 1905
T.ecc	*Thalassiosira eccentrica* (Ehrenberg) Cleve 1904
T.gra	*Thalassiosira gravida* Cleve
T.lep	*Thalassiosira* cf. *leptopus* (Grunow) Hasle and Fryxell 1977
	Thalassiosira minima Gaarder 1951
T.nor	*Thalassiosira nordenskioeldii* Cleve 1873
T.pac	*Thalassioisra pacifica* Gran and Angst 1931
	Thalassiosira rotula Meunier 1910
T.ten	*Thalassiosira tenera* Proschkina-Lavrenko 1961
	Thalassiosira sp. (S8-23) (cf. *T. eccentrica*)
	Thalassiosira sp. (S8-27)

were used from the freeze core. The samples were then plotted as passive (supplemental) variables in the final freeze core DCCA ordination.

RESULTS

Sediment Description

As described in Chapter 4, Slab 8 contains well-preserved laminae, and the couplets show a distinct thinning upward trend. Compaction of sediments at the depth at which this slab was recovered is not an important issue, so thickness of couplets from the bottom and top of the slab can be compared directly. Sediment accumulation rates (or couplet thickness) in this slab range from 0.8 to 3.5 mm/yr, with a mean rate of 1.82 mm/yr (Table 4.3; Appendix B2). At least 62 well-defined couplets have been identified from inspection of the slab itself and from the thin sections (Appendix D, Slides 8A-E), although the top 13 mm of the thin section record are missing due to damage of the sediment during the epoxy embedding process.

Sedimentary couplets are thicker (2–3 mm) at the bottom of the slab than at the top of the slab (1–2 mm). The thicker couplets at the bottom of the slab contain thicker diatomaceous laminae than the thinner couplets toward the top of the slab. Near monospecific sublaminae containing *Skeletonema costatum* and *Chaetoceros* resting spores are thicker and more common in the thicker couplets (Appendix D, Slides 8A–E). As the couplets become thinner toward the top of the slab, near monospecific laminae become thinner and silty diatomaceous laminae become thicker and more common. The general trend shows that terrigenous debris become more prominent in the thinner

couplets as diatomaceous laminae become thinner at the top of the slab. The thickness of terrigenous laminae shows no trends (Appendix B2, Appendix D).

There are three thin nonlaminated intervals, each approximately 1 cm thick, situated at the bottom, middle and top of the slab (Figure 7.2). These intervals have sharp and bedding-parallel contacts, and a homogeneous texture and brown colour in hand sample. No grading was evident in the upper- and lowermost intervals at both the macroscopic and microscopic levels. Subtle normal grading was seen in thin section in the middle interval where slightly larger wood fragments and terrigenous debris were found near the base. All nonlaminated intervals are composed of a mixture of silt, organic debris and diatom remains. This composition appears to be between that of terrigenous and diatomaceous laminae.

Diatom Abundance and Assemblages

The mean abundance of diatoms counted from the 67 samples is estimated at 4.53×10^8 valves/g (Figure 7.2; Appendix H2). The highest abundance occurs in sample S8-64 (1.38×10^9 valves/g) and the lowest is in sample S8-59 (7.63×10^7 valves/g). The mean abundance of *Chaetoceros* resting spores (CRS) is estimated at 1.26×10^8 valves/g. Highest abundance occurs in sample S8-33 (4.83×10^8 valves/g) and the lowest occurs in sample S8-31 (2.05×10^7 valves/g). Mean silicoflagellate abundance is 3.65×10^6 skeletons/g, with the highest abundance in sample S8-53 (1.24×10^7 skeletons/g) and the lowest in samples S8-18 and 24 where no silicoflagellates were counted. There is a general decrease in diatoms, CRS and silicoflagellates toward the top of the slab,

FIGURE 7.2. X-ray positive image of Slab 8, core TUL99B03, and diatom abundance. **A.** Couplet labels from thin section analyses (Appendix D). Thin sections did not cover the top 1.3 cm of the slab due to loss of sediment during the epoxy embedding process (Chapter 4). Couplet labels with a single asterisk represent 4-component couplets; double asterisks represent 3-component couplets (Chapter 4, Appenidx D). **B.** X-radiograph positive image. **C.** Subsample labels for high-resolution diatom analyses. Each couplet represents one year of deposition; most diatom subsamples are equivalent to the thin section couplet designations, except in the nonlaminated interval at 876.7–878.2 cm, where extra subsamples were taken to determine the composition of slightly different textures visible in the interval. **D.** Total diatom abundance (millions of valves/g of dry sediment).

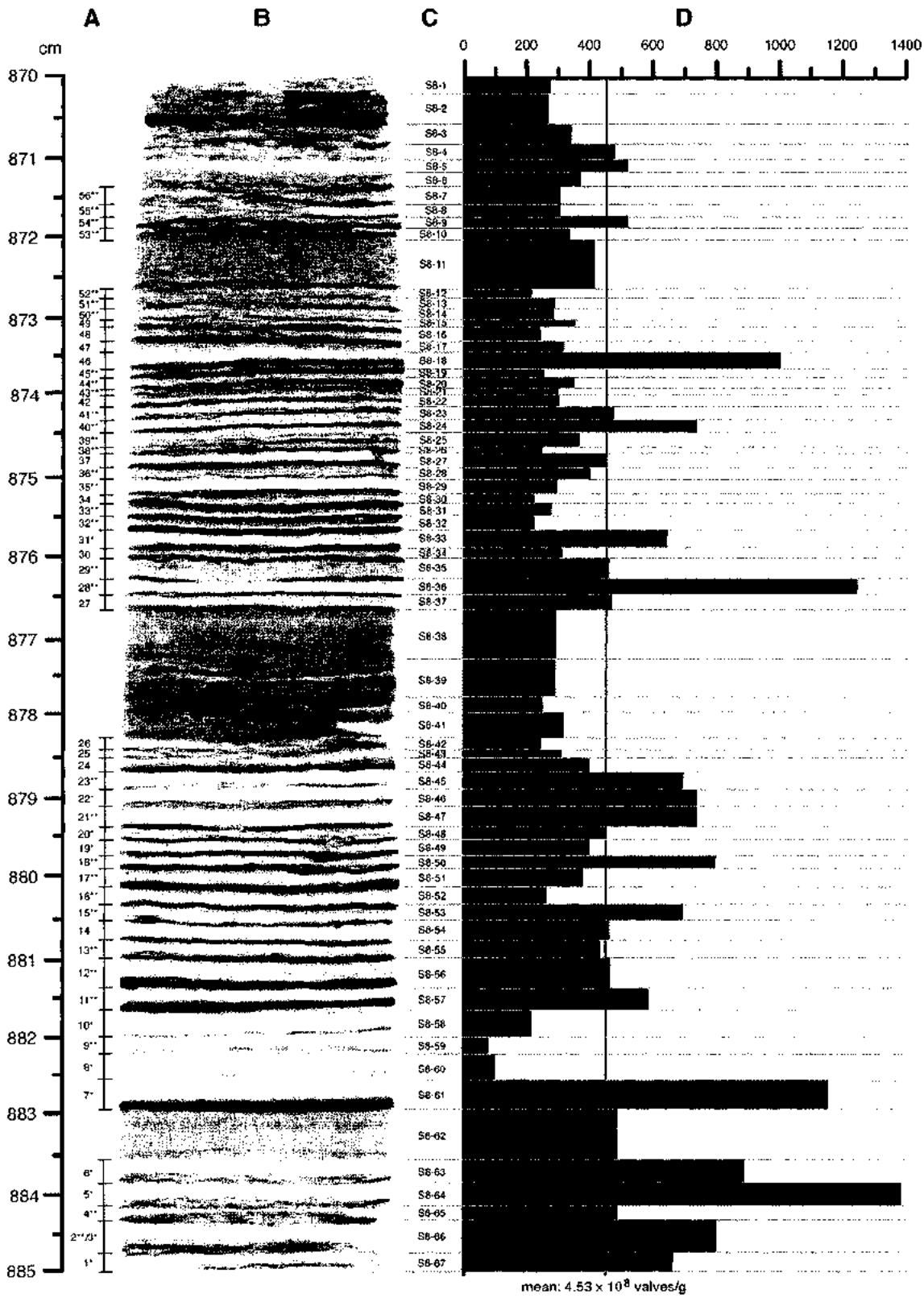
A
B
C
D
cm
870
871
872
873
874
875
876
877
878
879
880
881
882
883
884
885
0
200
400
600
800
1000
1200
1400
mean: 4.53 x 10^8 valves/g

following the thinning upward pattern of the couplets (Figures 7.2, 7.3, 7.4).

The weakly silicified form of *Skeletonema costatum* is the most dominant taxon at the bottom of the slab, with a maximum relative abundance of 82% and absolute abundance of 9.52×10^8 valves/ g (sample S8-61). Other dominant diatoms, all of which have concentrations greater than 1×10^8 valves/g are, in order of decreasing abundance, *Skeletonema costatum* (nominal or robust form), *Thalassiosira nordenskioeldii*, *Thalassiosira decipiens*, and *Fragilariopsis pseudonana*. Other dominant taxa include *Thalassionema nitzschioides* (maximum abundance 9.58×10^8 valves/g) and *Thalassiosira pacifica* (maximum abundance 8.50×10^8 valves/g) (Figures 7.5, 7.6, Appendices H3, H4).

Although total diatom abundance shows a general decrease as couplets become thinner toward the top of the slab, a comparison between brackish water taxa, total benthic diatoms and marine diatoms shows that many brackish water and benthic taxa actually increase in abundance toward the top of the slab where the couplets are thinner. Both relative and absolute abundance profiles show this trend, although the relative abundance plot shows the trend more clearly (Figures 7.3, 7.4, 7.5, 7.6). Taxa such as *Achnanthes minutissima*, *Cocconeis* spp., *Navicula perminuta*, *Nitzschia frustulum*, *Planothidium delicatulum*, and *Paralia sulcata* show definite increases in abundance in thinner couplets. Total *Thalassionema* spp. and total *Thalassiosira* spp. show a slight increase toward the top of the slab as well. *Achnanthes minutissima*, *Planothidium*

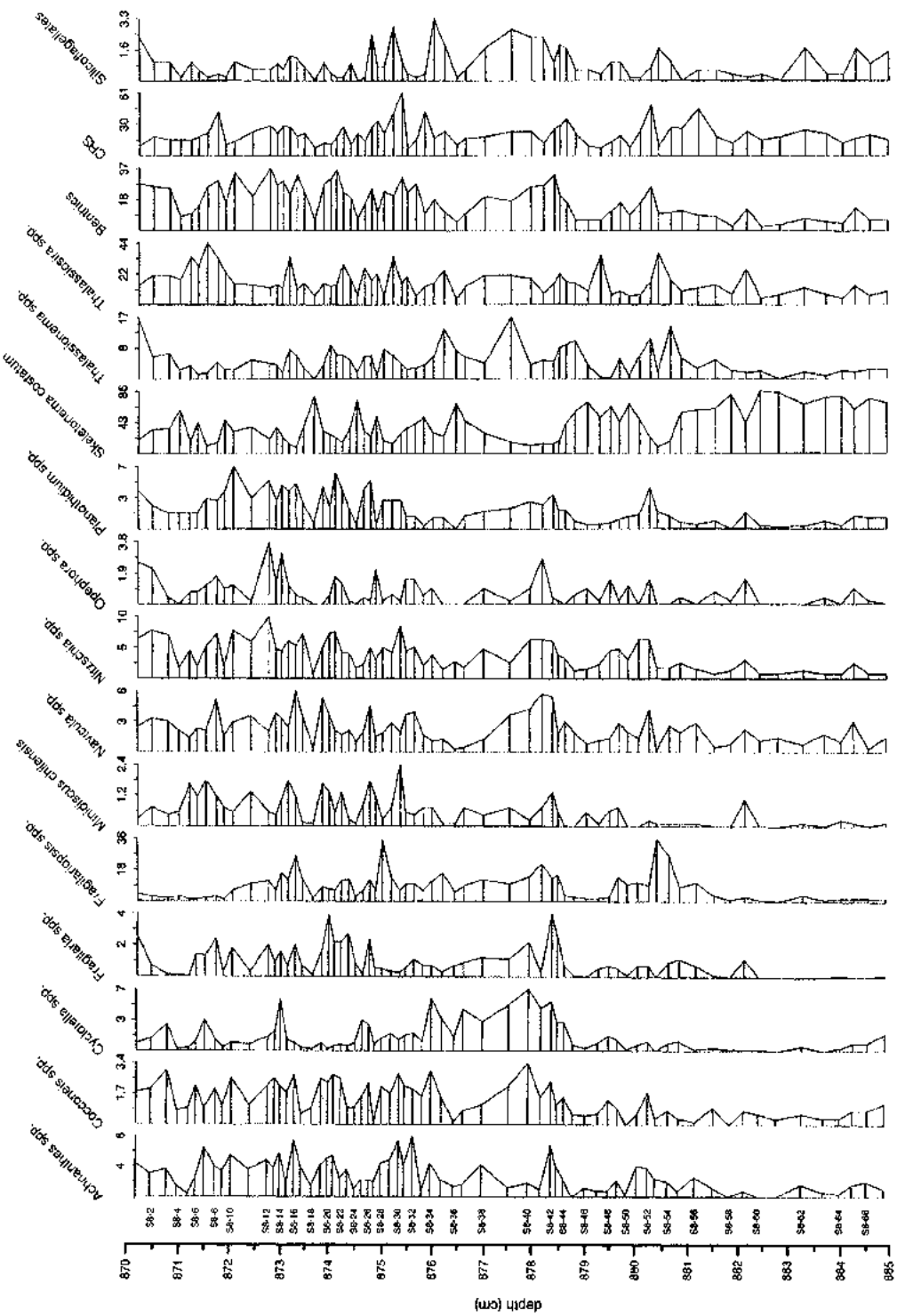

FIGURE 7.3. Relative abundance data (%) for major diatom taxa, total benthic diatoms, CRS and silicoflagellates for Slab 8, core TUL99B03. Only even-numbered sample labels are shown.

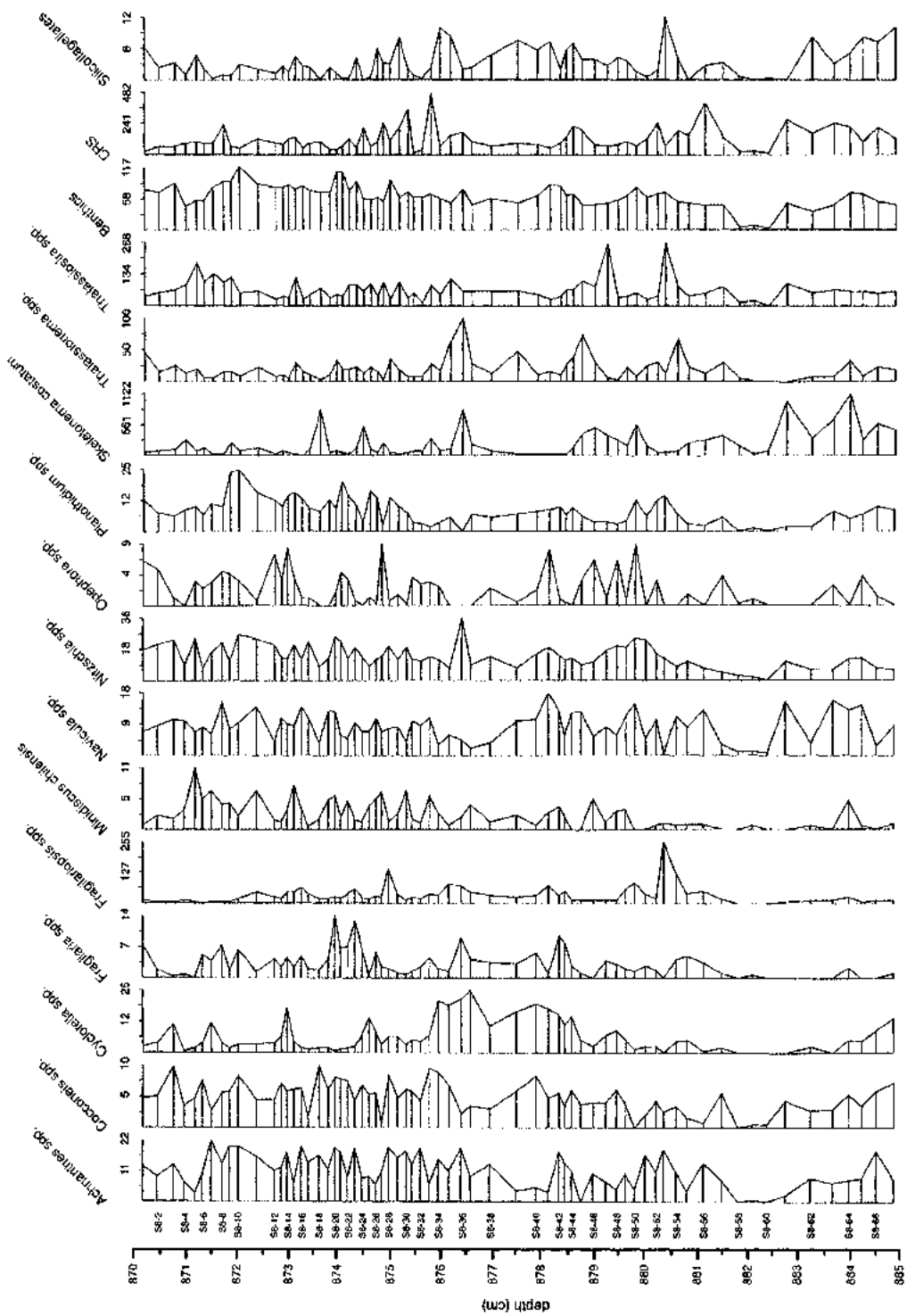

FIGURE 7.4. Absolute abundance data ($\times 10^6$ valves/g) for major diatom taxa, total benthic diatoms, CRS and silicoflagellates for Slab 8, core TUL99B03. Only even-numbered sample labels are shown.

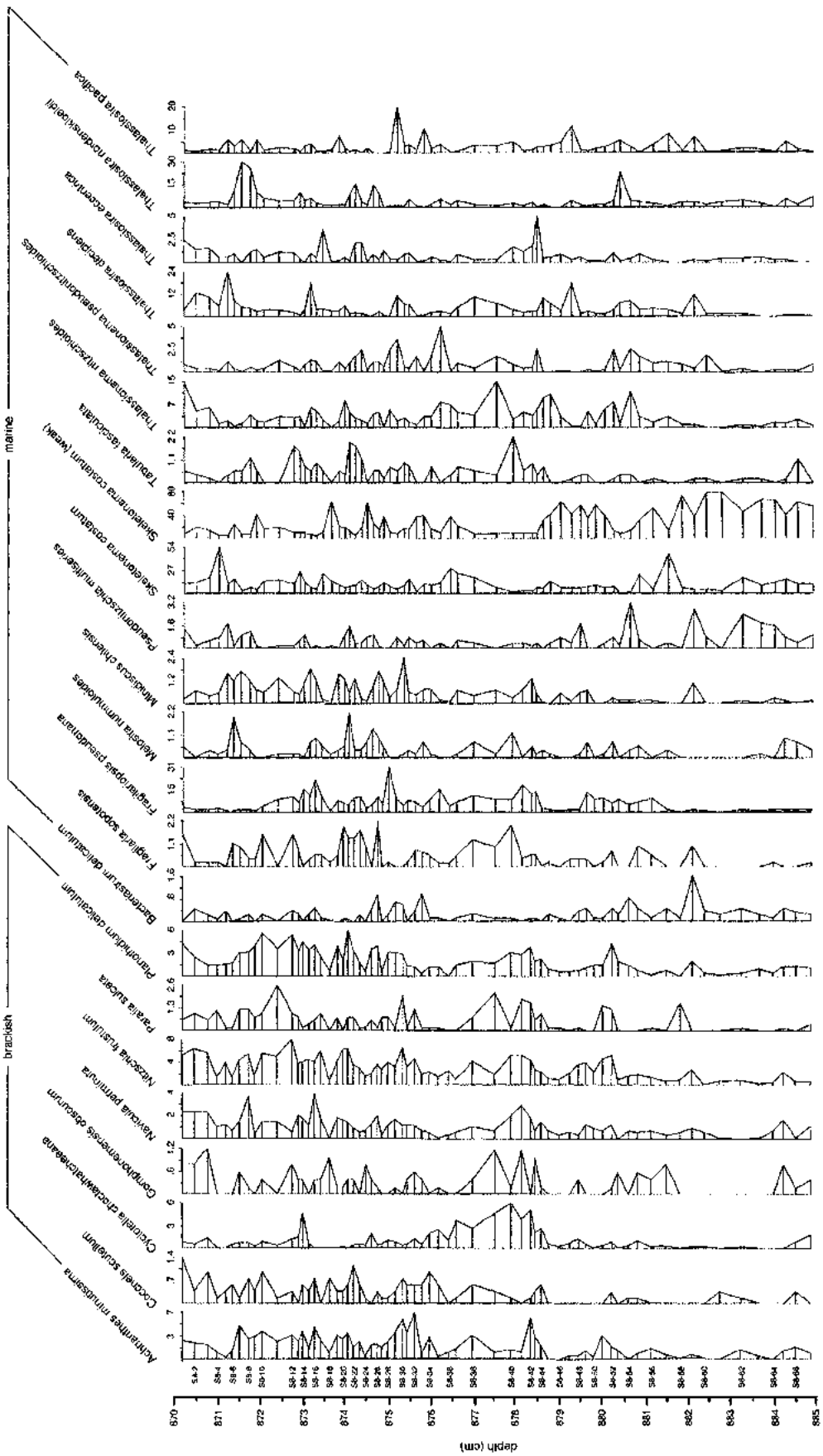

FIGURE 7.5. Relative abundance data (%) for selected major diatom taxa from Slab 8, core TUL99B03. Only even-numbered sample labels are shown. Data for other major taxa are presented in Appendix H3.

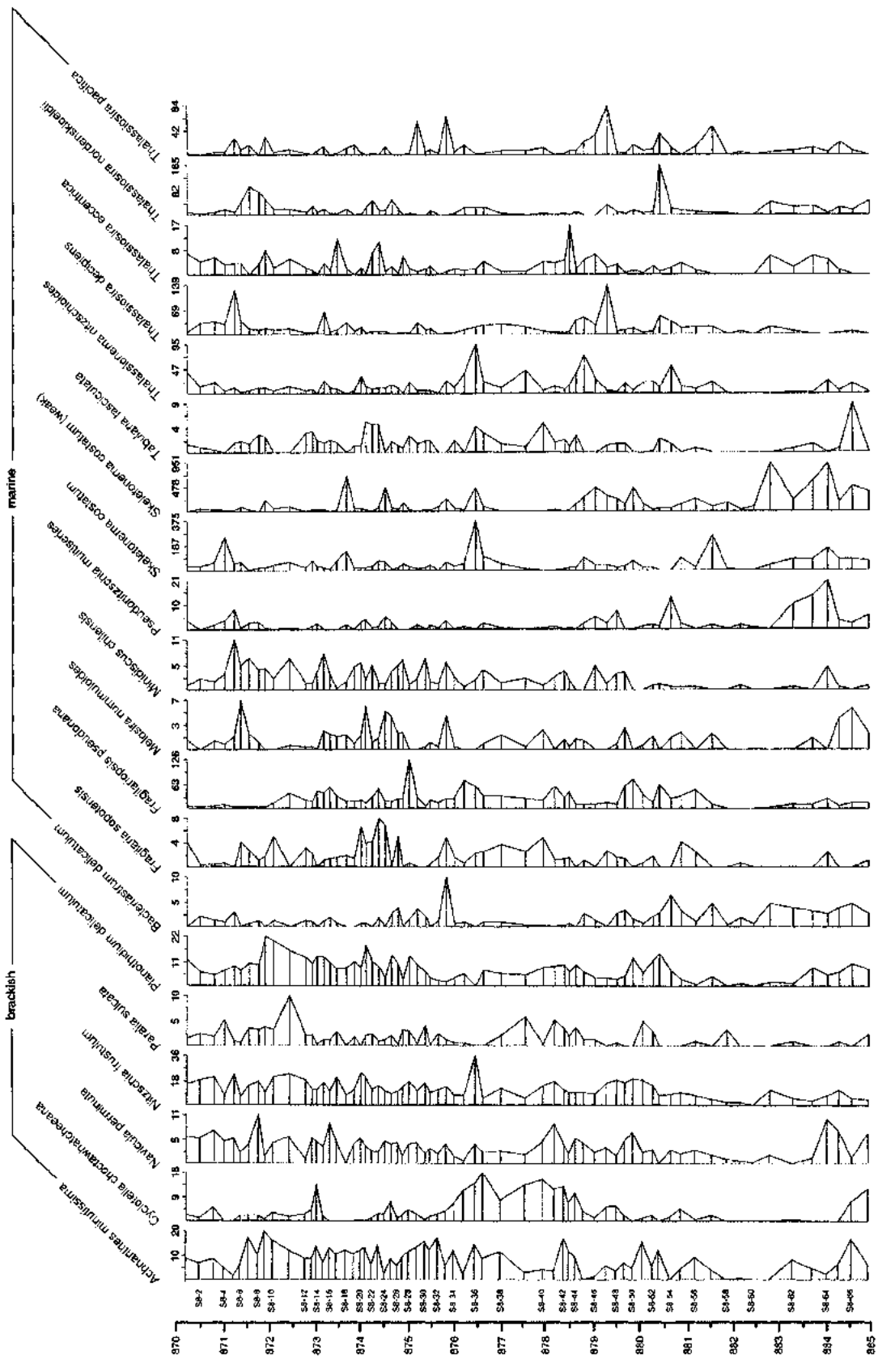

FIGURE 7.6. Absolute abundance data ($\times 10^6$ valves/g) for selected major diatom taxa from Slab 8, core TUL99B03. Only even-numbered sample labels are shown. Data for other major taxa are presented in Appendix H4.

delicatulum and *P. sulcata* show slight increases in the nonlaminated interval from the top of the slab, but not the interval at the bottom of the slab. *Cyclotella choctawhatcheeana* shows an increase in the graded interval in the middle of the slab. Unidentified benthic foraminifera were found in the uppermost and middle nonlaminated intervals (Appendix D, Slides 8C–E).

Species Assemblages and Environmental Variables

The final DCCA ordination from freeze core TUL99B04 was used as a template to explain the variation in species data from Slab 8. Environmental variables for sea surface temperature (SST), sea surface salinity (SSS) and the Aleutian Low Pressure Index (ALPI) were used in the joint ordination. As a result, the first four axes of the DCCA ordination explained 25.5% of variance in the species data, and the environmental data explained 43.9% of this variation along the second axis (Table 7.2). The first two axes are the most important, although only explaining 2.6% of the variance, because the data along these axes were constrained to the environmental variables. Axes 3 and 4 (22.9%) were less important because the data along these axes were not constrained to the environmental variables, and hence a zero species-environmental value on these axes (Table 7.2). Variable ALPI is strongly correlated with axis 2, while SST is less strongly correlated with axis 2. Variable SSS is strongly correlated with axis 1 (Figure 7.7).

The positions of the plotted samples and species on the final ordination diagram give a qualitative indication of their environmental optima (Figure 7.7A). Samples from the thicker couplets at the bottom of the slab (samples S8-44 to 67) tend to plot at the

TABLE 7.2. Summary of statistics for the first four axes of a detrended canonical correspondence analysis (DCCA) performed on species-environment data from Slab 8, using freeze core TUL99B04 DCCA as a template.

	Axis 1	Axis 2	Axis 3	Axis 4
Eigenvalues	0.016	0.010	0.164	0.065
Species-environment correlations	0.425	0.439	0.000	0.000

FIGURE 7.7. Final detrended canonical correspondence analysis (DCCA) ordination diagram of species-environment relationships for Slab 8, core TUL99B03, using the DCCA ordination from freeze core TUL99B04 as a template. **A.** Sample distribution of 67 samples plotted passively on DCCA. Active sample points from freeze core TUL99B04 have been removed to reduce clutter of the diagram. **B.** Species distribution of 35 major diatom species found in common between TUL99B04 and Slab 8. Codes for species names are found in Table 7.1.

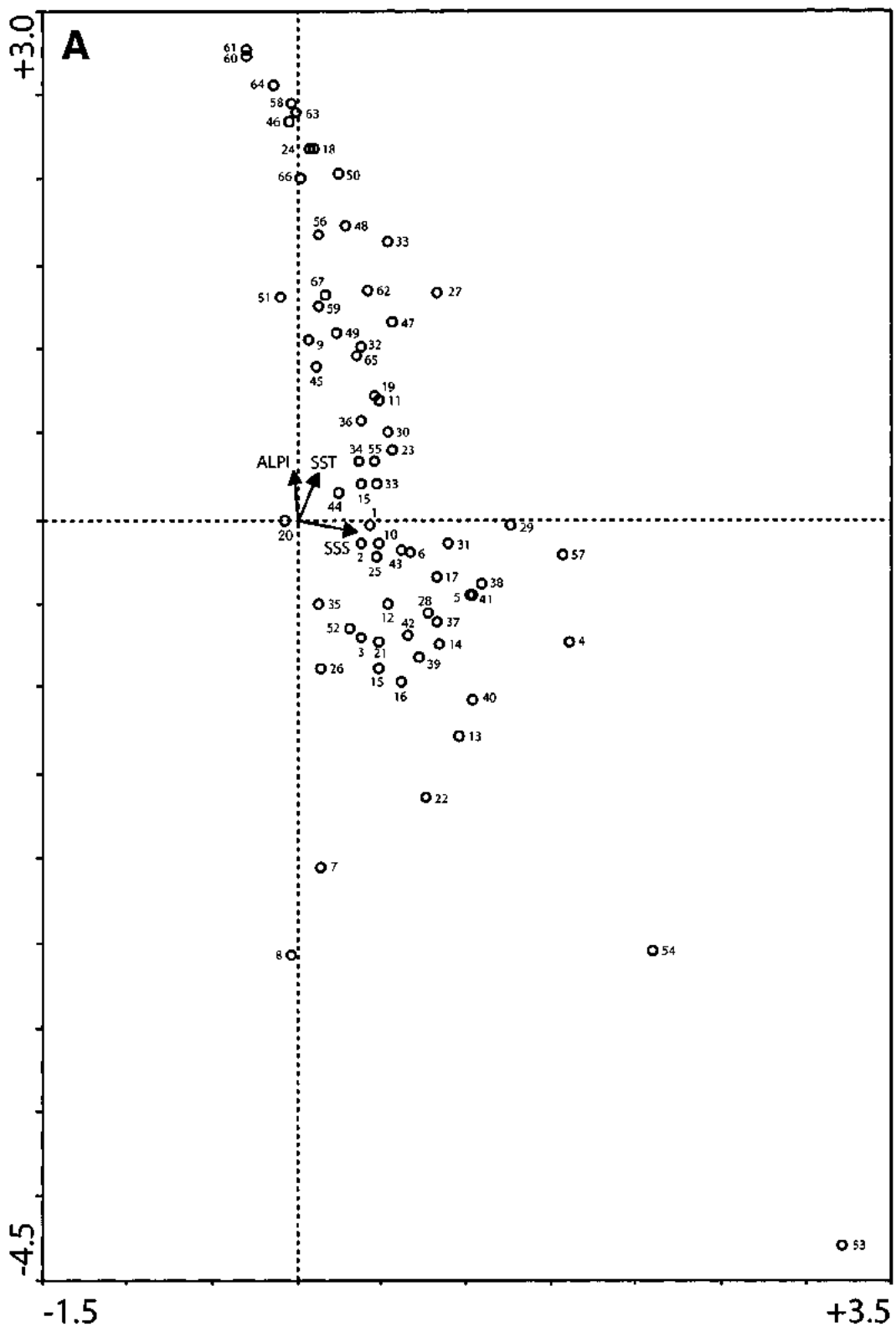
A
+3.0
-4.5
-1.5
+3.5
ALPI
SST
SSS
61
60
64
58
63
46
24
18
66
50
56
48
33
67
51
62
27
59
47
49
9
32
65
45
19
11
36
30
34
55
23
33
44
15
1
20
29
10
2
6
31
57
43
25
17
38
5
41
35
12
28
42
37
52
3
21
14
4
39
26
15
16
40
13
22
7
8
54
53

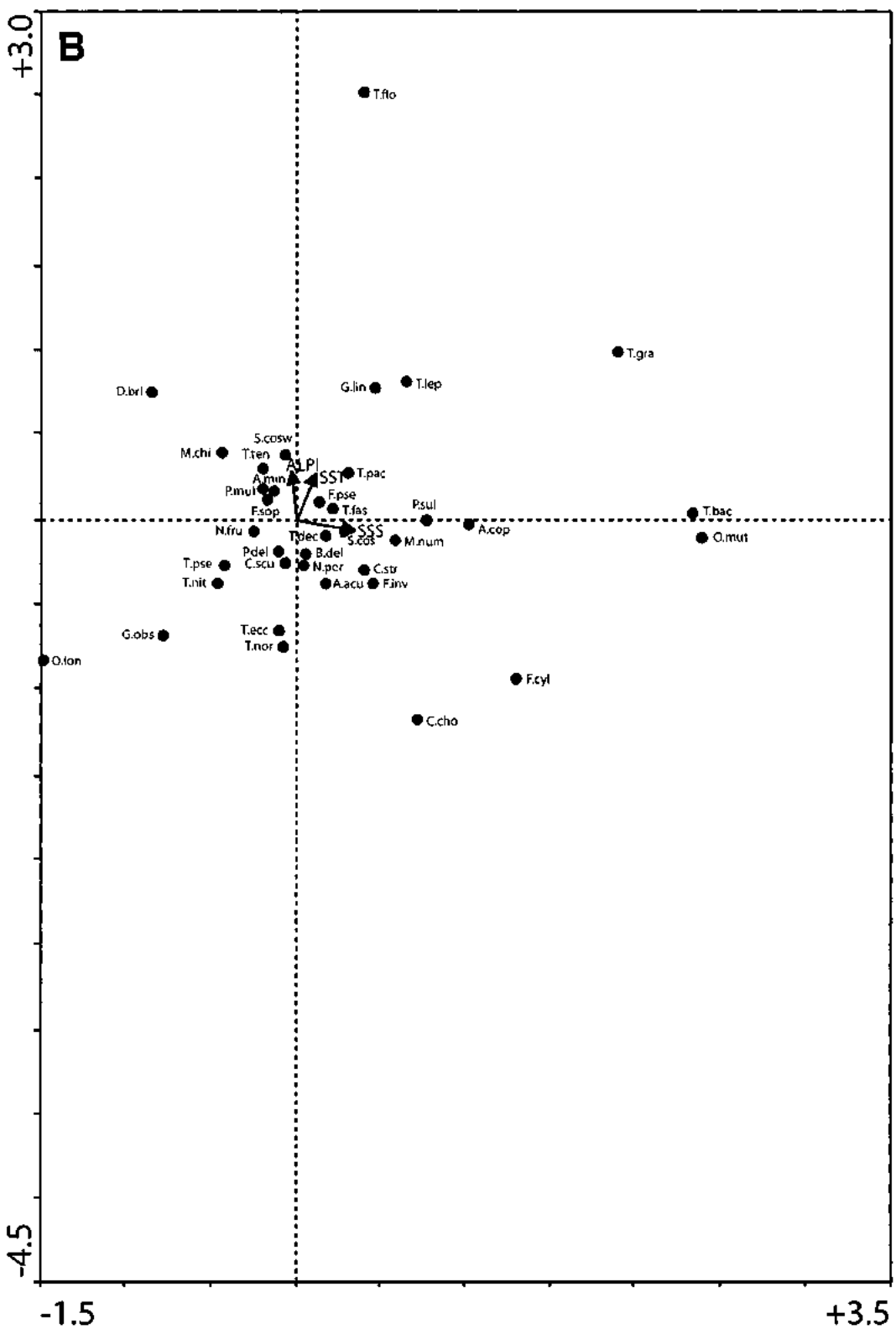
B
+3.0
-4.5
-1.5
+3.5
T.flo
T.gra
G.lin
T.lep
D.bri
S.cosw
M.chi
T.ten
ALP
SST
T.pac
A.mun
P.mul
F.pse
F.sop
T.fas
P.sul
T.bac
N.fru
T.dec
SSS
S.cos
M.num
A.cop
O.mut
P.del
B.del
C.scu
T.pse
N.per
C.str
T.nit
A.acu
F.inv
G.obs
T.ecc
T.nor
O.lon
F.cyl
C.cho

high end of the ALPI and SST vectors, except for samples S8-53 and 54, which have low abundances of the robust form of *Skeletonema costatum*. Samples from the thinner couplets at the top of the slab (samples S8-1 to 37) tend to plot on the low end of ALPI and SST and on the high end of the SSS vector. Exceptions again are samples S8-7 and 8, which plot farther away because they have low amounts of *S. costatum*. Sample S8-62 from the bottom nonlaminated interval and sample S8-11 from the top nonlaminated interval plot on the high end of the SST vector. In contrast, samples S8-38, 39 and 40 from the middle nonlaminated interval plot on the high end of the SSS vector and relatively lower SST than the other two nonlaminated interval samples.

The distribution of the diatom taxa in the joint DCCA is similar to the distribution derived from the freeze core DCCA (Figure 7.7B). *Thalassionema bacillare*, *Opephora mutabilis*, *Cyclotella chochtawhatcheeana*, *Amphora copulata*, *Thalassiosira gravida*, *Paralia sulcata*, *Melosira nummuloides*, *Fragilaria investiens*, *Cyclotella striata* and *Fragialriopsis cylindriformis* had optima on the high side of salinity. *Thalassiosira* cf. *leptopus*, *Tabellaria flocculosa*, *Gomphonemopsis lindae*, *Ditylum brightwellii* and *T. gravida* had high temperature optima. These same diatoms, along with taxa such as *Minidiscus chilensis* and *Skeletonema costatum* (weak), appeared when ALPI was high.

Cyclostratigraphy

Using wavelet analysis, significant cycles have been detected in both the sediment grey value and absolute diatom abundance. Significant and stationary cycles detected in sediment grey value were ~8–9 year cycles (Figure 7.8A). In diatom abundance,

FIGURE 7.8. Wavelet scalograms for Slab 8, core TUL99B03. Horizontal axis at the bottom represents the depth scale, vertical axes on scalograms represent the logarithmic scaled wavelength (or period); orange and yellow colours mark high wavelet coefficients (high spectral power or amplitude), and blue colour marks low wavelet coefficients (low spectral power or absent amplitude) at specific wavelengths at specific locations. Raw data are provided in Appendices H5 and H6. **A.** Scalogram of varve thickness in the time domain. **B.** Scalogram of diatom abundance in the time domain. **C.** Three most pronounced cycles of diatoms in the time domain. **D.** Scalogram of diatom abundance in the depth domain. **E.** Diatom abuundance plotted against depth (cm), as from Figure 7.2D. **F.** X-radiograph positive image as from Figure 7.2B.

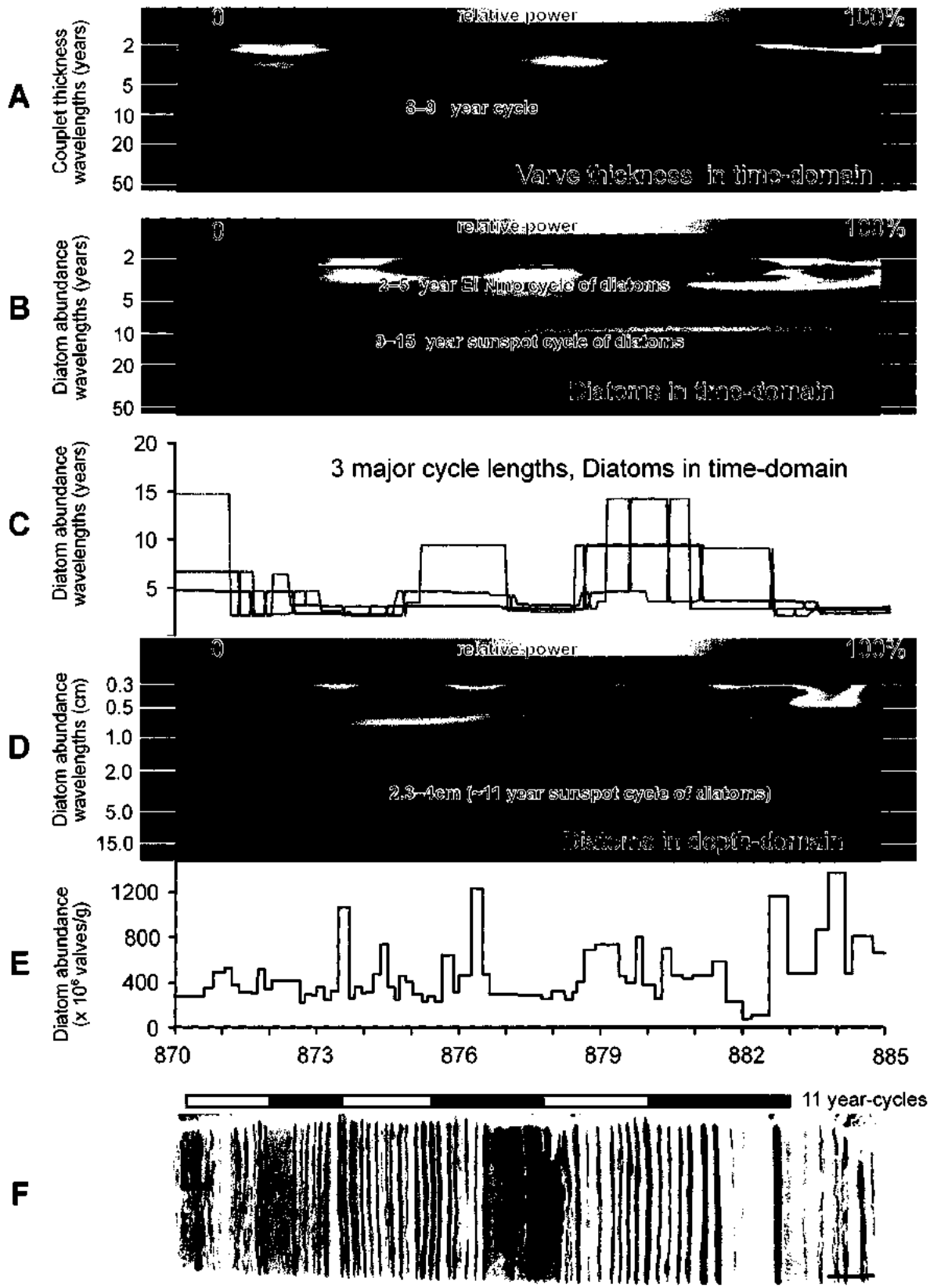
A
Couplet thickness wavelengths (years)
0
relative power
100%
2
5
10
20
50
8–9 year cycle
Varve thickness in time-domain
B
Diatom abundance wavelengths (years)
2–5 year El Niño cycle of diatoms
9–15 year sunspot cycle of diatoms
Diatoms in time-domain
C
Diatom abundance wavelengths (years)
20
15
10
5
3 major cycle lengths, Diatoms in time-domain
D
Diatom abundance wavelengths (cm)
0.3
0.5
1.0
2.0
5.0
15.0
2.3–4cm (~11 year sunspot cycle of diatoms)
Diatoms in depth-domain
E
Diatom abundance (x 10⁶ valves/g)
1200
800
400
0
870
873
876
879
882
885
F
11 year-cycles

significant cycles occurred at 2.3-4 cm in the depth domain, and 2–5 years and 9–15 years in the time domain (Figure 7.8B, D). The three most prominent diatom cycles in the time domain occurred at 2.5 years, 9 years and 15 years (Figure 7.8C).

DISCUSSION

Comparisons with Thin Sections, Sediment Traps and Freeze Core Samples

Quantitative diatom counts and species proportions determined in this study were in agreement with the diatom descriptions from thin sections analysis for taxa visible at 400× magnification (Chapter 4). Dominant taxa described for each diatomaceous lamina from the thin sections appeared as proportionately dominant taxa in equivalent subsamples, which was to be expected (compare Appendix D, Slides 8A–E with Appendix H3). For example, near-monospecific *Skeletonema costatum* sublaminae were more prominent in the thicker couplets at the bottom of the slab (Slides 8A, B) than in the thinner couplets at the top of the slab (Slide 8E). This result is reflected in the relative and absolute abundances of this taxon (Figures 7.3, 7.4). The only discrepancy between the thin section descriptions and quantitative counts is in the abundance of small (< 10 μm) taxa that could not be seen at 400×. Thus, the semi-quantitative proportion estimates performed on the thin sections provide a quick and accurate assessment of large and dominant taxa present in each lamina type.

When compared to the sediment trap samples, preservation of the diatoms in Slab 8 is similar to freeze core TUL99B04 when species proportions are considered. As with the freeze core sediments, lightly silicified diatoms such as *S. costatum* maintain

relatively the same proportions between the water column and the sediments, while various *Thalassiosira* species (e.g., *T. nordenskioeldii*, *T. pacifica*) increase in abundance in the sediments (compare Figures 5.7, 6.8 and 7.5). Some species proportions between freeze core and sediment slab samples differ likely because these two sample sets represent two different climate states, with the freeze core from modern conditions, and Slab 8 from conditions warmer than modern (Figure 4.14). For example, the warm to temperate water diatom *Thalassionema pseudonitzschioides* is slightly more abundant in Slab 8 than it is in the freeze core. *T. pseudonitzschioides* is all but absent in the inner basin sediment trap, with slightly elevated abundances in the trap at the mouth of the inlet (Appendices E4, G3, H3). In addition, brackish water diatoms such as *Cyclotella choctawhatcheeana*, *Navicula perminuta* and *Planothidium delicatulum* are more abundant in Slab 8 than in the freeze core. This appearance of more brackish species at ~4450 cal yr BP may be due to higher sea surface salinities caused by generally warmer temperatures and increased evaporation (Figures 6.8, 7.5).

Interannual Variability of Diatom Assemblages

An analysis of the thin section images and lamina measurements reveals that the thickness of terrigenous laminae do not become thinner or thicker as couplet thickness decreases toward the top of the slab (Appendix B2), but that the diatomaceous laminae become thinner, causing overall couplet thickness to decrease. Although there is interannual variability in the thickness of the terrigenous laminae throughout the slab, the lack of a trend in the change in thickness suggests that winter terrigenous input into the

inner basin was relatively stable throughout the 62 or so years of deposition. However, silt content within the diatomaceous laminae (i.e., the occurrence of silty diatomaceous laminae) gradually increases over time. This suggests that seasonality became weaker over time as the spring and summer seasons became wetter than usual, delivering more terrigenous debris to the basin via increased runoff year-round (Chang et al., 1998). The amount of rainfall is positively correlated to the amount of detritus washed into the inlet from runoff, as was evident in the autumn and winter sediment trap studies in Effingham Inlet and in other sites where hemipelagic sediments accumulate (e.g., Soutar and Crill, 1977). Hence, a progressive increase in precipitation over time led to continental runoff and delivery of terrigenous debris into the inlet, resulting in a higher silt and terrigenous debris content in the thinner couplets. Although Slab 8 occurs during an overall warm climate state, as defined from pollen stratigraphies for southern Vancouver Island (Hebda, 1995), the increase in precipitation signaled by increasing silt content is likely a high-resolution overprint of cooler and wetter conditions experienced during the 62 years of deposition.

The absolute abundance of total diatoms shows a progressive decrease toward the top of Slab 8 in concert with decreasing couplet thickness. This decrease in diatom abundance is governed by the amount of the dominant taxon *Skeletonema costatum* (weak form) and other marine species. Imprinted on this overall decrease in diatom abundance is an increase in the relative abundance of various brackish water and benthic species. The increase in benthic and brackish water species over time may also be a response to increased precipitation and runoff. Diatoms such as *Achnanthes minutissima*,

Navicula perminuta, *Paralia sulcata* and *Planothidium delicatulum* are both benthic and brackish water species and are more common in thinner couplets at the top of the slab (Figures 7.5, 7.6). These taxa can be easily sloughed off from benthic habitats during storm activity or heightened runoff caused by increased rainfall (McQuoid and Hobson, 1998). An alternative explanation for the observed increase in benthic species is a rise in sea level (McQuoid and Hobson, 1998). An increase in sea level can cause flooding of shallow areas along the margins of the inlet, increasing the available habitat for benthic species. However, as of yet no evidence has been found for sea level change or shoreline reconfiguration in Effingham Inlet at ~4450 yr BP.

An increase in both silt content and benthic species in the thinner couplets suggests that precipitation became more prominent over time. A decrease in marine species suggests that overall productivity and likely upwelling and nutrient delivery weakened over time.

Diatom Assemblages and Environmental Variables

The positions of the samples plotted on the DCCA ordination diagram suggest that the thicker couplets (samples S8-44 to 67) were deposited during conditions with a stronger AL and higher SST, and the thinner couplets (samples S8-1 to 37) deposited during a weaker AL and lower SST. Thus, this ordination suggests that the AL weakened and SST gradually decreased throughout the 62-year depositional interval as thicker couplets became thinner with the decrease in abundance of coastal marine species. A gradual weakening of the AL and decrease in SST over time would reflect the onset of

conditions typical of the cool phase of the Pacific Decadal Oscillation (PDO) in the north Pacific (Chavez et al., 2003). However, a cool PDO phase would result in the increase of upwelling and coastal productivity (Chavez et al., 2003), and not a decrease as observed. Nevertheless, the interpretation of increased precipitation over time also fits the cool PDO phase. As a caveat, the distribution of passively plotted samples using the DCCA ordination from another core as a template must be interpreted with caution, as the distribution may not portray the actual environmental conditions at the time of deposition.

The distribution of species plotted on the DCCA diagram, however, is similar to the distribution represented in freeze core samples because many of the same species from both sample sets were plotted (Figures 6.10C, 7.7B). Hence, the environmental affinities of taxa are similar between modern and ancient sediments.

Interpretation of Nonlaminated Intervals

The three nonlaminated intervals in the slab may have a similar physical appearance macroscopically, but their origins and modes of formation are different based on the diatom assemblages. Samples from the three intervals also show different environmental affinities on the DCCA ordination diagram, as described in the results section. Benthic brackish water taxa such as *Achnanthes minutissima*, *Navicula perminuta*, *Paralia sulcata* and *Planothidium delicatulum* are found in slightly elevated abundance in the uppermost interval, yet the pelagic brackish water species *C. chcotawhatcheeana* is found in elevated abundance in the slightly graded interval in the

middle of the slab but not at the top of the slab (Figures 7.2, 7.5, 7.6). All brackish water species are then almost absent in the interval at the bottom of the slab.

The nonlamianted interval at the bottom of the slab contains abundant *Skeletonema costatum*, and other diatom proportions are similar to the diatom compositions from the couplets immediately above and below the interval. This interval may represent an oxygenation event whereby increased oxygen levels introduced bioturbating macrobenthos to the bottom of the inlet (cf. Schimmelamnn et al., 1992; Dallimore, 2001). Bioturbation of the sediments would then destroy diatom frustules and original laminae and homogenize the sediment. Other than homogenized sediment and a relatively lower diatom abundance when compared to adjacent couplets, there is no obvious indication of bioturbation, in the form of burrows, either within the interval or in the couplets below the interval, as is generally found in other bioturbated laminated sediments (e.g., Chang and Grimm, 1999; Grimm and Föllmi, 1994).

The increased abundance of benthic brackish species in the uppermost nonlaminated interval suggests that these benthic species could have been swept into the inlet from littoral zones during precipitation events or other sediment-destabilizing mechanisms. The occurrence of unidentified benthic foraminifera in the uppermost interval, and in the slightly graded interval from the middle of the slab, may indicate that the sediment source was allochthonous and from above the anoxic bottom waters (Blais, 1995). This evidence implies that the sediment source was delivered to the inlet bottom via some sort of gravity flow or sloughing off of sediments from the sides of the inlet by another mechanism. The event was likely small-scale (or small-volume) as the

nonlaminated intervals are thin and there is no evidence of an erosional or scour base that is associated with debris flows (Blais, 1995). With the evidence provided, it is difficult to discern whether or not couplets below the slightly graded interval have been eroded by a gravity flow based on a simple examination of the sediments from a 3-cm wide sediment slab and 1-cm wide thin sections. The slight fining upwards texture of the middle graded interval does support the gravity flow interpretation, but does not explain why there is an increase in abundance of the pelagic species *Cyclotella choctawhatcheeana*. A detailed analysis of the grain size and composition of nonlaminated sediments is required in order to differentiate the origins of such sediments. The triggering mechanism for the formation of the upper two nonlaminated intervals, and hence increased benthic and brackish water species, may have involved extraordinary precipitation events causing sediment instability in low-lying areas such as marshes. This mechanism supports the interpretation that overall precipitation increased toward the top of the slab.

Cyclostratigraphy and Long-term Environmental Implications

Morlet wavelet analysis has revealed significant cycles in both the sedimentary grey values (from x-radiographs) and total diatom abundance. The most pronounced cycles in the time domain are the annual cycle, the 2–5 year cycle and the 8–15 year cycle. The 2–5 year cycle most likely represents the ENSO cycle, whereas the 8–15 year could represent the sunspot cycle or a modulated longer term ENSO cycle, although wavelet analysis performed on a correlative section of core (depth 873–910 cm) by Patterson et al. (in review B) detected a ~10–12 year cycle which correlates with the

known sunspot cycle. The discrepancy in determining a more precise sunspot cycle in Slab 8 may lie in the fact that laminae in the x-ray image were blurry at the top of the slab due to x-ray beam parallax (Chapter 4) and laminae were indistinct below the middle massive layer. The scanner therefore may not have detected the discrete couplets. The x-ray images from Patterson et al. (in review B) were sharp and clear from which cycles could be easily detected. As with freeze core TUL99B04, the detection of ENSO and sunspot cycles suggests that diatom productivity, and the resulting sedimentation pattern, are affected not only by large-scale ocean-atmosphere perturbations, but also by solar forcing on scales other than the annual cycle. Moreover, these cycles were detected in sediments deposited during two different climate states, indicating that such sub-decadal to decadal scale cycles are persistent at least throughout the last 5000 years of deposition.

Analysis of fish scale abundance was used as a proxy of pelagic fish productivity for core TUL99B03 (Patterson et al., in review B). The proportions of northern anchovy and Pacific herring scales were compared and, focusing on the 873–910 cm interval, showed that anchovy scales began increasing in abundance from 873–885 cm after an interval of low abundance from 885–910 cm (Figure 7.9). The abundance of herring scales remained relatively low throughout the sediment record. Herring is often associated with sardine populations, so the low abundance of herring and the increasing anchovy scales toward the top of the laminated section suggest that the climate experienced cool PDO conditions in the progressively thinner couplets. This evidence supports the positions of the samples plotted on the DCCA ordination diagram, and the interpretation of increasing precipitation through time.

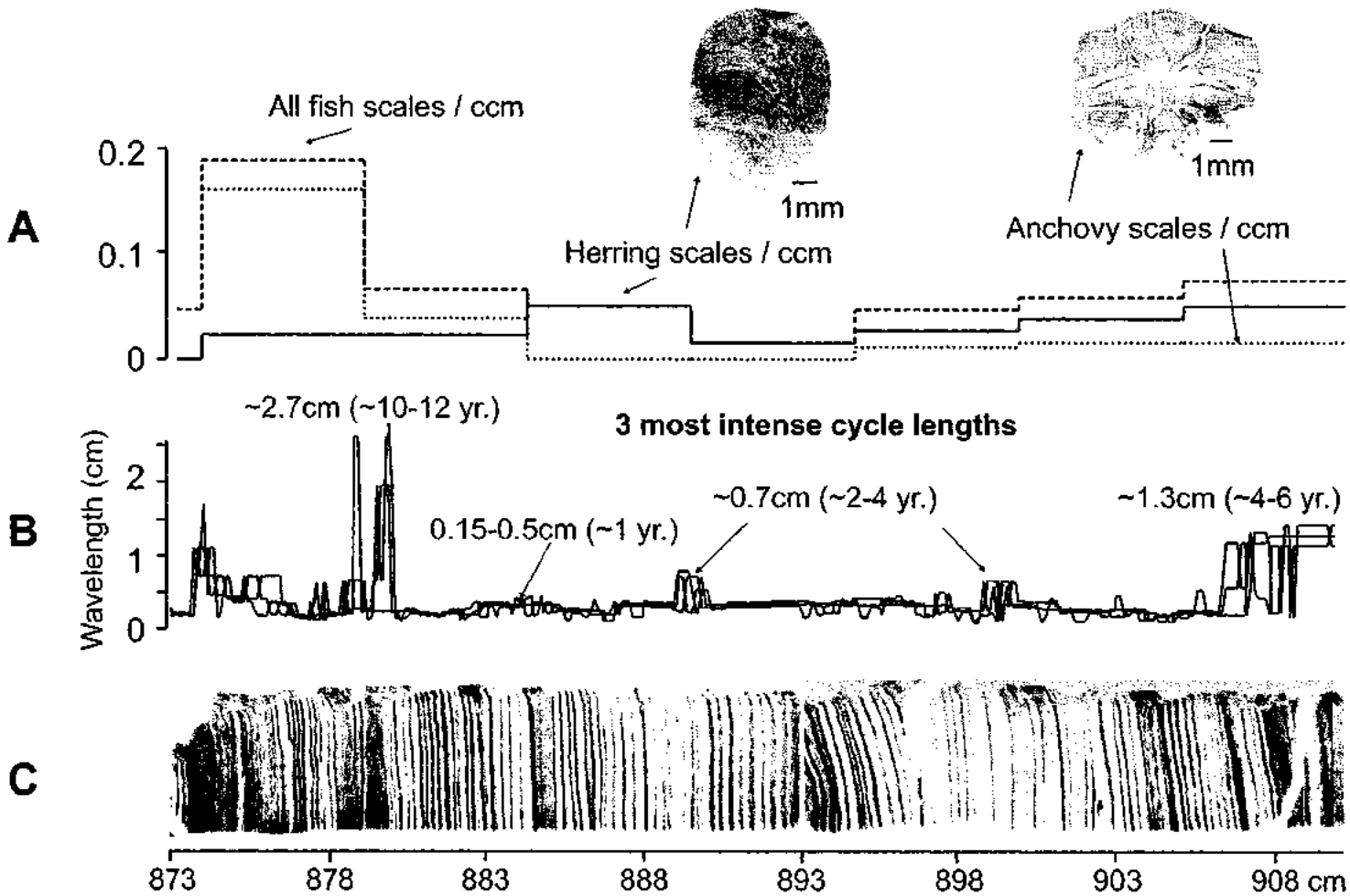

FIGURE 7.9. Fish scale abundance and cyclostratigraphy of interval 873–910 cm from core TUL99B03. **A.** Fish scale abundance data (per cubic centimeter, ccm), including micrographs of typical herring and anchovy scales recovered from the core. **B.** Three most intense cycles from sediment grey values. **C.** X-radiographs. Modified from Patterson et al. (in review B).

CONCLUSION

The stratigraphy of Slab 8 from core TUL99B03 suggests that major environmental change can occur over a time span of a few decades. The progressive decrease in thickness of sedimentary couplets and changes in diatom assemblages indicate that the productivity of marine species decreased over time. The increase in silt content and nonlaminated intervals with benthic species suggest that precipitation and continental runoff increased over the 62 years of deposition. These findings support interpretations that the sediments were deposited during the cool phase of the Pacific Decal Oscillation despite the fact that Slab 8 was deposited during an overall warm climate state.

Cyclostratigraphic results show that both ~2–5 year ENSO and ~11-year sunspot cycles may have been present in the sediment pattern and total diatom abundance. The presence of these cycles indicates that basin-wide ocean-atmosphere teleconnections and solar forcing had similar effects on productivity at ~4450 yr BP as they do in modern sediments, suggesting that such cycles are long-lived throughout the Holocene.

CHAPTER 8

CONCLUSION

The high-resolution stratigraphic approach to studying laminated diatomaceous sediments from Effingham Inlet has revealed a wealth of depositional, climatic and oceanographic information for the late Holocene of southwest British Columbia. In Chapter 4, the laminated sediments from throughout the late Holocene were found to be annual in nature in which a distinctive seasonal succession was preserved. Lamina types and couplet styles revealed that there were three distinct climate states throughout the late Holocene that agreed with climate states derived from pollen and neoglacial studies. A seasonal succession of diatom deposition was determined in modern sediments from a 1.5-year long sediment trap study detailed in Chapter 5, where the timing of the spring bloom was resolved and absolute diatom abundances were determined. In Chapter 6, late 20^{th} century diatom ecology and climate cycles were described from a freeze core. Some diatom abundance trends preserved in the core and environmental data taken from meteorological stations around Effingham Inlet reflect the 1976–1977 regime shift from cooler to warmer conditions in the north Pacific. Cyclostratigraphy showed that diatom abundance and sedimentation patterns had cycles similar to the 2–5 year El Niño cycle and the 11-year sunspot cycle. Finally, mid-Holocene diatom paleoecology was described in Chapter 7 from a sediment slab dating from approximately 4450 cal yr BP. This slab contained couplets that became thinner over time, where overall marine diatom productivity decreased and benthic diatoms increased. Climate conditions similar to the

cool phase of the Pacific Decadal Oscillation were likely responsible for these trends. Cyclostratigraphy also revealed the 2–5 year El Niño cycle and the 11-year sunspot cycle in sediment patterns and diatom abundance, suggesting that large-scale ocean-atmosphere fluctuations and solar forcing have been operating consistently throughout the late Holocene.

High-resolution climate and environmental change studies are continuing along the coast of British Columbia. In one project, there is on-going research in Effingham Inlet with the multidisciplinary examination of a 40-m long sediment core taken during the IMAGES coring program. Fourteen radiocarbon dates have constrained the age of the core to 12000 yr BP, providing an opportunity to study environmental change from the Pleistocene-Holocene boundary and throughout the Holocene. The project is headed by Dr. T.F. Pedersen and is based at the University of Victoria in Victoria, British Columbia. In another project, research has moved further north along the British Columbia coast to the inlets of the Seymour-Belize inlet complex on the BC mainland, just northwest of the northern tip of Vancouver Island. This inlet complex lies in the Coastal Transition Upwelling Domain, whereas Effingham Inlet was in the Coastal Upwelling Domain (Ware and Thomson, 1991). Several cores have been extracted from the inlets, as well as in marshes and small lakes, to document climate and sea level fluctuations throughout the Holocene. This project is headed by Dr. R.T. Patterson and is based at Carleton University.

Work from these various studies will provide a more complete and high-resolution picture of British Columbia's environmental history from the end of the last

ice age to the most recent times. Records of primary productivity, pelagic fish abundance, climate change and sediment patterns will be used to help differentiate natural variability from the imprint of anthropogenic activity before and after the advent of modern industrialization. The utilization of long sediment records, which go far beyond the ~100 year instrumental record, is crucial for reconstructing past environmental variability.

REFERENCES

* denotes contribution to the NSERC strategic grant project

Aebischer, N.J., Coulson, J.C., and Colebrook, J.M. 1990. Parallel long-term trends across four marine trophic levels and weather. Nature, 347: 753–755.

Algeo, T.J., Phillips, M., Jaminski, J., and Fenwick, M. 1994. High-resolution x-radiography of laminated sediment cores. Journal of Sedimentary Research, A64: 665–667.

Alldredge, A.L. and Gotschalk, C.C. 1989. Direct observations of the mass flocculation of diatom blooms: characteristics, settling velocities and formation of diatom aggregates. Deep-Sea Research, 36: 159–171.

Alley, N.F. and Chatwin, S.C. 1979. Late Pleistocene history and geomorphololgy, southeastern Vancouver Island, B.C. Canadian Journal of Earth Sciences, 16: 1645–1657.

Anderson, R.Y. 1990. Solar cycle modulations of ENSO: A possible source of climate change. *In* Betancourt, J.L. and MacKay, A.M. (eds.), Proceedings of the Sixth Annual Pacific Climate (PACLIM) Workshop. Technical Report no. 23, California Department of Water Resources: 77–81.

Anderson, R.Y., Linsley, B.K. and Gardner, J.V. 1990. Expression of seasonal and ENSO forcing in climatic variability at lower than ENSO frequencies: Evidence from Pleistocene marine varves off California. Paleogeography, Paleoclimatology, Paleoecology, 78: 287–300.

Barber, T.B. and Chavez, F.P. 1983. Biological consequences of El Niño. Science, 228: 1203–1210.

Barlow, R.G. 1984. Dynamics of the decline of a phytoplankton bloom after an upwelling event. Marine Ecology Progress Series, 16: 121–126.

Baumgartner, T.R. and Ferreira-Bartrina, V. 1993. Decadal to centennial variability in ocean climate inferred from fish scale deposition in the Santa Barbara Basin, California. EOS Transactions, American Geophysical Union, 74: 372.

Baumgartner, T., Ferreira, V., Cayan, D., and Soutar, A. 1994. Interdecadal variability of sardine and anchovy populations in the California Current. EOS Transactions, American Geophysical Union, Ocean Sciences Meeting Supplement, 75: 34.

Beamish, R.J. and Bouillon D.R. 1993. Pacific salmon production trends in relation to climate. Canadian Journal of Fisheries and Aquatic Sciences, 50: 1002–1016.

Beamish, R.J., Neville, C-E.M. and Cass, A.J. 1997. Production of Fraser River sockeye salmon (*Oncorhynchus nerka*) in relation to decadal-scale changes in the climate and the ocean. Canadian Journal of Fisheries and Aquatic Sciences, 54: 543–554.

Bérard-Therriault, L., Poulin, M., and Bossé, L. 1999. Guide d'identification du phytoplankton marin de l'estuaire et du Golfe du Saint-Laurent incluant également certains protozoaires. Publication spéciale canadienne de sciences halieutiques et aquatiques 128: 387 p.

*Bertram, M. et al. In preparation. Seasonal variability in the composition and flux of sedimenting particulate matter in a fjord on Vancouver Island: Implications for interpreting laminated sediments.

Birks, H.J.B. 1995. Quantitative paleoenvironmental reconstructions. *In* Maddy, D. and Brew, J.S. (eds.), Statistical Modelling of Quaternary Science Data. Quaternary Research Association, Cambridge, Technical Guide 5: 161–254.

Blais, A. 1995. Foraminiferal biofacies and Holocene sediments from Saanich Inlet, B.C.: Implications for environmental and neotectonic research. Unpublished Ph.D. dissertation, Carleton University, Ottawa; 275 p.

Blais-Stevens, A., Clague, J.J., Bobrowsky, P.T. and Patterson, R.T. 1997. Late Holocene sedimentation in Saanich Inlet, British Columbia, and its paleoseismic implications. Canadian Journal of Earth Sciences, 34: 1345–1357.

Braarud, T., Hofsvang, B.F., Hjelmfoss, P., and Överland, A.K. 1974. The natural history of the Hardangerfjord. 10. The phytoplankton in 1955–1956: The quantitative phytoplankton cycle in the fjord and in the offshore coastal waters. Sarsia, 55: 63–98.

Campeau, S., Pienitz, R. and Héquette, A. 1999. Diatoms from the Beaufort Sea Coast, southern Arctic Ocean (Canada): Modern Analogues for Reconstructing Late Quaternary Environments and Relative Sea Levels. Bibliotheca Diatomologica, Band 42. J. Cramer in der Gebrüder Borntraeger Verlagsbuchhandlung, Berlin: 244 p.

Carslaw, K.S., Harrison, R.G. and Kirkby, J. 2002. Cosmic rays, clouds and climate. Science, 298: 1732–1737.

Chang, A.S. and Grimm, K.A. 1999. Speckled beds: Distinctive gravity-flow deposits in finely laminated diatomaceous sediments, Miocene Monterey Formation, California. Journal of Sedimentary Research, 69: 122–134.

Chang, A.S., Grimm, K.A., and White, L.D. 1998. Diatomoaceous sediments from the Miocene Monterey Formation, California: a lamina-scale investigation of biological, ecological and sedimentary processes. Palaios, 13: 458–469.

*Chang, A.S., Patterson, R.T. and McNeely, R. 2003. Seasonal sediment and diatom record from Late Holocene laminated sediments, Effingham Inlet, British Columbia, Canada. Palaios, 18: 477–494.

Chavez, F.P., Ryan, J., Lluch-Cota, S.E. and Ñiquen C, M. 2003. From anchovies to sardines and back: Multidecadal change in the Pacific Ocean. Science, 299: 217–221.

Chamberlain, V.E. and Lambert, R. St. J. 1985. Cordillera: A newly defined Canadian microcontinent. Nature, 314: 707–713.

Clague, J.J. 1981. Late Quaternary geology and geochronology of British Columbia. Part 2: Summary and discussion of radiocarbon-dated Quaternary history. Geological Survey of Canada, Paper 80-35: 41 p.

Clague, J.J. 1983. Glacio-isostatic effects of the Cordilleran Ice Sheet, British Columbia, Canada. *In* Smith, D.E. and Dawson, A.G. (ed.), Shorelines and Isostacy. Academic Press, London, England: 321–343.

Clague, J.J. 1989a. Bedrock geology (Canadian Cordillera). *In* Fulton, R.J. (ed.), Quaternary Geology of Canada and Greenland, Geology of Canada, No. 1. Geological Survey of Canada: 22–25.

Clague, J. J. 1989b. Character and distribution of Quaternary deposits (Canadian Cordillera). *In* Fulton, R.J. (ed.), Quaternary Geology of Canada and Greenland, Geology of Canada, No. 1. Geological Survey of Canada: 34–38.

Clemons, M.J. and Miller, C.B. 1984. Blooms of large diatoms in the oceanic, subarctic Pacific. Deep-Sea Research, 31: 85–95.

Coney, P.J., Jones, D.L., and Monger, J.W.H. 1980. Cordilleran suspect terranes. Nature, 288: 329–333.

Crawford, R.M. 1980. Some considerations of size reduction in diatom cell walls. Proceedings of the 6th Symposium on recent and Fossil Diatoms: 253–266.

Crawford, R.M. 1995. The role of sex in the sedimentation of a marine diatom bloom. Limnology and Oceanography, 40: 200–204.

Cumming, B.E., Wilson, S.E., Hall, R.I., and Smol, J.P. 1995. Diatoms from British Columbia (Canada) Lakes and their Relationship to Salinity, Nutrients and Other Limnological Variables. Bibliotheca Diatomologica, Band 31. J. Cramer in der Gebrüder Borntraeger Verlagsbuchhandlung, Berlin: 207 p.

Cupp, E.E. 1943. Marine plankton diatoms of the west coast of North America. Bulletin of the Scripps Institute of Oceanography, 5: 1–238.

Cury, P. and Roy, C. 1989. Optimal environmental window and pelagic fish recruitment success in upwelling areas. Canadian Journal of Fisheries and Aquatic Sciences, 46: 670–680.

*Dallimore, A. 2001 Late Holocene geologic, oceanographic and climate history of an anoxic fjord; Effingham Inlet, west coast Vancouver Island. Unpublished Ph.D. Dissertation, Carleton University, Ottawa: 465 p.

Davis, J.R. 1986. Statistics and Data Analysis in Geology. 2nd Edition Revised. York. Wiley.

Denman, K.L., Mackas, D.L., Freeland, H.J., Austin, M.J. and Hill, S.H. 1981. Persistent upwelling and mesoscale zones of high productivity off the west coast of Vancouver Island, Canada. *In* Richards, F.A. (ed.), Coastal Upwelling, America Geophysical Union, Washington, D.C.: 514–521.

Deuser, W.G., Muller-Karger, F.E. and Hemleben, C. 1988. Temporal variations of particle fluxes in the deep subtropical and tropical North Atlantic: Eulerian versus Lagrangian effects. Journal of Geophysical Research, 93: 6857–6862.

Dymond, J. 1984. Sediment traps, particle fluxes, and benthic boundary layer processes. *In* Worshop on the Global Ocean Flux Study Proceedings, National Academy Press: 260–284.

Favorite, F., Dodimead, A.J. and Nasu, K. 1976. Oceanography of the subarctic Pacific region, 1960–71. International North Pacific Fisheries Commission Bulletin, 33: 187 p.

Freeland, H.J. and Denman, K.L. 1982. A topographically controlled upwelling center off southern Vancouver Island. Journal of Marine Research, 40: 1069–1093.

French, F.W. and Hargraves, P.E. 1980. Physiological characteristics of phytoplankton resting spores. Marine Biology Letters, 1: 185–195.

Frost, B.W. 1996. Phytoplankton bloom on iron rations. Nature, 383: 475–476.

Gauch, H.G. 1982. Multivariate Analysis in Community Ecology. Cambridge University Press, Cambridge: 298 p.

Griffin, D.A. and LeBlond, P.H. 1990. Estuary/ocean exchange controlled by spring-neap tidal mixing. Estuarine and Coastal Shelf Science, 30: 275–297.

Grimm, K.A. and Föllmi, K.B. 1994. Doomed pioneers: Allochthonous crustacean traacemakers in anaerobic basinal strata, Oligo-Miocene San Gregario Formation, Baja California Sur, Mexico. Palaios, 9: 313–334.

Grimm, K.A., Lange, C.B., and Gill, A.S. 1996. Biological forcing of hemipelagic sedimentary laminae: Evidence from ODP Site 893, Santa Barbara Basin, California. Journal of Sedimentary Research, 66: 613–624.

Grimm, K.A., Lange, C.B., and Gill, A.S. 1997. Self-sedimentation of fossil phytoplankton blooms in the geologic record. Sedimentary Geology, 110: 151–161.

Grossman, A. and Morlet, J. 1984. Decompositions of Hardy functions into square integrable wavelets of constant shape. SIAM J. Mathematische Annalen, 15: 732–736.

Guillard, R.R.L. and Kilham, P. 1977. The ecology of marine planktonic diatoms. *In* Werner, D. (ed.), The Biology of Diatoms. Botanical Monographs, v. 13. Blackwell Scientific Publications: 372–469.

Haigh, R., Taylor, F.J.R., and Sutherland, T.F. 1992. Phytoplankton ecology of Sechelt Inlet, a fjord system on the British Columbia coast. I. General features of the nano- and microplankton. Marine Ecology Progress Series, 89: 117–134.

Hall, R.I. and Smol, J. P. 1992. A weighted-averaging regression-calibration model for inferring total phosphorus concentration from diatoms in British Columbia (Canada) lakes. Freshwater Biology, 27: 417–434.

Hallegraeff, G.M. and Bolch, C.J. 1992. Transport of diatom and dinoflagellate resting spores in ships' ballast water: Implication for plankton biogeography and aquaculture. Journal of Phytoplankton Research, 14: 1067–1084.

Harrison, P.J., Fulton, J.D., Taylor, F.J.R., and Parsons, T.R. 1983. Review of the biological oceanography of the Strait of Georgia: pelagic environment. Canadian Journal of Fisheries and Aquatic Sciences, 40: 1064–1094.

Hasle, G.R. and Fryxell, G.A. 1970. Diatoms: Cleaning and mounting for light and electron microscopy. Transactions of the American Microscopical Society, 89: 469–474.

*Hay, M.B. and Pienitz, R. In preparation. Diatom record of late Holocene oceanography and climate along the west coast of Vancouver Island, British Columbia (Canada)

*Hay, M.B., Pienitz, R., and Thomson, R.E. 2003. Distribution of diatom surface sediment assemblages within Effingham Inlet, a temperate fjord on the west coast of Vancouver Island (Canada). Marine Micropaleontology, 48: 291–320.

Hebda, R.J. 1983. Late-glacial and postglacial vegetation history at Bear Cove Bog, northeast Vancouver Island, British Columbia. Canadian Journal of Botany, 61: 3172–3192.

Hebda, R.J., 1995. British Columbia vegetation and climate history with focus on 6 ka BP. Géographie Physique et Quaternaire, 49: 55–79.

Hedges, J.I., Clark, W.A. and Cowie, G.L. 1988. Fluxes and reactivities of organic matter in a coastal marine bay. Limnology and Oceanography, 33: 1137–1152.

Hemphill-Haley, E. and Fourtanier, E. 1995. A diatom record spanning 114,000 years from Site 893, Santa Barbara Basin. Proceedings of the Ocean Drilling Program, Scientific Results, 146 (Part 2): 223–249.

Heusser, L.E. 1983. Palynology and paleoecology of postglacial sediments in an anoxic basin, Saanich Inlet British Columbia. Canadian Journal of Earth Sciences, 20: 873–885.

Hickey, B.M. 1979. The California Current system—hypotheses and facts. Progress in Oceanography, 8: 191–279.

Hjort, J. and Gran, H.H. 1900. Hydrographic-biological investigations of the Skagerrak and the Christiania fjord. Report of the Norwegian Fisheries Marine Investigations, 1: 1–40.

Holmgren, D. 2001. Decadal-centennial variability in marine ecosystems of the northeast Pacific Ocean: the use of fish scales deposition in sediments. Unpublished Ph.D. dissertation, University of Washington, Seattle: 122 p.

Honjo, S. 1982. Seasonality and interaction of biogenic and lithogenic particulate flux at the Panama Basin. Science, 218: 883–884.

Hughen, K.A., Overpeck, J.T., Peterson, L.C. and Anderson, R.F., 1996. The nature of varved sedimentation in the Cariaco Basin, Venezuela. *In* Kemp, A.E.S. (ed.), Palaeoclimatology and Palaeoceanography from Laminated Sediments, Geological Society Special Publication, No. 116.: 171–183.

Ikeda, M. and Emery, W.J. 1984. A continental shelf upwelling event off Vancouver Island as revealed by satellite infrared imagery. Journal of Marine Research, 42: 303–317.

Jewson, D.H. 1992. Size reduction, reproductive strategy and the life cycle of centric diatom. Philosophical Transactions of the Royal Society of London, B 336: 191–213.

Jongman, R.H.G., ter Braak, C.J.F., and van Tongeren, O.F.R. (eds.) 1995. Data Analysis in Community and Landscape Ecology. Cambridge University Press, Cambridge, UK: 299 p.

Juggins, S. 1997. Calibrate version 0.70: A C++ program for analysing and visualizing species environment relationships and for predicting environmental values from species assemblages. User Guide Version 1.0.

Kaiho, K. 1994. Benthic foraminiferal dissolved-oxygen index and dissolved-oxygen levels in the modern ocean. Geology, 22: 719–722.

Karentz, D. and Smayda, T.J. 1984. Temperature and seasonal occurrence patterns of 30 dominant phytoplankton species in Narragansett Bay over a 22-year period (1959–1980). Marine Ecology Progress Series, 18: 277–293.

Keller, G.H. 1983. Coastal upwelling: Its influence on the geotechnical properties and stability characteristics of submarine deposits. *In* Thiede, J. and Suess, E. (eds.), Coastal Upwelling: Its Sediment Record, Part A. Plenum Press, New York: 181–199.

Kemp, A.E.S., 1990. Sedimentary fabric and cariations in lamination style in Peru continental margin upwelling sediments. Proceedings of the Ocean Drilling Program, Scientific Results (College Station, TX, Ocean Drilling Program), 112: 43–58.

Kemp, A.E.S., 1995. Laminated sediments from coastal and open ocean upwelling zones: What variability do they record? *In* Summerhayes, C.P., Emeis, K.-C., Angel, M.V., Smith, R.L. and Zeitschel, B. (eds.), Upwelling in the Ocean: Modern Processes and Ancient Records. Wiley, Chichester: 239–257.

Kemp, A.E.S. and Baldauf, J.G. 1993. Vast Neogene laminate diatom mat deposits from the eastern equatorial Pacific Ocean. Nature, 362: 141–144.

Kemp, A.E.S., Pike, J. Pearce, R.B. and Lange, C.B. 2000. The "Fall dump" — a new perspective on the role of a "shade flora" in the annual cycle of diatom production and export flux. Deep-Sea Research II, 47: 2129–2154.

*Kumar, A. and Patterson, R.T. 2002. Dinoflagellate cyst assemblages from Effingham Inlet, Vancouver Island, British Columbia, Canada. Palaeogeography, Palaeoclimatology, Palaeoecology, 180: 187–206.

Lamoureux, S. F. 1994. Embedding unfrozen lake sediments for thin section preparation. Journal of Paleolimnology, 10: 141–146.

Lange, C.B., Burke, S.K., and Berger, W.H. 1990. Biological production off southern California is linked to climate change. Climate Change, 16: 319–329.

Lange, C.B. Hasle, G.R. and Syvertsen, E.E. 1992. Seasonal cycle of diatoms in the Skagerrak, North Atlantic, with emphasis on the period 1980–1990. Sarsia, 77: 173–187.

Lange, C.B., Weinheimer, A.L., Reid, F.M.H., and Thunell, R.C. 1997. Sedimentation patters of diatoms, radiolarians, and silicoflagellates in Santa Barbara Basin, California. CalCOFI Report, 38: 161–170.

Lange, C.B., Weinheimer, A.L., Reid, F.M.H., Tappa, E., and Thunell, R.C. 2000. Repsonse of siliceous microplankton from the Santa Barbara Basin to the 1997–1998 El Niño event. CalCOFI Report, 41: 186–193.

Laws, R.A. 1983. Preparing strewn slides for quantitative microscopical analysis: A test using calibrated microspheres. Micropaleontology, 29: 60–65.

Lewis, W.M., Jr. 1984. The diatom sex clock and its evolutionary significance. American Naturalist, 123: 73–80.

Lipps, F.H. (ed.) 1993. Fossils Prokaryotes and Protists. Blackwell Scientific Publications, Boston: 342 p.

Lowden, J.A. and Blake, W., Jr. 1968. Geological Survey of Canada radiocarbon dates VII. Radiocarbon, v. 10, p. 207-245.

Lowden, J.A. and Blake, W., Jr. 1975. Radiocarbon dates XV. Geological Survey of Canada, Paper 75-7: 61 p.

Luternauer, J.L. and Murray, J.W. 1983. Late Quaternary morphologic development and sedimentation, central British Columbia continental shelf. Geological Survey of Canada, Paper 83-21: 38 p.

Mackas, D.L. and Sefton, H.A. 1982. Plankton species assemblages off southern Vancouver Island: Geographic patterns and temporal variability. Journal of Marine Science, 40: 1173–1198.

Mann, M.E., Park, J. and Bradley, R.S. 1995. Global interdecadal and century-scale climate oscillations during the past five centuries. Nature, 378: 266–267.

Mantua, N.J., Hare, S.R. Zhang, Y., Wallace, J.M. and Francis, R.C. 1997. A Pacific interdecadal climate oscillation with impacts on salmon production. Bulletin of the America Meteorological Society, 78: 1069–1079.

Margalef, R. 1958. Temporal succession and spatial heterogeneity in phytoplankton. *In* Traverso, A.A. (ed.), Perspectives in Marine Biology. University of California Press, Berkeley: 323–249.

Marsh, N.D. and Svensmark, H. 2000. Low cloud properties influenced by cosmic rays. Physical Review Letters, 85: 5004-5007.

Mathewes, R.W. 1985. Paleobotanical evidence for climatic change in southern British Columbia during late-glacial and Holocene time. *In* Harrington, C.R. (ed.), Climatic Change in Canada 5, Critical Periods in the Quaternary Climatic History of Northern North America. National Museums of Canada, National Museum of Natural Sciences, Syllogeus Series, No. 55: 397–422.

Mathewes, R.W. and Huesser, L.E .1981. A 12,000-year palynological record of temperature and precipitation trends in southwestern British Columbia. Canadian Journal of Botany, 51: 707–710.

McFarlane, G.A. and Beamish, R.J. 1992. Climatic influence linking copepod production with strong year-classes in the sablefish, Anoplopoma fimbria. Canadian Journal of Fisheries and Aquatic Sciences, 49: 743–753.

McMinn, A. 1995. Comparison of diatom preservation between oxic and anoxic basins in Ellis Fjord, Antarctica. Diatom Research, 10: 145–151.

McQuoid, M.R. and Hobson, L.A. 1997. A 91-year record of seasonal and interannual variability of diatoms from laminated sediments in Saanich Inlet, British Columbia. Journal of Plankton Research, 19: 173–194.

McQuoid, M.R. and Hobson, L.A. 1998. Assessment of palaeoenvironmental conditions on southern Vancouver Island, British Columbia, Canada, using the marine tychoplankter *Paralia sulcata*. Diatom Research, 13: 311–321.

McQuoid, M.R. and Hobson, L.A. 2001. A Holocene record of diatom and silicicoflagellate microfossils in sediments of Saanich Inlet, ODP Leg 169S. Marine Geology, 174: 111–124.

Middleton, G.V. and Hampton, M.A. 1976. Subaqueous sediment transport and deposition by sediment gravity flows. *In* Stanley, D.J. and Swift, D.J.P. (eds.), Marine Sediment Transport and Environmental Management. Wiley and Sons, New York: 197–218.

Minobe, S. 1997. A 50–70 year climatic oscillation over the North Pacific and North America. Geophysical Research Letters, 24: 683–686.

Minobe, S. 1999. Resonance in bidecadal and pentadecadal climate oscillations over the North Pacific: Role in climatic regime shifts. Geophysical Research Letters, 26: 855–858.

Morlet, J., Arehs, G., Fourgeau, I and Girard, D. 1982. Wave propagation and sampling theory. Geophysics, 47: 203.

Nissembaum, A., Presley, B.J., and Kaplan, I.R. 1972. Early diagenesis in a reducing fjord, Saanich Inlet, British Columbia. I. Chemical and isotopic changes in major components of interstitial water. Geochimica et Cosmochima Acta, 36: 1007–1027.

Patterson, R.T. and Fishbein, E. 1989. Re-examination of the statistical methods used to determine the number of point counts needed for micropaleontological quantitative research. Journal of Paleontology, 63: 245–248.

*Patterson, R.T., Guilbault, J.-P., and Thomson, R.E. 2000. Oxygen level control on foraminiferal distribution in Effingham Inlet, Vancouver Island, British Columbia, Canada. Journal of Foraminiferal Research, 30: 321–335.

*Patterson, R.T., Prokoph, A. and Chang, A.S. In review A. Late Holocene sedimentary response to solar and cosmic ray activity influenced climate variability in the NE Pacific. Sedimentary Geology.

*Patterson, R.T., Prokoph, A., Kumar, A. and Chang, A.S. In review B. Impact of Holocene solar variability on pelagic fish and phytoplankton productivity in the NE Pacific Ocean. The Holocene.

*Patterson, R.T., Wright, C., Chang, A.S., Taylor, L.A., Lyons, P.D., Kumar, A. and Dallimore, A. 2002. Atlas of common squamatological (fish scale) material in coastal British Columbia, and an assessment of the utility of various scale types in paleofisheries reconstruction. Palaeontologia Electronica, 4 (2): 88 p. <http://palaeo-electronica.org>

Pellatt, M.G., Hebda, R.J. and Mathewes, R.W. 2001. High-resolution Holocene vegetation history and climate from Hole 1034B, ODP leg 169S, Saanich Inlet, Canada. Marine Geology, 174: 211–226.

Pickard, G.L. 1961. Oceanographic features of inles in the British Columbia mainland coast. Journal, Fisheries Research Board of Canada, 18: 907–999

Pickard, G.L. 1963. Oceanographic charateristics of inlets of Vancouver Island, British Columbia. Journal, Fisheries Research Board of Canada, 20: 1109–1144.

Pike, J. and Kemp, A.E.S. 1996. Records of seasonal flux in Holocene laminated sediments, Gulf of California. *In* Kemp, A.E.S. (ed.), Palaeoclimatology and Palaeoceanography from Laminated Sediments. Geological Society (London) Special Publication No. 116: 157–169.

Pitcher, G.C. 1990. Phytoplankton seed population of the Cape Peninsula upwelling plume, with particular reference to resting spores of Chaetoceros (Bacillariophyceae) and their role in seeding upwelling waters. Estuarine, Coastal and Shelf Science, 31: 283–301.

Pisias, N. 1978. Paleoceanography of the Santa Barbara basin during the last 8000 years. Quaternary Research, 10: 366–384.

Polysciences, Inc.1995. Spurr low-viscosity embedding media. Data Sheet #127. Warington, PA: 2 p.

Porter, S.C. and Denton, G.H. 1967. Chronology of neoglaciation in the North American Cordillera. American Journal of Science, 265: 177–210.

Prokoph, A. and Barthelmes, F. 1996. Detection of nonstationaries in geological times series: Wavelet transform of chaotic and cyclic sequences. Computers and Geoscience, 22: 1097–1108.

Prokoph, A. and Patterson, R.T. In press. From depth scale to time scale: Transforming sediment image color data into a high-resolution time series. *In* Francus, P. (ed.),

Image Analysis, Sediment and Paleoenvironments. Kluwer Academic Publishers, Dordrecht, The Netherlands.

Quayle, D.B. 1988. Pacific Oyster Culture in British Columbia. Canadian Bulletin of Fisheries and Aquatic Sciences. No. 218: 241 p.

Quinn, W.H., Neal, V.T., and Antunez de Mayolo, S.E. 1987. El Niño occurrences over the past four and a half centuries. Journal of Geophysical Research, 92 (C13): 14,449–14,461.

Redmond, K.T. and Koch, R.W. 1991. Surface climate and streamflow variability in the western United States and their relationship to large-scale circulation indices. Water Resource Research, 27: 2381-2399.

Reed, R.K. and Halpern, D. 1976. Observations of the California Undercurrent off Washington and Vancouver Island. Limnology and Oceanography, 21: 389–398.

Robinson, S.N. and Thomson, G. 1981. Radiocarbon corrections for marine shell dates with application to southern Pacific northwest coast prehistory. Syesis, 14: 45–57.

Roelofs, A.K. 1983. The distribution of diatoms in the surface sediments of British Columbia inlets. Ph.D. dissertation, University of British Columbia, Canada: 267 p.

Rogers, G.C. 1980. A documentation of soil failure during the British Columbia earthquake of 23 June, 1946. Canadian Geotechnical Journal, 17: 122–127.

Round, F.E, Crawford, R.M., and Mann, D.G. (eds.) 1990. Diatoms: Biology and Morphology of the Genera. Cambridge University Press, New York: 747 p.

Ryder, J.M. 1989. Climate (Canadian Cordillera). *In* Fulton, R.J. (ed.), Quaternary Geology of Canada and Greenland, Geology of Canada, No. 1. Geological Survey of Canada: 26–31.

Ryder, J.M., and Thomson, B. 1986. Neoglaciation in the southern Coast Mountains of British Columbia: chronology prior to the late Neoglacial maximum. Canadian Journal of Earth Sciences, 23: 273–287.

Ryther, J.H. 1969. Photosynthesis and fish production in the sea. Science, 166: 72–76.

Sancetta, C. 1989a. Spatial and temporal trends of diatom flux in British Columbian fjords. Journal of Plankton Research, 11: 503–520.

Sancetta, C. 1989b. Processes controlling the accumulation of diatoms in sediments: a model derived from British Columbia fjords. Paleoceanography, 4: 235–251.

Sancetta, C. 1990. Seasonal occurrence of silicoflagellate morphologies in different environments of the eastern Pacific Ocean. Marine Micropaleontology, 16: 285–291.

Sancetta, C. 1996. Laminated diatomaceous sediments: Controls on formation and strategies for analyses. *In* Kemp, A.E.S. (ed.), Palaeoclimatology and Palaeoceanography from Laminated Sediments. Geological Society (London) Special Publication No. 116: 17–21.

Sancetta, C. and Calvert, S.E. 1988. The annual cycle of sedimentation in Saanich Inlet, British Columbia: Implications for the interpretation of diatom fossil assemblages. Deep-Sea Research, 35: 71–90.

Sautter, L. R. and Sancetta, C. 1992. Seasonal associations of phytoplankton and planktic foraminifera in an upwelling region and their contribution to the seafloor. Marine Micropaleontology, 18: 263–278.

Schimmelmann, A., Lange, C.B., and Berger, W.H. 1990. Climatically controlled marker layers in Santa Barbara Basin Sediments, and fine-scale core-to-core correlation. Limnology and Oceanography, 35: 165–173.

Schimmelmann, A., Lange, C.B., Berger, W.H., Simon, A., Burke, S.K. and Dunbar, R.B. 1992. Extreme climatic conditions recorded in Santa Barbara Basin laminated sediments: the 1835-1840 *Macoma* event. Marine Geology, 106: 279–299.

Schrader, H.J. and Gersonde, G. 1978. Diatoms and silicoflagellates. Utrecht Micropaleontological Bulletin, 17: 129–176.

Scott, D.B. and Hermelin, J.O.R. 1993. A device for precision splitting of micropaleontological samples in liquid suspension. Journal of Paleontology, 67: 151–154.

Shapiro, J. 1958. The freeze-corer: A new sampler for lake sediments. Ecology, 39: 748.

Shaviv, N.J. and Veizer, J. 2003. Celestial driver of Phanerozoic climate? GSA Today, 13: 4–10.

Silver, M. and Alldredge, A. 1981. Bathypelagic marine snow: deep-sea algal and detrital community. Journal of Marine Research, 39: 501–530.

Silver, E.A. and Smith, R.B. 1983. Comparison of terrane accretion in modern Southeast Asia and the Mesozoic North American Cordillera. Geology, 11: 198–202.

Simonsen, R. 1974. The diatom plankton of the Indian Ocean Expedition of RV "Meteor" 1964-1965. "Meteor" Forschungsergebnisse Reihe D, 19: 1–107.

Smayda, T.J. 1957. Plankton studies in lower Narrangansett Bay. Limnology and Oceanography, 2: 342–354.

Smayda, T.J. 1973. The growth of *Skeletonema costatum* during a winter–spring bloom in Narragansett Bay. Norweigen Journal of Botany, 20: 219–247.

Smetacek, V. 1985. Role of sinking in diatom life-history cycles: Ecological, evolutionary and geological significance. Marine Biology, 84: 239–251.

Smetacek, V. Scharek, R., Gordon, L.I., Eicken, H., Fahrbach, E., Rohardt, G., and Moore, S. 1992. Early spring phytoplankton blooms in ice platelet layers of the southern Weddell Sea, Antarctica. Deep-Sea Research, 39: 153–168.

Sorgente, D., Frignani, M., Longone, L., and Ravaioli, M., 1999, Chronology of Marine Sediments: Interpretation of Activity-Depth Profiles of ^{210}Pb and other Radioactive Tracers, Part I: Technical Report n. 54: Consiglio Nazionale delle Ricerche Inistituto per la Geologia Marina Bologna: 32 p.

Soutar, A. and Crill, P. 1977. Sedimentation and climatic patterns in the Santa Barbara Basin during the 19th and 20th centuries. Geological Society of America Bulletin, 88: 1161–1172.

Stronach, J.A., Ng, M.K., Foreman, M.G., and Murty, T.S. 1993. Tides and currents in Barkley Sound and Alberni Inlet. Marine Geodesy, 16: 1-41.

Stuiver, M. and Braziunas, T.F. 1993. Radiocarbon and 14C ages of marine samples to 10,000 B.C. Radiocarbon, 35: 137–189.

Stuiver, M, Reimer, P.J., Bard, E., Beck, J.W., Burr, G.S., Hughen, K.A., Kromer, B. McCormac, F.G., Plight, J. and Spurk, M. 1998a. INTCAL 98 radiocarbon age calibration 24,000–0 cal BP. Radiocarbon, 40: 1041–1083.

Stuiver, M., Reimer, P.J. and Braziunas, T.F. 1998b. High-precision radiocarbon age calibration for terrestrial and marine samples. Radiocarbon, 40: 1127–1151.

Subbotina, M.M., Thomson, R.E., and Rabinovich, A.B. 2001. Spectral characteristics of sea level variability along the west coast of North America during the 1982–83 and 1997-98 El Niño Events. Progress in Oceanography, 49: 353–372.

Syvertsen, E.E. 1977. *Thalassiosira rotula* and *T. gravida*: Ecology and morphology. Nova Hedwigia, 54: 99–112.

Syvitski, J.P.M. and Shaw, J., 1996. Sedimentology and geomorphology of fjords. Chapter 5, *In* Geomorphology and Sedimentology of Estuaries, Perillo, G.M.E. (ed.), Developments on Sedimentology (Elsevier) 53: 113–178.

Tabata, S. 1989. Trends and long-term variability of ocean properties at ocean station P in the northeast Pacific Ocean. *In* Petersen, D.H. (ed.), Aspects of Climate Variability in the Pacific and the Western Americas. Geophysical Monographs, 55: 113–132.

Takahashi, K. 1986. Seasonal fluxes of pelagic diatoms in the subarctic Pacific, 1982–1983. Deep-Sea Research, 33: 1225–1251.

Takahashi, K. 1987. Response of subarctic Pacific diatom fluxes to the 1982–1983 El Niño disturbance. Journal of Geophysical Research, 92 (C13): 14,387–14, 392.

Takahashi, M., Seibert, D.L. and Thomas, W.H. 1977. Occasional blooms of phytoplankton during summer in Saanich inlet, B.C., Canada. Deep-Sea Research, 24: 775–780.

Taylor, F.J.R. and Haigh, R. 1996. Spatial and temporal distributions of microplankton during the summers of 1992–1993 in Barkley Sound, British Columbia, with emphasis on harmful species. Canadian Journal of Fisheries and Aquatic Sciences, 53: 2310–2322.

ter Braak, C.J.F. 1986. Canonical correspondence analysis: a new eigenvector technique for multivariate direct gradient analysis. Ecology, 67: 1167–1179.

ter Braak, C.J.F. and Prentice, I.C. 1988. A theory of gradient analysis. Advances in Ecological Research, 18: 272–313.

ter Braak, C.J.F. and Smilauer, P. 1998. CANOCO reference Manual and User's Guide to Canoco for Windows: Software for Canonical Community Ordination (version 4). Microcomputer Power, Ithica, NY: 352 p.

Thomson, R.E. 1981. Oceanography of the British Columbia Coast. Canadian Special Publication of Fisheries and Aquatic Sciences No. 56: 291 p.

Thomson, R.E., Hickey, B.M., and LeBlond, P.H. 1989. The Vancouver Island Coastal Current: Fisheries barrier and conduit. *In* Beamish, R.J. and MacFarlane, G.A. (eds.), Effects of Ocean Variability on recruitment and an Evaluation of Parameters Used in Stock Assessment Models. Canadian Special Publication of Fisheries and Aquatic Sciences No. 108: 265–296.

Thomson, R.E. and Gower, J.F.R. 1998. A basin-scale oceanic instability event in the Gulf of Alaska. Journal of Geophysical Research, 103 (C2): 3033–3040.

Thunell, R., Pride, C., Tappa, E. and Muller-Karger, F. 1993. Varve formation in the Gulf of California: Insights from time series sediment trap sampling and remote sensing. Quaternary Science Reviews, 12: 451–464.

Timothy, D.A. and Pond, S. 1997. Describing additional fluxes to deep sediment traps and water-column decay in a coastal environment. Journal of Marine Research, 55: 383–406.

Timothy, D.A. and Soon, M.Y.S. 2001. Primary production and deep-water oxygen content of two British Columbian fjords. Marine Chemistry, 73: 37–51.

Tipper, H.W., Woodsworth, G.J., and Gabrielse, H. (coordinators) 1981. Tectonic assemblage map of the Canadian Cordillera and adjacent parts of the United States of America. Geological Survey of Canada Map, 1505A.

Todd, M.C. and Kniveton, D.R. 2001. Changes in cloud cover associated with Forbush decreases of galactic cosmic rays. Journal of Geophysical Research—Atmospheres, 106: 32031–32041.

Tomas, C.R. (ed.) 1997. Identifying Marine Phytoplankton. Academic Press, San Diego: 858 p.

Tully, J.P., 1949. Oceanography and prediction of pulp-mill pollution in Alberni Inlet. Fisheries Research Board of Canada, Bulletin 83: 169.

Venrick, E.L., McGowan, J.A., Cayan, D.R. and Hayward, T.L. 1987. Climate and chlorophyll a: Long-term trends in the central North Pacific Ocean. Science, 238: 70–72.

Waite, A., Bienfang, P.K., and Harrison, P.J. 1992. Spring bloom sedimentation in a subarctic ecosystem. II. Succession and sedimentation. Marine Biology, 114: 131–138.

Ware, D.M. and Thomson, R.E. 1991. Link between long-term variability in upwelling and fish production in the northeast Pacific Ocean. Canadian Journal of Fisheries and Aquatic Sciences, 48: 2296–2306.

Ware, D.M. and Thomson, R.E. 2000. Interannual to multidecadal timescale climate variations in the Northeast Pacific. Journal of Climate, 13: 3209–3220.

Werner, D. (ed.) 1977. The Biology of Diatoms. Botanical Monographs, v. 13. Blackwell Scientific Publications, Oxford, UK: 498 p.

Wilkerson, F.P., Dugdale, R.C., and Barber, R.T. 1987. Effects of El Niño on new, regenerated, and total production in eastern boundary upwelling systems. Journal of Geophysical Research, 92 (C13): 14,347–14,353.

Witkowski, A., Lange-Bertalot, H., and Metzeltin, D. 2000. Diatom Flora of Marine Coasts I. Iconographia Diatomologica Annotated Diatom Monographs, v. 7. A.R.G. Gantner Verlag K.G.: 925 p.

Wright, H.E. 1980. Cores of soft lake sediments. Boreas, 9: 107–114.

Yorath, C.J. and Naismith, H.W. 1995. The Geology of Southern Vancouver Island: a Field Guide. Orca Book Publishers, Victoria, B.C., Canada: 172 p.

APPENDIX A

AMS Radiocarbon (^{14}C) Dating Results from Piston Cores

The following is a facsimile of the original report supplied by Dr. Roelf Beukens of IsoTrace Laboratories, University of Toronto, for dating of all piston cores recovered during the October 1999 research cruise to Effingham Inlet. The dates represent calibrated radiocarbon years before present.

60 St. George Street
IsoTrace Radiocarbon Laboratory Toronto (Ont.) Canada M5S 1A7
Accelerator Mass Spectrometry Facility
at the University of Toronto
Telephone: (416) 978 - 4628
Fax: (416) 978 - 4711
Email: roelf.beukens@utoronto.ca

Radiocarbon Analysis Report

October 21, 2000

Submitter: R.T. Patterson, Dept of Earth Sciences, Carleton Univ, Ottawa ON

These results are the average of 2 separate analyses (normal precision) and are corrected for natural and sputtering fractionation to a base of $\delta^{13}C = -25‰$. The sample ages are quoted as uncalibrated conventional radiocarbon dates in years before present (BP), using the Libby ^{14}C meanlife of 8033 years. The errors represent 68.3 % confidence limits.

Before hydrolysis, the outer 50–75% of shell samples TO-8672, TO-8675, and TO-8687 was removed by HCl leaching to ensure that clean, unaltered carbonate material was used. The remaining shell samples were too small for a preleach. Marine reservoir corrections have not been applied to the results for these shell samples.

Sample Identification	Description	Weight used (mg)	IsoTrace Lab Number	Age (years BP)
RC03S101	wood frags	476	TO-8671	160 ± 40
RC03S201	shell valves	88	TO-8672	1770 ± 60
RC03S301	wood frags	135	TO-8673	2050 ± 70
RC03S501	wood frag	545	TO-8674	2830 ± 60
RC03S601	shell valves	355	TO-8675	3890 ± 80
RC03S701	wood frag	562	TO-8676	4190 ± 80
RC06S301	wood twig	184	TO-8677	1080 ± 50
RC06S302	wood frag	498	TO-8678	1340 ± 50
RC06S502	wood twigs	380	TO-8679	2050 ± 80
RC06S801	wood twig	147	TO-8680	3590 ± 50
RC09S302	wood frag	430	TO-8681	1890 ± 50
RC09S601	shell valves	40	TO-8682	4100 ± 60
RC11S501	shell valve frag	46	TO-8683	2460 ± 90
RC11S801A	shell frag	24	TO-8684	2830 ± 60
RC11S801	wood frag	291	TO-8685	2570 ± 100
RC11S802	shell frags	82	TO-8686	1820 ± 60
RC13S401	wood twig	506	TO-8687	1080 ± 60
RC13S502	wood twig	441	TO-8688	2140 ± 60
RC13S603	wood frag	627	TO-8689	3170 ± 50
RC13S701	wood frags	600	TO-8690	3640 ± 50

ISOTRACE RADIOCARBON CALIBRATION REPORT
Output by calibration program C14CAL98

06-Feb-01

TO-8671 RC03S101 wood frags

Radiocarbon date : 160 ± 40 BP

All solutions, with a probability of 50% or greater for the calibrated age of this radiocarbon date, have been calculated from the dendro calibration data. The 68% and 95% confidence intervals, which are the 1σ and 2σ limits for a normal distribution, are also given. A probability of 100% means the radiocarbon date intersects the dendro calibration curve at this age.
All results are rounded to the nearest multiple of 5 years.

Probability	cal Age	68.3 % c.i.	95.5 % c.i.
100 %	1675 cal AD	1665 AD - 1690 AD	1655 AD - 1895 AD
100 %	1735 cal AD	1725 AD - 1780 AD	1655 AD - 1895 AD
100 %	1750 cal AD	1725 AD - 1780 AD	1655 AD - 1895 AD
100 %	1755 cal AD	1725 AD - 1780 AD	1655 AD - 1895 AD
100 %	1805 cal AD	1795 AD - 1810 AD	1655 AD - 1895 AD
100 %	1935 cal AD	1915 AD - 1945 AD	1905 AD - 1955 AD
100 %	1955 cal AD	1950 AD - 1955 AD	1905 AD - 1955 AD

Calibrated with the standard data set INTCAL98 from:
M.Stuiver et al.; Radiocarbon 40#3 (1998) p1041

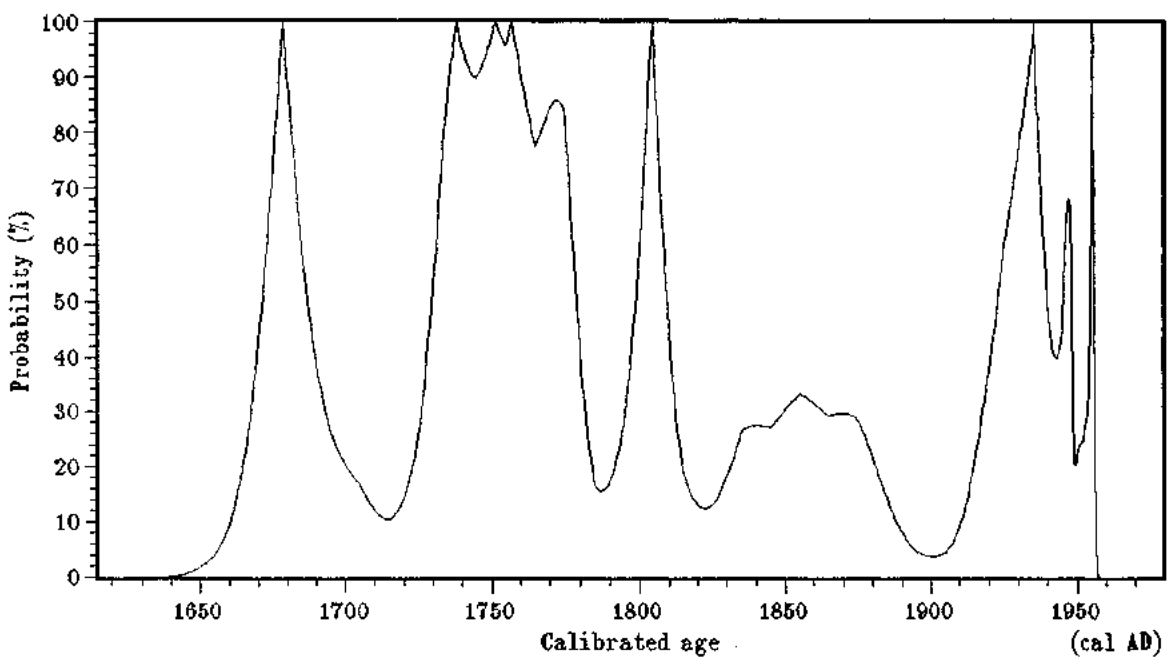

ISOTRACE RADIOCARBON CALIBRATION REPORT
Output by calibration program C14CAL98

06-Feb-01

TO-8672 RC03S201 shell valves

Radiocarbon date : 1770 ± 60 BP

All solutions, with a probability of 50% or greater for the calibrated age of this radiocarbon date, have been calculated from the dendro calibration data. The 68% and 95% confidence intervals, which are the 1σ and 2σ limits for a normal distribution, are also given. A probability of 100% means the radiocarbon date intersects the dendro calibration curve at this age.
All results are rounded to the nearest multiple of 5 years.

Probability	cal Age	68.3 % c.i.	95.5 % c.i.
100 %	1025 cal AD	975 AD - 1065 AD	895 AD - 1165 AD

Calibrated with the marine data set MARINE98 from:
M.Stuiver, P.J.Reimer, and Th.F.Braziunas; Radiocarbon 40#3 (1998) p1127

Delta R reservoir correction = 390 ± 25 years
from M.Stuiver and T.F.Braziunas; Radiocarbon 35#1 (1993) p156

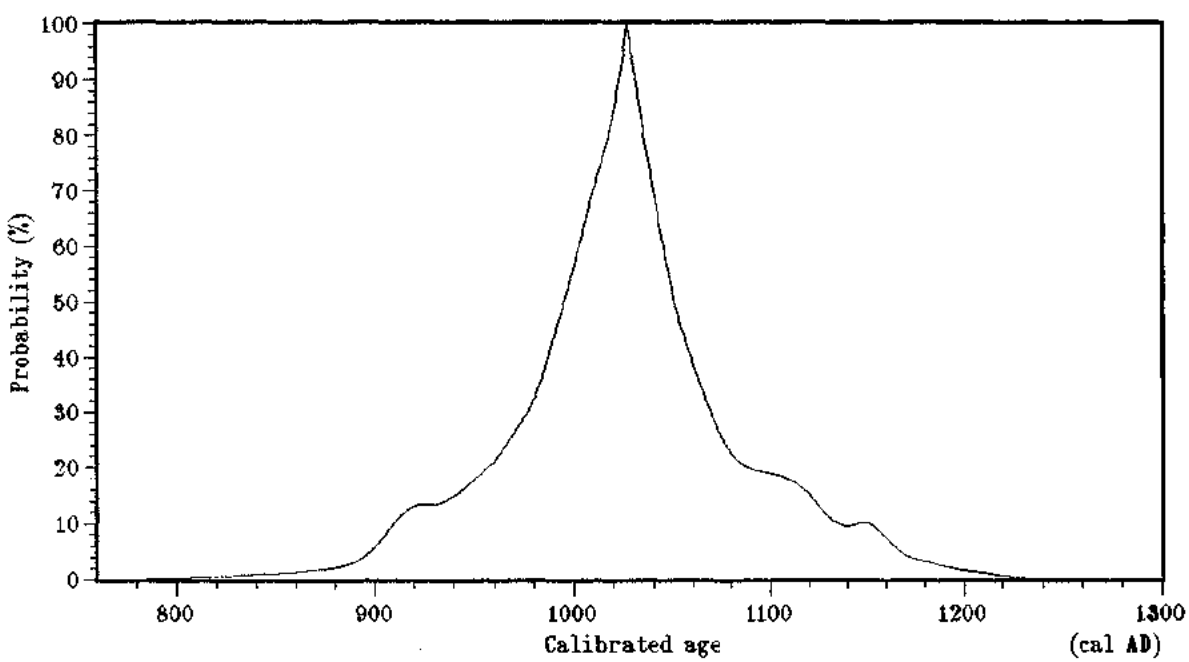

ISOTRACE RADIOCARBON CALIBRATION REPORT
Output by calibration program C14CAL98

06-Feb-01

TO-8673 RC03S301 wood frags

Radiocarbon date : 2050 ± 70 BP

All solutions, with a probability of 50% or greater for the calibrated age of this radiocarbon date, have been calculated from the dendro calibration data. The 68% and 95% confidence intervals, which are the 1σ and 2σ limits for a normal distribution, are also given. A probability of 100% means the radiocarbon date intersects the dendro calibration curve at this age. All results are rounded to the nearest multiple of 5 years.

Probability	cal Age	68.3 % c.i.	95.5 % c.i.
100 %	45 cal BC	165 BC - 25 AD	205 BC - 80 AD

Calibrated with the standard data set INTCAL98 from:
M.Stuiver et al.; Radiocarbon 40#3 (1998) p1041

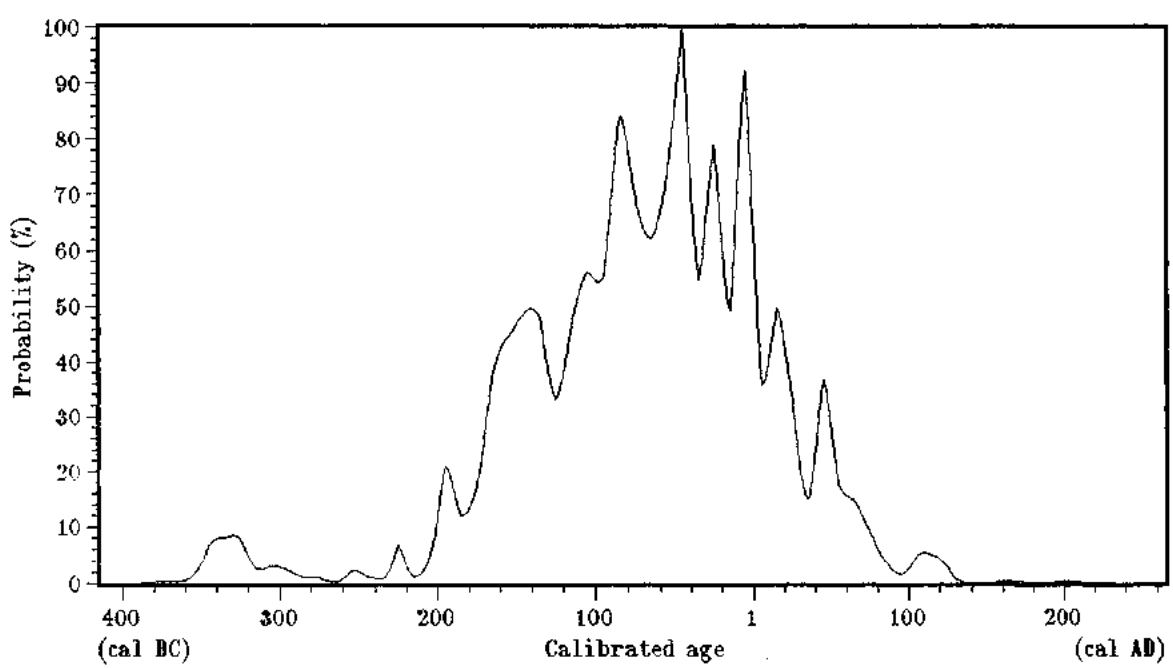

ISOTRACE RADIOCARBON CALIBRATION REPORT
Output by calibration program C14CAL98

06-Feb-01

TO-8674 RC03S501 wood frag

Radiocarbon date : 2830 ± 60 BP

All solutions, with a probability of 50% or greater for the calibrated age of this radiocarbon date, have been calculated from the dendro calibration data. The 68% and 95% confidence intervals, which are the 1σ and 2σ limits for a normal distribution, are also given. A probability of 100% means the radiocarbon date intersects the dendro calibration curve at this age.
All results are rounded to the nearest multiple of 5 years.

Probability	cal Age	68.3 % c.i.	95.5 % c.i.
100 %	995 cal BC	1045 BC - 900 BC	1130 BC - 830 BC
100 %	985 cal BC	1045 BC - 900 BC	1130 BC - 830 BC
100 %	975 cal BC	1045 BC - 900 BC	1130 BC - 830 BC
100 %	945 cal BC	1045 BC - 900 BC	1130 BC - 830 BC

Calibrated with the standard data set INTCAL98 from:
M.Stuiver et al.; Radiocarbon 40#3 (1998) p1041

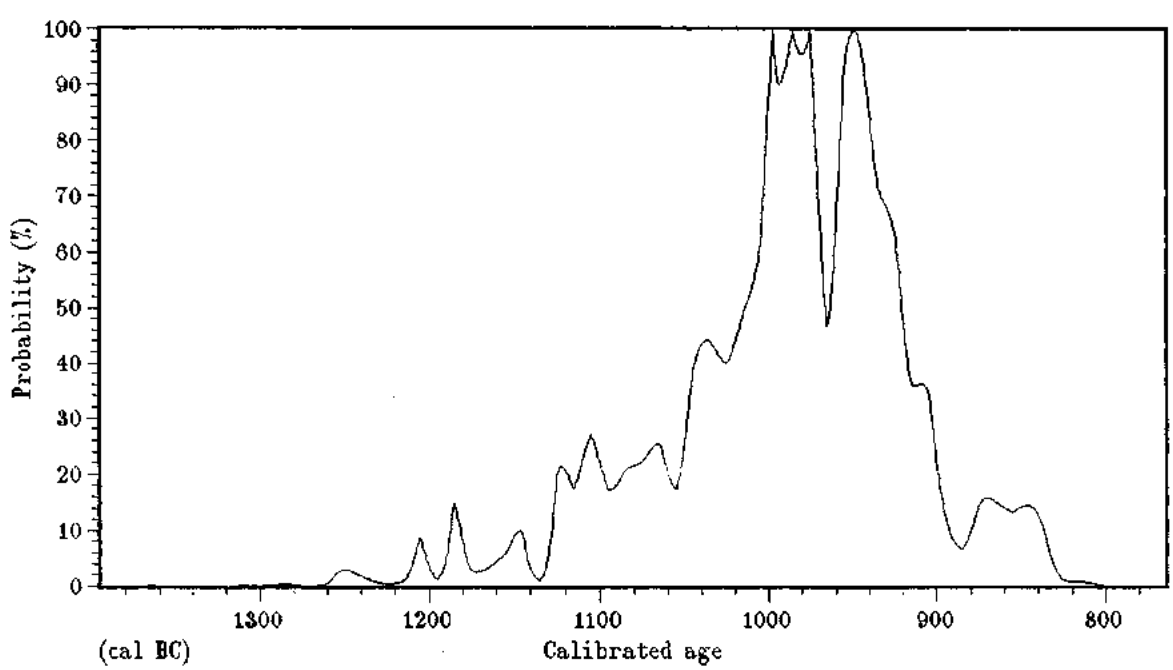

ISOTRACE RADIOCARBON CALIBRATION REPORT
Output by calibration program C14CAL98

06-Feb-01

TO-8675 RC03S601 shell valves

Radiocarbon date : 3890 ± 80 BP

All solutions, with a probability of 50% or greater for the calibrated age of this radiocarbon date, have been calculated from the dendro calibration data. The 68% and 95% confidence intervals, which are the 1σ and 2σ limits for a normal distribution, are also given. A probability of 100% means the radiocarbon date intersects the dendro calibration curve at this age.
All results are rounded to the nearest multiple of 5 years.

Probability	cal Age	68.3 % c.i.	95.5 % c.i.
100 %	1420 cal BC	1510 BC - 1355 BC	1620 BC - 1245 BC

Calibrated with the marine data set MARINE98 from:
M.Stuiver, P.J.Reimer, and Th.F.Braziunas; Radiocarbon 40#3 (1998) p1127

Delta R reservoir correction = 390 ± 25 years
from M.Stuiver and T.F.Braziunas; Radiocarbon 35#1 (1993) p156

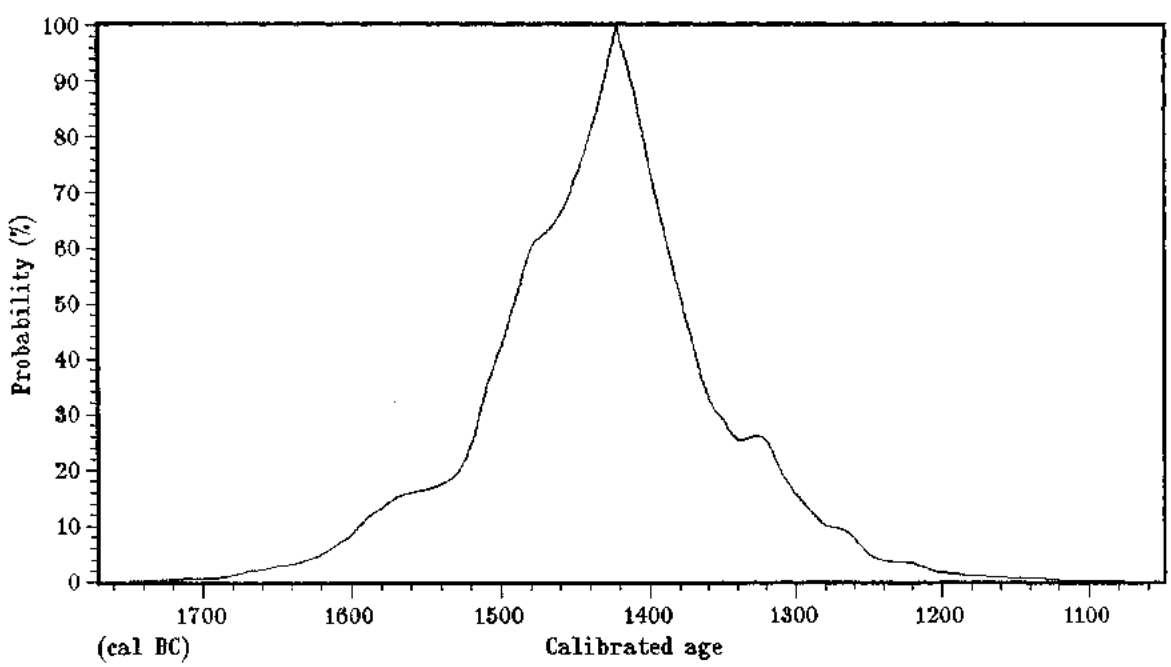

ISOTRACE RADIOCARBON CALIBRATION REPORT
Output by calibration program C14CAL98

06-Feb-01

TO-8676 RC03S701 wood frag

Radiocarbon date : 4190 ± 80 BP

All solutions, with a probability of 50% or greater for the calibrated age of this radiocarbon date, have been calculated from the dendro calibration data. The 68% and 95% confidence intervals, which are the 1σ and 2σ limits for a normal distribution, are also given. A probability of 100% means the radiocarbon date intersects the dendro calibration curve at this age. All results are rounded to the nearest multiple of 5 years.

Probability	cal Age	68.3 % c.i.	95.5 % c.i.
100 %	2870 cal BC	2885 BC - 2830 BC	2920 BC - 2565 BC
100 %	2800 cal BC	2820 BC - 2660 BC	2920 BC - 2565 BC
100 %	2785 cal BC	2820 BC - 2660 BC	2920 BC - 2565 BC
99 %	2765 cal BC	2820 BC - 2660 BC	2920 BC - 2565 BC

Calibrated with the standard data set INTCAL98 from:
M.Stuiver et al.; Radiocarbon 40#3 (1998) p1041

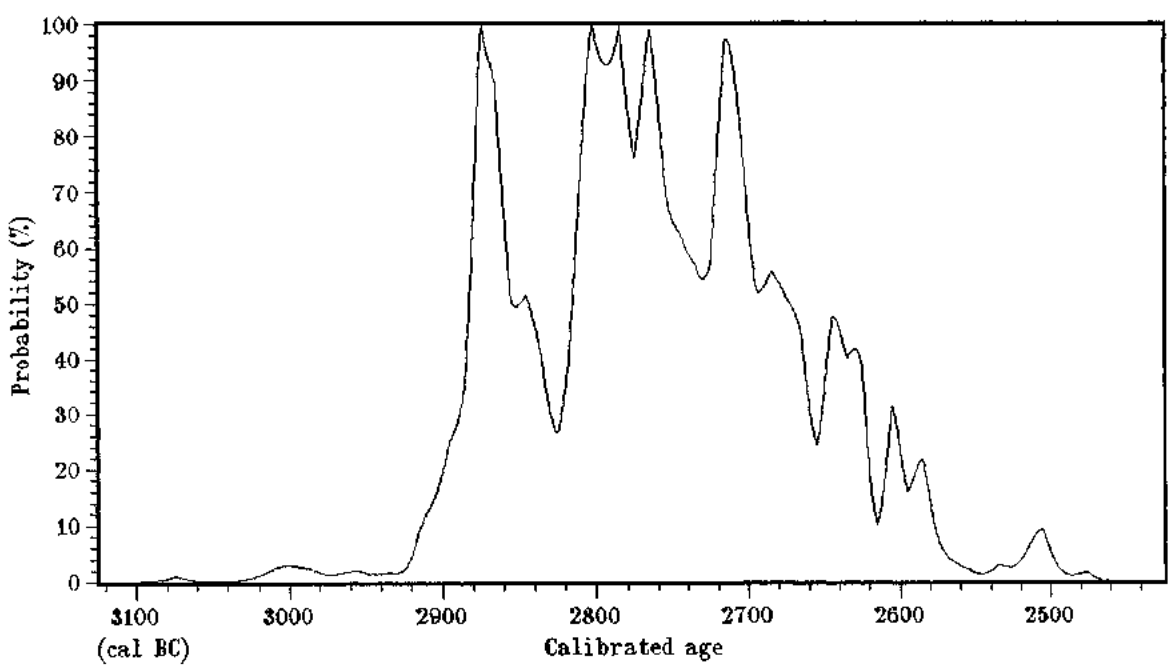

ISOTRACE RADIOCARBON CALIBRATION REPORT
Output by calibration program C14CAL98

06-Feb-01

TO-8677 RC06S301 wood twig

Radiocarbon date : 1080 ± 50 BP

All solutions, with a probability of 50% or greater for the calibrated age of this radiocarbon date, have been calculated from the dendro calibration data. The 68% and 95% confidence intervals, which are the 1σ and 2σ limits for a normal distribution, are also given. A probability of 100% means the radiocarbon date intersects the dendro calibration curve at this age.
All results are rounded to the nearest multiple of 5 years.

Probability	cal Age	68.3 % c.i.	95.5 % c.i.
77 %	905 cal AD	895 AD - 920 AD	880 AD - 1025 AD
100 %	980 cal AD	940 AD - 1000 AD	880 AD - 1025 AD

Calibrated with the standard data set INTCAL98 from:
M.Stuiver et al.; Radiocarbon 40#3 (1998) p1041

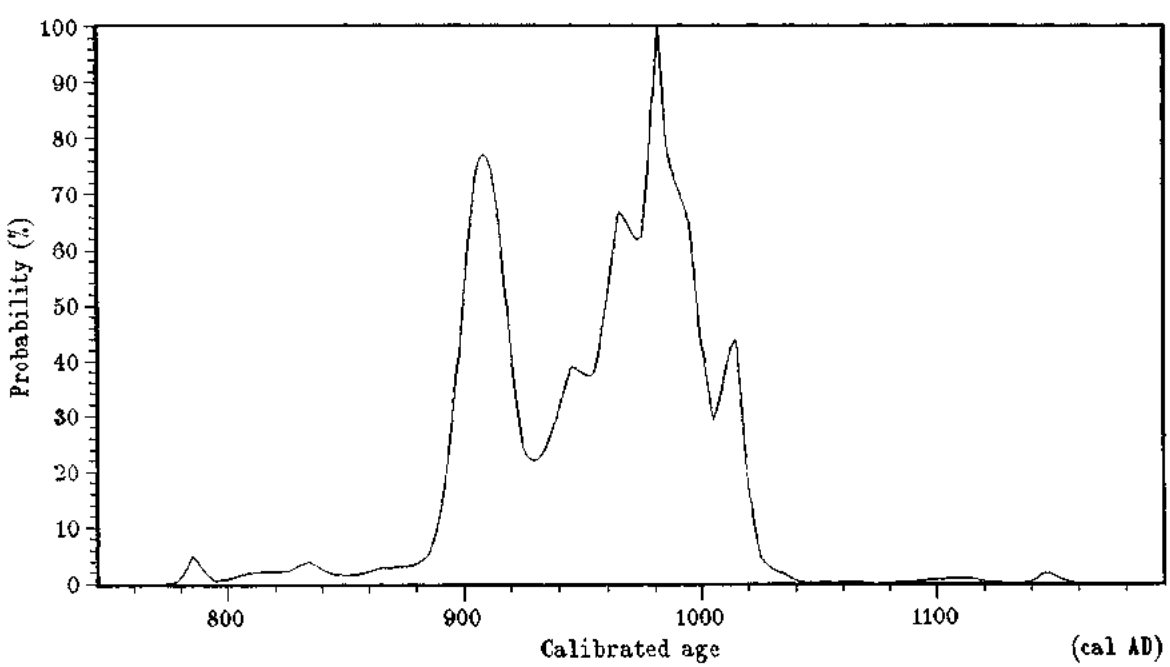

ISOTRACE RADIOCARBON CALIBRATION REPORT
Output by calibration program C14CAL98

06-Feb-01

TO-8678 RC06S302 wood frag

Radiocarbon date : 1340 ± 50 BP

All solutions, with a probability of 50% or greater for the calibrated age of this radiocarbon date, have been calculated from the dendro calibration data. The 68% and 95% confidence intervals, which are the 1σ and 2σ limits for a normal distribution, are also given. A probability of 100% means the radiocarbon date intersects the dendro calibration curve at this age.
All results are rounded to the nearest multiple of 5 years.

Probability	cal Age	68.3 % c.i.	95.5 % c.i.
100 %	665 cal AD	655 AD - 690 AD	635 AD - 775 AD

Calibrated with the standard data set INTCAL98 from:
M.Stuiver et al.; Radiocarbon 40#3 (1998) p1041

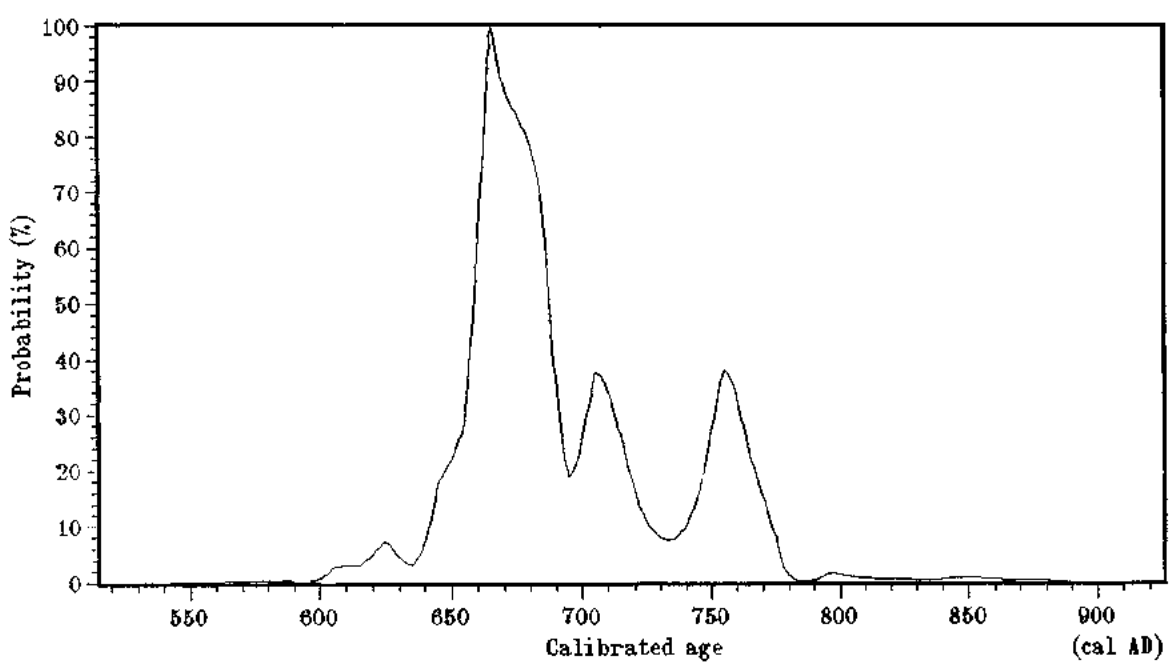

ISOTRACE RADIOCARBON CALIBRATION REPORT
Output by calibration program C14CAL98

06-Feb-01

TO-8679 RC06S502 wood twigs

Radiocarbon date : 2050 ± 80 BP

All solutions, with a probability of 50% or greater for the calibrated age of this radiocarbon date, have been calculated from the dendro calibration data. The 68% and 95% confidence intervals, which are the 1σ and 2σ limits for a normal distribution, are also given. A probability of 100% means the radiocarbon date intersects the dendro calibration curve at this age.
All results are rounded to the nearest multiple of 5 years.

Probability	cal Age	68.3 % c.i.	95.5 % c.i.
100 %	45 cal BC	170 BC - 25 AD	205 BC - 90 AD

Calibrated with the standard data set INTCAL98 from:
M.Stuiver et al.; Radiocarbon 40#3 (1998) p1041

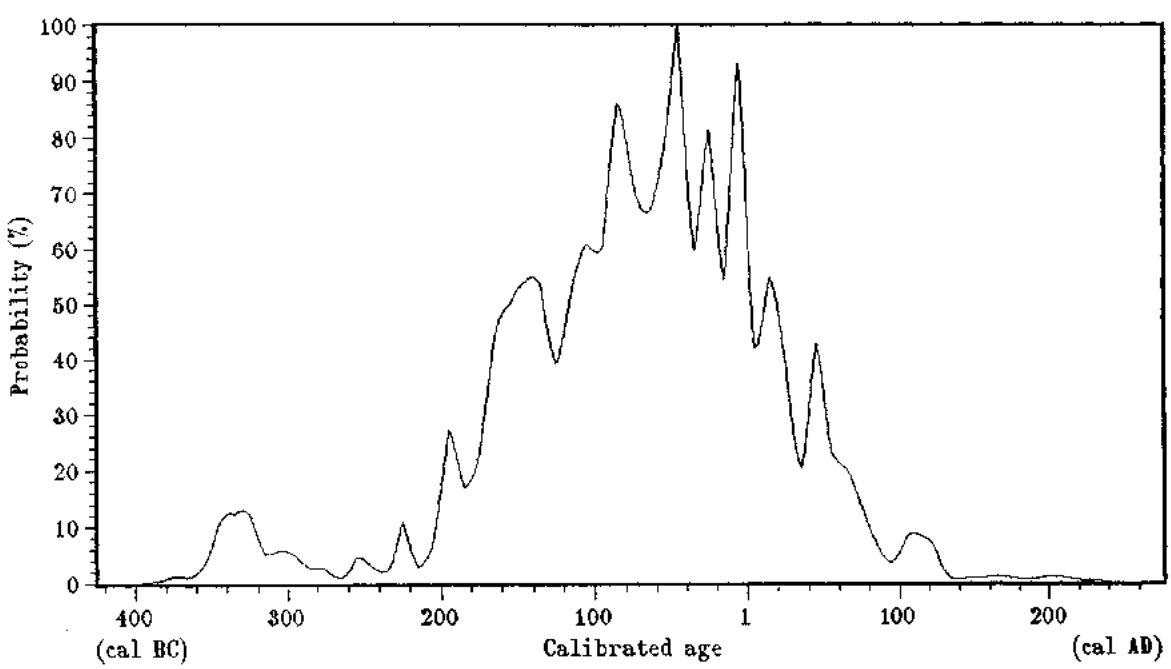

ISOTRACE RADIOCARBON CALIBRATION REPORT
Output by calibration program C14CAL98

06-Feb-01

TO-8680 RC06S801 wood twig

Radiocarbon date : 3590 ± 50 BP

All solutions, with a probability of 50% or greater for the calibrated age of this radiocarbon date, have been calculated from the dendro calibration data. The 68% and 95% confidence intervals, which are the 1σ and 2σ limits for a normal distribution, are also given. A probability of 100% means the radiocarbon date intersects the dendro calibration curve at this age. All results are rounded to the nearest multiple of 5 years.

Probability	cal Age	68.3 % c.i.	95.5 % c.i.
67 %	2005 cal BC	2025 BC - 1995 BC	2040 BC - 1860 BC
100 %	1935 cal BC	1980 BC - 1880 BC	2040 BC - 1860 BC
100 %	1925 cal BC	1980 BC - 1880 BC	2040 BC - 1860 BC
100 %	1920 cal BC	1980 BC - 1880 BC	2040 BC - 1860 BC

Calibrated with the standard data set INTCAL98 from:
M.Stuiver et al.; Radiocarbon 40#3 (1998) p1041

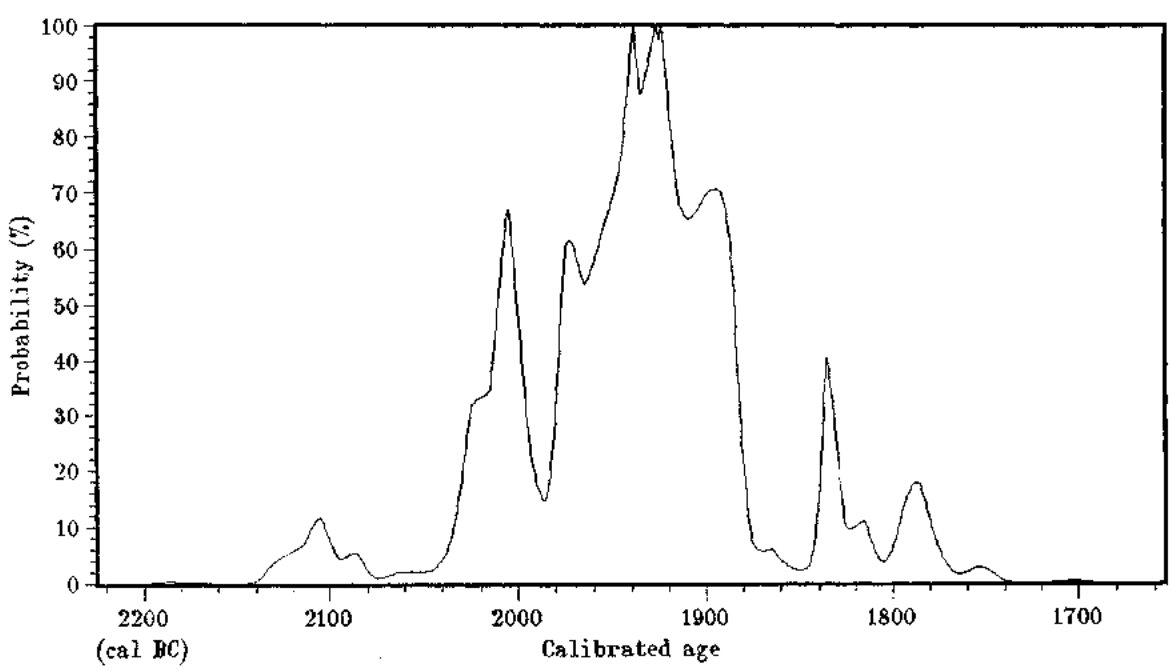

ISOTRACE RADIOCARBON CALIBRATION REPORT
Output by calibration program C14CAL98

06-Feb-01

TO-8681 RC09S302 wood frag

Radiocarbon date : 1890 ± 50 BP

All solutions, with a probability of 50% or greater for the calibrated age of this radiocarbon date, have been calculated from the dendro calibration data. The 68% and 95% confidence intervals, which are the 1σ and 2σ limits for a normal distribution, are also given. A probability of 100% means the radiocarbon date intersects the dendro calibration curve at this age.
All results are rounded to the nearest multiple of 5 years.

Probability	cal Age	68.3 % c.i.	95.5 % c.i.
100 %	90 cal AD	65 AD - 130 AD	20 AD - 240 AD
100 %	95 cal AD	65 AD - 130 AD	20 AD - 240 AD
100 %	125 cal AD	65 AD - 130 AD	20 AD - 240 AD

Calibrated with the standard data set INTCAL98 from:
M.Stuiver et al.; Radiocarbon 40#3 (1998) p1041

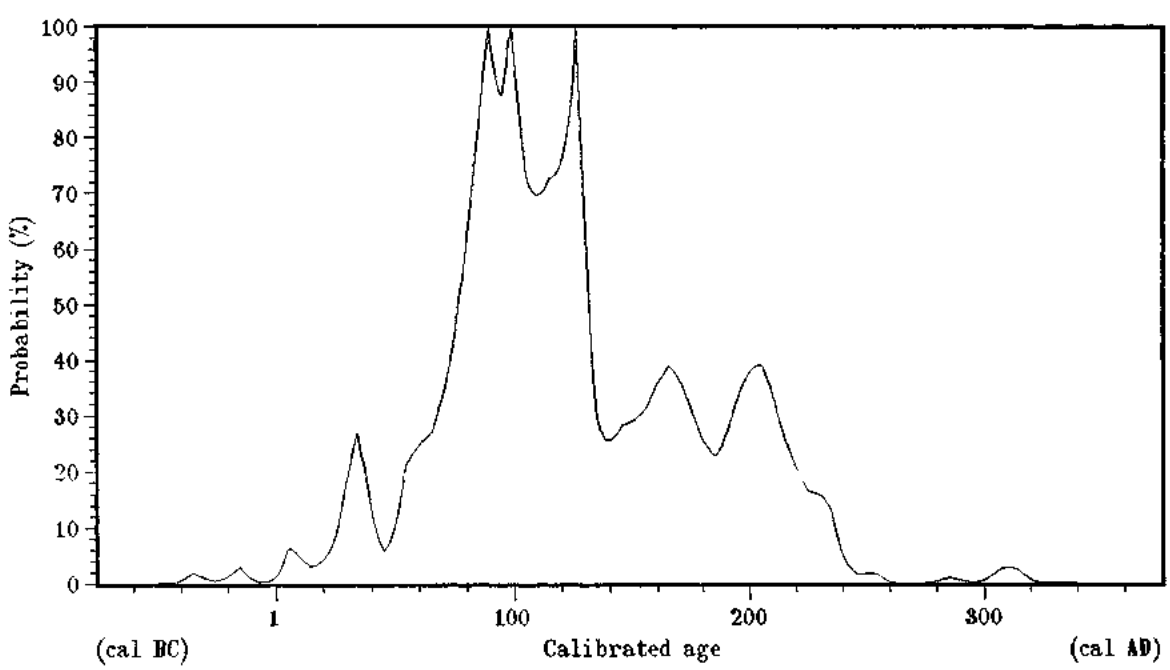

ISOTRACE RADIOCARBON CALIBRATION REPORT
Output by calibration program C14CAL98

06-Feb-01

TO-8682 RC09S601 shell valves

Radiocarbon date : 4100 ± 60 BP

All solutions, with a probability of 50% or greater for the calibrated age of this radiocarbon date, have been calculated from the dendro calibration data. The 68% and 95% confidence intervals, which are the 1σ and 2σ limits for a normal distribution, are also given. A probability of 100% means the radiocarbon date intersects the dendro calibration curve at this age.
All results are rounded to the nearest multiple of 5 years.

Probability	cal Age	68.3 % c.i.	95.5 % c.i.
100 %	1675 cal BC	1740 BC - 1595 BC	1860 BC - 1505 BC

Calibrated with the marine data set MARINE98 from:
M.Stuiver, P.J.Reimer, and Th.F.Braziunas; Radiocarbon 40#3 (1998) p1127

Delta R reservoir correction = 390 ± 25 years
from M.Stuiver and T.F.Braziunas; Radiocarbon 35#1 (1993) p156

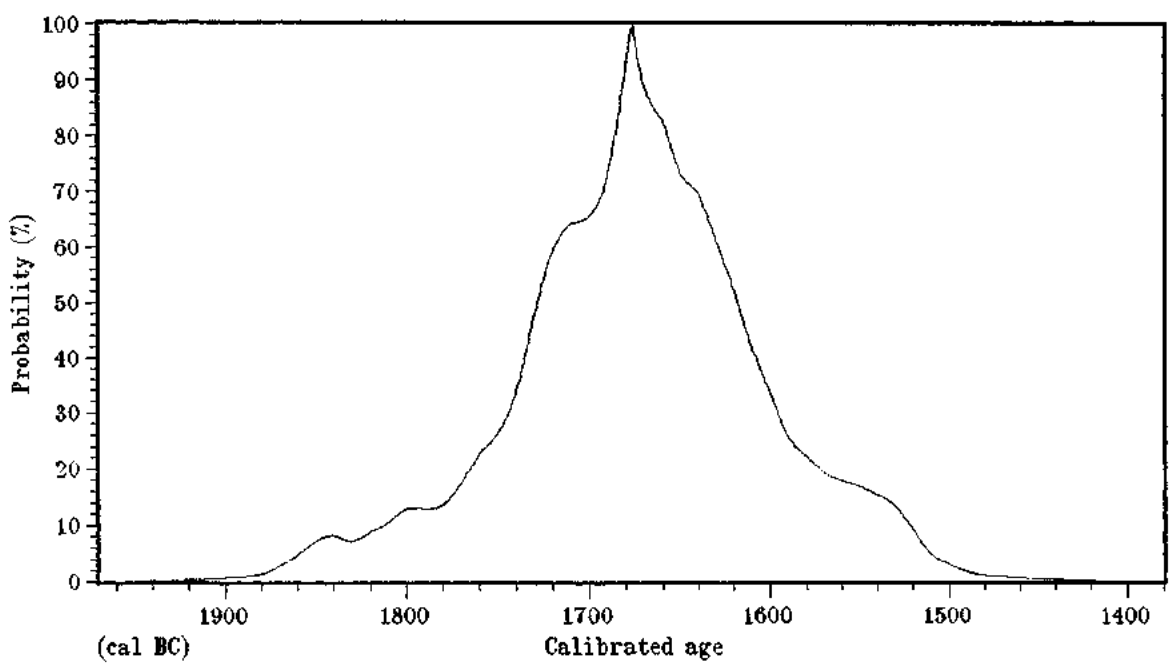

ISOTRACE RADIOCARBON CALIBRATION REPORT
Output by calibration program C14CAL98

06-Feb-01

TO-8683 RC11S501 shell valve frag

Radiocarbon date : 2460 ± 90 BP

All solutions, with a probability of 50% or greater for the calibrated age of this radiocarbon date, have been calculated from the dendro calibration data. The 68% and 95% confidence intervals, which are the 1σ and 2σ limits for a normal distribution, are also given. A probability of 100% means the radiocarbon date intersects the dendro calibration curve at this age.
All results are rounded to the nearest multiple of 5 years.

Probability	cal Age	68.3 % c.i.	95.5 % c.i.
100 %	320 cal AD	195 AD - 425 AD	85 AD - 535 AD

Calibrated with the marine data set MARINE98 from:
M.Stuiver, P.J.Reimer, and Th.F.Braziunas; Radiocarbon 40#3 (1998) p1127

Delta R reservoir correction = 390 ± 25 years
from M.Stuiver and T.F.Braziunas; Radiocarbon 35#1 (1993) p156

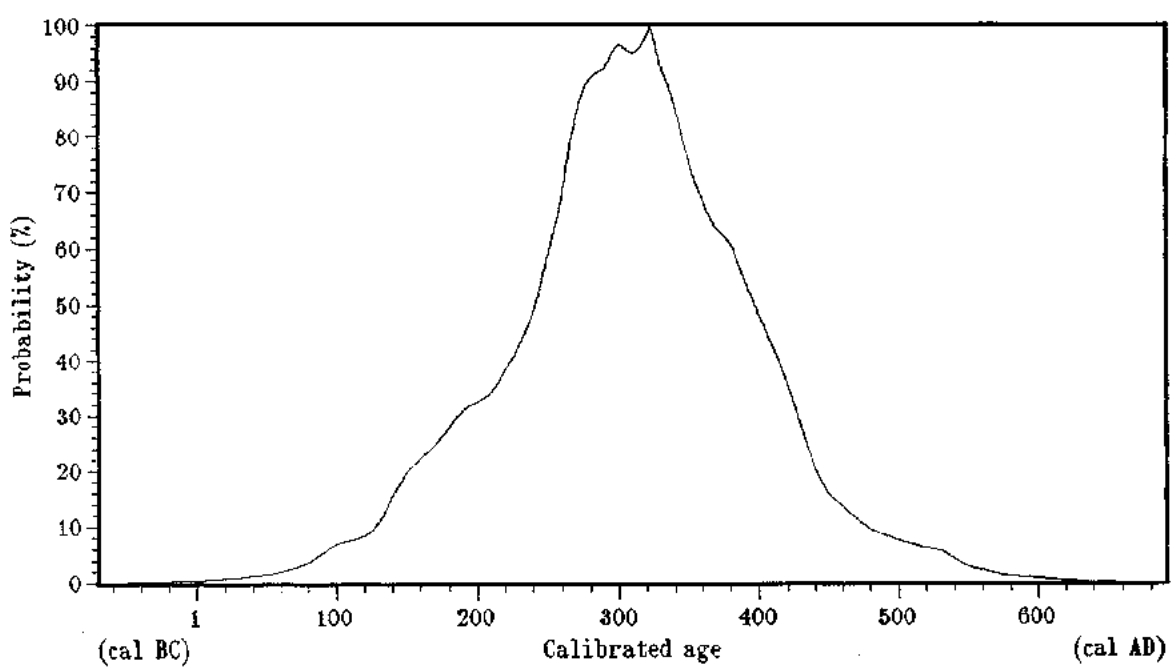

ISOTRACE RADIOCARBON CALIBRATION REPORT
Output by calibration program C14CAL98

06-Feb-01

TO-8684 RC11S801A shell frag

Radiocarbon date : 2830 ± 60 BP

All solutions, with a probability of 50% or greater for the calibrated age of this radiocarbon date, have been calculated from the dendro calibration data. The 68% and 95% confidence intervals, which are the 1σ and 2σ limits for a normal distribution, are also given. A probability of 100% means the radiocarbon date intersects the dendro calibration curve at this age.
All results are rounded to the nearest multiple of 5 years.

Probability	cal Age	68.3 % c.i.	95.5 % c.i.
100 %	130 cal BC	195 BC - 35 BC	335 BC - 30 AD

Calibrated with the marine data set MARINE98 from:
M.Stuiver, P.J.Reimer, and Th.F.Braziunas; Radiocarbon 40#3 (1998) p1127

Delta R reservoir correction = 390 ± 25 years
from M.Stuiver and T.F.Braziunas; Radiocarbon 35#1 (1993) p156

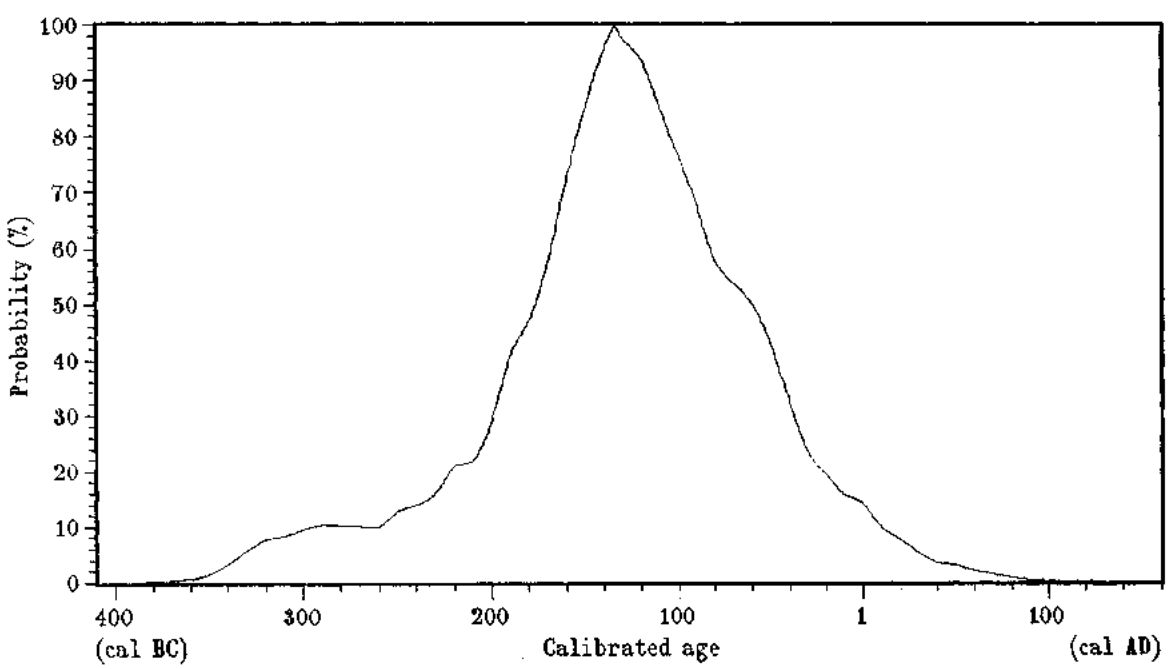

ISOTRACE RADIOCARBON CALIBRATION REPORT
Output by calibration program C14CAL98

06-Feb-01

TO-8685 RC11S801 wood frag

Radiocarbon date : 2570 ± 100 BP

All solutions, with a probability of 50% or greater for the calibrated age of this radiocarbon date, have been calculated from the dendro calibration data. The 68% and 95% confidence intervals, which are the 1σ and 2σ limits for a normal distribution, are also given. A probability of 100% means the radiocarbon date intersects the dendro calibration curve at this age. All results are rounded to the nearest multiple of 5 years.

Probability	cal Age	68.3 % c.i.	95.5 % c.i.
100 %	790 cal BC	820 BC - 755 BC	915 BC - 400 BC
65 %	675 cal BC	715 BC - 535 BC	915 BC - 400 BC

Calibrated with the standard data set INTCAL98 from:
M.Stuiver et al.; Radiocarbon 40#3 (1998) p1041

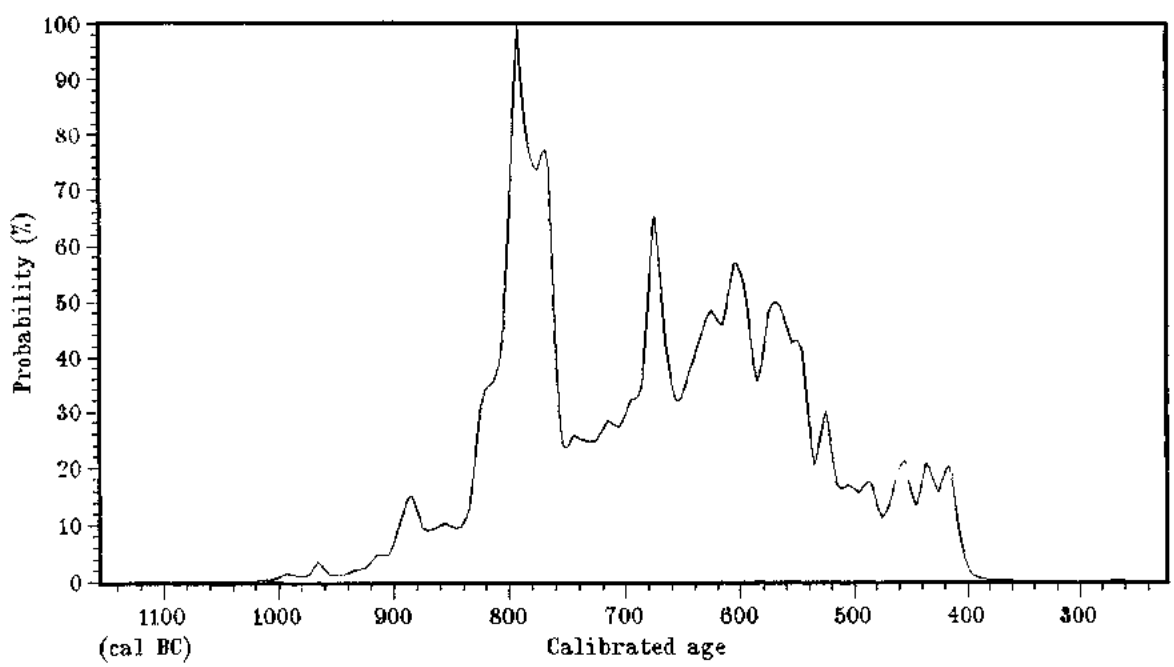

ISOTRACE RADIOCARBON CALIBRATION REPORT
Output by calibration program C14CAL98

06-Feb-01

TO-8686 RC11S802 shell frags

Radiocarbon date : 1820 ± 60 BP

All solutions, with a probability of 50% or greater for the calibrated age of this radiocarbon date, have been calculated from the dendro calibration data. The 68% and 95% confidence intervals, which are the 1σ and 2σ limits for a normal distribution, are also given. A probability of 100% means the radiocarbon date intersects the dendro calibration curve at this age.
All results are rounded to the nearest multiple of 5 years.

Probability	cal Age	68.3 % c.i.	95.5 % c.i.
100 %	990 cal AD	905 AD - 1035 AD	825 AD - 1080 AD

Calibrated with the marine data set MARINE98 from:
M.Stuiver, P.J.Reimer, and Th.F.Braziunas; Radiocarbon 40#3 (1998) p1127

Delta R reservoir correction = 390 ± 25 years
from M.Stuiver and T.F.Braziunas; Radiocarbon 35#1 (1993) p156

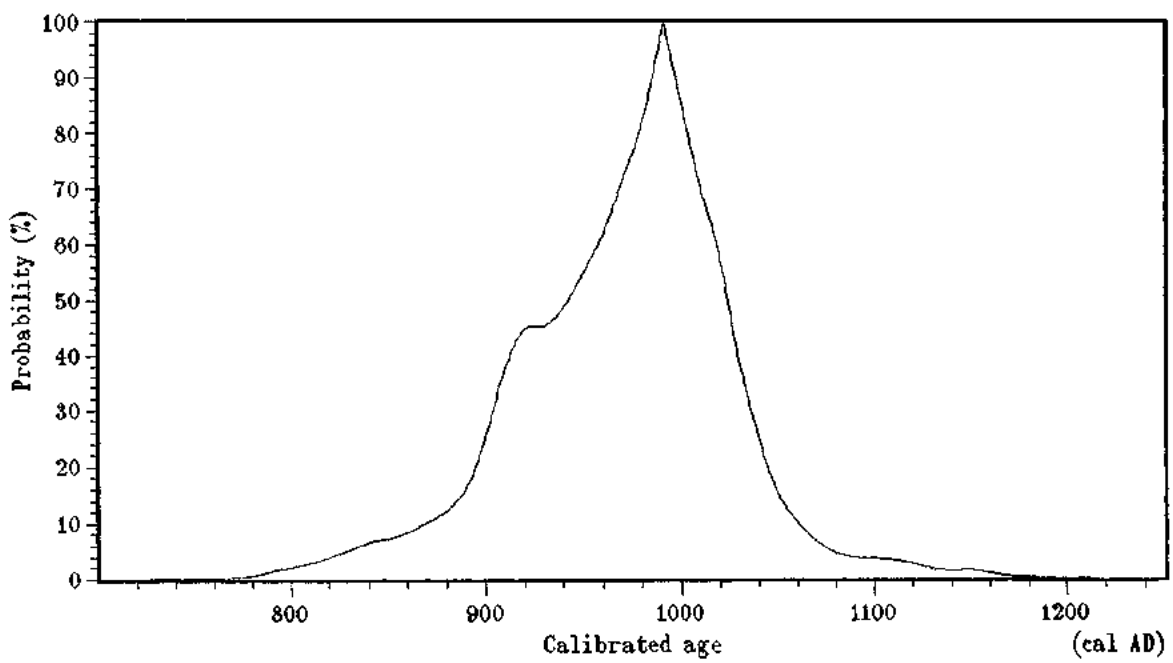

ISOTRACE RADIOCARBON CALIBRATION REPORT
Output by calibration program C14CAL98

06-Feb-01

TO-8687 RC13S401 wood twig

Radiocarbon date : 1080 ± 60 BP

All solutions, with a probability of 50% or greater for the calibrated age of this radiocarbon date, have been calculated from the dendro calibration data. The 68% and 95% confidence intervals, which are the 1σ and 2σ limits for a normal distribution, are also given. A probability of 100% means the radiocarbon date intersects the dendro calibration curve at this age.
All results are rounded to the nearest multiple of 5 years.

Probability	cal Age	68.3 % c.i.	95.5 % c.i.
81 %	905 cal AD	890 AD - 925 AD	850 AD - 1035 AD
100 %	980 cal AD	930 AD - 1015 AD	855 AD - 1030 AD

Calibrated with the standard data set INTCAL98 from:
M.Stuiver et al.; Radiocarbon 40#3 (1998) p1041

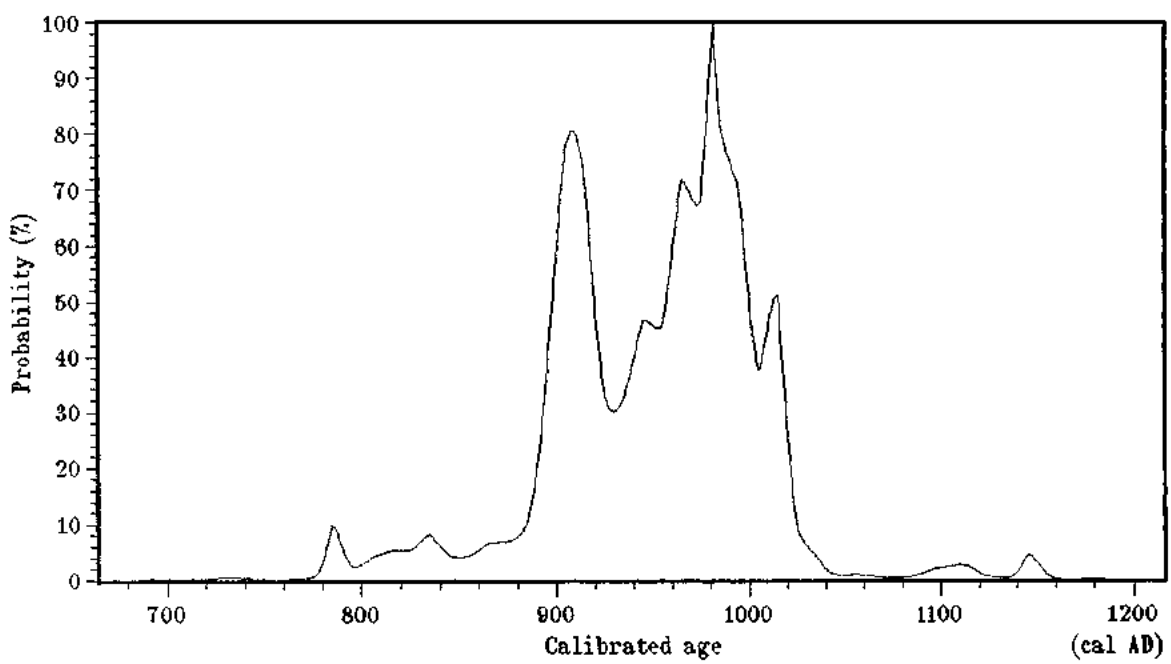

ISOTRACE RADIOCARBON CALIBRATION REPORT
Output by calibration program C14CAL98

06-Feb-01

TO-8688 RC13S502 wood twig

Radiocarbon date : 2140 ± 60 BP

All solutions, with a probability of 50% or greater for the calibrated age of this radiocarbon date, have been calculated from the dendro calibration data. The 68% and 95% confidence intervals, which are the 1σ and 2σ limits for a normal distribution, are also given. A probability of 100% means the radiocarbon date intersects the dendro calibration curve at this age.
All results are rounded to the nearest multiple of 5 years.

Probability	cal Age	68.3 % c.i.	95.5 % c.i.
56 %	335 cal BC	350 BC - 295 BC	380 BC - 35 BC
58 %	330 cal BC	350 BC - 295 BC	380 BC - 35 BC
50 %	225 cal BC	230 BC - 215 BC	380 BC - 35 BC
100 %	195 cal BC	205 BC - 90 BC	375 BC - 35 BC
100 %	170 cal BC	205 BC - 90 BC	375 BC - 35 BC

Calibrated with the standard data set INTCAL98 from:
M.Stuiver et al.; Radiocarbon 40#3 (1998) p1041

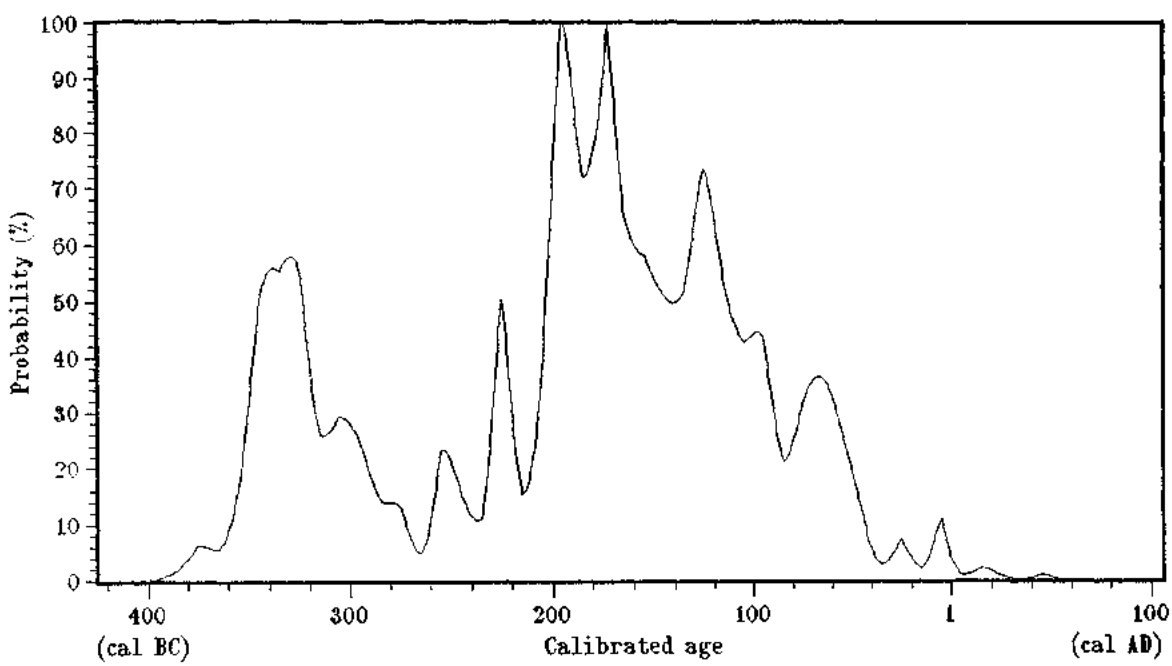

ISOTRACE RADIOCARBON CALIBRATION REPORT
Output by calibration program C14CAL98

06-Feb-01

TO-8689 RC13S603 wood frag

Radiocarbon date : 3170 ± 50 BP

All solutions, with a probability of 50% or greater for the calibrated age of this radiocarbon date, have been calculated from the dendro calibration data. The 68% and 95% confidence intervals, which are the 1σ and 2σ limits for a normal distribution, are also given. A probability of 100% means the radiocarbon date intersects the dendro calibration curve at this age.
All results are rounded to the nearest multiple of 5 years.

Probability	cal Age	68.3 % c.i.	95.5 % c.i.
100 %	1430 cal BC	1500 BC - 1405 BC	1520 BC - 1370 BC

Calibrated with the standard data set INTCAL98 from:
M.Stuiver et al.; Radiocarbon 40#3 (1998) p1041

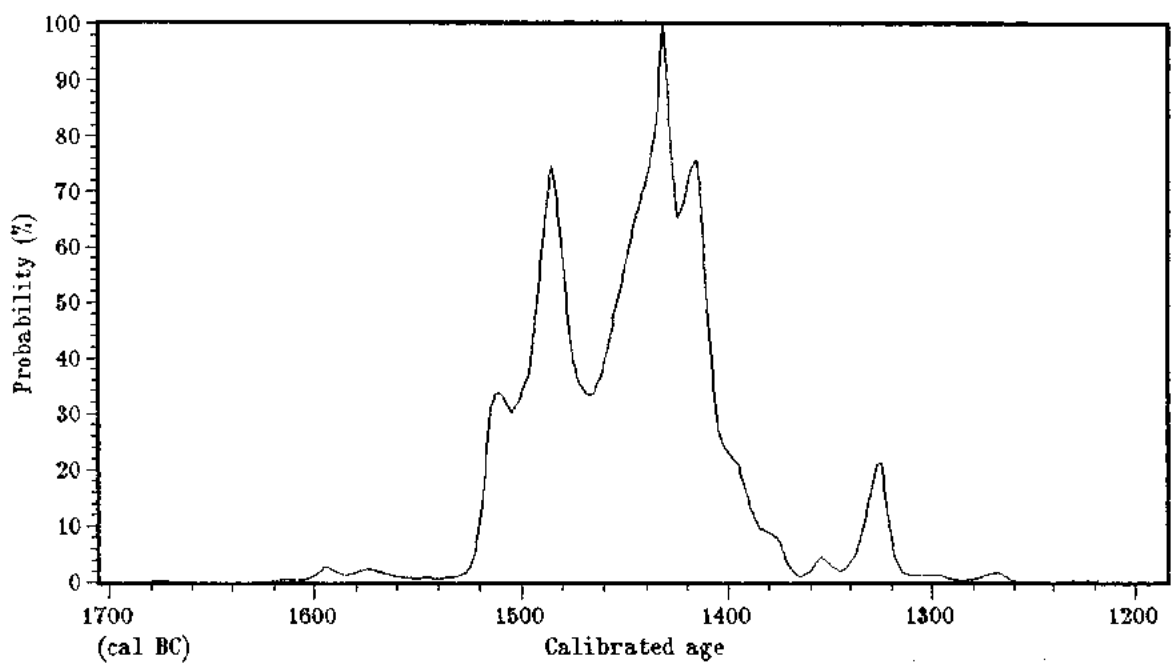

ISOTRACE RADIOCARBON CALIBRATION REPORT
Output by calibration program C14CAL98

06-Feb-01

TO-8690 RC13S701 wood frags

Radiocarbon date : 3640 ± 50 BP

All solutions, with a probability of 50% or greater for the calibrated age of this radiocarbon date, have been calculated from the dendro calibration data. The 68% and 95% confidence intervals, which are the 1σ and 2σ limits for a normal distribution, are also given. A probability of 100% means the radiocarbon date intersects the dendro calibration curve at this age.
All results are rounded to the nearest multiple of 5 years.

Probability	cal Age	68.3 % c.i.	95.5 % c.i.
55 %	2105 cal BC	2130 BC - 2080 BC	2140 BC - 1880 BC
100 %	2015 cal BC	2035 BC - 1935 BC	2140 BC - 1880 BC
100 %	1995 cal BC	2035 BC - 1935 BC	2140 BC - 1880 BC
100 %	1980 cal BC	2035 BC - 1935 BC	2140 BC - 1880 BC

Calibrated with the standard data set INTCAL98 from:
M.Stuiver et al.; Radiocarbon 40#3 (1998) p1041

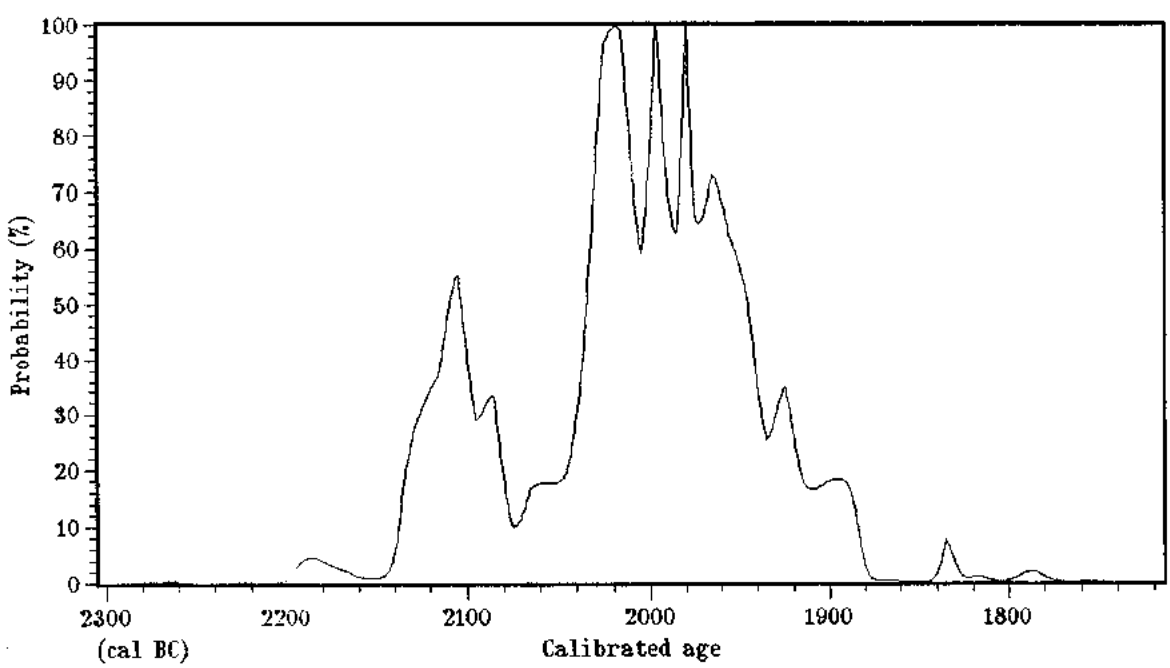

ISOTRACE RADIOCARBON CALIBRATION SUMMARY
Output by calibration program C14CAL98

06-Feb-01

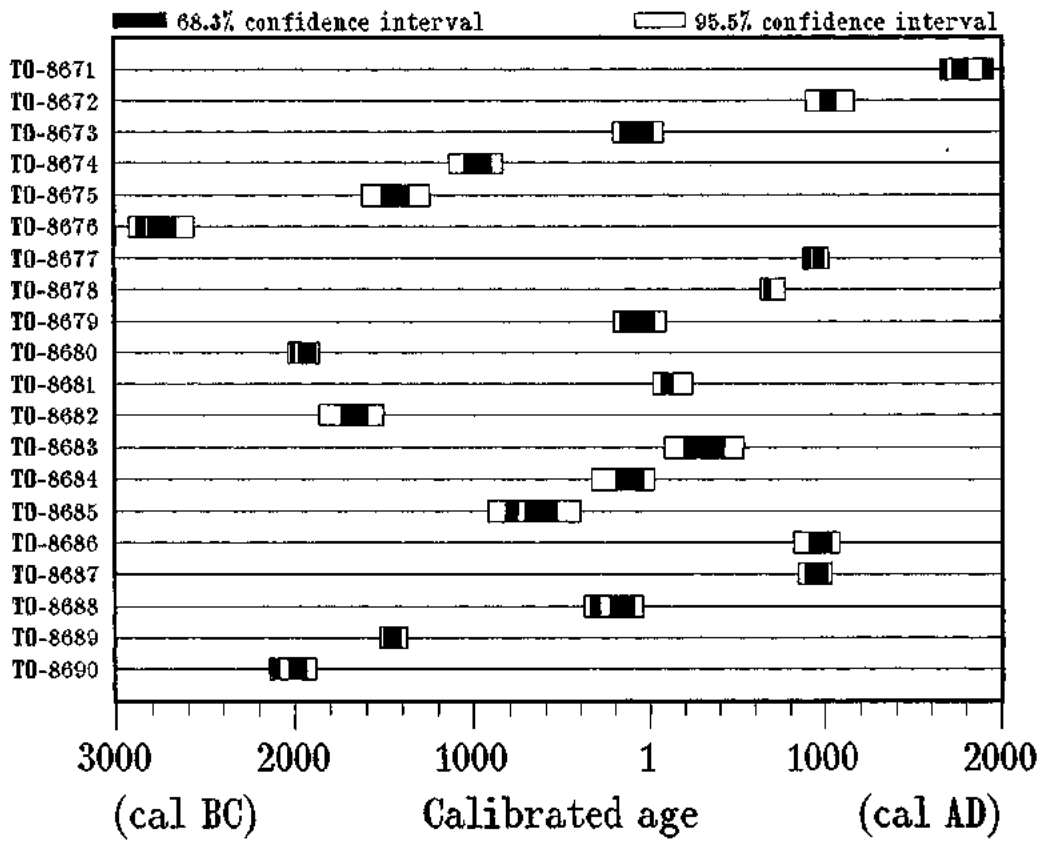

ISOTRACE RADIOCARBON CALIBRATION REPORT
Output by calibration program C14CAL98

06-Feb-01

TO-8672 RC03S201 shell valves

Radiocarbon date : 1770 ± 60 BP

All solutions, with a probability of 50% or greater for the calibrated age of this radiocarbon date, have been calculated from the dendro calibration data. The 68% and 95% confidence intervals, which are the 1σ and 2σ limits for a normal distribution, are also given. A probability of 100% means the radiocarbon date intersects the dendro calibration curve at this age.
All results are rounded to the nearest multiple of 5 years.

Probability	cal Age	68.3 % c.i.	95.5 % c.i.
100 %	530 cal AD	430 AD - 605 AD	345 AD - 665 AD

Calibrated with the marine data set MARINE98 from:
M.Stuiver, P.J.Reimer, and Th.F.Braziunas; Radiocarbon 40#3 (1998) p1127

Delta R reservoir correction = -120 ± 45 years
Based on results for RC11S801A and RC11S801

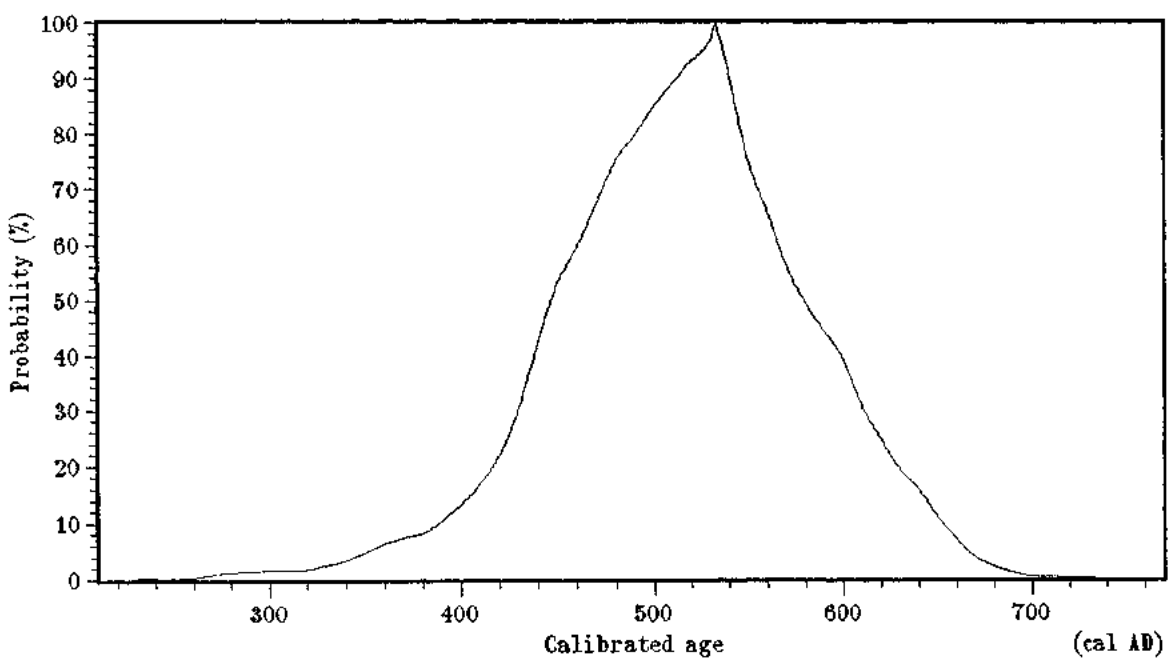

ISOTRACE RADIOCARBON CALIBRATION REPORT
Output by calibration program C14CAL98

06-Feb-01

TO-8675 RC03S601 shell valves

Radiocarbon date : 3890 ± 80 BP

All solutions, with a probability of 50% or greater for the calibrated age of this radiocarbon date, have been calculated from the dendro calibration data. The 68% and 95% confidence intervals, which are the 1σ and 2σ limits for a normal distribution, are also given. A probability of 100% means the radiocarbon date intersects the dendro calibration curve at this age.
All results are rounded to the nearest multiple of 5 years.

Probability	cal Age	68.3 % c.i.	95.5 % c.i.
100 %	2045 cal BC	2190 BC - 1935 BC	2330 BC - 1840 BC

Calibrated with the marine data set MARINE98 from:
M.Stuiver, P.J.Reimer, and Th.F.Braziunas; Radiocarbon 40#3 (1998) p1127

Delta R reservoir correction = -120 ± 45 years
Based on results for RC11S801A and RC11S801

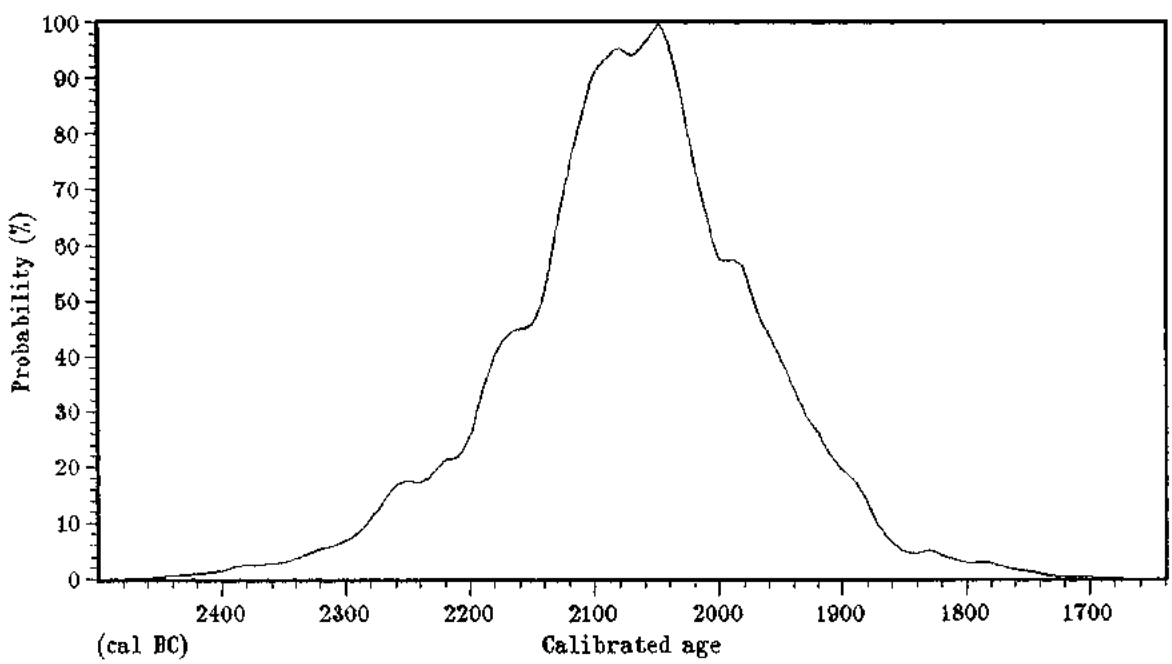

ISOTRACE RADIOCARBON CALIBRATION REPORT
Output by calibration program C14CAL98

06-Feb-01

TO-8682 RC09S601 shell valves

Radiocarbon date : 4100 ± 60 BP

All solutions, with a probability of 50% or greater for the calibrated age of this radiocarbon date, have been calculated from the dendro calibration data. The 68% and 95% confidence intervals, which are the 1σ and 2σ limits for a normal distribution, are also given. A probability of 100% means the radiocarbon date intersects the dendro calibration curve at this age.
All results are rounded to the nearest multiple of 5 years.

Probability	cal Age	68.3 % c.i.	95.5 % c.i.
100 %	2375 cal BC	2455 BC - 2265 BC	2555 BC - 2135 BC

Calibrated with the marine data set MARINE98 from:
M.Stuiver, P.J.Reimer, and Th.F.Braziunas; Radiocarbon 40#3 (1998) p1127

Delta R reservoir correction = -120 ± 45 years
Based on results for RC11S801A and RC11S801

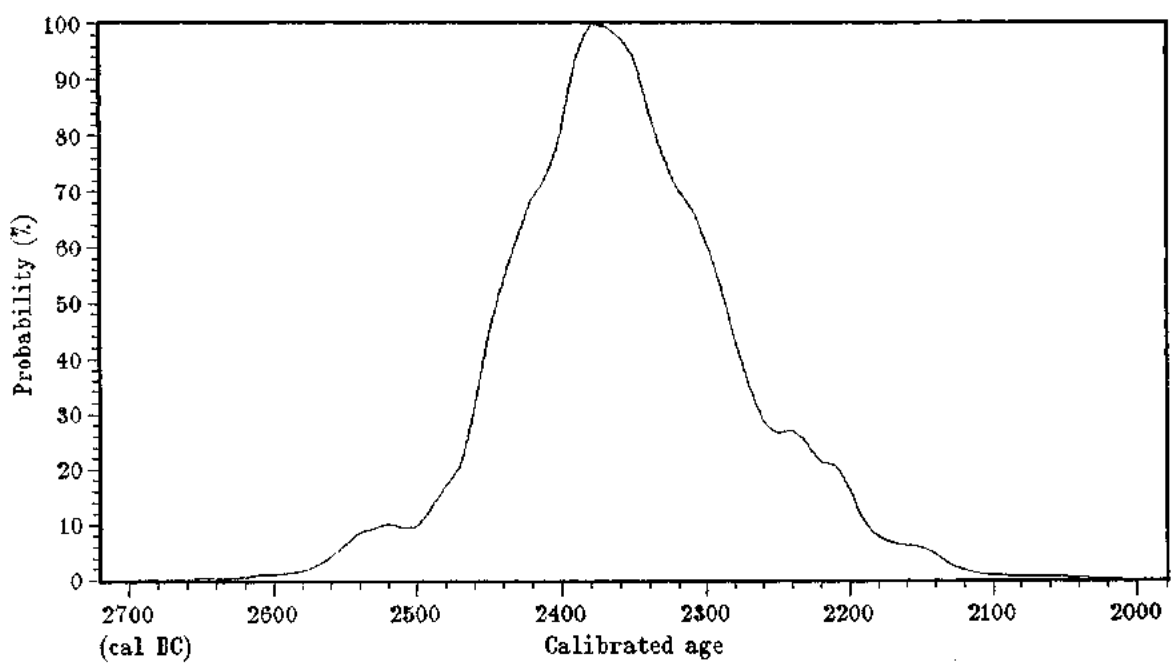

ISOTRACE RADIOCARBON CALIBRATION REPORT
Output by calibration program C14CAL98

06-Feb-01

TO-8683 RC11S501 shell valve frag

Radiocarbon date : 2460 ± 90 BP

All solutions, with a probability of 50% or greater for the calibrated age of this radiocarbon date, have been calculated from the dendro calibration data. The 68% and 95% confidence intervals, which are the 1σ and 2σ limits for a normal distribution, are also given. A probability of 100% means the radiocarbon date intersects the dendro calibration curve at this age.
All results are rounded to the nearest multiple of 5 years.

Probability	cal Age	68.3 % c.i.	95.5 % c.i.
100 %	340 cal BC	390 BC - 170 BC	535 BC - 40 BC

Calibrated with the marine data set MARINE98 from:
M.Stuiver, P.J.Reimer, and Th.F.Braziunas; Radiocarbon 40#3 (1998) p1127

Delta R reservoir correction = -120 ± 45 years
Based on results for RC11S801A and RC11S801

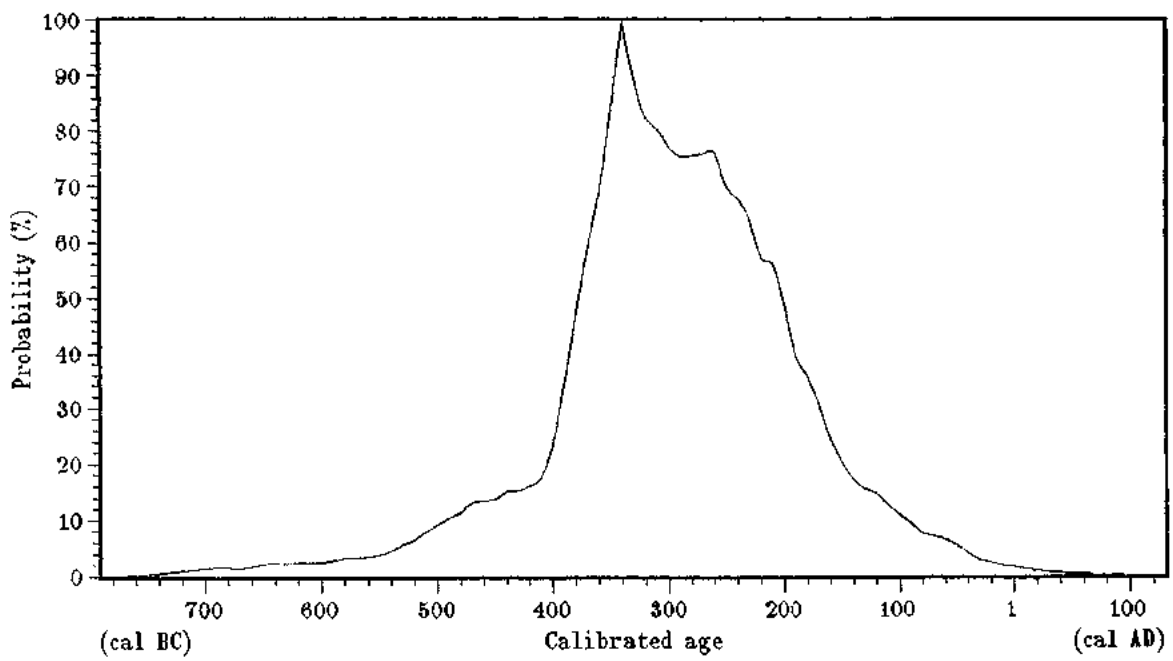

ISOTRACE RADIOCARBON CALIBRATION REPORT
Output by calibration program C14CAL98

06-Feb-01

TO-8684 RC11S801A shell frag

Radiocarbon date : 2830 ± 60 BP

All solutions, with a probability of 50% or greater for the calibrated age of this radiocarbon date, have been calculated from the dendro calibration data. The 68% and 95% confidence intervals, which are the 1σ and 2σ limits for a normal distribution, are also given. A probability of 100% means the radiocarbon date intersects the dendro calibration curve at this age.
All results are rounded to the nearest multiple of 5 years.

Probability	cal Age	68.3 % c.i.	95.5 % c.i.
100 %	780 cal BC	820 BC - 740 BC	910 BC - 580 BC

Calibrated with the marine data set MARINE98 from:
M.Stuiver, P.J.Reimer, and Th.F.Braziunas; Radiocarbon 40#3 (1998) p1127

Delta R reservoir correction = -120 ± 45 years
Based on results for RC11S801A and RC11S801

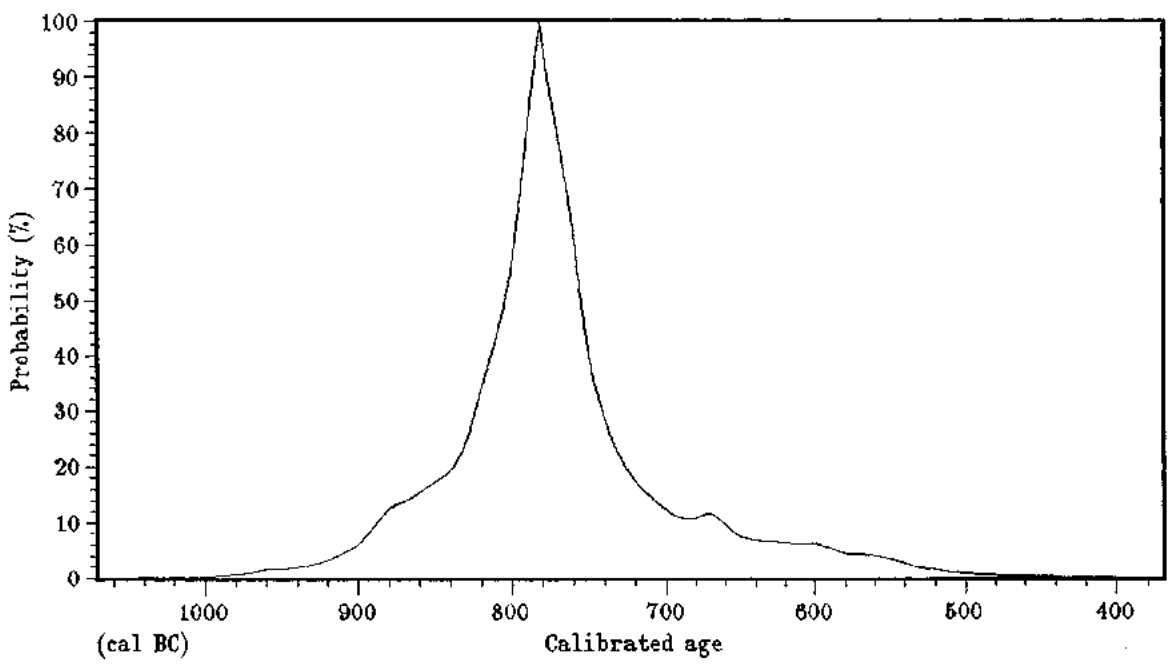

ISOTRACE RADIOCARBON CALIBRATION REPORT
Output by calibration program C14CAL98

06-Feb-01

TO-8686 RC11S802 shell frags

Radiocarbon date : 1820 ± 60 BP

All solutions, with a probability of 50% or greater for the calibrated age of this radiocarbon date, have been calculated from the dendro calibration data. The 68% and 95% confidence intervals, which are the 1σ and 2σ limits for a normal distribution, are also given. A probability of 100% means the radiocarbon date intersects the dendro calibration curve at this age.
All results are rounded to the nearest multiple of 5 years.

Probability	cal Age	68.3 % c.i.	95.5 % c.i.
100 %	445 cal AD	385 AD - 550 AD	265 AD - 630 AD

Calibrated with the marine data set MARINE98 from:
M.Stuiver, P.J.Reimer, and Th.F.Braziunas; Radiocarbon 40#3 (1998) p1127

Delta R reservoir correction = -120 ± 45 years
Based on results for RC11S801A and RC11S801

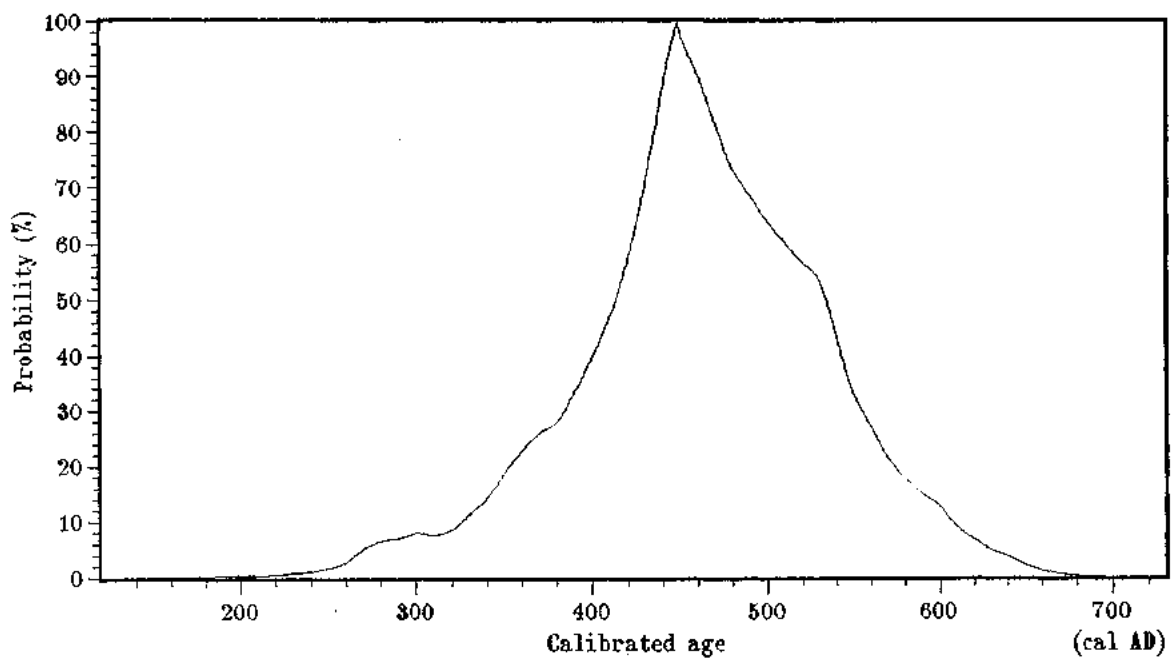

ISOTRACE RADIOCARBON CALIBRATION SUMMARY
Output by calibration program C14CAL98

06-Feb-01

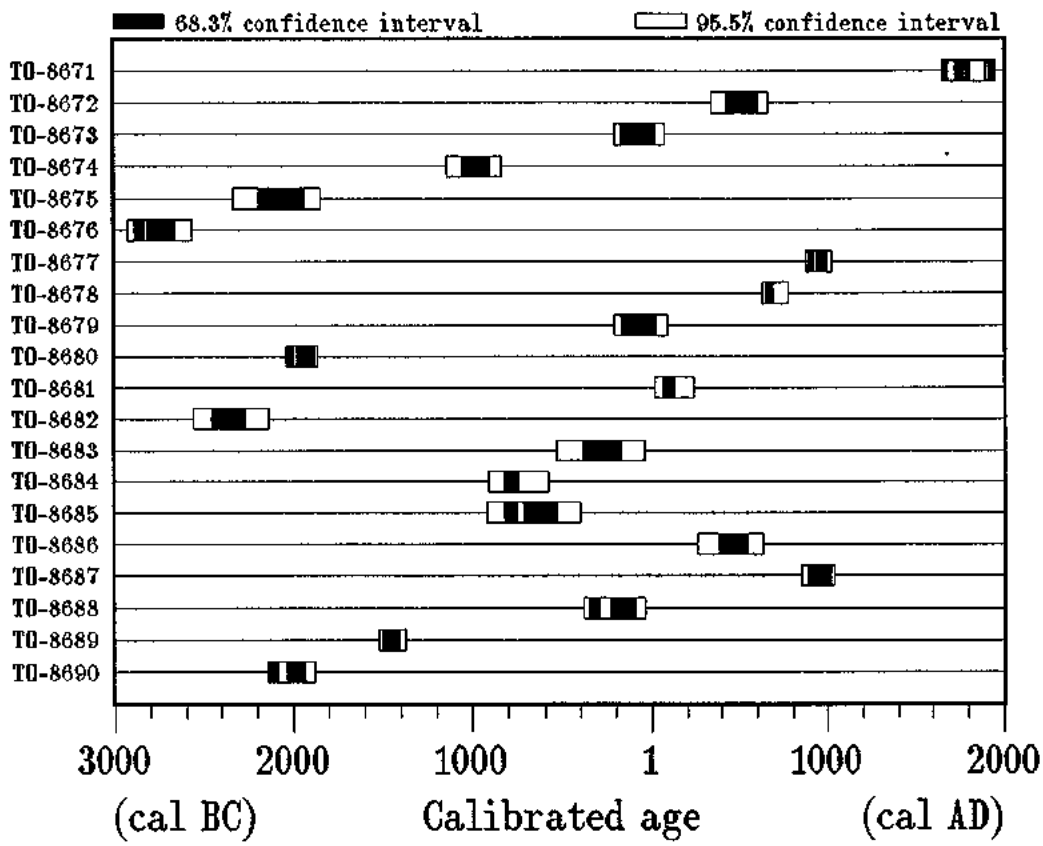

APPENDIX B

Lamina Thickness Measurements from Thin Sections

APPENDIX B1. Summary of cumulative lamina thickness measurements (in millimetres) per slide.

Slab	Slide	T	n	D	n	
1	1A	1.16	1	0.73	1	
	1B	5.50	10	17.01	10	x
	1C	4.53	7	11.51	7	
	1D	6.23	6	7.31	6	
2	2B	4.15	10	18.16	10	
	2C	5.41	9	19.31	10	
	2D	2.92	5	8.30	5	
3	3B	4.94	6	9.61	6	
	3C	5.49	8	21.96	8	
	3D	4.89	7	15.69	7	
	3E	4.20	7	15.62	7	
4	4B	6.79	11	21.38	12	
	4C	2.73	7	11.63	7	
	4D	3.60	6	13.69	6	
	4E	0.63	1	2.14	1	
5	5A	7.14	11	18.38	11	
	5B	8.00	15	19.27	15	
	5C	5.49	8	19.71	8	
	5D	3.84	7	16.24	7	
	5E	6.81	11	18.06	11	
6	6A	7.83	8	20.48	8	
	6B	6.39	8	20.93	8	
	6C	6.20	11	18.26	11	
	6D	5.20	9	17.53	9	
	6E	5.27	9	10.87	9	
7	7B	5.32	9	11.35	9	
	7C	9.10	13	19.61	13	
	7D	4.22	8	19.14	8	
	7E	6.34	13	25.79	13	
	7F	4.90	10	21.96	10	
8	8A	2.09	6	11.62	6	
	8B	4.88	10	21.48	10	
	8C	5.30	10	12.41	10	
	8D	6.73	15	15.74	15	
	8E	4.49	15	17.24	15	
9	9A	4.39	5	10.53	5	
	9B	3.66	8	24.57	8	
	9C	1.73	6	16.69	6	
	9D	4.40	9	19.49	9	
	9E	2.91	8	16.45	8	
	9F	3.63	7	17.47	7	
10	10A	3.42	8	16.20	8	
	10B	2.59	5	8.71	5	
	10C	6.78	12	18.94	12	
	10D	4.92	10	17.63	10	
	10E	4.12	8	18.74	9	
	10F	6.77	12	19.82	12	
Total		228.03	405	755.36	408	
Average		0.56		1.85		2.41 mm/yr

T = terrigenous
D = diatomaceous

APPENDIX B2. Detailed lamina thickness measurements

T = terrigenous, D = diatomaceous; s.d. = standard deviation; all measurements in millimetres

					Couplet Type		Total	Total	Average		Average			
Slab	Slide	Couplet	T	D	4-com	3-com	T	D	T	s.d.	D	s.d.	Couplet	s.d.
1	1A	1	1.16	0.73			17.42	36.56	0.73	0.46	1.52	0.67	2.25	0.69
	1B	2	0.52	1.88	●									
		3	0.45	2.17										
		4	0.55	1.05	●									
		5	0.49	2.82	●									
		6	0.93	1.96		●								
		7	0.88	3.16	●									
		8	0.26	1.09										
		9	0.20	1.37		●								
		10	0.59	0.83										
		11	0.63	0.68										
	1C	12	0.41	2.81										
		13	1.42	0.99										
		14	0.59	1.38		●								
		15	0.24	1.72	●									
		16	0.21	1.78										
		17	0.34	1.35										
		18	1.32	1.48										
	1D	19	1.95	1.20		●								
		20	1.24	1.02		●								
		21	0.86	1.53		●								
		22	0.47	1.26		●								
		23	1.30	0.99	●									
		24	0.41	1.31										
2	2B	1	0.58	1.96		●	12.48	45.77	0.52	0.22	1.83	0.78	2.35	0.88
		2	0.38	3.15										
		3	0.81	2.58	●									
		4	0.43	1.65		●								
		5	0.28	1.07										
		6	0.28	2.21		●								
		7	0.31	0.97										
		8	0.49	2.09										
		9	0.28	1.74	●									
		10	0.31	0.74										
	2C	11		3.69	●									
		12	0.31	1.27		●								
		13	0.50	2.75		●								
		14	0.66	1.88	●									
		15	0.71	1.33	●									
		16	0.71	1.41	●									
		17	0.74	2.26										
		18	0.47	0.71										
		19	0.49	2.61	●									
		20	0.82	1.40										
	2D	21	1.17	2.75										
		22	0.63	1.88		●								
		23	0.35	1.24		●								
		24	0.36	0.86	●									
		25	0.41	1.57	●									

APPENDIX B2 (continued)

Slab	Slide	Couplet	T	D	Couplet Type 4-com	Couplet Type 3-com	Total T	Total D	Average T	s.d.	Average D	s.d.	Couplet	s.d.
3	3B	1	0.93	0.67			19.52	62.88	0.70	0.46	2.25	1.42	2.95	1.31
		2	0.46	0.57										
		3	0.51	0.43										
		4	0.30	1.79										
		5	2.49	3.16		●								
		6	0.25	2.99	●									
	3C	7	0.42	3.81	●									
		8	1.06	3.27										
		9	0.52	3.00										
		10	0.24	1.79	●									
		11	0.60	1.04		●								
		12	0.52	2.02		●								
		13	1.01	1.36										
		14	1.12	5.67										
	3D	15	0.38	1.00										
		16	0.29	1.58										
		17	1.21	5.58		●								
		18	0.56	1.53		●								
		19	1.25	0.68		●								
		20	0.66	1.21										
		21	0.54	4.11										
	3E	22	0.33	2.68	●									
		23	0.65	0.99		●								
		24	0.38	0.89		●								
		25	0.88	2.69	●									
		26	0.49	3.22	●									
		27	0.57	2.18	●									
		28	0.90	2.97		●								
4	4B	1		1.81	●		13.75	48.84	0.55	0.28	1.88	0.70	2.43	0.86
		2	0.79	1.59	●									
		3	0.71	1.85		●								
		4	0.95	1.00										
		5	0.56	1.65	●									
		6	0.76	1.69		●								
		7	0.75	2.62		●								
		8	0.76	2.56	●									
		9	0.32	1.75		●								
		10	0.48	1.94	●									
		11	0.27	1.02										
		12	0.44	1.90										
	4C	13	0.23	0.86										
		14	0.31	1.16										
		15	0.23	1.11										
		16	0.45	0.93		●								
		17	0.66	2.16	●									
		18	0.62	2.32	●									
		19	0.23	3.09	●									
	4D	20	1.48	1.90	●									
		21	0.46	2.50										
		22	0.40	2.37	●									
		23	0.40	2.97										
		24	0.25	0.78		●								
		25	0.61	3.17										
	4E	26	0.63	2.14										

APPENDIX B2 (continued)

Slab	Slide	Couplet	T	D	Couplet Type 4-com	Couplet Type 3-com	Total T	Total D	Average T	s.d.	Average D	s.d.	Couplet	s.d.
5	5A	1	1.77	1.90			31.28	91.66	0.60	0.29	1.76	0.88	2.36	0.87
		2	0.58	0.82										
		3	0.62	2.26	●									
		4	0.73	1.17										
		5	0.31	3.49	●									
		6	0.45	0.39										
		7	0.31	0.72										
		8	0.44	0.62										
		9	0.63	1.17										
		10	0.54	2.33										
		11	0.76	3.51										
	5B	12	0.28	1.11										
		13	0.55	0.69		●								
		14	0.68	1.04		●								
		15	0.65	1.38		●								
		16	1.02	0.86		●								
		17	0.43	1.44		●								
		18	0.50	0.81		●								
		19	0.63	1.34		●								
		20	0.52	1.40										
		21	0.49	1.64		●								
		22	0.40	2.06		●								
		23	0.72	1.72	●									
		24	0.16	1.05		●								
		25	0.39	0.94		●								
		26	0.58	1.79		●								
	5C	27	1.06	0.98										
		28	0.31	2.09	●									
		29	0.85	1.64		●								
		30	0.16	2.02		●								
		31	0.47	4.36	●									
		32	0.83	4.05		●								
		33	0.83	1.86		●								
		34	0.98	2.71	●									
	5D	35	0.83	2.16		●								
		36	0.59	2.30		●								
		37	0.52	2.53		●								
		38	0.22	3.43		●								
		39	0.45	1.78		●								
		40	0.67	1.73		●								
		41	0.56	2.31		●								
	5E	42	0.27	1.15										
		43	0.58	2.18		●								
		44	0.68	1.18		●								
		45	0.86	1.05										
		46	0.85	1.32	●									
		47	0.32	2.90	●									
		48	0.52	1.52										
		49	0.45	1.46										
		50	0.31	1.96	●									
		51	0.72	1.15		●								
		52	1.25	2.19		●								

APPENDIX B2 (continued)

Slab	Slide	Couplet	T	D	Couplet Type 4-com	Couplet Type 3-com	Total T	Total D	Average T	SD	Average D	SD	Couplet	SD
6	6A	1	0.76	2.02	●		30.95	88.01	0.69	0.63	1.96	0.97	2.65	1.03
		2	3.91	2.29	●									
		3	0.79	1.87										
		4	0.39	3.04	●									
		5	0.23	3.36		●								
		6	0.65	2.47	●									
		7	0.53	3.92										
		8	0.57	1.51	●									
	6B	9	0.22	1.24		●								
		10	0.51	2.17		●								
		11	1.10	2.05	●									
		12	0.53	2.08	●									
		13	2.51	4.04	●									
		14	0.78	2.01		●								
		15	0.65	2.57	●									
		16	0.15	4.71		●								
	6C	17	0.29	1.92										
		18	1.05	2.62		●								
		19	0.25	2.82										
		20	0.78	1.09		●								
		21	0.52	2.69										
		22	0.77	1.23		●								
		23	0.92	1.34		●								
		24	0.46	0.83										
		25	0.17	0.43		●								
		26	0.45	1.54	●									
		27	0.54	1.75	●									
	6D	28	0.94	3.37	●									
		29	0.54	2.52	●									
		30	0.36	1.22	●									
		31	0.17	2.58	●									
		32	0.77	1.45		●								
		33	0.28	2.91	●									
		34	0.38	1.15		●								
		35	0.77	1.51	●									
		36	0.99	0.82										
	6E	37	0.23	1.08		●								
		38	0.59	1.16	●									
		39	1.01	1.90	●									
		40	0.68	1.11		●								
		41	0.29	0.93		●								
		42	0.46	0.68										
		43	0.43	1.39		●								
		44	0.36	0.59		●								
		45	1.22	2.03		●								

APPENDIX B2 (continued)

Slab	Slide	Couplet	T	D	Couplet Type 4-com	Couplet Type 3-com	Total T	Total D	Average T	s.d.	Average D	s.d.	Couplet	s.d.
7	7B	1	0.76	1.55		●	29.88	97.85	0.56	0.20	1.85	0.80	2.41	0.87
		2	0.42	0.70										
		3	0.73	2.09										
		4	0.62	1.02										
		5	0.51	0.91		●								
		6	0.68	0.78	●									
		7	0.31	1.16		●								
		8	0.58	1.09		●								
		9	0.71	2.05		●								
	7C	10	0.68	1.06										
		11	0.87	1.35	●									
		12	0.93	1.62		●								
		13	0.99	1.67										
		14	0.77	1.39		●								
		15	0.75	1.76	●									
		16	0.58	1.30		●								
		17	0.90	1.67	●									
		18	0.30	2.70		●								
		19	0.68	1.28		●								
		20	0.45	2.00		●								
		21	0.81	0.65										
		22	0.39	1.16		●								
	7D	23	0.26	2.95	●									
		24	0.69	2.49	●									
		25	0.63	0.86										
		26	0.52	1.74		●								
		27	0.49	1.92										
		28	0.71	1.40	●									
		29	0.55	3.89										
		30	0.37	3.89		●								
	7E	31	0.31	1.42		●								
		32	0.48	2.92	●									
		33	0.54	3.33	●									
		34	0.29	1.28		●								
		35	0.76	3.42	●									
		36	0.22	1.85		●								
		37	0.76	1.45		●								
		38	0.71	1.49	●									
		39	0.22	1.16	●									
		40	0.62	1.89		●								
		41	0.20	1.29		●								
		42	0.46	2.00	●									
		43	0.77	2.29		●								
	7F	44	0.29	2.21		●								
		45	0.40	1.88		●								
		46	0.37	1.25	●									
		47	0.37	1.76	●									
		48	0.37	3.15	●									
		49	0.38	1.62	●									
		50	0.72	2.57	●									
		51	0.63	2.21		●								
		52	0.74	2.24		●								
		53	0.63	3.07	●									

APPENDIX B2 (continued)

Stab	Slide	Couplet	T	D	Couplet Type 4-com	Couplet Type 3-com	Total T	Total D	Average T	s.d.	Average D	s.d.	Couplet	s.d.
8	8A	1	0.46	1.81	●		23.49	78.49	0.42	0.19	1.40	0.70	1.82	0.71
		2	0.28	0.49		●								
		3	0.22	2.76	●									
		4	0.35	1.71		●								
		5	0.29	2.46	●									
		6	0.49	2.39	●									
	8B	7	0.51	2.74	●									
		8	0.22	3.27	●									
		9	0.29	1.92		●								
		10	0.59	2.64	●									
		11	0.66	2.11		●								
		12	0.72	2.73		●								
		13	0.40	1.39		●								
		14	0.41	1.61										
		15	0.40	1.07		●								
		16	0.68	2.00		●								
	8C	17	0.94	1.39		●								
		18	0.36	1.36		●								
		19	0.29	0.88	●									
		20	0.58	1.31	●									
		21	0.66	1.92		●								
		22	0.58	1.39	●									
		23	0.21	1.84		●								
		24	0.66	0.98										
		25	0.51	0.51										
		26	0.51	0.83		●								
	8D	27	0.31	1.23										
		28	0.41	1.04		●								
		29	0.38	2.19		●								
		30	0.77	0.58										
		31	0.93	1.33	●									
		32	0.55	0.67		●								
		33	0.36	1.08		●								
		34	0.55	0.20										
		35	0.15	1.45		●								
		36	0.35	1.17		●								
		37	0.51	1.05										
		38	0.36	0.66		●								
		39	0.44	1.08		●								
		40	0.44	1.43		●								
		41	0.22	0.58		●								
	8E	42	0.37	1.11										
		43	0.35	0.96		●								
		44	0.22	0.65		●								
		45	0.27	1.03		●								
		46	0.25	0.62										
		47	0.61	2.92										
		48	0.30	1.05										
		49	0.35	0.71										
		50	0.22	1.36		●								
		51	0.30	1.09		●								
		52	0.15	0.91										
		53	0.19	1.00		●								
		54	0.21	0.94		●								
		55	0.25	1.44		●								
		56	0.45	1.45		●								

APPENDIX B2 (continued)

Slab	Slide	Couplet	T	D	Couplet Type 4-com	Couplet Type 3-com	Total T	Total D	Average T	s.d.	Average D	s.d.	Couplet	s.d.
9	9A	1	1.19	1.49			20.72	105.20	0.48	0.26	2.45	1.02	2.93	1.23
		2	0.54	1.69		●								
		3	0.96	2.37		●								
		4	0.85	2.34	●									
		5	0.85	2.64	●									
	9B	6	0.23	1.43		●								
		7	0.54	2.61	●									
		8	0.23	1.97		●								
		9	0.45	1.65		●								
		10	0.62	3.58		●								
		11	0.30	2.55		●								
		12	0.23	5.46		●								
		13	1.06	5.32		●								
	9C	14	0.33	4.91	●									
		15	0.19	2.05		●								
		16	0.20	1.98		●								
		17	0.19	2.32	●									
		18	0.23	3.19	●									
		19	0.59	2.24		●								
	9D	20	0.52	2.39		●								
		21	0.55	3.19	●									
		22	0.66	3.34		●								
		23	0.38	1.61	●									
		24	0.43	1.12										
		25	0.54	0.97		●								
		26	0.44	2.93	●									
		27	0.26	2.82		●								
		28	0.62	1.12		●								
	9E	29	0.53	2.19		●								
		30	0.37	1.55		●								
		31	0.19	2.39		●								
		32	0.19	2.59	●									
		33	0.20	2.89	●									
		34	0.53	1.16		●								
		35	0.75	1.55		●								
		36	0.15	2.13		●								
	9F	37	0.53	2.89		●								
		38	0.37	2.40	●									
		39	0.76	2.62	●									
		40	0.80	2.52		●								
		41	0.44	3.11	●									
		42	0.50	2.82	●									
		43	0.23	1.11		●								

APPENDIX B2 (continued)

Slab	Slide	Couplet	T	D	Couplet Type 4-com	Couplet Type 3-com	Total T	Total D	Average T	s.d.	Average D	s.d.	Couplet	s.d.
10	10A	1	0.48	0.75			28.60	100.04	0.52	0.21	1.79	0.84	2.31	0.88
		2	0.54	1.12		●								
		3	0.40	3.10	●									
		4	0.54	1.09		●								
		5	0.34	1.99		●								
		6	0.64	4.43	●									
		7	0.23	2.09		●								
		8	0.25	1.63		●								
	10B	9	0.47	2.53		●								
		10	0.23	2.11		●								
		11	0.71	1.19		●								
		12	0.62	1.09	●									
		13	0.56	1.79	●									
	10C	14	0.30	2.51		●								
		15	0.44	1.89	●									
		16	0.65	1.18		●								
		17	0.22	2.13		●								
		18	0.44	1.70		●								
		19	0.53	0.68		●								
		20	0.38	0.88		●								
		21	0.50	1.11										
		22	0.80	1.11										
		23	0.66	3.02		●								
		24	0.87	0.59		●								
		25	0.99	2.14		●								
	10D	26	0.59	2.09		●								
		27	0.73	1.72		●								
		28	0.54	1.05		●								
		29	0.31	4.73	●									
		30	0.23	0.93		●								
		31	0.47	1.61		●								
		32	0.74	1.35		●								
		33	0.22	1.24		●								
		34	0.90	0.93		●								
		35	0.19	1.98	●									
	10E	36	0.34	2.27		●								
		37	0.50	1.76										
		38		2.11										
		39	0.53	1.96		●								
		40	0.35	2.27		●								
		41	0.50	1.27										
		42	0.50	2.06		●								
		43	0.49	3.19		●								
		44	0.91	1.85		●								
	10F	45	0.53	1.36		●								
		46	0.39	1.89	●									
		47	0.50	1.73	●									
		48	0.49	0.41		●								
		49	0.38	1.49		●								
		50	0.49	2.03		●								
		51	0.42	2.06	●									
		52	0.62	0.83										
		53	0.65	2.65		●								
		54	1.21	1.58										
		55	0.48	1.14		●								
		56	0.61	2.65		●								

APPENDIX B2 (continued)

Summary of lamina thickness measurements:

			Couplet Type		Total	Total	Average		Average			
	T	D	4-com	3-com	T	D	T	s.d.	D	s.d.	Couplet	s.d.
	0.56	1.85	115	195	228.09	755.30	0.56	0.35	1.85	0.93	2.41	0.95
% couplets with seasonal succession:			28.19	47.79								

APPENDIX C

List of Identified Taxa from All Samples

APPENDIX C. Taxa from all samples analyzed. Asterisks denote major taxa used in multivariate statistics. Values in brackets (e.g., 11C-3) indicate first sample in which that diatom was described.

DIATOMS

Achnanthes brevipes Agardh 1824
Achnanthes groenlandica (Cleve) Grunow in Cleve & Grunow 1880
* *Achnanthes kriegeri* Krasske 1943
Achnanthes lanceolata (Brébisson ex Kützing) Grunow in Cleve & Grunow 1880
* *Achnanthes lemmermannii* Hustedt 1933
* *Achnanthes minutissima* Kützing 1833
Achnanthes nodosa Cleve 1900
Achnanthes parvula Kützing
Achnanthes vistulana Witkowski 1994
Achnanthes sp. (11C-3)
Achnanthes sp. (11C-13)
* *Achnanthidium biasolettianum* (Grunow in Cleve and Grunow) Round & Bukhtiyarova 1996
* *Actinocyclus curvatulus* Janisch in A. Schmidt 1878
Actinocyclus normanii (Gregory) Hustedt 1957
Actinocyclus octonarius Ehrenberg 1838
Actinocyclus sp. (3A-5)
Actinocyclus sp. (3B-2)
Actinocyclus sp. (11C-11)
Actinocyclus sp. (11C-13)
Actinocyclus sp. (B04-13)
Actinocyclus sp. (B04-23)
Actinocyclus sp. (B04-35)
Actinoptychus senarius (Ehrenberg) Ehrenberg 1843
* *Actinoptychus vulgaris* Schumann 1867
* *Amphora acutiuscula* Kützing 1844
Amphora coffeaeformis (Agardh) Kützing 1844
* *Amphora copulata* (Kützing) Schoeman & Archibald 1986
Amphora exigua Gregory
* *Amphora helenensis* Giffen 1973
Amphora maletracta var. *constricta* (Heiden) Simonsen 1992
Amphora marina W. Smith 1857
Amphora sp. (3A-9)
Amphora sp. (3B-1)
Amphora sp. (3A-11x)
Amphora sp. (S8-21)
* *Asteromphalus heptactis* (Brébisson) Ralfs in Pritchard 1861
* *Asteromphalus sarcophagus* Wallich 1860
Asteromphalus sp. (B04-20)
Aulacoseira cf. *ambigua* (Grunow in van Heurck) Simonsen 1979
Aulacoseira islandica (O. Müller) Simonsen 1979
Aulacoseira italica ssp. *subarctica* (O Müller) Simonsen 1979
Aulacoseira sp. (B04-32)
Azpeitia spp.
Bacillaria paxillifer (O.F. Müller) Hendey 1951
* *Bacteriastrum delicatulum* Cleve 1897
* *Berkeleya rutilans* (Trentpohl) Grunow 1880
Brachysira vitrea (Grunow) Ross in Hartley 1986
Caloneis sp. (S8-9)
Chaetoceros spp. Ehrenberg 1844 (resting spores)
Cocconeis cf. *britannica* Naegeli in Kützing 1849
Cocconeis californica Grunow in van Heurck 1880
* *Cocconeis costata* Gregory 1885
* *Cocconeis disculus* (Schumann) Cleve in Cleve and Jentzsch 1895
Cocconeis distans Gregory
Cocconeis dirupta Gregory

APPENDIX C (continued)

Cocconeis cf. *dirupta*
Cocconeis cf. *molesta* Kützing
* *Cocconeis neothumensis* Krammer 1991
Cocconeis pellucida Grunow ex Hantzsch in Rabenhorst 1863
Cocconeis cf. *pellucida*
Cocconeis peltoides Hustedt 1939
Cocconeis pinnata Gregory ex Greville 1859
* *Cocconeis placentula* Ehrenberg 1838
* *Cocconeis scutellum* Ehrenberg 1838
* *Cocconeis stauroneiformis* (Rabenhorst) Okuno 1957
Cocconeis sp.? (3A-12x)
Cocconeis sp. (11C-3)
Cocconeis sp. (B04-21)
Cocconeis sp. (B04-23)
Cocconeis sp. (S8-32)
Cocconeis spp. (small)
Coscinodiscus diorama
Coscinodiscus radiatus Ehrenberg 1840
Coscinodiscus sp. (B04-15)
Ctenophora pulchella (Ralfs ex Kützing) Williams & Round 1986
* *Cyclotella choctawhatcheeana* Prasad 1990
Cyclotella pseudostelligera Hustedt 1939
Cyclotella "punctata"
Cyclotella rossii (Grunow) Håkansson 1990
Cyclotella stelligera Cleve & Grunow (in van Heurck) 1882
* *Cyclotella striata* (Kützing) Grunow 1880
Cyclotella stylorum Brightwell 1860
Cyclotella sp. (B04-15)
Cyclotella sp. (3A-3)
Cyclotella sp. (3A-13)
Cyclotella sp. (S8-6)
Cyclotella sp. (S8-19)
Cyclotella sp. (S8-25)
Cyclotella sp. (S8-35)
Cymbella cymbiformis Agardh 1930
Cymbella gracilis (Ehrenberg) Kützing
Cymbella lanceolata (Ehrenberg) Kirchner 1878
Cymbella minuta Hilse ex Rabenhorst 1862
Cymbella sp. (11C-3)
Cymbella sp. (B04-17)
Cymbella sp. (B04-19)
Cymbella sp. (B04-25)
Cymbella sp. (S8-12)
Cymbella sp. (S8-32)
Delphineis spp. G.W. Andrews
Denticula cf. *neritica* Holmes & Croll 1982
Denticula sp. (B04-18)
Diatoma tenue Agardh 1812
Diatoma mesodon (Ehrenberg) Kützing 1844
Diatoma sp. (3B-10)
Diatoma sp. (B04-21)
* *Diatomella minuta* Hustedt in A. Schmidt, Atlas 1874
Dimeragramma sp. (11C-6)
Dimeragramma sp. (S8-5)
Diploneis bomboides (A. Schmidt) Cleve 1894-1895
Diploneis bombus (Ehrenberg) Ehrenberg ex Cleve 1894
Diploneis cf. *sejuncta* (Schmidt) Jørgensen

APPENDIX C (continued)

Diploneis smithii (Brébisson) Cleve 1894
Diploneis smithii var. *recta*
Diploneis spp. (Ehrenberg) Cleve 1894
* *Ditylum brightwellii* (West) Grunow in van Heurck 1883
Ethomodiscus sp. (B04-19)
Eucampia spp. Ehrenberg 1839
* *Eunotia* spp. Ehrenberg 1837
Fallacia sp. (B04-29)
Fallacia sp. (B04-28)
Fallacia sp. (S8-2)
Fallacia spp.
Fallacia sp. (3A-2)
* *Fragilaria capucina* Desmazieres 1825 complex
Fragilaria construens (Ehrenberg) Grunow 1862
Fragilaria construens var. venter (Ehrenberg) Grunow 1881
Fragilaria investiens (W. Smith) Cleve-Euler
* *Fragilaria pinnata* Ehrenberg 1843
Fragilaria schulzii Brockmann 1950
* *Fragilaria* cf. *sopotensis* Witkowski & Lange-Bertalot 1993
Fragilaria cf. *tenera* (W. Smith) Lange-Bertalot 1980
Fragilaria sp. (11C-13)
Fragilaria sp. (B04-38)
Fragilaria sp. (S8-13)
* *Fragilariopsis atlantica* Paasche 1961
* *Fragilariopsis cylindriformis* (Hasle in Hasle & Booth) Hasle
* *Fragilariopsis pseudonana* (Hasle) Hasle 1993
Fragilariopsis sp. (3A-7)
Fragilariopsis sp. (S8-10)
Frustulia rhomboides (Ehrenberg) de Toni
Frustulia spp. Rabenhorst 1853
Gomphonema augustatum (Kützing) Rabenhorst 1864
Gomphonema augustum Agardh 1831
Gomphonema olivaceum (Hornemann) Brébisson 1838
Gomphonema sp. (side)
Gomphonema sp. (3A-8)
Gomphonema sp. (11C-6)
Gomphonema sp. (11C-10)
Gomphonema sp. (B04-25)
Gomphonema sp. (S8-3)
Gomphonema sp. (S8-31)
Gomphonema sp. (S8-32)
Gomphonemopsis exigua (Kützing) Medlin 1986
* *Gomphonemopsis lindae* Witkowski, Metzeltin & Lange-Bertalot in Metzeltin & Witkowski 1996
* *Gomphonemopsis obscurum* (Krasske) Lange-Bertalot
* *Grammatophora angulosa* Ehrenberg
Grammatophora marina (Lyngbye) Kützing 1844
Grammatophora oceanica Ehrenberg 1841
Grammatophora sp. (B04-14)
Grammatophora sp. (B04-28)
Grammatophora sp. (S8-43)
Grammatophora spp. Ehrenberg 1840
Gyrosigma spp. Hassall 1845
Hannaea arcus (Ehrenberg) Patrick in Patrick & Reimer 1966
* *Hyalodiscus scoticus* (Kützing) Grunow 1879
Leptocylindrus spp. (resting spores)
Licomorpha spp. Agardh 1827
Luticola mutica (Kützing) Mann 1990

APPENDIX C (continued)

Luticola (?) sp. (3A-13)
Mastogloia exigua Lewis 1861
Mastogloia smithii Thwaites 1856
Mastogloia sp. (B04-13)
Mastogloia sp. (B04-17)
Mastogloia sp. 1 (B04-21)
Mastogloia sp. 2 (B04-21)
Mastogloia sp. (B04-22)
Mastogloia sp. (B04-29)
Mastogloia sp. (B04-31)
* *Melosira nummuloides* (Dillwyn) C.A. Agardh 1824
Melosira spp. Agardh 1824
* *Minidiscus chilensis* Rivera & Koch 1984
Navicula cryptocephala Kützing 1844
Navicula cf. *digitoradiata* (Gregory) Ralfs in Pritchard 1861
Navicula directa (W. Smith) Ralfs in Pritchard 1861
* *Navicula gregaria* Donkin 1861
* *Navicula perminuta* Grunow in van Heurck 1880
Navicula phylleptosoma Lange-Bertalot in Lange-Bertalot & Genkal 1999
Navicula cf. *ramossisima* (Agardh) Cleve 1895
Navicula cf. *salinarum* Grunow in Cleve & Grunow 1880
Navicula sensu *tropicoidea*
Navicula sp. (3A-7)
Navicula sp. (3A-13)
Navicula sp. 1 (3B-1)
Navicula sp. 2 (3B-1)
Navicula sp. (3B-5)
Navicula sp. 1 (3C-1)
Navicula sp. 2 (3C-1)
Navicula sp. (11C-3)
Navicula sp. (11C-9)
Navicula sp. (11C-14)
Navicula sp. 1 (B04-3)
Navicula sp. 2 (B04-3)
Navicula sp. 1 (B04-4)
Navicula sp. 2 (B04-4)
Navicula sp. 1 (B04-8)
Navicula sp. (B04-9)
Navicula sp. 1 (B04-13)
Navicula sp. 2 (B04-13)
Navicula sp. 3 (B04-13)
Navicula sp. 1 (B04-15)
Navicula sp. 1 (B04-16)
Navicula sp. 2 (B04-16)
Navicula sp. (B04-17)
Navicula sp. 1 (B04-21)
Navicula sp. 2 (B04-21)
Navicula sp. (B04-24)
Navicula sp. 1 (B04-31)
Navicula sp. 2 (B04-31)
Navicula sp. 3 (B04-31)
Navicula sp. (B04-32)
Navicula sp. (B04-33)
Navicula sp. (B04-38)
Navicula sp. (S8-4)
Navicula sp. (S8-8)
Navicula sp. (S8-33)

APPENDIX C (continued)

Navicula sp. (S8-48)
Nitzschia amphibia Grunow 1862
* *Nitzschia coarctata* Grunow in Cleve & Moller 1878
Nitzschia dissipata (Kützing) Grunow 1862
Nitzschia fonticola Grunow in Cleve & Möller 1879
* *Nitzschia frustulum* (Kützing) Grunow in Cleve & Grunow 1880
Nitzschia hungarica Grunow 1862
Nitzschia inconspicua Grunow 1862
Nitzschia microcephala Grunow in Cleve & Möller 1878
* *Nitzschia perminuta* (Grunow) M. Peragallo 1903
Nitzschia cf. *sicula* (Castracane) Hustedt
Nitzschia valdestriata Aleem & Hustedt 1951
Nitzschia sp. (3A-3)
Nitzschia sp. (B04-3)
Nitzschia sp. (B04-11)
Nitzschia sp. (B04-13)
Nitzschia sp. (B04-22)
Nitzschia sp. (B04-37)
Nitzschia sp. (S8-1)
Nitzschia sp. (S8-17)
Nitzschia sp. (S8-34)
Nitzschia/Fragilaria sp. (3B-8)
Odontella aurita (Lyngbye) Agardh 1832
* *Odontella longicruris* (Greville) Hoban 1983
Odontella sp. (3C-3)
Opephora gemmeta (Grunow) Hustedt 1931
Opephora guenter-grassii (Witkowski & Lange-Bertalot) Sabbe & Vyverman
* *Opephora* cf. *horstiana* Witkowski 1994
* *Opephora marina* (Gregory) Petit 1888
* *Opephora minuta* (Cleve-Euler) Witkowski, Lange-Bertalot & Metzeltin 2000
* *Opephora mutabilis* (Grunow) Sabbe & Vyverman 1995
Opephora pacifica (Grunow) Petit 1888
Opephora sp. (11C-9)
* *Paralia sulcata* (Ehrenberg) Cleve 1873
Pinnularia cf. *quadratarea* (Schmidt) Cleve 1895
Plagiogramma interruptum (Gregory) Ralfs in Pritchard 1861
Plagiogramma staurophorum (Gregory) Hieberg 1863
* *Planothidium delicatulum* (Kützing) Round & Buktiyarova 1996
* *Planothidium* cf. *engelbrechtii* (Cholnoky) Round & Buktiyarova 1996
* *Planothidium hauckianum* (Grunow) Round & Buktiyarova 1996
* *Pleurosigma* spp. W. Smith 1852
Protokeelia cholnokyana
* *Pseudonitzschia multiseries* (Hasle) Hasle 1995
* *Pseudonitzschia seriata* (Cleve) H. Peragallo in H. and M. Peragallo 1897-1908
Reimeria sinuata (Gregory) Kociolek & Stoermer 1987
Reimeria spp.
* *Rhizosolenia* spp. Brightwell 1858 (mainly *R. setigera* Brightwell 1858 processes)
Rhoicosphenia abbreviata (Agardh) Lange-Bertalot 1980
Rhoicosphenia cf. *genuflexa*
Rhopalodia brebissonii Krammer 1987
Rhopalodia pacifica Krammer
Seminavis spp. Mann in Round et al. 1990
* *Skeletonema costatum* (Greville) Cleve 1878
* *Skeletonema costatum* (Greville) Cleve 1878 (weak)
Stephanodiscus spp. Ehrenberg 1845
Stephanopyxis turris (Greville & Walker-Arnott) Ralfs in Pritchard 1861
Stephanopyxis spp. Ehrenberg 1844 (resting spores)

APPENDIX C (continued)

Surirella brebissonii Krammer & Lange-Bertalot 1987
Synedra ulna (Nitzsch) Ehrenberg 1832
* *Tabellaria flocculosa* (Roth) Kutzing 1844
* *Tabularia fasciculata* (Agardh) Williams and Round 1986
* *Thalassionema bacillare* (Heiden) Kolbe 1955
* *Thalassionema nitzschioides* (Grunow) Mereschkowsky 1902
* *Thalassionema pseudonitzschioides* (Schuette and Schrader) Hasle in Hasle and Syvertsen 1996
Thalassiosira aestivalis Gran 1931
* *Thalassiosira angulata* (Gregory) Hasle 1978
Thalassiosira anguste-lineata (A. Schmidt) Fryxell & Hasle 1977
* *Thalassiosira binata* Fryxell
* *Thalassiosira bioculata* (Grunow) Ostenfeld 1903
Thalassiosira bioculata var. *exigua* (Grunow) Hustedt 1928
* *Thalassiosira conferta* Hasle in Hasle and Fryxell 1977
* *Thalassiosira decipiens* (Grunow) Jørgensen 1905
Thalassiosira decipiens (Grunow) Jørgensen 1905 (large)
* *Thalassiosira eccentrica* (Ehrenberg) Cleve 1904
Thalassiosira eccentrica (Ehrenberg) Cleve 1904 (large)
Thalassiosira cf. eccentrica
* *Thalassiosira gravida* Cleve
Thalassiosira hendeyi Hasle & Fryxell 1977
Thalassiosira hyalina (Grunow) Gran 1897
* *Thalassiosira kushirensis* Takano 1985
* *Thalassiosira* cf. *leptopus* (Grunow) Hasle and Fryxell 1977
Thalassiosira aff. *leptopus* (Grunow) Hasle and Fryxell 1977
Thalassiosira lundiana Fryxell
* *Thalassiosira minima* Gaarder 1951
Thalassiosira nodulolineata (Hendey) Hasle & Fryxell 1977
* *Thalassiosira nordenskioeldii* Cleve 1873
Thalassiosira oceanica Hasle 1983
* *Thalassiosira oestrupii* (Ostenfeld) Hasle 1972
* *Thalassiosira pacifica* Gran and Angst 1931
Thalassiosira poroseriata (Ramsfjell) Hasle 1972
* *Thalassiosira punctigera* (Castracane) Hasle 1983
* *Thalassiosira rotula* Meunier 1910
* *Thalassiosira tealata* Takano 1980
* *Thalassiosira tenera* Proschkina-Lavrenko 1961
* *Thalassiosira* sp. (cf. *tenera)* Proschkina-Lavrenko 1961
Thalassiosira sp. 1 (3A-2)
Thalassiosira sp. 2 (3A-2)
Thalassiosira sp. (3A-6)
Thalassiosira sp. (3C-2)
Thalassiosira sp. (3C-8)
Thalassiosira sp. (3C-11)
Thalassiosira sp. (B04-2)
Thalassiosira sp. 1 (B04-12)
Thalassiosira sp. 2 (B04-12)
Thalassiosira sp. 2 (B04-15)
Thalassiosira sp. (B04-16)
Thalassiosira sp. (B04-21)
Thalassiosira sp. (B04-23)
Thalassiosira sp. (B04-24)
Thalassiosira sp. (B04-25)
Thalassiosira sp. (B04-27)
Thalassiosira sp. (B04-36)
Thalassiosira sp. (B04-40)
Thalassiosira sp. (S8-12)

APPENDIX C (continued)

Thalassiosira sp. (S8-27)
Thalassiosira sp. (S8-31)
Thalassiosira sp. (S8-35)
Thalassiothrix longissima Cleve & Grunow 1880
Trachyneis aspera (Ehrenberg) Cleve 1894
Triceratium spp. Ehrenberg 1844
Tryblionella cf. *acuminata* Smith 1853
Tryblionella aerophila (Hustedt) Mann 1990
Tryblionella sp. (3A-9)
Tryblionella sp.
Tryblionella sp. (3C-11)
Tryblionella sp. (S8-1)
Unknown pennate (3A-13)
Unknown pennate 1 (3B-1)
Unknown pennate 2 (3B-1)
Unknown pennate 1 (3B-5)
Unknown pennate 2 (3B-5)
Unknown pennate 1 (3B-7)
Unknown spennate 2 (3B-7)
Unknown pennate (3C-8)
Unknown pennate (3C-9)
Unknown centric (B04-6)
Unknown centric (B04-7)
Unknown pennate 1 (B04-9)
Unknown pennate (B04-14)
Unknown pennate 1 (B04-18)
Unknown centric (B04-20)
Unknown sp. 1 (B04-20)
Unknown pennate 2 (B04-20)
Unknown pennate 3 (B04-20)
Unknown centric (B04-21)
Unknown sp. 2 (B04-21)
Unknown centric (B04-23)
Unknown pennate 1 (B04-23)
Unknown pennate 2 (B04-23)
Unknown pennate 3 (B04-23)
Unknown centric (B04-37)
Unknown pennate (B04-37)
Unknown centric (S8-4)
Unknown pennate (S8-7)
Unknown pennate 2 (S8-8)
Unknown pennate (S8-32)
Unknown pennate (S8-36)
Unknown centric (S8-39)
Unknown pennate 1 (S8-41)
Unknown pennate 2 (S8-41)
Unknown pennate (S8-50)
Unknown pennate (S8-52)

SILICOFLAGELLATES

Dictyocha fibula Ehrenberg 1839
Dictyocha speculum Ehrenberg 1839
Octactis octonaria (Ehrenberg) Hovasse 1946 (including rare *Dictyocha octonaria* (Ehrenberg 1844))

diatom taxa, n=387; silicoflagellate taxa, n=3; total samples (thin sections and strewn slides), n=216

APPENDIX D

Sediment Slab Thin Section Record

This appendix contains images of all thin section slides analyzed in Chapter 4. Below is a guide illustrating how to read the images. The next two pages show where in the sediment slabs each slide comes from. Readers may wish to consult Figure 4.4 to see where in the core the slabs are located.

Reading the image. **A.** Slide name: numeral indicates the slab number, letter indicates slide location on the slab. **B.** This area contains the scale bar and occasional descriptions. **C.** Thin section photomosaic. **D.** Couplet interval and numeric label: **bold** labels indicate 4-component seasonal succession, *italic* labels indicate 3-component seasonal succession, and plain labels indicate no seasonal succession. **E.** Sediment lithology (see below for key). **F.** Lamina description. Read the slide from the bottom up as this simulates the temporal succession of deposition. Taxa mentioned for the first time are spelled out in entirety toward the bottom of the image. Abundant taxa and sedimentary components are listed first, followed by less abundant taxa and components. An exclamation mark after a taxon name implies a strongly near-monospecific bloom lamina. An asterisk beside a couplet label denotes silt-rich (possibly El Niño) couplets.

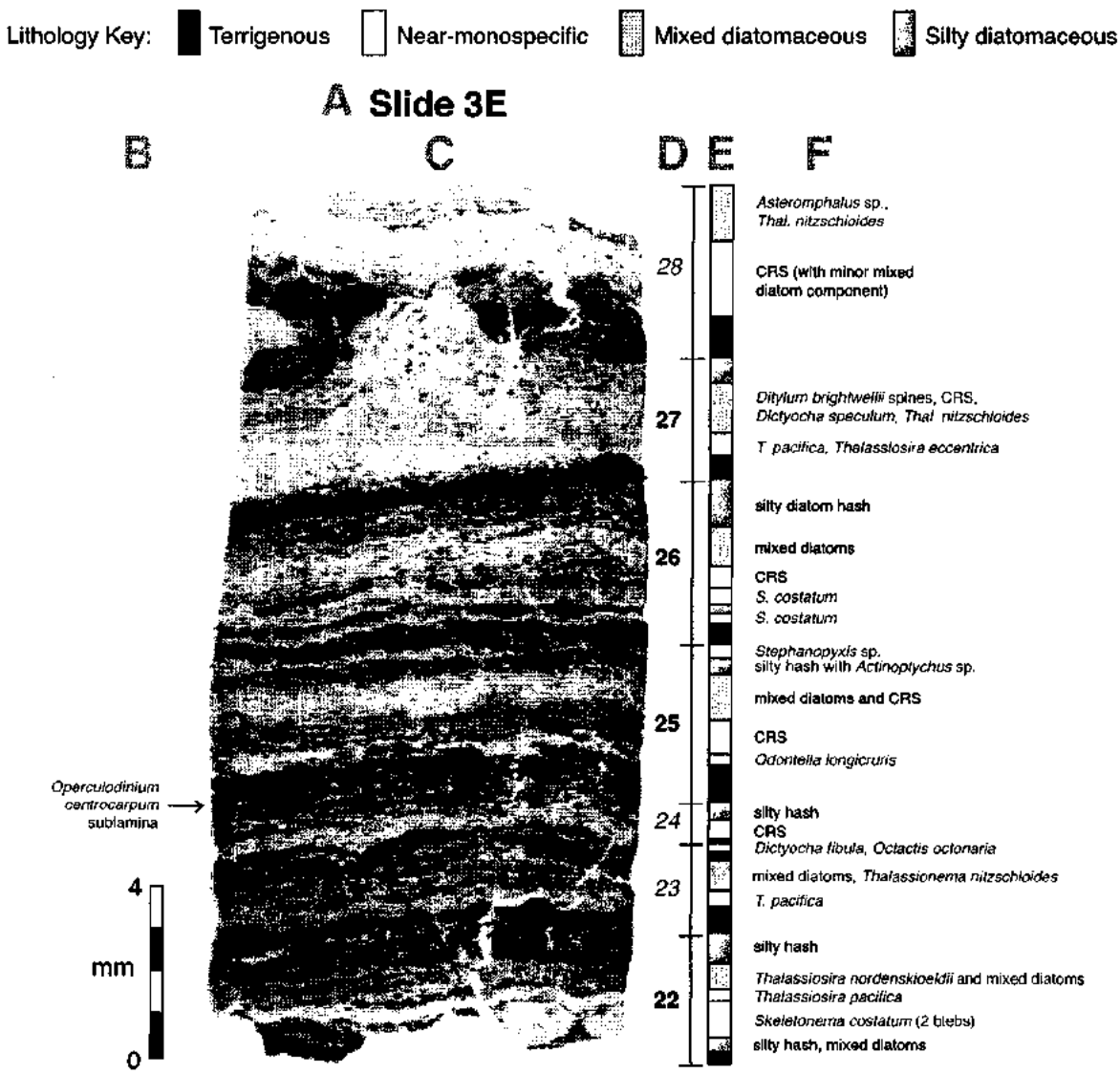

Appendix D (continued).

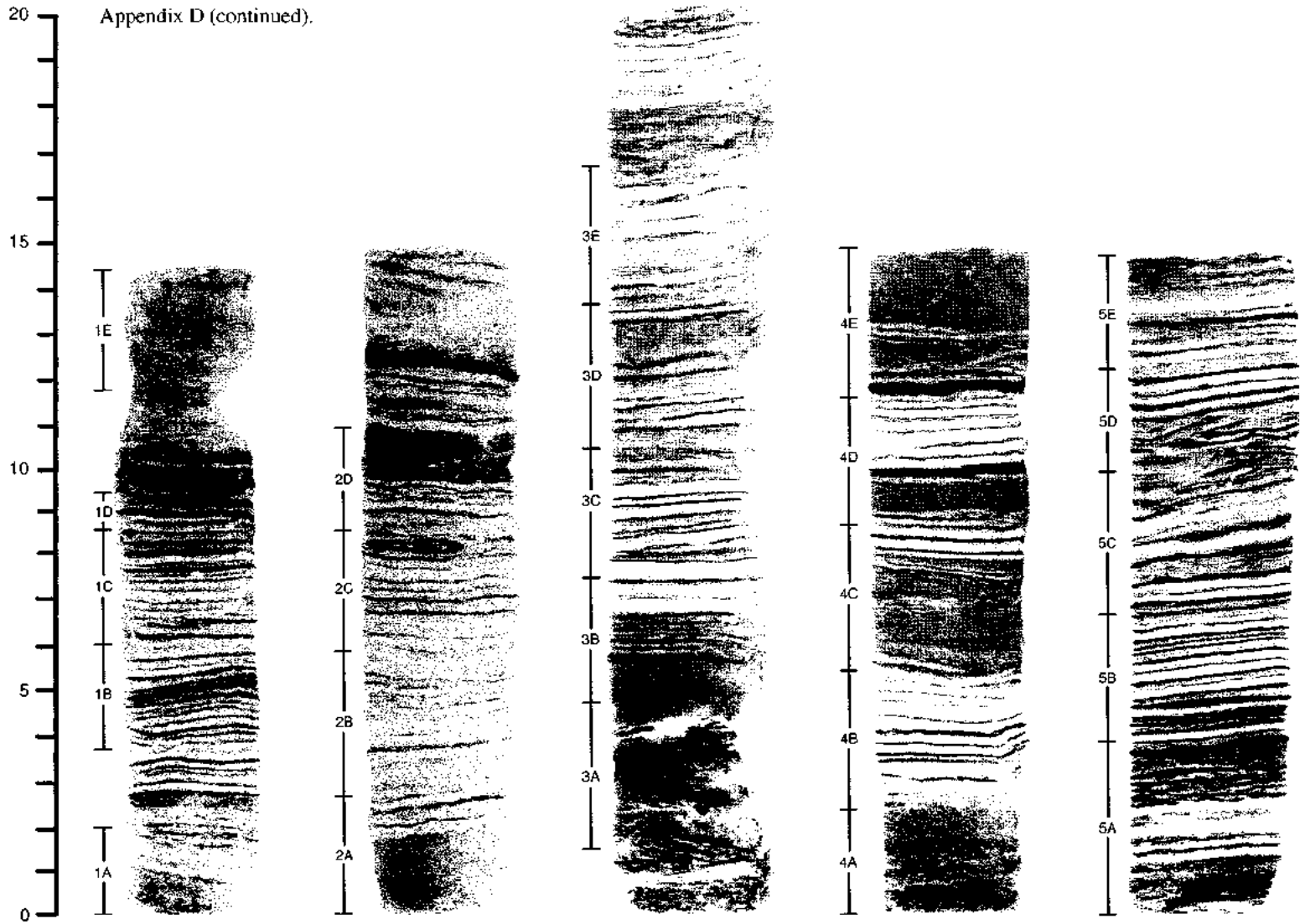

SLAB 1
78 - 93 cm

SLAB 2
142 - 157 cm

SLAB 3
373 - 388 cm

SLAB 4
469 - 484 cm

SLAB 5
682 - 697 cm

Appendix D (continued).

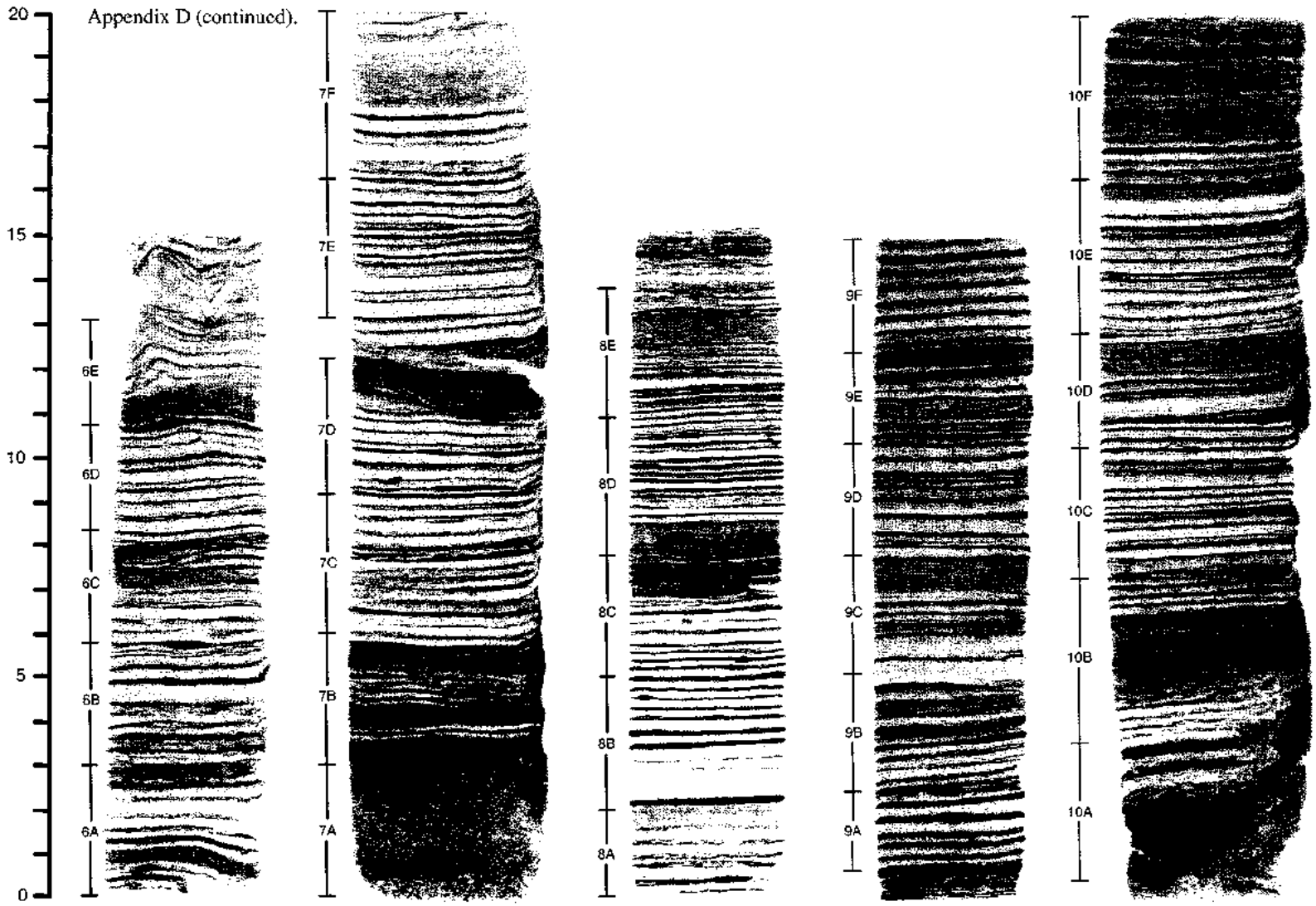

SLAB 6
682 - 697 cm

SLAB 7
753 - 768 cm

SLAB 8
870 - 885 cm

SLAB 9
889 - 904 cm

SLAB 10
1119 - 1134 cm

Slide 1A

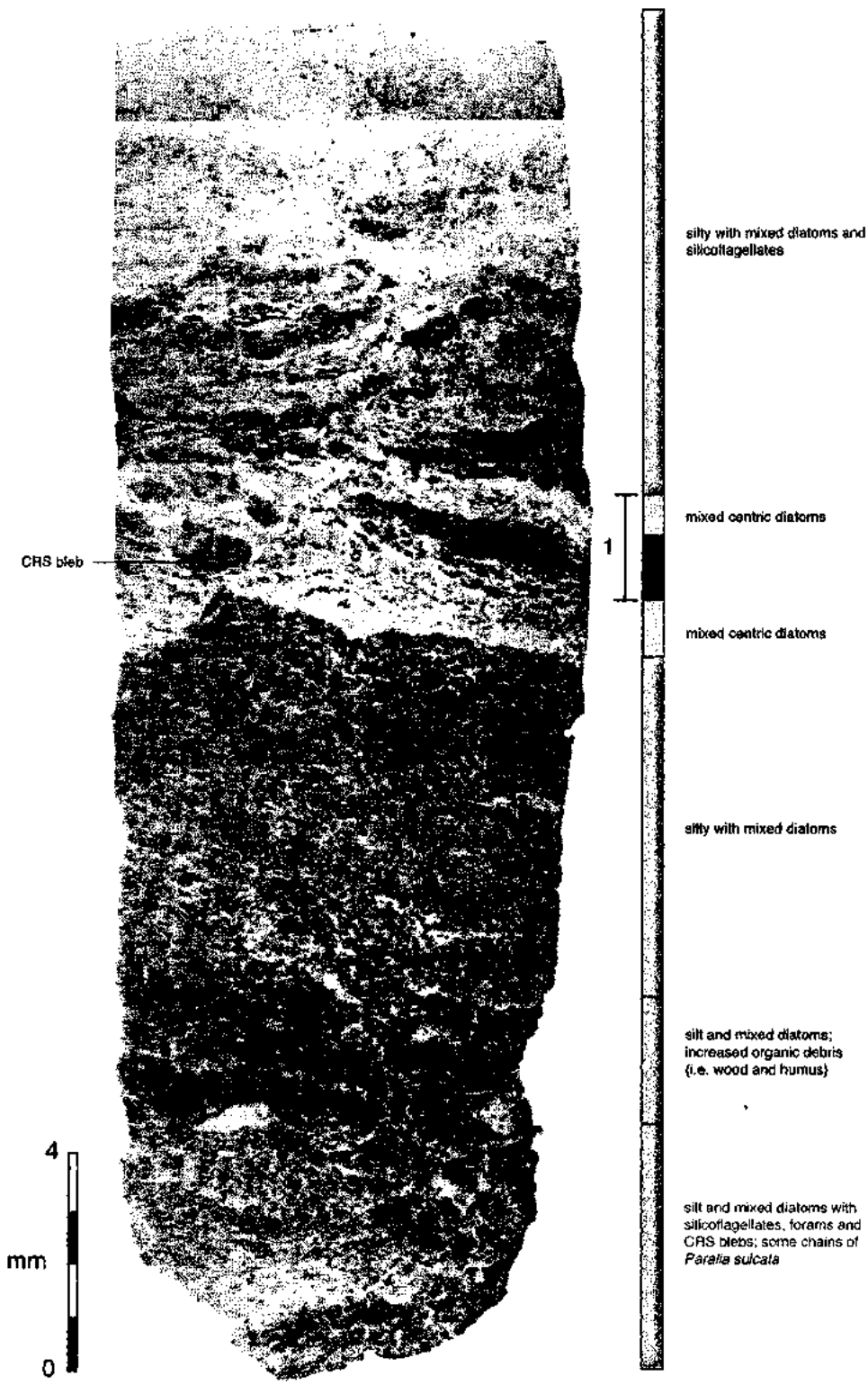
CRS bleb
1
4
mm
0
silty with mixed diatoms and silicoflagellates
mixed centric diatoms
mixed centric diatoms
silty with mixed diatoms
silt and mixed diatoms; increased organic debris (i.e. wood and humus)
silt and mixed diatoms with silicoflagellates, forams and CRS blebs; some chains of *Paralia sulcata*

Slide 1B

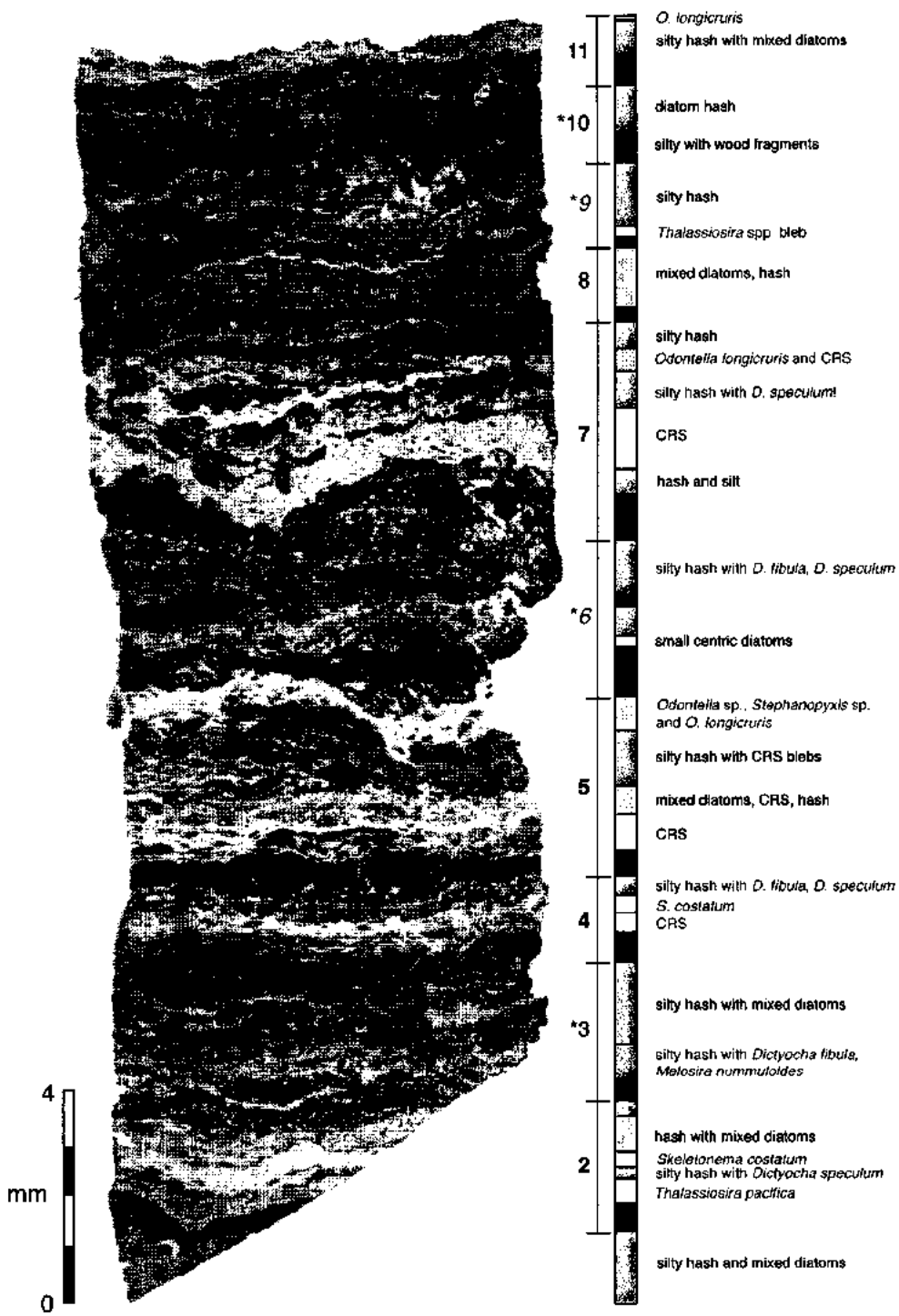
11
*10
*9
8
7
*6
5
4
*3
2
4
mm
0
O. longicruris
silty hash with mixed diatoms
diatom hash
silty with wood fragments
silty hash
Thalassiosira spp bleb
mixed diatoms, hash
silty hash
Odontella longicruris and CRS
silty hash with D. speculum
CRS
hash and silt
silty hash with D. fibula, D. speculum
small centric diatoms
Odontella sp., Stephanopyxis sp.
and O. longicruris
silty hash with CRS blebs
mixed diatoms, CRS, hash
CRS
silty hash with D. fibula, D. speculum
S. costatum
CRS
silty hash with mixed diatoms
silty hash with Dictyocha fibula,
Melosira nummuloides
hash with mixed diatoms
Skeletonema costatum
silty hash with Dictyocha speculum
Thalassiosira pacifica
silty hash and mixed diatoms

Slide 1C

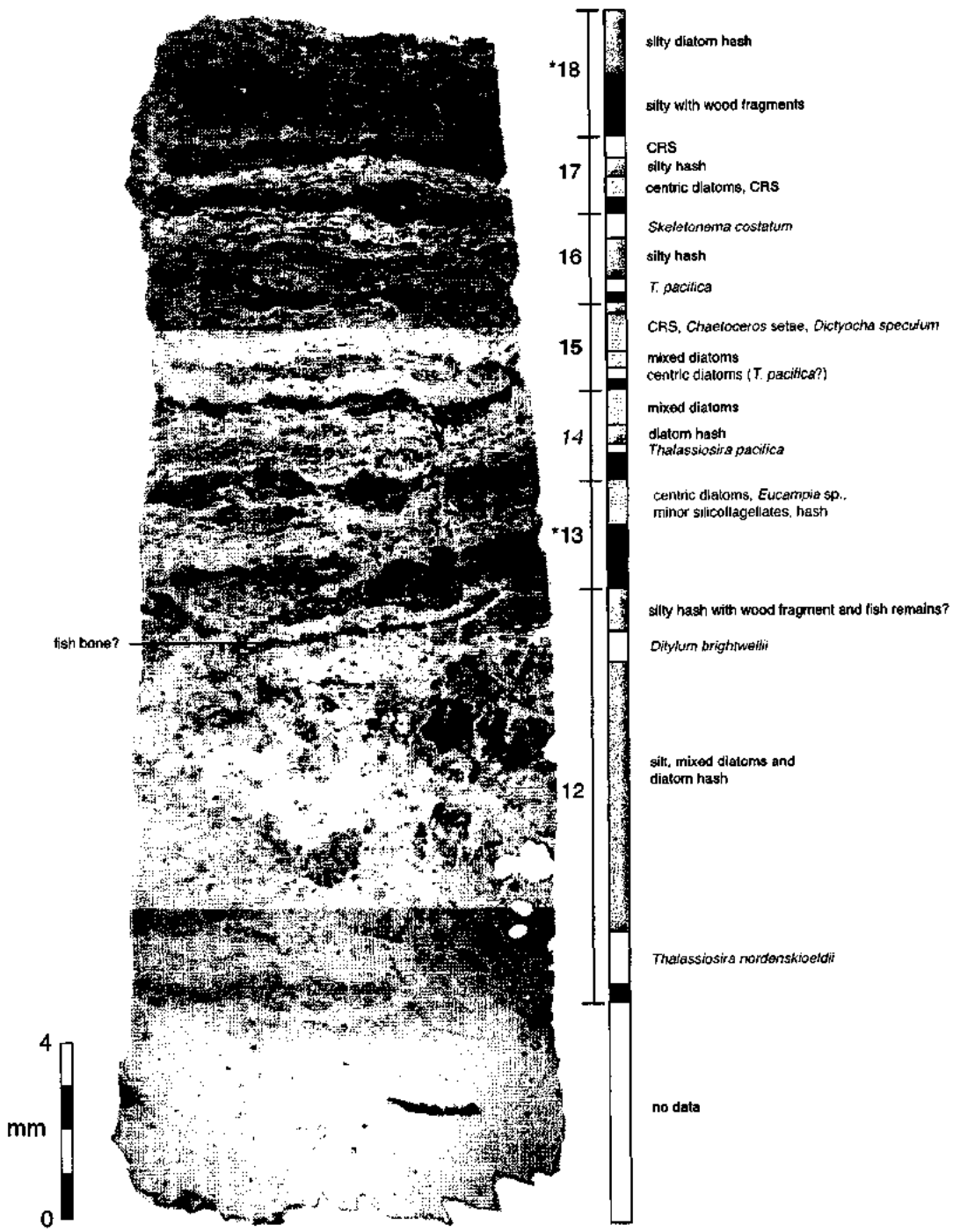
*18
17
16
15
14
*13
12
silty diatom hash
silty with wood fragments
CRS
silty hash
centric diatoms, CRS
Skeletonema costatum
silty hash
T. pacifica
CRS, Chaetoceros setae, Dictyocha speculum
mixed diatoms
centric diatoms (T. pacifica?)
mixed diatoms
diatom hash
Thalassiosira pacifica
centric diatoms, Eucampia sp.,
minor silicoflagellates, hash
silty hash with wood fragment and fish remains?
Ditylum brightwellii
silt, mixed diatoms and
diatom hash
Thalassiosira nordenskioeldii
no data
fish bone?
4
mm
0

Slide 1D

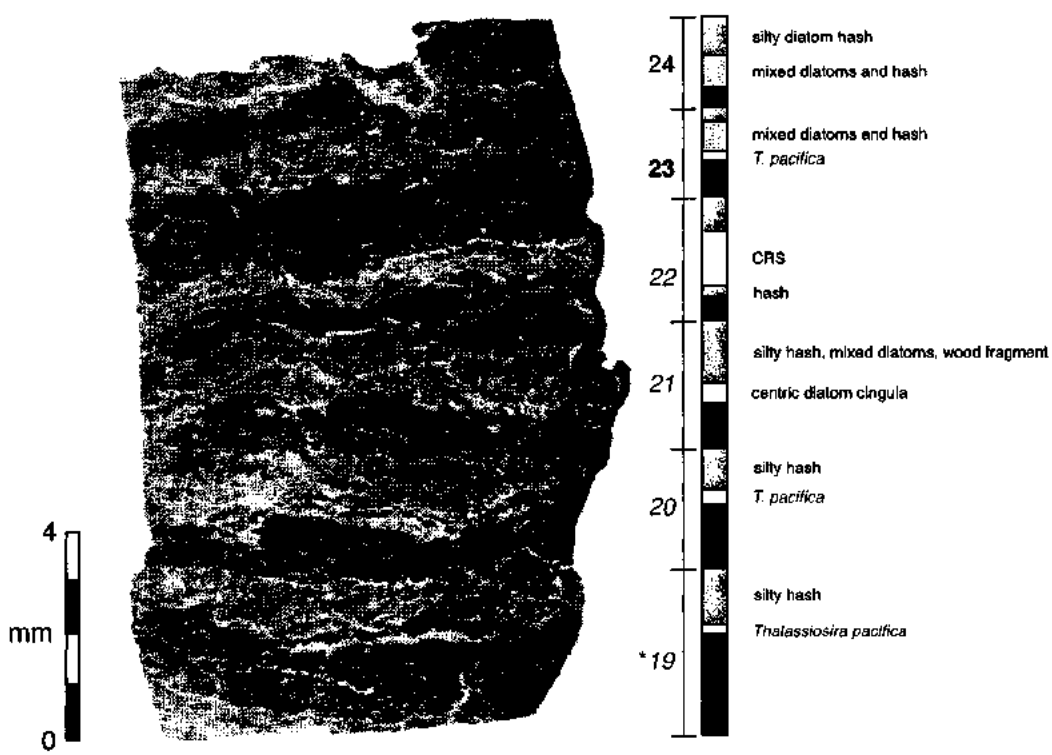
4
mm
0
24
23
22
21
20
*19
silty diatom hash
mixed diatoms and hash
mixed diatoms and hash
T. pacifica
CRS
hash
silty hash, mixed diatoms, wood fragment
centric diatom cingula
silty hash
T. pacifica
silty hash
Thalassiosira pacifica

Slide 1E

massive interval with silt and terrigenous organic material; microfossils include mixed diatoms, benthic forams, silicoflagellates and fecal pellets; chains of *Paralia sulcata* visible

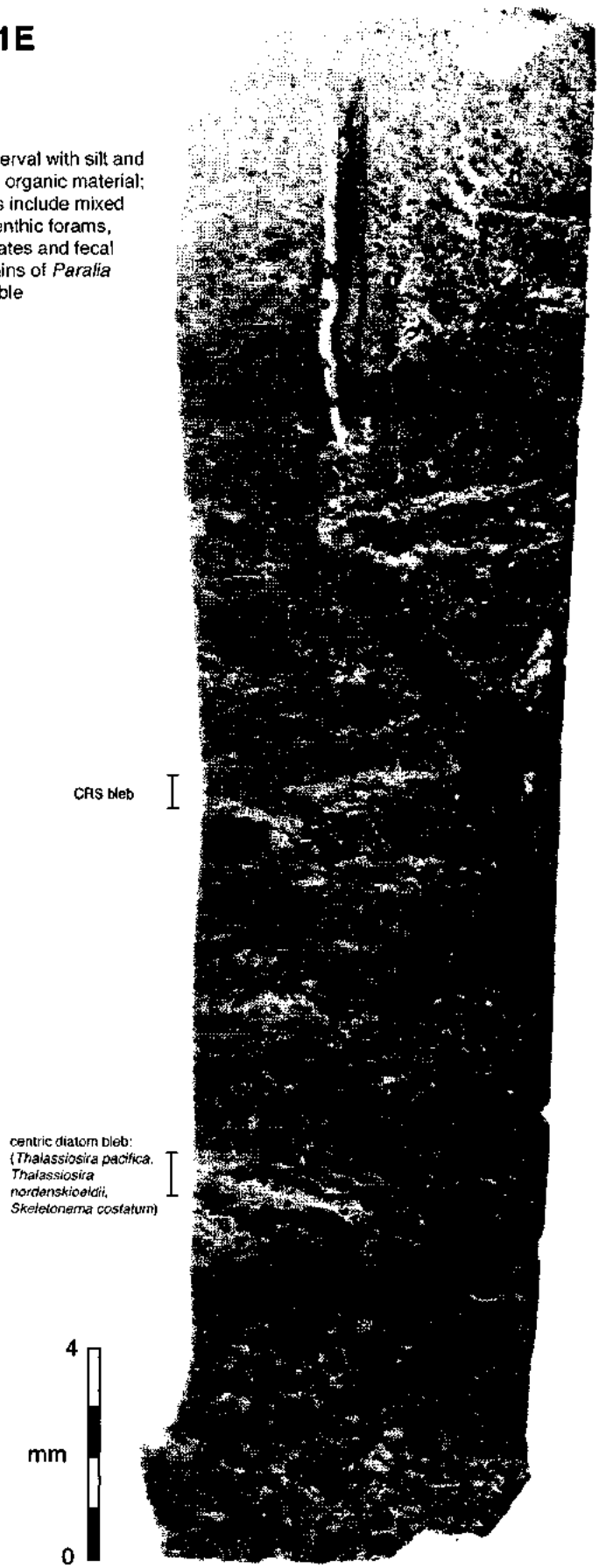

Slide 2A

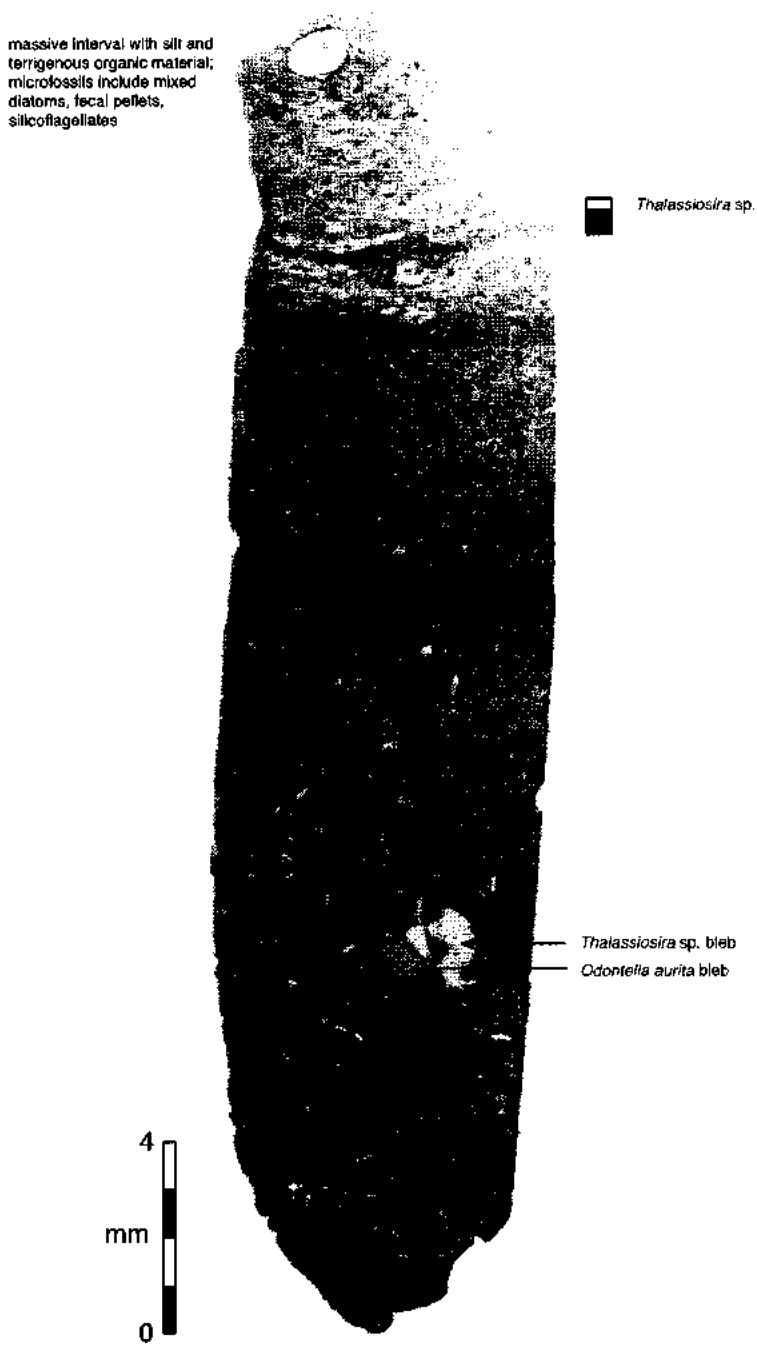
massive interval with silt and terrigenous organic material; microfossils include mixed diatoms, fecal pellets, silicoflagellates
Thalassiosira sp.
Thalassiosira sp. bleb
Odontella aurita bleb
4
mm
0

Slide 2B

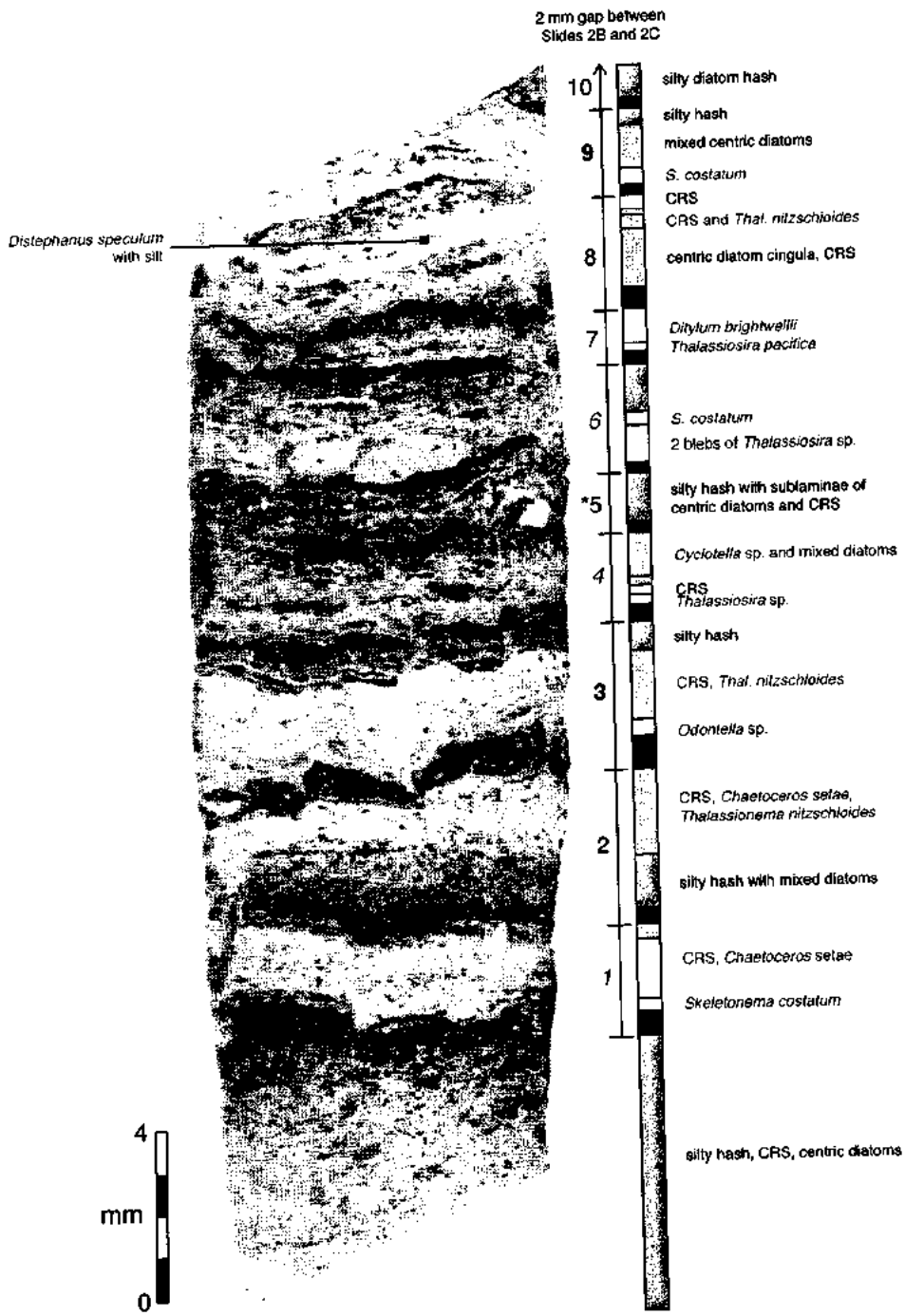
2 mm gap between
Slides 2B and 2C
Distephanus speculum
with silt
10
9
8
7
6
*5
4
3
2
1
silty diatom hash
silty hash
mixed centric diatoms
S. costatum
CRS
CRS and Thal. nitzschioides
centric diatom cingula, CRS
Ditylum brightwellii
Thalassiosira pacifica
S. costatum
2 blebs of Thalassiosira sp.
silty hash with sublaminae of
centric diatoms and CRS
Cyclotella sp. and mixed diatoms
CRS
Thalassiosira sp.
silty hash
CRS, Thal. nitzschioides
Odontella sp.
CRS, Chaetoceros setae,
Thalassionema nitzschioides
silty hash with mixed diatoms
CRS, Chaetoceros setae
Skeletonema costatum
silty hash, CRS, centric diatoms
4
mm
0

Slide 2C

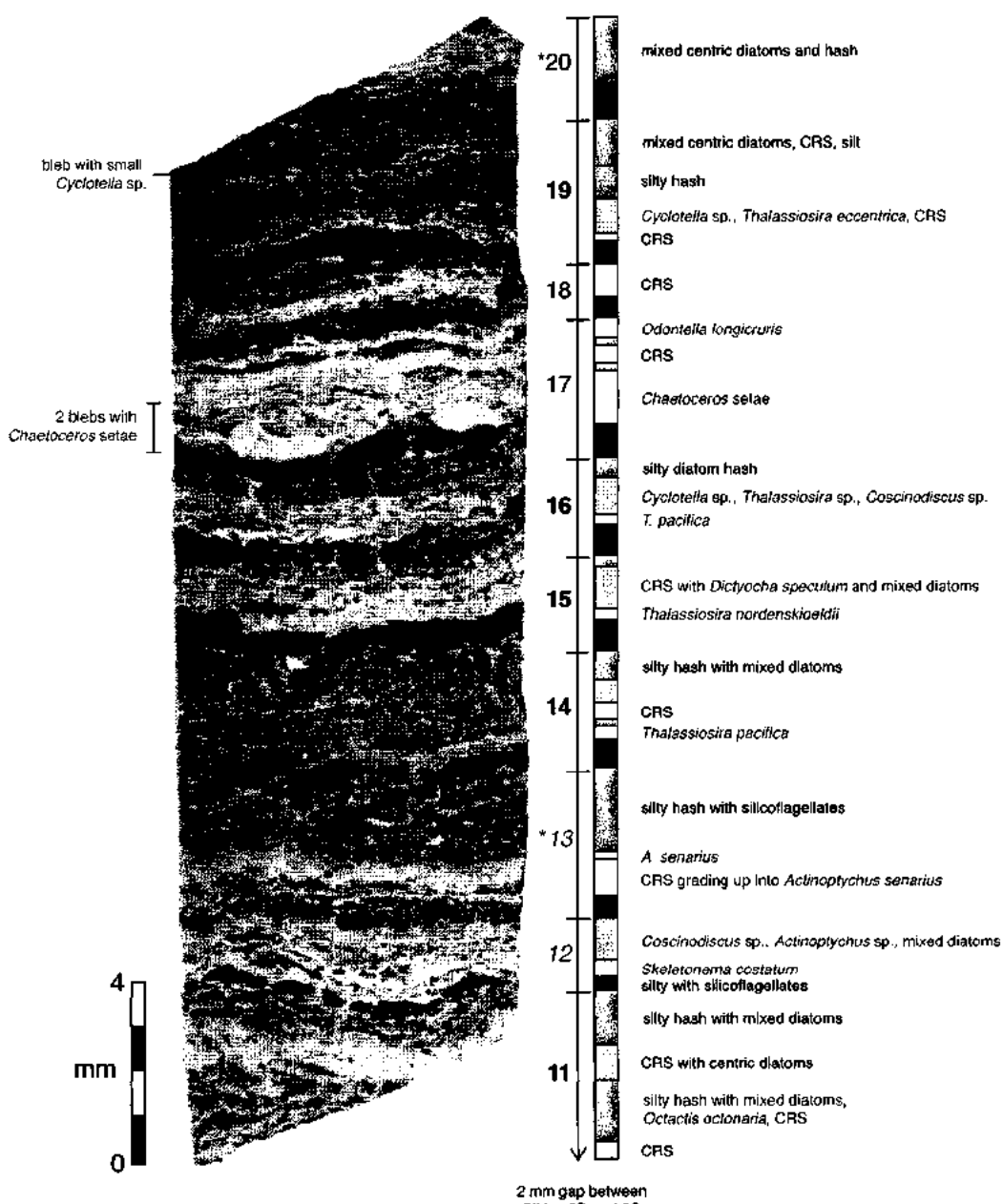
bleb with small
Cyclotella sp.
2 blebs with
Chaetoceros setae
4
mm
0
*20
19
18
17
16
15
14
*13
12
11
mixed centric diatoms and hash
mixed centric diatoms, CRS, silt
silty hash
Cyclotella sp., Thalassiosira eccentrica, CRS
CRS
CRS
Odontella longicruris
CRS
Chaetoceros setae
silty diatom hash
Cyclotella sp., Thalassiosira sp., Coscinodiscus sp.
T. pacifica
CRS with Dictyocha speculum and mixed diatoms
Thalassiosira nordenskioeldii
silty hash with mixed diatoms
CRS
Thalassiosira pacifica
silty hash with silicoflagellates
A. senarius
CRS grading up into Actinoptychus senarius
Coscinodiscus sp., Actinoptychus sp., mixed diatoms
Skeletonema costatum
silty with silicoflagellates
silty hash with mixed diatoms
CRS with centric diatoms
silty hash with mixed diatoms,
Octactis octonaria, CRS
CRS
2 mm gap between
Slides 2B and 2C

Slide 2D

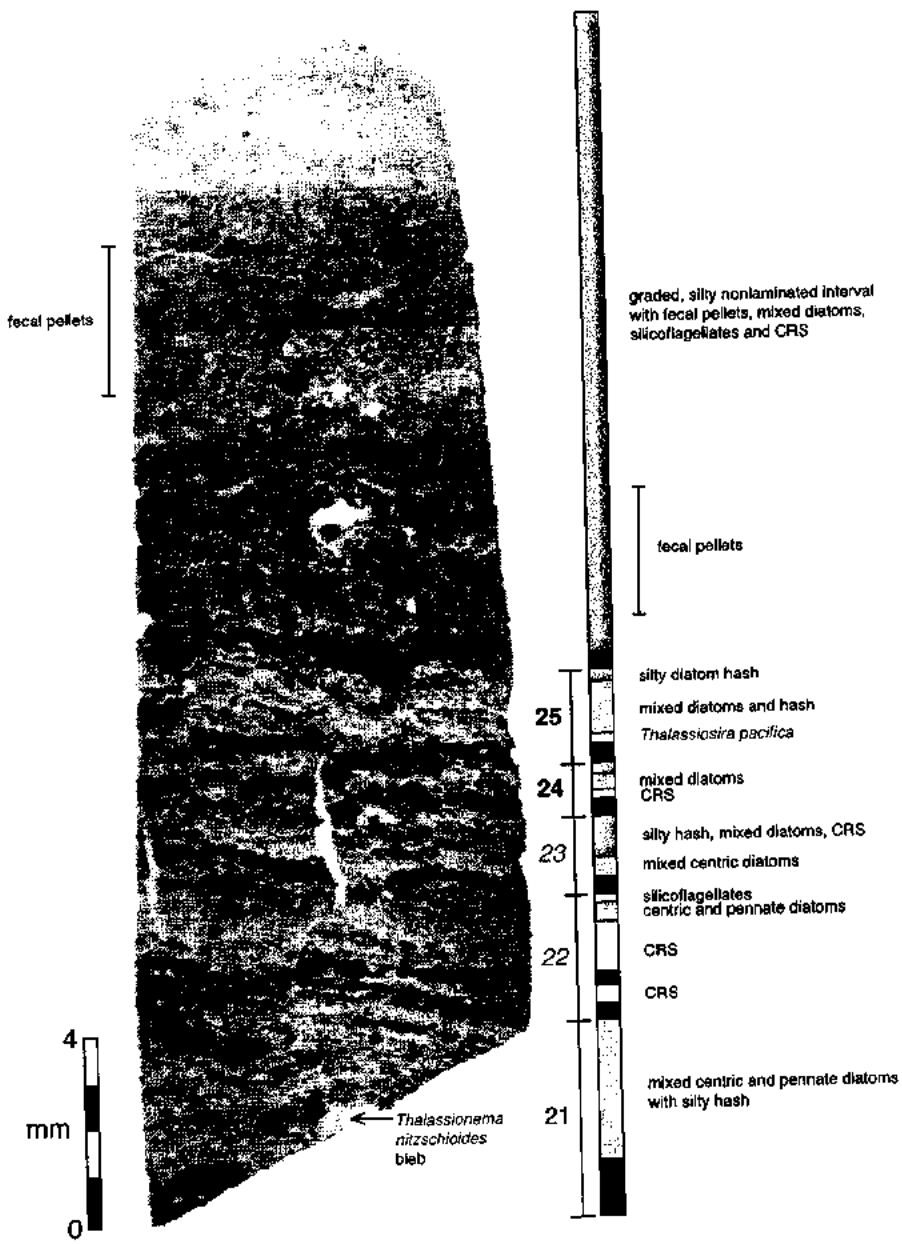
fecal pellets
graded, silty nonlaminated interval with fecal pellets, mixed diatoms, silicoflagellates and CRS
fecal pellets
silty diatom hash
mixed diatoms and hash
25
Thalassiosira pacifica
mixed diatoms
24
CRS
silty hash, mixed diatoms, CRS
23
mixed centric diatoms
silicoflagellates
centric and pennate diatoms
22
CRS
CRS
mixed centric and pennate diatoms
with silty hash
21
4
mm
0
Thalassionema
nitzschioides
bleb

Slide 3A

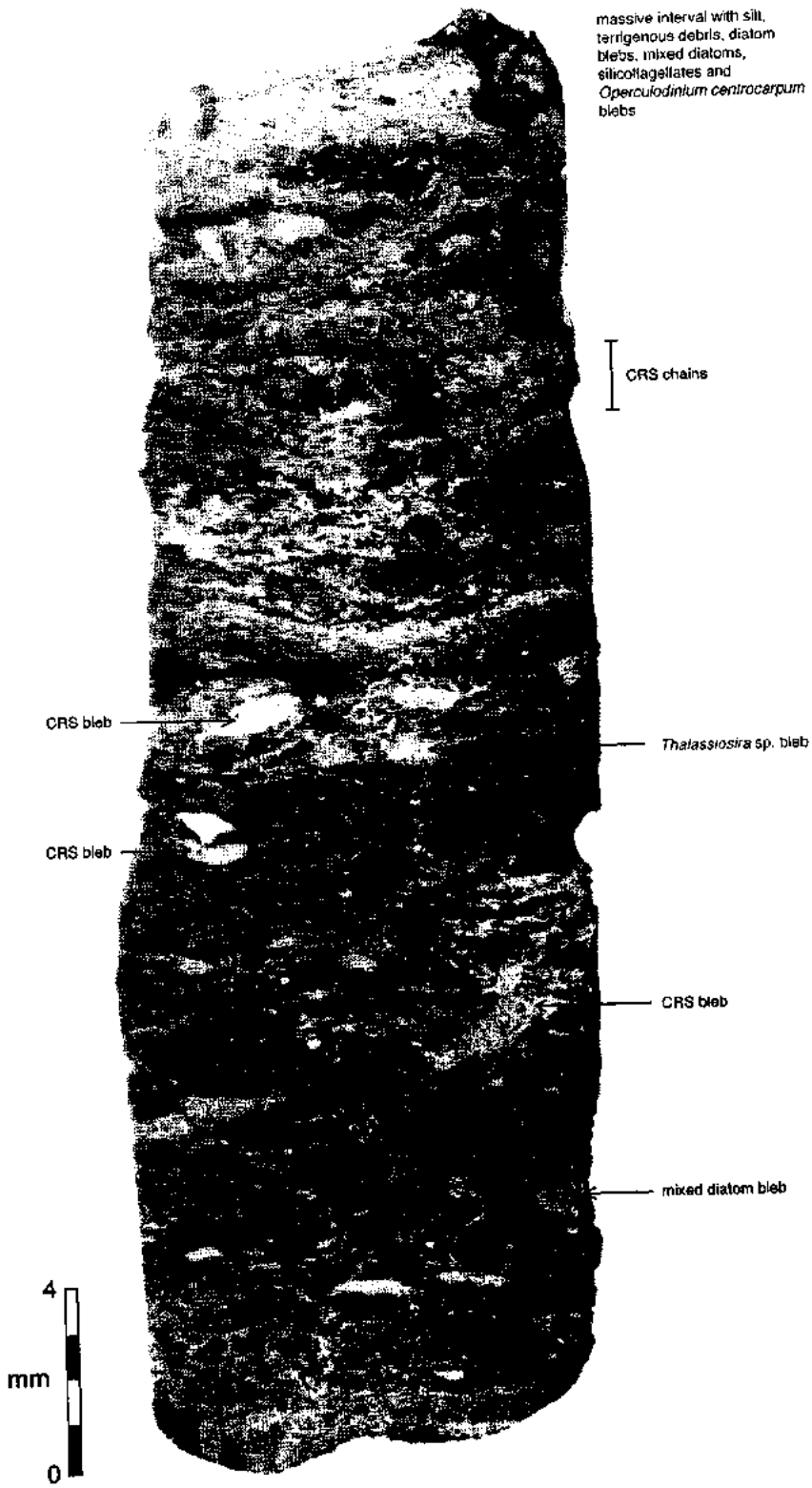
massive interval with silt, terrigenous debris, diatom blebs, mixed diatoms, silicoflagellates and *Operculodinium centrocarpum* blebs
CRS chains
CRS bleb
CRS bleb
Thalassiosira sp. bleb
CRS bleb
mixed diatom bleb
4
mm
0

Slide 3B

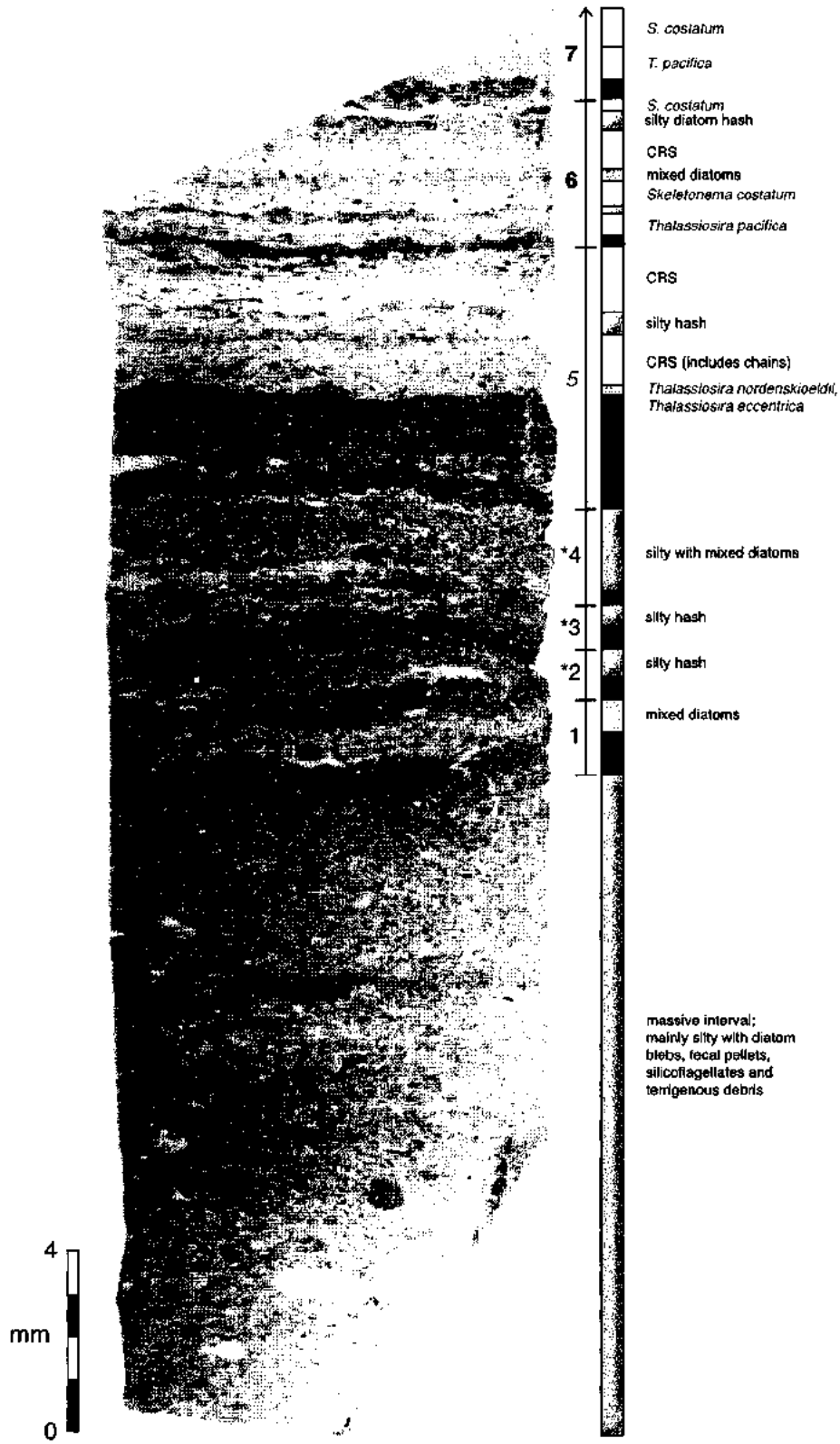
7
6
5
*4
*3
*2
1
S. costatum
T. pacifica
S. costatum
silty diatom hash
CRS
mixed diatoms
Skeletonema costatum
Thalassiosira pacifica
CRS
silty hash
CRS (includes chains)
Thalassiosira nordenskioeldii,
Thalassiosira eccentrica
silty with mixed diatoms
silty hash
silty hash
mixed diatoms
massive interval;
mainly silty with diatom
blebs, fecal pellets,
silicoflagellates and
terrigenous debris
4
mm
0

Slide 3C

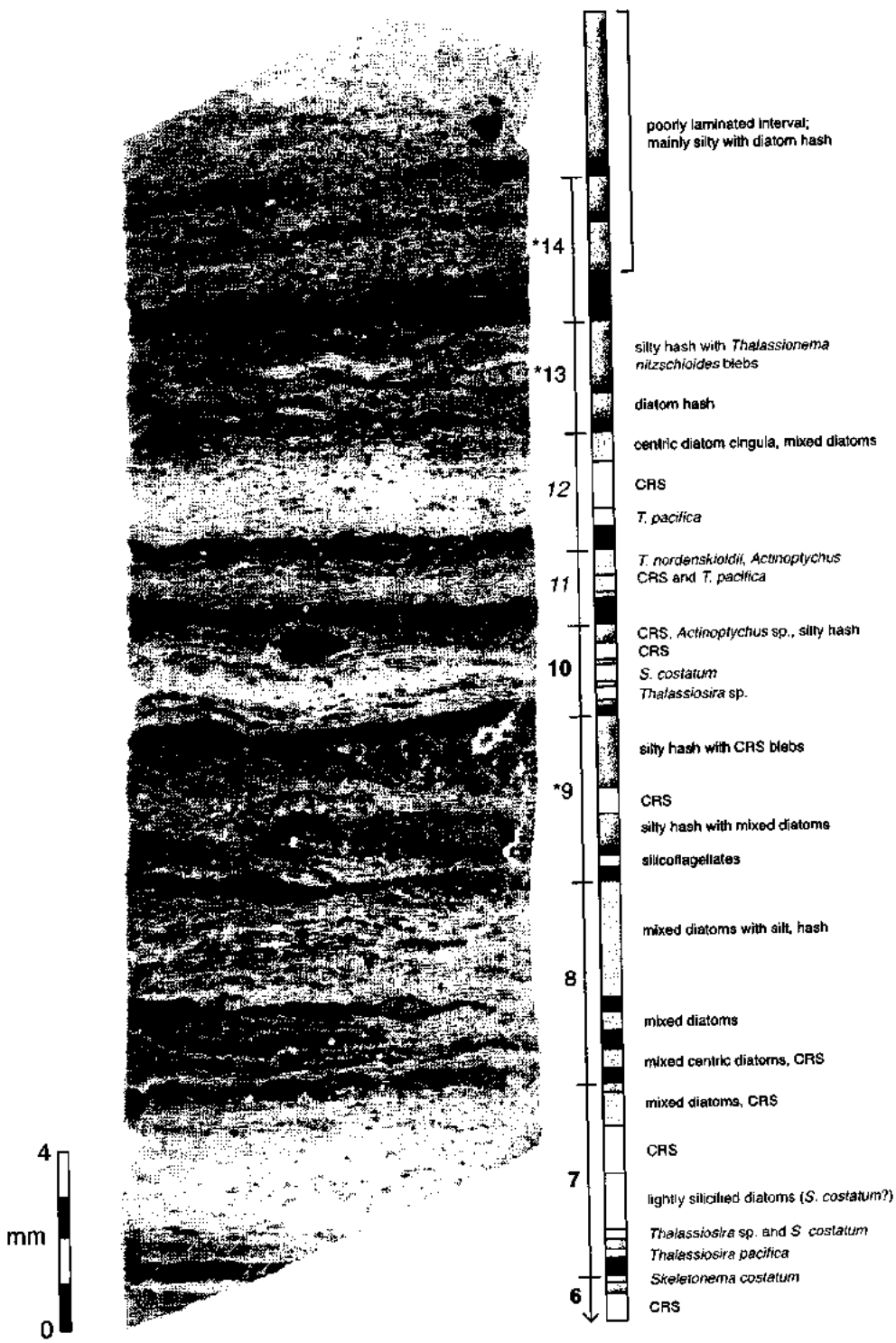
poorly laminated interval;
mainly silty with diatom hash
*14
silty hash with Thalassionema nitzschioides blebs
*13
diatom hash
centric diatom cingula, mixed diatoms
12
CRS
T. pacifica
T. nordenskioldii, Actinoptychus
CRS and T. pacifica
11
CRS, Actinoptychus sp., silty hash
CRS
10
S. costatum
Thalassiosira sp.
silty hash with CRS blebs
*9
CRS
silty hash with mixed diatoms
silicoflagellates
mixed diatoms with silt, hash
8
mixed diatoms
mixed centric diatoms, CRS
mixed diatoms, CRS
CRS
7
lightly silicified diatoms (S. costatum?)
Thalassiosira sp. and S. costatum
Thalassiosira pacifica
Skeletonema costatum
6
CRS
4
mm
0

Slide 3D

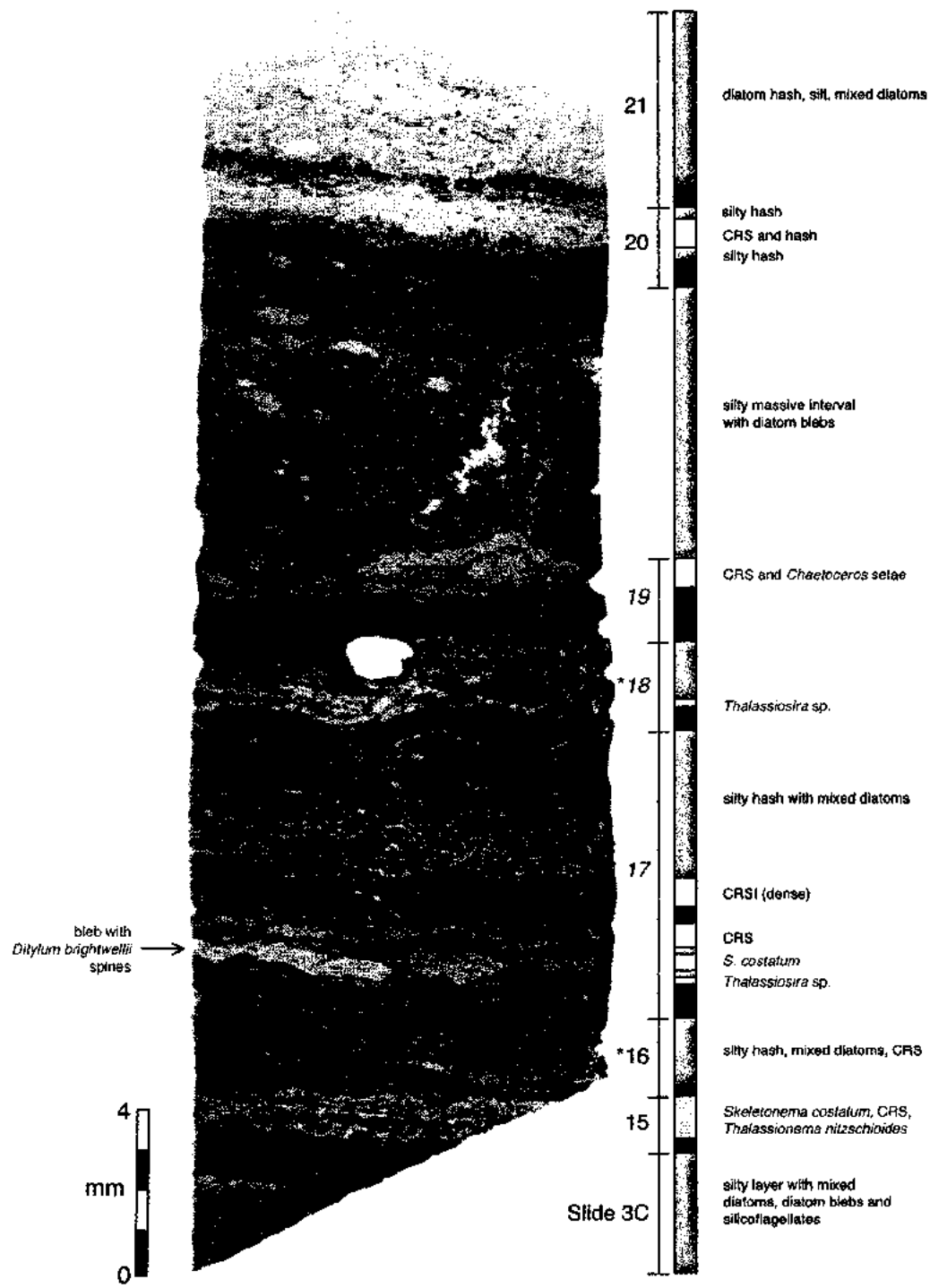
21
diatom hash, silt, mixed diatoms
silty hash
20
CRS and hash
silty hash
silty massive interval
with diatom blebs
CRS and Chaetoceros setae
19
*18
Thalassiosira sp.
silty hash with mixed diatoms
17
CRSI (dense)
CRS
S. costatum
Thalassiosira sp.
bleb with
Ditylum brightwellii
spines
*16
silty hash, mixed diatoms, CRS
15
Skeletonema costatum, CRS,
Thalassionema nitzschioides
silty layer with mixed
diatoms, diatom blebs and
silicoflagellates
Slide 3C
4
mm
0

Slide 3E

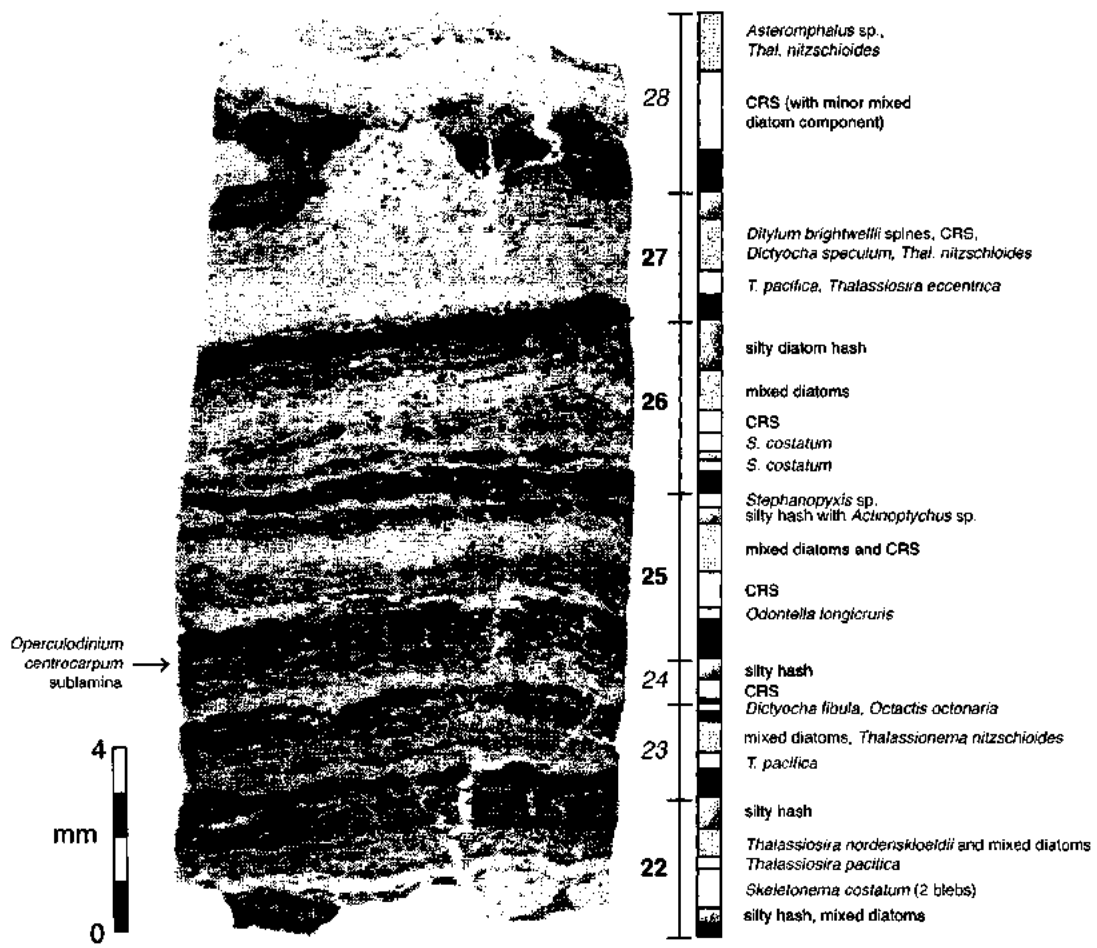
Operculodinium centrocarpum sublamina
4
mm
0
28
27
26
25
24
23
22
Asteromphalus sp., Thal. nitzschioides
CRS (with minor mixed diatom component)
Ditylum brightwellii spines, CRS, Dictyocha speculum, Thal. nitzschioides
T. pacifica, Thalassiosira eccentrica
silty diatom hash
mixed diatoms
CRS
S. costatum
S. costatum
Stephanopyxis sp.
silty hash with Actinoptychus sp.
mixed diatoms and CRS
CRS
Odontella longicruris
silty hash
CRS
Dictyocha fibula, Octactis octonaria
mixed diatoms, Thalassionema nitzschioides
T. pacifica
silty hash
Thalassiosira nordenskioeldii and mixed diatoms
Thalassiosira pacifica
Skeletonema costatum (2 blebs)
silty hash, mixed diatoms

Slide 4A

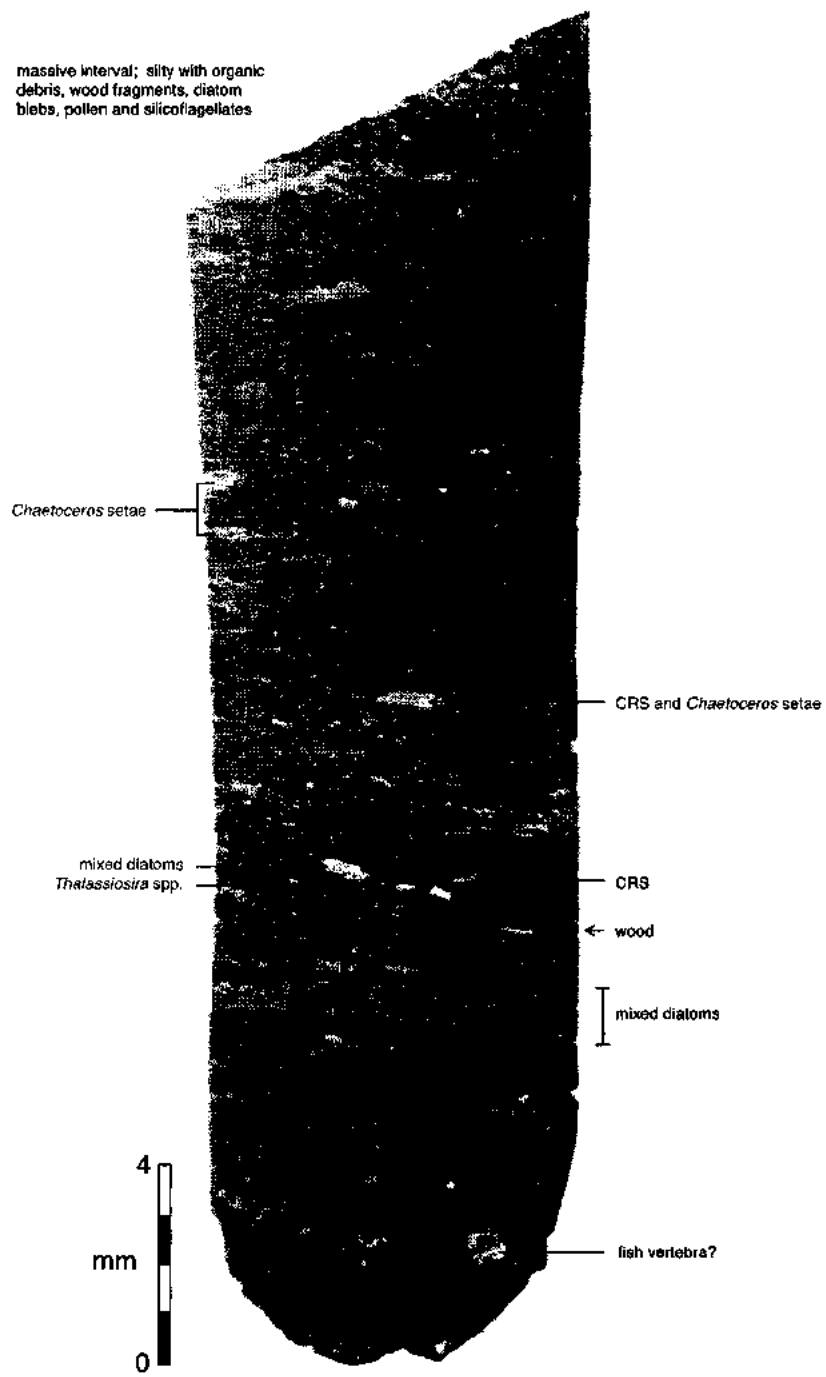
massive interval; silty with organic debris, wood fragments, diatom blebs, pollen and silicoflagellates
Chaetoceros setae
CRS and *Chaetoceros* setae
mixed diatoms
Thalassiosira spp.
CRS
wood
mixed diatoms
4
mm
0
fish vertebra?

Slide 4B

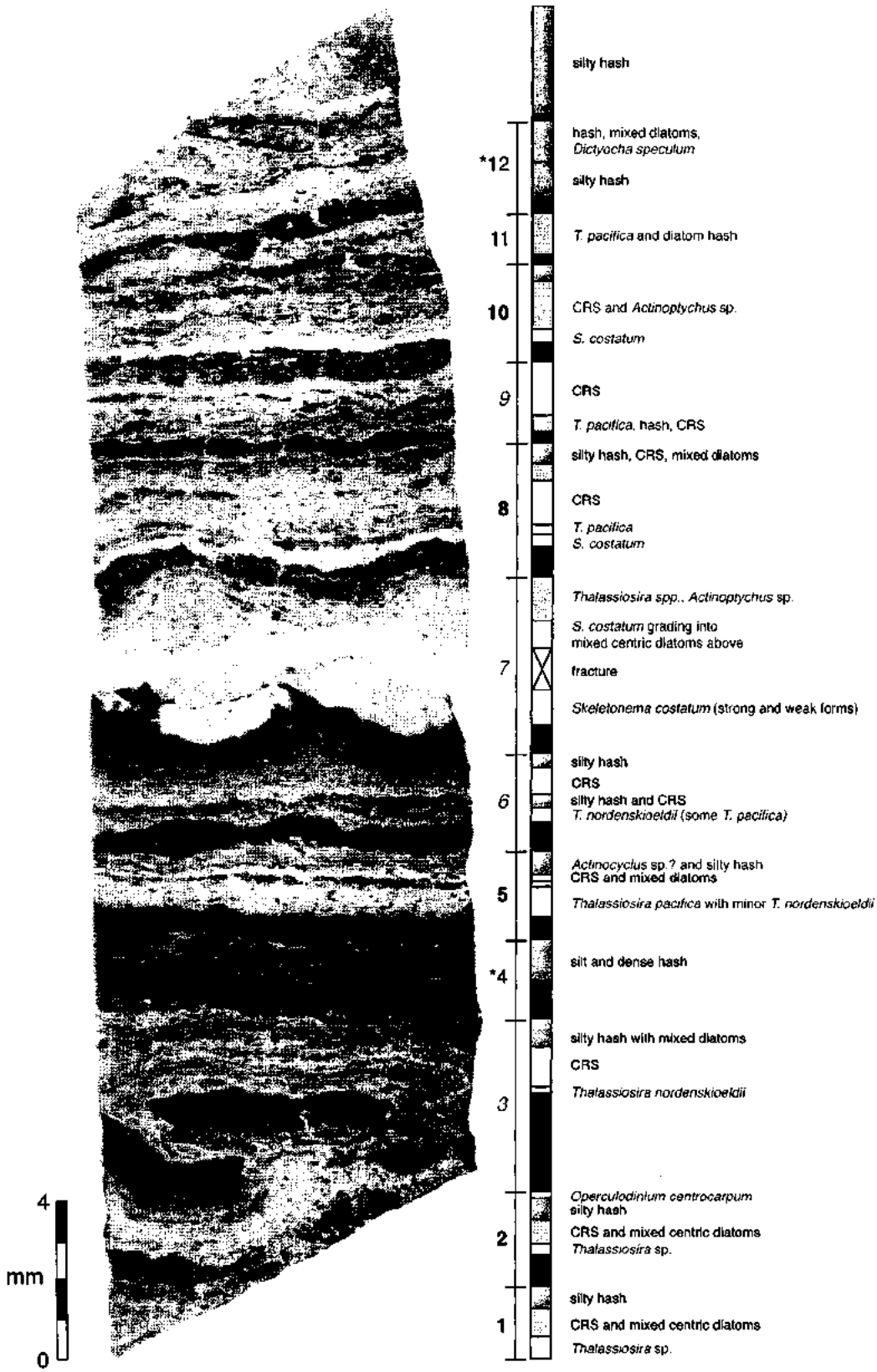
silty hash
hash, mixed diatoms,
Dictyocha speculum
*12
silty hash
11
T. pacifica and diatom hash
10
CRS and Actinoptychus sp.
S. costatum
9
CRS
T. pacifica, hash, CRS
silty hash, CRS, mixed diatoms
8
CRS
T. pacifica
S. costatum
Thalassiosira spp., Actinoptychus sp.
S. costatum grading into
mixed centric diatoms above
7
fracture
Skeletonema costatum (strong and weak forms)
silty hash
CRS
6
silty hash and CRS
T. nordenskioeldii (some T. pacifica)
Actinocyclus sp.? and silty hash
CRS and mixed diatoms
5
Thalassiosira pacifica with minor T. nordenskioeldii
*4
silt and dense hash
silty hash with mixed diatoms
CRS
3
Thalassiosira nordenskioeldii
Operculodinium centrocarpum
silty hash
2
CRS and mixed centric diatoms
Thalassiosira sp.
silty hash
1
CRS and mixed centric diatoms
Thalassiosira sp.
4
mm
0

Slide 4C

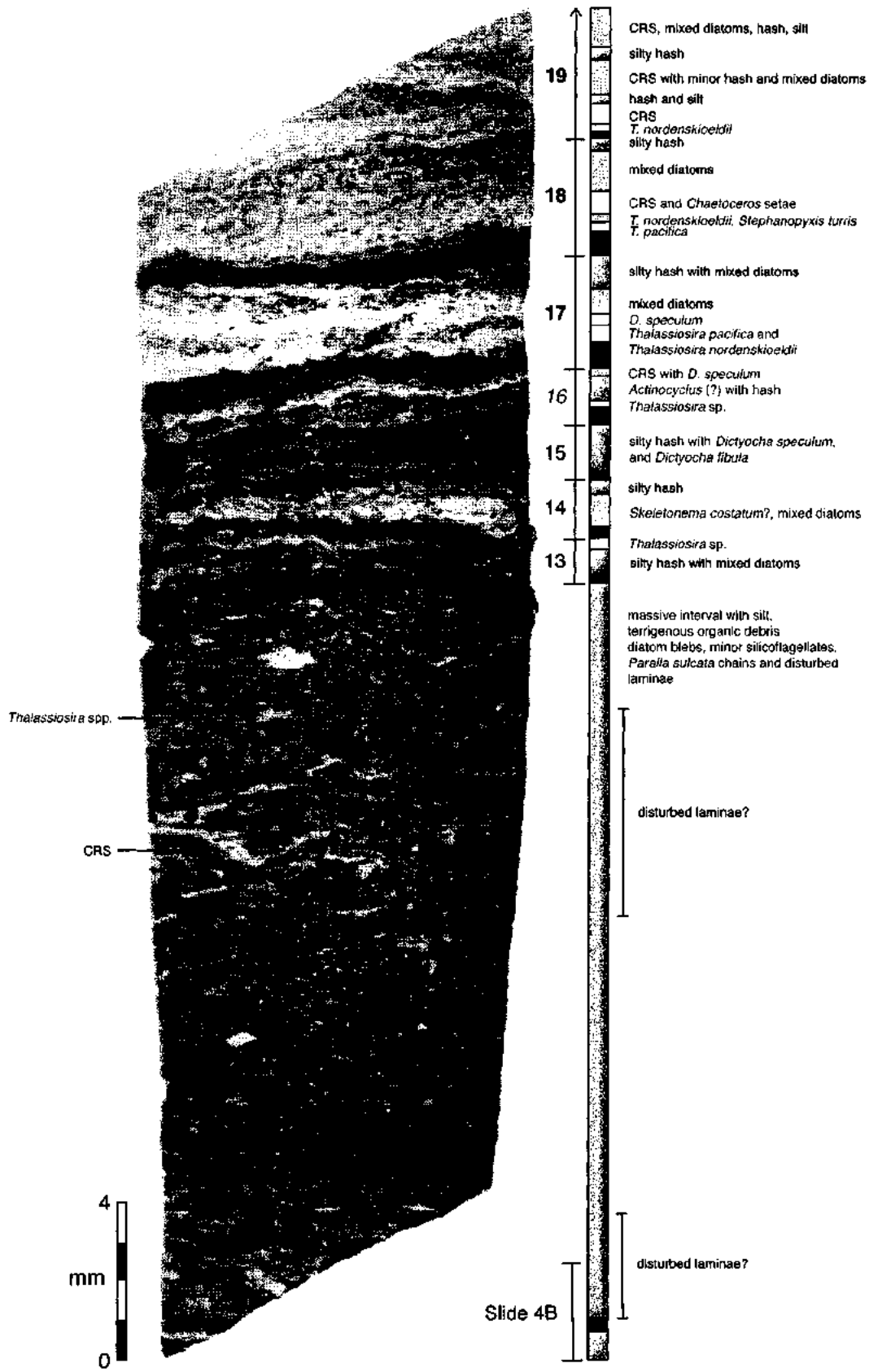
CRS, mixed diatoms, hash, silt
silty hash
19
CRS with minor hash and mixed diatoms
hash and silt
CRS
T. nordenskioeldii
silty hash
mixed diatoms
18
CRS and Chaetoceros setae
T. nordenskioeldii, Stephanopyxis turris
T. pacifica
silty hash with mixed diatoms
mixed diatoms
17
D. speculum
Thalassiosira pacifica and
Thalassiosira nordenskioeldii
CRS with D. speculum
16
Actinocyclus (?) with hash
Thalassiosira sp.
silty hash with Dictyocha speculum,
15
and Dictyocha fibula
silty hash
14
Skeletonema costatum?, mixed diatoms
Thalassiosira sp.
13
silty hash with mixed diatoms
massive interval with silt,
terrigenous organic debris
diatom blebs, minor silicoflagellates,
Paralia sulcata chains and disturbed
laminae
Thalassiosira spp.
disturbed laminae?
CRS
4
mm
0
disturbed laminae?
Slide 4B

Slide 4D

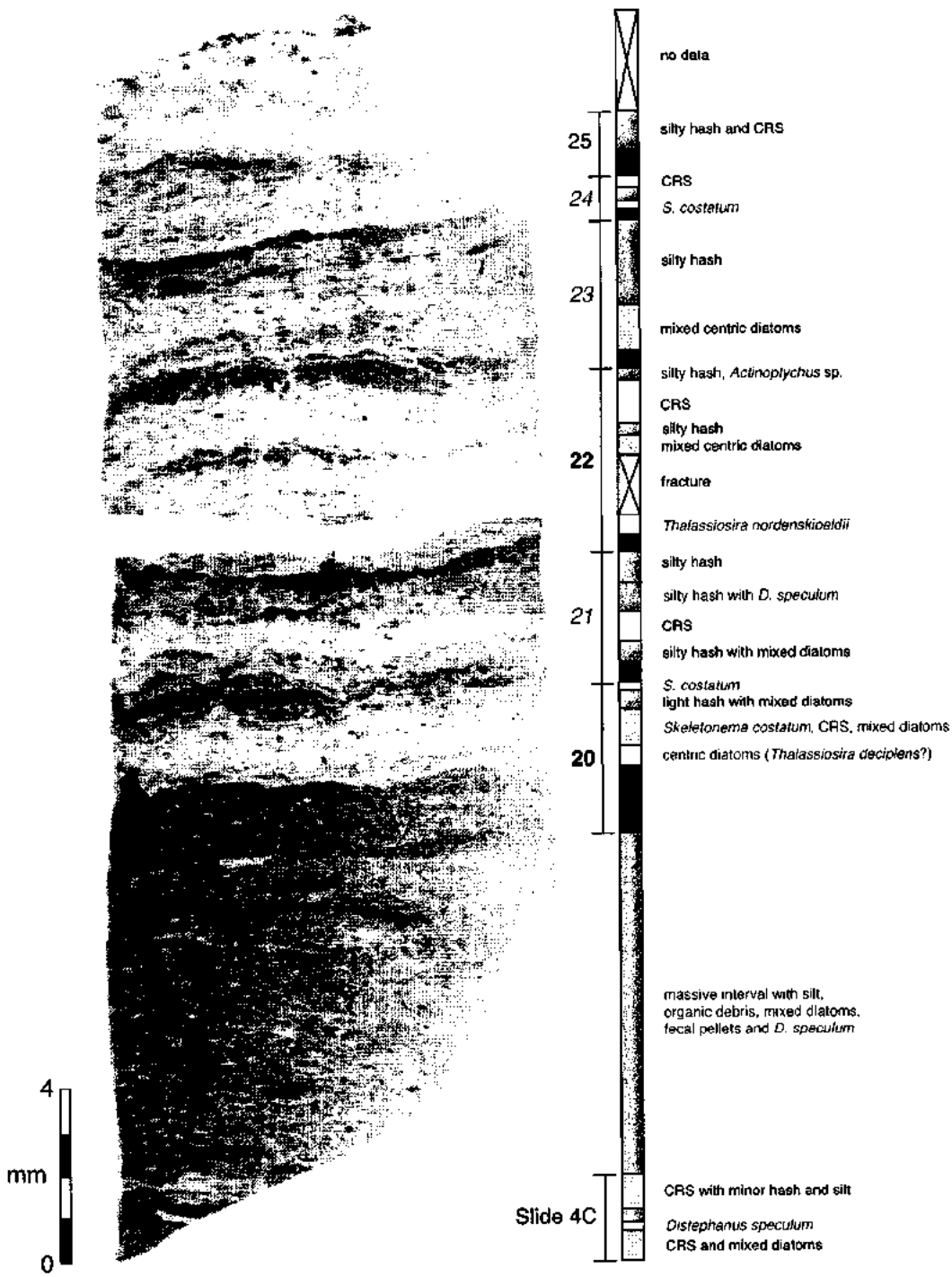
no data
25
silty hash and CRS
CRS
24
S. costatum
silty hash
23
mixed centric diatoms
silty hash, Actinoptychus sp.
CRS
silty hash
mixed centric diatoms
22
fracture
Thalassiosira nordenskioeldii
silty hash
silty hash with D. speculum
21
CRS
silty hash with mixed diatoms
S. costatum
light hash with mixed diatoms
Skeletonema costatum, CRS, mixed diatoms
20
centric diatoms (Thalassiosira deciplens?)
massive interval with silt,
organic debris, mixed diatoms,
fecal pellets and D. speculum
CRS with minor hash and silt
Slide 4C
Distephanus speculum
CRS and mixed diatoms
4
mm
0

Slide 4E

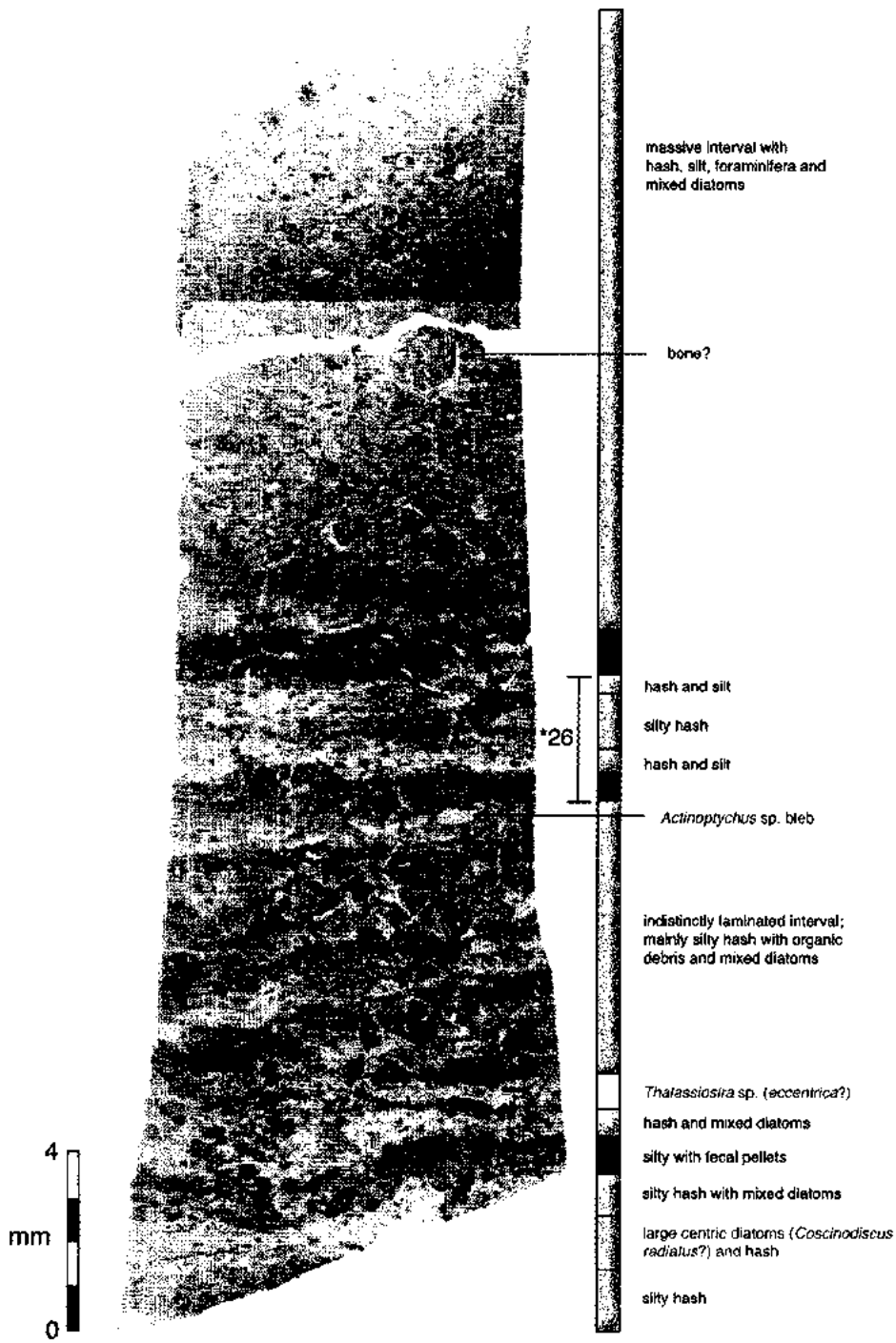
massive interval with hash, silt, foraminifera and mixed diatoms
bone?
hash and silt
silty hash
hash and silt
*26
Actinoptychus sp. bleb
indistinctly laminated interval; mainly silty hash with organic debris and mixed diatoms
Thalassiosira sp. (eccentrica?)
hash and mixed diatoms
silty with fecal pellets
silty hash with mixed diatoms
large centric diatoms (Coscinodiscus radiatus?) and hash
silty hash
4
mm
0

Slide 5A

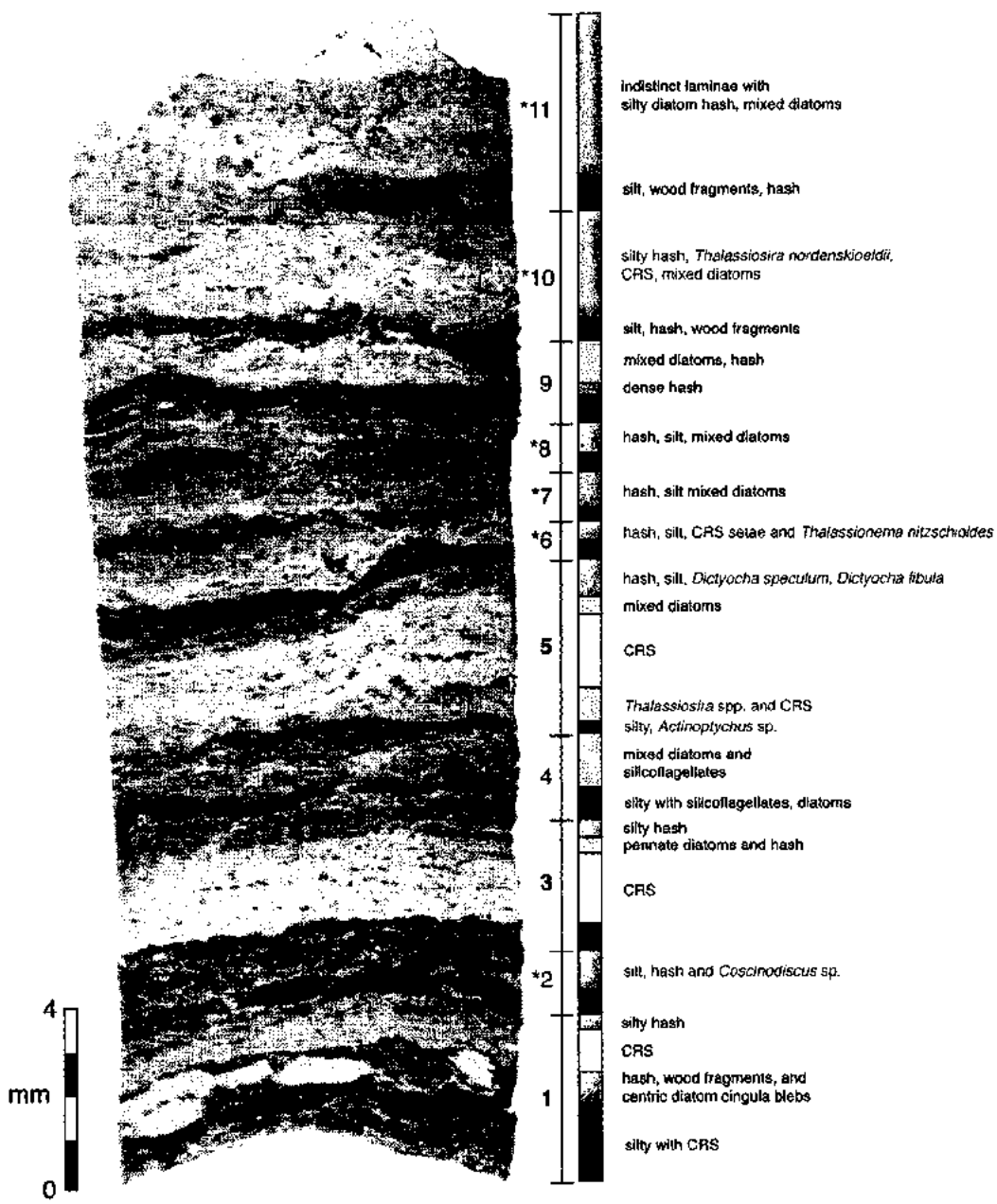
*11
indistinct laminae with
silty diatom hash, mixed diatoms
silt, wood fragments, hash
*10
silty hash, Thalassiosira nordenskioeldii,
CRS, mixed diatoms
silt, hash, wood fragments
mixed diatoms, hash
9
dense hash
*8
hash, silt, mixed diatoms
*7
hash, silt mixed diatoms
*6
hash, silt, CRS setae and Thalassionema nitzschioides
hash, silt, Dictyocha speculum, Dictyocha fibula
mixed diatoms
5
CRS
Thalassiosira spp. and CRS
silty, Actinoptychus sp.
mixed diatoms and
silicoflagellates
4
silty with silicoflagellates, diatoms
silty hash
pennate diatoms and hash
3
CRS
*2
silt, hash and Coscinodiscus sp.
silty hash
CRS
hash, wood fragments, and
centric diatom cingula blebs
1
silty with CRS
4
mm
0

Slide 5B

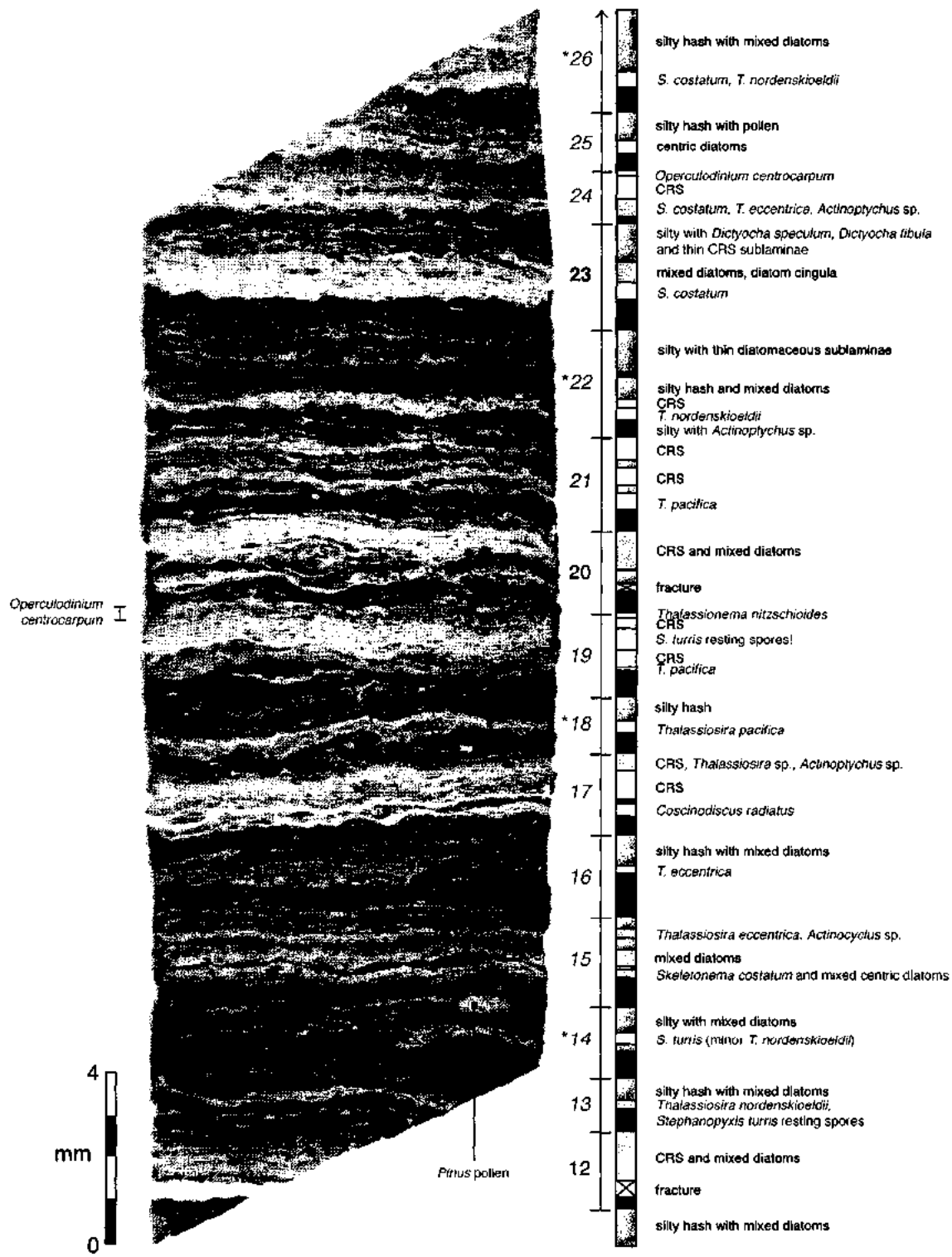
*26
silty hash with mixed diatoms
S. costatum, T. nordenskioeldii
25
silty hash with pollen
centric diatoms
Operculodinium centrocarpum
24
CRS
S. costatum, T. eccentrica, Actinoptychus sp.
silty with Dictyocha speculum, Dictyocha fibula and thin CRS sublaminae
23
mixed diatoms, diatom cingula
S. costatum
silty with thin diatomaceous sublaminae
*22
silty hash and mixed diatoms
CRS
T. nordenskioeldii
silty with Actinoptychus sp.
CRS
21
CRS
T. pacifica
CRS and mixed diatoms
20
fracture
Thalassionema nitzschioides
CRS
S. turris resting spores!
19
CRS
T. pacifica
silty hash
*18
Thalassiosira pacifica
CRS, Thalassiosira sp., Actinoptychus sp.
17
CRS
Coscinodiscus radiatus
silty hash with mixed diatoms
16
T. eccentrica
Thalassiosira eccentrica, Actinocyclus sp.
15
mixed diatoms
Skeletonema costatum and mixed centric diatoms
silty with mixed diatoms
*14
S. turris (minor T. nordenskioeldii)
silty hash with mixed diatoms
13
Thalassiosira nordenskioeldii,
Stephanopyxis turris resting spores
CRS and mixed diatoms
12
fracture
silty hash with mixed diatoms
Operculodinium centrocarpum
Pinus pollen
4
mm
0

Slide 5C

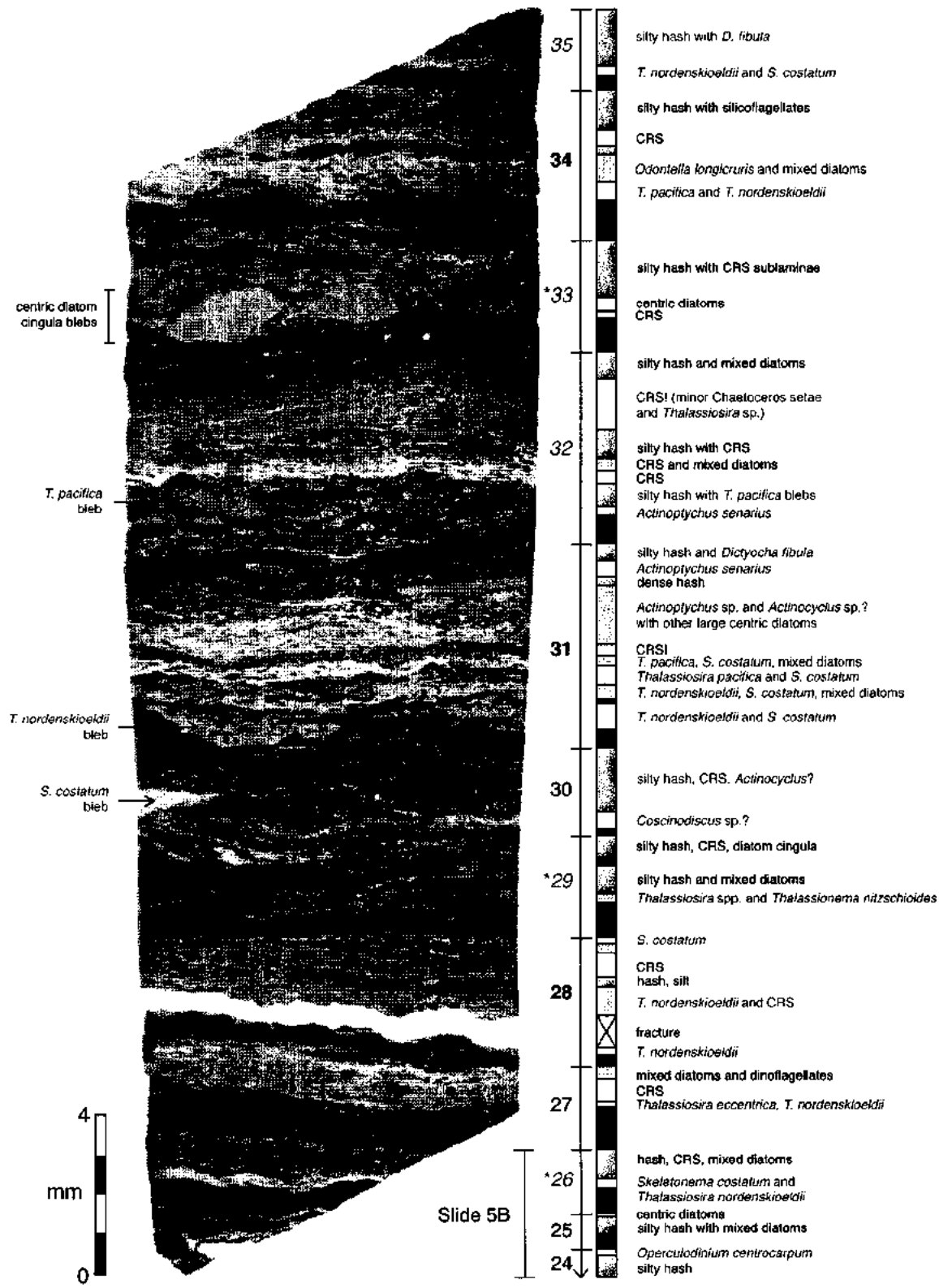
centric diatom cingula blebs
T. pacifica bleb
T. nordenskioeldii bleb
S. costatum bleb
4
mm
0
Slide 5B
35
34
*33
32
31
30
*29
28
27
*26
25
24
silty hash with D. fibula
T. nordenskioeldii and S. costatum
silty hash with silicoflagellates
CRS
Odontella longicruris and mixed diatoms
T. pacifica and T. nordenskioeldii
silty hash with CRS sublaminae
centric diatoms
CRS
silty hash and mixed diatoms
CRS! (minor Chaetoceros setae and Thalassiosira sp.)
silty hash with CRS
CRS and mixed diatoms
CRS
silty hash with T. pacifica blebs
Actinoptychus senarius
silty hash and Dictyocha fibula
Actinoptychus senarius
dense hash
Actinoptychus sp. and Actinocyclus sp.? with other large centric diatoms
CRS!
T. pacifica, S. costatum, mixed diatoms
Thalassiosira pacifica and S. costatum
T. nordenskioeldii, S. costatum, mixed diatoms
T. nordenskioeldii and S. costatum
silty hash, CRS. Actinocyclus?
Coscinodiscus sp.?
silty hash, CRS, diatom cingula
silty hash and mixed diatoms
Thalassiosira spp. and Thalassionema nitzschioides
S. costatum
CRS
hash, silt
T. nordenskioeldii and CRS
fracture
T. nordenskioeldii
mixed diatoms and dinoflagellates
CRS
Thalassiosira eccentrica, T. nordenskioeldii
hash, CRS, mixed diatoms
Skeletonema costatum and Thalassiosira nordenskioeldii
centric diatoms
silty hash with mixed diatoms
Operculodinium centrocarpum
silty hash

Slide 5D

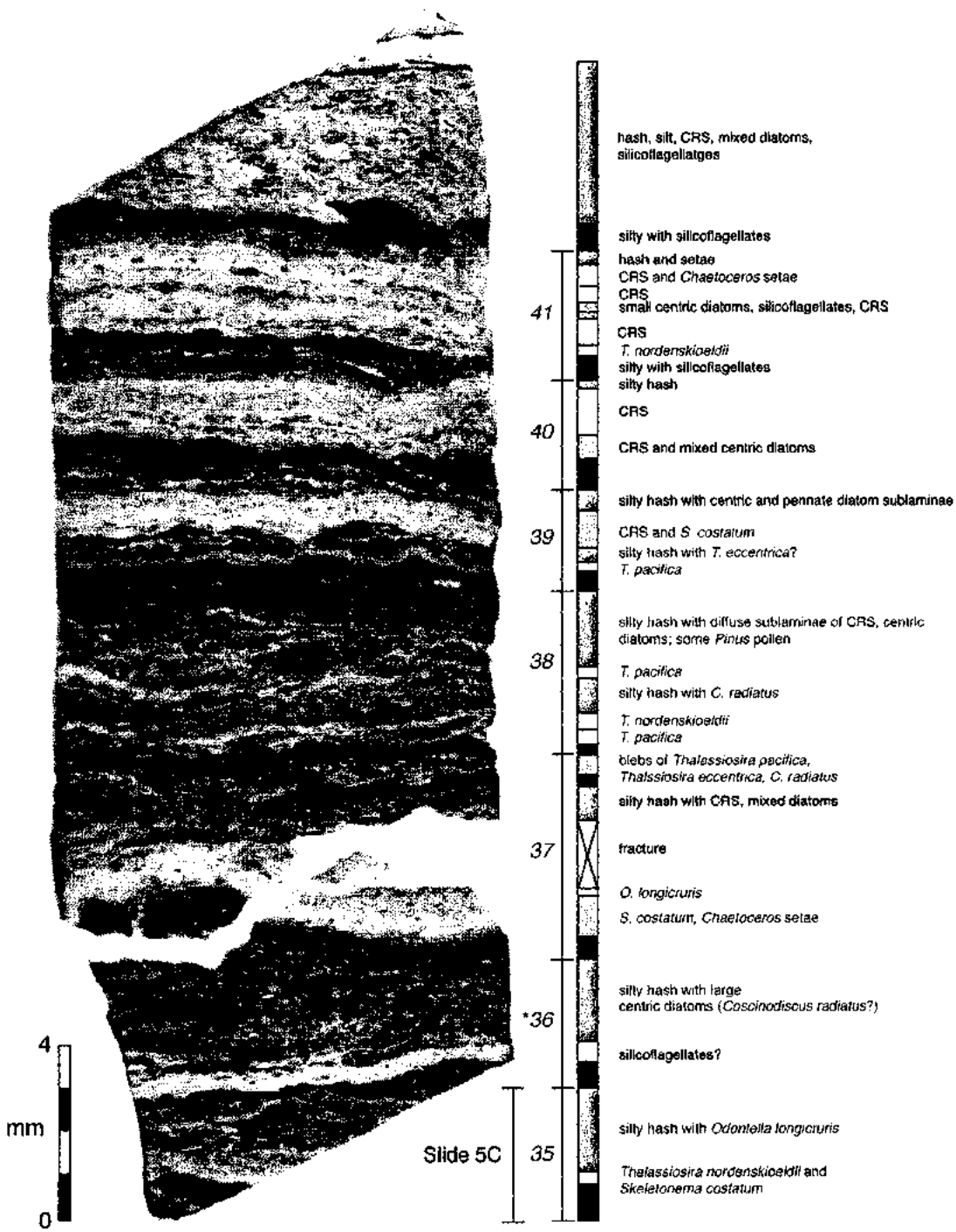
4
mm
0
Slide 5C
41
40
39
38
37
*36
35
hash, silt, CRS, mixed diatoms, silicoflagellatges
silty with silicoflagellates
hash and setae
CRS and Chaetoceros setae
CRS
small centric diatoms, silicoflagellates, CRS
CRS
T. nordenskioeldii
silty with silicoflagellates
silty hash
CRS
CRS and mixed centric diatoms
silty hash with centric and pennate diatom sublaminae
CRS and S. costatum
silty hash with T. eccentrica?
T. pacifica
silty hash with diffuse sublaminae of CRS, centric diatoms; some Pinus pollen
T. pacifica
silty hash with C. radiatus
T. nordenskioeldii
T. pacifica
blebs of Thalassiosira pacifica, Thalssiosira eccentrica, C. radiatus
silty hash with CRS, mixed diatoms
fracture
O. longicruris
S. costatum, Chaetoceros setae
silty hash with large centric diatoms (Coscinodiscus radiatus?)
silicoflagellates?
silty hash with Odontella longicruris
Thalassiosira nordenskioeldii and Skeletonema costatum

Slide 5E

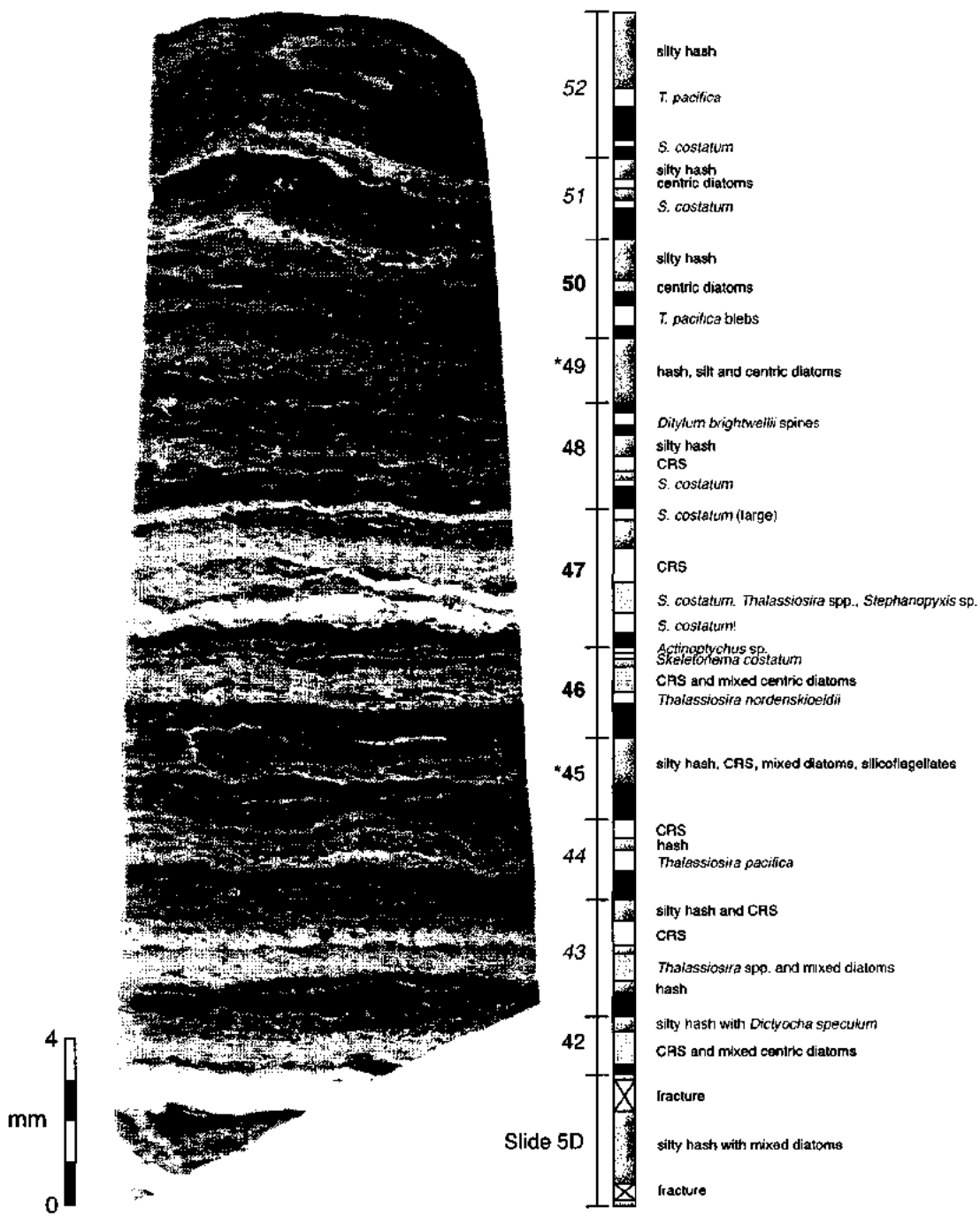
4
mm
0
Slide 5D
52
51
50
*49
48
47
46
*45
44
43
42
silty hash
T. pacifica
S. costatum
silty hash
centric diatoms
S. costatum
silty hash
centric diatoms
T. pacifica blebs
hash, silt and centric diatoms
Ditylum brightwellii spines
silty hash
CRS
S. costatum
S. costatum (large)
CRS
S. costatum, Thalassiosira spp., Stephanopyxis sp.
S. costatum!
Actinoptychus sp.
Skeletonema costatum
CRS and mixed centric diatoms
Thalassiosira nordenskioeldii
silty hash, CRS, mixed diatoms, silicoflagellates
CRS
hash
Thalassiosira pacifica
silty hash and CRS
CRS
Thalassiosira spp. and mixed diatoms
hash
silty hash with Dictyocha speculum
CRS and mixed centric diatoms
fracture
silty hash with mixed diatoms
fracture

Slide 6A

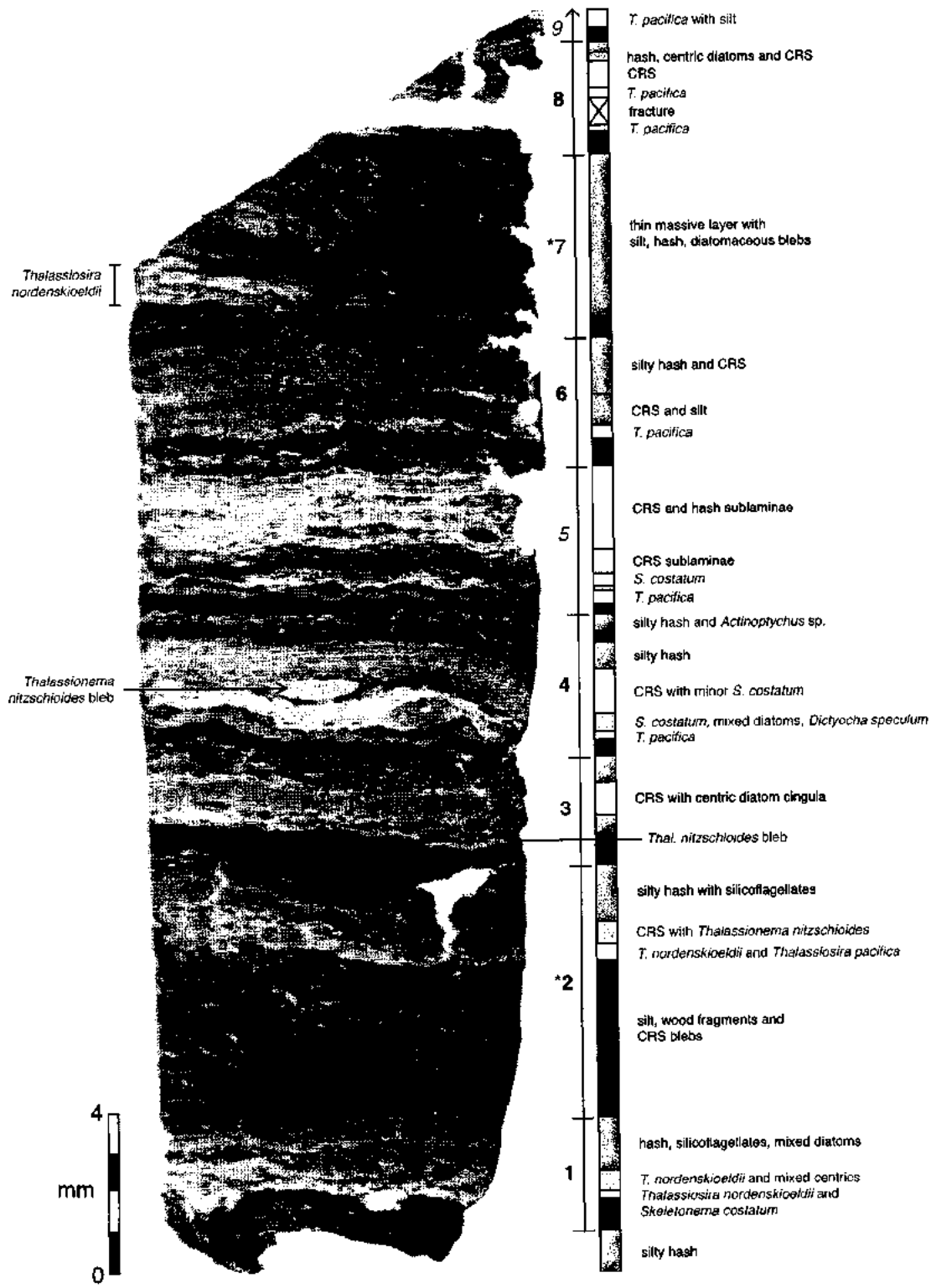
Thalassiosira nordenskioeldii
Thalassionema nitzschioides bleb
4
mm
0
9
8
*7
6
5
4
3
*2
1
T. pacifica with silt
hash, centric diatoms and CRS
CRS
T. pacifica
fracture
T. pacifica
thin massive layer with silt, hash, diatomaceous blebs
silty hash and CRS
CRS and silt
T. pacifica
CRS and hash sublaminae
CRS sublaminae
S. costatum
T. pacifica
silty hash and Actinoptychus sp.
silty hash
CRS with minor S. costatum
S. costatum, mixed diatoms, Dictyocha speculum
T. pacifica
CRS with centric diatom cingula
Thal. nitzschioides bleb
silty hash with silicoflagellates
CRS with Thalassionema nitzschioides
T. nordenskioeldii and Thalassiosira pacifica
silt, wood fragments and CRS blebs
hash, silicoflagellates, mixed diatoms
T. nordenskioeldii and mixed centrics
Thalassiosira nordenskioeldii and Skeletonema costatum
silty hash

Slide 6B

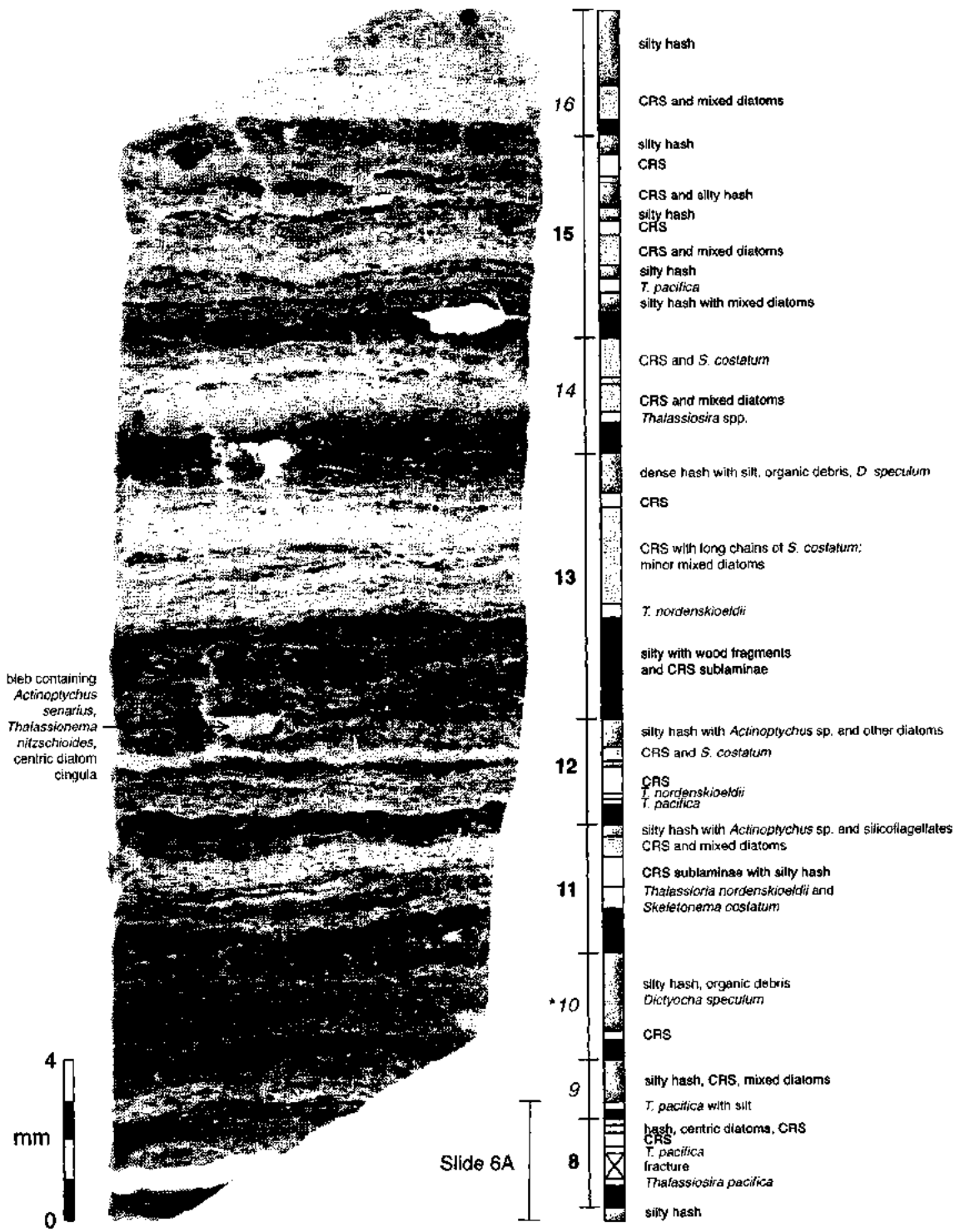
silty hash
16
CRS and mixed diatoms
silty hash
CRS
CRS and silty hash
silty hash
CRS
15
CRS and mixed diatoms
silty hash
T. pacifica
silty hash with mixed diatoms
CRS and S. costatum
14
CRS and mixed diatoms
Thalassiosira spp.
dense hash with silt, organic debris, D. speculum
CRS
CRS with long chains of S. costatum;
minor mixed diatoms
13
T. nordenskioeldii
silty with wood fragments
and CRS sublaminae
bleb containing
Actinoptychus
senarius,
Thalassionema
nitzschioides,
centric diatom
cingula
silty hash with Actinoptychus sp. and other diatoms
CRS and S. costatum
12
CRS
T. nordenskioeldii
T. pacifica
silty hash with Actinoptychus sp. and silicoflagellates
CRS and mixed diatoms
CRS sublaminae with silty hash
11
Thalassiothrix nordenskioeldii and
Skeletonema costatum
silty hash, organic debris
*10
Dictyocha speculum
CRS
silty hash, CRS, mixed diatoms
9
T. pacifica with silt
hash, centric diatoms, CRS
CRS
T. pacifica
8
fracture
Thalassiosira pacifica
silty hash
Slide 6A
4
mm
0

Slide 6C

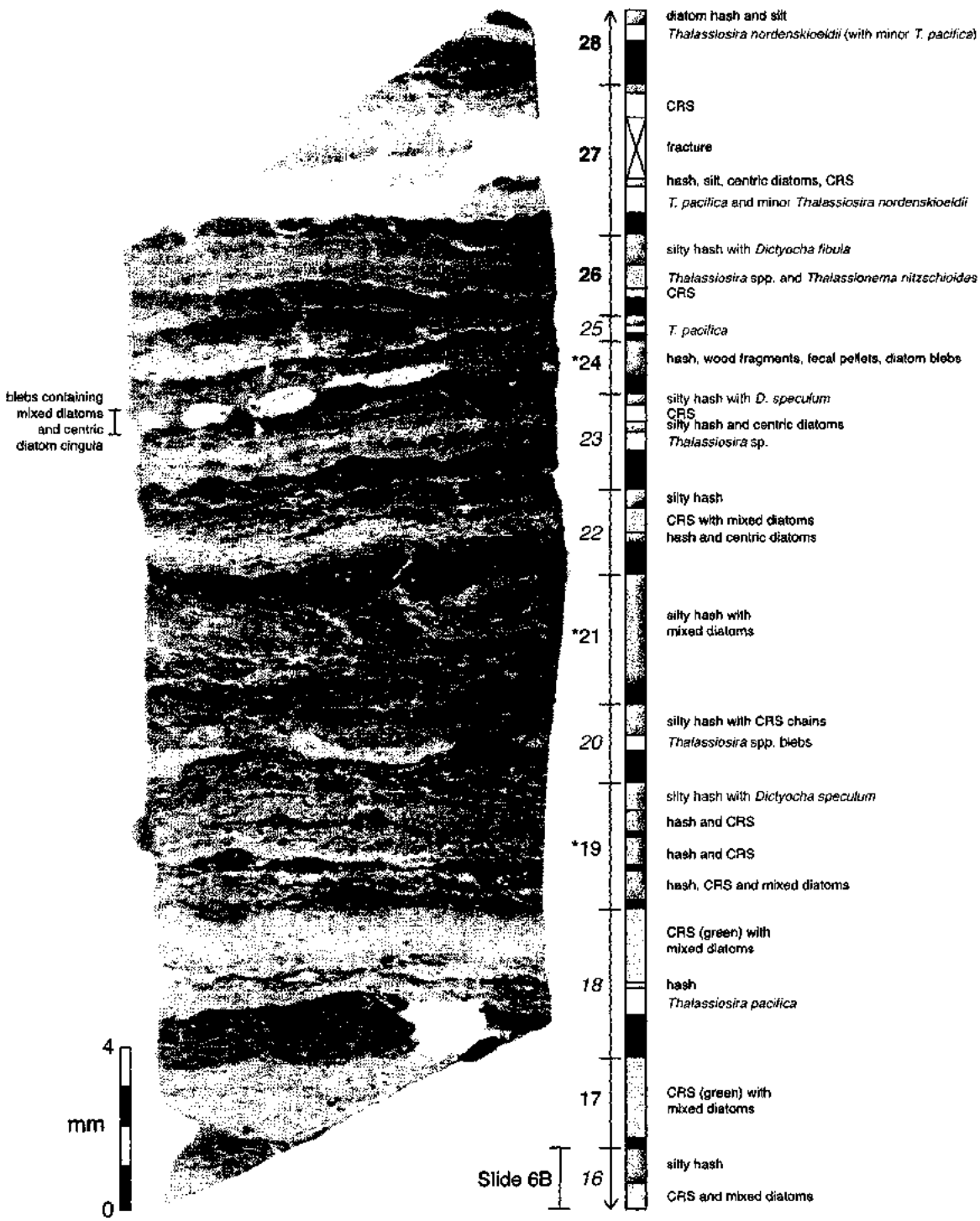
blebs containing mixed diatoms and centric diatom cingula
4
mm
0
Slide 6B
28
27
26
25
*24
23
22
*21
20
*19
18
17
16
diatom hash and silt
Thalassiosira nordenskioeldii (with minor T. pacifica)
CRS
fracture
hash, silt, centric diatoms, CRS
T. pacifica and minor Thalassiosira nordenskioeldii
silty hash with Dictyocha fibula
Thalassiosira spp. and Thalassionema nitzschioides
CRS
T. pacifica
hash, wood fragments, fecal pellets, diatom blebs
silty hash with D. speculum
CRS
silty hash and centric diatoms
Thalassiosira sp.
silty hash
CRS with mixed diatoms
hash and centric diatoms
silty hash with
mixed diatoms
silty hash with CRS chains
Thalassiosira spp. blebs
silty hash with Dictyocha speculum
hash and CRS
hash and CRS
hash, CRS and mixed diatoms
CRS (green) with
mixed diatoms
hash
Thalassiosira pacifica
CRS (green) with
mixed diatoms
silty hash
CRS and mixed diatoms

Slide 6D

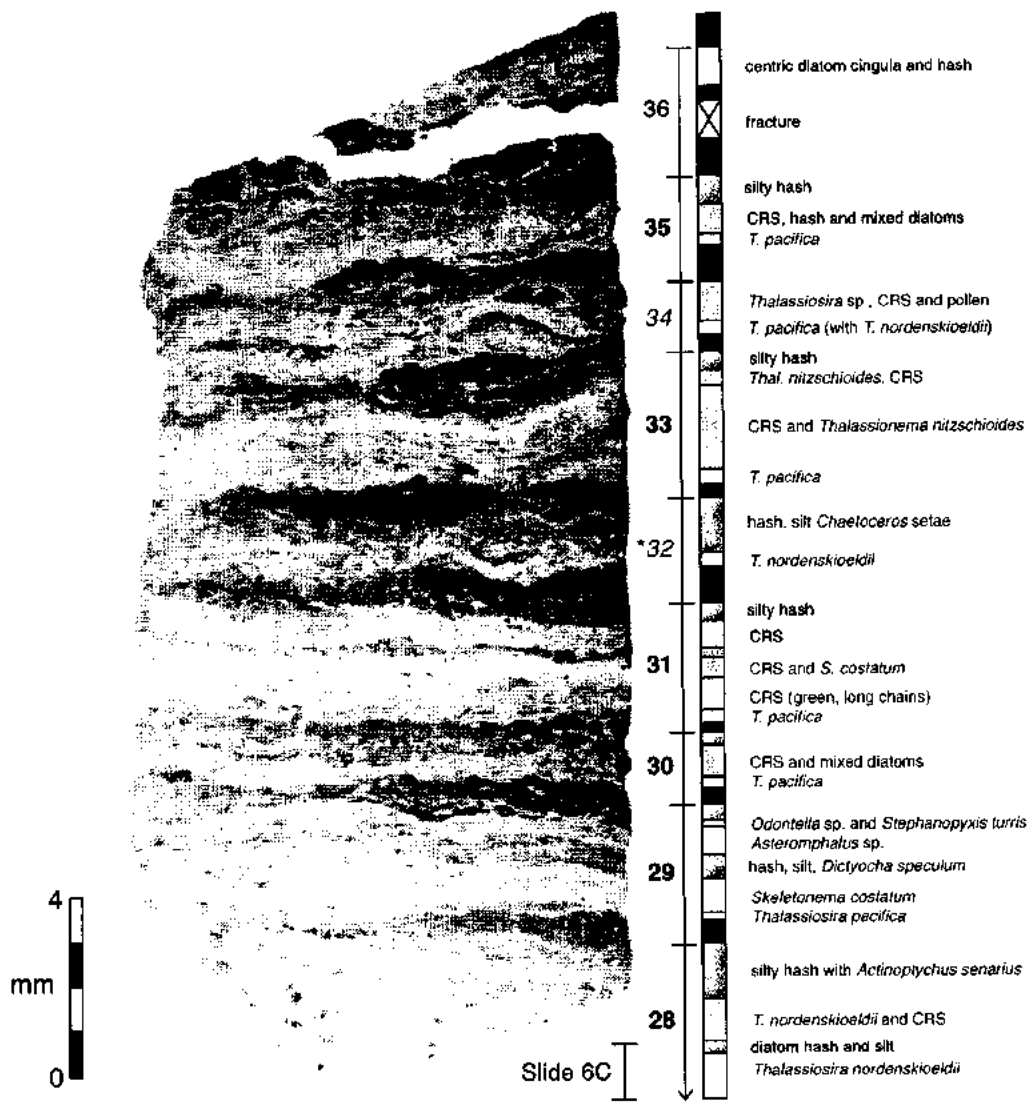
centric diatom cingula and hash
36
fracture
silty hash
CRS, hash and mixed diatoms
T. pacifica
35
Thalassiosira sp., CRS and pollen
34
T. pacifica (with T. nordenskioeldii)
silty hash
Thal. nitzschioides, CRS
33
CRS and Thalassionema nitzschioides
T. pacifica
hash, silt Chaetoceros setae
*32
T. nordenskioeldii
silty hash
CRS
31
CRS and S. costatum
CRS (green, long chains)
T. pacifica
30
CRS and mixed diatoms
T. pacifica
Odontella sp. and Stephanopyxis turris
Asteromphalus sp.
29
hash, silt, Dictyocha speculum
Skeletonema costatum
Thalassiosira pacifica
silty hash with Actinoptychus senarius
28
T. nordenskioeldii and CRS
diatom hash and silt
Thalassiosira nordenskioeldii
Slide 6C
4
mm
0

Slide 6E

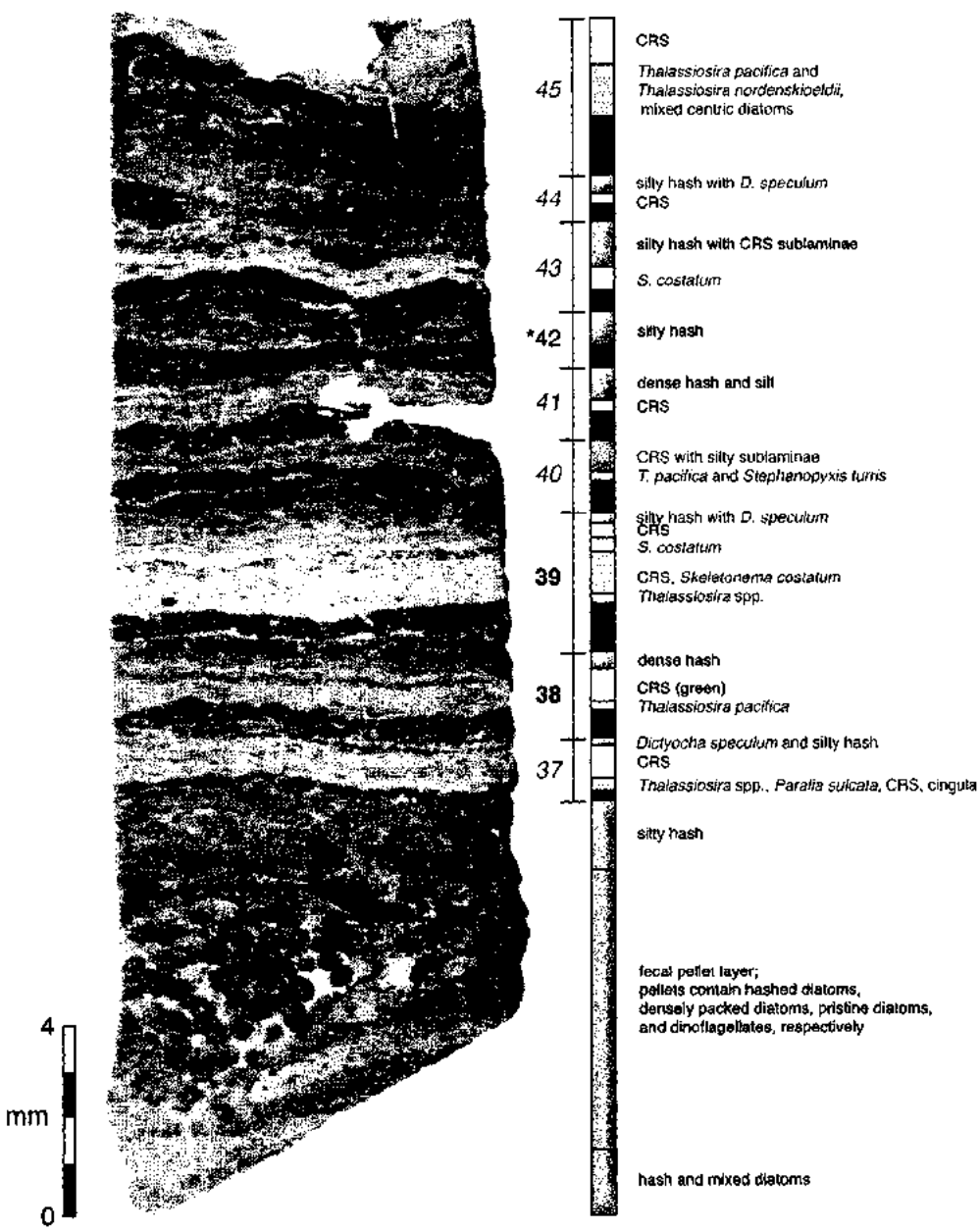
CRS
Thalassiosira pacifica and
Thalassiosira nordenskioeldii,
mixed centric diatoms
45
silty hash with D. speculum
CRS
44
silty hash with CRS sublaminae
S. costatum
43
silty hash
*42
dense hash and silt
CRS
41
CRS with silty sublaminae
T. pacifica and Stephanopyxis turris
40
silty hash with D. speculum
CRS
S. costatum
CRS, Skeletonema costatum
Thalassiosira spp.
39
dense hash
CRS (green)
Thalassiosira pacifica
38
Dictyocha speculum and silty hash
CRS
Thalassiosira spp., Paralia sulcata, CRS, cingula
37
silty hash
fecal pellet layer;
pellets contain hashed diatoms,
densely packed diatoms, pristine diatoms,
and dinoflagellates, respectively
hash and mixed diatoms
4
mm
0

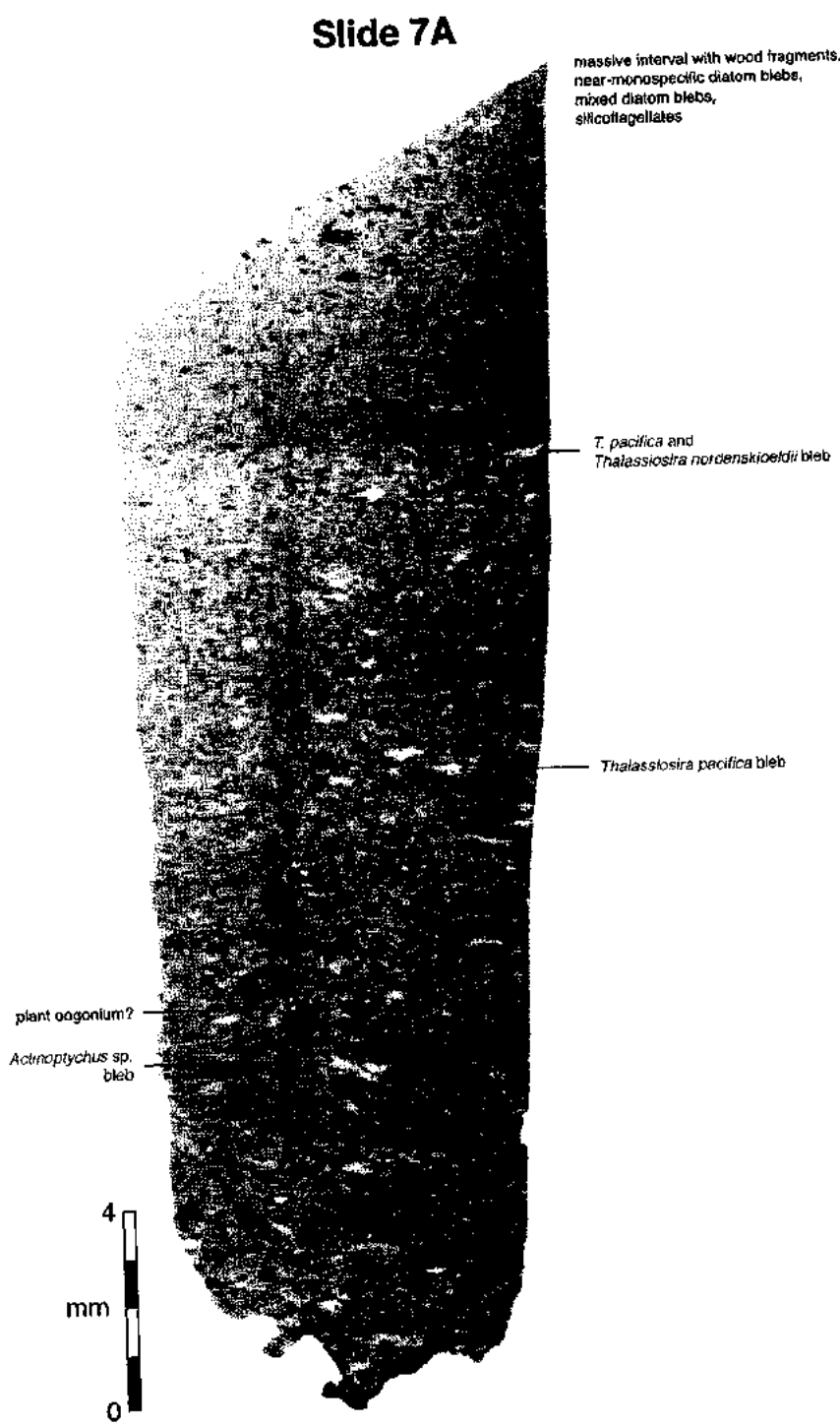
Slide 7A
massive interval with wood fragments,
near-monospecific diatom blebs,
mixed diatom blebs,
silicoflagellates
T. pacifica and
Thalassiosira nordenskioeldii bleb
Thalassiosira pacifica bleb
plant oogonium?
Actinoptychus sp.
bleb
4
mm
0

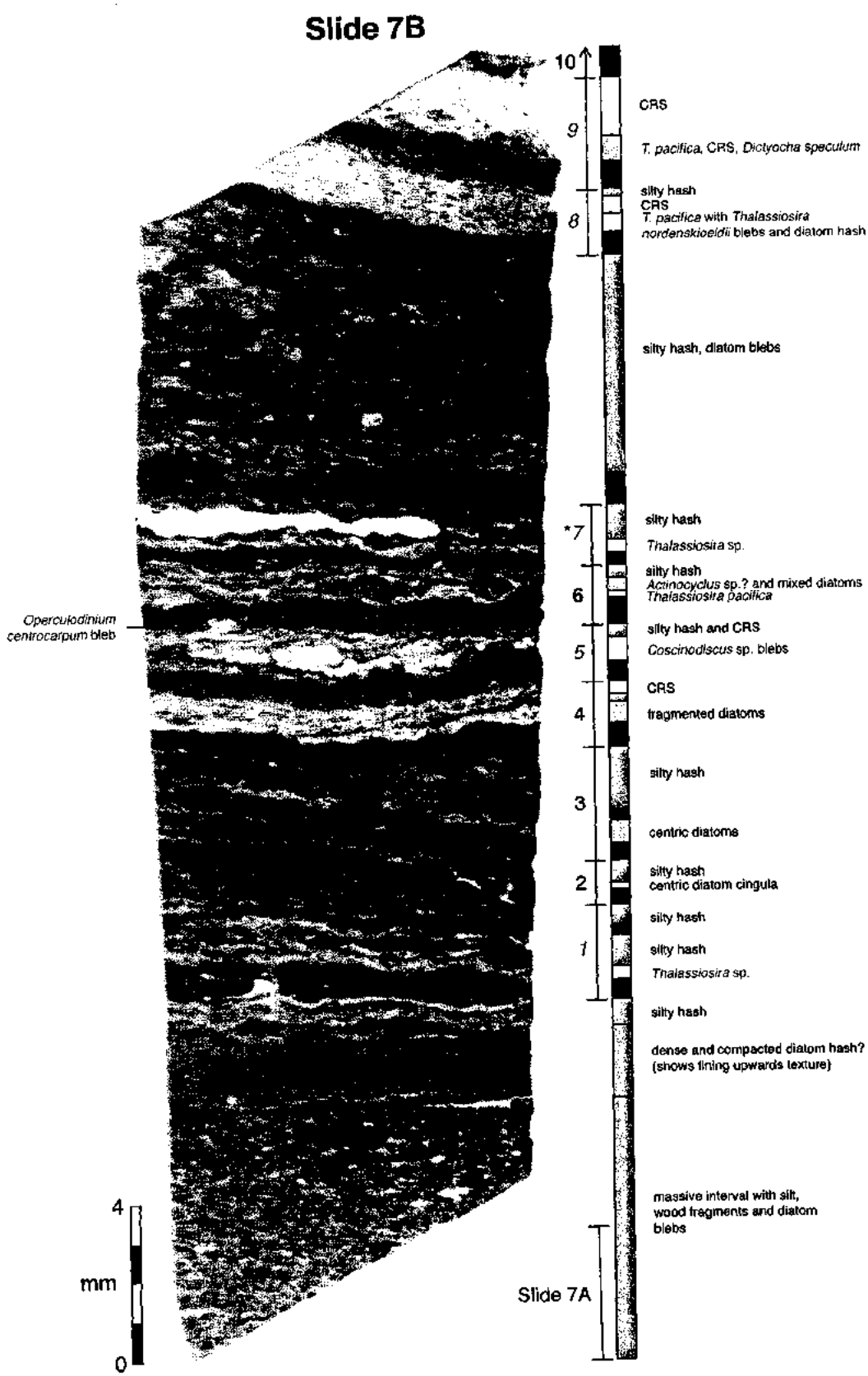
Slide 7B
10
9
8
*7
6
5
4
3
2
1
CRS
T. pacifica, CRS, Dictyocha speculum
silty hash
CRS
T. pacifica with Thalassiosira nordenskioeldii blebs and diatom hash
silty hash, diatom blebs
silty hash
Thalassiosira sp.
silty hash
Actinocyclus sp.? and mixed diatoms
Thalassiosira pacifica
silty hash and CRS
Coscinodiscus sp. blebs
CRS
fragmented diatoms
silty hash
centric diatoms
silty hash
centric diatom cingula
silty hash
silty hash
Thalassiosira sp.
silty hash
dense and compacted diatom hash?
(shows fining upwards texture)
massive interval with silt,
wood fragments and diatom
blebs
Operculodinium centrocarpum bleb
4
mm
0
Slide 7A

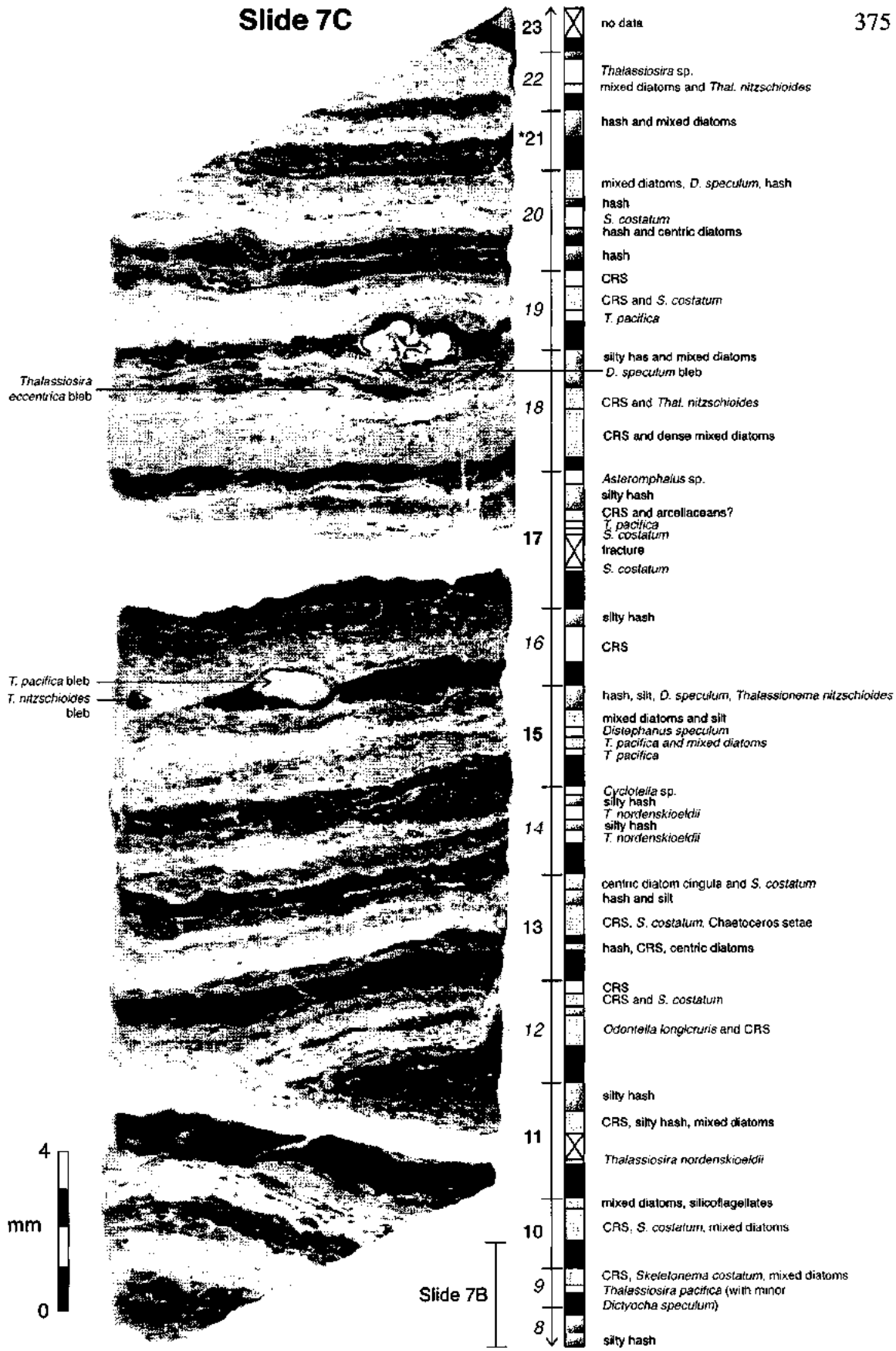
Slide 7C
Thalassiosira eccentrica bleb
T. pacifica bleb
T. nitzschioides bleb
4
mm
0
Slide 7B
23
22
*21
20
19
18
17
16
15
14
13
12
11
10
9
8
no data
Thalassiosira sp.
mixed diatoms and Thal. nitzschioides
hash and mixed diatoms
mixed diatoms, D. speculum, hash
hash
S. costatum
hash and centric diatoms
hash
CRS
CRS and S. costatum
T. pacifica
silty has and mixed diatoms
D. speculum bleb
CRS and Thal. nitzschioides
CRS and dense mixed diatoms
Asteromphalus sp.
silty hash
CRS and arcellaceans?
T. pacifica
S. costatum
fracture
S. costatum
silty hash
CRS
hash, silt, D. speculum, Thalassionema nitzschioides
mixed diatoms and silt
Distephanus speculum
T. pacifica and mixed diatoms
T. pacifica
Cyclotella sp.
silty hash
T. nordenskioeldii
silty hash
T. nordenskioeldii
centric diatom cingula and S. costatum
hash and silt
CRS, S. costatum, Chaetoceros setae
hash, CRS, centric diatoms
CRS
CRS and S. costatum
Odontella longicruris and CRS
silty hash
CRS, silty hash, mixed diatoms
Thalassiosira nordenskioeldii
mixed diatoms, silicoflagellates
CRS, S. costatum, mixed diatoms
CRS, Skeletonema costatum, mixed diatoms
Thalassiosira pacifica (with minor
Dictyocha speculum)
silty hash

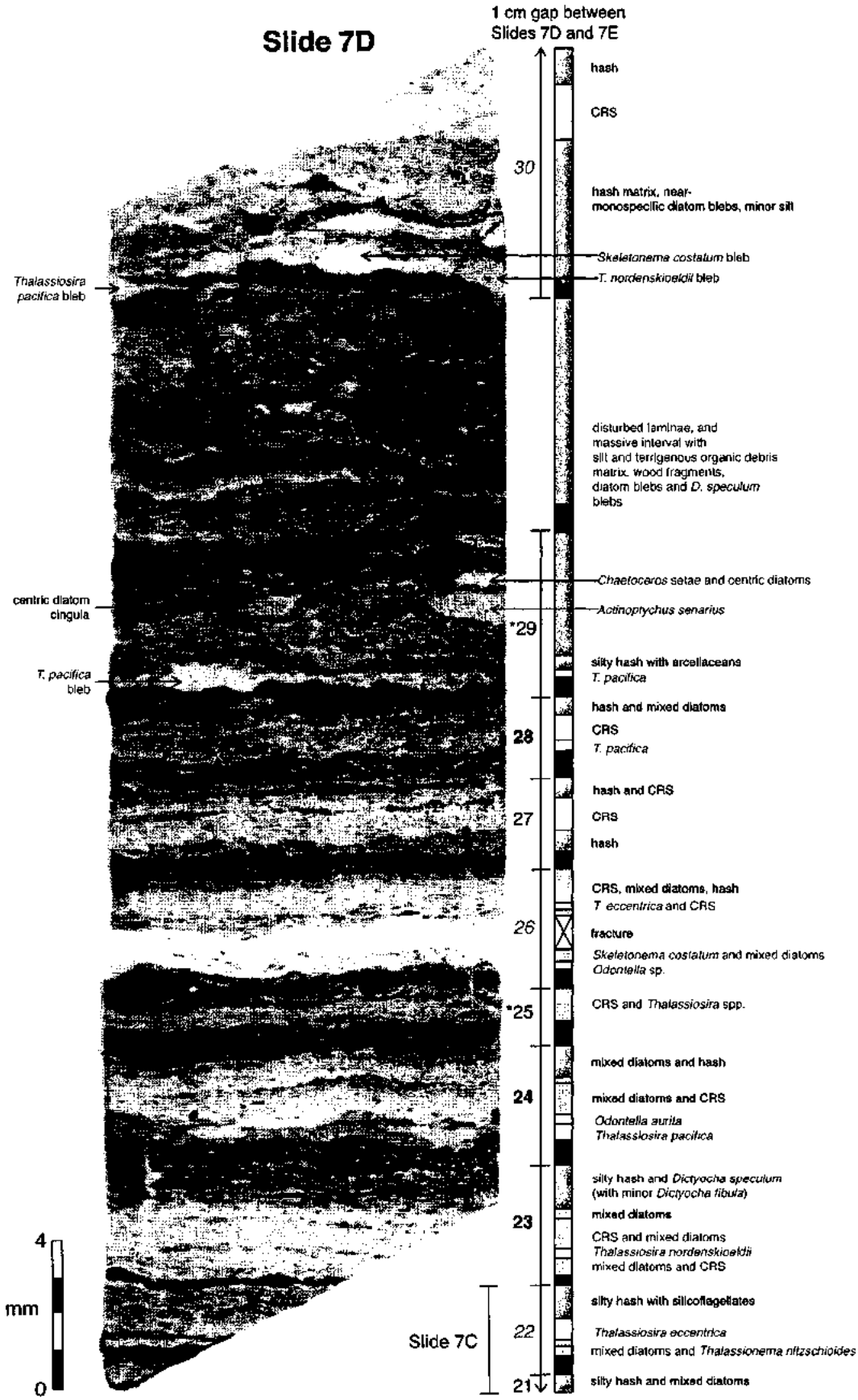
Slide 7D
1 cm gap between
Slides 7D and 7E
hash
CRS
30
hash matrix, near-
monospecific diatom blebs, minor silt
Skeletonema costatum bleb
T. nordenskioeldii bleb
Thalassiosira
pacifica bleb
disturbed laminae, and
massive interval with
silt and terrigenous organic debris
matrix, wood fragments,
diatom blebs and D. speculum
blebs
Chaetoceros setae and centric diatoms
centric diatom
cingula
Actinoptychus senarius
*29
silty hash with arcellaceans
T. pacifica
T. pacifica
bleb
hash and mixed diatoms
CRS
28
T. pacifica
hash and CRS
CRS
27
hash
CRS, mixed diatoms, hash
T. eccentrica and CRS
26
fracture
Skeletonema costatum and mixed diatoms
Odontella sp.
*25
CRS and Thalassiosira spp.
mixed diatoms and hash
24
mixed diatoms and CRS
Odontella aurita
Thalassiosira pacifica
silty hash and Dictyocha speculum
(with minor Dictyocha fibula)
mixed diatoms
23
CRS and mixed diatoms
Thalassiosira nordenskioeldii
mixed diatoms and CRS
silty hash with silicoflagellates
Slide 7C
22
Thalassiosira eccentrica
mixed diatoms and Thalassionema nitzschioides
21
silty hash and mixed diatoms
4
mm
0

Slide 7E

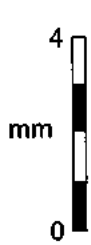

44
T. nordenskioeldii

Octactis octonaria
hash and mixed diatoms

43
CRS, hash, *Chaetoceros* setae, *O. longicruris*

CRS

Dictyocha speculum, *Thal. nitzschioides*, hash
Operculodinium centrocarpum

42
CRS and *S. costatum*
S. costatum
T. nordenskioeldii
CRS
T. pacifica

CRS
41
S. costatum

S. costatum
CRS and *Chaetoceros* setae
silty hash, silicoflagellates, mixed diatoms

40
CRS, *Ditylum brightwellii* spines, *Odontella longicurris*

T. pacifica
S. costatum
hash, CRS

39
CRS and hash
T. pacifica

silty hash with mixed diatoms

38
CRS and mixed diatoms
T. pacifica

CRS and mixed diatoms

37
T. pacifica (minor *T. nordenskioeldii*)

*36
silty hash with *Actinoptychus* sp.
and silicoflagellates

T. nordenskioeldii and CRS
silty hash with mixed diatoms

CRS, *Actinoptychus* sp., mixed diatoms

35
S. costatum
T. pacifica
fracture
Thalassioira pacifica

Actinoptychus sp., *Thalassionema nitzschioides*, hash
34
CRS and *Thalassiosira nordenskioeldii*
mixed diatoms

silty hash with *Asteromphalus* sp.

CRS
33
S. costatum, CRS, hash

Thalassiosira eccentrica with minor hash

CRS

silty hash with mixed diatoms

32
CRS, *S. costatum*

Skeletonema costatum

CRS
31
CRS and *Chaetoceros* setae
Stephanopyxis sp. and mixed diatoms

1 cm gap between
Slides 7D and 7E

Slide 7F

mixed diatom and hash

CRS and silty hash

CRS, *Chaetoceros* setae

CRS, mixed diatoms, hash

53

CRS

O. longicruris

CRS, *Thalassiosira* sp. sublaminae

CRS

52

dense CRS

T. pacifica

CRS

graded bed with wood fragments at base; matrix organic and silty with mixed diatoms, CRS, *Chaetoceros* setae, *Thalassiosira* sp. blebs

silty hash

Skeletonema costatum

51

CRS, *S. costatum*, *Thal. nitzschioides*

mixed diatoms, CRS, hash

T. eccentrica, CRS, hash

CRS, *Thalassiosira eccentrica*

S. costatum, CRS

50

Thalassiosira spp., *Ditylum brightwellii* spines, *Chaetoceros* setae

T. pacifica

silty hash with large centric diatoms

49

Thal. nitzschioides, mixed diatoms

CRS

hash, silt, CRS, *Thalassionema nitzschioides*, mixed diatoms

S. costatum

hash

48

hash and *Octactis octonaria*

CRS, *Skeletonema costatum*, centric diatoms

CRS, *Chaetoceros* setae

T. pacifica (?) and hash

setae, hash, CRS, 6-spine silicoflagellates

hash and silt

47

Thalassiosira spp., CRS

CRS

Thalassiosira pacifica

hash, mixed diatoms, *Dictyocha speculum*

46

CRS, *Odontella longicruris*

T. nordenskioeldii

CRS and hash

CRS

45

T. nordenskioeldii

setae, mixed diatoms, CRS, hash, silt

44

Thalassiosira nordenskioeldii

Slide 8A

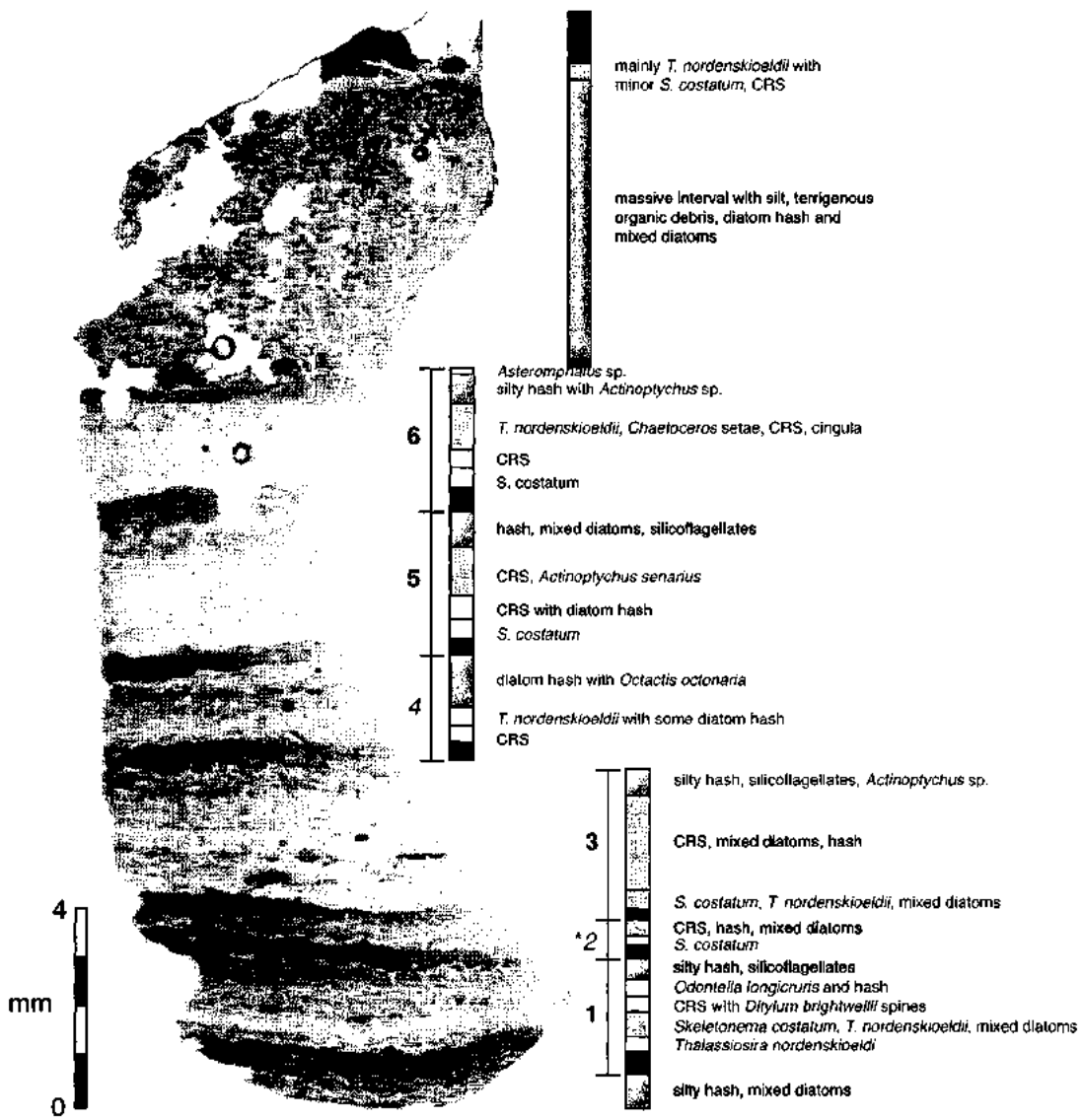
mainly T. nordenskioeldii with minor S. costatum, CRS
massive interval with silt, terrigenous organic debris, diatom hash and mixed diatoms
Asteromphalus sp.
silty hash with Actinoptychus sp.
6
T. nordenskioeldii, Chaetoceros setae, CRS, cingula
CRS
S. costatum
hash, mixed diatoms, silicoflagellates
5
CRS, Actinoptychus senarius
CRS with diatom hash
S. costatum
diatom hash with Octactis octonaria
4
T. nordenskioeldii with some diatom hash
CRS
silty hash, silicoflagellates, Actinoptychus sp.
3
CRS, mixed diatoms, hash
S. costatum, T. nordenskioeldii, mixed diatoms
CRS, hash, mixed diatoms
*2
S. costatum
silty hash, silicoflagellates
Odontella longicruris and hash
CRS with Ditylum brightwellii spines
1
Skeletonema costatum, T. nordenskioeldii, mixed diatoms
Thalassiosira nordenskioeldi
silty hash, mixed diatoms
4
mm
0

Slide 8B

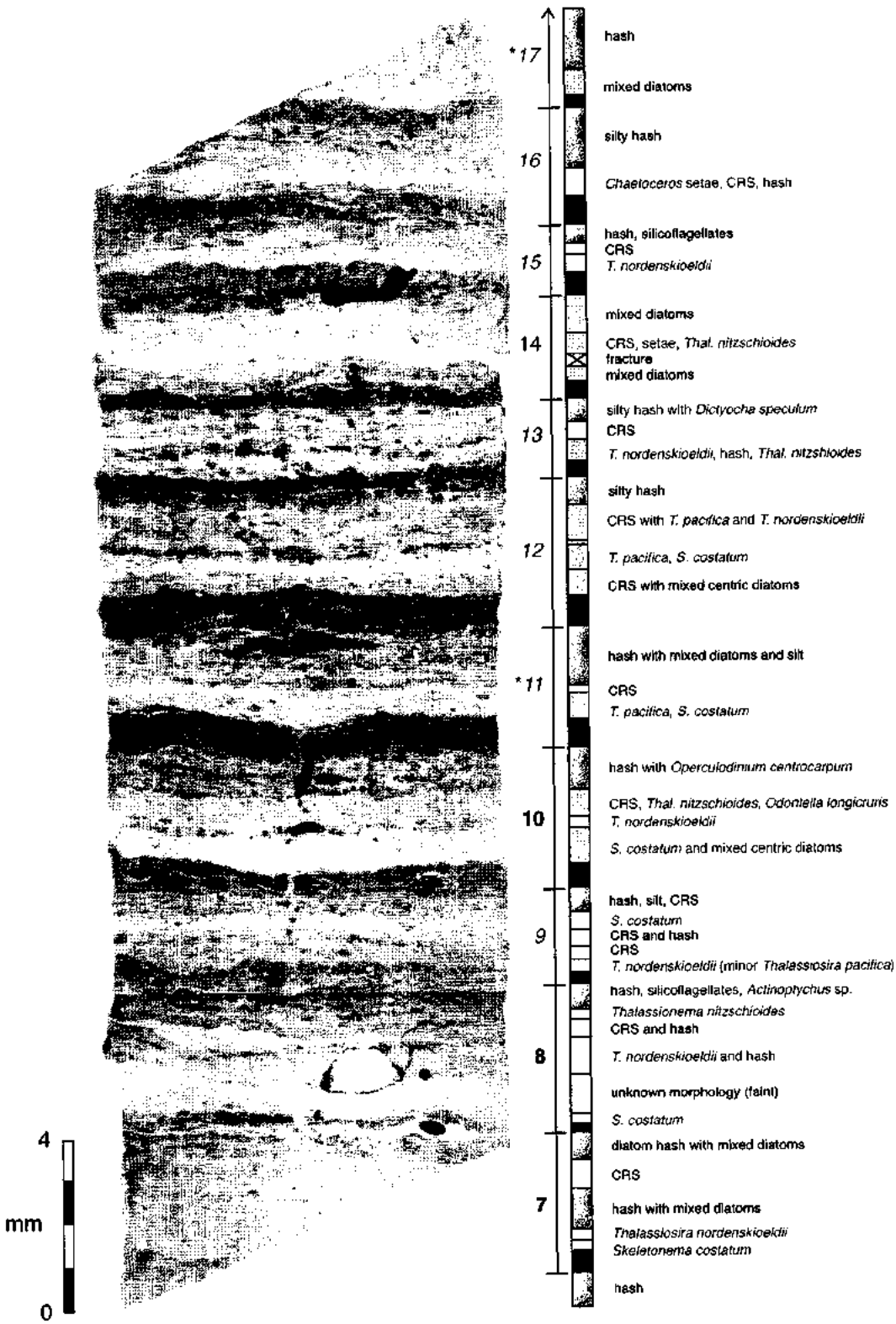
*17
hash
mixed diatoms
16
silty hash
Chaetoceros setae, CRS, hash
15
hash, silicoflagellates
CRS
T. nordenskioeldii
14
mixed diatoms
CRS, setae, Thal. nitzschioides
fracture
mixed diatoms
13
silty hash with Dictyocha speculum
CRS
T. nordenskioeldii, hash, Thal. nitzshioides
12
silty hash
CRS with T. pacifica and T. nordenskioeldii
T. pacifica, S. costatum
CRS with mixed centric diatoms
*11
hash with mixed diatoms and silt
CRS
T. pacifica, S. costatum
10
hash with Operculodinium centrocarpum
CRS, Thal. nitzschioides, Odontella longicruris
T. nordenskioeldii
S. costatum and mixed centric diatoms
9
hash, silt, CRS
S. costatum
CRS and hash
CRS
T. nordenskioeldii (minor Thalassiosira pacifica)
8
hash, silicoflagellates, Actinoptychus sp.
Thalassionema nitzschioides
CRS and hash
T. nordenskioeldii and hash
unknown morphology (faint)
S. costatum
7
diatom hash with mixed diatoms
CRS
hash with mixed diatoms
Thalassiosira nordenskioeldii
Skeletonema costatum
hash
4
mm
0

Slide 8C

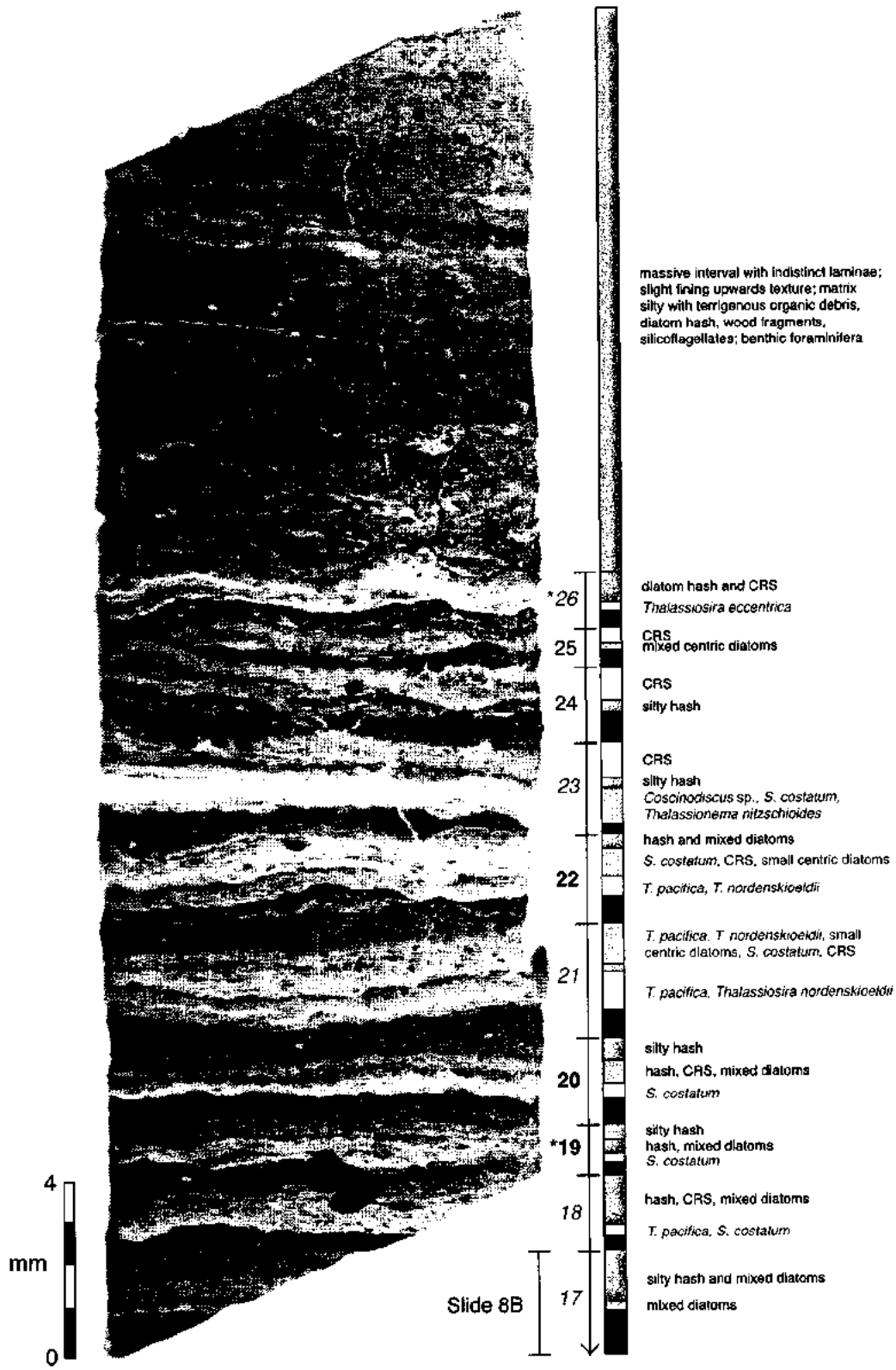
massive interval with indistinct laminae; slight fining upwards texture; matrix silty with terrigenous organic debris, diatom hash, wood fragments, silicoflagellates; benthic foraminifera
*26
diatom hash and CRS
Thalassiosira eccentrica
25
CRS
mixed centric diatoms
24
CRS
silty hash
23
CRS
silty hash
Coscinodiscus sp., S. costatum, Thalassionema nitzschioides
22
hash and mixed diatoms
S. costatum, CRS, small centric diatoms
T. pacifica, T. nordenskioeldii
21
T. pacifica, T. nordenskioeldii, small centric diatoms, S. costatum, CRS
T. pacifica, Thalassiosira nordenskioeldii
20
silty hash
hash, CRS, mixed diatoms
S. costatum
*19
silty hash
hash, mixed diatoms
S. costatum
18
hash, CRS, mixed diatoms
T. pacifica, S. costatum
17
silty hash and mixed diatoms
mixed diatoms
Slide 8B
4
mm
0

Slide 8D

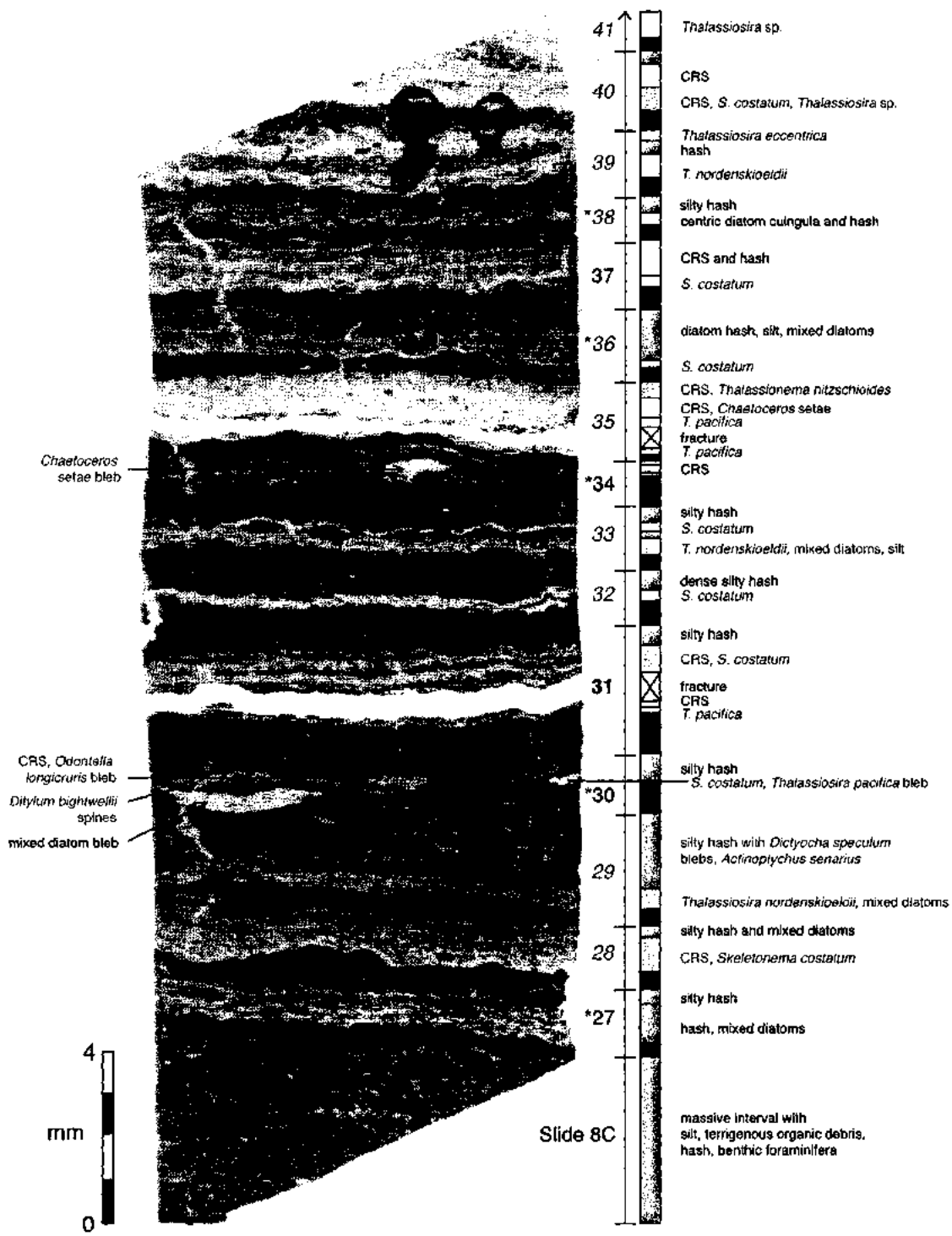
41
Thalassiosira sp.
40
CRS
CRS, S. costatum, Thalassiosira sp.
39
Thalassiosira eccentrica hash
T. nordenskioeldii
*38
silty hash
centric diatom cingula and hash
37
CRS and hash
S. costatum
*36
diatom hash, silt, mixed diatoms
S. costatum
CRS, Thalassionema nitzschioides
35
CRS, Chaetoceros setae
T. pacifica
fracture
T. pacifica
CRS
Chaetoceros setae bleb
*34
silty hash
33
S. costatum
T. nordenskioeldii, mixed diatoms, silt
32
dense silty hash
S. costatum
silty hash
CRS, S. costatum
31
fracture
CRS
T. pacifica
CRS, Odontella longicruris bleb
Dityfum bightwellii spines
mixed diatom bleb
silty hash
S. costatum, Thalassiosira pacifica bleb
*30
silty hash with Dictyocha speculum blebs, Actinoptychus senarius
29
Thalassiosira nordenskioeldii, mixed diatoms
silty hash and mixed diatoms
28
CRS, Skeletonema costatum
silty hash
*27
hash, mixed diatoms
4
mm
0
Slide 8C
massive interval with silt, terrigenous organic debris, hash, benthic foraminifera

Slide 8E

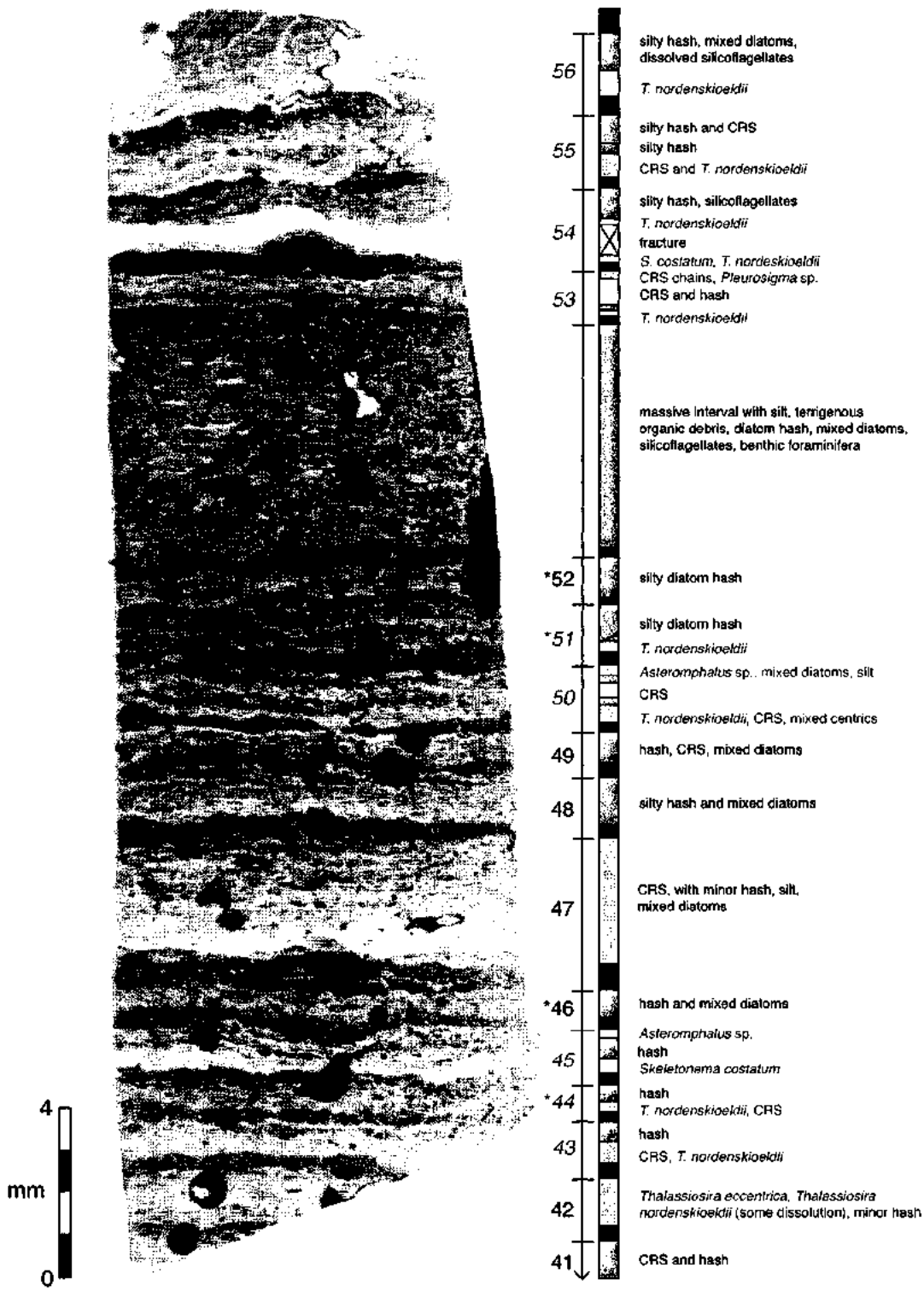
4
mm
0
56
silty hash, mixed diatoms, dissolved silicoflagellates
T. nordenskioeldii
55
silty hash and CRS
silty hash
CRS and T. nordenskioeldii
54
silty hash, silicoflagellates
T. nordenskioeldii
fracture
S. costatum, T. nordeskioeldii
CRS chains, Pleurosigma sp.
53
CRS and hash
T. nordenskioeldii
massive interval with silt, terrigenous organic debris, diatom hash, mixed diatoms, silicoflagellates, benthic foraminifera
*52
silty diatom hash
*51
silty diatom hash
T. nordenskioeldii
Asteromphalus sp., mixed diatoms, silt
50
CRS
T. nordenskioeldii, CRS, mixed centrics
49
hash, CRS, mixed diatoms
48
silty hash and mixed diatoms
47
CRS, with minor hash, silt, mixed diatoms
*46
hash and mixed diatoms
Asteromphalus sp.
45
hash
Skeletonema costatum
*44
hash
T. nordenskioeldii, CRS
43
hash
CRS, T. nordenskioeldii
42
Thalassiosira eccentrica, Thalassiosira nordenskioeldii (some dissolution), minor hash
41
CRS and hash

Slide 9A

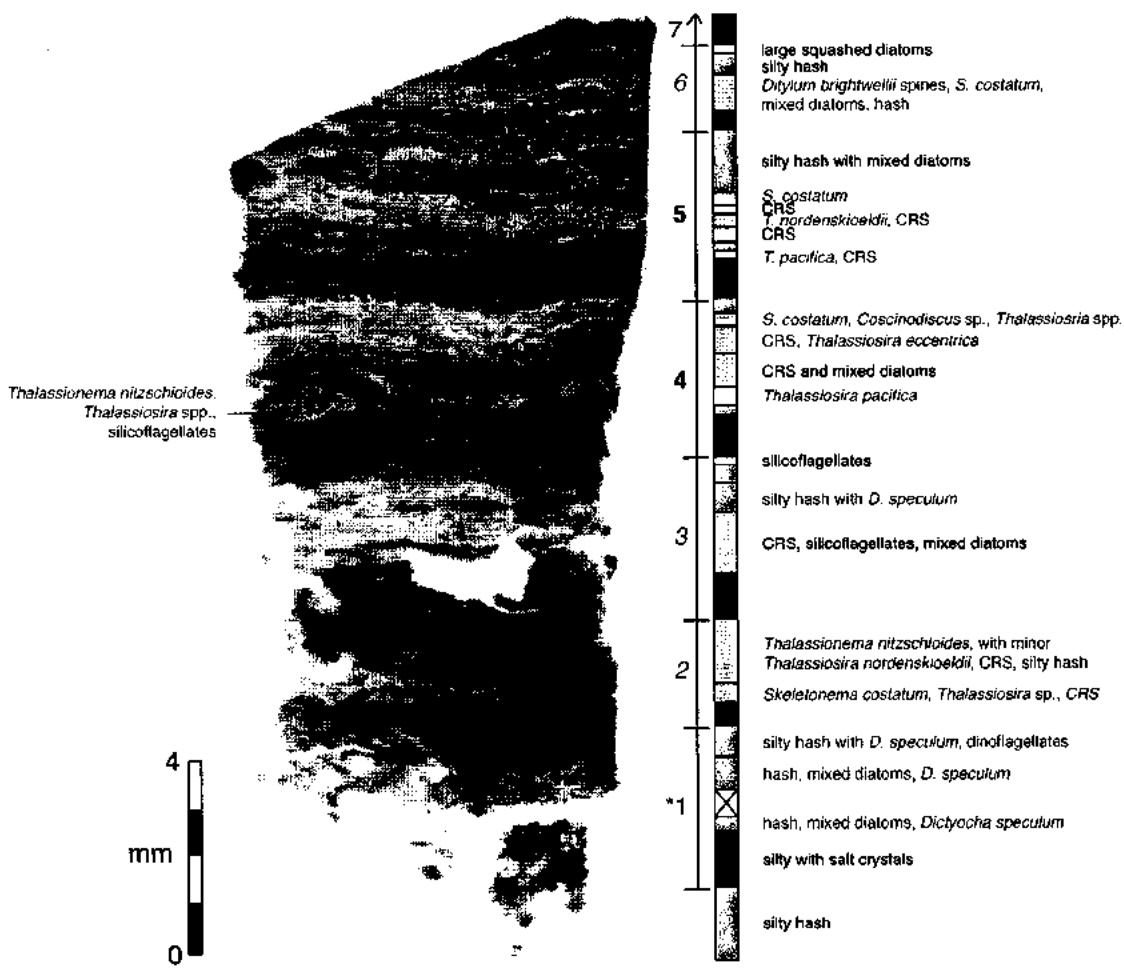

lower 1.05 cm of thin section missing

Slide 9B

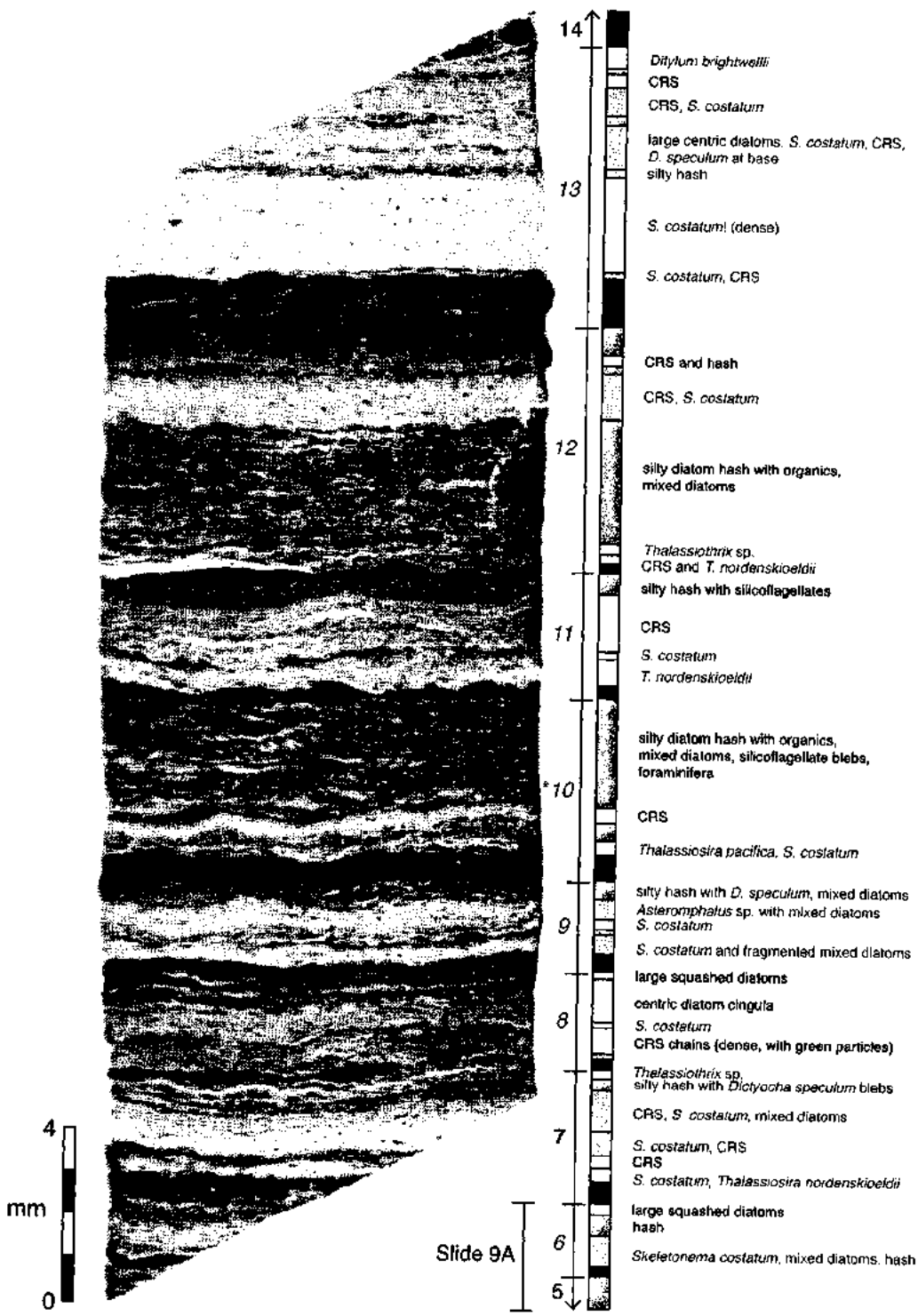
14
13
12
11
10
9
8
7
6
5
4
mm
0
Slide 9A
Ditylum brightwellii
CRS
CRS, S. costatum
large centric diatoms. S. costatum, CRS, D. speculum at base
silty hash
S. costatum! (dense)
S. costatum, CRS
CRS and hash
CRS, S. costatum
silty diatom hash with organics, mixed diatoms
Thalassiothrix sp.
CRS and T. nordenskioeldii
silty hash with silicoflagellates
CRS
S. costatum
T. nordenskioeldii
silty diatom hash with organics, mixed diatoms, silicoflagellate blebs, foraminifera
CRS
Thalassiosira pacifica, S. costatum
silty hash with D. speculum, mixed diatoms
Asteromphalus sp. with mixed diatoms
S. costatum
S. costatum and fragmented mixed diatoms
large squashed diatoms
centric diatom cingula
S. costatum
CRS chains (dense, with green particles)
Thalassiothrix sp.
silty hash with Dictyocha speculum blebs
CRS, S. costatum, mixed diatoms
S. costatum, CRS
CRS
S. costatum, Thalassiosira nordenskioeldii
large squashed diatoms
hash
Skeletonema costatum, mixed diatoms, hash

Slide 9C

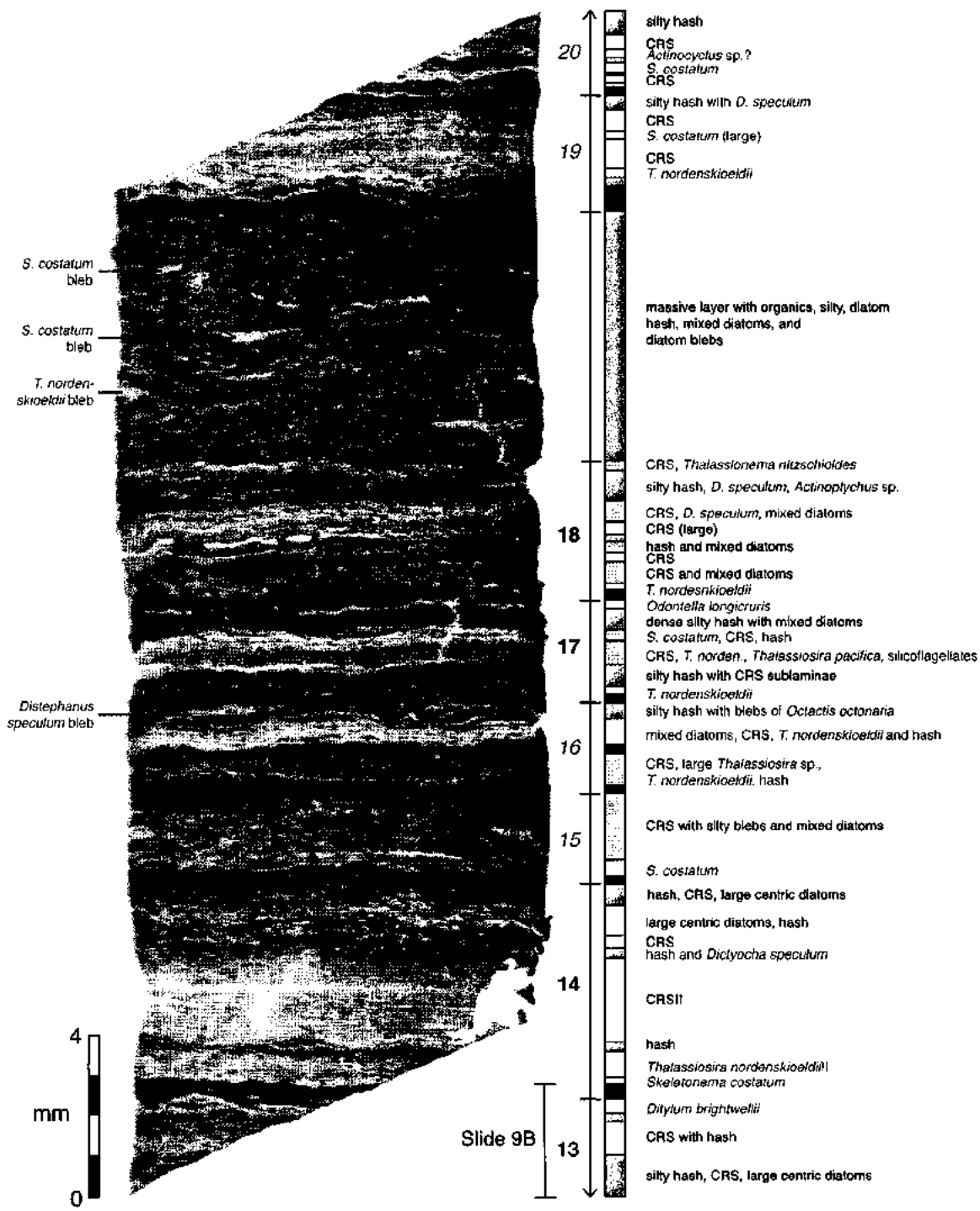
S. costatum bleb
S. costatum bleb
T. norden-skioeldii bleb
Distephanus speculum bleb
4
mm
0
Slide 9B
20
19
18
17
16
15
14
13
silty hash
CRS
Actinocyclus sp.?
S. costatum
CRS
silty hash with D. speculum
CRS
S. costatum (large)
CRS
T. nordenskioeldii
massive layer with organics, silty, diatom hash, mixed diatoms, and diatom blebs
CRS, Thalassionema nitzschioides
silty hash, D. speculum, Actinoptychus sp.
CRS, D. speculum, mixed diatoms
CRS (large)
hash and mixed diatoms
CRS
CRS and mixed diatoms
T. nordesnkioeldii
Odontella longicruris
dense silty hash with mixed diatoms
S. costatum, CRS, hash
CRS, T. norden., Thalassiosira pacifica, silicoflagellates
silty hash with CRS sublaminae
T. nordenskioeldii
silty hash with blebs of Octactis octonaria
mixed diatoms, CRS, T. nordenskioeldii and hash
CRS, large Thalassiosira sp., T. nordenskioeldii. hash
CRS with silty blebs and mixed diatoms
S. costatum
hash, CRS, large centric diatoms
large centric diatoms, hash
CRS
hash and Dictyocha speculum
CRSII
hash
Thalassiosira nordenskioeldii
Skeletonema costatum
Ditylum brightwellii
CRS with hash
silty hash, CRS, large centric diatoms

Slide 9D

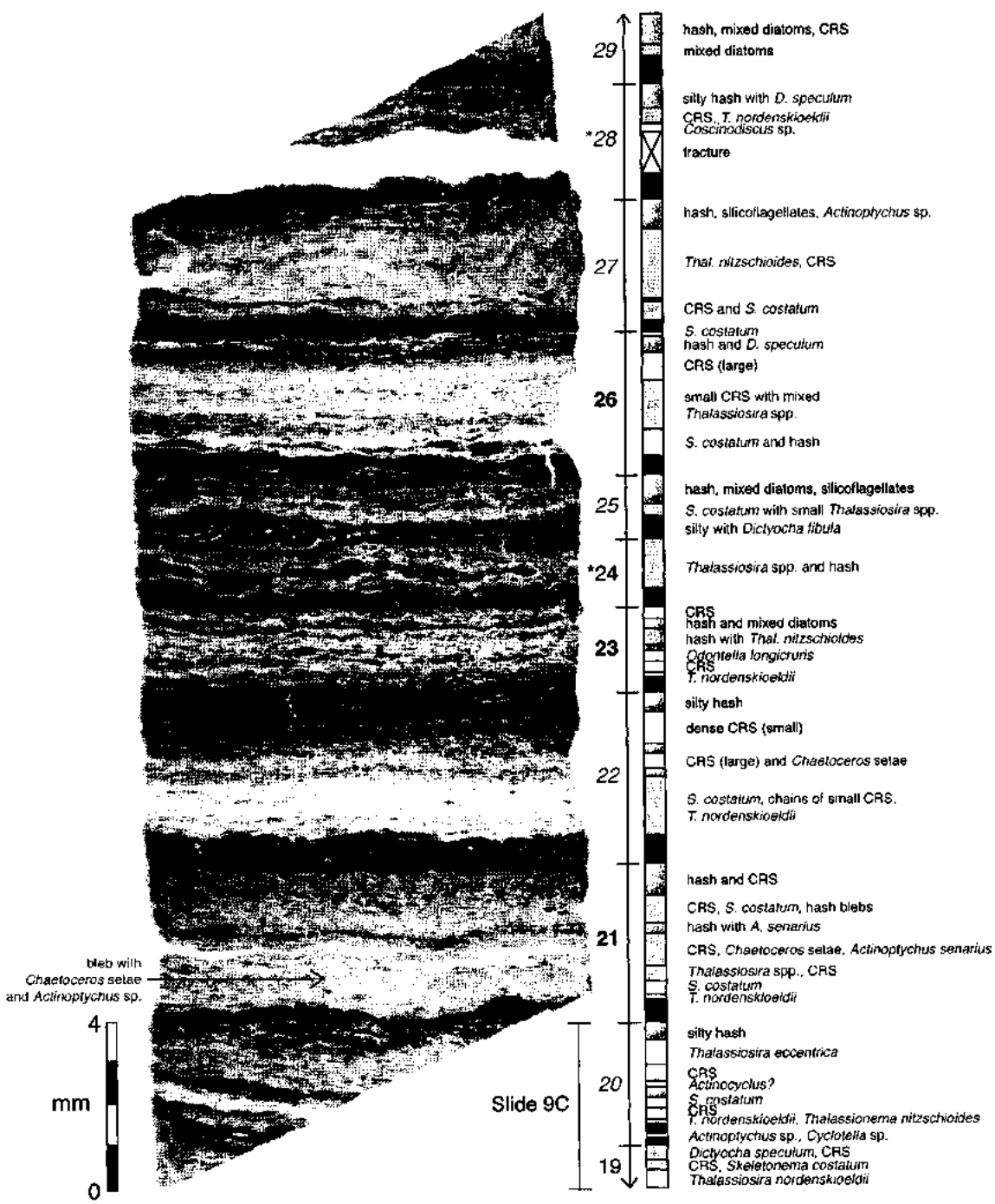
29
*28
27
26
25
*24
23
22
21
20
19
hash, mixed diatoms, CRS
mixed diatoms
silty hash with D. speculum
CRS., T. nordenskioeldii
Coscinodiscus sp.
fracture
hash, silicoflagellates, Actinoptychus sp.
Thal. nitzschioides, CRS
CRS and S. costatum
S. costatum
hash and D. speculum
CRS (large)
small CRS with mixed
Thalassiosira spp.
S. costatum and hash
hash, mixed diatoms, silicoflagellates
S. costatum with small Thalassiosira spp.
silty with Dictyocha fibula
Thalassiosira spp. and hash
CRS
hash and mixed diatoms
hash with Thal. nitzschioides
Odontella longicruris
CRS
T. nordenskioeldii
silty hash
dense CRS (small)
CRS (large) and Chaetoceros setae
S. costatum, chains of small CRS,
T. nordenskioeldii
hash and CRS
CRS, S. costatum, hash blebs
hash with A. senarius
CRS, Chaetoceros setae, Actinoptychus senarius
Thalassiosira spp., CRS
S. costatum
T. nordenskioeldii
silty hash
Thalassiosira eccentrica
CRS
Actinocyclus?
S. costatum
CRS
T. nordenskioeldii, Thalassionema nitzschioides
Actinoptychus sp., Cyclotella sp.
Dictyocha speculum, CRS
CRS, Skeletonema costatum
Thalassiosira nordenskioeldii
bleb with
Chaetoceros setae
and Actinoptychus sp.
4
mm
0
Slide 9C

Slide 9E

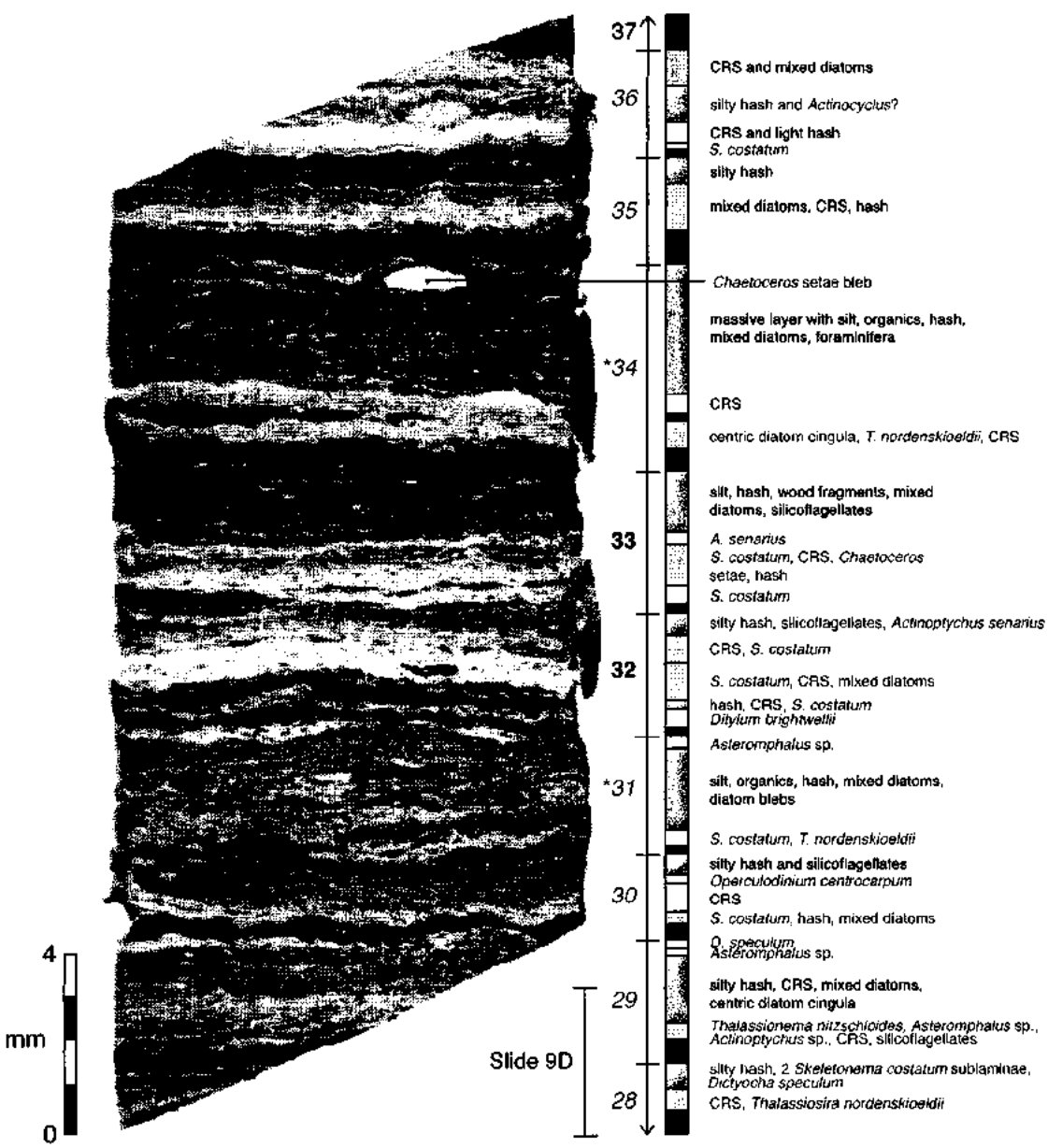
37
CRS and mixed diatoms
36
silty hash and Actinocyclus?
CRS and light hash
S. costatum
silty hash
35
mixed diatoms, CRS, hash
Chaetoceros setae bleb
massive layer with silt, organics, hash, mixed diatoms, foraminifera
*34
CRS
centric diatom cingula, T. nordenskioeldii, CRS
silt, hash, wood fragments, mixed diatoms, silicoflagellates
33
A. senarius
S. costatum, CRS, Chaetoceros setae, hash
S. costatum
silty hash, silicoflagellates, Actinoptychus senarius
CRS, S. costatum
32
S. costatum, CRS, mixed diatoms
hash, CRS, S. costatum
Ditylum brightwellii
Asteromphalus sp.
*31
silt, organics, hash, mixed diatoms, diatom blebs
S. costatum, T. nordenskioeldii
silty hash and silicoflagellates
Operculodinium centrocarpum
30
CRS
S. costatum, hash, mixed diatoms
D. speculum
Asteromphalus sp.
silty hash, CRS, mixed diatoms, centric diatom cingula
29
Thalassionema nitzschioides, Asteromphalus sp., Actinoptychus sp., CRS, silicoflagellates
silty hash, 2 Skeletonema costatum sublaminae, Dictyocha speculum
28
CRS, Thalassiosira nordenskioeldii
Slide 9D
4
mm
0

Slide 9F

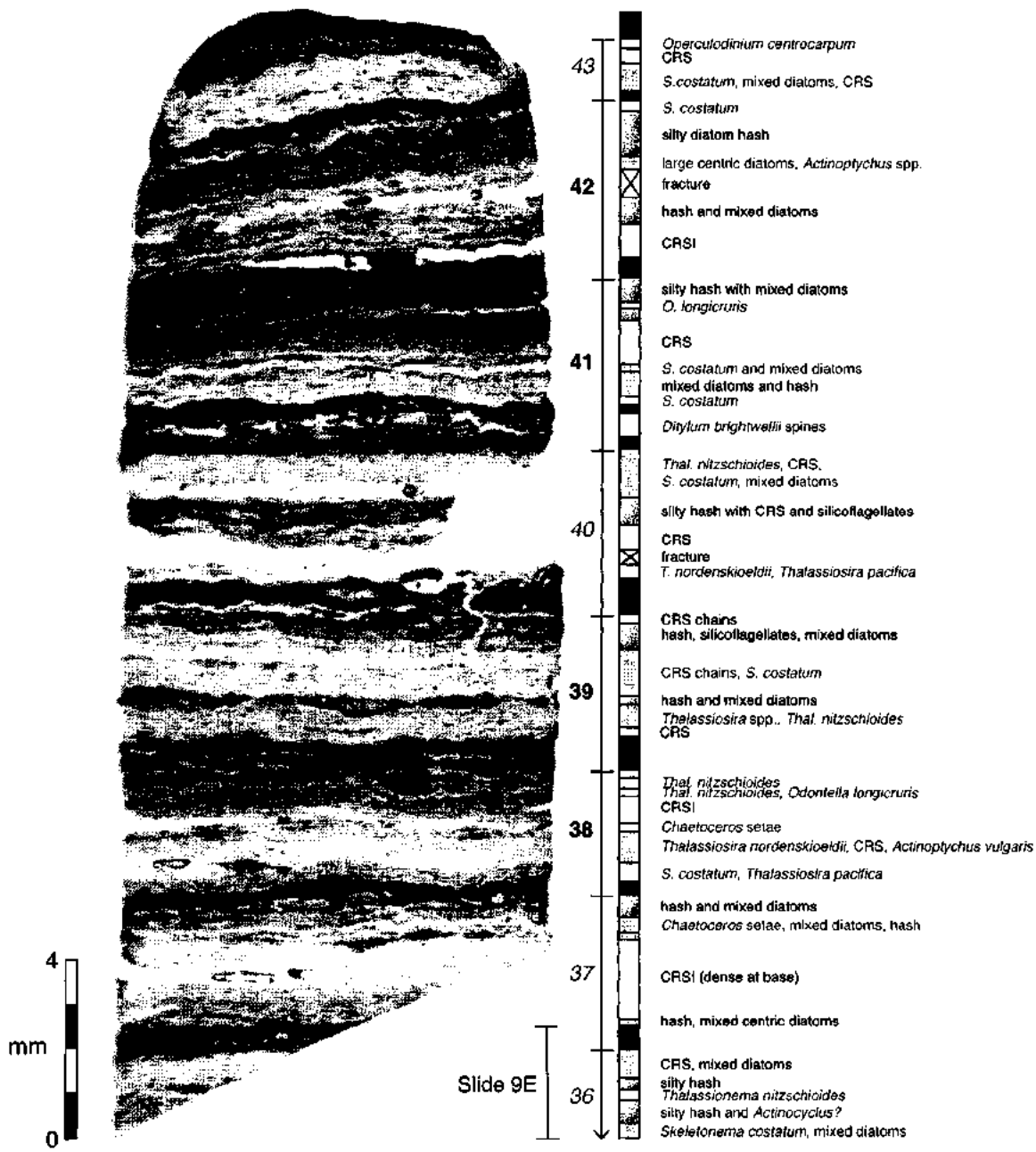
4
mm
0
Slide 9E
43
42
41
40
39
38
37
36
Operculodinium centrocarpum
CRS
S.costatum, mixed diatoms, CRS
S. costatum
silty diatom hash
large centric diatoms, *Actinoptychus* spp.
fracture
hash and mixed diatoms
CRSI
silty hash with mixed diatoms
O. longicruris
CRS
S. costatum and mixed diatoms
mixed diatoms and hash
S. costatum
Ditylum brightwellii spines
Thal. nitzschioides, CRS,
S. costatum, mixed diatoms
silty hash with CRS and silicoflagellates
CRS
fracture
T. nordenskioeldii, Thalassiosira pacifica
CRS chains
hash, silicoflagellates, mixed diatoms
CRS chains, *S. costatum*
hash and mixed diatoms
Thalassiosira spp., *Thal. nitzschioides*
CRS
Thal. nitzschioides
Thal. nitzschioides, Odontella longicruris
CRSI
Chaetoceros setae
Thalassiosira nordenskioeldii, CRS, *Actinoptychus vulgaris*
S. costatum, Thalassiosira pacifica
hash and mixed diatoms
Chaetoceros setae, mixed diatoms, hash
CRSI (dense at base)
hash, mixed centric diatoms
CRS, mixed diatoms
silty hash
Thalassionema nitzschioides
silty hash and *Actinocyclus?*
Skeletonema costatum, mixed diatoms

Slide 10A

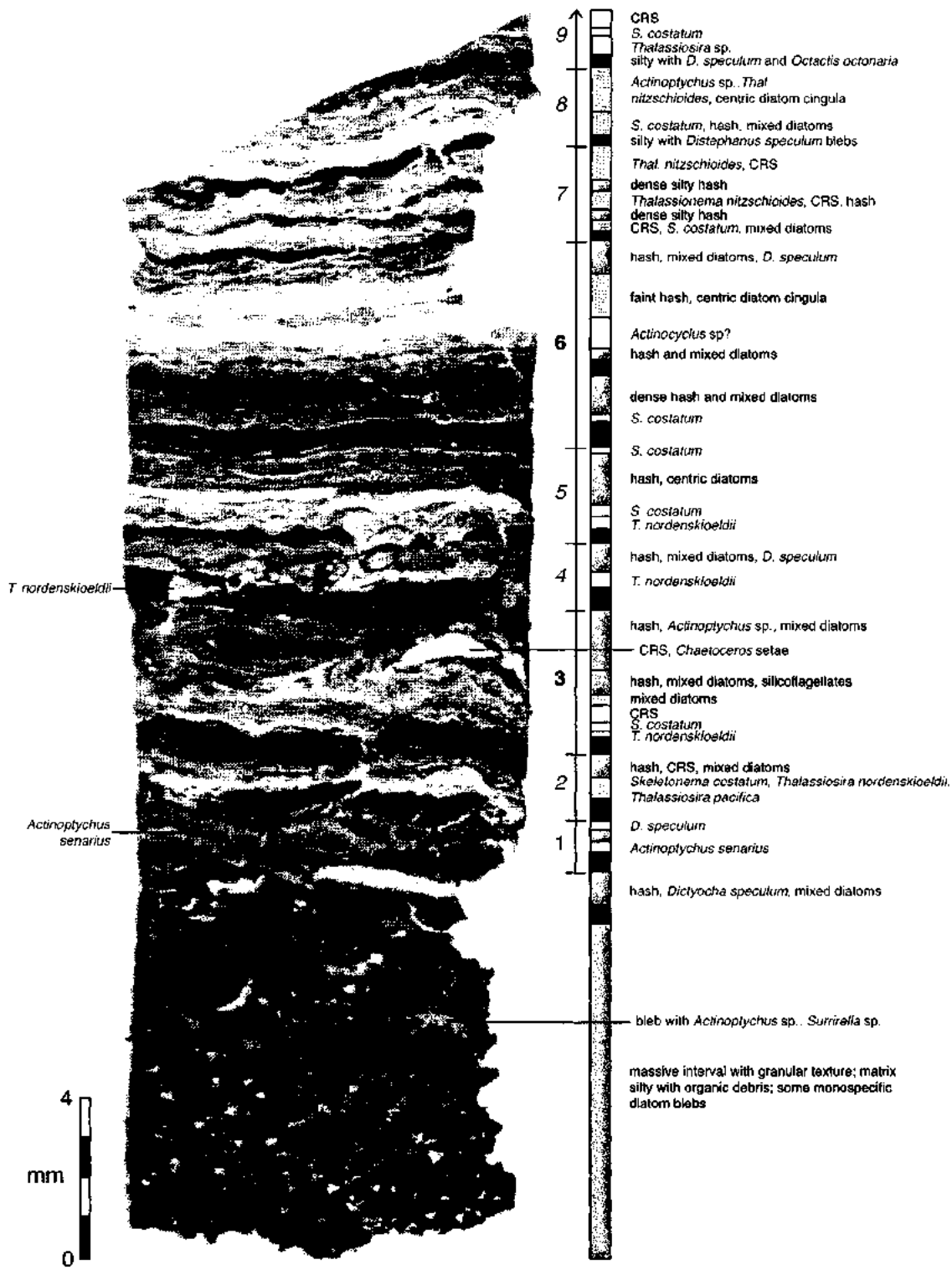
9
8
7
6
5
4
3
2
1
CRS
S. costatum
Thalassiosira sp.
silty with D. speculum and Octactis octonaria
Actinoptychus sp., Thal nitzschioides, centric diatom cingula
S. costatum, hash, mixed diatoms
silty with Distephanus speculum blebs
Thal. nitzschioides, CRS
dense silty hash
Thalassionema nitzschioides, CRS, hash
dense silty hash
CRS, S. costatum, mixed diatoms
hash, mixed diatoms, D. speculum
faint hash, centric diatom cingula
Actinocyclus sp?
hash and mixed diatoms
dense hash and mixed diatoms
S. costatum
S. costatum
hash, centric diatoms
S. costatum
T. nordenskioeldii
hash, mixed diatoms, D. speculum
T. nordenskioeldii
hash, Actinoptychus sp., mixed diatoms
CRS, Chaetoceros setae
hash, mixed diatoms, silicoflagellates
mixed diatoms
CRS
S. costatum
T. nordenskioeldii
hash, CRS, mixed diatoms
Skeletonema costatum, Thalassiosira nordenskioeldii,
Thalassiosira pacifica
D. speculum
Actinoptychus senarius
hash, Dictyocha speculum, mixed diatoms
bleb with Actinoptychus sp., Surirella sp.
massive interval with granular texture; matrix
silty with organic debris; some monospecific
diatom blebs
T. nordenskioeldii
Actinoptychus senarius
4
mm
0

Slide 10B

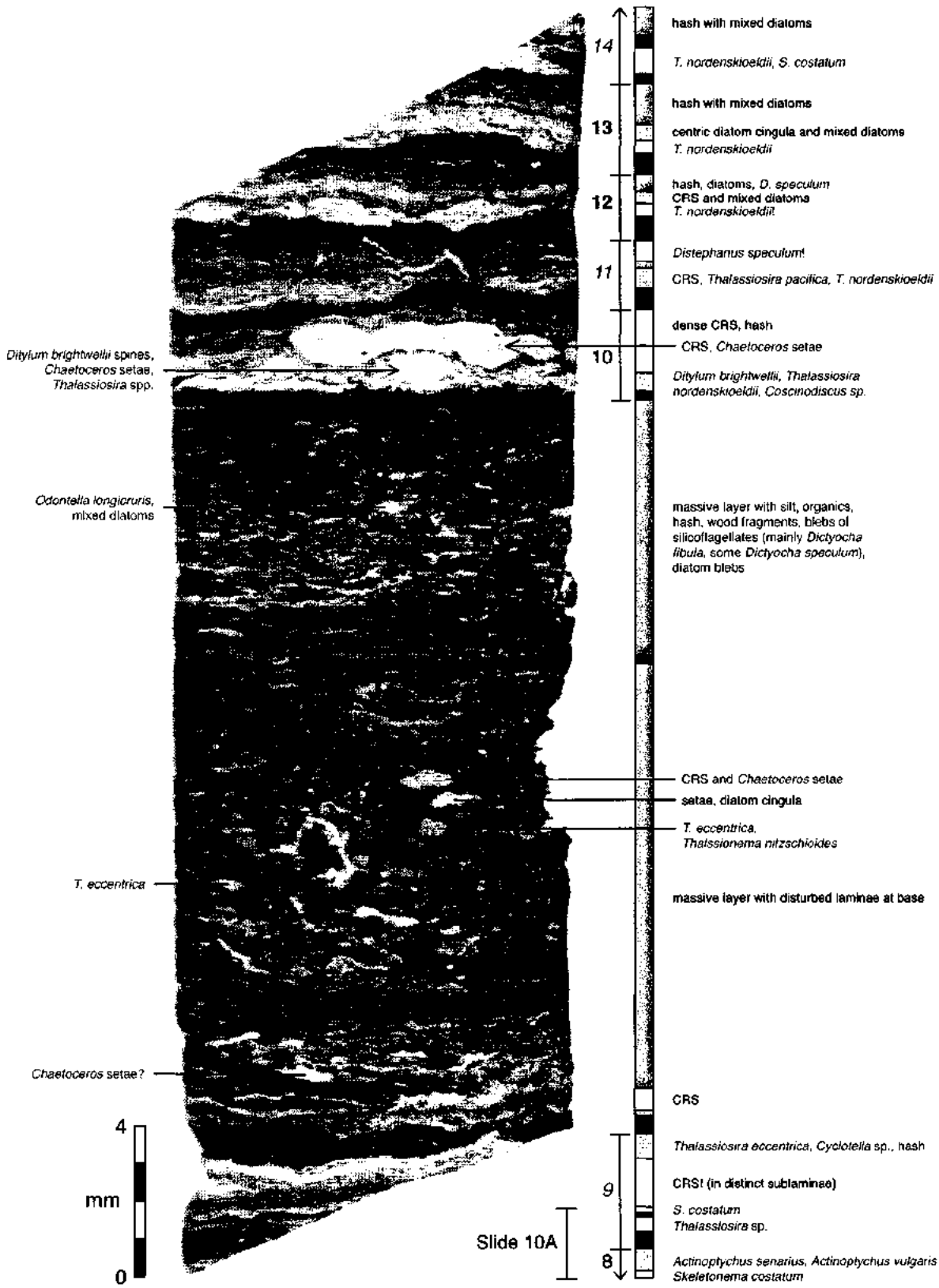
14
13
12
11
10
9
8
hash with mixed diatoms
T. nordenskioeldii, S. costatum
hash with mixed diatoms
centric diatom cingula and mixed diatoms
T. nordenskioeldii
hash, diatoms, D. speculum
CRS and mixed diatoms
T. nordenskioeldii
Distephanus speculum
CRS, Thalassiosira pacifica, T. nordenskioeldii
dense CRS, hash
CRS, Chaetoceros setae
Ditylum brightwellii, Thalassiosira nordenskioeldii, Coscinodiscus sp.
massive layer with silt, organics, hash, wood fragments, blebs of silicoflagellates (mainly Dictyocha fibula, some Dictyocha speculum), diatom blebs
CRS and Chaetoceros setae
setae, diatom cingula
T. eccentrica, Thalssionema nitzschioides
massive layer with disturbed laminae at base
CRS
Thalassiosira eccentrica, Cyclotella sp., hash
CRS! (in distinct sublaminae)
S. costatum
Thalassiosira sp.
Actinoptychus senarius, Actinoptychus vulgaris
Skeletonema costatum
Ditylum brightwellii spines, Chaetoceros setae, Thalassiosira spp.
Odontella longicruris, mixed diatoms
T. eccentrica
Chaetoceros setae?
4
mm
0
Slide 10A

Slide 10C

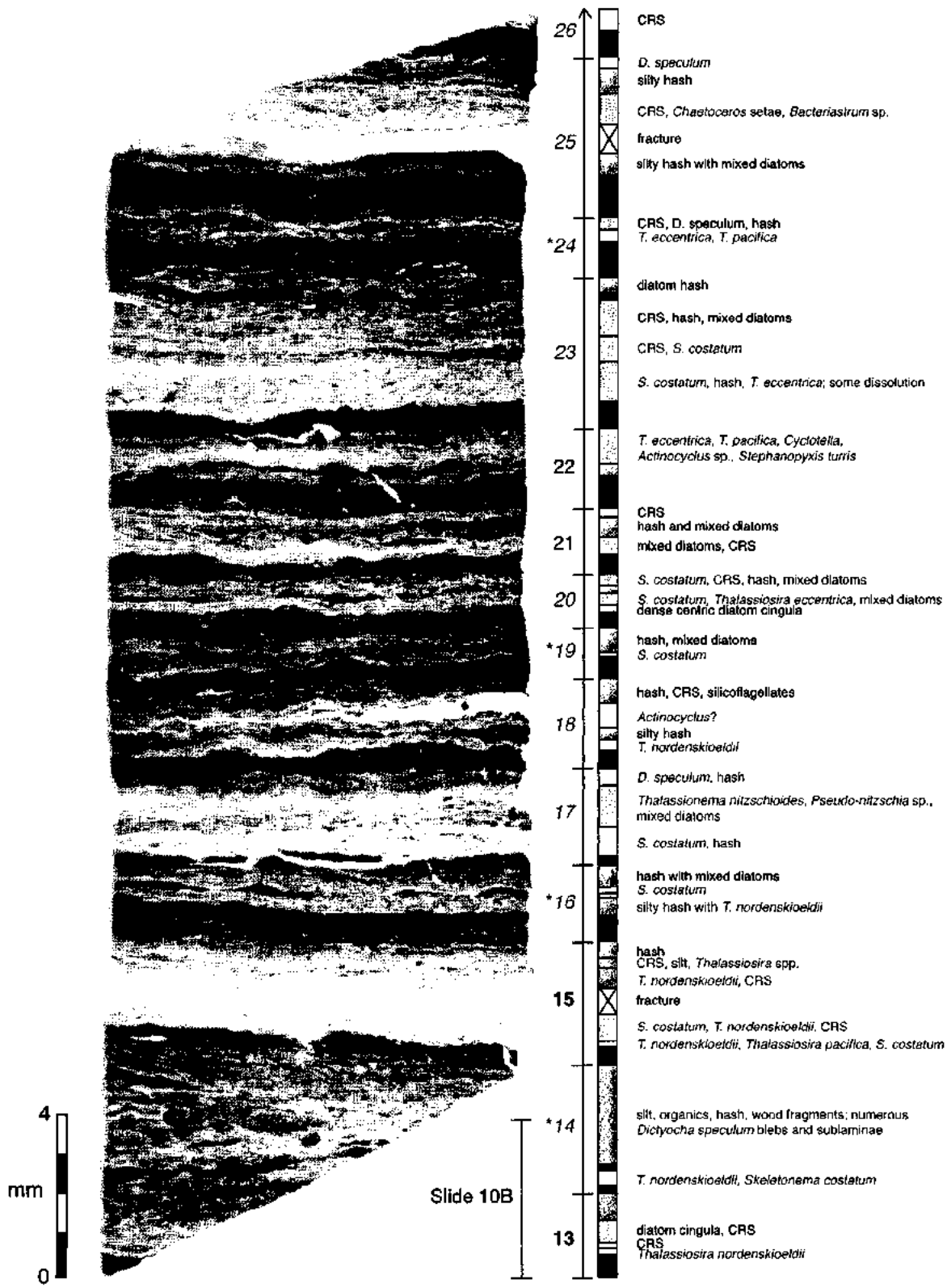
26
CRS
D. speculum
silty hash
CRS, Chaetoceros setae, Bacteriastrum sp.
25
fracture
silty hash with mixed diatoms
CRS, D. speculum, hash
*24
T. eccentrica, T. pacifica
diatom hash
CRS, hash, mixed diatoms
23
CRS, S. costatum
S. costatum, hash, T. eccentrica; some dissolution
T. eccentrica, T. pacifica, Cyclotella,
22
Actinocyclus sp., Stephanopyxis turris
CRS
hash and mixed diatoms
21
mixed diatoms, CRS
S. costatum, CRS, hash, mixed diatoms
20
S. costatum, Thalassiosira eccentrica, mixed diatoms
dense centric diatom cingula
hash, mixed diatoms
*19
S. costatum
hash, CRS, silicoflagellates
Actinocyclus?
18
silty hash
T. nordenskioeldii
D. speculum, hash
Thalassionema nitzschioides, Pseudo-nitzschia sp.,
17
mixed diatoms
S. costatum, hash
hash with mixed diatoms
S. costatum
*16
silty hash with T. nordenskioeldii
hash
CRS, silt, Thalassiosira spp.
T. nordenskioeldii, CRS
15
fracture
S. costatum, T. nordenskioeldii, CRS
T. nordenskioeldii, Thalassiosira pacifica, S. costatum
silt, organics, hash, wood fragments; numerous
*14
Dictyocha speculum blebs and sublaminae
T. nordenskioeldii, Skeletonema costatum
diatom cingula, CRS
13
CRS
Thalassiosira nordenskioeldii
Slide 10B
4
mm
0

Slide 10D

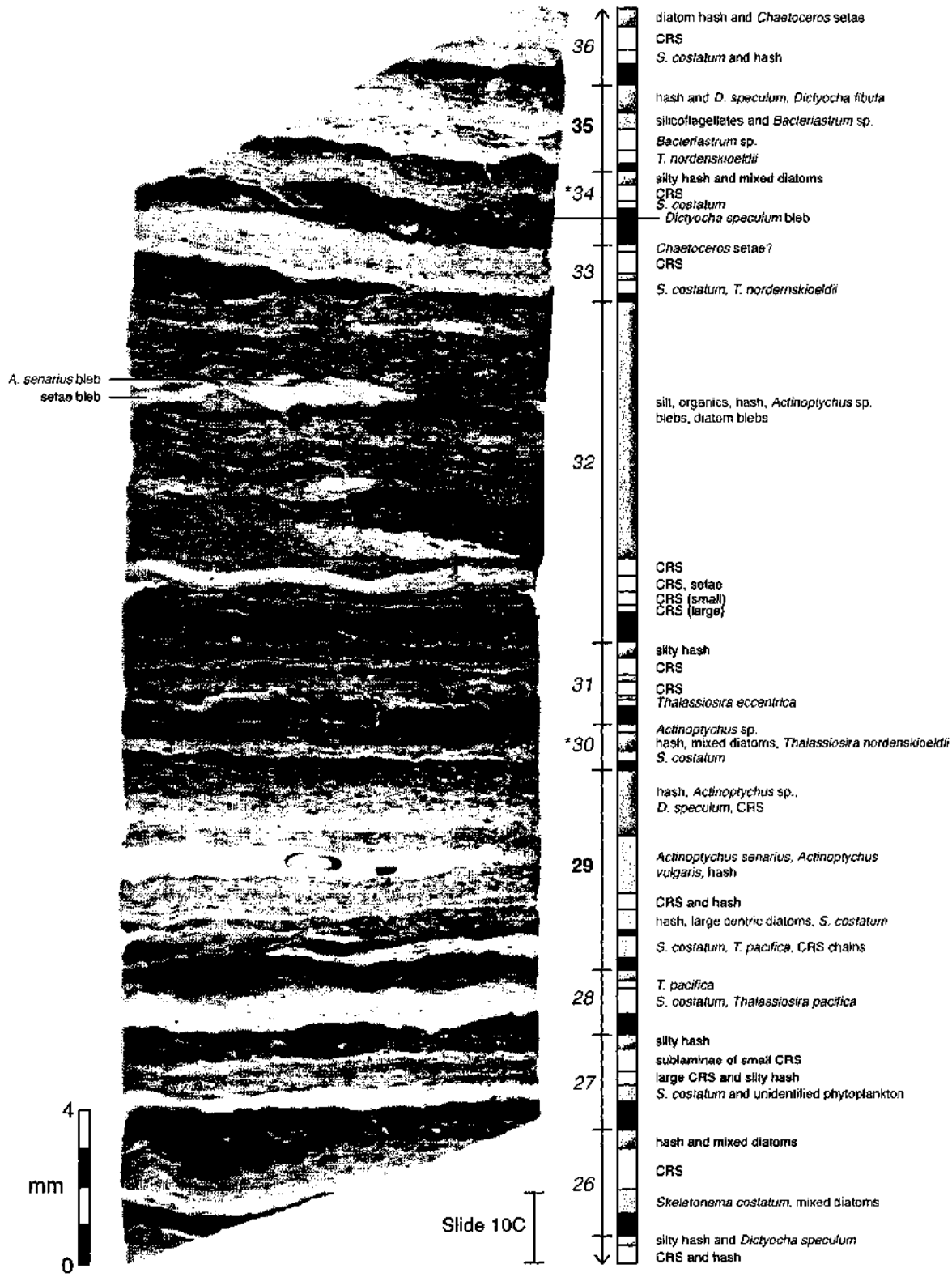
A. senarius bleb
setae bleb
4
mm
0
Slide 10C
36
35
*34
33
32
31
*30
29
28
27
26
diatom hash and Chaetoceros setae
CRS
S. costatum and hash
hash and D. speculum, Dictyocha fibula
silicoflagellates and Bacteriastrum sp.
Bacteriastrum sp.
T. nordenskioeldii
silty hash and mixed diatoms
CRS
S. costatum
Dictyocha speculum bleb
Chaetoceros setae?
CRS
S. costatum, T. nordenskioeldii
silt, organics, hash, Actinoptychus sp.
blebs, diatom blebs
CRS
CRS, setae
CRS (small)
CRS (large)
silty hash
CRS
CRS
Thalassiosira eccentrica
Actinoptychus sp.
hash, mixed diatoms, Thalassiosira nordenskioeldii
S. costatum
hash, Actinoptychus sp.,
D. speculum, CRS
Actinoptychus senarius, Actinoptychus
vulgaris, hash
CRS and hash
hash, large centric diatoms, S. costatum
S. costatum, T. pacifica, CRS chains
T. pacifica
S. costatum, Thalassiosira pacifica
silty hash
sublaminae of small CRS
large CRS and silty hash
S. costatum and unidentified phytoplankton
hash and mixed diatoms
CRS
Skeletonema costatum, mixed diatoms
silty hash and Dictyocha speculum
CRS and hash

Slide 10E

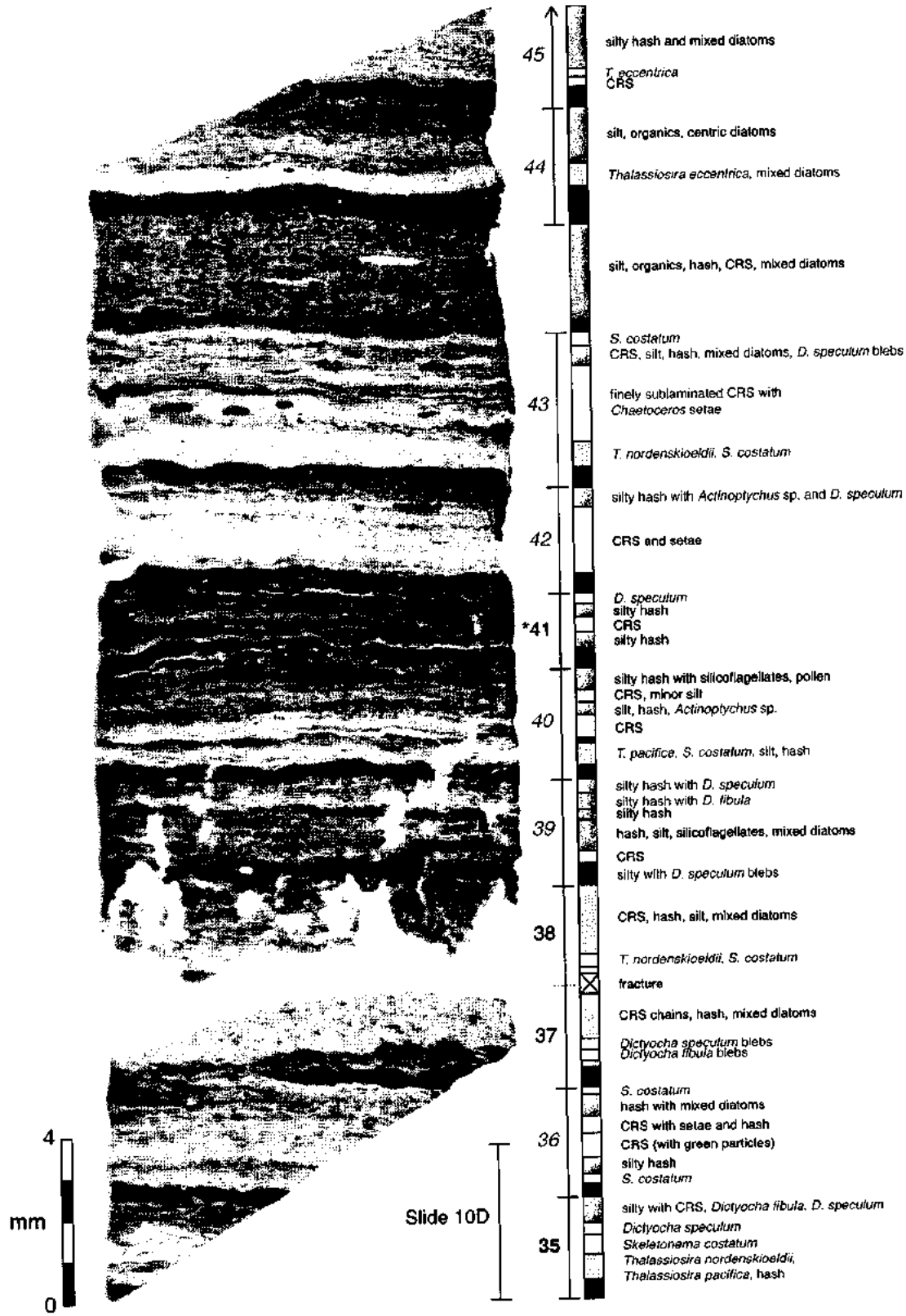
45
silty hash and mixed diatoms
T. eccentrica
CRS
silt, organics, centric diatoms
44
Thalassiosira eccentrica, mixed diatoms
silt, organics, hash, CRS, mixed diatoms
S. costatum
CRS, silt, hash, mixed diatoms, D. speculum blebs
43
finely sublaminated CRS with
Chaetoceros setae
T. nordenskioeldii, S. costatum
silty hash with Actinoptychus sp. and D. speculum
42
CRS and setae
D. speculum
silty hash
CRS
*41
silty hash
silty hash with silicoflagellates, pollen
CRS, minor silt
silt, hash, Actinoptychus sp.
40
CRS
T. pacifica, S. costatum, silt, hash
silty hash with D. speculum
silty hash with D. fibula
silty hash
39
hash, silt, silicoflagellates, mixed diatoms
CRS
silty with D. speculum blebs
CRS, hash, silt, mixed diatoms
38
T. nordenskioeldii, S. costatum
fracture
CRS chains, hash, mixed diatoms
37
Dictyocha speculum blebs
Dictyocha fibula blebs
S. costatum
hash with mixed diatoms
CRS with setae and hash
36
CRS (with green particles)
silty hash
S. costatum
silty with CRS, Dictyocha fibula, D. speculum
Dictyocha speculum
Skeletonema costatum
35
Thalassiosira nordenskioeldii,
Thalassiosira pacifica, hash
4
mm
0
Slide 10D

Slide 10F

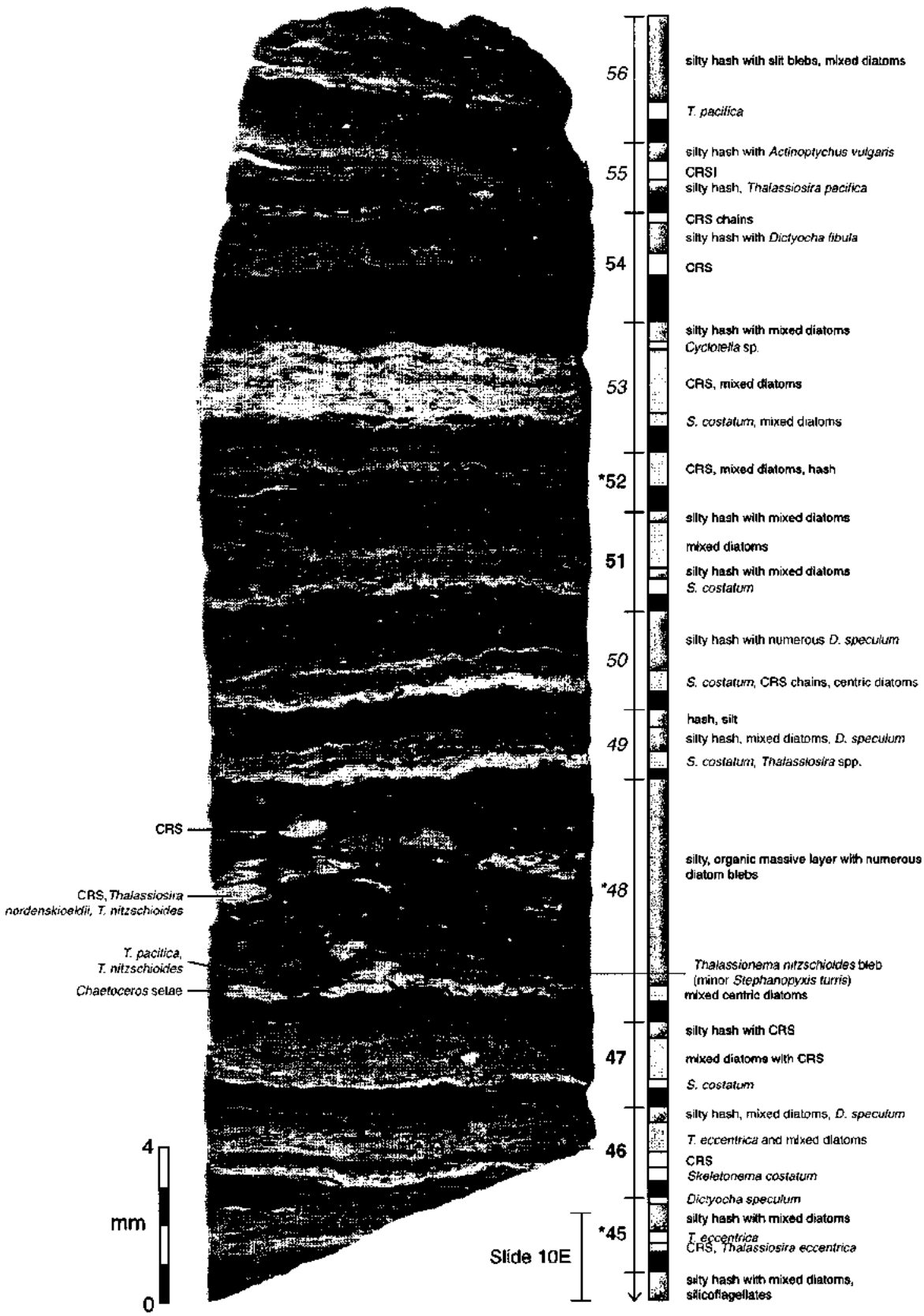
56
silty hash with slit blebs, mixed diatoms
T. pacifica
silty hash with Actinoptychus vulgaris
55
CRSI
silty hash, Thalassiosira pacifica
CRS chains
silty hash with Dictyocha fibula
54
CRS
silty hash with mixed diatoms
Cyclotella sp.
53
CRS, mixed diatoms
S. costatum, mixed diatoms
*52
CRS, mixed diatoms, hash
silty hash with mixed diatoms
mixed diatoms
51
silty hash with mixed diatoms
S. costatum
silty hash with numerous D. speculum
50
S. costatum, CRS chains, centric diatoms
hash, silt
49
silty hash, mixed diatoms, D. speculum
S. costatum, Thalassiosira spp.
CRS
silty, organic massive layer with numerous diatom blebs
CRS, Thalassiosira nordenskioeldii, T. nitzschioides
*48
T. pacifica, T. nitzschioides
Chaetoceros setae
Thalassionema nitzschioides bleb
(minor Stephanopyxis turris)
mixed centric diatoms
silty hash with CRS
47
mixed diatoms with CRS
S. costatum
silty hash, mixed diatoms, D. speculum
T. eccentrica and mixed diatoms
46
CRS
Skeletonema costatum
Dictyocha speculum
silty hash with mixed diatoms
*45
T. eccentrica
CRS, Thalassiosira eccentrica
silty hash with mixed diatoms, silicoflagellates
Slide 10E
4
mm
0

APPENDIX E

Data from Sediment Traps CTC3 and CTC11

APPENDIX E1. Sediment trap microfossil counts

Sample	3A-1	3A-2	3A-3	3A-4	3A-5	3A-6	3A-7	3A-8	3A-9	3A-10	3A-11X	3A-12X	3A-13	3B-1	3B-2	3B-3	3B-4	3B-5	3B-6
Date Opened	5/29/99	6/6/99	6/15/99	6/24/99	7/3/99	7/12/99	7/21/99	7/30/99	8/7/99	8/16/99	8/25/99	9/3/99	9/12/99	10/11/99	10/26/99	11/11/99	11/27/99	12/12/99	12/28/99
DIATOMS																			
A. brevipes								1		2									
A. kriegeri									2	3	1	4	2	2	2	2	4	2	4
A. lanceolata																1			
A. lemmermannii							1			4									
A. minutissima	8	2	9	4	10	3	9	16	8	1	19	24	9	11	11	32	40	43	48
A. nodosa			1			2													
Achnanthidium biasolettianum								2				2		2	3	1	2	1	4
Achnanthes sp. (11C-3)																			
Achnanthes sp. (11C-13)																			
Actinocyclus curvatulus		2	4	5	2			3	2		1	2	1						
A. normanii			1																
A. octonarius			1	2	1		3	1	1			2						1	
Actinocyclus sp. (3A-5)					3														
Actinocyclus sp. (3B-2)															1				
Actinocyclus sp. (11C-11)																			
Actinocyclus sp. (11C-13)																			
Actinoptychus senarius				1						1	1				2				
A. vulgaris		4	1	2	6	2	5	2	1	4	3	5	2		1		1		
Amphora acutiuscula					1	1			1			1		2			1	2	
A. coffeaeformis														1					
A. copulata	2						1			1	2	1				3	2	1	3
A. exigua	1			1		1		1		2	2			2				2	
A. helenensis						2		2			2	2		4		1		5	
A. maletracta var. *constricta*										1							1		
A. marina			2																
Amphora sp. (3A-9)									2										
Amphora sp. (3A-11x)											1								
Amphora sp. (3B-1)														1	1				
Asteromphalus heptacis			1					2		1			1				1		1
A. sarcophagus															1		1		
Aulacoseira ambigua																		2	
A. italica var. *subarctica*																			
Bacillaria paxillifer								1						1		1			
Bacteriastrum delicatulum	2	1		2			2	3	2		1	2	1	3	3		1	2	
Berkeleya rutilans	2	2	1	1	1	1			1		1	5		3		5	1	2	2
Brachysira sp.	2					2					1				1				1
Cocconeis californica																			
C. costata complex								1		1									1
C. disculus		1	3	1	4		3	3	2	3	1	6	2	5	3	1	1	1	
C. distans	1							1	1				1		2			2	
C. neothumensis												4	3	2	1	2		2	1
Cocconeis cf. *pellucida*											1			1	1				
C. peltoides					1					1									
C. pinnata	1				1		1												
C. placentula		2	5		1	1	2	3	7	2	6	4	2	4	3	2	2	5	5
C. scutellum	2			1		2	2	1	1		2	4	2	3	5	3	6		4
C. stauroneiformis	2	3		1	3		1	2	2	3	2			4		1	8		3
Cocconeis sp.? (3A-12x)												1							
Cocconeis sp. (11C-3)																			
Cocconeis spp. (small)					2		1		1	3	2	1	1	2	2	2	1	1	1
Coscinodiscus diorama																			1
C. radiatus			1										1						1
Ctenophora pulchella					1									1		2	1		
C. choctawhatcheeana	3	1			1		1	1	4	3	3	2		1	1	1	4	3	

APPENDIX E1 (continued)

Sample	3A-1	3A-2	3A-3	3A-4	3A-5	3A-6	3A-7	3A-8	3A-9	3A-10	3A-11x	3A-12x	3A-13	3B-1	3B-2	3B-3	3B-4	3B-5	3B-6
Date Opened	5/29/99	6/6/99	6/15/99	6/24/99	7/3/99	7/12/99	7/21/99	7/30/99	8/7/99	8/16/99	8/25/99	9/3/99	9/12/99	10/11/99	10/26/99	11/11/99	11/27/99	12/12/99	12/28/99
Cyclotella "punctata"																			
C. rossii									1										
C. stelligera	1	2			1	1	1		1			1				1	3	3	1
Cyclotella striata	2	2	1		4	2	2	3	3	1	2	1	2						1
C. stylorum				1								1						1	
Cyclotella sp. (B04-15)											1								1
Cyclotella sp. (3A-3)			1																
Cyclotella sp. (3A-13)													1						
Cymbella cymbiformis						1							1					1	
C. minuta					1	3		1			3				3		5		
Cymbella sp. (11C-3)																			
Delphineis spp.	3						1	3	2	2	1	1		2	1		1	1	1
Denticula cf. *neritica*				1															
Diatoma tenue			1			1													
D. mesodon										2		1				1		1	
Diatoma sp. (3B-10)																			
Diatomella minuta						1						2							2
Dimeragramma sp. (11C-6)																			
Diploneis bombus																			
Diploneis smithii																			
Diploneis sp.													1						
Ditylum brightwellii				3	2					1		1		1	1		2		
Eucampia spp.								2						1	1	2	1	3	3
Eunotia spp.		1	1			1						1					1	1	1
Fallacia sp. (B04-29)																1	1	1	
Fallacia sp. (B04-28)																			
Fallacia sp.		1			1		1		8	3					1				
Fallacia sp. (3A-2)		2																	
Fragilaria capucina complex		2	3	1	1			4			1	2	1		1	2	1	1	
F. construens var. *construens*																			
F. investiens		4	1		2	1			2	3	1	2	1					2	
F. pinnata			1												1		1	2	
Fragilaria cf. *sopotensis*	1	4		1	3	1	2	4	6		2				3		1	2	
Fragilaria sp. (11C-13)																			
Fragilariopsis atlantica	102	94	155	204	132	105	120	103	93	105	89	91	45	6	13	11	9	6	5
F. cylindriformis		1	3	3	2	1		4				1							
F. pseudonana	39	36	41	10	19	18	11	17	13	13	14	13	2	6	10	9	10	20	19
Fragilariopsis cf. *tenera*											1								
Fragilariopsis sp. (3A-7)							2	5	1	8	2	1			1	1	4		
Gomphonema augustatum													2						
G. augustum							2												
G. olivaceum																			
Gomphonema sp.								2	2		2	2				2	8	4	
Gomphonema sp. (3A-8)								1											
Gomphonema sp. (11C-6)																			
Gomphonema sp. (11C-10)																			
Gomphonemopsis exigua				1		2	3					1		4		1	4	3	
G. lindae		1		1							1						2		
G. obscurum	1		1	2			5	2		5	2	2	2	8		3		3	4
Grammatophora angulosa														2					
G. marina																			
G. oceanica								2						1			2	1	
Grammatophora sp. (B04-14)	2				2										4	2			
Hannea arcus			1		2		4			2	1	1		1	2	1		1	
Hyalodiscus scoticus				1	1						2	1	1	6	5	4		2	

APPENDIX E1 (continued)

Sample	3A-1	3A-2	3A-3	3A-4	3A-5	3A-6	3A-7	3A-8	3A-9	3A-10	3A-11x	3A-12x	3A-13	3B-1	3B-2	3B-3	3B-4	3B-5	3B-6
Date Opened	5/29/99	6/6/99	6/15/99	6/24/99	7/3/99	7/12/99	7/21/99	7/30/99	8/7/99	8/16/99	8/25/99	9/3/99	9/12/99	10/11/99	10/26/99	11/11/99	11/27/99	12/12/99	12/28/99
Licomorpha spp.																			
Luticola mutica											1	1							2
Luticola (?) sp. (3A-13)													1						
Mastogloia exigua									2			1		2					1
M. smithii						1								2		1			
Melosira nummuloides					1	3	4		3					17	2	2	5	4	3
Melosira sp.					1			4	2	1	1	1	1	2		3	3		3
Minidiscus chilensis	19	48	28	14	35	53	35	40	50	42	29	52	22	33	70	43	49	46	63
Navicula cryptocephala								2			1	2			2		1		
Navicula cf. *digitoradiata*																			
N. directa				1									1	3		1		1	1
N. gregaria		2				3		1	1	1	3	4	3	1	4	2	4	2	1
N. perminuta	5	11	12	5	6	7	1	8	9	15	12	7	4	15	8	15	14	14	8
N. phylleptosoma	1		1			1	1		1		1	2					1		2
Navicula cf. *ramossisima*								3	2	1	2	2		1	1	1		2	
Navicula aff. *salinarum*											1						2		1
Navicula sp. (3A-7)							3												
Navicula sp. (3A-13)													1						
Navicula sp. 1 (3B-1)														1					
Navicula sp. 2 (3B-1)														2					
Navicula sp. (3B-5)																		1	
Navicula sp. 1 (3C-1)																			
Navicula sp. 2 (3C-1)																			
Navicula sp. (11C-3)																			
Navicula sp. (11C-9)																			
Navicula sp. (11C-14)																			
Nitzschia amphibia			1																
N. coarctata									1				1				2		
N. dissipata			1		1	1	1	1								3			
N. fonticola				2					1		1	1		1		3	2	1	2
N. frustulum	27	25	33	15	19	33	36	35	40	43	38	32	5	32	23	41	35	27	25
N. inconspicua					2	1	1												
N. microcephala	2				1														
N. perminuta											2								
Nitzschia cf. *sicula* (B04-12)												1	1				1		1
N. valdestriata					1			2	1			1	1	3		1		1	
Nitzschia sp. (3A-3)			1																
Nitzschia sp. (B04-3)																			
Nitzschia hungarica												1							
Nitzschia/Fragilaria sp. (3B-8)																			
Odontella aurita/pulchella																			1
O. longicruris																	1		1
Odontella sp. (3C-3)																			
Opephora gemmeta												1							
O. gunter-grassi		1																	
Opephora cf. *horstiana*												1	3	1			1		3
O. marina	1				1			2			3	2		2		1		3	2
O. minuta	1	1	1								1	1							1
O. mutabilis		2		1		3		4	8	3				1	1	1		1	
Opephora sp. (11C-9)																			
Paralia sulcata	2		1			1		2		7	1				4		1	2	1
Planothidium delicatulum	5	6	9	5	6	4	13	5	10	12	14	14	5	21	7	23	10	10	9
Planothidium cf. *engelbretchii*					1						1	1							
P. hauckianum	3	1	4	1	3		1	2	1		3	4					6	1	2
Pleurosigma spp.		5	6	10	6	15	14	13	16	13	11	20	7					2	

APPENDIX E1 (continued)

Sample	3A-1	3A-2	3A-3	3A-4	3A-5	3A-6	3A-7	3A-8	3A-9	3A-10	3A-11x	3A-12x	3A-13	3B-1	3B-2	3B-3	3B-4	3B-5	3B-6
Date Opened	5/29/99	6/6/99	6/15/99	6/24/99	7/3/99	7/12/99	7/21/99	7/30/99	8/7/99	8/16/99	8/25/99	9/3/99	9/12/99	10/11/99	10/26/99	11/11/99	11/27/99	12/12/99	12/28/99
Pseudonitzschia multiseries	1	1			3	1	2	3	1	6	3	2	3	4	7	7	9	5	7
P. seriata	1				1			1	1							3	2	3	1
Reimeria sinuata	1															2	2		
Rhizosolenia spp. (spines)	3	1	1		1	1		1	3	1	2	3	2	5	7	18	24	15	13
Rhoichosphenia curvata														2					
Rhopalodia brebissonii																1			
R. pacifica														2					
Seminavis spp.		1	2	1								2							
Skeletonema costatum	141	99	73	85	80	97	89	98	79	88	80	55	37	114	173	140	111	114	132
Skeletonema costatum (weak)	59	36	17	15	38	38	33	15	19	15	28	19	11	21	28	30	28	37	48
Stephanodiscus spp.						1													
Stephanopyxis turris						2				4		2					1		
Surirella brebissonii																			
Synedra ulna																		3	
Tabellaria flocculosa	2					1						1					3		
Tabularia fasciculata		2	2	3	1	3		3	5	8	3	4		5	1	7	5	2	1
Thalassionema cf. *bacillare*	7	1	3	5	3	2	6	1	1	2		4	2		1				2
T. nitzschioides	11	26	12	21	26	29	25	23	25	21	30	20	16	34	24	28	22	22	16
T. pseudonitzschioides																			
Thalassiosira aestivalis		1		1				1						1	1				
T. angulata	1	7	4	4	1	1	4	1									1		1
T. binata	1		1	1	2				1			3				1			
T. bioculata			1													1			
T. conferta	10	4	3	3	5	8	2			2	8	4	1	1	2	2		1	
T. decipiens		2	4	1		1		1	4	2	1	2	6	5	8	4	1	4	3
T. decipiens (large)					2				5	2			1					1	1
T. eccentrica	2	2	2	5	2	5	4		1	1	5	4	2	4	1	6	3		6
T. eccentrica (large)	1			4	1					1							1		
T. gravida																			
T. kushirensis																			
Thalassiosira cf. *leptopus*	1	8	3	9	8	3	13	7	8	8	5	8	2	1	3	1	1	3	4
Thalassiosira aff. *leptopus*										1									
T. lundiana					1				1					3	1			1	
T. minima	3	11	3	5	5	1	1	3	1						1			1	1
T. nodulolineata																	1		
T. nordenskioeldii	2		1			1		1	1	1	1		1		4	1	3	2	3
T. oceanica	2	2	1	2		2	2		3			2			1		1	2	2
T. oestrupii	6	11	21	21	13	11	10	11	14	11	13	8	10			1	1	3	2
T. pacifica	1	1	1	2	3	1	6	4	1	2	9	3	6	8	8	6	5	10	2
T. poroseriata												1							
T. punctigera		1		2		1	1		1		1			1			1	4	
T. rotula		1	1	1							2		1			3	3	1	1
T. tealata	1	4	5	3	2	4	1	1	5	2	1	1							
T. tenera		3			1		1						1	3	2	2	2	3	5
Thalassiosira cf. *tenera*		2	3		5	1	2	1	2	4	3	4	3	1	6	4	1	2	2
Thalassiosira sp. 1 (3A-2)		2																	
Thalassiosira sp. 2 (3A-2)		1		3		2													
Thalassiosira sp. (3A-6)						1													
Thalassiosira sp. (3C-2)																			
Thalassiosira sp. (3C-8)																			
Thalassiosira sp. (3C-11)																			
Thalssiothrix longissima									1										
Trachyneis aspera					2										1				
Tryblionella cf. *acuminata*														1				1	
T. aerophila						1	2		2								2		

APPENDIX E1 (continued)

Sample	3A-1	3A-2	3A-3	3A-4	3A-5	3A-6	3A-7	3A-8	3A-9	3A-10	3A-11x	3A-12x	3A-13	3B-1	3B-2	3B-3	3B-4	3B-5	3B-6
Date Opened	5/29/99	6/6/99	6/15/99	6/24/99	7/3/99	7/12/99	7/21/99	7/30/99	8/7/99	8/16/99	8/25/99	9/3/99	9/12/99	10/11/99	10/26/99	11/11/99	11/27/99	12/12/99	12/28/99
Tryblionella sp. (3A-9)									1										
Tryblionella sp.													1						
Tryblionella sp. (3C-11)																			
Unknown centric (B04-7)											2								
Unknown centric 2 (B04-21)								1										1	
Unknown centric 3 (B04-23)															2				
Unknown pennate (3A-13)													1						
Unknown pennate 1 (3B-1)														49	1	1			
Unknown pennate 2 (3B-1)														2					
Unknown pennate 1 (3B-5)																		2	
Unknown pennate 2 (3B-5)																		3	1
Unknown pennate 1 (3B-7)																			
Unknown pennate 2 (3B-7)																			
Unknown pennate (3C-8)																			
Unknown pennate (3C-9)																			
TOTAL	500	500	502	501	501	500	500	500	504	501	500	502	250	500	496	511	506	500	505
DIATOM RESTING SPORES																			
Chaetoceros spp.	12	36	25	32	47	30	35	34	34	30	38	36	26	27	41	32	32	33	39
Leptocylindrus spp.		1	1			2	3		2	2	1	6	1		3	4		1	3
Stephanopyxis spp.			1																
TOTAL	12	37	27	32	47	32	38	34	36	32	39	42	27	27	44	36	32	34	42
SILICOFLAGELLATES																			
Dictyocha fibula			1	2			1									2			
D. speculum		1		5	3	7		2	2	5		1		2	3	2	3	6	1
Octactis sp.										3	1		1						
TOTAL	0	1	1	7	3	7	1	2	2	8	1	1	1	2	3	4	3	6	1

APPENDIX E1 (continued)

Sample	3B-7	3B-8	3B-9	3B-10	3B-11	3B-12	3B-13	3B-14	3C-1	3C-2	3C-3	3C-4	3C-5	3C-6	3C-7	3C-8	3C-9	3C-10	3C-11
Date Opened	1/13/00	1/29/00	2/13/00	2/29/00	3/16/00	3/31/00	4/16/00	5/2/00	5/15/00	5/24/00	6/3/00	6/13/00	6/23/00	7/3/00	7/12/00	7/22/00	8/1/00	8/11/00	8/21/00
DIATOMS																			
A. brevipes					1	2													
A. kriegeri	1	2	2	5	2				1	3						1	1		3
A. lanceolata		1																1	
A. lemmermannii	2																		
A. minutissima	21	24	16	25	4	18	9	6	17	21	2	1	4		6	3	2		5
A. nodosa			2			1		1											
Achnanthidium biasolettianum		1	1	1	5		1		1	2									
Achnanthes sp. (11C-3)																			
Achnanthes sp. (11C-13)																			
Actinocyclus curvatulus	1				1					1	1								
A. normanii																			
A. octonarius						2													
Actinocyclus sp. (3A-5)																			
Actinocyclus sp. (3B-2)																			
Actinocyclus sp. (11C-11)																			
Actinocyclus sp. (11C-13)																			
Actinoptychus senarius	1	1			1					2									
A. vulgaris						1										1	1		
Amphora acutiuscula						1			1				1				2	3	
A. coffeaeformis										1									
A. copulata	2			1	1	1	2		1	4						1	3		1
A. exigua			2	1	2				1	1					1			1	1
A. helenensis			3						3	1	1		1				2	1	
A. maletracta var. *constricta*	1	1	1			1			1	1			1						
A. marina						1		1		2									
Amphora sp. (3A-9)																			
Amphora sp. (3A-11x)																			
Amphora sp. (3B-1)																			
Asteromphalus heptacis		2			3					1				1					
A. sarcophagus		1		1								2	3	1	2	1	3	2	2
Aulacoseira ambigua																			
A. italica var. *subarctica*																			
Bacillaria paxillifer				1						3		1					1		
Bacteriastrum delicatulum	2			2		1	1	2	9	3	3	2	6	2		7	4	1	10
Berkeleya rutilans									1	5				1		2			1
Brachysira sp.		2	1																
Cocconeis californica																			
C. costata complex	1			1	2			1	2	3									
C. disculus	1	1				2	1										1		1
C. distans	1		1				1	1		1									
C. neothumensis	1	4		2	3		1		2							2			
Cocconeis cf. *pellucida*									1										
C. peltoides	1			2	1				1										
C. pinnata	2			1		1													
C. placentula	5	3	2	3	4		2	1	4	3	1	1				1	2	1	5
C. scutellum	3	5	2		5	3	6		2	7		2				2		3	2
C. stauroneiformis		3	1	6	4	6	5	1	3	6		1			1	3		1	3
Cocconeis sp.? (3A-12x)																			
Cocconeis sp. (11C-3)																			
Cocconeis spp. (small)		1	7	1	2	3		2	1	1									2
Coscinodiscus diorama																			
C. radiatus					1										1				
Ctenophora pulchella			1				2						1			1			1
C. choctawhatcheeana	1	1			3	4	1	2		1	3								

APPENDIX E1 (continued)

Sample	3B-7	3B-8	3B-9	3B-10	3B-11	3B-12	3B-13	3B-14	3C-1	3C-2	3C-3	3C-4	3C-5	3C-6	3C-7	3C-8	3C-9	3C-10	3C-11
Date Opened	1/13/00	1/29/00	2/13/00	2/29/00	3/16/00	3/31/00	4/16/00	5/2/00	5/15/00	5/24/00	6/3/00	6/13/00	6/23/00	7/3/00	7/12/00	7/22/00	8/1/00	8/11/00	8/21/00
Cyclotella "punctata"	1		2	3	1			1											
C. rossii				1		1													
C. stelligera	2	1	3		2		1		1	1									
Cyclotella striata			1	1															
C. stylorum	1		1			2		2	1										
Cyclotella sp. (B04-15)							2												
Cyclotella sp. (3A-3)																			
Cyclotella sp. (3A-13)																			
Cymbella cymbiformis					1						1	1						1	
C. minuta		1								1						1			
Cymbella sp. (11C-3)																			
Delphineis spp.	2	1	2			1		3		1					1			1	
Denticula cf. *nerilica*																			
Diatoma tenue			1															1	
D. mesodon	3									3			1						
Diatoma sp. (3B-10)				2															
Diatomella minuta	2	2		3	2					6	2					1			
Dimeragramma sp. (11C-6)																			
Diploneis bombus				3															
Diploneis smithii																			
Diploneis sp.																			
Ditylum brightwellii	1	3		1	1	2	2	19	6	5	1				2	3	2	2	3
Eucampia spp.	2	1	1	1															
Eunotia spp.	5	1	4	5	1	1				1						1			
Fallacia sp. (B04-29)	1	1											2			1			1
Fallacia sp. (B04-28)			1																
Fallacia sp.	1	1	1			2			2	1								3	
Fallacia sp. (3A-2)																			
Fragilaria capucina complex	3		1	2	1				4	2						1		1	
F. construens var. *construens*																			
F. investiens	2			1	2	2	2	1	2	2									1
F. pinnata			3		2	1				1									
Fragilaria cf. *sopotensis*		3		7	1		1		2								1		
Fragilaria sp. (11C-13)																			
Fragilariopsis atlantica	3	10	13	6	14	4	5	2	1	5	1		1				5		3
F. cylindriformis						1			1	4		1			1				1
F. pseudonana	37	34	27	30	11	33	9	14	10	7	4	15	9	5	7	9	15	18	18
Fragilariopsis cf. *tenera*																			
Fragilariopsis sp. (3A-7)		2	2	1			1		2	8	3	2					1		
Gomphonema augustatum																			
G. augustum	1									1						2			
G. olivaceum													1						
Gomphonema sp.				1	2	2												4	
Gomphonema sp. (3A-8)																			
Gomphonema sp. (11C-6)																			
Gomphonema sp. (11C-10)																			
Gomphonemopsis exigua				1	2	1						1							
G. lindae	2	2							4	9	1				1			2	2
G. obscurum	2	3	1	4	2	6	6	4	15	8	1		2			2	6		1
Grammatophora angulosa			1	1															
G. marina		1							1										
G. oceanica														1					
Grammatophora sp. (B04-14)	2		2				1												
Hannea arcus	1	2		1													1		1
Hyalodiscus scoticus	2		2	1	1											1		2	

APPENDIX E1 (continued)

Sample	3B-7	3B-8	3B-9	3B-10	3B-11	3B-12	3B-13	3B-14	3C-1	3C-2	3C-3	3C-4	3C-5	3C-6	3C-7	3C-8	3C-9	3C-10	3C-11
Date Opened	1/13/00	1/29/00	2/13/00	2/29/00	3/16/00	3/31/00	4/16/00	5/2/00	5/15/00	5/24/00	6/3/00	6/13/00	6/23/00	7/3/00	7/12/00	7/22/00	8/1/00	8/11/00	8/21/00
Licomorpha spp.																			2
Luticola mutica	1			2						1									
Luticola (?) sp. (3A-13)																			
Mastogloia exigua							1												
M. smithii																			
Melosira nummuloides	2	6		4	3	2	10	3	6	8				1					1
Melosira sp.		2	1		2							1						1	1
Minidiscus chilensis	69	64	61	64	57	135	91	53	80	35	9	5	8	1	2	8	13	3	9
Navicula cryptocephala			1	2		1													
Navicula cf. *digitoradiata*					2														
N. directa			1	1	1	1	1			2									
N. gregaria	1		5	2	1	3	2		1	1		1					1	1	1
N. perminuta	10	13	19	4	5	10	6	1	30	20	1	1	2		3	5	9	3	4
N. phylleptosoma	1						1		2										
Navicula cf. *ramossisima*	1	3	2	1		2	3			4		1	1	1		2		3	5
Navicula aff. *salinarum*																			
Navicula sp. (3A-7)																			
Navicula sp. (3A-13)																			
Navicula sp. 1 (3B-1)																7			
Navicula sp. 2 (3B-1)																			
Navicula sp. (3B-5)																			
Navicula sp. 1 (3C-1)									15	16	2	2	2		1		5	9	2
Navicula sp. 2 (3C-1)									1										
Navicula sp. (11C-3)																			
Navicula sp. (11C-9)																			
Navicula sp. (11C-14)																			
Nitzschia amphibia																			
N. coarctata			7			1													
N. dissipata				2		1	1		1					2					
N. fonticola	1	1		1															
N. frustulum	33	18	10	16	16	21	20	13	40	63	15	9	4	3	3	5	7	11	23
N. inconspicua					1			2	2				1		2	2			1
N. microcephala						1			1	1									
N. perminuta					2	1	1		1										
Nitzschia cf. *sicula* (B04-12)					1												1		
N. valdestriata		2		1		1			1	1	1				1	3			
Nitzschia sp. (3A-3)																			
Nitzschia sp. (B04-3)	1																		
Nitzschia hungarica																			
Nitzschia/Fragilaria sp. (3B-8)		1																	
Odontella aurita/pulchella				1															
O. longicruris			1														1		2
Odontella sp. (3C-3)											5			1					
Opephora gemmeta															1				
O. gunter-grassi																			
Opephora cf. *horstiana*	1			2		2			1	2					1	4			1
O. marina		3	2	1					3	1							2		
O. minuta	3			2		1													
O. mutabilis			3	2	1				1	1	1								
Opephora sp. (11C-9)																			
Paralia sulcata		5		2	4	4	1	1	1	1		4							1
Planothidium delicatulum	10	15	1	6	8	11	12	4	24	20	4		6		1	2	6	8	8
Planothidium cf. *engelbretchii*				4	2	6			1	5								4	
P. hauckianum		2	2	1		3			2	5						1	1		1
Pleurosigma spp.		3	1	2	3	1			2	1									

APPENDIX E1 (continued)

Sample	3B-7	3B-8	3B-9	3B-10	3B-11	3B-12	3B-13	3B-14	3C-1	3C-2	3C-3	3C-4	3C-5	3C-6	3C-7	3C-8	3C-9	3C-10	3C-11
Date Opened	1/13/00	1/29/00	2/13/00	2/29/00	3/16/00	3/31/00	4/16/00	5/2/00	5/15/00	5/24/00	6/3/00	6/13/00	6/23/00	7/3/00	7/12/00	7/22/00	8/1/00	8/11/00	8/21/00
Pseudonitzschia multiseries	7	6	10	4	5	5	2		2	2		7		1	8	7	7	2	10
P. seriata	3	4	4	5	1		1		3	3	4	11	11	4	11	10	16	19	34
Reimeria sinuata										1									
Rhizosolenia spp. (spines)	13	19	18	8	11	3	5	4		3							3	1	2
Rhoichosphenia curvata					2														
Rhopalodia brebissonii																			
R. pacifica				1															
Seminavis spp.				3	1			4			1								
Skeletonema costatum	144	103	129	122	111	44	98	142	61	56	377	207	295	470	384	260	258	290	251
Skeletonema costatum (weak)	33	43	47	43	48	54	72	157	13	19	28	201	92	34	56	75	54	43	29
Stephanodiscus spp.		2																	
Stephanopyxis turris					1		1												
Surirella brebissonii				1						2									
Synedra ulna				1						2									
Tabellaria flocculosa					1														
Tabularia fasciculata	3	2	2	2	7		5		4	12	3		7	2		1	2	5	
Thalassionema bacillare					1														
T. nitzschioides	13	22	25	25	67	38	43	18	46	36	8	6	13	6	5	32	32	21	19
T. pseudonitzschioides					3				12	9		2	4			2	2	2	3
Thalassiosira aestivalis		1		1		1													
T. angulata		1										1		1	1	1			1
T. binata				2		1							1						
T. bioculata																			
T. conferta	3	5	2		1	1	2	1			2	5	1						
T. decipiens	4	9	7	8	15	13	17	7	10	7	2		1				1	2	2
T. decipiens (large)	2	1			1			1	1										
T. eccentrica	1	1	2	3	1	2	1		4	5	11	5	8		2	5	5	6	5
T. eccentrica (large)					1	1						1							
T. gravida				2															
T. kushirensis					1														
Thalassiosira cf. *leptopus*	3	3	5	3	2	1	2	2	1		2		2		1	1	1	1	1
Thalassiosira aff. *leptopus*																			
T. lundiana		1			1	1	1		3	2									
T. minima	2		1		1	2							1			1			
T. nodulolineata								1								1	1		
T. nordenskioeldii		1	2	5	2	1		2	4	1	2	2	6	2	2	4	3	3	4
T. oceanica	1	1				1	1	1	1	2	2		2	2	1	1			
T. oestrupii	1	2	3	2	4	3			6	1		2		1	4	4	1	2	3
T. pacifica	4	4	5	8	6	7	25	10	3	3		1	1	2		2	4	3	
T. poroseriata																			
T. punctigera		2			3		2			2							1		
T. rotula						2	5	5			2	2	1			1	2		1
T. tealata		1		1		1				1		2	2	1				1	
T. tenera	2		3			3		2	7	1	10	4		1			3	6	4
Thalassiosira cf. *tenera*	1	5	9	3	8	8	6	3	1	1		1		1		1	1		3
Thalassiosira sp. 1 (3A-2)																			
Thalassiosira sp. 2 (3A-2)																			
Thalassiosira sp. (3A-6)																			
Thalassiosira sp. (3C-2)										2									
Thalassiosira sp. (3C-8)																1			
Thalassiosira sp. (3C-11)																			4
Thalssiothrix longissima								1							1	2	3		2
Trachyneis aspera	1																		
Tryblionella cf. *acuminata*																			
T. aerophila		2					1		1				1			1			

APPENDIX E1 (continued)

Sample	3B-7	3B-8	3B-9	3B-10	3B-11	3B-12	3B-13	3B-14	3C-1	3C-2	3C-3	3C-4	3C-5	3C-6	3C-7	3C-8	3C-9	3C-10	3C-11
Date Opened	1/13/00	1/29/00	2/13/00	2/29/00	3/16/00	3/31/00	4/16/00	5/2/00	5/15/00	5/24/00	6/3/00	6/13/00	6/23/00	7/3/00	7/12/00	7/22/00	8/1/00	8/11/00	8/21/00
Tryblionella sp. (3A-9)																			
Tryblionella sp.																			
Tryblionella sp. (3C-11)																			1
Unknown centric (B04-7)																			
Unknown centric 2 (B04-21)																			
Unknown centric 3 (B04-23)																			
Unknown pennate (3A-13)																			
Unknown pennate 1 (3B-1)																			
Unknown pennate 2 (3B-1)																			
Unknown pennate 1 (3B-5)																			
Unknown pennate 2 (3B-5)	1					1												1	
Unknown pennate 1 (3B-7)	1																		
Unknown pennate 2 (3B-7)	2																		
Unknown pennate (3C-8)																2			
Unknown pennate (3C-9)																	1		
TOTAL	502	501	502	505	506	509	502	502	503	500	517	514	506	548	514	501	500	500	509
DIATOM RESTING SPORES																			
Chaetoceros spp.	38	34	39	39	38	30	26	411	201	106	20	16	52	39	18	57	76	68	44
Leptocylindrus spp.	1	2	2		4	2										1		1	
Stephanopyxis spp.																			
TOTAL	39	36	41	39	42	32	26	411	201	106	20	16	52	39	18	58	76	69	44
SILICOFLAGELLATES																			
Dictyocha fibula						1	1												
D. speculum	3	5	2	2	9	2	4		5	3	2	8	3		3	3	3	8	5
Octactis sp.																			1
TOTAL	3	5	2	2	9	3	5	0	5	3	2	8	3	0	3	3	3	8	6

APPENDIX E1 (continued)

Sample	3C-12	3C-13	3C-14	11C-1	11C-2	11C-3	11C-4	11C-5	11C-6	11C-7	11C-8	11C-9	11C-10	11C-11	11C-12	11C-13	11C-14
Date Opened	8/31/00	9/9/00	9/19/00	5/15/00	5/24/00	6/3/00	6/13/00	6/23/00	7/3/00	7/12/00	7/22/00	8/1/00	8/11/00	8/21/00	8/31/00	9/9/00	9/19/00
DIATOMS																	
A. brevipes							1										
A. kriegeri	1		3	4	1				3	1							1
A. lanceolata					1												
A. lemmermannii																	
A. minutissima	4	8	4	1	6	1	4	5	4	1		5	2	1	2		6
A. nodosa																	
Achnanthidium biasolettianum										3							
Achnanthes sp. (11C-3)						2											
Achnanthes sp. (11C-13)																1	
Actinocyclus curvatulus																	
A. normanii																	
A. octonarius																	
Actinocyclus sp. (3A-5)																	
Actinocyclus sp. (3B-2)																	
Actinocyclus sp. (11C-11)														1			1
Actinocyclus sp. (11C-13)																1	
Actinoptychus senarius							2			1				1		1	1
A. vulgaris										1	1	2				1	
Amphora acutiuscula						2		1			1	1					1
A. coffeaeformis				1				1									
A. copulata		2	1	3				1	1			1		4		3	
A. exigua				1	1		1	1					1	1		1	
A. helenensis					1		2		2	1			2				7
A. maletracta var. *constricta*				2		1		1		1				1	1		
A. marina			1													1	1
Amphora sp. (3A-9)																	
Amphora sp. (3A-11x)																	
Amphora sp. (3B-1)																	
Asteromphalus heptacis		1															
A. sarcophagus	1	2	3					1		1							
Aulacoseira ambigua															1		
A. italica var. *subarctica*																2	
Bacillaria paxillifer									1			1					
Bacteriastrum delicatulum	2	8	1	1			3	1	2	9	1	1	2		1	2	
Berkeleya rutilans	1			4					1				1		1		
Brachysira sp.																	
Cocconeis californica						2		1	1						2		1
C. costata complex	1		1	2	1		3		1		2	1	1	2			1
C. diculus		1	1	1	1	1				1	2	1				4	1
C. distans	1			3	2	3	2	1			1		1	1		2	1
C. neothumensis		1		1													
Cocconeis cf. *pellucida*																	
C. peltoides							1	1	1	2		2		1			
C. pinnata						1								1		2	
C. placentula	1	3	2	2	7	2		2	2	3	4	4	1	4	7	2	2
C. scutellum		2		5	7	4	1	4	7	4	3	4	5	5	1	2	5
C. stauroneiformis		1	1	1	3	1	1		1	1							1
Cocconeis sp.? (3A-12x)																	
Cocconeis sp. (11C-3)						1											
Cocconeis spp. (small)			1	1										1		1	
Coscinodiscus diorama						1											
C. radiatus						1	1		2		2		1				1
Ctenophora pulchella			1												1		
C. choctawhatcheeana		1	1	1	2	2	3			1	1	1	1		2	1	2

APPENDIX E1 (continued)

Sample	3C-12	3C-13	3C-14	11C-1	11C-2	11C-3	11C-4	11C-5	11C-6	11C-7	11C-8	11C-9	11C-10	11C-11	11C-12	11C-13	11C-14
Date Opened	8/31/00	9/9/00	9/19/00	5/15/00	5/24/00	6/3/00	6/13/00	6/23/00	7/3/00	7/12/00	7/22/00	8/1/00	8/11/00	8/21/00	8/31/00	9/9/00	9/19/00
Cyclotella "punctata"						2						1		1			
C. rossii												3					
C. stelligera			1			4		2		1		2	1	1	1		
Cyclotella striata	2			1	1				3		2	1	4		1		2
C. stylorum								1									
Cyclotella sp. (B04-15)														1			
Cyclotella sp. (3A-3)																	
Cyclotella sp. (3A-13)																	
Cymbella cymbiformis																	
C. minuta						2		1	1								
Cymbella sp. (11C-3)						2											
Delphineis spp.		1			1	1	1		1	1	2			1		1	3
Denticula cf. *nerütica*																	
Diatoma tenue		1															
D. mesodon																	
Diatoma sp. (3B-10)				1			1										1
Diatomella minuta				2							2						
Dimeragramma sp. (11C-6)									2							1	1
Diploneis bombus				1													
Diploneis smithii											1						
Diploneis sp.																	
Ditylum brightwellii	2	2	1	4	2	1			1			1	1	1		2	
Eucampia spp.			1							12	1	28	5	8	4	3	6
Eunotia spp.		2		1													
Fallacia sp. (B04-29)					1			1		1		1					
Fallacia sp. (B04-28)								1									
Fallacia sp.											1		4			1	
Fallacia sp. (3A-2)																	
Fragilaria capucina complex	1			1													1
F. construens var. *construens*						1											
F. investiens		1	1	7		3			1	1	2		2		1	2	1
F. pinnata				3			2									2	1
Fragilaria cf. *sopotensis*			2	1						1							
Fragilaria sp. (11C-13)																1	
Fragilariopsis atlantica		1		1				1		3	3	2	1		3	1	
F. cylindriformis		1			1					1		2					8
F. pseudonana	3	17	9	9	13	13	11	9	12	12	9	13	10	3	3	5	5
Fragilariopsis cf. *tenera*																	
Fragilariopsis sp. (3A-7)		1		1			3										
Gomphonema augustatum																	
G. augustum						1	2										
G. olivaceum																	
Gomphonema sp.						2											
Gomphonema sp. (3A-8)																	
Gomphonema sp. (11C-6)									2								
Gomphonema sp. (11C-10)													2				
Gomphonemopsis exigua	1			3				2			1				1	5	1
G. lindae	1		2	2	1						1		1				
G. obscurum	3	2	1	1	1	2	1	2	5				2		2		3
Grammatophora angulosa																	
G. marina				1												1	
G. oceanica				3	3	1											
Grammatophora sp. (B04-14)																	
Hannea arcus																	
Hyalodiscus scoticus					1			1			1						

APPENDIX E1 (continued)

Sample	3C-12	3C-13	3C-14	11C-1	11C-2	11C-3	11C-4	11C-5	11C-6	11C-7	11C-8	11C-9	11C-10	11C-11	11C-12	11C-13	11C-14
Date Opened	8/31/00	9/9/00	9/19/00	5/15/00	5/24/00	6/3/00	6/13/00	6/23/00	7/3/00	7/12/00	7/22/00	8/1/00	8/11/00	8/21/00	8/31/00	9/9/00	9/19/00
Licomorpha spp.							2						1	1			
Luticola mutica								2	1								
Luticola (?) sp. (3A-13)																	
Mastogloia exigua																	
M. smithii								1									
Melosira nummuloides			1		4						1						
Melosira sp.			1			4		1	1		1		1				
Minidiscus chilensis	4	17	20	201	236	177	127	117	113	95	102	193	207	215	165	184	168
Navicula cryptocephala																	
Navicula cf. *digitoradiata*																	
N. directa						1				1		1			1		
N. gregaria		1	2			1				1							
N. perminuta	1	8	4		6	4	1	10	3	1	4	6	2	4	8	9	4
N. phylleptosoma																	
Navicula cf. *ramossisima*	1	3	6					1		3							4
Navicula aff. *salinarum*																	
Navicula sp. (3A-7)																	
Navicula sp. (3A-13)																	
Navicula sp. 1 (3B-1)																	
Navicula sp. 2 (3B-1)																	
Navicula sp. (3B-5)																	
Navicula sp. 1 (3C-1)	6	8	6	6	8			6	5	4		6	5	11		3	2
Navicula sp. 2 (3C-1)											9						
Navicula sp. (11C-3)						6											
Navicula sp. (11C-9)												2					
Navicula sp. (11C-14)																	2
Nitzschia amphibia																	
N. coarctata		1			1												
N. dissipata		1			2		1										
N. fonticola																	
N. frustulum	12	22	14	13	6	9	10	12	6	2	10	8	8	4	11	8	6
N. inconspicua	1																
N. microcephala																	
N. perminuta																2	
Nitzschia cf. *sicula* (B04-12)			1												1		
N. valdestriata					1	1		1				1			1		
Nitzschia sp. (3A-3)																	
Nitzschia sp. (B04-3)																	
Nitzschia hungarica																	
Nitzschia/Fragilaria sp. (3B-8)																	
Odontella aurita/pulchella																	
O. longicruris				1			1			1						1	
Odontella sp. (3C-3)																	2
Opephora gemmeta																	
O. gunter-grassi																	
Opephora cf. *horstiana*	1		3		3			1					1				
O. marina			1		2			1			2						
O. minuta		2															
O. mutabilis	1	1			1	1		2	2	2		2				1	
Opephora sp. (11C-9)												1					
Paralia sulcata				2	5	11	7		6		5	3	1		4	15	7
Planothidium delicatulum	9	4	4	4	6	9	6	2		4	6	6	1	4	1	2	6
Planothidium cf. *engelbretchii*													2				
P. hauckianum	2				1			2	1		2			1			1
Pleurosigma spp.	2								1						1		

APPENDIX E1 (continued)

Sample	3C-12	3C-13	3C-14	11C-1	11C-2	11C-3	11C-4	11C-5	11C-6	11C-7	11C-8	11C-9	11C-10	11C-11	11C-12	11C-13	11C-14
Date Opened	8/31/00	9/9/00	9/19/00	5/15/00	5/24/00	6/3/00	6/13/00	6/23/00	7/3/00	7/12/00	7/22/00	8/1/00	8/11/00	8/21/00	8/31/00	9/9/00	9/19/00
Pseudonitzschia multiseries	7	10	4	2	2	2	17	5	6	2	3	2	4	2	5	2	2
P. seriata	19	29	15	2	1	9	26	14	7	26	16	10	6	11	11	13	4
Reimeria sinuata																	
Rhizosolenia spp. (spines)		3	2	3	4	8	2	7	1	4	9	13	7	28	143	53	49
Rhoichosphenia curvata							2										
Rhopalodia brebissonii																	
R. pacifica																	
Seminavis spp.																	
Skeletonema costatum	336	248	287	22	27	32	51	56	151	175	118	64	65	56	32	40	52
Skeletonema costatum (weak)	23	22	37	12	9	18	75	42	42	17	17	9	5	10	5	6	15
Stephanodiscus spp.			1		1									1		1	
Stephanopyxis turris																	
Surirella brebissonii																	
Synedra ulna																	
Tabellaria flocculosa							1			1							
Tabularia fasciculata	3	2	4	4		3			3					2			1
Thalassionema bacillare	2													1			1
T. nitzschioides	21	33	29	80	62	84	59	76	31	37	82	54	85	61	54	62	73
T. pseudonitzschioides	4	3	4	14	11	5	4	3	3	2	3	2	4	3	2	1	2
Thalassiosira aestivalis					1								3	1			1
T. angulata							1	1	1	1		1					
T. binata							1		1			2					
T. bioculata																	
T. conferta				2		1	1	2		5				2	1	1	1
T. decipiens		2	1	27	23	17	12	17	16	8	14	13	13	16	6	11	12
T. decipiens (large)						5		1	3			2		6		3	4
T. eccentrica	4	6	11	9	2	4	5	4	10	2	11	3	13	5	5	6	3
T. eccentrica (large)						1			1								
T. gravida										1							
T. kushirensis		1		2	2			1		1	1	2	1	1		2	
Thalassiosira cf. *leptopus*	5	2	2					4	1	1			1				1
Thalassiosira aff. *leptopus*																	
T. lundiana																	
T. minima												1	1				
T. nodulolineata							1						1				
T. nordenskioeldii	3	4	3	3	2		6	1	4	10	8	3	2	1	2	1	1
T. oceanica	1	3	1														
T. oestrupii	2	2		2	3	1		2	3		3			3	1	3	7
T. pacifica	1	1		7	8	8	26	54	11	12	14	5	1	9	4	9	1
T. poroseriata																	
T. punctigera							1	1									
T. rotula	2		1			1	1	1		2						1	
T. tealata							2	2					1				1
T. tenera	1	4	4	4	5	9	4	5	8	8	12	7	6	6	3	8	6
Thalassiosira cf. *tenera*	3		1	2	2		1						1				
Thalassiosira sp. 1 (3A-2)																	
Thalassiosira sp. 2 (3A-2)																	
Thalassiosira sp. (3A-6)																	
Thalassiosira sp. (3C-2)																	
Thalassiosira sp. (3C-8)																	
Thalassiosira sp. (3C-11)																	
Thalssiothrix longissima	5	1					2		1	7	3		1	1			
Trachyneis aspera																	
Tryblionella cf. *acuminata*																	
T. aerophila					2	2											

APPENDIX E1 (continued)

Sample	3C-12	3C-13	3C-14	11C-1	11C-2	11C-3	11C-4	11C-5	11C-6	11C-7	11C-8	11C-9	11C-10	11C-11	11C-12	11C-13	11C-14
Date Opened	8/31/00	9/9/00	9/19/00	5/15/00	5/24/00	6/3/00	6/13/00	6/23/00	7/3/00	7/12/00	7/22/00	8/1/00	8/11/00	8/21/00	8/31/00	9/9/00	9/19/00
Tryblionella sp. (3A-9)																	
Tryblionella sp.																	
Tryblionella sp. (3C-11)																	
Unknown centric (B04-7)																	
Unknown centric 2 (B04-21)		1					1										
Unknown centric 3 (B04-23)																	
Unknown pennate (3A-13)																	
Unknown pennate 1 (3B-1)																	
Unknown pennate 2 (3B-1)																	
Unknown pennate 1 (3B-5)																	
Unknown pennate 2 (3B-5)						1											
Unknown pennate 1 (3B-7)																	
Unknown pennate 2 (3B-7)																	
Unknown pennate (3C-8)																	
Unknown pennate (3C-9)																	
TOTAL	507	504	509	501	507	495	503	500	500	500	500	500	501	506	502	500	505
DIATOM RESTING SPORES																	
Chaetoceros spp.	42	83	62	111	68	64	25	66	70	138	118	103	135	86	52	76	93
Leptocylindrus spp.			1			1		2	1		3		1	7			
Stephanopyxis spp.																	
TOTAL	42	83	63	111	68	65	25	68	71	138	121	103	136	93	52	76	93
SILICOFLAGELLATES																	
Dictyocha fibula				1						1					1		1
D. speculum	2	8	11	4	3	4	9	3	5	1	6	7	5	7	3	5	9
Octactis sp.		1														2	
TOTAL	2	9	11	5	3	4	9	3	5	2	6	7	5	7	4	7	10

APPENDIX E2. Sediment trap microfossil absolute abundance (concentration) and flux

$C_a = \frac{Nadv_s}{fAwv_p}$

N = number of valves or skeletons counted
a = area of cover slip (18 × 18 mm = 324000000 μm^2)
d = dilution factor
v_s = initial volume of slurry (mL)
f = number of fields of view examined
A = area of field of view (radius at 1000 × is 105 μm = 34636 μm^2)
w = initial sediment mass (g)
v_p = volume of slurry plated onto cover slip (mL)

$Flux = \frac{C_a m}{tc}$

C_a = concentration (valves or skeletons/g)
m = total dry mass (g)
t = number of days opened
c = sediment trap cone collection area (0.49 m^2)

Sample	Date opened	Days opened	Total dry mass in cylinder (g)	Estimated initial mass after split* (g)	Initial slurry volume (mL)	Dilution Factor	Volume plated (mL)	Diatom count (valves)	CRS count (valves)	Silico. count (skeletons)	Fields of view examined	Diatom concentration (millions of valves/g)	Diatom flux (millions of valves/m^2/d)	CRS concentration (millions of valves/g)	CRS flux (millions of valves/m^2/d)	Silicoflagellate concnetration (millions of skeletons/g)	Silicoflagellate flux (millions of skeletons/m^2/d)
		t	m	w	v_s	d	v_p	N	N	N	f	C_a		C_a		C_a	
Inner Basin																	
3A-1	5/29/99	8.86	2.4916	0.1162	20.5	15	0.5	500	12	0	145	170.67	97.95	4.10	2.35	0.00	0.000
3A-2	6/6/99	8.86	3.6775	0.1325	20.5	15	0.5	500	36	1	116	187.16	158.54	11.23	11.41	0.37	0.317
3A-3	6/15/99	8.86	1.7520	0.0620	19.5	15	0.5	502	25	1	115	385.15	155.43	15.34	7.74	0.77	0.310
3A-4	6/24/99	8.86	0.6999	0.0231	20.0	2.5	0.5	501	32	7	116	174.70	28.16	10.46	1.80	2.44	0.394
3A-5	7/3/99	8.86	2.1488	0.0771	20.5	15	0.5	501	47	3	180	207.80	102.85	17.83	9.65	1.24	0.616
3A-6	7/12/99	8.86	10.4767	0.3717	20.5	15	0.5	500	30	7	51	151.73	366.15	8.50	21.97	2.12	5.126
3A-7	7/21/99	8.86	11.3764	0.4259	20.8	15	0.5	500	35	1	43	158.98	416.61	10.49	29.16	0.32	0.833
3A-8	7/30/99	8.86	3.6052	0.1305	20.0	15	0.5	500	34	2	58	370.69	307.82	23.72	20.93	1.48	1.231
3A-9	8/7/99	8.86	2.2025	0.0821	19.5	15	0.5	504	34	2	74	453.81	230.23	30.61	15.53	1.80	0.914
3A-10	8/16/99	8.86	1.6518	0.0551	21.3	5	0.5	501	30	8	84	215.12	81.85	12.02	4.90	3.43	1.307
3A-11X	8/25/99	8.86	1.1221	0.1722	20.5	2.5	0.5	500	38	1	99	28.12	7.27	2.08	0.55	0.06	0.015
3A-12X	9/3/99	8.86	0.3801	0.0742	20.5	2.5	0.5	502	36	1	169	38.38	3.36	2.52	0.24	0.08	0.007
3A-13	9/12/99	8.86	0.3434	0.0120	21.0	5	0.5	250	26	1	188	218.23	17.26	20.95	1.80	0.87	0.069
3B-1	10/11/99	15	3.7945	0.1025	21.5	5	0.5	500	27	2	40	245.30	126.64	13.25	6.84	0.98	0.507
3B-2	10/26/99	15	4.7903	0.1169	19.5	15	0.5	496	41	3	52	446.62	291.08	33.32	24.06	2.70	1.761
3B-3	11/11/99	15	6.6867	0.1785	19.5	15	0.5	511	32	4	51	307.12	279.40	16.23	17.50	2.40	2.187
3B-4	11/27/99	15	7.1006	0.1828	20.5	15	0.5	506	32	3	60	265.46	256.46	14.69	16.22	1.57	1.520
3B-5	12/12/99	15	7.2576	0.1902	21.0	5	0.5	500	33	6	66	78.24	77.25	4.38	5.10	0.94	0.927
3B-6	12/28/99	15	5.4358	0.1426	19.5	15	0.5	505	39	1	59	328.37	242.85	23.41	18.75	0.65	0.481
3B-7	1/13/00	15	5.1897	0.1418	20.0	15	0.5	502	38	3	71	279.76	197.54	19.51	14.95	1.67	1.180
3B-8	1/29/00	15	5.5824	0.1391	20.0	15	0.5	501	34	5	97	208.41	158.29	13.73	10.74	2.08	1.580
3B-9	2/13/00	15	5.9475	0.1529	19.5	15	0.5	503	39	2	89	202.28	163.68	15.68	12.69	0.80	0.651
3B-10	2/29/00	15	9.7448	0.2513	20.5	15	0.5	505	39	2	60	192.68	255.46	14.88	19.73	0.76	1.012
3B-11	3/16/00	15	8.2253	0.2318	22.5	5	0.5	506	38	9	42	109.39	122.41	8.21	9.19	1.95	2.177
3B-12	3/31/00	15	5.1413	0.1273	20.5	15	0.5	509	30	3	85	270.71	189.36	15.96	11.16	1.60	1.116
3B-13	4/16/00	15	5.0437	0.1249	20.5	15	0.5	502	26	5	62	372.94	255.92	19.32	13.25	3.71	2.549
3B-14	5/2/00	15	14.2878	0.2902	20.5	30	0.5	502	411	0	45	442.25	859.69	354.15	703.85	0.00	0.000

APPENDIX E2 (continued)

Sample	Date opened	Days opened	Total dry mass in cylinder (g)	Estimated initial mass after split* (g)	Initial slurry volume (mL)	Dilution Factor	Volume plated (mL)	Diatom count (valves)	CRS count (valves)	Silico. count (skeletons)	Fields of view examined	Diatom concentration (millions of valves/g)	Diatom flux (millions of valves/m²/d)	CRS concentration (millions of valves/g)	CRS flux (millions of valves/m²/d)	Silicoflagellate concnetration (millions of skeletons/g)	Silicoflagellate flux (millions of skeletons/m²/d)
		t	m	w	v_s	d	v_p	N	N	N	f	C_a		C_a		C_a	
3C-1	5/15/00	9.82	1.2245	1.2245	21.5	5	0.5	503	201	5	79	10.46	2.66	3.83	1.06	0.10	0.026
3C-2	5/24/00	9.82	1.2961	1.2961	20.5	5	0.5	500	106	3	69	10.72	2.89	2.04	0.61	0.06	0.017
3C-3	6/3/00	9.82	1.2497	1.2497	20.0	5	0.5	517	20	2	16	48.38	12.56	1.68	0.49	0.19	0.049
3C-4	6/13/00	9.82	4.3800	4.3800	20.3	15	0.5	514	16	8	13	51.30	46.70	1.60	1.45	0.80	0.727
3C-5	6/23/00	9.82	2.9406	2.9406	20.5	15	0.5	506	52	3	23	43.04	26.30	3.91	2.70	0.26	0.156
3C-6	7/3/00	9.82	2.4494	2.4494	20.0	15	0.5	548	39	0	13	96.59	49.17	5.99	3.50	0.00	0.000
3C-7	7/12/00	9.82	0.0526	0.0526	24.8	2.5	0.5	514	18	3	16	706.85	7.73	19.25	0.27	4.13	0.045
3C-8	7/22/00	9.82	0.0433	0.0433	20.5	2.5	0.5	501	57	3	65	170.83	1.54	18.07	0.17	1.02	0.009
3C-9	8/1/00	9.82	0.0407	0.0407	20.5	2.5	0.5	501	76	3	59	200.10	1.69	29.56	0.26	1.20	0.010
3C-10	8/11/00	9.82	0.0481	0.0481	20.5	2.5	0.5	500	68	8	44	226.43	2.26	29.44	0.31	3.62	0.036
3C-11	8/21/00	9.82	0.0586	0.0586	20.0	2.5	0.5	509	44	6	46	176.63	2.15	14.57	0.19	2.08	0.025
3C-12	8/31/00	9.82	0.0710	0.0710	23.0	2.5	0.5	507	42	2	42	182.99	2.70	14.44	0.22	0.72	0.011
3C-13	9/9/00	9.82	0.0940	0.0940	20.5	2.5	0.5	504	83	9	52	98.82	1.93	15.49	0.32	1.76	0.034
3C-14	9/19/00	9.82	0.0777	0.0777	20.0	2.5	0.5	509	62	11	50	122.60	1.98	13.25	0.24	2.65	0.043
Average for CTC3C												153.27	11.59	12.37	0.84	1.33	0.085
Average for all samples												211.12	136.87	22.19	24.97	1.35	0.731
Mouth of Inlet																	
11C-1	5/15/00	9.82	7.0447	0.1822	21.5	15	0.5	501	111	5	65	255.20	373.63	56.54	82.78	2.55	3.729
11C-2	5/24/00	9.82	5.5464	0.1392	21.0	15	0.5	507	68	3	78	275.21	317.23	36.91	42.55	1.63	1.877
11C-3	6/3/00	9.82	12.4024	0.3010	21.3	30	0.5	496	64	4	53	370.80	955.75	47.85	123.32	2.99	7.708
11C-4	6/13/00	9.82	17.8210	0.4607	22.3	30	0.5	503	25	9	61	223.52	827.84	11.11	41.15	4.00	14.812
11C-5	6/23/00	9.82	7.5605	0.1974	22.0	15	0.5	500	66	3	85	183.95	289.03	24.28	38.15	1.10	1.734
11C-6	7/3/00	9.82	7.6046	0.1935	21.0	15	0.5	500	70	5	73	208.56	329.62	28.36	46.15	2.09	3.296
11C-7	7/12/00	9.82	7.5154	0.1900	22.0	15	0.5	500	138	2	80	203.06	317.16	54.83	87.54	0.81	1.269
11C-8	7/22/00	9.82	10.3998	0.2814	21.8	30	0.5	500	118	6	92	235.74	509.51	54.22	120.24	2.83	6.114
11C-9	8/1/00	9.82	4.1777	0.1111	22.8	15	0.5	500	103	7	92	312.31	271.15	64.33	55.86	4.37	3.796
11C-10	8/11/00	9.82	12.7689	0.3616	22.9	60	0.5	501	135	5	111	320.54	850.62	82.54	229.21	3.20	8.489
11C-11	8/21/00	9.82	5.2469	0.1425	22.0	15	0.5	506	86	7	85	258.00	281.32	40.79	47.81	3.57	3.892
11C-12	8/31/00	9.82	7.0161	0.1834	22.5	30	0.5	502	52	4	99	349.21	509.17	33.39	52.74	2.78	4.057
11C-13	9/9/00	9.82	8.6803	0.2234	21.5	30	0.5	500	76	7	103	262.25	473.08	39.86	71.91	3.67	6.623
11C-14	9/19/00	9.82	5.1766	0.1378	23.0	15	0.5	505	93	10	77	307.14	330.42	56.56	60.85	6.08	6.543
Average												268.96	473.97	45.11	78.59	2.98	5.281

X = analysis performed on extra sample
n.s. = no sample
* samples from series CTC3C not split

APPENDX E3. Sediment trap diatom specific diversity index

$$S.D.I. = \frac{S_i - 1}{\ln(N_i)}$$

S_i = number of taxa in sample *i*
N_i = total number of valves counted in sample *i*

Sample	Date Opened	N_i	S_i	S.D.I.
3A-1	5/29/99	500	50	7.88
3A-2	6/6/99	500	56	8.85
3A-3	6/15/99	502	58	9.17
3A-4	6/24/99	501	54	8.53
3A-5	7/3/99	501	66	10.46
3A-6	7/12/99	500	62	9.82
3A-7	7/21/99	500	54	8.53
3A-8	7/30/99	500	66	10.46
3A-9	8/7/99	504	68	10.77
3A-10	8/16/99	501	58	9.17
3A-11X	8/25/99	500	72	11.42
3A-12X	9/3/99	502	80	12.70
3A-13	9/12/99	250	57	10.14
3B-1	10/11/99	500	70	11.10
3B-2	10/26/99	496	64	10.15
3B-3	11/11/99	511	68	10.74
3B-4	11/27/99	506	78	12.37
3B-5	12/12/99	500	79	12.55
3B-6	12/28/99	505	68	10.76
3B-7	1/13/00	502	73	11.58
3B-8	1/29/00	501	71	11.26
3B-9	2/13/00	502	65	10.29
3B-10	2/29/00	505	80	12.69
3B-11	3/16/00	506	77	12.21
3B-12	3/31/00	509	73	11.55
3B-13	4/16/00	502	54	8.52
3B-14	5/2/00	502	42	6.59
3C-1	5/15/00	503	72	11.41
3C-2	5/24/00	500	82	13.03
3C-3	6/3/00	517	37	5.76
3C-4	6/13/00	514	38	5.93
3C-5	6/23/00	506	38	5.94
3C-6	7/3/00	548	26	3.96
3C-7	7/12/00	514	31	4.81
3C-8	7/22/00	501	54	8.53
3C-9	8/1/00	500	50	7.88
3C-10	8/11/00	500	45	7.08
3C-11	8/21/00	509	56	8.82
3C-12	8/31/00	507	44	6.90
3C-13	9/9/00	504	51	8.04
3C-14	9/19/00	509	50	7.86
11C-1	5/15/00	501	58	9.17
11C-2	5/24/00	507	54	8.51
11C-3	6/3/00	495	59	9.19
11C-4	6/13/00	503	52	8.20
11C-5	6/23/00	500	58	9.17
11C-6	7/3/00	500	53	8.37
11C-7	7/12/00	500	54	8.53
11C-8	7/22/00	500	47	7.40
11C-9	8/1/00	500	50	7.88
11C-10	8/11/00	501	52	8.20
11C-11	8/21/00	506	48	7.55
11C-12	8/31/00	502	41	6.43
11C-13	9/9/00	500	55	8.69
11C-14	9/19/00	505	58	9.16

Summary			
Inner Basin Mean Diversity			
spring/summer 1999	9.84	n=13	range: 7.9-12.7
fall/winter	11.43	n=11	range: 10.2-12.7
spring/summer 2000	7.80	n=17	range: 4.0-13.0
Inlet Mouth Mean Diversity			
spring/summer 2000	8.32	n=14	range: 6.4-9.2

APPENDIX E4. Sediment trap major taxa relative abundance (%)*

Sample	3A-1	3A-2	3A-3	3A-4	3A-5	3A-6	3A-7	3A-8	3A-9	3A-10
Date opened	5/29/99	6/6/99	6/15/99	6/24/99	7/3/99	7/12/99	7/21/99	7/30/99	8/7/99	8/16/99
Achnanthes minutissima	1.60	0.40	1.79	0.80	2.00	0.60	1.80	2.67	1.59	0.20
Actinocyclus curvatulus		0.40	0.80	1.00	0.40			0.60	0.40	
Actinoptychus vulgaris		0.80	0.20	0.40	1.20	0.40	1.00	0.40	0.20	0.80
Amphora helenensis						0.40		0.40		
Bacteriastrum delicatulum	0.40	0.20		0.40			0.40	0.60	0.40	
Berkeleya rutilans	0.40	0.40	0.20	0.20	0.20	0.20			0.20	
Cocconeis disculus		0.20	0.60	0.20	0.80		0.60	0.60	0.40	0.60
Cocconeis neothumensis										
Cocconeis placentula		0.40	1.00		0.20	0.20	0.40	0.60	1.39	0.40
Cocconeis scutellum	0.40			0.20		0.40	0.40	0.20	0.20	
Cocconeis stauroneiformis	0.40	0.60		0.20	0.60		0.20	0.40	0.40	0.60
Diatomella minuta						0.20				
Ditylum brightwellii				0.60	0.40					0.20
Eunotia spp.		0.20	0.20			0.20				
Fragilaria cf. *sopotensis*	0.20	0.80		0.20	0.60	0.20	0.40	0.80	1.19	
Fragilariopsis atlantica	20.40	18.80	30.88	40.72	26.35	21.00	24.00	20.60	18.45	20.96
Fragilariopsis pseudonana	7.80	7.20	8.17	2.00	3.79	3.60	2.20	3.40	2.58	2.59
Gomphonemopsis lindae		0.20		0.20						
Gomphonemopsis obscurum	0.20		0.20	0.40			1.00	0.40		1.00
Hyalodiscus scoticus				0.20	0.20					
Melosira nummuloides					0.20	0.60	0.80		0.60	
Minidiscus chilensis	3.80	9.60	5.58	2.79	6.99	10.60	7.00	8.00	9.92	8.38
Navicula gregaria		0.40				0.60		0.20	0.20	0.20
Navicula perminuta	1.00	2.20	2.39	1.00	1.20	1.40	0.20	1.60	1.79	2.99
Nitzschia coarctata									0.20	
Nitzschia frustulum	5.40	5.00	6.57	2.99	3.79	6.60	7.20	7.00	7.94	8.58
Opephora cf. *horstiana*										
Opephora mutabilis		0.40		0.20		0.60		0.80	1.59	0.60
Paralia sulcata	0.40		0.20			0.20		0.40		1.40
Planothidium delicatulum	1.00	1.20	1.79	1.00	1.20	0.80	2.60	1.00	1.98	2.40
Planothidium cf. *engelbretchii*					0.20					
Planothidium hauckianum	0.60	0.20	0.80	0.20	0.60		0.20	0.40	0.20	
Pleurosigma spp.		1.00	1.20	2.00	1.20	3.00	2.80	2.60	3.17	2.59
Pseudonitzschia multiseries	0.20	0.20			0.60	0.20	0.40	0.60	0.20	1.20
Pseudonitzschia seriata	0.20				0.20			0.20	0.20	
Rhizosolenia spp.	0.60	0.20	0.20		0.20	0.20		0.20	0.60	0.20
Skeletonema costatum	28.20	19.80	14.54	16.97	15.97	19.40	17.80	19.60	15.67	17.56
Skeletonema costatum (weak)	11.80	7.20	3.39	2.99	7.58	7.60	6.60	3.00	3.77	2.99
Tabularia fasciculata		0.40	0.40	0.60	0.20	0.60		0.60	0.99	1.60
Thalassionema bacillare	1.40	0.20	0.60	1.00	0.60	0.40	1.20	0.20	0.20	0.40
Thalassionema nitzschioides	2.20	5.20	2.39	4.19	5.19	5.80	5.00	4.60	4.96	4.19
Thalassionema pseudonitzschioides										
Thalassiosira angulata	0.20	1.40	0.80	0.80	0.20	0.20	0.80	0.20		
Thalassiosira conferta	2.00	0.80	0.60	0.60	1.00	1.60	0.40			0.40
Thalassiosira decipiens		0.40	0.80	0.20	0.40	0.20	0.00	0.20	1.79	0.80
Thalassiosira eccentrica	0.40	0.40	0.40	1.00	0.40	1.00	0.80		0.20	0.20
Thalassiosira cf. *leptopus*	0.20	1.60	0.60	1.80	1.60	0.60	2.60	1.40	1.59	1.60
Thalassiosira minima	0.60	2.20	0.60	1.00	1.00	0.20	0.20	0.60	0.20	
Thalassiosira nordenskioeldii	0.40		0.20			0.20		0.20	0.20	0.20
Thalassiosira oestrupii	1.20	2.20	4.18	4.19	2.59	2.20	2.00	2.20	2.78	2.20
Thalassiosira parifica	0.20	0.20	0.20	0.40	0.60	0.20	1.20	0.80	0.20	0.40
Thalassiosira rotula		0.20	0.20	0.20						
Thalassiosira tealata	0.20	0.80	1.00	0.60	0.40	0.80	0.20	0.20	0.99	0.40
Thalassiosira tenera		0.60			0.20		0.20			
Thalassiosira sp. (cf. *tenera*)		0.40	0.60		1.00	0.20	0.40	0.20	0.40	0.80
Total relative abundance	94.00	95.00	94.27	94.44	92.05	93.40	93.00	88.67	89.93	89.63
Benthics	13.80	14.80	18.13	9.18	15.17	15.40	18.60	22.80	25.00	22.55
CRS	2.34	6.72	4.74	6.00	8.58	5.66	6.54	6.37	6.32	5.65
Silicoflagellates		0.20	0.20	1.38	0.60	1.38	0.20	0.40	0.40	1.57

* major taxa defined as those which appeared in at least three samples and at least 1% in one sample; no entry for zero values

APPENDIX E4 (continued)

Sample	3A-11	3A-12	3A-13	3B-1	3B-2	3B-3	3B-4	3B-5	3B-6
Date opened	8/25/99	9/3/99	9/12/99	10/11/99	10/26/99	11/11/99	11/27/99	12/12/99	12/28/99
Achnanthes minutissima	3.80	4.78	3.60	2.20	2.22	6.26	7.91	8.60	9.50
Actinocyclus curvatulus	0.20	0.40	0.40						
Actinoptychus vulgaris	0.60	1.00	0.80		0.20		0.20		
Amphora helenensis	0.40	0.40		0.80		0.20		1.00	
Bacteriastrum delicatulum	0.20	0.40	0.40	0.60	0.60		0.20	0.40	
Berkeleya rutilans	0.20	1.00		0.60		0.98	0.20	0.40	0.40
Cocconeis disculus	0.20	1.20	0.80	1.00	0.60	0.20	0.20	0.20	
Cocconeis neothumensis		0.80	1.20	0.40	0.20	0.39		0.40	0.20
Cocconeis placentula	1.20	0.80	0.80	0.80	0.60	0.39	0.40	1.00	0.99
Cocconeis scutellum	0.40	0.80	0.80	0.60	1.01	0.59	1.19		0.79
Cocconeis stauroneiformis	0.40			0.80		0.20	1.58		0.59
Diatomella minuta		0.40							0.40
Ditylum brightwellii		0.20		0.20	0.20		0.40		
Eunotia spp.		0.20					0.20	0.20	0.20
Fragilaria cf. *sopotensis*	0.40				0.60		0.20	0.40	
Fragilariopsis atlantica	17.80	18.13	18.00	1.20	2.62	2.15	1.78	1.20	0.99
Fragilariopsis pseudonana	2.80	2.59	0.80	1.20	2.02	1.76	1.98	4.00	3.76
Gomphonemopsis lindae	0.20						0.40		
Gomphonemopsis obscurum	0.40	0.40	0.80	1.60		0.59		0.60	0.79
Hyalodiscus scoticus	0.40	0.20	0.40	1.20	1.01	0.78		0.40	
Melosira nummuloides				3.40	0.40	0.39	0.99	0.80	0.59
Minidiscus chilensis	5.80	10.36	8.80	6.60	14.11	8.41	9.68	9.20	12.48
Navicula gregaria	0.60	0.80	1.20	0.20	0.81	0.39	0.79	0.40	0.20
Navicula perminuta	2.40	1.39	1.60	3.00	1.61	2.94	2.77	2.80	1.58
Nitzschia coarctata			0.40				0.40		
Nitzschia frustulum	7.60	6.37	2.00	6.40	4.64	8.02	6.92	5.40	4.95
Opephora cf. *horstiana*		0.20	1.20	0.20			0.20		0.59
Opephora mutabilis				0.20	0.20	0.20		0.20	
Paralia sulcata	0.20				0.81		0.20	0.40	0.20
Planothidium delicatulum	2.80	2.79	2.00	4.20	1.41	4.50	1.98	2.00	1.78
Planothidium cf. *engelbretchii*	0.20	0.20							
Planothidium hauckianum	0.60	0.80					1.19	0.20	0.40
Pleurosigma spp.	2.20	3.98	2.80					0.40	
Pseudonitzschia multiseries	0.60	0.40	1.20	0.80	1.41	1.37	1.78	1.00	1.39
Pseudonitzschia seriata						0.59	0.40	0.60	0.20
Rhizosolenia spp.	0.40	0.60	0.80	1.00	1.41	3.52	4.74	3.00	2.57
Skeletonema costatum	16.00	10.96	14.80	22.80	34.88	27.40	21.94	22.80	26.14
Skeletonema costatum (weak)	5.60	3.78	4.40	4.20	5.65	5.87	5.53	7.40	9.50
Tabularia fasciculata	0.60	0.80		1.00	0.20	1.37	0.99	0.40	0.20
Thalassionema bacillare		0.80	0.80		0.20				0.40
Thalassionema nitzschioides	6.00	3.98	6.40	6.80	4.84	5.48	4.35	4.40	3.17
Thalassionema pseudonitzschioides									
Thalassiosira angulata							0.20		0.20
Thalassiosira conferta	1.60	0.80	0.40	0.20	0.40	0.39		0.20	
Thalassiosira decipiens	0.20	0.40	2.80	1.00	1.61	0.78	0.20	1.00	0.79
Thalassiosira eccentrica	1.00	0.80	0.80	0.80	0.20	1.17	0.59		1.19
Thalassiosira cf. *leptopus*	1.00	1.59	0.80	0.20	0.60	0.20	0.20	0.60	0.79
Thalassiosira minima					0.20			0.20	0.20
Thalassiosira nordenskioeldii	0.20		0.40		0.81	0.20	0.59	0.40	0.59
Thalassiosira oestrupii	2.60	1.59	4.00			0.20	0.20	0.60	0.40
Thalassiosira pacifica	1.80	0.60	2.40	1.60	1.61	1.17	0.99	2.00	0.40
Thalassiosira rotula	0.40		0.40			0.59	0.59	0.20	0.20
Thalassiosira tealata	0.20	0.20							
Thalassiosira tenera			0.40	0.60	0.40	0.39	0.40	0.60	0.99
Thalassiosira sp. (cf. *tenera*)	0.60	0.80	1.20	0.20	1.21	0.78	0.20	0.40	0.40
Total relative abundance	90.80	88.69	90.80	78.60	91.50	90.81	85.85	86.40	91.10
Benthics	27.40	29.08	22.00	30.20	18.15	32.09	34.98	31.40	28.12
CRS	7.06	6.69	9.42	5.12	7.64	5.89	5.95	6.19	7.17
Silicoflagellates	0.20	0.20	0.40	0.40	0.60	0.78	0.59	1.19	0.20

APPENDIX E4 (continued)

Sample	3B-7	3B-8	3B-9	3B-10	3B-11	3B-12	3B-13	3B-14	3C-1	3C-2
Date opened	1/13/00	1/29/00	2/13/00	2/29/00	3/16/00	3/31/00	4/16/00	5/2/00	5/15/00	5/24/00
Achnanthes minutissima	4.18	4.79	3.19	4.95	0.79	3.54	1.79	1.20	3.38	4.20
Actinocyclus curvatulus	0.20				0.20					0.20
Actinoptychus vulgaris						0.20				
Amphora helenensis			0.60						0.60	0.20
Bacteriastrum delicatulum	0.40			0.40		0.20	0.20	0.40	1.79	0.60
Berkeleya rutilans									0.20	1.00
Cocconeis disculus	0.20	0.20				0.39	0.20			
Cocconeis neothumensis	0.20	0.80		0.40	0.59		0.20		0.40	
Cocconeis placentula	1.00	0.60	0.40	0.59	0.79		0.40	0.20	0.80	0.60
Cocconeis scutellum	0.60	1.00	0.40		0.99	0.59	1.20		0.40	1.40
Cocconeis stauroneiformis		0.60	0.20	1.19	0.79	1.18	1.00	0.20	0.60	1.20
Diatomella minuta	0.40	0.40		0.59	0.40					1.20
Ditylum brightwellii	0.20	0.60		0.20	0.20	0.39	0.40	3.78	1.19	1.00
Eunotia spp.	1.00	0.20	0.80	0.99	0.20	0.20				0.20
Fragilaria cf. *sopotensis*		0.60		1.39	0.20		0.20		0.40	
Fragilariopsis atlantica	0.60	2.00	2.59	1.19	2.77	0.79	1.00	0.40	0.20	1.00
Fragilariopsis pseudonana	7.37	6.79	5.38	5.94	2.17	6.48	1.79	2.79	1.99	1.40
Gomphonemopsis lindae	0.40	0.40							0.80	1.80
Gomphonemopsis obscurum	0.40	0.60	0.20	0.79	0.40	1.18	1.20	0.80	2.98	1.60
Hyalodiscus scoticus	0.40		0.40	0.20	0.20					
Melosira nummuloides	0.40	1.20		0.79	0.59	0.39	1.99	0.60	1.19	1.60
Minidiscus chilensis	13.75	12.77	12.15	12.67	11.26	26.52	18.13	10.56	15.90	7.00
Navicula gregaria	0.20		1.00	0.40	0.20	0.59	0.40		0.20	0.20
Navicula perminuta	1.99	2.59	3.78	0.79	0.99	1.96	1.20	0.20	5.96	4.00
Nitzschia coarctata			1.39			0.20				
Nitzschia frustulum	6.57	3.59	1.99	3.17	3.16	4.13	3.98	2.59	7.95	12.60
Opephora cf. *horstiana*	0.20			0.40		0.39			0.20	0.40
Opephora mutabilis			0.60	0.40	0.20				0.20	0.20
Paralia sulcata		1.00		0.40	0.79	0.79	0.20	0.20	0.20	0.20
Planothidium delicatulum	1.99	2.99	0.20	1.19	1.58	2.16	2.39	0.80	4.77	4.00
Planothidium cf. *engelbretchii*				0.79	0.40	1.18			0.20	1.00
Planothidium hauckianum		0.40	0.40	0.20		0.59			0.40	1.00
Pleurosigma spp.		0.60	0.20	0.40	0.59	0.20			0.40	0.20
Pseudonitzschia multiseries	1.39	1.20	1.99	0.79	0.99	0.98	0.40		0.40	0.40
Pseudonitzschia seriata	0.60	0.80	0.80	0.99	0.20		0.20		0.60	0.60
Rhizosolenia spp.	2.59	3.79	3.59	1.58	2.17	0.59	1.00	0.80		0.60
Skeletonema costatum	28.69	20.56	25.70	24.16	21.94	8.64	19.52	28.29	12.13	11.20
Skeletonema costatum (weak)	6.57	8.58	9.36	8.51	9.49	10.61	14.34	31.27	2.58	3.80
Tabularia fasciculata	0.60	0.40	0.40	0.40	1.38		1.00		0.80	2.40
Thalassionema bacillare					0.20					
Thalassionema nitzschioides	2.59	4.39	4.98	4.95	13.24	7.47	8.57	3.59	9.15	7.20
Thalassionema pseudonitzschioides					0.59				2.39	1.80
Thalassiosira angulata		0.20								
Thalassiosira conferta	0.60	1.00	0.40		0.20	0.20	0.40	0.20		
Thalassiosira decipiens	1.20	2.00	1.39	1.58	3.16	2.55	3.39	1.59	2.19	1.40
Thalassiosira eccentrica	0.20	0.20	0.40	0.59	0.20	0.39	0.20		0.80	1.00
Thalassiosira cf. *leptopus*	0.60	0.60	1.00	0.59	0.40	0.20	0.40	0.40	0.20	
Thalassiosira minima	0.40		0.20		0.20	0.39				
Thalassiosira nordenskioeldii		0.20	0.40	0.99	0.40	0.20		0.40	0.80	0.20
Thalassiosira oestrupii	0.20	0.40	0.60	0.40	0.79	0.59			1.19	0.20
Thalassiosira pacifica	0.80	0.80	1.00	1.58	1.19	1.38	4.98	1.99	0.60	0.60
Thalassiosira rotula						0.39	1.00	1.00		
Thalassiosira tealata		0.20		0.20		0.20				0.20
Thalassiosira tenera	0.40		0.60			0.59		0.40	1.39	0.20
Thalassiosira sp. (cf. *tenera*)	0.20	1.00	1.79	0.59	1.58	1.57	1.20	0.60	0.20	0.20
Total relative abundance	90.28	91.04	90.47	88.32	88.77	91.18	94.47	95.25	88.72	82.00
Benthics	24.90	23.75	21.51	24.95	17.79	23.77	17.53	7.97	39.76	46.60
CRS	7.04	6.36	7.20	7.17	6.99	5.57	4.92	45.02	28.55	17.49
Silicoflagellates	0.59	0.99	0.40	0.39	1.75	0.59	0.99		0.98	0.60

APPENDIX E4 (continued)

Sample	3C-3	3C-4	3C-5	3C-6	3C-7	3C-8	3C-9	3C-10	3C-11	3C-12
Date opened	6/3/00	6/13/00	6/23/00	7/3/00	7/12/00	7/22/00	8/1/00	8/11/00	8/21/00	8/31/00
Achnanthes minutissima	0.39	0.19	0.79		1.17	0.60	0.40		0.98	0.79
Actinocyclus curvatulus	0.19									
Actinoptychus vulgaris						0.20	0.20			
Amphora helenensis	0.19		0.20				0.40	0.20		
Bacteriastrum delicatulum	0.58	0.39	1.19	0.36		1.40	0.80	0.20	1.96	0.39
Berkeleya rutilans				0.18		0.40			0.20	0.20
Cocconeis disculus							0.20		0.20	
Cocconeis neothumensis						0.40				
Cocconeis placentula	0.19	0.19				0.20	0.40	0.20	0.98	0.20
Cocconeis scutellum		0.39				0.40		0.60	0.39	
Cocconeis stauroneiformis		0.19			0.19	0.60		0.20	0.59	
Diatomella minuta	0.39					0.20				
Ditylum brightwellii	0.19				0.39	0.60	0.40	0.40	0.59	0.39
Eunotia spp.						0.20				
Fragilaria cf. *sopotensis*							0.20			
Fragilariopsis atlantica	0.19		0.20				1.00		0.59	
Fragilariopsis pseudonana	0.77	2.92	1.78	0.91	1.36	1.80	3.00	3.60	3.54	0.59
Gomphonemopsis lindae	0.19				0.19			0.40	0.39	0.20
Gomphonemopsis obscurum	0.19		0.40			0.40	1.20		0.20	0.59
Hyalodiscus scoticus						0.20		0.40		
Melosira nummuloides				0.18					0.20	
Minidiscus chilensis	1.74	0.97	1.58	0.18	0.39	1.60	2.60	0.60	1.77	0.79
Navicula gregaria		0.19					0.20	0.20	0.20	
Navicula perminuta	0.19	0.19	0.40		0.58	1.00	1.80	0.60	0.79	0.20
Nitzschia coarctata										
Nitzschia frustulum	2.90	1.75	0.79	0.55	0.58	1.00	1.40	2.20	4.52	2.37
Opephora cf. *horstiana*					0.19	0.80			0.20	0.20
Opephora mutabilis	0.19									0.20
Paralia sulcata		0.78							0.20	
Planothidium delicatulum	0.77		1.19		0.19	0.40	1.20	1.60	1.57	1.78
Planothidium cf. *engelbretchii*								0.80		
Planothidium hauckianum						0.20	0.20		0.20	0.39
Pleurosigma spp.										0.39
Pseudonitzschia multiseries		1.36		0.18	1.56	1.40	1.40	0.40	1.96	1.38
Pseudonitzschia seriata	0.77	2.14	2.17	0.73	2.14	2.00	3.20	3.80	6.68	3.75
Rhizosolenia spp.							0.60	0.20	0.39	
Skeletonema costatum	72.92	40.27	58.30	85.77	74.71	51.90	51.60	58.00	49.31	66.27
Skeletonema costatum (weak)	5.42	39.11	18.18	6.20	10.89	14.97	10.80	8.60	5.70	4.54
Tabularia fasciculata	0.58		1.38	0.36		0.20	0.40	1.00		0.59
Thalassionema bacillare										0.39
Thalassionema nitzschioides	1.55	1.17	2.57	1.09	0.97	6.39	6.40	4.20	3.73	4.14
Thalassionema pseudonitzschioides		0.39	0.79			0.40	0.40	0.40	0.59	0.79
Thalassiosira angulata		0.19		0.18	0.19	0.20			0.20	
Thalassiosira conferta	0.39	0.97	0.20							
Thalassiosira decipiens	0.39		0.20				0.20	0.40	0.39	0.00
Thalassiosira eccentrica	2.13	0.97	1.58		0.39	1.00	1.00	1.20	0.98	0.79
Thalassiosira cf. *leptopus*	0.39		0.40		0.19	0.20	0.20	0.20	0.20	0.99
Thalassiosira minima			0.20			0.20				
Thalassiosira nordenskioeldii	0.39	0.39	1.19	0.36	0.39	0.80	0.60	0.60	0.79	0.59
Thalassiosira oestrupii		0.39		0.18	0.78	0.80	0.20	0.40	0.59	0.39
Thalassiosira pacifica		0.19	0.20	0.36		0.40	0.80	0.60		0.20
Thalassiosira rotula	0.39	0.39	0.20			0.20	0.40		0.20	0.39
Thalassiosira tealata		0.39	0.40	0.18				0.20		
Thalassiosira tenera	1.93	0.78		0.18			0.60	1.20	0.79	0.20
Thalassiosira sp. (cf. *tenera*)		0.19		0.18		0.20	0.20		0.59	0.59
Total relative abundance	96.50	97.44	96.48	98.31	97.44	93.86	94.60	93.60	93.35	95.66
Benthics	6.38	4.09	5.93	1.28	4.28	11.18	10.40	12.20	15.13	9.66
CRS	3.72	3.02	9.32	6.64	3.38	10.22	13.17	11.97	7.96	7.65
Silicoflagellates	0.39	1.53	0.59		0.58	0.60	0.60	1.57	1.17	0.39

APPENDIX E4 (continued)

Sample	3C-13	3C-14	11C-1	11C-2	11C-3	11C-4	11C-5	11C-6	11C-7	11C-8
Date opened	9/9/00	9/19/00	5/15/00	5/24/00	6/3/00	6/13/00	6/23/00	7/3/00	7/12/00	7/22/00
Achnanthes minutissima	1.59	0.79	0.20	1.18	0.20	0.80	1.00	0.80	0.20	
Actinocyclus curvatulus										
Actinoptychus vulgaris									0.20	0.20
Amphora helenensis				0.20		0.40		0.40	0.20	
Bacteriastrum delicatulum	1.59	0.20	0.20			0.60	0.20	0.40	1.80	0.20
Berkeleya rutilans			0.80					0.20		
Cocconeis disculus	0.20	0.20	0.20	0.20	0.20				0.20	0.40
Cocconeis neothumensis	0.20		0.20							
Cocconeis placentula	0.60	0.39	0.40	1.38	0.40		0.40	0.40	0.60	0.80
Cocconeis scutellum	0.40		1.00	1.38	0.81	0.20	0.80	1.40	0.80	0.60
Cocconeis stauroneiformis	0.20	0.20	0.20	0.59	0.20	0.20		0.20	0.20	
Diatomella minuta			0.40							0.40
Ditylum brightwellii	0.40	0.20	0.80	0.39	0.20			0.20		
Eunotia spp.	0.40		0.20							
Fragilaria cf. *sopotensis*		0.39	0.20						0.20	
Fragilariopsis atlantica	0.20		0.20				0.20		0.60	0.60
Fragilariopsis pseudonana	3.37	1.77	1.80	2.56	2.63	2.19	1.80	2.40	2.40	1.80
Gomphonemopsis lindae		0.39	0.40	0.20						0.20
Gomphonemopsis obscurum	0.40	0.20	0.20	0.20	0.40	0.20	0.40	1.00		
Hyalodiscus scoticus				0.20			0.20			0.20
Melosira nummuloides		0.20		0.79						0.20
Minidiscus chilensis	3.37	3.93	40.12	46.55	35.76	25.25	23.40	22.60	19.00	20.40
Navicula gregaria	0.20	0.39			0.20				0.20	
Navicula perminuta	1.59	0.79		1.18	0.81	0.20	2.00	0.60	0.20	0.80
Nitzschia coarctata	0.20			0.20						
Nitzschia frustulum	4.37	2.75	2.59	1.18	1.82	1.99	2.40	1.20	0.40	2.00
Opephora cf. *horstiana*		0.59		0.59			0.20			
Opephora mutabilis	0.20			0.20	0.20		0.40	0.40	0.40	
Paralia sulcata			0.40	0.99	2.22	1.39		1.20		1.00
Planothidium delicatulum	0.79	0.79	0.80	1.18	1.82	1.19	0.40		0.80	1.20
Planothidium cf. *engelbretchii*										
Planothidium hauckianum				0.20			0.40	0.20		0.40
Pleurosigma spp.								0.20		
Pseudonitzschia multiseries	1.98	0.79	0.40	0.39	0.40	3.38	1.00	1.20	0.40	0.60
Pseudonitzschia seriata	5.75	2.95	0.40	0.20	1.82	5.17	2.80	1.40	5.20	3.20
Rhizosolenia spp.	0.60	0.39	0.60	0.79	1.62	0.40	1.40	0.20	0.80	1.80
Skeletonema costatum	49.21	56.39	4.39	5.33	6.46	10.14	11.20	30.20	35.00	23.60
Skeletonema costatum (weak)	4.37	7.27	2.40	1.78	3.64	14.91	8.40	8.40	3.40	3.40
Tabularia fasciculata	0.40	0.79	0.80		0.61			0.60		
Thalassionema bacillare										
Thalassionema nitzschioides	6.55	5.70	15.97	12.23	16.97	11.73	15.20	6.20	7.40	16.40
Thalassionema pseudonitzschioides	0.60	0.79	2.79	2.17	1.01	0.80	0.60	0.60	0.40	0.60
Thalassiosira angulata						0.20	0.20	0.20	0.20	
Thalassiosira conferta			0.40		0.20	0.20	0.40		1.00	
Thalassiosira decipiens	0.40	0.20	5.39	4.54	4.44	2.39	3.60	3.80	1.60	2.80
Thalassiosira eccentrica	1.19	2.16	1.80	0.39	0.81	0.99	0.80	2.00	0.40	2.20
Thalassiosira cf. *leptopus*	0.40	0.39					0.80	0.20	0.20	
Thalassiosira minima										
Thalassiosira nordenskioeldii	0.79	0.59	0.60	0.39		1.19	0.20	0.80	2.00	1.60
Thalassiosira oestrupii	0.40		0.40	0.59	0.20		0.40	0.60		0.60
Thalassiosira pacifica	0.20		1.40	1.58	1.62	5.17	10.80	2.20	2.40	2.80
Thalassiosira rotula		0.20			0.20	0.20	0.20		0.40	
Thalassiosira tealata						0.40	0.40			
Thalassiosira tenera	0.79	0.79	0.80	0.99	1.82	0.80	1.00	1.60	1.60	2.40
Thalassiosira sp. (cf. *tenera*)		0.20	0.40	0.39		0.20				
Total relative abundance	93.90	93.77	90.25	93.30	89.69	92.88	93.60	94.00	90.80	93.40
Benthics	14.68	12.38	14.97	14.40	13.74	7.75	13.00	10.40	10.20	10.60
CRS	14.14	10.86	18.14	11.83	11.43	4.73	11.66	12.28	21.63	19.09
Silicoflagellates	1.75	2.12	0.79	0.59	0.80	1.76	0.60	0.99	0.20	1.19

APPENDIX E4 (continued)

Sample	11C-9	11C-10	11C-11	11C-12	11C-13	11C-14
Date opened	8/1/00	8/11/00	8/21/00	8/31/00	9/9/00	9/19/00
Achnanthes minutissima	1.00	0.40	0.20	0.40		1.19
Actinocyclus curvatulus						
Actinoptychus vulgaris	0.40				0.20	
Amphora helenensis		0.40				1.39
Bacteriastrum delicatulum	0.2	0.4		0.2	0.4	
Berkeleya rutilans		0.20		0.20		
Cocconeis disculus	0.20				0.80	0.20
Cocconeis neothumensis						
Cocconeis placentula	0.80	0.20	0.79	1.39	0.40	0.40
Cocconeis scutellum	0.80	1.00	0.99	0.20	0.40	0.99
Cocconeis stauroneiformis						0.20
Diatomella minuta						
Ditylum brightwellii	0.20	0.20	0.20		0.40	
Eunotia spp.						
Fragilaria cf. *sopotensis*						
Fragilariopsis atlantica	0.40	0.20		0.60	0.20	
Fragilariopsis pseudonana	2.60	2.00	0.59	0.60	1.00	0.99
Gomphonemopsis lindae		0.20				
Gomphonemopsis obscrurum		0.40		0.40		0.59
Hyalodiscus scoticus						
Melosira nummuloides						
Minidiscus chilensis	38.60	41.32	42.49	32.87	36.80	33.27
Navicula gregaria						
Navicula perminuta	1.20	0.40	0.79	1.59	1.80	0.79
Nitzschia coarctata						
Nitzschia frustulum	1.60	1.60	0.79	2.19	1.60	1.19
Opephora cf. *horstiana*		0.20				
Opephora mutabilis	0.40				0.20	
Paralia sulcata	0.60	0.20		0.80	3.00	1.39
Planothidium delicatulum	1.20	0.20	0.79	0.20	0.40	1.19
Planothidium cf. *engelbretchii*		0.40				
Planothidium hauckianum			0.20			0.20
Pleurosigma spp.				0.20		
Pseudonitzschia multiseries	0.40	0.80	0.40	1.00	0.40	0.40
Pseudonitzschia seriata	2.00	1.20	2.17	2.19	2.60	0.79
Rhizosolenia spp.	2.60	1.40	5.53	28.49	10.60	9.70
Skeletonema costatum	12.80	12.97	11.07	6.37	8.00	10.30
Skeletonema costatum (weak)	1.80	1.00	1.98	1.00	1.20	2.97
Tabularia fasciculata			0.40			0.20
Thalassionema bacillare			0.20			0.20
Thalassionema nitzschioides	10.80	16.97	12.06	10.76	12.40	14.46
Thalassionema pseudonitzschioides	0.40	0.80	0.59	0.40	0.20	0.40
Thalassiosira angulata	0.20					
Thalassiosira conferta			0.40	0.20	0.20	0.20
Thalassiosira decipiens	3.00	2.59	4.35	1.20	2.80	3.17
Thalassiosira eccentrica	0.60	2.59	0.99	1.00	1.20	0.59
Thalassiosira cf. *leptopus*		0.20				0.20
Thalassiosira minima	0.20	0.20				
Thalassiosira nordenskioeldii	0.60	0.40	0.20	0.40	0.20	0.20
Thalassiosira oestrupii			0.59	0.20	0.60	1.39
Thalassiosira pacifica	1.00	0.20	1.78	0.80	1.80	0.20
Thalassiosira rotula					0.20	
Thalassiosira tealata		0.20				0.20
Thalassiosira tenera	1.40	1.20	1.19	0.60	1.60	1.19
Thalassiosira sp. (cf. *tenera*)		0.20				
Total relative abundance	88.00	92.84	91.73	96.45	91.60	90.74
Benthics	16.20	9.78	10.67	8.96	11.80	13.27
CRS	17.08	21.23	14.53	9.39	13.19	15.55
Silicoflagellates	1.38	0.99	1.36	0.59	1.38	1.75

APPENDIX E5. Sediment trap major taxa absolute abundance ($\times 10^6$ valves/g) data*

Sample	3A-1	3A-2	3A-3	3A-4	3A-5	3A-6	3A-7	3A-8	3A-9	3A-10
Date opened	5/29/99	6/6/99	6/15/99	6/24/99	7/3/99	7/12/99	7/21/99	7/30/99	8/7/99	8/16/99
Achnanthes minutissima	2.73	0.75	6.89	1.40	4.16	0.91	2.86	9.90	7.22	0.43
Actinocyclus curvatulus		0.75	3.08	1.75	0.83			2.22	1.82	
Actinoptychus vulgaris		1.50	0.77	0.70	2.49	0.61	1.59	1.48	0.91	1.72
Amphora helenensis						0.61		1.48		
Bacteriastrum delicatulum	0.68	0.37		0.70			0.64	2.22	1.82	
Berkeleya rutilans	0.68	0.75	0.77	0.35	0.42	0.30			0.91	
Cocconeis disculus		0.37	2.31	0.35	1.66		0.95	2.22	1.82	1.29
Cocconeis neothumensis										
Cocconeis placentula		0.75	3.85		0.42	0.30	0.64	2.22	6.31	0.86
Cocconeis scutellum	0.68			0.35		0.61	0.64	0.74	0.91	
Cocconeis stauroneiformis	0.68	1.12		0.35	1.25	0.00	0.32	1.48	1.82	1.29
Diatomella minuta						0.30				
Ditylum brightwellii				1.05	0.83					0.43
Eunotia spp.		0.37	0.77			0.30				
Fragilaria cf. *sopotensis*	0.34	1.50		0.35	1.25	0.30	0.64	2.97	5.40	
Fragilariopsis atlantica	34.82	35.19	118.93	71.14	54.75	31.86	38.16	76.36	83.73	45.09
Fragilariopsis pseudonana	13.31	13.48	31.47	3.49	7.88	5.46	3.50	12.60	11.71	5.57
Gomphonemopsis lindae		0.37		0.35						
Gomphonemopsis obscurum	0.34		0.77	0.70			1.59	1.48		2.15
Hyalodiscus scoticus				0.35	0.42					
Melosira nummuloides					0.42	0.91	1.27		2.72	
Minidiscus chilensis	6.49	17.97	21.49	4.87	14.53	16.08	11.13	29.65	45.02	18.03
Navicula gregaria		0.75				0.91		0.74	0.91	0.43
Navicula perminuta	1.71	4.12	9.21	1.75	2.49	2.12	0.32	5.93	8.12	6.43
Nitzschia coarctata									0.91	
Nitzschia frustulum	9.22	9.36	25.30	5.22	7.88	10.01	11.45	25.95	36.03	18.46
Opephora cf. *horstiana*										
Opephora mutabilis		0.75		0.35		0.91		2.97	7.22	1.29
Paralia sulcata	0.68		0.77			0.30		1.48		3.01
Planothidium delicatulum	1.71	2.25	6.89	1.75	2.49	1.21	4.13	3.71	8.99	5.16
Planothidium cf. engelbretchii					0.42					
Planothidium hauckianum	1.02	0.37	3.08	0.35	1.25		0.32	1.48	0.91	
Pleurosigma spp.		1.87	4.62	3.49	2.49	4.55	4.45	9.64	14.39	5.57
Pseudonitzschia multiseries	0.34	0.37			1.25	0.30	0.64	2.22	0.91	2.58
Pseudonitzschia seriata	0.34				0.42			0.74	0.91	
Rhizosolenia spp.	1.02	0.37	0.77		0.42	0.30		0.74	2.72	0.43
Skeletonema costatum	48.13	37.06	56.00	29.65	33.19	29.44	28.30	72.65	71.11	37.77
Skeletonema costatum (weak)	20.14	13.48	13.06	5.22	15.75	11.53	10.49	11.12	17.11	6.43
Tabularia fasciculata		0.75	1.54	1.05	0.42	0.91		2.22	4.49	3.44
Thalassionema bacillare	2.39	0.37	2.31	1.75	1.25	0.61	1.91	0.74	0.91	0.86
Thalassionema nitzschioides	3.75	9.73	9.21	7.32	10.78	8.80	7.95	17.05	22.51	9.01
Thalassionema pseudonitzschioides										
Thalassiosira angulata	0.34	2.62	3.08	1.40	0.42	0.30	1.27	0.74		
Thalassiosira conferta	3.41	1.50	2.31	1.05	2.08	2.43	0.64			0.86
Thalassiosira decipiens		0.75	3.08	0.35	0.83	0.30		0.74	8.12	1.72
Thalassiosira eccentrica	0.68	0.75	1.54	1.75	0.83	1.52	1.27		0.91	0.43
Thalassiosira cf. *leptopus*	0.34	2.99	2.31	3.14	3.32	0.91	4.13	5.19	7.22	3.44
Thalassiosira minima	1.02	4.12	2.31	1.75	2.08	0.30	0.32	2.22	0.91	
Thalassiosira nordenskioeldii	0.68		0.77			0.30		0.74	0.91	0.43
Thalassiosira oestrupii	2.05	4.12	16.10	7.32	5.38	3.34	3.18	8.16	12.62	4.73
Thalassiosira pacifica	0.34	0.37	0.77	0.70	1.25	0.30	1.91	2.97	0.91	0.86
Thalassiosira rotula		0.37	0.77	0.35						
Thalassiosira tealata	0.34	1.50	3.85	1.05	0.83	1.21	0.32	0.74	4.49	0.86
Thalassiosira tenera		1.12			0.42		0.32			
Thalassiosira sp. (cf. *tenera*)		0.75	2.31		2.08	0.30	0.64	0.74	1.82	1.72
Benthics	23.55	27.70	69.83	16.04	31.52	23.37	29.57	84.52	113.45	48.51

* major taxa defined as those which appeared in at least three samples in at least 1% in one sample; no entry for zero values

APPENDIX E5 (continued)

Sample	3A-11	3A-12	3A-13	3B-1	3B-2	3B-3	3B-4	3B-5	3B-6
Date opened	8/25/99	9/3/99	9/12/99	10/11/99	10/26/99	11/11/99	11/27/99	12/12/99	12/28/99
Achnanthes minutissima	1.07	1.83	7.86	5.40	9.91	19.23	21.00	6.73	31.20
Actinocyclus curvatulus	0.06	0.15	0.87						
Actinoptychus vulgaris	0.17	0.38	1.75		0.89		0.53		
Amphora helenensis	0.11	0.15		1.96		0.61		0.78	
Bacteriastrum delicatulum	0.06	0.15	0.87	1.47	2.68		0.53	0.31	
Berkeleya rutilans	0.06	0.38		1.47		3.01	0.53	0.31	1.31
Cocconeis disculus	0.06	0.46	1.75	2.45	2.68	0.61	0.53	0.16	
Cocconeis neothumensis		0.31	2.62	0.98	0.89	1.20		0.31	0.66
Cocconeis placentula	0.34	0.31	1.75	1.96	2.68	1.20	1.06	0.78	3.25
Cocconeis scutellum	0.11	0.31	1.75	1.47	4.51	1.81	3.16		2.59
Cocconeis stauroneiformis	0.11			1.96		0.61	4.19		1.94
Diatomella minuta		0.15							1.31
Ditylum brightwellii		0.08		0.49	0.89		1.06		
Eunotia spp.		0.08					0.53	0.16	0.66
Fragilaria cf. *sapotensis*	0.11				2.68		0.53	0.31	
Fragilariopsis atlantica	5.01	6.96	39.28	2.94	11.70	6.60	4.73	0.94	3.25
Fragilariopsis pseudonana	0.79	0.99	1.75	2.94	9.02	5.41	5.26	3.13	12.35
Gomphonemopsis lindae	0.06						1.06		
Gomphonemopsis obscrurum	0.11	0.15	1.75	3.92		1.81		0.47	2.59
Hyalodiscus scoticus	0.11	0.08	0.87	2.94	4.51	2.40		0.31	
Melosira nummuloides				8.34	1.79	1.20	2.63	0.63	1.94
Minidiscus chilensis	1.63	3.98	19.20	16.19	63.02	25.83	25.70	7.20	40.98
Navicula gregaria	0.17	0.31	2.62	0.49	3.62	1.20	2.10	0.31	0.66
Navicula perminuta	0.67	0.53	3.49	7.36	7.19	9.03	7.35	2.19	5.19
Nitzschia coarctata			0.87				1.06	0.00	
Nitzschia frustulum	2.14	2.45	4.36	15.70	20.72	24.63	18.37	4.22	16.25
Opephora cf. *horstiana*		0.08	2.62	0.49			0.53		1.94
Opephora mutabilis				0.49	0.89	0.61		0.16	
Paralia sulcata	0.06				3.62		0.53	0.31	0.66
Planothidium delicatulum	0.79	1.07	4.36	10.30	6.30	13.82	5.26	1.56	5.85
Planothidium cf. engelbretchii	0.06	0.08							
Planothidium hauckianum	0.17	0.31					3.16	0.16	1.31
Pleurosigma spp.	0.62	1.53	6.11					0.31	
Pseudonitzschia multiseries	0.17	0.15	2.62	1.96	6.30	4.21	4.73	0.78	4.56
Pseudonitzschia seriata						1.81	1.06	0.47	0.66
Rhizosolenia spp.	0.11	0.23	1.75	2.45	6.30	10.81	12.58	2.35	8.44
Skeletonema costatum	4.50	4.21	32.30	55.93	155.78	84.15	58.24	17.84	85.84
Skeletonema costatum (weak)	1.57	1.45	9.60	10.30	25.23	18.03	14.68	5.79	31.20
Tabularia fasciculata	0.17	0.31		2.45	0.89	4.21	2.63	0.31	0.66
Thalassionema bacillare		0.31	1.75		0.89				1.31
Thalassionema nitzschioides	1.69	1.53	13.97	16.68	21.62	16.83	11.55	3.44	10.41
Thalassionema pseudonitzschioides									
Thalassiosira angulata							0.53		0.66
Thalassiosira conferta	0.45	0.31	0.87	0.49	1.79	1.20		0.16	
Thalassiosira decipiens	0.06	0.15	6.11	2.45	7.19	2.40	0.53	0.78	2.59
Thalassiosira eccentrica	0.28	0.31	1.75	1.96	0.89	3.59	1.57		3.91
Thalassiosira cf. *leptopus*	0.28	0.61	1.75	0.49	2.68	0.61	0.53	0.47	2.59
Thalassiosira minima					0.89			0.16	0.66
Thalassiosira nordenskioeldii	0.06		0.87		3.62	0.61	1.57	0.31	1.94
Thalassiosira oestrupii	0.73	0.61	8.73			0.61	0.53	0.47	1.31
Thalassiosira pacifica	0.51	0.23	5.24	3.92	7.19	3.59	2.63	1.56	1.31
Thalassiosira rotula	0.11		0.87			1.81	1.57	0.16	0.66
Thalassiosira tealata	0.06	0.08							
Thalassiosira tenera			0.87	1.47	1.79	1.20	1.06	0.47	3.25
Thalassiosira sp. (cf. *tenera*)	0.17	0.31	2.62	0.49	5.40	2.40	0.53	0.31	1.31
Benthics	7.70	11.16	48.01	74.08	81.06	98.55	92.86	24.57	92.34

APPENDIX E5 (continued)

Sample	3B-7	3B-8	3B-9	3B-10	3B-11	3B-12	3B-13	3B-14	3C-1	3C-2
Date opened	1/13/00	1/29/00	2/13/00	2/29/00	3/16/00	3/31/00	4/16/00	5/2/00	5/15/00	5/24/00
Achnanthes minutissima	11.69	9.98	6.45	9.54	0.86	9.58	6.68	5.31	0.35	0.45
Actinocyclus curvatulus	0.56				0.22					0.02
Actinoptychus vulgaris						0.54				
Amphora helenensis			1.21						0.06	0.02
Bacteriastrum delicatulum	1.12			0.77		0.54	0.75	1.77	0.19	0.06
Berkeleya rutilans									0.02	0.11
Cocconeis disculus	0.56	0.42				1.06	0.75		0.00	
Cocconeis neothumensis	0.56	1.67		0.77	0.65		0.75		0.04	
Cocconeis placentula	2.80	1.25	0.81	1.14	0.86		1.49	0.88	0.08	0.06
Cocconeis scutellum	1.68	2.08	0.81		1.08	1.60	4.48		0.04	0.15
Cocconeis stauroneiformis		1.25	0.40	2.29	0.86	3.19	3.73	0.88	0.06	0.13
Diatomella minuta	1.12	0.83		1.14	0.44					0.13
Ditylum brightwellii	0.56	1.25		0.39	0.22	1.06	1.49	16.72	0.12	0.11
Eunotia spp.	2.80	0.42	1.62	1.91	0.22	0.54				0.02
Fragilaria cf. *sopotensis*		1.25		2.68	0.22		0.75		0.04	
Fragilariopsis atlantica	1.68	4.17	5.24	2.29	3.03	2.14	3.73	1.77	0.02	0.11
Fragilariopsis pseudonana	20.62	14.15	10.88	11.45	2.37	17.54	6.68	12.34	0.21	0.15
Gomphonemopsis lindae	1.12	0.83							0.08	0.19
Gomphonemopsis obscurum	1.12	1.25	0.40	1.52	0.44	3.19	4.48	3.54	0.31	0.17
Hyalodiscus scoticus	1.12		0.81	0.39	0.22					
Melosira nummuloides	1.12	2.50		1.52	0.65	1.06	7.42	2.65	0.12	0.17
Minidiscus chilensis	38.47	26.61	24.58	24.41	12.32	71.79	67.61	46.70	1.66	0.75
Navicula gregaria	0.56		2.02	0.77	0.22	1.60	1.49		0.02	0.02
Navicula perminuta	5.57	5.40	7.65	1.52	1.08	5.31	4.48	0.88	0.62	0.43
Nitzschia coarctata			2.81			0.54				
Nitzschia frustulum	18.38	7.48	4.03	6.11	3.46	11.18	14.84	11.45	0.83	1.35
Opephora cf. *horstiana*	0.56			0.77		1.06			0.02	0.04
Opephora mutabilis			1.21	0.77	0.22				0.02	0.02
Paralia sulcata		2.08		0.77	0.86	2.14	0.75	0.88	0.02	0.02
Planothidium delicatulum	5.57	6.23	0.40	2.29	1.73	5.85	8.91	3.54	0.50	0.43
Planothidium cf. engelbretchii				1.52	0.44	3.19			0.02	0.11
Planothidium hauckianum		0.83	0.81	0.39		1.60			0.04	0.11
Pleurosigma spp.		1.25	0.40	0.77	0.65	0.54			0.04	0.02
Pseudonitzschia multiseries	3.89	2.50	4.03	1.52	1.08	2.65	1.49		0.04	0.04
Pseudonitzschia seriata	1.68	1.67	1.62	1.91	0.22		0.75		0.06	0.06
Rhizosolenia spp.	7.25	7.90	7.26	3.04	2.37	1.60	3.73	3.54		0.06
Skeletonema costatum	80.26	42.85	51.98	46.55	24.00	23.39	72.80	125.11	1.27	1.20
Skeletonema costatum (weak)	18.38	17.88	18.93	16.40	10.38	28.72	53.48	138.29	0.27	0.41
Tabularia fasciculata	1.68	0.83	0.81	0.77	1.51		3.73		0.08	0.26
Thalassionema bacillare					0.22					
Thalassionema nitzschioides	7.25	9.15	10.07	9.54	14.48	20.22	31.96	15.88	0.96	0.77
Thalassionema pseudonitzschioides					0.65				0.25	0.19
Thalassiosira angulata		0.42								
Thalassiosira conferta	1.68	2.08	0.81		0.22	0.54	1.49	0.88		
Thalassiosira decipiens	3.36	4.17	2.81	3.04	3.46	6.90	12.64	7.03	0.23	0.15
Thalassiosira eccentrica	0.56	0.42	0.81	1.14	0.22	1.06	0.75		0.08	0.11
Thalassiosira cf. *leptopus*	1.68	1.25	2.02	1.14	0.44	0.54	1.49	1.77	0.02	
Thalassiosira minima	1.12		0.40		0.22	1.06				
Thalassiosira nordenskioeldii		0.42	0.81	1.91	0.44	0.54		1.77	0.08	0.02
Thalassiosira oestrupii	0.56	0.83	1.21	0.77	0.86	1.60			0.12	0.02
Thalassiosira pacifica	2.24	1.67	2.02	3.04	1.30	3.74	18.57	8.80	0.06	0.06
Thalassiosira rotula						1.06	3.73	4.42		
Thalassiosira tealata		0.42		0.39		0.54				0.02
Thalassiosira tenera	1.12		1.21			1.60		1.77	0.15	0.02
Thalassiosira sp. (cf. *tenera*)	0.56	2.08	3.62	1.14	1.73	4.25	4.48	2.65	0.02	0.02
Benthics	69.66	49.50	43.51	48.07	19.46	64.35	65.38	35.25	4.16	5.00

APPENDIX E5 (continued)

Sample	3C-3	3C-4	3C-5	3C-6	3C-7	3C-8	3C-9	3C-10	3C-11	3C-12
Date opened	6/3/00	6/13/00	6/23/00	7/3/00	7/12/00	7/22/00	8/1/00	8/11/00	8/21/00	8/31/00
Achnanthes minutissima	0.19	0.10	0.34		8.27	1.02	0.80	0.00	1.73	1.45
Actinocyclus curvatulus	0.09									
Actinoptychus vulgaris						0.34	0.40			
Amphora helenensis	0.09		0.09				0.80	0.45		
Bacteriastrum delicatulum	0.28	0.20	0.51	0.35		2.39	1.60	0.45	3.46	0.71
Berkeleya rutilans				0.17		0.68			0.35	0.37
Cocconeis disculus							0.40		0.35	
Cocconeis neothumensis						0.68				
Cocconeis placentula	0.09	0.10				0.34	0.80	0.45	1.73	0.37
Cocconeis scutellum		0.20				0.68		1.36	0.69	
Cocconeis stauroneiformis		0.10			1.34	1.02		0.45	1.04	
Diatomella minuta	0.19					0.34				
Ditylum brightwellii	0.09				2.76	1.02	0.80	0.91	1.04	0.71
Eunotia spp.						0.34				
Fragilaria cf. *sopotensis*							0.40			
Fragilariopsis atlantica	0.09		0.09				2.00		1.04	
Fragilariopsis pseudonana	0.37	1.50	0.77	0.88	9.61	3.07	6.00	8.15	6.25	1.08
Gomphonemopsis lindae	0.09				1.34			0.91	0.69	0.37
Gomphonemopsis obscurum	0.09		0.17			0.68	2.40		0.35	1.08
Hyalodiscus scoticus						0.34		0.91		
Melosira nummuloides				0.17					0.35	
Minidiscus chilensis	0.84	0.50	0.68	0.17	2.76	2.73	5.20	1.36	3.13	1.45
Navicula gregaria		0.10					0.40	0.45	0.35	
Navicula perminuta	0.09	0.10	0.17		4.10	1.71	3.60	1.36	1.40	0.37
Nitzschia coarctata										
Nitzschia frustulum	1.40	0.90	0.34	0.53	4.10	1.71	2.80	4.98	7.98	4.34
Opephora cf. *horstiana*					1.34	1.37			0.35	0.37
Opephora mutabilis	0.09									0.37
Paralia sulcata		0.40							0.35	
Planothidium delicatulum	0.37		0.51		1.34	0.68	2.40	3.62	2.77	3.26
Planothidium cf. engelbretchii								1.81		
Planothidium hauckianum						0.34	0.40		0.35	0.71
Pleurosigma spp.										0.71
Pseudonitzschia multiseries		0.70		0.17	11.03	2.39	2.80	0.91	3.46	2.53
Pseudonitzschia seriata	0.37	1.10	0.93	0.71	15.13	3.42	6.40	8.60	11.80	6.86
Rhizosolenia spp.							1.20	0.45	0.69	
Skeletonema costatum	35.28	20.66	25.09	82.85	528.09	88.66	103.25	131.33	87.10	121.27
Skeletonema costatum (weak)	2.62	20.06	7.82	5.99	76.98	25.57	21.61	19.47	10.07	8.31
Tabularia fasciculata	0.28		0.59	0.35		0.34	0.80	2.26		1.08
Thalassionema bacillare										0.71
Thalassionema nitzschioides	0.75	0.60	1.11	1.05	6.86	10.92	12.81	9.51	6.59	7.58
Thalassionema pseudonitzschioides		0.20	0.34			0.68	0.80	0.91	1.04	1.45
Thalassiosira angulata		0.10		0.17	1.34	0.34			0.35	
Thalassiosira conferta	0.19	0.50	0.09							
Thalassiosira decipiens	0.19	0.00	0.09				0.40	0.91	0.69	
Thalassiosira eccentrica	1.03	0.50	0.68		2.76	1.71	2.00	2.72	1.73	1.45
Thalassiosira cf. *leptopus*	0.19		0.17		1.34	0.34	0.40	0.45	0.35	1.81
Thalassiosira minima			0.09			0.34				0.00
Thalassiosira nordenskioeldii	0.19	0.20	0.51	0.35	2.76	1.37	1.20	1.36	1.40	1.08
Thalassiosira oestrupii		0.20		0.17	5.51	1.37	0.40	0.91	1.04	0.71
Thalassiosira pacifica		0.10	0.09	0.35		0.68	1.60	1.36		0.37
Thalassiosira rotula	0.19	0.20	0.09			0.34	0.80		0.35	0.71
Thalassiosira tealata		0.20	0.17	0.17				0.45		
Thalassiosira tenera	0.93	0.40		0.17			1.20	2.72	1.40	0.37
Thalassiosira sp. (cf. *tenera*)		0.10		0.17		0.34	0.40		1.04	1.08
Benthics	3.09	2.10	2.55	1.24	30.25	19.10	20.81	27.62	26.72	17.68

APPENDIX E5 (continued)

Sample	3C-13	3C-14	11C-1	11C-2	11C-3	11C-4	11C-5	11C-6	11C-7	11C-8
Date opened	9/9/00	9/19/00	5/15/00	5/24/00	6/3/00	6/13/00	6/23/00	7/3/00	7/12/00	7/22/00
Achnanthes minutissima	1.57	0.97	0.51	3.25	0.74	1.79	1.84	1.67	0.41	
Actinocyclus curvatulus										
Actinoptychus vulgaris									0.41	0.47
Amphora helenensis				0.55		0.89		0.83	0.41	
Bacteriastrum delicatulum	1.57	0.25	0.51			1.33	0.37	0.83	3.66	0.47
Berkeleya rutilans			2.04					0.42		
Cocconeis diculus	0.20	0.25	0.51	0.55	0.74				0.41	0.94
Cocconeis neothumensis	0.20		0.51							
Cocconeis placentula	0.59	0.48	1.02	3.80	1.48		0.74	0.83	1.22	1.89
Cocconeis scutellum	0.40		2.55	3.80	3.00	0.45	1.47	2.92	1.62	1.41
Cocconeis stauroneiformis	0.20	0.25	0.51	1.62	0.74	0.45		0.42	0.41	
Diatomella minuta			1.02							0.94
Ditylum brightwellii	0.40	0.25	2.04	1.07	0.74			0.42		
Eunotia spp.	0.40		0.51							
Fragilaria cf. *sopotensis*		0.48	0.51						0.41	
Fragilariopsis atlantica	0.20		0.51				0.37		1.22	1.41
Fragilariopsis pseudonana	3.33	2.17	4.59	7.05	9.75	4.90	3.31	5.01	4.87	4.24
Gomphonemopsis lindae		0.48	1.02	0.55						0.47
Gomphonemopsis obscurum	0.40	0.25	0.51	0.55	1.48	0.45	0.74	2.09		
Hyalodiscus scoticus				0.55			0.37			0.47
Melosira nummuloides		0.25		2.17						0.47
Minidiscus chilensis	3.33	4.82	102.39	128.11	132.60	56.44	43.04	47.14	38.58	48.09
Navicula gregaria	0.20	0.48			0.74				0.41	
Navicula perminuta	1.57	0.97		3.25	3.00	0.45	3.68	1.25	0.41	1.89
Nitzschia coarctata	0.20			0.55						
Nitzschia frustulum	4.32	3.37	6.61	3.25	6.75	4.45	4.41	2.50	0.81	4.71
Opephora cf. *horstiana*		0.72		1.62			0.37			
Opephora mutabilis	0.20			0.55	0.74		0.74	0.83	0.81	
Paralia sulcata			1.02	2.72	8.23	3.11		2.50		2.36
Planothidium delicatulum	0.78	0.97	2.04	3.25	6.75	2.66	0.74		1.62	2.83
Planothidium cf. engelbretchii										
Planothidium hauckianum				0.55			0.74	0.42		0.94
Pleurosigma spp.								0.42		
Pseudonitzschia multiseries	1.96	0.97	1.02	1.07	1.48	7.56	1.84	2.50	0.81	1.41
Pseudonitzschia seriata	5.68	3.62	1.02	0.55	6.75	11.56	5.15	2.92	10.56	7.54
Rhizosolenia spp.	0.59	0.48	1.53	2.17	6.01	0.89	2.58	0.42	1.62	4.24
Skeletonema costatum	48.63	69.13	11.20	14.67	23.95	22.67	20.60	62.99	71.07	55.63
Skeletonema costatum (weak)	4.32	8.91	6.12	4.90	13.50	33.33	15.45	17.52	6.90	8.02
Tabularia fasciculata	0.40	0.97	2.04		2.26			1.25		
Thalassionema bacillare										
Thalassionema nitzschioides	6.47	6.99	40.76	33.66	62.93	26.22	27.96	12.93	15.03	38.66
Thalassionema pseudonitzschioides	0.59	0.97	7.12	5.97	3.75	1.79	1.10	1.25	0.81	1.41
Thalassiosira angulata						0.45	0.37	0.42	0.41	
Thalassiosira conferta			1.02		0.74	0.45	0.74		2.03	
Thalassiosira decipiens	0.40	0.25	13.76	12.49	16.46	5.34	6.62	7.93	3.25	6.60
Thalassiosira eccentrica	1.18	2.65	4.59	1.07	3.00	2.21	1.47	4.17	0.81	5.19
Thalassiosira cf. *leptopus*	0.40	0.48					1.47	0.42	0.41	
Thalassiosira minima										
Thalassiosira nordenskioeldii	0.78	0.72	1.53	1.07		2.66	0.37	1.67	4.06	3.77
Thalassiosira oestrupii	0.40		1.02	1.62	0.74		0.74	1.25		1.41
Thalassiosira pacifica	0.20		3.57	4.35	6.01	11.56	19.87	4.59	4.87	6.60
Thalassiosira rotula		0.25			0.74	0.45	0.37		0.81	
Thalassiosira tealata						0.89	0.74			
Thalassiosira tenera	0.78	0.97	2.04	2.72	6.75	1.79	1.84	3.34	3.25	5.66
Thalassiosira sp. (cf. *tenera*)		0.25	1.02	1.07		0.45				
Benthics	14.51	15.18	38.20	39.63	50.95	17.32	23.91	21.69	20.71	24.99

APPENDIX E5 (continued)

Sample	11C-9	11C-10	11C-11	11C-12	11C-13	11C-14
Date opened	8/1/00	8/11/00	8/21/00	8/31/00	9/9/00	9/19/00
Achnanthes minutissima	3.12	1.28	0.52	1.40	0.00	3.65
Actinocyclus curvatulus						
Actinoptychus vulgaris	1.25				0.52	
Amphora helenensis		1.28				4.27
Bacteriastrum delicatulum	0.62	1.28		0.70	1.05	
Berkeleya rutilans		0.64		0.70		
Cocconeis disculus	0.62				2.10	0.61
Cocconeis neothumensis						
Cocconeis placentula	2.50	0.64	2.04	4.85	1.05	1.23
Cocconeis scutellum	2.50	3.21	2.55	0.70	1.05	3.04
Cocconeis stauroneiformis						0.61
Diatomella minuta						
Ditylum brightwellii	0.62	0.64	0.52		1.05	
Eunotia spp.						
Fragilaria cf. *sopotensis*						
Fragilariopsis atlantica	1.25	0.64		2.10	0.52	
Fragilariopsis pseudonana	8.12	6.41	1.52	2.10	2.62	3.04
Gomphonemopsis lindae		0.64				
Gomphonemopsis obscrurum		1.28		1.40		1.81
Hyalodiscus scoticus						
Melosira nummuloides						
Minidiscus chilensis	120.55	132.45	109.62	114.78	96.51	102.19
Navicula gregaria						
Navicula perminuta	3.75	1.28	2.04	5.55	4.72	2.43
Nitzschia coarctata						
Nitzschia frustulum	5.00	5.13	2.04	7.65	4.20	3.65
Opephora cf. *horstiana*		0.64				
Opephora mutabilis	1.25				0.52	
Paralia sulcata	1.87	0.64		2.79	7.87	4.27
Planothidium delicatulum	3.75	0.64	2.04	0.70	1.05	3.65
Planothidium cf. engelbretchii		1.28				
Planothidium hauckianum			0.52			0.61
Pleurosigma spp.				0.70		
Pseudonitzschia multiseries	1.25	2.56	1.03	3.49	1.05	1.23
Pseudonitzschia seriata	6.25	3.85	5.60	7.65	6.82	2.43
Rhizosolenia spp.	8.12	4.49	14.27	99.49	27.80	29.79
Skeletonema costatum	39.98	41.57	28.56	22.24	20.98	31.64
Skeletonema costatum (weak)	5.62	3.21	5.11	3.49	3.15	9.12
Tabularia fasciculata			1.03			0.61
Thalassionema bacillare			0.52			0.61
Thalassionema nitzschioides	33.73	54.40	31.11	37.57	32.52	44.41
Thalassionema pseudonitzschioides	1.25	2.56	1.52	1.40	0.52	1.23
Thalassiosira angulata	0.62					
Thalassiosira conferta			1.03	0.70	0.52	0.61
Thalassiosira decipiens	9.37	8.30	11.22	4.19	7.34	9.74
Thalassiosira eccentrica	1.87	8.30	2.55	3.49	3.15	1.81
Thalassiosira cf. *leptopus*		0.64				0.61
Thalassiosira minima	0.62	0.64				
Thalassiosira nordenskioeldii	1.87	1.28	0.52	1.40	0.52	0.61
Thalassiosira oestrupii			1.52	0.70	1.57	4.27
Thalassiosira pacifica	3.12	0.64	4.59	2.79	4.72	0.61
Thalassiosira rotula					0.52	
Thalassiosira tealata		0.64				0.61
Thalassiosira tenera	4.37	3.85	3.07	2.10	4.20	3.65
Thalassiosira sp. (cf. *tenera*)		0.64				
Benthics	50.59	31.35	27.53	31.29	30.94	40.76

APPENDIX E6. Sediment trap major taxa flux data ($\times 10^6$ valves/m^2/day)*

Sample	3A-1	3A-2	3A-3	3A-4	3A-5	3A-6	3A-7	3A-8	3A-9	3A-10
Date opened	5/29/99	6/6/99	6/15/99	6/24/99	7/3/99	7/12/99	7/21/99	7/30/99	8/7/99	8/16/99
Achnanthes minutissima	1.57	0.63	2.78	0.23	2.06	2.20	7.50	8.22	3.66	0.16
Actinocyclus curvatulus		0.63	1.24	0.28	0.41			1.85	0.92	
Actinoptychus vulgaris		1.27	0.31	0.11	1.23	1.46	4.17	1.23	0.46	0.65
Amphora helenensis						1.46		1.23		
Bacteriastrum delicatulum	0.39	0.32		0.11			1.67	1.85	0.92	
Berkeleya rutilans	0.39	0.63	0.31	0.06	0.21	0.73			0.46	
Cocconeis disculus		0.32	0.93	0.06	0.82		2.50	1.85	0.92	0.49
Cocconeis neothumensis										
Cocconeis placentula		0.63	1.55		0.21	0.73	1.67	1.85	3.20	0.33
Cocconeis scutellum	0.39			0.06		1.46	1.67	0.62	0.46	
Cocconeis stauroneiformis	0.39	0.95		0.06	0.62		0.83	1.23	0.92	0.49
Diatomella minuta						0.73				
Ditylum brightwellii				0.17	0.41					0.16
Eunotia spp.		0.32	0.31			0.73				
Fragilaria cf. *sopotensis*	0.20	1.27		0.06	0.62	0.73	1.67	2.46	2.74	
Fragilariopsis atlantica	19.98	29.81	48.00	11.47	27.10	76.89	99.99	63.41	42.48	17.16
Fragilariopsis pseudonana	7.64	11.41	12.70	0.56	3.90	13.18	9.17	10.47	5.94	2.12
Gomphonemopsis lindae		0.32		0.06						
Gomphonemopsis obscurum	0.20		0.31	0.11			4.17	1.23		0.82
Hyalodiscus scoticus				0.06	0.21					
Melosira nummuloides					0.21	2.20	3.33		1.38	
Minidiscus chilensis	3.72	15.22	8.67	0.79	7.19	38.81	29.16	24.63	22.84	6.86
Navicula gregaria		0.63				2.20		0.62	0.46	0.16
Navicula perminuta	0.98	3.49	3.71	0.28	1.23	5.13	0.83	4.93	4.12	2.45
Nitzschia coarctata									0.46	
Nitzschia frustulum	5.29	7.93	10.21	0.84	3.90	24.17	30.00	21.55	18.28	7.02
Opephora cf. *horstiana*										
Opephora mutabilis		0.63		0.06		2.20		2.46	3.66	0.49
Paralia sulcata	0.39		0.31			0.73		1.23		1.15
Planothidium delicatulum	0.98	1.90	2.78	0.28	1.23	2.93	10.83	3.08	4.56	1.96
Planothidium cf. engelbretchii					0.21					
Planothidium hauckianum	0.59	0.32	1.24	0.06	0.62		0.83	1.23	0.46	
Pleurosigma spp.		1.59	1.87	0.56	1.23	10.98	11.67	8.00	7.30	2.12
Pseudonitzschia multiseries	0.20	0.32			0.62	0.73	1.67	1.85	0.46	0.98
Pseudonitzschia seriata	0.20				0.21			0.62	0.46	
Rhizosolenia spp.	0.59	0.32	0.31		0.21	0.73		0.62	1.38	0.16
Skeletonema costatum	27.62	31.39	22.60	4.78	16.43	71.03	74.16	60.33	36.08	14.37
Skeletonema costatum (weak)	11.56	11.41	5.27	0.84	7.80	27.83	27.50	9.23	8.68	2.45
Tabularia fasciculata		0.63	0.62	0.17	0.21	2.20		1.85	2.28	1.31
Thalassionema bacillare	1.37	0.32	0.93	0.28	0.62	1.46	5.00	0.62	0.46	0.33
Thalassionema nitzschioides	2.15	8.24	3.71	1.18	5.34	21.24	20.83	14.16	11.42	3.43
Thalassionema pseudonitzschioides										
Thalassiosira angulata	0.20	2.22	1.24	0.23	0.21	0.73	3.33	0.62		
Thalassiosira conferta	1.96	1.27	0.93	0.17	1.03	5.86	1.67			0.33
Thalassiosira decipiens		0.63	1.24	0.06	0.41	0.73		0.62	4.12	0.65
Thalassiosira eccentrica	0.39	0.63	0.62	0.28	0.41	3.66	3.33		0.46	0.16
Thalassiosira cf. *leptopus*	0.20	2.54	0.93	0.51	1.65	2.20	10.83	4.31	3.66	1.31
Thalassiosira minima	0.59	3.49	0.93	0.28	1.03	0.73	0.83	1.85	0.46	
Thalassiosira nordenskioeldii	0.39		0.31			0.73		0.62	0.46	0.16
Thalassiosira oestrupii	1.18	3.49	6.50	1.18	2.66	8.06	8.33	6.77	6.40	1.80
Thalassiosira pacifica	0.20	0.32	0.31	0.11	0.62	0.73	5.00	2.46	0.46	0.33
Thalassiosira rotula		0.32	0.31	0.06						
Thalassiosira tealata	0.20	1.27	1.55	0.17	0.41	2.93	0.83	0.62	2.28	0.33
Thalassiosira tenera		0.95			0.21		0.83			
Thalassiosira sp. (cf. *tenera*)		0.63	0.93		1.03	0.73	1.67	0.62	0.92	0.65

* major taxa defined as those which appeared in at least three samples and at least 1% in one sample; no entry for zero values

APPENDIX E6 (continued)

Sample	3A-11	3A-12	3A-13	3B-1	3B-2	3B-3	3B-4	3B-5	3B-6
Date opened	8/25/99	9/3/99	9/12/99	10/11/99	10/26/99	11/11/99	11/27/99	12/12/99	12/28/99
Achnanthes minutissima	0.28	0.16	0.62	2.79	6.46	17.49	20.29	6.64	23.07
Actinocyclus curvatulus	0.01	0.01	0.07						
Actinoptychus vulgaris	0.04	0.03	0.14		0.58		0.51		
Amphora helenensis	0.03	0.01		1.01		0.56		0.77	
Bacteriastrum delicatulum	0.01	0.01	0.07	0.76	1.75		0.51	0.31	
Berkeleya rutilans	0.01	0.03		0.76		2.74	0.51	0.31	0.97
Cocconeis disculus	0.01	0.04	0.14	1.27	1.75	0.56	0.51	0.15	
Cocconeis neothumensis		0.03	0.21	0.51	0.58	1.09		0.31	0.49
Cocconeis placentula	0.09	0.03	0.14	1.01	1.75	1.09	1.03	0.77	2.40
Cocconeis scutellum	0.03	0.03	0.14	0.76	2.94	1.65	3.05		1.92
Cocconeis stauroneiformis	0.03			1.01		0.56	4.05		1.43
Diatomella minuta		0.01							0.97
Ditylum brightwellii		0.01		0.25	0.58		1.03		
Eunotia spp.		0.01					0.51	0.15	0.49
Fragilaria cf. *sopotensis*	0.03				1.75		0.51	0.31	
Fragilariopsis atlantica	1.29	0.61	3.11	1.52	7.63	6.01	4.56	0.93	2.40
Fragilariopsis pseudonana	0.20	0.09	0.14	1.52	5.88	4.92	5.08	3.09	9.13
Gomphonemopsis lindae	0.01						1.03		
Gomphonemopsis obscurum	0.03	0.01	0.14	2.03		1.65		0.46	1.92
Hyalodiscus scoticus	0.03	0.01	0.07	1.52	2.94	2.18		0.31	
Melosira nummuloides				4.31	1.16	1.09	2.54	0.62	1.43
Minidiscus chilensis	0.42	0.35	1.52	8.36	41.07	23.50	24.82	7.11	30.31
Navicula gregaria	0.04	0.03	0.21	0.25	2.36	1.09	2.03	0.31	0.49
Navicula perminuta	0.17	0.05	0.28	3.80	4.69	8.21	7.10	2.16	3.84
Nitzschia coarctata			0.07				1.03		
Nitzschia frustulum	0.55	0.21	0.35	8.10	13.51	22.41	17.75	4.17	12.02
Opephora cf. *horstiana*		0.01	0.21	0.25			0.51		1.43
Opephora mutabilis				0.25	0.58	0.56		0.15	
Paralia sulcata	0.01				2.36		0.51	0.31	0.49
Planothidium delicatulum	0.20	0.09	0.35	5.32	4.10	12.57	5.08	1.55	4.32
Planothidium cf. engelbretchii	0.01	0.01							
Planothidium hauckianum	0.04	0.03					3.05	0.15	0.97
Pleurosigma spp.	0.16	0.13	0.48					0.31	
Pseudonitzschia multiseries	0.04	0.01	0.21	1.01	4.10	3.83	4.56	0.77	3.38
Pseudonitzschia seriata						1.65	1.03	0.46	0.49
Rhizosolenia spp.	0.03	0.02	0.14	1.27	4.10	9.84	12.16	2.32	6.24
Skeletonema costatum	1.16	0.37	2.55	28.87	101.53	76.56	56.27	17.61	63.48
Skeletonema costatum (weak)	0.41	0.13	0.76	5.32	16.45	16.40	14.18	5.72	23.07
Tabularia fasciculata	0.04	0.03		1.27	0.58	3.83	2.54	0.31	0.49
Thalassionema bacillare		0.03	0.14		0.58				0.97
Thalassionema nitzschioides	0.44	0.13	1.10	8.61	14.09	15.31	11.16	3.40	7.70
Thalassionema pseudonitzschioides									
Thalassiosira angulata							0.51		0.49
Thalassiosira conferta	0.12	0.03	0.07	0.25	1.16	1.09		0.15	
Thalassiosira decipiens	0.01	0.01	0.48	1.27	4.69	2.18	0.51	0.77	1.92
Thalassiosira eccentrica	0.07	0.03	0.14	1.01	0.58	3.27	1.51		2.89
Thalassiosira cf. *leptopus*	0.07	0.05	0.14	0.25	1.75	0.56	0.51	0.46	1.92
Thalassiosira minima					0.58			0.15	0.49
Thalassiosira nordenskioeldii	0.01		0.07		2.36	0.56	1.51	0.31	1.43
Thalassiosira oestrupii	0.19	0.05	0.69			0.56	0.51	0.46	0.97
Thalassiosira pacifica	0.13	0.02	0.41	2.03	4.69	3.27	2.54	1.55	0.97
Thalassiosira rotula	0.03		0.07			1.65	1.51	0.15	0.49
Thalassiosira tealata	0.01	0.01							
Thalassiosira tenera			0.07	0.76	1.16	1.09	1.03	0.46	2.40
Thalassiosira sp. (cf. *tenera*)	0.04	0.03	0.21	0.25	3.52	2.18	0.51	0.31	0.97

APPENDIX E6 (continued)

Sample	3B-7	3B-8	3B-9	3B-10	3B-11	3B-12	3B-13	3B-14	3C-1	3C-2
Date opened	1/13/00	1/29/00	2/13/00	2/29/00	3/16/00	3/31/00	4/16/00	5/2/00	5/15/00	5/24/00
Achnanthes minutissima	8.26	7.58	5.22	12.65	0.97	6.70	4.58	10.32	0.09	0.12
Actinocyclus curvatulus	0.40				0.24					0.01
Actinoptychus vulgaris						0.38				
Amphora helenensis			0.98						0.02	0.01
Bacteriastrum delicatulum	0.79			1.02		0.38	0.51	3.44	0.05	0.02
Berkeleya rutilans									0.01	0.03
Cocconeis disculus	0.40	0.32				0.74	0.51			
Cocconeis neothumensis	0.40	1.27		1.02	0.72		0.51		0.01	
Cocconeis placentula	1.98	0.95	0.65	1.51	0.97		1.02	1.72	0.02	0.02
Cocconeis scutellum	1.19	1.58	0.65		1.21	1.12	3.07		0.01	0.04
Cocconeis stauroneiformis		0.95	0.33	3.04	0.97	2.23	2.56	1.72	0.02	0.03
Diatomella minuta	0.79	0.63		1.51	0.49					0.03
Ditylum brightwellii	0.40	0.95		0.51	0.24	0.74	1.02	32.50	0.03	0.03
Eunotia spp.	1.98	0.32	1.31	2.53	0.24	0.38				0.01
Fragilaria cf. *sopotensis*		0.95		3.55	0.24		0.51		0.01	
Fragilariopsis atlantica	1.19	3.17	4.24	3.04	3.39	1.50	2.56	3.44	0.01	0.03
Fragilariopsis pseudonana	14.56	10.75	8.81	15.17	2.66	12.27	4.58	23.99	0.05	0.04
Gomphonemopsis lindae	0.79	0.63							0.02	0.05
Gomphonemopsis obscurum	0.79	0.95	0.33	2.02	0.49	2.23	3.07	6.88	0.08	0.05
Hyalodiscus scoticus	0.79		0.65	0.51	0.24					0.00
Melosira nummuloides	0.79	1.90		2.02	0.72	0.74	5.09	5.16	0.03	0.05
Minidiscus chilensis	27.16	20.21	19.89	32.37	13.78	50.22	46.40	90.78	0.42	0.20
Navicula gregaria	0.40		1.64	1.02	0.24	1.12	1.02		0.01	0.01
Navicula perminuta	3.93	4.10	6.19	2.02	1.21	3.71	3.07	1.72	0.16	0.12
Nitzschia coarctata			2.28			0.38				
Nitzschia frustulum	12.98	5.68	3.26	8.10	3.87	7.82	10.19	22.27	0.21	0.36
Opephora cf. *horstiana*	0.40			1.02		0.74			0.01	0.01
Opephora mutabilis			0.98	1.02	0.24				0.01	0.01
Paralia sulcata		1.58		1.02	0.97	1.50	0.51	1.72	0.01	0.01
Planothidium delicatulum	3.93	4.73	0.33	3.04	1.93	4.09	6.12	6.88	0.13	0.12
Planothidium cf. engelbretchii				2.02	0.49	2.23			0.01	0.03
Planothidium hauckianum		0.63	0.65	0.51		1.12			0.01	0.03
Pleurosigma spp.		0.95	0.33	1.02	0.72	0.38			0.01	0.01
Pseudonitzschia multiseries	2.75	1.90	3.26	2.02	1.21	1.86	1.02		0.01	0.01
Pseudonitzschia seriata	1.19	1.27	1.31	2.53	0.24		0.51		0.02	0.02
Rhizosolenia spp.	5.12	6.00	5.88	4.04	2.66	1.12	2.56	6.88		0.02
Skeletonema costatum	56.67	32.54	42.07	61.72	26.86	16.36	49.96	243.21	0.32	0.32
Skeletonema costatum (weak)	12.98	13.58	15.32	21.74	11.62	20.09	36.70	268.83	0.07	0.11
Tabularia fasciculata	1.19	0.63	0.65	1.02	1.69		2.56		0.02	0.07
Thalassionema bacillare					0.24					
Thalassionema nitzschioides	5.12	6.95	8.15	12.65	16.21	14.15	21.93	30.86	0.24	0.21
Thalassionema pseudonitzschioides					0.72				0.06	0.05
Thalassiosira angulata		0.32								
Thalassiosira conferta	1.19	1.58	0.65		0.24	0.38	1.02	1.72		
Thalassiosira decipiens	2.37	3.17	2.28	4.04	3.87	4.83	8.68	13.67	0.06	0.04
Thalassiosira eccentrica	0.40	0.32	0.65	1.51	0.24	0.74	0.51		0.02	0.03
Thalassiosira cf. *leptopus*	1.19	0.95	1.64	1.51	0.49	0.38	1.02	3.44	0.01	
Thalassiosira minima	0.79		0.33		0.24	0.74				
Thalassiosira nordenskioeldii		0.32	0.65	2.53	0.49	0.38		3.44	0.02	0.01
Thalassiosira oestrupii	0.40	0.63	0.98	1.02	0.97	1.12			0.03	0.01
Thalassiosira pacifica	1.58	1.27	1.64	4.04	1.46	2.61	12.74	17.11	0.02	0.02
Thalassiosira rotula						0.74	2.56	8.60		
Thalassiosira tealata		0.32		0.51		0.38				0.01
Thalassiosira tenera	0.79		0.98			1.12		3.44	0.04	0.01
Thalassiosira sp. (cf. *tenera*)	0.40	1.58	2.93	1.51	1.93	2.97	3.07	5.16	0.01	0.01

APPENDIX E6 (continued)

Sample	3C-3	3C-4	3C-5	3C-6	3C-7	3C-8	3C-9	3C-10	3C-11	3C-12
Date opened	6/3/00	6/13/00	6/23/00	7/3/00	7/12/00	7/22/00	8/1/00	8/11/00	8/21/00	8/31/00
Achnanthes minutissima	0.05	0.09	0.21	0.00	0.09	0.01	0.01	0.00	0.02	0.02
Actinocyclus curvatulus	0.02									
Actinoptychus vulgaris										
Amphora helenensis	0.02		0.05				0.01			
Bacteriastrum delicatulum	0.07	0.18	0.31	0.18		0.02	0.01		0.04	0.01
Berkeleya rutilans				0.09		0.01				0.01
Cocconeis disculus										
Cocconeis neothumensis						0.01				
Cocconeis placentula	0.02	0.09					0.01		0.02	0.01
Cocconeis scutellum		0.18				0.01		0.01	0.01	0.00
Cocconeis stauroneiformis		0.09			0.01	0.01			0.01	
Diatomella minuta	0.05									
Ditylum brightwellii	0.02				0.03	0.01	0.01	0.01	0.01	0.01
Eunotia spp.										
Fragilaria cf. *sopotensis*										
Fragilariopsis atlantica	0.02		0.05				0.02		0.01	
Fragilariopsis pseudonana	0.10	1.36	0.47	0.45	0.11	0.03	0.05	0.08	0.08	0.02
Gomphonemopsis lindae	0.02				0.01			0.01	0.01	0.01
Gomphonemopsis obscurum	0.02		0.11			0.01	0.02			0.02
Hyalodiscus scoticus								0.01		
Melosira nummuloides				0.09						
Minidiscus chilensis	0.22	0.45	0.42	0.09	0.03	0.02	0.04	0.01	0.04	0.02
Navicula gregaria		0.09								
Navicula perminuta	0.02	0.09	0.11		0.04	0.02	0.03	0.01	0.02	0.01
Nitzschia coarctata										0.00
Nitzschia frustulum	0.36	0.82	0.21	0.27	0.04	0.02	0.02	0.05	0.10	0.06
Opephora cf. *horstiana*					0.01	0.01				0.01
Opephora mutabilis	0.02									0.01
Paralia sulcata		0.36								
Planothidium delicatulum	0.10		0.31		0.01	0.01	0.02	0.04	0.03	0.05
Planothidium cf. engelbretchii								0.02		
Planothidium hauckianum										0.01
Pleurosigma spp.										0.01
Pseudonitzschia multiseries		0.64		0.09	0.12	0.02	0.02	0.01	0.04	0.04
Pseudonitzschia seriata	0.10	1.00	0.57	0.36	0.17	0.03	0.05	0.09	0.14	0.10
Rhizosolenia spp.					0.00		0.01		0.01	
Skeletonema costatum	9.16	18.80	15.33	42.17	5.77	0.80	0.87	1.31	1.06	1.79
Skeletonema costatum (weak)	0.68	18.26	4.78	3.05	0.84	0.23	0.18	0.19	0.12	0.12
Tabularia fasciculata	0.07		0.36	0.18	0.00		0.01	0.02		0.02
Thalassionema bacillare										0.01
Thalassionema nitzschioides	0.19	0.55	0.68	0.54	0.07	0.10	0.11	0.10	0.08	0.11
Thalassionema pseudonitzschioides		0.18	0.21			0.01	0.01	0.01	0.01	0.02
Thalassiosira angulata		0.09	0.00	0.09	0.01					
Thalassiosira conferta	0.05	0.45	0.05		0.00					
Thalassiosira decipiens	0.05		0.05					0.01	0.01	
Thalassiosira eccentrica	0.27	0.45	0.42		0.03	0.02	0.02	0.03	0.02	0.02
Thalassiosira cf. *leptopus*	0.05		0.11		0.01					0.03
Thalassiosira minima			0.05							
Thalassiosira nordenskioeldii	0.05	0.18	0.31	0.18	0.03	0.01	0.01	0.01	0.02	0.02
Thalassiosira oestrupii		0.18		0.09	0.06	0.01		0.01	0.01	0.01
Thalassiosira pacifica		0.09	0.05	0.18		0.01	0.01	0.01		0.01
Thalassiosira rotula	0.05	0.18	0.05				0.01			0.01
Thalassiosira tealata		0.18	0.11	0.09						
Thalassiosira tenera	0.24	0.36		0.09			0.01	0.03	0.02	0.01
Thalassiosira sp. (cf. *tenera*)		0.09		0.09					0.01	0.02

APPENDIX E6 (continued)

Sample	3C-13	3C-14	11C-1	11C-2	11C-3	11C-4	11C-5	11C-6	11C-7	11C-8
Date opened	9/9/00	9/19/00	5/15/00	5/24/00	6/3/00	6/13/00	6/23/00	7/3/00	7/12/00	7/22/00
Achnanthes minutissima	0.03	0.02	0.75	3.74	1.91	6.62	2.89	2.64	0.63	
Actinocyclus curvatulus										
Actinoptychus vulgaris									0.63	1.02
Amphora helenensis				0.63		3.31		1.32	0.63	
Bacteriastrum delicatulum	0.03		0.75			4.94	0.58	1.32	5.71	1.02
Berkeleya rutilans			2.99					0.66		
Cocconeis disculus			0.75	0.63	1.91				0.63	2.04
Cocconeis neothumensis			0.75							
Cocconeis placentula	0.01	0.01	1.49	4.38	3.82		1.16	1.32	1.90	4.08
Cocconeis scutellum	0.01		3.74	4.38	7.74	1.66	2.31	4.61	2.54	3.06
Cocconeis stauroneiformis			0.75	1.87	1.91	1.66		0.66	0.63	
Diatomella minuta			1.49							2.04
Ditylum brightwellii	0.01		2.99	1.24	1.91			0.66		
Eunotia spp.	0.01		0.75							
Fragilaria cf. *sopotensis*		0.01	0.75						0.63	
Fragilariopsis atlantica			0.75				0.58		1.90	3.06
Fragilariopsis pseudonana	0.07	0.04	6.73	8.12	25.14	18.13	5.20	7.91	7.61	9.17
Gomphonemopsis lindae		0.01	1.49	0.63						1.02
Gomphonemopsis obscrurum	0.01		0.75	0.63	3.82	1.66	1.16	3.30		
Hyalodiscus scoticus				0.63			0.58			1.02
Melosira nummuloides				2.51						1.02
Minidiscus chilensis	0.07	0.08	149.90	147.67	341.78	209.03	67.63	74.49	60.26	103.94
Navicula gregaria		0.01			1.91				0.63	
Navicula perminuta	0.03	0.02		3.74	7.74	1.66	5.78	1.98	0.63	4.08
Nitzschia coarctata				0.63						
Nitzschia frustulum	0.08	0.05	9.68	3.74	17.39	16.47	6.94	3.96	1.27	10.19
Opephora cf. *horstiana*		0.01		1.87			0.58			
Opephora mutabilis				0.63	1.91		1.16	1.32	1.27	
Paralia sulcata			1.49	3.14	21.22	11.51		3.96		5.10
Planothidium delicatulum	0.02	0.02	2.99	3.74	17.39	9.85	1.16		2.54	6.11
Planothidium cf. engelbretchii										
Planothidium hauckianum				0.63			1.16	0.66		2.04
Pleurosigma spp.								0.66		
Pseudonitzschia multiseries	0.04	0.02	1.49	1.24	3.82	27.98	2.89	3.96	1.27	3.06
Pseudonitzschia seriata	0.11	0.06	1.49	0.63	17.39	42.80	8.09	4.61	16.49	16.30
Rhizosolenia spp.	0.01	0.01	2.24	2.51	15.48	3.31	4.05	0.66	2.54	9.17
Skeletonema costatum	0.95	1.12	16.40	16.91	61.74	83.94	32.37	99.54	111.01	120.24
Skeletonema costatum (weak)	0.08	0.14	8.97	5.65	34.79	123.43	24.28	27.69	10.78	17.32
Tabularia fasciculata	0.01	0.02	2.99		5.83			1.98		
Thalassionema bacillare										
Thalassionema nitzschioides	0.13	0.11	59.67	38.80	162.19	97.11	43.93	20.44	23.47	83.56
Thalassionema pseudonitzschioides	0.01	0.02	10.42	6.88	9.65	6.62	1.73	1.98	1.27	3.06
Thalassiosira angulata						1.66	0.58	0.66	0.63	
Thalassiosira conferta			1.49		1.91	1.66	1.16		3.17	
Thalassiosira decipiens	0.01		20.14	14.40	42.44	19.79	10.40	12.53	5.07	14.27
Thalassiosira eccentrica	0.02	0.04	6.73	1.24	7.74	8.20	2.31	6.59	1.27	11.21
Thalassiosira cf. *leptopus*	0.01	0.01					2.31	0.66	0.63	
Thalassiosira minima										
Thalassiosira nordenskioeldii	0.02	0.01	2.24	1.24		9.85	0.58	2.64	6.34	8.15
Thalassiosira oestrupii	0.01		1.49	1.87	1.91		1.16	1.98		3.06
Thalassiosira pacifica			5.23	5.01	15.48	42.80	31.21	7.25	7.61	14.27
Thalassiosira rotula					1.91	1.66	0.58		1.27	
Thalassiosira tealata						3.31	1.16			
Thalassiosira tenera	0.02	0.02	2.99	3.14	17.39	6.62	2.89	5.27	5.07	12.23
Thalassiosira sp. (cf. *tenera*)			1.49	1.24		1.66				

APPENDIX E6 (continued)

Sample	11C-9	11C-10	11C-11	11C-12	11C-13	11C-14
Date opened	8/1/00	8/11/00	8/21/00	8/31/00	9/9/00	9/19/00
Achnanthes minutissima	2.71	3.40	0.56	2.04		3.93
Actinocyclus curvatulus						
Actinoptychus vulgaris	1.08				0.95	
Amphora helenensis		3.40				4.59
Bacteriastrum delicatulum	0.54	3.40		1.01	1.89	
Berkeleya rutilans		1.70		1.02		
Cocconeis disculus	0.54				3.78	0.66
Cocconeis neothumensis						
Cocconeis placentula	2.17	1.70	2.22	7.08	1.89	1.32
Cocconeis scutellum	2.17	8.51	2.79	1.02	1.89	3.27
Cocconeis stauroneiformis						0.66
Diatomella minuta						
Ditylum brightwellii	0.54	1.70	0.56		1.89	
Eunotia spp.						
Fragilaria cf. *sopotensis*						
Fragilariopsis atlantica	1.08	1.70		3.06	0.95	
Fragilariopsis pseudonana	7.05	17.01	1.66	3.06	4.73	3.27
Gomphonemopsis lindae		1.70				
Gomphonemopsis obscurum		3.40		2.04		1.95
Hyalodiscus scoticus						
Melosira nummuloides						
Minidiscus chilensis	104.66	351.47	119.53	167.37	174.09	109.93
Navicula gregaria						
Navicula perminuta	3.25	3.40	2.22	8.10	8.52	2.61
Nitzschia coarctata	0.00					
Nitzschia frustulum	4.34	13.61	2.22	11.15	7.57	3.93
Opephora cf. *horstiana*		1.70				
Opephora mutabilis	1.08				0.95	
Paralia sulcata	1.63	1.70		4.07	14.19	4.59
Planothidium delicatulum	3.25	1.70	2.22	1.02	1.89	3.93
Planothidium cf. engelbretchii		3.40				
Planothidium hauckianum			0.56			0.66
Pleurosigma spp.				1.02		
Pseudonitzschia multiseries	1.08	6.80	1.13	5.09	1.89	1.32
Pseudonitzschia seriata	5.42	10.21	6.10	11.15	12.30	2.61
Rhizosolenia spp.	7.05	11.91	15.56	145.06	50.15	32.05
Skeletonema costatum	34.71	110.32	31.14	32.43	37.85	34.03
Skeletonema costatum (weak)	4.88	8.51	5.57	5.09	5.68	9.81
Tabularia fasciculata			1.13			0.66
Thalassionema bacillare			0.56			0.66
Thalassionema nitzschioides	29.28	144.35	33.93	54.79	58.66	47.78
Thalassionema pseudonitzschioides	1.08	6.80	1.66	2.04	0.95	1.32
Thalassiosira angulata	0.54					
Thalassiosira conferta			1.13	1.02	0.95	0.66
Thalassiosira decipiens	8.13	22.03	12.24	6.11	13.25	10.47
Thalassiosira eccentrica	1.63	22.03	2.79	5.09	5.68	1.95
Thalassiosira cf. *lepiopus*		1.70				0.66
Thalassiosira minima	0.54	1.70				
Thalassiosira nordenskioeldii	1.63	3.40	0.56	2.04	0.95	0.66
Thalassiosira oestrupii		0.00	1.66	1.02	2.84	4.59
Thalassiosira pacifica	2.71	1.70	5.01	4.07	8.52	0.66
Thalassiosira rotula					0.95	
Thalassiosira tealata		1.70				0.66
Thalassiosira tenera	3.80	10.21	3.35	3.06	7.57	3.93
Thalassiosira sp. (cf. *tenera*)		1.70				

APPENDIX F

^{137}Cs and ^{210}Pb Analysis Results from Freeze Core TUL99B04

APPENDIX F1

^{137}Cs and ^{210}Pb analysis report

The following is a facsimile of the original report supplied by Dr. Bassam Ghaleb of GEOTOP Laboratories, University of Quebec at Montreal, for analyses of freeze core TUL99B04. The results represent raw data that have not been converted into calendar dates.

Sample	Depth cm	210Pb dpm/g	±	137Cs dpm/g	±
1	3.5	27.5892	1.1034	n.d.	n.d.
2	4.5	19.6896	0.663	n.d.	n.d.
3	5.5	15.0053	0.6637	n.d.	n.d.
4	6.5	14.8138	0.5626	n.d.	n.d.
5	7.5	19.1768	0.662	n.d.	n.d.
6	8.5	18.7678	0.5645	1.96754985	0.28785254
7	9.5	15.8521	0.5518	4.51410458	0.27445756
8	10.5	15.2466	0.4769	2.52343263	0.16225672
9	11.5	14.7841	0.3493	2.35062369	0.21461194
10	12.5	13.744	0.5087	2.41212976	0.14738113
11	13.5	12.4566	0.2737	3.19680807	0.21898135
12	14.5	12.4679	0.3264	3.05435374	0.20128191
13	15.5	13.3083	0.557	2.82462134	0.21890815
14	16.5	11.2877	0.5076	3.27395497	0.15354849
15	17.5	9.9365	0.2809	3.50669038	0.17533452
16	18.5	10.0903	0.2308	4.09675857	0.24170876
17	19.5	9.3052	0.3955	2.94326901	0.20750047
18	20.5	n.d.	n.d.	3.04705827	0.16636938
19	21.5	7.1394	0.2171	3.89986416	0.19538319
20	22.5	8.993	0.2326	6.95946778	0.40991265
21	23.5	7.9991	0.2132	6.34070022	0.24221475
22	24.5	6.9989	0.2233	3.40902231	0.15715593
23	25.5	7.3646	0.2298	3.49440137	0.19708424
24	26.5	7.2795	0.2417	n.d.	n.d.
25	27.5	6.9837	0.259	1.22748806	0.13244596
26	28.5	6.7459	0.2163	0.89821156	0.14407313
27	29.5	6.2885	0.1893	n.d.	n.d.
28	30.5	5.814	0.1688	n.d.	n.d.
29	31.5	3.8549	0.1151	n.d.	n.d.

dpm/g: disintegration per minute per gram of sample

±: correspond to 1 sigma error from counting statistic

n.d.: not determined

Le 03/08/2001 À 19:11:04

UqPo : 3129

ANALYSE ^{209}Po, ^{210}Po,

Terrain : 1.Chang 3-4cm
Masse : 0.1067 g

1. Caracteristiques des isotopes du Polonium

	^{209}Po	^{210}Po	Temps
Impulsions	1815	987	4008.9020 mn
Bruit Fond	108	73	15691.9970 mn
Cps	0.4459	0.2416	
Signa	±0.0106	±0.0078	

2. Traceurs et rendements

Traceur UqPo ^{209}PoRef d.p.m. = 5.4337 Au jour d'acquisition : 30Jul01
Rend. Chim. Po : 0.2931 Rend. Global. Po :0.0821

3. Concentration et activite de l'echantillon

^{209}Podpm/g	^{210}Podpm/g
10.7173	27.5892
±0.3592	±1.1034

Le 31/07/2001 à 15:52:09

UqPo : 3130

ANALYSE ^{209}Po, ^{210}Po,

Terrain : 2.Chang 4-5cm
Masse : 0.3009 g

1. Caracteristiques des isotopes du Polonium

	^{209}Po	^{210}Po	Temps
Impulsions	1696	1852	1430.4670 mn
Bruit Fond	44	91	15691.8907 mn
Cps	1.1828	1.2889	
Sigma	±0.0288	±0.0300	

2. Traceurs et rendements

Traceur UqPo ^{209}PoRef d.p.m. = 5.4371 Au jour d'acquisition : 30/07/01
Rend. Chim. Po : 0.7204 Rend. Global. Po :0.2175

3. Concentration et activite de l'echantillon

^{209}Podpm/g	^{210}Podpm/g
10.7177	19.6896
±0.3685	±0.6630

Le 31/07/2001 à 15:52:10

UqPo : 3131

ANALYSE ^{209}Po, ^{210}Po,

Terrain : 3.Chang 5-6cm
Masse : 0.3062 g

1. Caractéristiques des isotopes du Polonium

	^{209}Po	^{210}Po	Temps
Impulsions	1123	954	1430.3970 mn
Bruit fond	75	106	15691.7497 mn
Cps	0.7853	0.6602	
Sigma	±0.0234	±0.0215	

2. Traceurs et rendements

Traceur UqPo [illegible]Ref d.p.m. = 5.4306 [illegible] d'acquisition : 30041.01
Rend. Chim. Po : 0.4972 Rend. Global. Po :0.1437

3. Concentration et activité de l'echantillon

^{209}Podpm/g	^{210}Podpm/g
10.7177	15.0053
±0.4538	±0.6637

Le 31/07/2001 À 15:52:10

UqPo : 3132

ANALYSE ^{209}Po, ^{210}Po,

Terrain : 4.Chang 6-7cm
Masse : 0.3085 g

1. Caracteristiques des isotopes du Polonium

	^{209}Po	^{210}Po	Temps
Impulsions	1518	1283	1430.3147 mn
Bruit Fond	9	53	14284.7150 mn
Cps	1.0607	0.8933	
Sigma	±0.0272	±0.0250	

2. Traceurs et rendements

Traceur UqPo ^{209}PoRef d.p.m. = 5.4264 Au jour d'acquisition : 30Jul01
Rend. Chim. Po : 0.7041 Rend. Global. Po :0.1955

3. Concentration et activite de l'echantillon

^{209}Podpm/g	^{210}Podpm/g
10.7177	14.8138
±0.3892	±0.5626

Le 31/07/2001 à 15:52:10

UqPo : 3133

ANALYSE ^{209}Po, ^{210}Po,

Terrain : 5.Chang 7-8cm
Masse : 0.3019 g

1. Caracteristiques des isotopes du Polonium

	^{209}Po	^{210}Po	Temps
Impulsions	1643	1734	1430.2587 mn
Bruit Fond	80	80	14284.6687 mn
Cps	1.1431	1.2068	
Sigma	±0.0283	±0.0291	

2. Traceurs et rendements

Traceur UqPo ^{209}PoRef d.p.m. = 5.4842 Au jour d'acquisition : 30Jul01
Rend. Chim. Po : 0.7624 Rend. Global. Po :0.2084

3. Concentration et activite de l'echantillon

^{209}Podpm/g	^{210}Podpm/g
10.7177 ±0.3749	19.1768 ±0.6620

Le 31/07/2001 à 15:52:11

UqPo : 3134

ANALYSE ^{209}Po, ^{210}Po,

Terrain : 6.Chang 8-9cm
Masse : 0.3147 g

1. Caracteristiques des isotopes du Polonium

	^{209}Po	^{210}Po	Temps
Impulsions	2608	1944	1430.1990 mn
Bruit Fond	115	169	14284.6330 mn
Cps	1.8155	1.3474	
Sigma	±0.0356	±0.0307	

2. Traceurs et rendements

Traceur UqPo ^{209}PoRef d.p.m. = 7.9579 Au jour d'acquisition : 30Jul01
Rend. Chim. Po : 0.7658 Rend. Global. Po :0.2281

3. Concentration et activite de l'echantillon

^{209}Podpm/g	^{210}Podpm/g
10.7177 ±0.2975	18.7678 ±0.5645

Le 31/07/2001 à 15:52:11

UqPo : 3135

ANALYSE ^{209}Po, ^{210}Po,

Terrain : 7.Chang 9-10cm
Masse : 0.3066 g

1. Caracteristiques des isotopes du Polonium

	^{209}Po	^{210}Po	Temps
Impulsions	1758	1570	1430.1343 mn
Bruit Fond	27	119	15691.2793 mn
Cps	1.2275	1.0902	
Sigma	±0.0293	±0.0276	

2. Traceurs et rendements

Traceur UqPo ^{209}PoRef d.p.m. = 5.4724 Au jour d'acquisition : 30Jul01
Rend. Chim. Po : 0.7789 Rend. Global. Po :0.2243

3. Concentration et activite de l'echantillon

^{209}Podpm/g	^{210}Podpm/g
10.7177	15.8521
±0.3618	±0.5518

Le 03/08/2001 à 19:11:04

UqPo : 3136

ANALYSE ^{209}Po, ^{210}Po,

Terrain : 8.Chang 10-11cm
Masse : 0.3035 g

1. Caracteristiques des isotopes du Polonium

	^{209}Po	^{210}Po	Temps
Impulsions	2236	1904	1920.1253 mn
Bruit Fond	112	73	15691.9970 mn
Cpm	1.1574	0.9869	
Sigma	±0.0246	±0.0227	

2. Traceurs et rendements

Traceur UqPo ^{209}PoRef d.p.m. = 5.4263 Au jour d'acquisition : 02Aug01
Rend. Chim. Po : 0.7617 Rend. Global. Po :0.2133

3. Concentration et activite de l'echantillon

^{209}Podpm/g	^{210}Podpm/g
10.7176 ±0.3216	15.2466 ±0.4769

Le 23/07/2001 à 13:23:13

UqPo : 3120

ANALYSE ^{209}Po, ^{210}Po,

Terrain : 9.Chang 11-12cm
Masse : 0.3024 g

1. Caracteristiques des isotopes du Polonium

	^{209}Po	^{210}Po	Temps
Impulsions	4035	3264	4270.5703 mn
Bruit Fond	44	89	15691.8907 mn
Cpa	0.9420	0.7586	
Sigma	±0.0149	±0.0133	

2. Traceurs et rendements

Traceur UqPo ^{209}PoRef d.p.m. = 5.5516 Au jour d'acquisition : 20Jul01
Rend. Chim. Po : 0.5619 Rend. Global. Po :0.1697

3. Concentration et activite de l'echantillon

^{209}Podpm/g	^{210}Podpm/g
10.7173 ±0.2391	14.7841 ±0.3493

Le 20/07/2001 à 13:55:51

UqPo : 3121

ANALYSE ^{209}Po, ^{210}Po,

Terrain : 10. Chang 12-13cm
Masse : 0.3773 g

1. Caractéristiques des isotopes du Polonium

	^{209}Po	^{210}Po	Temps
Impulsions	1507	1428	1664.2497 mn
Fruit Fond	36	76	15691.8907 mn
Cpm	0.9032	0.8532	
Sigma	±0.0233	±0.0226	

2. Traceurs et rendements

Traceur UqPo ^{209}PoRef d.p.m. = 5.4896 Au jour d'acquisition : 19Juil1
Rend. Chim. Po : 0.5448 Rend. Global. Po : 0.1545

3. Concentrations en fonction de la soustraction

^{209}Podpm/g	^{210}Podpm/g
10.7177 ±0.3910	13.7440 ±0.5087

Le 06/08/2001 à 12:08:59

UqPo : 3140

ANALYSE ^{209}Po, ^{210}Po,

Terrain : 11.Chang 13-14cm
Masse : 0.3024 g

1. Caracteristiques des isotopes du Polonium

	^{209}Po	^{210}Po	Temps
Impulsions	5116	3516	3881.8297 mn
Bruit Fond	31	120	18829.8300 mn
Cps	1.3163	0.8994	
Sigma	±0.0184	±0.0152	

2. Traceurs et rendements

Traceur UqPo ^{209}PoRef d.p.m. = 5.5130 Au jour d'acquisition : 03Au,01
Rend. Chim. Po : 0.7752 Rend. Global. Po :0.2388

3. Concentration et activite de l'echantillon

^{209}Podpm/g	^{210}Podpm/g
10.7173	12.4566
±0.2121	±0.2737

Le 06/08/2001 à 12:08:59

UqPo : 3141

ANALYSE ^{209}Po, ^{210}Po,

Terrain : 12.Chang 14-15cm
Masse : 0.3005 g

1. Caractéristiques des isotopes du Polonium

	^{209}Po	^{210}Po	Temps
Impulsions	3612	2481	3881.8067 mn
Bruit Fond	47	88	15692.2973 mn
Cpm	0.9275	0.6335	
Sigma	±0.0155	±0.0128	

2. Traceurs et rendements

Traceur UqPo ^{209}PoRef d.p.m. = 5.4351 Au jour d'acquisition : 03Aug01
Rend. Chim. Po : 0.5544 Rend. Global. Po :0.1691

3. Concentration et activité de l'échantillon

^{209}Podpm/g	^{210}Podpm/g
10.7173 ±0.2527	12.4679 ±0.3264

Le 30/07/2001 à 13:55:51

UqPo : 3123

ANALYSE ^{209}Po, ^{210}Po,

Terrain : 13.Chang 15-16cm
Masse : 0.3047 g

1. Caracteristiques des isotopes du Polonium

	^{209}Po	^{210}Po	Temps
Impulsions	1348	1005	1664.2307 mn
Bruit Fond	67	91	15691.7497 mn
Cps	0.8057	0.5981	
Sigma	±0.0220	±0.0190	

2. Traceurs et rendements

Traceur UqPo ^{209}PoRef d.p.m. = 5.4628 Au jour d'acquisition : 19Jul01
Rend. Chim. Po : 0.5103 Rend. Global. Po :0.1475

3. Concentration et activite de l'echantillon

^{209}Podpm/g	^{210}Podpm/g
10.7177	13.3083
±0.4140	±0.5570

Le 20/07/2001 à 13:55:51

UqPo : 3124

ANALYSE ^{209}Po, ^{210}Po,

Terrain : 14.Chang 16-17cm
Masse : 0.3248 g

1. Caracteristiques des isotopes du Polonium

	^{209}Po	^{210}Po	Temps
Impulsions	1230	833	1664.1987 mn
Bruit Fond	9	44	14284.7150 mn
Cps	0.7385	0.4975	
Signa	±0.0211	±0.0173	

2. Traceurs et rendements

Traceur UqPo ^{209}PoRef d.p.m. = 5.4424 Au jour d'acquisition : 19Jul01
Rend. Chim. Po : 0.4888 Rend. Global. Po :0.1357

3. Concentration et activite de l'echantillon

^{209}Podpm/g	^{210}Podpm/g
10.7177	11.2877
±0.4324	±0.5076

Le 23/07/2001 à 13:23:12

UqPo : 3125

ANALYSE ^{209}Po, ^{210}Po,

Terrain : 15.Chang 17--18cm
Masse : 0.2931 g

1. Caracteristiques des isotopes du Polonium

	^{209}Po	^{210}Po	Temps
Impulsions	3656	1950	4270.5527 mn
Bruit Fond	83	115	15691.7497 mn
Cpm	0.8508	0.4493	
Sigma	±0.0141	±0.0103	

2. Traceurs et rendements

Traceur UqPo ^{209}PoRef d.p.m. = 5.5151 Au jour d'acquisition : 20Jul01
Rend. Chim. Po : 0.5338 Rend. Global. Po :0.1543

3. Concentration et activite de l'echantillon

^{209}Podpm/g	^{210}Podpm/g
10.7173 ±0.2517	9.9365 ±0.2809

Le 06/03/2001 à 12:08:59

UqPo : 3142

ANALYSE ^{209}Po, ^{210}Po,

Terrain : 16.Chang 18-19cm
Masse : 0.3143 g

1. Caracteristiques des isotopes du Polonium

	^{209}Po	^{210}Po	Temps
Impulsions	5210	3047	3881.7887 mn
Bruit Fond	44	82	15692.1783 mn
Cps	1.3394	0.7797	
Sigma	±0.0186	±0.0142	

2. Traceurs et rendements

Traceur UqPo ^{209}PoRef d.p.m. = 5.4476 Au jour d'acquisition : 03Aug01
Rend. Chim. Po : 0.8478 Rend. Global. Po :0.2459

3. Concentration et activite de l'echantillon

^{209}Podpm/g	^{210}Podpm/g
10.7173	10.0903
±0.2103	±0.2308

Le 23/07/2001 à 13:23:13

UqPo : 3126

ANALYSE ^{209}Po, ^{210}Po,

Terrain : 17.Chang 19-20cm
Masse : 0.3218 g

1. Caracteristiques des isotopes du Polonium

	^{209}Po	^{210}Po	Temps
Impulsions	1555	877	4270.5270 mn
Bruit Fond	9	43	14284.7150 mn
Cpm	0.3635	0.2024	
Sigma	±0.0092	±0.0069	

2. Traceurs et rendements

Traceur UqPo ^{209}PoRef d.p.m. = 5.3790 Au jour d'acquisition : 20Jul01
Rend. Chim. Po : 0.2434 Rend. Global. Po :0.0676

3. Concentration et activite de l'echantillon

^{209}Podpm/g	^{210}Podpm/g
10.7173	9.3052
±0.3848	±0.3955

Le 06/08/2001 à 12:09:00

UqPo : 3144

ANALYSE ^{209}Po, ^{210}Po,

Terrain : 19.Chang21-22cm
Masse : 0.3025 g

1. Caracteristiques des isotopes du Polonium

	^{209}Po	^{210}Po	Temps
Impulsions	3823	1539	3881.7733 mn
Bruit Fond	96	88	15692.0943 mn
Cps	0.9787	0.3909	
Signa	±0.0159	±0.0101	

2. Traceurs et rendements

Traceur UqPo ^{209}PoRef d.p.m. = 5.4080 Au jour d'acquisition : 03Aug01
Rend. Chim. Po : 0.6487 Rend. Global. Po :0.1810

3. Concentration et activite de l'echantillon

^{209}Podpm/g	^{210}Podpm/g
10.7173 ±0.2461	7.1394 ±0.2171

Le 06/08/2001 à 12:09:00

UqPo : 3145

ANALYSE ^{209}Po, ^{210}Po,

Terrain : 20.Chiang 22-23cm
Masse : 0.3138 g

1. Caracteristiques des isotopes du Polonium

	^{209}Po	^{210}Po	Temps
Impulsions	4384	2302	3881.7577 mn
Bruit Fond	110	75	15691.9970 mn
Cpm	1.1224	0.5883	
Sigma	±0.0170	±0.0123	

2. Traceurs et rendements

Traceur UqPo ^{209}PoRef d.p.m. = 5.3844 Au jour d'acquisition : 03Aug01
Rend. Chim. Po : 0.7445 Rend. Global. Po :0.2085

3. Concentration et activite de l'echantillon

^{209}Podpm/g	^{210}Podpm/g
10.7173 ±0.2298	8.9930 ±0.2326

Le 06/08/2001 à 12:09:00

UqPo : 3146

ANALYSE ^{209}Po, ^{210}Po,

Terrain : 21.Chang 23-24cm
Masse : 0.3264 g

1. Caracteristiques des isotopes du Polonium

	^{209}Po	^{210}Po	Temps
Impulsions	4358	2105	3881.6373 mn
Bruit Fond	80	56	14284.6687 mn
Cps	1.1171	0.5384	
Sigma	±0.0170	±0.0118	

2. Traceurs et rendements

Traceur UqPo ^{209}PoRef d.p.m. = 5.4176 Au jour d'acquisition : 03Aug01
Rend. Chim. Po : 0.7542 Rend. Global. Po :0.2062

3. Concentration et activite de l'echantillon

^{209}Podpm/g	^{210}Podpm/g
10.7173 ±0.2303	7.9991 ±0.2132

Le 08/08/2001 À 10:17:31

UqPo : 3147

ANALYSE ^{209}Po, ^{210}Po,

Terrain : 22.Chang 24-25cm
Masse : 0.3099 g

1. Caracteristiques des isotopes du Polonium

	^{209}Po	^{210}Po	Temps
Impulsions	3441	1375	2766.6310 mn
Bruit Fond	2	0	15692.6193 mn
Cps	1.2436	0.4970	
Signa	±0.0212	±0.0134	

2. Traceurs et rendements

Traceur UqPo ^{209}PoRef d.p.m. = 5.4274 Au jour d'acquisition : 06Aug01
Rend. Chim. Po : 0.7910 Rend. Global. Po :0.2291

3. Concentration et activite de l'echantillon

^{209}Podpm/g	^{210}Podpm/g
10.7175	6.9989
±0.2584	±0.2233

Le 08/08/2001 à 10:17:32

UqPo : 3148

ANALYSE ^{209}Po, ^{210}Po,

Terrain : 23.Chang 25-26cm
Masse : 0.3161 g

1. Caracteristiques des isotopes du Polonium

	^{209}Po	^{210}Po	Temps
Impulsions	3420	1485	2766.5903 mn
Bruit Fond	27	99	18829.8300 mn
Cps	1.2347	0.5315	
Signa	±0.0211	±0.0139	

2. Traceurs et rendements

Traceur UqPo ^{209}PoRef d.p.m. = 5.4081 Au jour d'acquisition : 06Aug01
Rend. Chim. Po : 0.7413 Rend. Global. Po :0.2283

3. Concentration et activite de l'echantillon

^{209}Podpm/g	^{210}Podpm/g
10.7175	7.3646
±0.2593	±0.2298

Le 10/08/2001 à 15:52:08

UqPo : 3149

ANALYSE ^{209}Po, ^{210}Po,

Terrain : 24.Chang 26-27cm
Masse : 0.3157 g

1. Caracteristiques des isotopes du Polonium

	^{209}Po	^{210}Po	Temps
Impulsions	3069	1287	3183.0220 mn
Bruit Fond	1	0	15692.6193 mn
Cps	0.9641	0.4043	
Signa	±0.0174	±0.0113	

2. Traceurs et rendements

Traceur UqPo ^{209}PoRef d.p.m. = 5.4798 Au jour d'acquisition : 08Aug01
Rend. Chim. Po : 0.6073 Rend. Global. Po :0.1759

3. Concentration et activite de l'echantillon

^{209}Podpm/g	^{210}Podpm/g
10.7175 ±0.2736	7.2795 ±0.2417

Le 10/08/2001 à 15:52:08

UqPo : 3150

ANALYSE ^{209}Po, ^{210}Po,

Terrain : 25.Chang 27-28cm
Masse : 0.3400 g

1. Caracteristiques des isotopes du Polonium

	^{209}Po	^{210}Po	Temps
Impulsions	2389	1066	3182.9867 mn
Bruit Fond	29	99	18829.8300 mn
Cpm	0.7490	0.3296	
Sigma	±0.0153	±0.0102	

2. Traceurs et rendements

Traceur UqPo ^{209}PoRef d.p.m. = 5.3952 Au jour d'acquisition : 08Aug01
Rend. Chim. Po : 0.4507 Rend. Global. Po :0.1388

3. Concentration et activite de l'echantillon

^{209}Podpm/g	^{210}Podpm/g
10.7175	6.9837
±0.3105	±0.2590

Le 13/08/2001 à 18:03:33

UqPo : 3151

ANALYSE ^{209}Po, ^{210}Po,

[illegible] : 25.01mg 25—29cm
Masse : 0.3367 g

1. Caractéristiques des Isotopes du Polonium

	^{209}Po	^{210}Po	Temps
Coups/cpm	3333	1417	4442.7257 mn
Coup fond	92	103	10631.0943 mn
Cpm	0.7444	0.3124	
Sigma	±0.0130	±0.0084	

2. Traceurs et rendements

Traceur UqPo ^{209}PoRef d.p.m. = 5.4122 Au jour d'acquisition : 10Aug01
Rend. Chim. Po : 0.4929 Rend. Global. Po : 0.[illegible]

3. Concentration et activité de l'échantillon

^{209}Podpm/g	^{210}Podpm/g
10.7173	6.7459
±0.2639	±0.2163

Le 16/08/2001 à 11:20:50

UqPo : 3152

ANALYSE ^{209}Po, ^{210}Po,

Terrain : 27.Chang 29-30cm
Masse : 0.2569 g

1. Caracteristiques des isotopes du Polonium

	^{209}Po	^{210}Po	Temps
Impulsions	4950	1506	8337.5403 mn
Bruit Fond	136	94	15691.9970 mn
Cps	0.5850	0.1746	
Sigma	±0.0084	±0.0046	

2. Traceurs et rendements

Traceur UqPo $^{209}PoRef$ d.p.m. = 5.4119 Au jour d'acquisition : 10Aug01
Rend. Chim. Po : 0.3861 Rend. Global. Po :0.1081

3. Concentration et activite de l'echantillon

$^{209}Podpm/g$	$^{210}Podpm/g$
10.7167	6.2885
±0.2179	±0.1893

Le 16/08/2001 à 11:20:51

UqPo : 3153

ANALYSE ^{209}Po, ^{210}Po,

Terrain : 28.Chang 30-31cm
Masse : 0.2407 g

1. Caracteristiques des isotopes du Polonium

	^{209}Po	^{210}Po	Temps
Impulsions	5838	1575	8337.4990 mn
Bruit Fond	45	103	15691.8907 mn
Cpm	0.6973	0.1823	
Signa	±0.0092	±0.0047	

2. Traceurs et rendements

Traceur UqPo $^{209}PoRef$ d.p.m. = 5.3519 Au jour d'acquisition : 10Aug01
Rend. Chim. Po : 0.4314 Rend. Global. Po :0.1303

3. Concentration et activite de l'echantillon

^{209}Podpm/g	^{210}Podpm/g
10.7167	5.8140
±0.1990	±0.1688

Le 16/08/2001 à 11:20:51

UqPo : 3154

ANALYSE ^{209}Po, ^{210}Po,

Terrain : 29.Chiang 31-32cm
Masse : 0.2587 g

1. Caracteristiques des isotopes du Polonium

	^{209}Po	^{210}Po	Temps
Impulsions	7420	1437	8337.4477 mn
Bruit Fond	89	141	15691.7497 mn
Cps	0.8843	0.1634	
Sigma	±0.0103	±0.0045	

2. Traceurs et rendements

Traceur UqPo ^{209}PoRef d.p.m. = 5.3980 Au jour d'acquisition : 10Aug01
Rend. Chim. Po : 0.5668 Rend. Global. Po :0.1638

3. Concentration et activite de l'echantillon

^{209}Podpm/g	^{210}Podpm/g
10.7167	3.8549
±0.1768	±0.1151

APPENDIX F2: Calculation of calendar years from ^{210}Pb dating of freeze core TUL99B04

Sample	Median Interval (cm)	Wet Weight (g)	Dry Weight (g)	Percent Water	Total Dry Density (g/cm^3)	Wet Density (g/cm^3)	Dry Density (g dry/cm^3 wet)	Powys (1987) formulae for porosity	Bulk Density [density*(1-porisity] (g/cm^3)
1	3.5	1.5	0.1	93.333	2.275	1.108	0.083	0.965	0.080
2	4.5	4.8	0.3	93.750	2.275	1.103	0.078	0.967	0.076
3	5.5	6.2	0.3	95.161	2.275	1.085	0.060	0.974	0.059
4	6.5	6.8	0.3	95.588	2.275	1.080	0.055	0.976	0.054
5	7.5	8.5	0.5	94.118	2.275	1.099	0.074	0.969	0.071
6	8.5	9.5	0.7	92.632	2.275	1.117	0.092	0.961	0.089
7	9.5	9.4	0.7	92.553	2.275	1.118	0.093	0.961	0.089
8	10.5	10.2	0.7	93.137	2.275	1.111	0.086	0.964	0.083
9	11.5	9.5	0.9	90.526	2.275	1.143	0.118	0.951	0.113
10	12.5	10.0	0.8	92.000	2.275	1.125	0.100	0.958	0.096
11	13.5	9.8	0.8	91.837	2.275	1.127	0.102	0.957	0.098
12	14.5	8.9	0.7	92.135	2.275	1.123	0.098	0.959	0.094
13	15.5	10.6	1.0	90.566	2.275	1.143	0.118	0.951	0.112
14	16.5	10.0	1.0	90.000	2.275	1.150	0.125	0.948	0.118
15	17.5	9.6	0.9	90.625	2.275	1.142	0.117	0.951	0.111
16	18.5	7.7	0.7	90.909	2.275	1.139	0.114	0.952	0.108
17	19.5	8.6	0.8	90.698	2.275	1.141	0.116	0.951	0.111
18	20.5	9.2	0.8	91.304	2.275	1.134	0.109	0.954	0.104
19	21.5	10.1	0.9	91.089	2.275	1.136	0.111	0.953	0.106
20	22.5	6.0	0.6	90.000	2.275	1.150	0.125	0.948	0.118
21	23.5	7.0	0.9	87.143	2.275	1.186	0.161	0.934	0.150
22	24.5	8.8	0.9	89.773	2.275	1.153	0.128	0.947	0.121
23	25.5	9.4	0.9	90.426	2.275	1.145	0.120	0.950	0.114
24	26.5	7.3	0.6	91.781	2.275	1.128	0.103	0.957	0.098
25	27.5	8.3	0.7	91.566	2.275	1.130	0.105	0.956	0.101
26	28.5	7.6	0.7	90.789	2.275	1.140	0.115	0.952	0.110
27	29.5	9.2	1.0	89.130	2.275	1.161	0.136	0.944	0.128
28	30.5	8.5	0.9	89.412	2.275	1.157	0.132	0.945	0.125
29	31.5	2.3	0.3	86.957	2.275	1.188	0.163	0.933	0.152

n.s. = no sample

avg from Box Core Core EFBC9703-2

1.025=density of sea water

sed rate = 0.666666667 mm/yr

Mass accumulation rate:
cumulative mass (sum of sediment flux)
2.989011853 g/cm^2

number of years		if	
45	yr	46	yr
0.066422486	g/cm^2/yr	0.064978519	g/cm^2/yr

APPENDIX F2 (continued)

Sample	Sediment Flux (bulk density* slice thickness) (g/cm^2)	Cumulative Density (bottom) (g/cm^2)	Cumulative Density (top) (g/cm^2)	Pb (dpm/g)	Pb (ln)	Years from Top (Box Core)	Chronology	Years from Top (Freeze Core)	Chronology
1	0.080	0.080	0.000	27.5892	3.3174	0.0000	1989.0	0.0000	1989.0
2	0.076	0.156	0.080	19.6896	2.9801	1.1964	1987.8	1.2103	1987.8
3	0.059	0.215	0.156	15.0053	2.7084	2.3206	1986.7	2.3474	1986.7
4	0.054	0.269	0.215	14.8138	2.6956	3.1974	1985.8	3.2344	1985.8
5	0.071	0.340	0.269	19.1768	2.9537	3.9988	1985.0	4.0450	1985.0
6	0.089	0.428	0.340	18.7678	2.9321	5.0588	1983.9	5.1173	1983.9
7	0.089	0.518	0.428	15.8521	2.7633	6.3763	1982.6	6.4500	1982.5
8	0.083	0.601	0.518	15.2466	2.7244	7.7073	1981.3	7.7964	1981.2
9	0.113	0.713	0.601	14.7841	2.6936	8.9376	1980.1	9.0409	1980.0
10	0.096	0.809	0.713	13.744	2.6206	10.6129	1978.4	10.7356	1978.3
11	0.098	0.907	0.809	12.4566	2.5223	12.0385	1977.0	12.1777	1976.8
12	0.094	1.001	0.907	12.4679	2.5232	13.4920	1975.5	13.6480	1975.4
13	0.112	1.113	1.001	13.3083	2.5884	14.8946	1974.1	15.0668	1973.9
14	0.118	1.231	1.113	11.2877	2.4237	16.5632	1972.4	16.7547	1972.2
15	0.111	1.343	1.231	9.9365	2.2962	18.3267	1970.7	18.5386	1970.5
16	0.108	1.451	1.343	10.0903	2.3116	19.9853	1969.0	20.2164	1968.8
17	0.111	1.562	1.451	9.3052	2.2306	21.5961	1967.4	21.8458	1967.2
18	0.104	1.665	1.562	n.s.	n.s.	23.2426	1965.8	23.5113	1965.5
19	0.106	1.772	1.665	7.1394	1.9656	24.7865	1964.2	25.0731	1963.9
20	0.118	1.890	1.772	8.993	2.1964	26.3669	1962.6	26.6718	1962.3
21	0.150	2.040	1.890	7.9991	2.0793	28.1304	1960.9	28.4557	1960.5
22	0.121	2.161	2.040	6.9989	1.9458	30.3645	1958.6	30.7156	1958.3
23	0.114	2.275	2.161	7.3646	1.9967	32.1659	1956.8	32.5378	1956.5
24	0.098	2.373	2.275	7.2795	1.9851	33.8581	1955.1	34.2496	1954.8
25	0.101	2.474	2.373	6.9837	1.9436	35.3211	1953.7	35.7295	1953.3
26	0.110	2.584	2.474	6.7459	1.9089	36.8206	1952.2	37.2464	1951.8
27	0.128	2.712	2.584	6.2885	1.8387	38.4516	1950.5	38.8962	1950.1
28	0.125	2.837	2.712	5.814	1.7603	40.3598	1948.6	40.8265	1948.2
29	0.152	2.989	2.837	3.8549	1.3493	42.2213	1946.8	42.7095	1946.3

2.98901 18534 = summed sediment flux

APPENDIX F3. Freeze core couplet thickness measured from x-radiographs

Year	Thickness (mm)	Comment
1993	5.0	no analysis
1992	8.0	mean thickness (1986-1992): 10.2 mm
1991	12.0	
1990	10.2	
1989	13.1	
1988	5.0	
1987	13.0	
1986	12.7	
1985	7.4	mean thickness (1971-1985): 6.3 mm
1984	8.4	
1983	7.5	
1982	7.2	
1981	6.0	
1980	4.7	
1979	4.6	
1978	7.0	
1977	7.0	
1976	7.5	
1975	5.1	
1974	6.2	
1973	5.0	
1972	7.0	
1971	4.0	
1970	6.0	mean thickness (1947-1970): 6.0 mm
1969	6.5	
1968	8.0	
1967	5.8	
1966	4.7	
1965	7.0	
1964	8.0	
1963	6.9	
1962	4.4	
1961	5.7	
1960	5.3	
1959	5.0	
1958	6.2	
1957	8.0	
1956	4.4	
1955	5.8	
1954	6.7	
1953	4.4	
1952	6.0	
1951	4.8	
1950	5.5	
1949	5.0	
1948	4.5	
1947	10.0	Total thickness (1947-1993): 318.2 mm

mean sediment accumulation rate (1947-1993): 6.9 mm/yr
mean sediment accumulation rate (1947-1985): 6.1 mm/yr

APPENDIX G

Data from Core Freeze Core TUL99B04

APPENDIX G1: Freeze core microfossil counts

Sample	B04-1	B04-2	B04-3	B04-4	B04-5	B04-6	B04-7	B04-8	B04-9	B04-10	B04-11	B04-12	B04-13	B04-14	B04-15	B04-16	B04-17
DIATOMS																	
A. brevipes					1							1			1	1	
A. kregeri															2		
A. lanceolata									1								
A. lemmermannii													1				1
A. minutissima	8	5	14	1	18	29	21	15	14	10	26	15	8	29	15	18	27
A. nodosa																	
A. parvula																	
Achnanthidium biasolettianum									1								
Actinocyclus curvatulus				1						1	2						
A. octonarius														1		1	
Actinocyclus sp. (B04-13)													1				
Actinocyclus sp. (B04-23)																	
Actinocyclus sp. (B04-35)																	
Actinoptychus senarius		1								1						2	
A. vulgaris				1													1
Amphora acutiuscula	1	1				2			1			1		6			1
A. coffaeformis								2		1				1			3
A. copulata	2	2			2		2	3					4	1			
A. exigua										1							
A. helenensis			2														
A. maletracta var. *constricta*			1			1								1		3	
A. marina							1										1
Asteromphalus heptacis					1	1		1		3							
A. sarcophagus	1									1						2	1
Asteromphalus sp. (B04-20)																	
Aulacoseira islandica																	
Aulacoseira italica var. *subarctica*								1						1			
Aulacoseira sp. (B04-32)																	
Bacillaria paxillifer				1							1			1	1	1	1
Bacteriastrum delicatulum	2	1	3	7	1	4			3	2	3	1			4	5	1
Berkeleya rutilans		2			1		2									1	
Brachysira sp.														1	3		
Cocconeis costata complex	1	1	1	2	1	2		1		1			1	1		2	4
C. dirupta											1						
C. disculus			2					1		1	2	1		1	1		2
C. distans							1										
C. neothumensis																	
Cocconeis cf. *pellucida*																	
C. peltoides	2		1			2		1	2	1	1			1		2	3
C. pinnata																	
C. placentula	1	1	5		3	2	1		2	1		1	2	3	4		
C. scutellum			5		1	1	1	3	1	1	4	3		2	2	4	4
C. stauroneiformis		2	3	7	2	1	2	4		1	3	6	4	4	2	4	5
Cocconeis sp. (B04-21)																	
Cocconeis sp. (B04-23)																	
Cocconeis spp. (small)	1		3	2	1	4	3	2		2	3	1	1	1	2	1	1
Coscinodiscus diorama					1												
C. radiatus		1														1	
Coscinodiscus sp. (B04-15)															1		
Craticula halophila			1														
Ctenophora pulchella		2	1						2					3			
C. choctawhatcheeana															3		1
C. "punctata"														1			
C. rossii	1		3				1				1						
C. stelligera			5					2		1	1			1	1	2	1
C. striata							1			2	1	1	2	2		2	
C. stylorum					2				2								
Cyclotella sp. (B04-15)															1		

APPENDIX G1 (continued)

Sample	B04-1	B04-2	B04-3	B04-4	B04-5	B04-6	B04-7	B04-8	B04-9	B04-10	B04-11	B04-12	B04-13	B04-14	B04-15	B04-16	B04-17
Cymbella cymbiformis	1							1									
C. gracilis			1											1			
C. lanceolata																	
C. minuta			1					2	3						2		
Cymbella sp. (B04-17)																	1
Cymbella sp. (B04-19)																	
Cymbella sp. (B04-25)																	
Delphineis sp.																	
Denticula sp. (B04-18)			2			2					2		1				
Diatoma mesodon																	
D. tenue							1		1								
Diatoma sp. (B04-21)																	
Diatomella minuta				2	1												
Diploneis spp.																	
Ditylum brightwellii	3	2	4	1	4	3	3	3	6	1	5	2		3	6	2	
Ethmodiscus sp. (B04-19)																	
Eunotia spp.						1	1	1		1			1	1			
Fallacia sp. (B04-29)									2								
Fallacia sp.																	5
Fragilaria capucina complex			1		3	2	1					4			4		4
F. construens var. *construens*													1				
Fragilaria fo. *venter*																1	
F. investiens												2	4	6		1	2
F. pinnata		1	4				1	2	2	1					2	1	1
Fragilaria cf. *sopotensis*			2		2	2	1		1						1	4	1
Fragilaria sp. (B04-38)																	
Fragilariopsis atlantica		2		2			1			1	2	3				1	
F. cylindriformis	1							2			1						
F. pseudonana	1	3	13	3	1	2	4	4	2	15	12	7	6	12	6	18	14
F. schulzii									1								
Gomphonema augustatum																	
G. augustum			1			2						2		3			
G. olivaceum		2						1									
Gomphonema sp. (B04-25)																	
Gomphonema spp. (side)						6					1	2					1
Gomphonemopsis exigua	1			2									4			1	
G. lindae	4	2	2					6		3	1	2					
G. obscurum		3	3						4	1	5	5	1	1	2	1	5
Grammatophora angulosa																	
G. marina										1							
G. oceanica																	
Grammatophora sp.			2						4								
Grammatophora sp. (B04-14)																2	
Grammatophora sp. (B04-28)																	
Hannea arcus			1			2				2	3	1	3	1			
Hyalodiscus scotica						3		1			2						
Licomorpha sp.						1											
Luticola mutica													1	2			
Mastogloia exigua			2														
M. smithii																	
Mastogloia sp. (B04-13)													2				
Mastogloia sp. (B04-17)																	1
Mastogloia sp. 1 (B04-21)																	
Mastogloia sp. 2 (B04-21)																	
Mastogloia sp. (B04-22)							2										
Mastogloia sp. (B04-29)																	
Mastogloia sp. (B04-31)																	
Melosira nummuloides	1		5	1	2	2	2	1	5	1	2	2	5	2	8		1
Melosira sp.																8	

APPENDIX G1 (continued)

Sample	B04-1	B04-2	B04-3	B04-4	B04-5	B04-6	B04-7	B04-8	B04-9	B04-10	B04-11	B04-12	B04-13	B04-14	B04-15	B04-16	B04-17
Minidiscus chilensis	20	55	35	15	31	91	29	79	59	56	161	36	29	61	70	32	38
Navicula cryptocephala							1		1		4	2		2			1
N. directa			1					2	3			3		1		2	1
N. gregaria			4		2	4	2	4	1	1	4	1	1	1	2	1	1
N. perminuta	2	1	9		3	8	2	7	4	3		8	7	11	6	2	6
N. phylleptosoma			2			2	1	1	1		1	1			1		
Navicula cf. *ramossisima*		1														2	2
Navicula aff. *salinarum*																	
Navicula sensu tropicoidea													1				
Navicula sp. 1 (B04-3)			1							1	1	2	2		3		
Navicula sp. 2 (B04-3)			1														
Navicula sp. 1 (B04-4)				1													
Navicula sp. 2 (B04-4)				8													
Navicula sp. 1 (B04-8)								5									
Navicula sp. (B04-9)									1								
Navicula sp. 1 (B04-13)										2			2				
Navicula sp. 2 (B04-13)													1				
Navicula sp. 3 (B04-13)													2				
Navicula sp. 1 (B04-15)															1		
Navicula sp. 1 (B04-16)																2	
Navicula sp. 2 (B04-16)																1	
Navicula sp. (B04-17)																	1
Navicula sp. 1 (B04-21)																	
Navicula sp. 2 (B04-21)																	
Navicula sp. (B04-24)																	
Navicula sp. 1 (B04-31)		1															
Navicula sp. 2 (B04-31)																	
Navicula sp. 3 (B04-31)																	
Navicula sp. (B04-32)																	
Navicula sp. (B04-33)																	
Navicula sp. (B04-38)																	
Nitzschia coarctata			2														1
N. dissipata			3		1						1	2					
N. fonticola		1	1	1		1		2	1			2	3	2			
N. frustulum	14	14	19	8	12	16	11	29	20	19	20	19	18	28	31	19	32
N. inconspicua		2	1	1	1	1	1		1		1	2	1	3	2	1	3
N. microcephala									1								
N. perminuta	1		2		1						1	1			2	2	
Nitzschia cf. *sicula* (B04-12)											1			5	4		
N. valdestriata									1	1	2						
Nitzschia sp. (B04-11)											1						
Nitzschia sp. (B04-13)													2				
Nitzschia sp. (B04-22)																	
Nitzschia sp. (B04-37)																	
Odontella aurita/pulchella																	
O. longicruris												1	1				
Opephora gemmeta		1						1	1					2			
O. horstiana								2									
O. marina	1	1	1	1				1	1					1			1
O. mutabilis	6													2			
O. pacifica																1	
Paralia sulcata	1	2	3		1	1		3		1	2	2	5	1	1	1	1
Plagiogramma interruptum													2				
Planothidium delicatulum		2	6	4	3	4	8		3	3	2	8	8	7	6	2	6
P. engelbrechtii	1	1		3	1	2	1	2	2		1			1	2		
P. hauckiana						2	1	1	1		1	1	3	1		1	2
Pleurosigma spp.												1				1	
Pseudonitzschia multiseries	9	4	3	5	14		16	7				1		1		2	3
P. seriata				4			1	5		1	1			1	1		1

APPENDIX G1 (continued)

Sample	B04-1	B04-2	B04-3	B04-4	B04-5	B04-6	B04-7	B04-8	B04-9	B04-10	B04-11	B04-12	B04-13	B04-14	B04-15	B04-16	B04-17
Reimeria sinuata														1			
Rhizosolenia spp.	20	10	12	7	54	29	3	2	1	7	33	14	9	12	13	10	92
Rhoichosphenia cf. *genflexa*																	
R. curvata						4											2
Rhopalodia brebissonii		1	2														1
R pacifica				2									2			1	3
Seminavis spp.			1				1										
Skeletonema costatum	306	189	118	203	118	69	183	145	151	236	62	131	178	93	159	121	57
S. costatum (weak)	23	45	44	165	164	32	107	18	26	36	26	67	138	58	28	57	32
Stephanodiscus spp.										1		1					
Stephanopyxis turris			1			1								1			
Surirella brebissonii	1		1								2	1					
Synedra ulna		1											1				
Tabellaria flocculosa			1							7	2			8			
Tabularia fasciculata		1	2	2	1	3	3	16	9	3	1	3	1	2	4	2	4
Thalassionema cf. *bacillare*										1				1	2		
T. nitzschioides	21	51	45	16	12	44	45	78	83	25	57	79	10	56	20	38	38
T. pseudonitzschioides	1	6	6	7	4	2	4	5	14	5	2			5	3	2	
Thalassiosira aestivalis					1	3											
T. angulata						1				1						1	
T. anguste-lineata									2								
T. binata									1							2	1
T. bioculata										6	3	2	1			2	1
T. conferta			2	1				1	1	1					1	1	1
T. decipiens	16	15	14	5	9	12	7	2	20	5	10	16	1	8	19	42	13
T. decipiens (large)										6						1	14
T. eccentrica	1	13	8	1	2		1	6	2		1	7	1	3	6	8	15
T. eccentrica (large)														1	5	1	
T. gravida												1	1				
T. kushirensis						4		1	2	1	1	3			4	1	3
Thalassiosira cf. *leptopus*	6	7	2	3	5	1	1		3	5				14	2	2	1
T. lundiana																	
T. minima																	
T. nodulolineata		1										2					
T. nordenskioeldii	1	22	3	2	4	11	11	2	2	1	1	5	16	2	16	7	5
T. oceanica																	
T. oestrupii		1		1				2	6	4	3	3	3	3		2	3
T. pacifica	7	12	39	6	8	69	6	10	14	5	4	5	2	4	5	11	23
T. poroseriata			1			5									1		
T punctigera	7	5	4										2	1			1
T. rotula										1		2	2		1		
T. tealata																	
T. tenera	1		5				1		1	2	4	3	2	8	3	12	6
Thalassiosira cf. *tenera*	2		2	1	1	1		2	1	2	1	1	2	2	3	6	
Thalassiosira sp. (B04-2)		1															
Thalassiosira sp. 1 (B04-12)	1																
Thalassiosira sp. 2 (B04-12)												1					
Thalassiosira sp. 2 (B04-15)															3		
Thalassiosira sp. (B04-16)																7	
Thalassiosira sp. (B04-21)																	
Thalassiosira sp. (B04-23)																	
Thalassiosira sp. (B04-24)																	
Thalassiosira sp. (B04-25)																	
Thalassiosira sp. (B04-27)																	
Thalassiosira sp. (B04-36)																	
Thalssiothrix longissima																	
Trachyneis aspera											1						
Triceratium sp.															1		
Tryblionella aerophila														2			

APPENDIX G1 (continued)

Sample	B04-1	B04-2	B04-3	B04-4	B04-5	B04-6	B04-7	B04-8	B04-9	B04-10	B04-11	B04-12	B04-13	B04-14	B04-15	B04-16	B04-17
Unknown centric (B04-6)						1											
Unknown centric (B04-7)							1										
Unknown pennate 1 (B04-9)									1								
Unknown pennate (B04-14)														1			
Unknown pennate 1 (B04-18)																	
Unknown centric (B04-20)																	
Unknown sp. 1 (B04-20)																	
Unknown pennate 2 (B04-20)																	
Unknown pennate 3 (B04-20)																	
Unknown centric (B04-21)																	1
Unknown centric (B04-23)																	
Unknown pennate 1 (B04-23)																	
Unknown pennate 2 (B04-23)																	
Unknown pennate 3 (B04-23)																	
Unknown centric (B04-37)																	
Unknown pennate (B04-37)																	
TOTAL	501	501	501	506	501	501	501	501	502	507	504	503	513	511	505	501	511
RESTING SPORES																	
Chaetoceros spp.	74	61	61	84	51	55	217	283	638	36	16	39	67	42	14	58	74
Leptocylindrus spp.																	
TOTAL	74	61	61	84	51	55	217	283	638	36	16	39	67	42	14	58	74
SILICOFLAGELLATES																	
Dictyocha fibula			1		1	1	2	3							2		
D. speculum	3	8	8	5	2	5	3	1	15	4	4	6	2	8	7	3	4
Octactis sp.							1				1	1					
TOTAL	3	8	9	5	3	6	6	4	15	4	5	7	2	8	9	3	4

APPENDIX G1 (continued)

Sample	B04-18	B04-19	B04-20	B04-21	B04-22	B04-23	B04-24	B04-25	B04-26	B04-27	B04-28	B04-29	B04-30	B04-31	B04-32	B04-33	B04-34
DIATOMS																	
A. brevipes					1								2				
A. kregeri		3	1	3			1		3		3			2	3		
A. lanceolata			1														
A. lemmermannii		1						1					1				
A. minutissima	12	8	20	26	34	24	13	9	13	2	8	29	9	26	26	19	13
A. nodosa		1															
A. parvula							1										
Achnanthidium biasolettianum	1					1			2								
Actinocyclus curvatulus					1			1						1			3
A. octonarius																	
Actinocyclus sp. (B04-13)																	
Actinocyclus sp. (B04-23)						2											
Actinocyclus sp. (B04-35)																	
Actinoptychus senarius							2				3						2
A. vulgaris					1		1	1									2
Amphora acutiuscula				1				1				2	3	1			
A. coffaeformis	1		1														1
A. copulata								2				2				4	6
A. exigua								1	1								
A. helensis						2											
A. maletracta var. *constricta*			2			1							1			1	
A. marina		1	2		2	1						2			4		
Asteromphalus heptactis		1				3		1	1	1	1	1		1			
A. sarcophagus	1	5	1	1					1						2	3	
Asteromphalus sp. (B04-20)			1			1											
Aulacoseira islandica					2												
Aulacoseira italica var. *subarctica*				3	3	2	3	1									1
Aulacoseira sp. (B04-32)															2		
Bacillaria paxillifer							2					1					
Bacteriastrum delicatulum	1	1		2	1	1	2			1		4	1	8	4	11	3
Berkeleya rutilans	2							1			6	1		1	1	2	1
Brachysira sp.	1																
Cocconeis costata complex		3	4	1	1	1				1		1	1	1	2	1	1
C. dirupta																	
C. disculus				12	16	2	2				1	1	1		1	1	
C. distans												1					
C. neothumensis			1		1												
Cocconeis cf. *pellucida*			1														
C. peltoides		2	1		1	3											
C. pinnata			1		1												
C. placentula		2		8	2		1	2				2	3	3	5	1	
C. scutellum	1	1	5	3		3	1	1			4	3	2	1	3	4	
C. stauroneiformis	1	4	8	1	4	1	1	4			1	2	2	3	1	5	1
Cocconeis sp. (B04-21)				1													
Cocconeis sp. (B04-23)						1											
Cocconeis spp. (small)	1	1	2		2	1	1					1				1	
Coscinodiscus diorama														1			
C. radiatus			1		1	1	1							3			
Coscinodiscus sp. (B04-15)		1															
Craticula halophila																	
Ctenophora pulchella			2					1					2	2		2	
C. choctawhatcheeana					3	3	1	1					1		1	5	3
C. "punctata"														1			
C. rossii			1	1													
C. stelligera		1			3		1	2				4	1				3
C. striata				3			1	6									
C. stylorum							1										
Cyclotella sp. (B04-15)																	

APPENDIX G1 (continued)

Sample	B04-18	B04-19	B04-20	B04-21	B04-22	B04-23	B04-24	B04-25	B04-26	B04-27	B04-28	B04-29	B04-30	B04-31	B04-32	B04-33	B04-34
Cymbella cymbiformis		1										4					1
C. gracilis																	
C. lanceolata													1				
C. minuta	1		1		1							3					
Cymbella sp. (B04-17)																	
Cymbella sp. (B04-19)		1															
Cymbella sp. (B04-25)								1									
Delphineis sp.			1														
Denticula sp. (B04-18)		2															
Diatoma mesodon							2										
D. tenue			2										1				
Diatoma sp. (B04-21)				1													
Diatomella minuta				2											4	3	
Diploneis spp.				2	1												
Ditylum brightwellii	1	7		2		2	3	1			1	1				1	1
Ethmodiscus sp. (B04-19)		1															
Eunotia spp.		1	2	1	1	4						2					
Fallacia sp. (B04-29)		1	1														
Fallacia sp.		1	2	4		1					1		1	2			
Fragilaria capucina complex		2			5							2	4				
F. construens var. *construens*															1		
Fragilaria fo. *venter*																	
F. investiens			3			1	2						2	1			
F. pinnata	1							1								2	
Fragilaria cf. *sopotensis*		1		1		2						1	5		2		
Fragilaria sp. (B04-38)																	
Fragilariopsis atlantica	1																
F. cylindriformis		2												4	1	5	1
F. pseudonana	13	2	6	4	2	2	6	4			13	3	11	22	28	17	2
F. schulzii																	
Gomphonema augustatum				1													
G. augustum	4		2		4							1			2	4	
G. olivaceum			1														
Gomphonema sp. (B04-25)								2									
Gomphonema spp. (side)							2				1				4		
Gomphonemopsis exigua	2						2										
G. lindae	1	1	3												2		
G. obscurum	7	7	8	8	2	5		2		1	3	5	1		6	10	8
Grammatophora angulosa							1										
G. marina														1			
G. oceanica					2						1	1					
Grammatophora sp.																	
Grammatophora sp. (B04-14)							2										
Grammatophora sp. (B04-28)											2						
Hannea arcus					4						1			2			
Hyalodiscus scotica		3		3	1	1		1				1	1		1	2	1
Licomorpha sp.																	
Luticola mutica		2	1									1		2	1		1
Mastogloia exigua															1		
M. smithii		2															
Mastogloia sp. (B04-13)																	
Mastogloia sp. (B04-17)																	
Mastogloia sp. 1 (B04-21)				2													
Mastogloia sp. 2 (B04-21)				2	3												
Mastogloia sp. (B04-22)																	
Mastogloia sp. (B04-29)												1					
Mastogloia sp. (B04-31)														1			
Melosira nummuloides	3	2		2	8	2			11		6	3	2	1		3	7
Melosira sp.			4														

APPENDIX G1 (continued)

Sample	B04-18	B04-19	B04-20	B04-21	B04-22	B04-23	B04-24	B04-25	B04-26	B04-27	B04-28	B04-29	B04-30	B04-31	B04-32	B04-33	B04-34
Minidiscus chilensis	28	51	69	131	43	62	41	43	70	60	27	39	23	53	73	30	32
Navicula cryptocephala		1				1						1			3		
N. directa																	
N. gregaria		2	1	1	2			2	3		3	4	1	1	2	3	
N. perminuta	5	19	8	12	13	9	2	1	7	2	7	11	4	7	15	10	1
N. phylleptosoma		1	3	1		2									1	1	
Navicula cf. *ramossisima*	1		1		1	1	2				3	1		1		1	
Navicula aff. *salinarum*		2							1								
Navicula sensu tropicoidea																	
Navicula sp. 1 (B04-3)																	
Navicula sp. 2 (B04-3)																	
Navicula sp. 1 (B04-4)																	
Navicula sp. 2 (B04-4)																	
Navicula sp. 1 (B04-8)																	
Navicula sp. (B04-9)																	
Navicula sp. 1 (B04-13)																	
Navicula sp. 2 (B04-13)																	
Navicula sp. 3 (B04-13)																	
Navicula sp. 1 (B04-15)																	
Navicula sp. 1 (B04-16)																	
Navicula sp. 2 (B04-16)																	
Navicula sp. (B04-17)																	
Navicula sp. 1 (B04-21)				1													
Navicula sp. 2 (B04-21)				1													
Navicula sp. (B04-24)							1										
Navicula sp. 1 (B04-31)																	
Navicula sp. 2 (B04-31)														1			
Navicula sp. 3 (B04-31)														1			
Navicula sp. (B04-32)															2		
Navicula sp. (B04-33)																2	
Navicula sp. (B04-38)																	
Nitzschia coarctata												1			1		
N. dissipata			2											1			
N. fonticola			1					1				3	3			1	
N. frustulum	21	24	29	34	20	14	17	13		2	8	40	26	24	22	22	8
N. inconspicua	4		1	1	2	1						1	1	2			
N. microcephala																	
N. perminuta			1	3		1			9								
Nitzschia cf. *sicula* (B04-12)																	3
N. valdestriata	1			1											2		
Nitzschia sp. (B04-11)																	
Nitzschia sp. (B04-13)																	
Nitzschia sp. (B04-22)					2												
Nitzschia sp. (B04-37)																	
Odontella aurita/pulchella		1														1	
O. longicruris		1	1		1	10	4				1	1					
Opephora gemmeta	1																
O. horstiana																	
O. marina														3	1	1	
O. mutabilis					1				2					1			
O. pacifica																	
Paralia sulcata			5	2	6	7	2		1				3		2	2	2
Plagiogramma interruptum																	
Planothidium delicatulum	2	6	12	6	7	4	2	4	4		6	11	6	14	16	9	5
P. engelbretchii		2	1														
P. haukiana	3	2	5	4	3	1	2				1		2	2	1		
Pleurosigma spp.			1													1	
Pseudonitzschia multiseries		1	8	2	2	3	12	1			2	7	4	2	2	1	
P. seriata	1	1		1	1	2		1		1	4	1			1	2	4

APPENDIX G1 (continued)

Sample	B04-18	B04-19	B04-20	B04-21	B04-22	B04-23	B04-24	B04-25	B04-26	B04-27	B04-28	B04-29	B04-30	B04-31	B04-32	B04-33	B04-34
Reimeria sinuata																	
Rhizosolenia spp.	47	37	36	8	14	3	2	18	10	1	70	3	25	30	31	33	11
Rhoichosphenia cf. *genflexa*					2		2										
R. curvata	2					2											
Rhopalodia brebissonii							1										
R. pacifica																	
Seminavis spp.																	
Skeletonema costatum	244	149	93	82	73	62	34	146	154	211	194	151	108	43	67	125	291
S. costatum (weak)	15	31	25	10	25	23		26	80	78	36	57	147	21	35	52	39
Stephanodiscus spp.				1													
Stephanopyxis turris			1														
Surirella brebissonii																	
Synedra ulna					2												
Tabellaria flocculosa													2		4	2	
Tabularia fasciculata	1	1			5	4	3	1			4	5	2	4	4	3	
Thalassionema cf. *bacillare*	1	1			2				1			1	2		1	2	
T. nitzschioides	36	37	41	46	105	163	247	139	53	17	10	39	44	62	23	19	17
T. pseudonitzschioides	1	7	9	7	7	4	5	3				2	3	8	2	2	
Thalassiosira aestivalis		1															
T. angulata					1		1		1		1						
T. anguste-lineata																	
T. binata				1	1		1	1						1			
T. bioculata	1			1					1								
T. conferta				1		1		2				1	1	1		3	2
T. decipiens	6	15	19	10	9	8	10	22	32	1		5	7	9	9	18	11
T. decipiens (large)	4		4	1			13	3	1					2	2		
T. eccentrica	2	1		1	1	2	11	2	1		2	4	1	6	5	4	5
T. eccentrica (large)				1													
T. gravida				1		1			12	7		3					
T. kushirensis			2	10	9	3	2	9	4	94	36	6	1				
Thalassiosira cf. *leptopus*							1	1				2	1	2			
T. lundiana		1			2					1							1
T. minima				2	2		2					1	1		1	5	3
T. nodulolineata	1																
T. nordenskioeldii	5	9	2	3	8	8	13	2	6	2	18	6	5	40	9	5	8
T. oceanica													3	1			
T. oestrupii		2	4	1			2	1	2				1	3	3	2	
T. pacifica	6	10	5	6	10	5	7	12	13	1	3	4	6	58	54	25	1
T. poroseriata	1																
T. punctigera		1	1									4	6	1		1	
T. rotula													4				
T. tealata				1													
T. tenera	4	6	8	1	3	4	2		3	2	1	2	1	3	3	2	1
Thalassiosira cf. *tenera*	1	1	4	2		3	1	1	2	1	1					4	
Thalassiosira sp. (B04-2)																	
Thalassiosira sp. 1 (B04-12)																	
Thalassiosira sp. 2 (B04-12)																	
Thalassiosira sp. 2 (B04-15)																	
Thalassiosira sp. (B04-16)																	
Thalassiosira sp. (B04-21)				1													
Thalassiosira sp. (B04-23)						1											
Thalassiosira sp. (B04-24)							1										
Thalassiosira sp. (B04-25)								2									
Thalassiosira sp. (B04-27)										20	6						
Thalassiosira sp. (B04-36)																	
Thalssiothrix longissima		1	1			4											
Trachyneis aspera																	
Triceratium sp.																	
Tryblionella aerophila				1		1											

APPENDIX G1 (continued)

Sample	B04-18	B04-19	B04-20	B04-21	B04-22	B04-23	B04-24	B04-25	B04-26	B04-27	B04-28	B04-29	B04-30	B04-31	B04-32	B04-33	B04-34
Unknown centric (B04-6)																	
Unknown centric (B04-7)								1									
Unknown pennate 1 (B04-9)																	
Unknown pennate (B04-14)																	
Unknown pennate 1 (B04-18)	1																
Unknown centric (B04-20)			1														
Unknown sp. 1 (B04-20)			1														
Unknown pennate 2 (B04-20)			2														
Unknown pennate 3 (B04-20)			1														
Unknown centric (B04-21)	1		1		1	2								1			
Unknown centric (B04-23)						1											
Unknown pennate 1 (B04-23)						2											
Unknown pennate 2 (B04-23)						1											
Unknown pennate 3 (B04-23)						2								1			
Unknown centric (B04-37)																	
Unknown pennate (B04-37)																	
TOTAL	503	500	503	501	500	502	502	506	505	507	500	503	503	501	505	501	507
RESTING SPORES																	
Chaetoceros spp.	29	55	110	93	90	129	145	41	45	13	138	81	44	115	37	15	12
Leptocylindrus spp.						2	1	7	2		2	2	5			1	
TOTAL	29	55	110	93	90	131	146	48	47	13	140	83	49	115	37	16	12
SILICOFLAGELLATES																	
Dictyocha fibula	2	1		1	1												
D. speculum	5	3	7	1	15	3	10		1		2	14	9	4	4	5	
Octactis sp.			2					8									
TOTAL	7	4	9	2	16	3	10	8	1		2	14	9	4	4	5	

APPENDIX G1 (continued)

Sample	B04-35	B04-36	B04-37	B04-38	B04-39	B04-40	B04-41	B04-42
DIATOMS								
A. brevipes								
A. kregeri	2						2	2
A. lanceolata							1	
A. lemmermannii						1	1	2
A. minutissima	2	3	13	28	7	15	14	14
A. nodosa								
A. parvula								
Achnanthidium biasolettianum			1	1	1		1	2
Actinocyclus curvatulus	2		1					1
A. octonarius								2
Actinocyclus sp. (B04-13)						1		
Actinocyclus sp. (B04-23)								
Actinocyclus sp. (B04-35)	1							
Actinoptychus senarius				1				
A. vulgaris				1				
Amphora acutiuscula								
A. coffaeformis								
A. copulata			2					4
A. exigua								
A. helensis								2
A. maletracta var. *constricta*						2		
A. marina								
Asteromphalus heptactis	1	2				2	2	1
A. sarcophagus							1	4
Asteromphalus sp. (B04-20)								1
Aulacoseira islandica								
Aulacoseira italica var. *subarctica*								
Aulacoseira sp. (B04-32)								
Bacillaria paxillifer							2	
Bacteriastrum delicatulum	1	2		1	2	3	15	2
Berkeleya rutilans								2
Brachysira sp.		1		1	2			
Cocconeis costata complex						1	1	
C. dirupta								
C. disculus	2	1	1		1		2	2
C. distans								
C. neothumensis								
Cocconeis cf. *pellucida*								
C. peltoides								2
C. pinnata					1			
C. placentula	1			2	1	2	1	3
C. scutellum	1		1	2	2	3	7	1
C. stauroneiformis		4	3	2	5		4	1
Cocconeis sp. (B04-21)								
Cocconeis sp. (B04-23)								
Cocconeis spp. (small)			1	1	1	1	1	1
Coscinodiscus diorama								
C. radiatus								
Coscinodiscus sp. (B04-15)								
Craticula halophila								
Ctenophora pulchella		1	3					
C. choctawhatcheeana	2			4		4	6	10
C. "punctata"								
C. rossii								
C. stelligera			1	1				1
C. striata			1	2	3		3	2
C. stylorum								
Cyclotella sp. (B04-15)								

APPENDIX G1 (continued)

Sample	B04-35	B04-36	B04-37	B04-38	B04-39	B04-40	B04-41	B04-42
Cymbella cymbiformis							1	1
C. gracilis								
C. lanceolata								
C. minuta			1				1	
Cymbella sp. (B04-17)								
Cymbella sp. (B04-19)								
Cymbella sp. (B04-25)								
Delphineis sp.								
Denticula sp. (B04-18)						1		
Diatoma mesodon	1			1				
D. tenue								
Diatoma sp. (B04-21)								
Diatomella minuta							1	1
Diploneis spp.								
Ditylum brightwellii		3	1	1	1	2		1
Ethmodiscus sp. (B04-19)								
Eunotia spp.								
Fallacia sp. (B04-29)			1				1	
Fallacia sp.								
Fragilaria capucina complex						1		
F. construens var. *construens*			1					1
Fragilaria fo. *venter*								
F. investiens			2					
F. pinnata	2	1						1
Fragilaria cf. *sopotensis*					1	2		7
Fragilaria sp. (B04-38)				2				
Fragilariopsis atlantica	1							
F. cylindriformis		1	3			1	3	13
F. pseudonana	1	2	6	11	13	16	23	19
F. schulzii								
Gomphonema augustatum								
G. augustum								
G. olivaceum								
Gomphonema sp. (B04-25)								
Gomphonema spp. (side)					2		1	2
Gomphonemopsis exigua		1	2					4
G. lindae						1		
G. obscurum	2	1		2	6	8	2	
Grammatophora angulosa								
G. marina						1		
G. oceanica							1	
Grammatophora sp.								
Grammatophora sp. (B04-14)							2	
Grammatophora sp. (B04-28)								
Hannea arcus					2			4
Hyalodiscus scotica			1	1				1
Licamorpha sp.								
Luticola mutica								
Mastogloia exigua						1	2	
M. smithii								
Mastogloia sp. (B04-13)								
Mastogloia sp. (B04-17)								
Mastogloia sp. 1 (B04-21)								
Mastogloia sp. 2 (B04-21)								
Mastogloia sp. (B04-22)								
Mastogloia sp. (B04-29)								
Mastogloia sp. (B04-31)								
Melosira nummuloides	1		2		4		2	5
Melosira sp.								

APPENDIX G1 (continued)

Sample	B04-35	B04-36	B04-37	B04-38	B04-39	B04-40	B04-41	B04-42
Minidiscus chilensis	9	42	46	17	30	50	42	31
Navicula cryptocephala							2	1
N. directa		1	1				1	
N. gregaria	1		1		3	1	1	
N. perminuta	6	4	1	4	8	6	5	14
N. phylleptosoma								1
Navicula cf. *ramossisima*								
Navicula aff. *salinarum*								
Navicula sensu tropicoidea								
Navicula sp. 1 (B04-3)								
Navicula sp. 2 (B04-3)								
Navicula sp. 1 (B04-4)								
Navicula sp. 2 (B04-4)								
Navicula sp. 1 (B04-8)								
Navicula sp. (B04-9)								
Navicula sp. 1 (B04-13)								
Navicula sp. 2 (B04-13)								
Navicula sp. 3 (B04-13)								
Navicula sp. 1 (B04-15)								
Navicula sp. 1 (B04-16)								
Navicula sp. 2 (B04-16)								
Navicula sp. (B04-17)								
Navicula sp. 1 (B04-21)								
Navicula sp. 2 (B04-21)								
Navicula sp. (B04-24)								
Navicula sp. 1 (B04-31)								
Navicula sp. 2 (B04-31)								
Navicula sp. 3 (B04-31)								
Navicula sp. (B04-32)								
Navicula sp. (B04-33)								
Navicula sp. (B04-38)				1				
Nitzschia coarctata								
N. dissipata				1				
N. fonticola				1	1	1		
N. frustulum	5	5	4	14	19	18	17	21
N. inconspicua		2		2		3		
N. microcephala								
N. perminuta								
Nitzschia cf. *sicula* (B04-12)					2			
N. valdestriata				1				1
Nitzschia sp. (B04-11)								
Nitzschia sp. (B04-13)								
Nitzschia sp. (B04-22)								
Nitzschia sp. (B04-37)			2					
Odontella aurita/pulchella								
O. longicruris				1	1			
Opephora gemmeta								
O. horstiana								
O. marina				1	1		2	
O. mutabilis					3			
O. pacifica								
Paralia sulcata			8	2	1			3
Plagiogramma interruptum								
Planothidium delicatulum	4	4	2	3	2	9	7	8
P. engelbretchii						1		
P. haukiana								1
Pleurosigma spp.								
Pseudonitzschia multiseries	1	2	3		1	2		3
P. seriata	2			2		1		3

APPENDIX G1 (continued)

Sample	B04-35	B04-36	B04-37	B04-38	B04-39	B04-40	B04-41	B04-42
Reimeria sinuata		1						1
Rhizosolenia spp.	5	2	5	18	17	48	66	48
Rhoicosphenia cf. *genflexa*								1
R. curvata								
Rhopalodia brebissonii								
R. pacifica	1							
Seminavis spp.								
Skeletonema costatum	371	262	254	197	200	110	61	118
S. costatum (weak)	16	51	37	89	73	35	11	51
Stephanodiscus spp.						1		
Stephanopyxis turris								
Surirella brebissonii						1		
Synedra ulna						1		
Tabellaria flocculosa		1						
Tabularia fasciculata		2	6	2	1		3	
Thalassionema cf. *bacillare*		1	6			1	2	
T. nitzschioides	37	23	21	31	12	46	116	42
T. pseudonitzschioides	5	3	3	2		4	10	1
Thalassiosira aestivalis							1	
T. angulata				1				
T. anguste-lineata								
T. binata	1	1					1	
T. bioculata						1		
T. conferta	1		1		1	1		2
T. decipiens	10	12	20	14	16	14	13	2
T. decipiens (large)				1	1	2		
T. eccentrica	5	2	4	5	5	4	3	2
T. eccentrica (large)	1							
T. gravida		1				1		
T. kushirensis					1	5		1
Thalassiosira cf. *leptopus*			1		1			
T. lundiana	1	1				1		
T. minima		2	4	2	2	4	1	1
T. nodulolineata	1							
T. nordenskioeldii	2	39	3	7	27	21	6	
T. oceanica								
T. oestrupii	1		2					2
T. pacifica	8	7	14	13	11	30	16	17
T. poroseriata								
T. punctigera							7	1
T. rotula		3				4		
T. tealata								1
T. tenera		1					2	3
Thalassiosira cf. *tenera*					3	2	1	1
Thalassiosira sp. (B04-2)								
Thalassiosira sp. 1 (B04-12)								
Thalassiosira sp. 2 (B04-12)								
Thalassiosira sp. 2 (B04-15)								
Thalassiosira sp. (B04-16)								
Thalassiosira sp. (B04-21)								
Thalassiosira sp. (B04-23)								
Thalassiosira sp. (B04-24)								
Thalassiosira sp. (B04-25)								
Thalassiosira sp. (B04-27)								
Thalassiosira sp. (B04-36)		3			1	1		
Thalssiothrix longissima								
Trachyneis aspera			2					
Triceratium sp.								
Tryblionella aerophila	1							

APPENDIX G1 (continued)

Sample	B04-35	B04-36	B04-37	B04-38	B04-39	B04-40	B04-41	B04-42
Unknown centric (B04-6)								
Unknown centric (B04-7)								
Unknown pennate 1 (B04-9)								
Unknown pennate (B04-14)								
Unknown pennate 1 (B04-18)								
Unknown centric (B04-20)								
Unknown sp. 1 (B04-20)								
Unknown pennate 2 (B04-20)								
Unknown pennate 3 (B04-20)								
Unknown centric (B04-21)				2		2		
Unknown centric (B04-23)								
Unknown pennate 1 (B04-23)								
Unknown pennate 2 (B04-23)								
Unknown pennate 3 (B04-23)								
Unknown centric (B04-37)			1					
Unknown pennate (B04-37)			1	1				
TOTAL	518	501	501	500	499	501	501	504
RESTING SPORES								
Chaetoceros spp.	21	49	43	44	35	17	184	170
Leptocylindrus spp.		1		2	1	3	2	2
TOTAL	21	50	43	46	36	20	186	172
SILICOFLAGELLATES								
Dictyocha fibula								
D. speculum		1	1	1	1	3	3	3
Octactis sp.								
TOTAL		1	1	1	1	3	3	3

APPENDIX G2. Freeze core microfossil absolute abundance (concentration)

$C_a = \frac{Nadv_s}{fAwv_v}$

N = number of valves or skeletons counted
a = area of cover slip (18 × 18 mm = 324000000 μm^2)
d = dilution factor
v_s = initial volume of slurry (mL)
f = number of fields of view examined
A = area of field of view (radius at 1000 × is 105 μm = 34636.14 μm^2)
w = initial sediment mass (g)
v_v = volume of slurry plated onto cover slip (mL)

Sample	Top interval (cm)	Bottom interval (cm)	Midpoint (cm)	Year (Top)	Year (Bottom)	Time interval (years)	Initial mass (g)	Initial slurry volume (mL)	Dilution Factor	Volume plated (mL)	Diatom count (valves)	CRS count (valves)	Silico. count (skeletons)	Fields of view examined	Diatom Concentration ($\times 10^6$ valves/g)	CRS Concentration ($\times 10^6$ valves/g)	Siliceoflagellate Concentration ($\times 10^6$ skel./g)
							w	v_s	d	v_v	N	N	N	f			
B04-1	0.5	1.3	0.90	1993.0	1992.0	1.0	0.0394	22.5	5	0.5	501	74	3	56	477.92	70.59	2.86
B04-2	1.3	2.4	1.85	1992.0	1991.0	1.0	0.0412	23.0	5	0.5	501	54	8	70	373.75	40.28	5.97
B04-3	2.4	4.0	3.20	1991.0	1989.5	1.5	0.0440	22.0	5	0.5	501	54	9	103	227.50	24.52	4.09
B04-4	4.0	4.8	4.40	1989.5	1989.0	0.5	0.0399	22.0	5	0.5	506	82	5	49	532.62	86.31	5.26
B04-5	4.8	5.3	5.05	1989.0	1988.0	1.0	0.0406	22.0	5	0.5	501	50	3	57	445.53	44.46	2.67
B04-6	5.3	6.3	5.80	1988.0	1987.0	1.0	0.0444	22.0	5	0.5	501	53	6	125	185.77	19.65	2.22
B04-7	6.3	7.7	7.00	1987.0	1986.0	1.0	0.0398	21.0	5	0.5	501	217	6	68	363.65	157.51	4.36
B04-8	7.7	8.6	8.15	1986.0	1985.0	1.0	0.0406	21.0	5	0.5	501	282	4	87	278.63	156.83	2.22
B04-9	8.6	9.1	8.85	1985.0	1984.0	1.0	0.0381	22.5	5	0.5	502	628	15	111	249.84	312.54	7.47
B04-10	9.1	9.7	9.40	1984.0	1983.5	0.5	0.0394	21.5	5	0.5	507	36	4	73	354.52	25.17	2.80
B04-11	9.7	10.2	9.95	1983.5	1983.0	0.5	0.0409	22.0	5	0.5	504	16	5	104	243.84	7.74	2.42
B04-12	10.2	11.0	10.60	1983.0	1982.0	1.0	0.0412	22.0	5	0.5	503	39	7	140	179.47	13.91	2.50
B04-13	11.0	11.8	11.40	1982.0	1980.5	1.5	0.0402	21.5	5	0.5	513	62	2	122	210.37	25.42	0.82
B04-14	11.8	12.6	12.20	1980.5	1979.0	1.5	0.0411	21.5	5	0.5	511	42	8	166	150.63	12.38	2.36
B04-15	12.6	13.2	12.90	1979.0	1978.0	1.0	0.0402	22.0	5	0.5	505	14	9	134	192.93	5.35	3.44
B04-16	13.2	14.3	13.75	1978.0	1976.5	1.5	0.0406	21.0	5	0.5	501	58	3	118	205.43	23.78	1.23
B04-17	14.3	14.8	14.55	1976.5	1976.0	0.5	0.0415	22.0	5	0.5	511	74	4	141	179.72	26.03	1.41
B04-18	14.8	15.4	15.10	1976.0	1975.0	1.0	0.0395	22.0	5	0.5	503	29	7	84	311.98	17.99	4.34
B04-19	15.4	16.0	15.70	1975.0	1974.0	1.0	0.0399	21.5	5	0.5	500	55	4	124	203.25	22.36	1.63
B04-20	16.0	16.5	16.25	1974.0	1973.0	1.0	0.0392	21.0	5	0.5	503	110	9	108	233.40	51.04	4.18
B04-21	16.5	17.0	16.75	1973.0	1972.0	1.0	0.0413	22.0	5	0.5	501	92	2	116	215.21	39.52	0.86
B04-22	17.0	18.2	17.60	1972.0	1969.8	2.3	0.0409	21.0	5	0.5	500	90	16	174	138.02	24.84	4.42
B04-23	18.2	18.7	18.45	1969.8	1968.8	1.0	0.0397	21.0	5	0.5	502	129	3	103	241.16	61.97	1.44
B04-24	18.7	19.7	19.20	1968.8	1967.8	1.0	0.0415	22.0	5	0.5	502	145	10	62	401.52	115.98	8.00
B04-25	19.7	21.0	20.35	1967.8	1965.0	2.8	0.0414	22.0	5	0.5	506	39	8	54	465.79	35.90	7.36
B04-26	21.0	22.0	21.50	1965.0	1964.0	1.0	0.0400	22.0	5	0.5	505	42	1	43	604.23	50.25	1.20
B04-27	22.0	22.5	22.25	1964.0	1963.5	0.5	0.0414	22.0	5	0.5	507	13	0	25	1008.11	25.85	0.00
B04-28	22.5	23.0	22.75	1963.5	1962.5	1.0	0.0398	22.0	5	0.5	500	132	2	78	331.46	87.51	1.33
B04-29	23.0	23.7	23.35	1962.5	1961.0	1.5	0.0416	20.5	5	0.5	503	81	14	119	194.85	31.38	5.42
B04-30	23.7	24.4	24.05	1961.0	1960.0	1.0	0.0395	21.5	5	0.5	503	44	9	104	246.26	21.54	4.41

APPENDIX G2 (continued)

Sample	Top interval (cm)	Bottom interval (cm)	Midpoint (cm)	Year (Top)	Year (Bottom)	Time interval (years)	Initial mass (g)	Initial slurry volume (mL)	Dilution Factor	Volume plated (mL)	Diatom count (valves)	CRS count (valves)	Silico. count (skeletons)	Fields of view examined	Diatom Concentration ($\times 10^6$ valves/g)	CRS Concentration ($\times 10^6$ valves/g)	Silicoflagellate Concentration ($\times 10^5$ skel./g)
							w	v_s	d	v_p	N	N	N	f			
B04-31	24.4	24.8	24.60	1960.0	1959.0	1.0	0.0397	21.5	5	0.5	501	111	4	106	239.44	53.05	1.91
B04-32	24.8	25.3	25.05	1959.0	1958.0	1.0	0.0398	21.0	5	0.5	505	37	4	150	166.17	12.17	1.32
B04-33	25.3	25.8	25.55	1958.0	1957.4	0.6	0.0408	22.0	5	0.5	501	15	5	82	308.18	9.23	3.08
B04-34	25.8	26.4	26.10	1957.4	1956.3	1.1	0.0396	21.5	5	0.5	507	12	0	63	408.72	9.67	0.00
B04-35	26.4	27.0	26.70	1956.3	1955.3	1.0	0.0413	21.0	5	0.5	518	21	0	28	879.95	35.67	0.00
B04-36	27.0	27.4	27.20	1955.3	1954.8	0.5	0.0397	21.0	5	0.5	501	49	1	36	688.62	67.35	1.37
B04-37	27.4	27.8	27.60	1954.8	1954.3	0.5	0.0404	22.0	5	0.5	501	43	1	49	520.83	44.70	1.04
B04-38	27.8	28.2	28.00	1954.3	1953.3	1.0	0.0402	22.0	5	0.5	500	44	1	89	287.60	25.31	0.58
B04-39	28.2	29.0	28.60	1953.3	1952.0	1.3	0.0401	22.0	5	0.5	499	35	1	60	426.82	29.94	0.86
B04-40	29.0	30.0	29.50	1952.0	1950.0	2.0	0.0396	22.0	5	0.5	501	17	3	79	329.57	11.18	1.97
B04-41	30.0	31.0	30.50	1950.0	1948.0	2.0	0.0409	22.0	5	0.5	501	184	3	97	259.88	95.45	1.56
B04-42	31.0	32.0	31.50	1948.0	1947.0	1.0	0.0403	22.0	5	0.5	504	170	3	84	306.40	103.35	1.82
Average							0.0405								339.75	50.85	2.72

APPENDIX G3. Freeze core major taxa relative abundance (%)*

Sample	B04-1	B04-2	B04-3	B04-4	B04-5	B04-6	B04-7	B04-8	B04-9	B04-10	B04-11
Achnanthes minutissima	1.60	1.00	2.79	0.20	3.59	5.79	4.19	2.99	2.79	1.97	5.16
Amphora acutiuscula	0.20	0.20				0.40			0.20		
Amphora copulata	0.40	0.40			0.40		0.40	0.60			
Asteromphalus sarcophagus	0.20									0.20	
Bacteriastrum delicatulum	0.40	0.20	0.60	1.38	0.20	0.80			0.60	0.39	0.60
Berkeleya rutilans		0.40			0.20		0.40				
Cocconeis disculus			0.40					0.20		0.20	0.40
Cocconeis placentula	0.20	0.20	1.00		0.60	0.40	0.20		0.40	0.20	
Cocconeis scutellum			1.00		0.20	0.20	0.20	0.60	0.20	0.20	0.79
Cocconeis stauroneiformis		0.40	0.60	1.38	0.40	0.20	0.40	0.80		0.20	0.60
Cyclotella choctawhatcheeana											
Cyclotella striata							0.20			0.39	0.20
Ditylum brightwellii	0.60	0.40	0.80	0.20	0.80	0.60	0.60	0.60	1.20	0.20	0.99
Fragilaria capucina complex			0.20		0.60	0.40	0.20				
Fragilaria investiens											
Fragilaria cf. *sopotensis*			0.40		0.40	0.40	0.20		0.20		
Fragilariopsis cylindriformis	0.20							0.40			0.20
Fragilariopsis pseudonana	0.20	0.60	2.59	0.59	0.20	0.40	0.80	0.80	0.40	2.96	2.38
Gomphonemopsis lindae	0.80	0.40	0.40					1.20		0.59	0.20
Gomphonemopsis obscurum		0.60	0.60						0.80	0.20	0.99
Melosira nummuloides	0.20		1.00	0.20	0.40	0.40	0.40	0.20	1.00	0.20	0.40
Minidiscus chilensis	3.99	10.98	6.99	2.96	6.19	18.16	5.79	15.77	11.78	11.05	31.94
Navicula perminuta	0.40	0.20	1.80		0.60	1.60	0.40	1.40	0.80	0.59	
Nitzschia frustulum	2.79	2.79	3.79	1.58	2.40	3.19	2.20	5.79	3.99	3.75	3.97
Nitzschia perminuta	0.20		0.40		0.20						0.20
Odontella longicruris											
Opephora mutabilis	1.20										
Paralia sulcata	0.20	0.40	0.60		0.20	0.20		0.60		0.20	0.40
Planothidium delicatulum		0.40	1.20	0.79	0.60	0.80	1.60		0.60	0.59	0.40
Pseudonitzschia multiseries	1.80	0.80	0.60	0.99	2.79		3.19	1.40			
Rhizosolenia spp.	3.99	2.00	2.40	1.38	10.78	5.79	0.60	0.40	0.20	1.38	6.55
Skeletonema costatum	61.08	37.72	23.55	40.12	23.55	13.77	36.53	28.94	30.14	46.55	12.30
Skeletonema costatum (weak)	4.59	8.98	8.78	32.61	32.73	6.39	21.36	3.59	5.19	7.10	5.16
Tabellaria flocculosa			0.20							1.38	0.40
Tabularia fasciculata		0.20	0.40	0.40	0.20	0.60	0.60	3.19	1.80	0.59	0.20
Thalassionema bacillare										0.20	
Thalassionema nitzschioides	4.19	10.18	8.98	3.16	2.40	8.78	8.98	15.57	16.57	4.93	11.31
Thalassionema pseudonitzschioides	0.20	1.20	1.20	1.38	0.80	0.40	0.80	1.00	2.79	0.99	0.40
Thalassiosira bioculata										1.18	0.60
Thalassiosira decipiens	3.19	2.99	2.79	0.99	1.80	2.40	1.40	0.40	3.99	2.17	1.98
Thalassiosira eccentrica	0.20	2.59	1.60	0.20	0.40		0.20	1.20	0.40		0.20
Thalassiosira gravida											
Thalassiosira kushirensis						0.80		0.20	0.40	0.20	0.20
Thalassiosira cf. *leptosus*	1.20	1.40	0.40	0.59	1.00	0.20	0.20		0.60	0.99	
Thalassiosira nordenskioeldii	0.20	4.39	0.60	0.40	0.80	2.20	2.20	0.40	0.40	0.20	0.20
Thalassiosira oestrupii		0.20		0.20				0.40	1.20	0.79	0.60
Thalassiosira pacifica	1.40	2.40	7.78	1.19	1.60	13.77	1.20	2.00	2.79	0.99	0.79
Thalassiosira punctigera	1.40	1.00	0.80								
Thalassiosira tenera	0.20		1.00				0.20		0.20	0.39	0.79
Thalassiosira sp. (cf. *tenera*)	0.40		0.40	0.20	0.20	0.20		0.40	0.20	0.39	0.20
Total relative abundance	97.82	95.62	88.64	93.09	97.23	89.24	95.64	91.04	91.83	94.50	91.70
Benthics	6.80	6.00	17.00	5.70	8.00	14.00	9.60	15.00	10.00	9.50	15.00
CRS to Diatom	12.87	9.73	9.73	13.95	9.07	9.57	30.22	36.02	55.58	6.63	3.08
Silicoflagellates	0.60	1.57	1.76	0 98	0.60	1 18	1.18	0.79	2.90	0.78	0.98

*major taxa defined as those which appeared in at least three samples with at least 1% in one sample; no entry for zero values

APPENDIX G3 (continued)

Sample	B04-12	B04-13	B04-14	B04-15	B04-16	B04-17	B04-18	B04-19	B04-20	B04-21	B04-22
Achnanthes minutissima	2.98	1.56	5.68	2.97	3.59	5.29	2.39	1.60	3.99	5.19	6.81
Amphora acutiuscula	0.20		1.17			0.20				0.20	
Amphora copulata		0.78	0.20								
Asteromphalus sarcophagus					0.40	0.20	0.20	1.00	0.20	0.20	
Bacteriastrum delicatulum	0.20			0.79	1.00	0.20	0.20	0.20		0.40	0.20
Berkeleya rutilans					0.20		0.40				
Cocconeis disculus	0.20		0.20	0.20		0.39				2.40	3.21
Cocconeis placentula	0.20	0.39	0.59	0.79				0.40		1.60	0.40
Cocconeis scutellum	0.60		0.39	0.40	0.80	0.78	0.20	0.20	1.00	0.60	
Cocconeis stauroneiformis	1.19	0.78	0.78	0.40	0.80	0.98	0.20	0.80	1.60	0.20	0.80
Cyclotella choctawhatcheeana				0.60		0.20					0.60
Cyclotella striata	0.20	0.39	0.39		0.40					0.60	
Ditylum brightwellii	0.40		0.59	1.19	0.40		0.20	1.40		0.40	
Fragilaria capucina complex	0.80			0.79		0.78		0.40			1.00
Fragilaria investiens	0.40	0.78	1.17		0.20	0.39			0.60		
Fragilaria cf. *sopotensis*				0.20	0.80	0.20		0.20		0.20	
Fragilariopsis cylindriformis								0.40			
Fragilariopsis pseudonana	1.39	1.17	2.35	1.19	3.59	2.75	2.59	0.40	1.20	0.80	0.40
Gomphonemopsis lindae	0.40						0.20	0.20	0.60		
Gomphonemopsis obscurum	0.99	0.19	0.20	0.40	0.20	0.98	1.39	1.40	1.60	1.60	0.40
Melosira nummuloides	0.40	0.97	0.39	1.58		0.20	0.60	0.40		0.40	1.60
Minidiscus chilensis	7.16	5.65	11.94	13.86	6.39	7.45	5.58	10.20	13.77	26.15	8.62
Navicula perminuta	1.59	1.36	2.15	1.19	0.40	1.18	1.00	3.80	1.60	2.40	2.61
Nitzschia frustulum	3.78	3.51	5.48	6.14	3.79	6.27	4.18	4.80	5.79	6.79	4.01
Nitzschia perminuta	0.20			0.40	0.40				0.20	0.60	
Odontella longicruris	0.20	0.19						0.20	0.20		0.20
Opephora mutabilis			0.39								0.20
Paralia sulcata	0.40	0.97	0.20	0.20	0.20	0.20			1.00	0.40	1.20
Planothidium delicatulum	1.59	1.56	1.37	1.19	0.40	1.18	0.40	1.20	2.40	1.20	1.40
Pseudonitzschia multiseries	0.20		0.20		0.40	0.59		0.20	1.60	0.40	0.40
Rhizosolenia spp.	2.78	1.75	2.35	2.57	2.00	18.04	9.36	7.40	7.19	1.60	2.81
Skeletonema costatum	26.04	34.70	18.20	31.49	24.15	11.18	48.61	29.80	18.56	16.37	14.63
Skeletonema costatum (weak)	13.32	26.90	11.35	5.54	11.38	6.27	2.99	6.20	4.99	2.00	5.01
Tabellaria flocculosa			1.57								
Tabularia fasciculata	0.60	0.19	0.39	0.79	0.40	0.78	0.20	0.20			1.00
Thalassionema bacillare			0.20	0.40			0.20	0.20			0.40
Thalassionema nitzschioides	15.71	1.95	10.96	3.96	7.58	7.45	7.17	7.40	8.18	9.18	21.04
Thalassionema pseudonitzschioides			0.98	0.59	0.40		0.20	1.40	1.80	1.40	1.40
Thalassiosira bioculata	0.40	0.19			0.40	0.20	0.20			0.20	
Thalassiosira decipiens	3.18	0.19	1.57	3.76	8.58	5.29	1.99	3.00	4.59	2.20	1.80
Thalassiosira eccentrica	1.39	0.19	0.59	1.19	1.60	2.94	0.40	0.20		0.20	0.20
Thalassiosira gravida	0.20	0.19								0.20	
Thalassiosira kushirensis	0.60			0.79	0.20	0.59			0.40	2.00	1.80
Thalassiosira cf. *leptosus*			2.74	0.40	0.40	0.20					
Thalassiosira nordenskioeldii	0.99	3.12	0.39	3.17	1.40	0.98	1.00	1.80	0.40	0.60	1.60
Thalassiosira oestrupii	0.60	0.58	0.59		0.40	0.59		0.40	0.80	0.20	
Thalassiosira pacifica	0.99	0.39	0.78	0.99	2.20	4.51	1.20	2.00	1.00	1.20	2.00
Thalassiosira punctigera		0.39	0.20			0.20		0.20	0.20		
Thalaysiosira tenera	0.60	0.39	1.57	0.59	2.40	1.18	0.80	1.20	1.60	0.20	0.60
Thalassiosira sp. (cf. *tenera*)	0.20	0.39	0.39	0.59	1.20		0.20	0.20	0.80	0.40	
Total relative abundance	93.27	91.76	90.65	91.30	89.05	90.81	94.25	91.00	87.86	90.68	88.35
Benthics	15.00	11.00	19.00	12.00	15.00	20.00	11.00	15.00	18.00	19.00	20.00
CRS	7.20	10.78	7.59	2.70	10.38	12.65	5.45	9.91	17.94	15.51	15.25
Silicoflagellates	1.37	0.39	1.54	1.75	0.60	0.78	1.37	0.79	1.76	0.40	3.10

APPENDIX G3 (continued)

Sample	B04-23	B04-24	B04-25	B04-26	B04-27	B04-28	B04-29	B04-30	B04-31	B04-32	B04-33
Achnanthes minutissima	4.80	2.59	1.78	2.57	0.39	1.60	5.77	1.79	5.20	5.15	3.79
Amphora acutiuscula			0.20				0.40	0.60	0.20		
Amphora copulata			0.40				0.40				0.80
Asteromphalus sarcophagus				0.20						0.40	0.60
Bacteriastrum delicatulum	0.20	0.40			0.20		0.80	0.20	1.60	0.79	2.20
Berkeleya rutilans			0.20			1.20	0.20		0.20	0.20	0.40
Cocconeis disculus	0.40	0.40				0.20	0.20	0.20		0.20	0.20
Cocconeis placentula		0.20	0.40				0.40	0.60	0.60	0.99	0.20
Cocconeis scutellum	0.60	0.20	0.20			0.80	0.60	0.40	0.20	0.59	0.80
Cocconeis stauroneiformis	0.20	0.20	0.79			0.20	0.40	0.40	0.60	0.20	1.00
Cyclotella choctawhatcheeana	0.60	0.20	0.20					0.20		0.20	1.00
Cyclotella striata		0.20	1.19								
Ditylum brightwellii	0.40	0.60	0.20			0.20	0.20				0.20
Fragilaria capucina complex							0.40	0.80			
Fragilaria investiens	0.20	0.40						0.40	0.20		
Fragilaria cf. *sopotensis*	0.40						0.20	0.99		0.40	
Fragilariopsis cylindriformis									1.00	0.20	1.00
Fragilariopsis pseudonana	0.40	1.20	0.79			2.60	0.60	2.19	4.40	5.54	3.39
Gomphonemopsis lindae										0.40	
Gomphonemopsis obscurum	1.00		0.40		0.20	0.60	0.99	0.20		1.19	2.00
Melosira nummuloides	0.40			2.18		1.20	0.60	0.40	0.20		0.60
Minidiscus chilensis	12.40	8.17	8.50	13.86	11.83	5.40	7.75	4.57	10.60	14.46	5.99
Navicula perminuta	1.80	0.40	0.20	1.39	0.39	1.40	2.19	0.80	1.40	2.97	2.00
Nitzschia frustulum	2.80	3.39	2.57		0.39	1.60	7.95	5.17	4.80	4.36	4.39
Nitzschia perminuta	0.20			1.78							
Odontella longicruris	2.00	0.80				0.20	0.20				
Opephora mutabilis				0.40					0.20		
Paralia sulcata	1.40	0.40		0.20				0.60		0.40	0.40
Planothidium delicatulum	0.80	0.40	0.79	0.79		1.20	2.19	1.19	2.80	3.17	1.80
Pseudonitzschia multiseries	0.60	2.39	0.20			0.40	1.39	0.80	0.40	0.40	0.20
Rhizosolenia spp.	0.60	0.40	3.56	1.98	0.20	14.00	0.60	4.97	6.00	6.14	6.59
Skeletonema costatum	12.40	6.77	28.85	30.50	41.62	38.80	30.02	21.47	8.60	13.27	24.95
Skeletonema costatum (weak)	4.60		5.14	15.84	15.38	7.20	11.33	29.22	4.20	6.93	10.38
Tabellaria flocculosa								0.40		0.79	0.40
Tabularia fasciculata	0.80	0.60	0.20			0.80	0.99	0.40	0.80	0.79	0.60
Thalassionema bacillare				0.20			0.20	0.40		0.20	0.40
Thalassionema nitzschioides	32.60	49.20	27.47	10.50	3.35	2.00	7.75	8.75	12.40	4.55	3.79
Thalassionema pseudonitzschioides	0.80	1.00	0.59				0.40	0.60	1.60	0.40	0.40
Thalassiosira bioculata				0.20							
Thalassiosira decipiens	1.60	4.58	4.94	6.53	0.20	0.00	0.99	1.39	2.20	2.18	3.59
Thalassiosira eccentrica	0.40	2.19	0.40	0.20		0.40	0.80	0.20	1.20	0.99	0.80
Thalassiosira gravida	0.20			2.38	1.38		0.60				
Thalassiosira kushirensis	0.60	0.40	1.78	0.79	18.54	7.20	1.19	0.20			
Thalassiosira cf. *leptosus*		0.20	0.20				0.40	0.20	0.40		
Thalassiosira nordenskioeldii	1.60	2.59	0.40	1.19	0.39	3.60	1.19	0.99	8.00	1.78	1.00
Thalassiosira oestrupii		0.40	0.20	0.40				0.20	0.60	0.59	0.40
Thalassiosira pacifica	1.00	1.39	2.37	2.57	0.20	0.60	0.80	1.19	11.60	10.69	4.99
Thalassiosira punctigera							0.80	1.19	0.20		0.20
Thalassiosira tenera	0.80	0.40		0.59	0.39	0.20	0.40	0.20	0.60	0.59	0.40
Thalassiosira sp. (cf. *tenera*)	0.60	0.20	0.20	0.40	0.20	0.20					0.80
Total relative abundance	90.20	92.86	95.31	97.64	95.25	93.80	92.29	94.47	93.00	92.10	92.65
Benthics	13.00	7.60	6.70	6.30	1.20	9.60	17.00	11.00	16.00	22.00	19.00
CRS	20.44	22.41	7.16	7.68	2.50	20.89	13.87	8.04	18.14	6.83	2.91
Silicoflagellates	0.59	1.95	1.56	0.20	0.00	0.40	2.71	1.76	0.79	0.79	0.99

APPENDIX G3 (continued)

Sample	B04-34	B04-35	B04-36	B04-37	B04-38	B04-39	B04-40	B04-41	B04-42
Achnanthes minutissima	2.56	0.39	0.60	2.59	5.60	1.40	2.99	2.79	2.78
Amphora acutiuscula									
Amphora copulata	1.18			0.40					0.79
Asteromphalus sarcophagus								0.20	0.79
Bacteriastrum delicatulum	0.59	0.19	0.40		0.20	0.40	0.60	2.99	0.40
Berkeleya rutilans	0.20								0.40
Cocconeis disculus		0.39	0.20	0.20		0.20	0.20	0.40	0.40
Cocconeis placentula		0.19			0.40	0.20	0.40	0.20	0.60
Cocconeis scutellum		0.19		0.20	0.40	0.40	0.60	1.40	0.20
Cocconeis stauroneiformis	0.20		0.80	0.60	0.40	1.00		0.80	0.20
Cyclotella choctawhatcheeana	0.59	0.39			0.80		0.80	1.20	2.00
Cyclotella striata				0.20	0.40	0.60		0.60	0.40
Ditylum brightwellii	0.20		0.60	0.20	0.20	0.20	0.40		0.20
Fragilaria capucina complex							0.20		
Fragilaria investiens				0.40					
Fragilaria cf. *sopotensis*						0.20	0.40		1.39
Fragilariopsis cylindriformis	0.20		0.20	0.60			0.20	0.60	2.58
Fragilariopsis pseudonana	0.39	0.19	0.40	0.60	2.20	2.61	3.19	4.59	3.77
Gomphonemopsis lindae							0.20		
Gomphonemopsis obscurum	1.57	0.39	0.20		0.40	1.20	1.59	0.40	
Melosira nummuloides	1.38	0.19		0.40		0.80		0.40	0.99
Minidiscus chilensis	6.30	1.74	8.40	9.18	3.40	6.01	9.96	8.38	6.15
Navicula perminuta	0.20	1.16	0.80	0.20	0.80	1.60	1.20	1.00	2.78
Nitzschia frustulum	1.57	0.97	1.00	0.80	2.80	3.81	3.59	3.39	4.17
Nitzschia perminuta									
Odontella longicruris					0.20	0.20			
Opephora mutabilis						0.60			
Paralia sulcata	0.39			1.60	0.40	0.20			0.60
Planothidium delicatulum	0.98	0.77	0.80	0.40	0.60	0.40	1.79	1.40	1.59
Pseudonitzschia multiseries		0.19	0.40	0.60		0.20	0.40		0.60
Rhizosolenia spp.	2.17	0.97	0.40	1.00	3.60	3.41	9.56	13.17	9.52
Skeletonema costatum	57.28	71.62	52.40	50.70	39.40	40.08	21.91	12.18	23.41
Skeletonema costatum (weak)	7.68	3.09	10.20	7.39	17.80	14.63	6.97	2.20	10.12
Tabellaria flocculosa			0.20						
Tabularia fasciculata			0.40	1.20	0.40	0.20		0.60	
Thalassionema bacillare			0.20	1.20			0.20	0.40	
Thalassionema nitzschioides	3.35	7.14	4.60	4.19	6.20	2.40	9.16	23.15	8.33
Thalassionema pseudonitzschioides		0.97	0.40	0.60	0.40		0.80	2.00	0.20
Thalassiosira bioculata							0.20		
Thalassiosira decipiens	2.17	1.93	2.40	3.99	3.00	3.41	3.19	2.59	0.40
Thalassiosira eccentrica	0.98	0.97	0.40	0.80	1.00	1.00	0.80	0.60	0.40
Thalassiosira gravida			0.20				0.20		
Thalassiosira kushirensis						0.20	1.00		0.20
Thalassiosira cf. *leptosus*				0.20		0.20			
Thalassiosira nordenskioeldii	1.57	0.39	7.80	0.60	1.40	5.41	4.18	1.20	
Thalassiosira oestrupii	0.20	0.19		0.40					0.40
Thalassiosira pacifica		1.54	1.40	2.79	2.60	2.20	5.98	3.19	3.37
Thalassiosira punctigera								1.40	0.20
Thalassiosira tenera	0.20		0.20					0.40	0.60
Thalassiosira sp. (cf. *tenera*)						0.60	0.40	0.20	0.20
Total relative abundance	94.10	96.15	96.00	94.23	95.00	95.97	93.26	94.02	91.13
Benthics	6.90	4.10	4.00	8.20	11.00	11.00	13.00	16.00	20.00
CRS	2.31	3.90	8.91	7.90	8.09	6.55	3.28	26.86	25.22
Silicoflagellates			0.20	0.20	0.20	0.20	0.60	0.60	0.59

APPENDIX G4. Freeze core major taxa absolute abundance (× 10^6 valves/g) *

Sample	B04-1	B04-2	B04-3	B04-4	B04-5	B04-6	B04-7	B04-8	B04-9	B04-10	B04-11
Achnanthes minutissima	7.65	3.74	6.35	1.07	15.99	10.76	15.24	8.33	6.97	6.98	12.58
Amphora acutiuscula	0.96	0.75				0.74			0.50		
Amphora copulata	1.91	1.50			1.78		1.45	1.67			
Asteromphalus sarcophagus	0.96									0.71	
Bacteriastrum delicatulum	1.91	0.75	1.37	7.35	0.89	1.49			1.50	1.38	1.46
Berkeleya rutilans		1.50			0.89		1.45				
Cocconeis disculus			0.91					0.56		0.71	0.98
Cocconeis placentula	0.96	0.75	2.28		2.67	0.74	0.73		1.00	0.71	
Cocconeis scutellum			2.28		0.89	0.37	0.73	1.67	0.50	0.71	1.93
Cocconeis stauroneiformis		1.50	1.37	7.35	1.78	0.37	1.45	2.23		0.71	1.46
Cyclotella choctawhatcheeana											
Cyclotella striata							0.73			1.38	0.49
Ditylum brightwellii	2.87	1.50	1.82	1.07	3.56	1.11	2.18	1.67	3.00	0.71	2.41
Fragilaria capucina complex			0.46		2.67	0.74	0.73				
Fragilaria investiens											
Fragilaria cf. *sopotensis*			0.91		1.78	0.74	0.73		0.50		
Fragilariopsis cylindriformis	0.96						0.00	1.11			0.49
Fragilariopsis pseudonana	0.96	2.24	5.89	3.14	0.89	0.74	2.91	2.23	1.00	10.49	5.80
Gomphonemopsis lindae	3.82	1.50	0.91					3.34		2.09	0.49
Gomphonemopsis obscurum		2.24	1.37						2.00	0.71	2.41
Melosira nummuloides	0.96		2.28	1.07	1.78	0.74	1.45	0.56	2.50	0.71	0.98
Minidiscus chilensis	19.07	41.04	15.90	15.77	27.58	33.74	21.06	43.94	29.43	39.17	77.88
Navicula perminuta	1.91	0.75	4.10		2.67	2.97	1.45	3.90	2.00	2.09	
Nitzschia frustulum	13.33	10.43	8.62	8.42	10.69		8.00	16.13	9.97	13.29	9.68
Nitzschia perminuta	0.96		0.91		0.89	0.00					0.49
Odontella longicruris											
Opephora mutabilis	5.73										
Paralia sulcata	0.96	1.50	1.37		0.89	0.37		1.67		0.71	0.98
Planothidium delicatulum		1.50	2.73	4.21	2.67	1.49	5.82		1.50	2.09	0.98
Pseudonitzschia multiseries	8.60	2.99	1.37	5.27	12.43		11.60	3.90			
Rhizosolenia spp.	19.07	7.48	5.46	7.35	48.03	10.76	2.18	1.11	0.50	4.89	15.97
Skeletonema costatum	291.91	140.98	53.58	213.69	104.92	25.58	132.84	80.64	75.30	165.03	29.99
Skeletonema costatum (weak)	21.94	33.56	19.97	173.69	145.82	11.87	77.68	10.00	12.97	25.17	12.58
Tabellaria flocculosa			0.46							4.89	0.98
Tabularia fasciculata		0.75	0.91	2.13	0.89	1.11	2.18	8.89	4.50	2.09	0.49
Thalassionema bacillare										0.71	
Thalassionema nitzschioides	20.02	38.05	20.43	16.83	10.69	16.31	32.66	43.38	41.40	17.48	27.58
Thalassionema pseudonitzschioides	0.96	4.49	2.73	7.35	3.56	0.74	2.91	2.79	6.97	3.51	0.98
Thalassiosira bioculata										4.18	1.46
Thalassiosira decipiens	15.25	11.18	6.35	5.27	8.02	4.46	5.09	1.11	9.97	7.69	4.83
Thalassiosira eccentrica	0.96	9.68	3.64	1.07	1.78		0.73	3.34	1.00		0.49
Thalassiosira gravida											
Thalassiosira kushirensis						1.49		0.56	1.00	0.71	0.49
Thalassiosira cf. *leptosus*	5.73	5.23	0.91	3.14	4.46	0.37	0.73		1.50	3.51	
Thalassiosira nordenskioeldii	0.96	16.41	1.37	2.13	3.56	4.09	8.00	1.11	1.00	0.71	0.49
Thalassiosira oestrupii		0.75		1.07				1.11	3.00	2.80	1.46
Thalassiosira pacifica	6.69	8.97	17.70	6.34	7.13	25.58	4.36	5.57	6.97	3.51	1.93
Thalassiosira punctigera	6.69	3.74	1.82								
Thalassiosira tenera	0.96		2.28				0.73		0.50	1.38	1.93
Thalassiosira sp. (cf. *tenera*)	1.91		0.91	1.07	0.89	0.37		1.11	0.50	1.38	0.49

*major taxa defined as those which appeared in at least three samples with at least 1% in one sample; no entry for zero values

APPENDIX G4 (continued)

Sample	B04-12	B04-13	B04-14	B04-15	B04-16	B04-17	B04-18	B04-19	B04-20	B04-21	B04-22
Achnanthes minutissima	5.35	3.28	8.56	5.73	7.37	9.51	7.46	3.25	9.31	11.17	9.40
Amphora acutiuscula	0.36		1.76			0.36				0.43	
Amphora copulata		1.64	0.30								
Asteromphalus sarcophagus					0.82	0.36	0.62	2.03	0.47	0.43	
Bacteriastrum delicatulum	0.36			1.52	2.05	0.36	0.62	0.41		0.86	0.28
Berkeleya rutilans					0.41		1.25				
Cocconeis disculus	0.36		0.30	0.39		0.70				5.17	4.43
Cocconeis placentula	0.36	0.82	0.89	1.52				0.81		3.44	0.55
Cocconeis scutellum	1.08		0.59	0.77	1.64	1.40	0.62	0.41	2.33	1.29	
Cocconeis stauroneiformis	2.14	1.64	1.17	0.77	1.64	1.76	0.62	1.63	3.73	0.43	1.10
Cyclotella choctawhatcheeana				1.16		0.36					0.83
Cyclotella striata	0.36	0.82	0.59		0.82					1.29	
Ditylum brightwellii	0.72		0.89	2.30	0.82		0.62	2.85		0.86	
Fragilaria capucina complex	1.44			1.52		1.40		0.81			1.38
Fragilaria investiens	0.72	1.64	1.76		0.41	0.70			1.40		
Fragilaria cf. *sopotensis*				0.39	1.64	0.36		0.41		0.43	
Fragilariopsis cylindriformis								0.81			
Fragilariopsis pseudonana	2.49	2.46	3.54	2.30	7.37	4.94	8.08	0.81	2.80	1.72	0.55
Gomphonemopsis lindae	0.72						0.62	0.41	1.40		
Gomphonemopsis obscurum	1.78	0.40	0.30	0.77	0.41	1.76	4.34	2.85	3.73	3.44	0.55
Melosira nummuloides	0.72	2.04	0.59	3.05		0.36	1.87	0.81		0.86	2.21
Minidiscus chilensis	12.85	11.89	17.99	26.74	13.13	13.39	17.41	20.73	32.14	56.28	11.90
Navicula perminuta	2.85	2.86	3.24	2.30	0.82	2.12	3.12	7.72	3.73	5.17	3.60
Nitzschia frustulum	6.78	7.38	8.25	11.85	7.79	11.27	13.04	9.76	13.51	14.61	5.53
Nitzschia perminuta	0.36			0.77	0.82				0.47	1.29	
Odontella longicruris	0.36	0.40						0.41	0.47		0.28
Opephora mutabilis			0.59								0.28
Paralia sulcata	0.72	2.04	0.30	0.39	0.41	0.36			2.33	0.86	1.66
Planothidium delicatulum	2.85	3.28	2.06	2.30	0.82	2.12	1.25	2.44	5.60	2.58	1.93
Pseudonitzschia multiseries	0.36		0.30		0.82	1.06		0.41	3.73	0.86	0.55
Rhizosolenia spp.	4.99	3.68	3.54	4.96	4.11	32.42	29.20	15.04	16.78	3.44	3.88
Skeletonema costatum	46.73	73.00	27.42	60.75	49.61	20.09	151.65	60.57	43.32	35.23	20.19
Skeletonema costatum (weak)	23.90	56.59	17.10	10.69	23.38	11.27	9.33	12.60	11.65	4.30	6.91
Tabellaria flocculosa			2.36								
Tabularia fasciculata	1.08	0.40	0.59	1.52	0.82	1.40	0.62	0.41			1.38
Thalassionema bacillare			0.30	0.77			0.62	0.41			0.55
Thalassionema nitzschioides	28.19	4.10	16.51	7.64	15.57	13.39	22.37	15.04	19.09	19.76	29.04
Thalassionema pseudonitzschioides			1.48	1.14	0.82		0.62	2.85	4.20	3.01	1.93
Thalassiosira bioculata	0.72	0.40			0.82	0.36	0.62			0.43	
Thalassiosira decipiens	5.71	0.40	2.36	7.25	17.63	9.51	6.21	6.10	10.71	4.73	2.48
Thalassiosira eccentrica	2.49	0.40	0.89	2.30	3.29	5.28	1.25	0.41		0.43	0.28
Thalassiosira gravida	0.36	0.40								0.43	
Thalassiosira kushirensis	1.08			1.52	0.41	1.06			0.93	4.30	2.48
Thalassiosira cf. *leptosus*			4.13	0.77	0.82	0.36					
Thalassiosira nordenskioeldii	1.78	6.56	0.59	6.12	2.88	1.76	3.12	3.66	0.93	1.29	2.21
Thalassiosira oestrupii	1.08	1.22	0.89		0.82	1.06		0.81	1.87	0.43	
Thalassiosira pacifica	1.78	0.82	1.17	1.91	4.52	8.11	3.74	4.06	2.33	2.58	2.76
Thalassiosira punctigera		0.82	0.30			0.36		0.41	0.47		
Thalassiosira tenera	1.08	0.82	2.36	1.14	4.93	2.12	2.50	2.44	3.73	0.43	0.83
Thalassiosira sp. (cf. *tenera*)	0.36	0.82	0.59	1.14	2.47		0.62	0.41	1.87	0.86	

APPENDIX G4 (continued)

Sample	B04-23	B04-24	B04-25	B04-26	B04-27	B04-28	B04-29	B04-30	B04-31	B04-32	B04-33
Achnanthes minutissima	11.58	10.40	8.29	15.53	3.93	5.30	11.24	4.41	12.45	8.56	11.68
Amphora acutiuscula			0.93				0.78	1.48	0.48		
Amphora copulata			1.86				0.78				2.47
Asteromphalus sarcophagus				1.21						0.66	1.85
Bacteriastrum delicatulum	0.48	1.61			2.02		1.56	0.49	3.83	1.31	6.78
Berkeleya rutilans			0.93			3.98	0.39		0.48	0.33	1.23
Cocconeis disculus	0.96	1.61				0.66	0.39	0.49		0.33	0.62
Cocconeis placentula		0.80	1.86				0.78	1.48	1.44	1.65	0.62
Cocconeis scutellum	1.45	0.80	0.93			2.65	1.17	0.99	0.48	0.98	2.47
Cocconeis stauroneiformis	0.48	0.80	3.68			0.66	0.78	0.99	1.44	0.33	3.08
Cyclotella choctawhatcheeana	1.45	0.80	0.93					0.49		0.33	3.08
Cyclotella striata		0.80	5.54								
Ditylum brightwellii	0.96	2.41	0.93			0.66	0.39				0.62
Fragilaria capucina complex							0.78	1.97			
Fragilaria investiens	0.48	1.61						0.99	0.48		
Fragilaria cf. *sopotensis*	0.96						0.39	2.44		0.66	
Fragilariopsis cylindriformis									2.39	0.33	3.08
Fragilariopsis pseudonana	0.96	4.82	3.68			8.62	1.17	5.39	10.54	9.21	10.45
Gomphonemopsis lindae										0.66	
Gomphonemopsis obscurum	2.41		1.86		2.02	1.99	1.93	0.49		1.98	6.16
Melosira nummuloides	0.96			13.17		3.98	1.17	0.99	0.48		1.85
Minidiscus chilensis	29.90	32.80	39.59	83.75	119.26	17.90	15.10	11.25	25.38	24.03	18.46
Navicula perminuta	4.34	1.61	0.93	8.40	3.93	4.64	4.27	1.97	3.35	4.94	6.16
Nitzschia frustulum	6.75	13.61	11.97		3.93	5.30	15.49	12.73	11.49	7.24	13.53
Nitzschia perminuta	0.48			10.76							
Odontella longicruris	4.82	3.21				0.66	0.39				
Opephora mutabilis				2.42					0.48		
Paralia sulcata	3.38	1.61		1.21				1.48		0.66	1.23
Planothidium delicatulum	1.93	1.61	3.68	4.77		3.98	4.27	2.93	6.70	5.27	5.55
Pseudonitzschia multiseries	1.45	9.60	0.93			1.33	2.71	1.97	0.96	0.66	0.62
Rhizosolenia spp.	1.45	1.61	16.58	11.96	2.02	46.40	1.17	12.24	14.37	10.20	20.31
Skeletonema costatum	29.90	27.18	134.38	184.29	419.57	128.61	58.49	52.87	20.59	22.05	76.89
Skeletonema costatum (weak)	11.09		23.94	95.71	155.05	23.87	22.08	71.96	10.06	11.52	31.99
Tabellaria flocculosa								0.99		1.31	1.23
Tabularia fasciculata	1.93	2.41	0.93			2.65	1.93	0.99	1.92	1.31	1.85
Thalassionema bacillare				1.21			0.39	0.99		0.33	1.23
Thalassionema nitzschioides	78.62	197.55	127.95	63.44	33.77	6.63	15.10	21.55	29.69	7.56	11.68
Thalassionema pseudonitzschioides	1.93	4.02	2.75				0.78	1.48	3.83	0.66	1.23
Thalassiosira bioculata				1.21							
Thalassiosira decipiens	3.86	18.39	23.01	39.46	2.02		1.93	3.42	5.27	3.62	11.06
Thalassiosira eccentrica	0.96	8.79	1.86	1.21		1.33	1.56	0.49	2.87	1.65	2.47
Thalassiosira gravida	0.48			14.38	13.91		1.17				
Thalassiosira kushirensis	1.45	1.61	8.29	4.77	186.90	23.87	2.32	0.49			
Thalassiosira cf. *leptosus*		0.80	0.93				0.78	0.49	0.96		
Thalassiosira nordenskioeldii	3.86	10.40	1.86	7.19	3.93	11.93	2.32	2.44	19.16	2.96	3.08
Thalassiosira oestrupii		1.61	0.93	2.42				0.49	1.44	0.98	1.23
Thalassiosira pacifica	2.41	5.58	11.04	15.53	2.02	1.99	1.56	2.93	27.77	17.76	15.38
Thalassiosira punctigera							1.56	2.93	0.48		0.62
Thalassiosira tenera	1.93	1.61		3.56	3.93	0.66	0.78	0.49	1.44	0.98	1.23
Thalassiosira sp. (cf. *tenera*)	1.45	0.80	0.93	2.42	2.02	0.66					2.47

APPENDIX G4 (continued)

Sample	B04-34	B04-35	B04-36	B04-37	B04-38	B04-39	B04-40	B04-41	B04-42
Achnanthes minutissima	10.46	3.43	4.13	13.49	16.11	5.98	9.85	7.25	8.52
Amphora acutiuscula									
Amphora copulata	4.82			2.08					2.42
Asteromphalus sarcophagus								0.52	2.42
Bacteriastrum delicatulum	2.41	1.67	2.75		0.58	1.71	1.98	7.77	1.23
Berkeleya rutilans	0.82								1.23
Cocconeis disculus		3.43	1.38	1.04		0.85	0.66	1.04	1.23
Cocconeis placentula		1.67			1.15	0.85	1.32	0.52	1.84
Cocconeis scutellum		1.67		1.04	1.15	1.71	1.98	3.64	0.61
Cocconeis stauroneiformis	0.82		5.51	3.12	1.15	4.27		2.08	0.61
Cyclotella choctawhatcheeana	2.41	3.43			2.30		2.64	3.12	6.13
Cyclotella striata				1.04	1.15	2.56	0.00	1.56	1.23
Ditylum brightwellii	0.82		4.13	1.04	0.58	0.85	1.32		0.61
Fragilaria capucina complex							0.66		
Fragilaria investiens				2.08					
Fragilaria cf. *sopotensis*						0.85	1.32		4.26
Fragilariopsis cylindriformis	0.82		1.38	3.12			0.66	1.56	7.91
Fragilariopsis pseudonana	1.59	1.67	2.75	3.12	6.33	11.14	10.51	11.93	11.55
Gomphonemopsis lindae							0.66		
Gomphonemopsis obscurum	6.42	3.43	1.38		1.15	5.12	5.24	1.04	
Melosira nummuloides	5.64	1.67		2.08		3.41	0.00	1.04	3.03
Minidiscus chilensis	25.75	15.31	57.84	47.81	9.78	25.65	32.83	21.78	18.84
Navicula perminuta	0.82	10.21	5.51	1.04	2.30	6.83	3.95	2.60	8.52
Nitzschia frustulum	6.42	8.54	6.89	4.17	8.05	16.26	11.83	8.81	12.78
Nitzschia perminuta									
Odontella longicruris					0.58	0.85			
Opephora mutabilis						2.56			
Paralia sulcata	1.59			8.33	1.15	0.85			1.84
Planothidium delicatulum	4.01	6.78	5.51	2.08	1.73	1.71	5.90	3.64	4.87
Pseudonitzschia multiseries		1.67	2.75	3.12		0.85	1.32		1.84
Rhizosolenia spp.	8.87	8.54	2.75	5.21	10.35	14.55	31.51	34.23	29.17
Skeletonema costatum	234.11	630.22	360.84	264.06	113.32	171.07	72.21	31.65	71.73
Skeletonema costatum (weak)	31.39	27.19	70.24	38.49	51.19	62.44	22.97	5.72	31.01
Tabellaria flocculosa			1.38						
Tabularia fasciculata			2.75	6.25	1.15	0.85		1.56	
Thalassionema bacillare			1.38	6.25			0.66	1.04	
Thalassionema nitzschioides	13.69	62.83	31.68	21.82	17.83	10.24	30.19	60.16	25.52
Thalassionema pseudonitzschioides		8.54	2.75	3.12	1.15		2.64	5.20	0.61
Thalassiosira bioculata							0.66		
Thalassiosira decipiens	8.87	16.98	16.53	20.78	8.63	14.55	10.51	6.73	1.23
Thalassiosira eccentrica	4.01	8.54	2.75	4.17	2.88	4.27	2.64	1.56	1.23
Thalassiosira gravida			1.38				0.66		
Thalassiosira kushirensis						0.85	3.30		0.61
Thalassiosira cf. *leptosus*				1.04		0.85			
Thalassiosira nordenskioeldii	6.42	3.43	53.71	3.12	4.03	23.09	13.78	3.12	
Thalassiosira oestrupii	0.82	1.67		2.08					1.23
Thalassiosira pacifica		13.55	9.64	14.53	7.48	9.39	19.71	8.29	10.33
Thalassiosira punctigera								3.64	0.61
Thalassiosira tenera	0.82		1.38					1.04	1.84
Thalassiosira sp. (cf. *tenera*)						2.56	1.32	0.52	0.61

APPENDIX G5. Freeze core cyclostratigraphy: Depth vs. diatom abundance

Depth (cm)	Diatom Abundance (valves/g)
0.5000	477915943.4
1.2999	477915943.4
1.3000	373753983.1
2.3999	373753983.1
2.4000	227502424.5
3.9999	227502424.5
4.0000	532622790.7
4.7999	532622790.7
4.8000	445528039.0
5.2999	445528039.0
5.3000	185773151.0
6.2999	185773151.0
6.3000	363647461.0
7.6999	363647461.0
7.7000	278629604.3
8.5999	278629604.3
8.6000	249835302.0
9.0999	249835302.0
9.1000	354521731.0
9.6999	354521731.0
9.7000	243844011.2
10.1999	243844011.2
10.2000	179465485.4
10.9999	179465485.4
11.0000	210370803.2
11.7999	210370803.2
11.8000	150634681.6
12.5999	150634681.6
12.6000	192929541.1
13.1999	192929541.1
13.2000	205430301.5
14.2999	205430301.5
14.3000	179718131.8
14.7999	179718131.8
14.8000	311982194.1
15.3999	311982194.1
15.4000	203249463.2
15.9999	203249463.2
16.0000	233395770.2
16.4999	233395770.2
16.5000	215212696.8
16.9999	215212696.8
17.0000	138016899.4
18.1999	138016899.4
18.2000	241163070.2
18.6999	241163070.2
18.7000	401515333.8
19.6999	401515333.8
19.7000	465794783.5
20.9999	465794783.5
21.0000	604228402.3
21.9999	604228402.3
22.0000	1008105105.0

Depth (cm) (continued)	Diatom Abundance (valves/g)
22.4999	1008105105.0
22.5000	331459548.3
22.9999	331459548.3
23.0000	194848505.0
23.6999	194848505.0
23.7000	246258672.4
24.3999	246258672.4
24.4000	239439246.7
24.7999	239439246.7
24.8000	166169711.4
25.2999	166169711.4
25.3000	308178200.6
25.7999	308178200.6
25.8000	408720299.3
26.3999	408720299.3
26.4000	879946960.1
26.9999	879946960.1
27.0000	688619849.1
27.3999	688619849.1
27.4000	520832990.4
27.7999	520832990.4
27.8000	287602163.8
28.1999	287602163.8
28.2000	426818393.9
28.9999	426818393.9
29.0000	329574539.0
29.9999	329574539.0
30.0000	259884805.2
30.9999	259884805.2
31.0000	306396929.6
31.9999	306396929.6

APPENDIX G6. Freeze core cyclostratigraphy: Time vs. diatom abundance

Year	Diatom Abundance (valves/g)
1993.000	477915943.4
1992.001	477915943.4
1992.000	373753983.1
1991.001	373753983.1
1991.000	227502424.5
1989.501	227502424.5
1989.500	532622790.7
1989.001	532622790.7
1989.000	445528039.0
1988.001	445528039.0
1988.000	185773151.0
1987.001	185773151.0
1987.000	363647461.0
1986.001	363647461.0
1986.000	278629604.3
1985.001	278629604.3
1985.000	249835302.0
1984.001	249835302.0
1984.000	354521731.0
1983.501	354521731.0
1983.500	243844011.2
1983.001	243844011.2
1983.000	179465485.4
1982.001	179465485.4
1982.000	210370803.2
1980.501	210370803.2
1980.500	150634681.6
1979.001	150634681.6
1979.000	192929541.1
1978.001	192929541.1
1978.000	205430301.5
1976.501	205430301.5
1976.500	179718131.8
1976.001	179718131.8
1976.000	311982194.1
1975.001	311982194.1
1975.000	203249463.2
1974.001	203249463.2
1974.000	233395770.2
1973.001	233395770.2
1973.000	215212696.8
1972.001	215212696.8
1972.000	138016899.4
1969.801	138016899.4
1969.750	241163070.2
1968.800	401515333.8
1968.751	241163070.2
1967.801	401515333.8
1967.750	465794783.5
1965.001	465794783.5
1965.000	604228402.3
1964.001	604228402.3
1964.000	1008105105.0

Year (continued)	Diatom Abundance (valves/g)
1963.501	1008105105.0
1963.500	331459548.3
1962.501	331459548.3
1962.500	194848505.0
1961.001	194848505.0
1961.000	246258672.4
1960.001	246258672.4
1960.000	239439246.7
1959.001	239439246.7
1959.000	166169711.4
1958.001	166169711.4
1958.000	308178200.6
1957.401	308178200.6
1957.400	408720299.3
1956.301	408720299.3
1956.300	879946960.1
1955.301	879946960.1
1955.300	688619849.1
1954.801	688619849.1
1954.800	520832990.4
1954.301	520832990.4
1954.300	287602163.8
1953.301	287602163.8
1953.300	426818393.9
1952.001	426818393.9
1952.000	329574539.0
1950.001	329574539.0
1950.000	259884805.2
1948.001	259884805.2
1948.000	306396929.6
1947.000	306396929.6

APPENDIX H

Data from Piston Core TUL99B03, Slab 8

APPENDIX H1. Sediment slab microfossil counts

Sample	S8-1	S8-2	S8-3	S8-4	S8-5	S8-6	S8-7	S8-8	S8-9	S8-10	S8-11	S8-12	S8-13	S8-14	S8-15	S8-16	S8-17
DIATOMS																	
A. brevipes														1		2	
A. groenlandica																	
A. kregeri		3	4	2	1	4	2	4		2	2	1	6	3		10	2
A. lanceolata	3																
A. lemmermanii							1			3		1		1			
A. minutissima	16	14	13	6	2	8	29	18	20	25	15	21	16	25	10	28	17
A. nedosa																	
A. vistulana																	
Achnanthidium biasolettianum	5		3			2	4	1			3	4		2		2	3
Actinocyclus curvatulus	3					1						1					
A. octonarius	1	2		1											1		
Actinoptychus senarius	1	1	1			3						1					
A. vulgaris	5	3				4		1		1			2	1			
Amphora aa utiuscula			1							1		1	3		2		1
A. coffaeformis			1			1			1	2		1		3			2
A. copulata		2	4	1	2		3			6		4	4	2	2	2	
A. exigua																	
Amphora cf. *helensis*	3		1					2		4		3		2	2		
A. maletracta var. *constricta*		1						1									
A. marina													5			2	
Amphora sp. (S8-21)																	
Asteromphalus heptacis			2	1	2	1	2	1	1		2	1	2	2		1	
A. sarcophagus	1	1					3	1	1	1		2	1	2			3
Aulacoseira cf. *ambigua*						2			1							4	
A. italica var. *subarctica*	1																
Azepeitia spp.								3									
Bacillaria paxillifer		1							1				1	2			1
Bacteriastrum delicatulum		4	2	1	3		1	2		2		3	2		2	4	1
Berkeleya rutilans			3				3		1		2		5		2		2
Brachysira spp.							1					1		2			
Caloneis sp. (S8-9)									1								
Cocconeis britannica																	
C. californica																	
C. costata complex			2	1	2	2	1	2	1			1	4		3		
Cocconeis cf. *dirupta*																	
C. disculus		2		2		1	1	3	1	2	2	4	1	2			
C. distans		2	1						1		1		2	1			
Cocconeis cf. *molesta*																	
C. neothumensis												1		1		1	
C. pellucida							1										1
C. peltoides			1			2				2			2				
C. pinnata			2					1		1						1	
C. placentula	2	3	3		1		1			2	2	3	3		2	4	
C. scutellum	7	2	5	1	2	3	1	4	2	5	1	2		3	2	4	
C. stauroneiformis		1	1			3			1	1			1	4	2	4	2
Cocconeis sp. (S8-32)																	
Coscinodiscus diorama				1										1			
C. radiatus													1				
Ctenophora pulchella								1			2		1				1
C. choctawhatcheeana	5	3	8	0	0	3	4	4	1	5	2	7	8	26	3	0	0
C. pseudostelligera												1				1	
Cyclotella rossii		1	1		2		2		1		1		2	1		1	
C. stelligera			1								1	1		1		1	2
C. striata		2	6			1	3	3					2		3	1	
C. stylorum		2	1	1			2							2		1	
Cyclotella sp. (B04-15/16)																	
Cyclotella sp. (S8-6)						2	9							4	1		
Cyclotella sp. (S8-19)																	
Cyclotella sp. (S8-25)																	

APPENDIX H1 (continued)

Sample	S8-1	S8-2	S8-3	S8-4	S8-5	S8-6	S8-7	S8-8	S8-9	S8-10	S8-11	S8-12	S8-13	S8-14	S8-15	S8-16	S8-17
Cyclotella sp. (S8-35)																	
Cymbella cymbiformis					1		2							1		1	
C. lanceolata																	
C. minuta			1														
Cymbella sp. (S8-12)												1					
Cymbella sp. (S8-32)																	
Delphineis spp.		3						3		3		1				2	
Denticula spp.																	
Diatoma mesodon														1			
Diatoma cf. *tenue*																	
Diatomella minuta	5							1	2			2			2	4	2
Dimeragramma sp. (11C-6)										2						2	
Dimeragramma sp. (S8-5)					1			1									
Diploneis cf. *bomboides*																	
D. bombus																	
Diploneis cf. *sejuncta*													1				
D. smithii						1				1	1						
D. smithii var. *recta*												1					
Diploneis spp.																	
Ditylum brightwellii	1					1		5		1	2	3	1	1		2	6
Eucampia spp.										1							
Eunotia spp.		3	1	1			1	2			1	1			3		2
Fallacia spp.								2		1			1		1	1	1
Fallacia sp. (B04-29)															2		
Fallacia sp. (S8-2)		1															
Fragilaria capucina complex	4																1
F. construens var. *construens*																1	
F. investiens	1	3				2	2	3		2	1	3	1	5	2	5	
F. pinnata	1							8			1			4		2	
F. sopotensis	8	1	1	1		6	5	2	2	8		8	4		2	3	3
Fragilaria sp. (S8-13)													1				
Fragilariopsis atlantica	1	1								1							1
F. cylindriformis	7	4		1	3	1	1	3	1	4	6	9	3	3	6	24	10
F. pseudonana	19	13	13	15	5	7	10	12	7	25	49	55	33	81	59	115	57
F. schulzii								1					1	2			
Fragilariopsis sp. (3A-7)										1				1		1	
Fragilariopsis sp. (S8-10)										2							
Frustulia rhomboides																	
Gomphonema angustum	2	2	2										2				2
G. angustatum		1				1											
G. olivaceum		2															
Gomphonema sp.			2				2		2				2				
Gomphonema sp. (S8-3)			2				1										
Gomphonema sp. (S8-31)																	
Gomphonema sp. (S8-32)																	
Gomphonemensis exigua				1		4			2			1		2		2	
G. lindae	2	1	2				4	2	6			6	2			1	1
G. obscurum	4	4	6				3	1		2		4	2	2		2	2
Grammatophora angulosa											1					1	
G. marina	2	1												1			
G. oceanica	1											6					
Grammatophora sp. (B04-14)								4		2							
Grammatophora sp. (S8-43)																	
Gyrosigma spp.																	
Hannea arcus							4		2	4							2
Hyalodiscus scoticus			2	2			2	1			1		2	2	1	1	
Licomorpha sp.																	
Luticola mutica	1	2				2			2								
Mastogloia exigua			2									1					
Melosira nummuloides	3		2	1	2	10	4	2			1	1	1		4	5	3

APPENDIX H1 (continued)

Sample	S8-1	S8-2	S8-3	S8-4	S8-5	S8-6	S8-7	S8-8	S8-9	S8-10	S8-11	S8-12	S8-13	S8-14	S8-15	S8-16	S8-17
Melosira spp.	1			1	1	1		1	1	1	1					1	
Minidiscus chilensis	2	5	3	4	11	8	12	8	5	4	9	4	3	7	12	8	1
Navicula cryptocephala		1		2		1			2		2						
N. directa				1		1	3			1			1				
N. gregaria	1		1	1		2			1	1	1	1	2	1	1		1
N. perminuta	12	12	12	6	6	4	8	20	2	8	8	3	11	10	6	21	9
N. phylleptosoma		2						1		3		2					2
Navicula cf. *ramosissima*		1	2		1	1		1	1			1	1				
Navicula sp. (3C-1)		1	1			3		3	2	2	4	2	5	6	5	10	6
Navicula sp. (S8-4)				1													
Navicula sp. (S8-8)								2			3	1			1		
Navicula sp. (S8-33)																	
Navicula sp. (S8-48)																	
Nitzschia coaretata			2					1									
N. dissipata		1			1	2	1	1				4	1		2	2	1
N. fonticola		1						3		1		1		1	4	1	1
N. frustulum	30	36	32	8	23	9	25	31	10	32	29	45	21	22	25	24	34
N. inconspicua	1	2					2	2		4	2		1				
N. microcephala	1									1							
N. perminuta									1								
Nitzschia cf. *sicula* (B04-12)												1					
N. valdestriata			2	2						2			2				
Nitzschia sp. (S8-1)	2																
Nitzschia sp. (S8-17)																	1
Nitzschia sp. (S8-34)																	
Odontella aurita																	
O. longicruris		1		2				2			2	1		1		2	
Opephora horstiana	5						3	1	5	4		10	1	6	4		
O. marina	2	3	1				2	4		1		4		7			
O. minuta		6										5		1	2	3	
O. mutabilis	6	2	1		4	4	1	4		1	1		6	2			2
O. pacifica																	
Paralia sulcata	3	5	3	6	1	1	6	6	4	5	13	5	4	1	2	3	5
Pinnularia cf. *quadraterea*																	
Plagiogramma staurophorum																	
Planothidium delicatulum	23	13	8	8	9	10	17	17	22	31	20	30	18	24	19	23	13
P. engelbretchtii		1													1		
P. haukiana	1	1	2	2	1		2	1	2	7				3	3	5	3
Pleurosigma spp.										1							
Protokeelia cholnokyana	1		2														
Pseudonitzschia multiseries	7	1	3	4	9	1	5	6	1		1	1	3	5		1	
P. seriata	1	2	3	3	117	2		1			1	3	2	1	1		
Reimeria spp.																	
Rhizolenia spp. (spines)		1	1							1							
Rhoicosphenia curvata																	
Rhopalodia pacifica										1		3				2	2
Seminavis spp.						1		2									1
Skeletonema costatum	61	64	95	282	56	90	17	36	30	73	84	57	136	67	35	29	122
S. costatum (weak)	42	102	78	30	33	139	45	41	218	90	105	51	52	57	39	24	64
Stephanodiscus spp.														1			
Stephanopyxis turris	1	4						1		1		1					
Surirella brebissonii			1				1				1		1				
Synedra ulna																	
Tabellaria flocculosa	22	2					5		5	4	14	1		1			
Tabularia fasciculata	3	2	1		2	3	3	6	3			9	7	4	3	5	3
Thalassionema cf. *bacillare*	6			5	2				1	1		2					1
T. nitzschioides	75	28	35	8	12	4	9	22	12	11	20	17	19	4	35	28	15
T. pseudonitzschioides	5	3	3	1	7	3		4	2	3	8	4	1	5	8	7	1
Thalassiosira aestivalis									2					1	1	2	3
T. angulata				3	1	2	2		1	1						1	1

APPENDIX H1 (continued)

Sample	S8-1	S8-2	S8-3	S8-4	S8-5	S8-6	S8-7	S8-8	S8-9	S8-10	S8-11	S8-12	S8-13	S8-14	S8-15	S8-16	S8-17
Thalassiosira binata	1	1	2		1						1			1	5	2	
T. bioculata var. *exigua*																1	
T. conferta	5	1	2		2	1	2		2	3	3		2	1	4		2
T. decipiens	17	54	44	24	88	35	14	20	15	16	16	12	7	13	86	15	21
T. decipiens (large)	2	12	10	8	37	15	14	2	2	4	5	2		6	9	4	2
T. eccentrica	14	9	9	4	4	6		7	9	4	7	6	3		6	4	21
T. eccentrica (large)	3							1			1				1		
Thalassiosira cf. *eccentrica*																	
T. gravida		2					1								1		
T. hendeyi																	
T. hyalina																	
T. kushirensis			3		1	1	1			1		1			2	2	
Thalassiosira cf. *leptopus*	3	5	2	1	1	4		3	1	4	3	6	1		4		5
T. lundiana																	
T. minima	1											2					
T. nodulineata																	
T. nordenskioeldii	18	15	19	22	12	60	156	134	54	33	25	25	57	25	32	14	12
T. oceanica	1	3		2					1	2							
T. oestrupii		3	2		1	3	3		1	4	3		3	1		1	1
T. pacifica	8	3	10	6	30	15	30	4	32	8	12	9	3	15	21	5	5
T. poroseriata							1										
T. punctigera																	
T. rotula				25													
T. tealata																	2
T. tenera			1			1				1	2					1	2
Thalassiosira cf. *tenera*			2				3	1							1	3	
Thalassiosira sp. (B04-40)																	
Thalassiosira sp. (S8-12)												1	2		3	4	3
Thalassiosira sp. (S8-27)																	
Thalassiosira sp. (S8-31)																	
Thalassiosira sp. (S8-35)																	
Thalassiothrix longissima					1												
Trachyneis aspera									1			2					
Tryblionella cf. *aerophila*										2				1			2
Tryblionella sp. (S8-1)	1																
Unknown centric 1 (B04-7)										1				2			
Unknown centric (B04-21)												1				1	
Unknown centric (S8-4)				1													
Unknown pennate (S8-7)							1										
Unknown pennate 2 (S8-8)								1						1			
Unknown pennate (S8-32)																	
Unknown pennate (S8-36)																	
Unknown centric (S8-39)																	
Unknown pennate 1 (S8-41)																	
Unknown pennate 2 (S8-41)																	
Unknown pennate (S8-50)																	
Unknown pennate (S8-52)																	
TOTAL	503	503	501	513	504	511	510	506	512	504	507	504	507	504	503	508	501
RESTING SPORES																	
Chaetoceros spp.	60	120	100	101	94	120	140	399	63	87	155	216	138	219	196	124	142
Leptocylindrus spp.						3	3	3	1	1	2	2	1	2	7	1	1
Stephanopyxis spp.																	
TOTAL	60	120	100	101	94	123	143	402	64	88	157	218	139	221	203	125	143
SILICOFLAGELLATES																	
Dictyocha fibula													1	1			
D. speculum	11	5	5	1	5	2	1	2	1	4	2		2	1	6	5	4
Octactis sp.	1					1				1	1	3	2	1	1	1	
TOTAL	12	5	5	1	5	3	1	2	1	5	3	3	5	3	7	6	4

APPENDIX H1 (continued)

Sample	S8-18	S8-19	S8-20	S8-21	S8-22	S8-23	S8-24	S8-25	S8-26	S8-27	S8-28	S8-29	S8-30	S8-31	S8-32	S8-33	S8-34
DIATOMS																	
A. brevipes				2							2	1	2				
A. groenlandica																	1
A. kregeri			2		2	3	2			1	5	2	2				4
A. lanceolata													2				
A. lemmermanii	2	2	2	1							2						
A. minutissima	6	21	18	23	11	16	2	13	13	11	15	24	35	23	40	5	20
A. nedosa																	
A. vistulana			2	2	1	2											
Achnanthidium biasolettianum		1	4	2			2				1			1	4		
Actinocyclus curvatulus												2	1	1	3	1	
A. octonarius												1	2				1
Actinoptychus senarius		1											2	1			1
A. vulgaris			1			1	1	2							1	1	3
Amphora acutiuscula		6	2		1							2	3				1
A. coffaeformis	1			3							1						
A. copulata		2	4	2					1	2			6	2	2		
A. exigua											2						
Amphora cf. *helensis*		2	4	2		2			2			2					
A. maletractata var. *constricta*									1					2			
A. marina	2				2					2							
Amphora sp. (S8-21)				1													
Asteromphalus heptactis		18	24	6				3		1	3	2	1		1	1	
A. sarcophagus				1		2		1						2		1	1
Aulacoseira cf. *ambigua*																	
A. italica var. *subarctica*																	
Azepeitia spp.					1									2			2
Bacillaria paxillifer	1		2	2	1									1			
Bacteriastrum delicatulum			1	1		2		4	8		2	6	5		3	8	1
Berkeleya rutilans				1	1			1	2	1			1	1			
Brachysira spp.		1	2					1			1		1			1	
Caloneis sp. (S8-9)																	
Cocconeis britannica																	
C. californica																	1
C. costata complex		3	3	1	3			2			1	2	1	1	3	1	4
Cocconeis cf. *dirupta*		2															
C. disculus		1	3	2	2		3		1		3	1	3	2		1	2
C. distans		1	1										1				
Cocconeis cf. *molesta*																	
C. neothumensis				1		1	1		2			2	2	4			
C. pellucida													1				
C. peltoides		1		1				3			2		1		1		
C. pinnata		1			1				1		1	1		1		2	1
C. placentula		1	3	3					4		2				2	1	1
C. scutellum	4	2	2	3	6	3	1		2	1	1	2	4	3	3	3	5
C. stauroneiformis	1	1		3	1	1		3	2		1	1	1				1
Cocconeis sp. (S8-32)															1		
Coscinodiscus diorama						1											
C. radiatus							1		1				1				
Ctenophora pulchella		1	1	2	1		1	1			2	2	1		1		
C. choctawhatcheeana			1		2	3	2	11	3	3	6	5	2	3	7	3	11
C. pseudostelligera																	
Cyclotella rossii	1	1		2	2		1							1			
C. stelligera										1	1	1	3	5	2	1	2
C. striata		1		1			2	2	4		1	2					3
C. styloram								2					2				2
Cyclotella sp. (B04-15/16)									4						2	1	
Cyclotella sp. (S8-6)		1						4	6			3		1		1	16
Cyclotella sp. (S8-19)		2															
Cyclotella sp. (S8-25)								1									

APPENDIX H1 (continued)

Sample	S8-18	S8-19	S8-20	S8-21	S8-22	S8-23	S8-24	S8-25	S8-26	S8-27	S8-28	S8-29	S8-30	S8-31	S8-32	S8-33	S8-34
Cyclotella sp. (S8-35)																	
Cymbella cymbiformis								1	1		3					1	2
C. lanceolata																	
C. minuta		1		2		1						1	2		1		
Cymbella sp. (S8-12)																	
Cymbella sp. (S8-32)															1		
Delphineis spp.		1				1											
Denticula spp.																	
Diatoma mesodon					1												1
Diatoma cf. *tenue*					2												
Diatomella minuta		4							1		2	6		2	2		2
Dimeragramma sp. (11C-6)					1		1		1				1	1			
Dimeragramma sp. (S8-5)												1					
Diploneis cf. *bomboides*																	
D. bombus				1	1								2				
Diploneis cf. *sejuncta*																	
D. smithii				1	1						1		1				
D. smithii var. *recta*																	
Diploneis spp.																	
Ditylum brightwellii					3	2						1	2		1	4	16
Eucampia spp.				1													
Eunotia spp.	1	1	1	6	2	1			1		1			2	2	1	1
Fallacia spp.		2			2	2							6		3	3	
Fallacia sp. (B04-29)			1														1
Fallacia sp. (S8-2)																	
Fragilaria capucina complex			3							1	1		2				
F. construens var. *construens*												1					
F. investiens		2	8	3	5			1		2	1			2			1
F. pinnata		4		2		6			2			1			2		
F. sopotensis	1	3	10	7	7	9	5		11		1			1	4	4	3
Fragilaria sp. (S8-13)																	
Fragilariopsis atlantica		1											1				1
F. cylindriformis	2	3	8	6	11	7	4	5	9	5	24	20	8	3	15	12	14
F. pseudonana	9	41	32	28	52	57	14	30	55	29	157	51	24	44	38	22	46
F. schulzii						1						1	1	3			
Fragilariopsis sp. (3A-7)						2			2		2			1		1	
Fragilariopsis sp. (S8-10)																	
Frustulia rhomboides				1													
Gomphonema angustum			3			4					4			1	2	1	
G. angustatum					1				2								
G. olivaceum										1							
Gomphonema sp.											4		4		2	2	
Gomphonema sp. (S8-3)																	
Gomphonema sp. (S8-31)														1			
Gomphonema sp. (S8-32)															2		
Gomphonemensis exigua		1	2	2		1								2			
G. lindae	1		1	5	5		2	1				3					3
G. obscurum	5	1	1	2	2		4	2	1			1		2	3	2	
Grammatophora angulosa									1								
G. marina			1		4				1								
G. oceanica				2				2	3					3			1
Grammatophora sp. (B04-14)				2		2					1				3	3	
Grammatophora sp. (S8-43)																	
Gyrosigma spp.	1			1				1			1						1
Hannea arcus	1			3	1	1											
Hyalodiscus scoticus		3	1		1			1						1			
Licomorpha sp.												2					
Luticola mutica					1	2							1	1			
Mastogloia exigua											2						
Melosira nummuloides	1	2	3	11	2	2	4	7	5	3			1	2	1	4	1

APPENDIX H1 (continued)

Sample	S8-18	S8-19	S8-20	S8-21	S8-22	S8-23	S8-24	S8-25	S8-26	S8-27	S8-28	S8-29	S8-30	S8-31	S8-32	S8-33	S8-34
Melosira spp.	1		3	4	1				2	1		1	3	2	1		
Minidiscus chilensis	1	11	9	4	9	2	1	6	12	8	2	5	16	4	3	5	5
Navicula cryptocephala						1											
N. directa		1		1	1				2			1		3	2	1	
N. gregaria			2		1	1		2	6	3		1	2	4	3	1	1
N. perminuta		10	9	8	5	3	4	7	11	2	6	9	6	7	6	4	3
N. phylleptosoma		2	2				1	1	2			1		1	3		
Navicula cf. *ramosissima*														1	4		
Navicula sp. (3C-1)	2	14	6	2	2	6			3	3	4	3	2	3	2	1	2
Navicula sp. (S8-4)																	
Navicula sp. (S8-8)																	
Navicula sp. (S8-33)																2	
Navicula sp. (S8-48)																	
Nitzschia coarctata			1			1								3			
N. dissipata		1	1			1											
N. fonticola		1				2	2		3		2		5	1			1
N. frustulum	4	24	36	37	20	17	8	12	22	16	23	19	38	19	26	11	13
N. inconspicua				2							1						2
N. microcephala												1					
N. perminuta									1								
Nitzschia cf. *sicula* (B04-12)												1					
N. valdestriata					2							1	1				3
Nitzschia sp. (S8-1)																	
Nitzschia sp. (S8-17)																	
Nitzschia sp. (S8-34)																	1
Odontella aurita																	
O. longicruris			1	1	5	3		2	4	1	1				5	1	3
Opephora horstiana			2	2	4			2		1	1					1	
O. marina																	1
O. minuta			1	2													
O. mutabilis				4	3	1				10		3		8	7	2	4
O. pacifica				1					1				1		1		
Paralia sulcata		4		4	4	1	1	3	1	4	4	1	10	1	6	1	1
Pinnularia cf. *quadraterea*				1													
Plagiogramma staurophorum																	4
Planothidium delicatulum	4	22	12	32	18	10	3	20	22	3	17	17	15	8	7	2	7
P. engelbretchtii																	
P. hauckiana		4	2	3	6	2		4	8		1	1	2		1		
Pleurosigma spp.		1				1		1			1					1	
Protokeelia cholnokyana																	
Pseudonitzschia multiseries	1		5	8	2	2	4	5	1			4	1	4	2	3	
P. seriata	3						1			3		1	1		1	17	
Reimeria spp.																	
Rhizolenia spp. (spines)																1	
Rhoicosphenia curvata																	4
Rhopalodia pacifica											2					2	
Seminavis spp.									2						1		
Skeletonema costatum	76	50	33	45	53	86	48	28	45	69	41	28	53	94	14	57	54
S. costatum (weak)	339	111	104	66	31	96	329	132	77	199	53	40	90	89	196	204	94
Stephanodiscus spp.			1														
Stephanopyxis turris													1				
Surirella brebissonii						1		1					1				
Synedra ulna																	
Tabellaria flocculosa						3							1			3	
Tabularia fasciculata		3	2	10	9	6		3	3	1	4	3	5	4			4
Thalassionema cf. *bacillare*		2		5	7			1	2			1	2		2	1	1
T. nitzschioides	1	12	47	26	17	13	8	24	25	1	30	12	16	11	5	20	20
T. pseudonitzschioides	1	7	3	6	10	14	2	7	7	4	14	21	4	3	10	1	10
Thalassiosira aestivalis		5			1							1					
T. angulata						2			1			4	1			1	

APPENDIX H1 (continued)

Sample	S8-18	S8-19	S8-20	S8-21	S8-22	S8-23	S8-24	S8-25	S8-26	S8-27	S8-28	S8-29	S8-30	S8-31	S8-32	S8-33	S8-34
Thalassiosira binata		1		1	2		3	1	5	47	9			1	4		5
T. bioculata var. *exigua*																	1
T. conferta		6	6	5	6		4	1	1	8					3		
T. decipiens	16	12	30	10	10	8	5	4	11	6	5	48	29	28	4	3	10
T. decipiens (large)	1	4	2		4	1	1		4			12	4	4		1	1
T. eccentrica	1	1	4	1	13	13	1	5	2	8	3	2	5	6	1	1	4
T. eccentrica (large)													2				
Thalassiosira cf. *eccentrica*						23	2	2	1				3				4
T. gravida	1	1			1												
T. hendeyi					1												
T. hyalina					2												
T. kushirensis	1								3				1			1	
Thalassiosira cf. *leptopus*	1	1	3	3	12	23	6	45	4		2	1	7			1	3
T. lundiana																	
T. minima														1			
T. nodulineata													1				
T. nordenskioeldii	11	9	9	44	81	20	10	77	48	4	8	5	5	29	5		9
T. oceanica													3				
T. oestrupii		1	3	3		1			3		1			2			3
T. pacifica	6	38	10	4	7	2	11	1	2	2	5	102	16	18	8	53	10
T. poroseriata					1	1											
T. punctigera																	
T. rotula								1	6	2			1	4	1		
T. tealata			1	1	2					2					1		
T. tenera					1	4					3		3	5	9	10	31
Thalassiosira cf. *tenera*				1	3	1		1		1		2	1				1
Thalassiosira sp. (B04-40)												3					
Thalassiosira sp. (S8-12)			3			1			1							1	
Thalassiosira sp. (S8-27)										38	2			3			2
Thalassiosira sp. (S8-31)														1			
Thalassiosira sp. (S8-35)																	
Thalassiothrix longissima																	
Trachyneis aspera																	2
Tryblionella cf. *aerophila*		3		2	1												2
Tryblionella sp. (S8-1)																	
Unknown centric 1 (B04-7)																	
Unknown centric (B04-21)			1		1		1		1								
Unknown centric (S8-4)																	
Unknown peanate (S8-7)																	
Unknown pennate 2 (S8-8)																	
Unknown pennate (S8-32)															1		
Unknown pennate (S8-36)																	
Unknown centric (S8-39)																	
Unknown pennate 1 (S8-41)																	
Unknown pennate 2 (S8-41)																	
Unknown pennate (S8-50)																	
Unknown pennate (S8-52)																	
TOTAL	511	505	511	503	502	511	509	504	508	511	505	508	500	501	503	506	504
CHAETOCEROS																	
Chaetoceros spp.	50	75	67	114	199	63	147	89	206	275	142	373	783	37	95	383	110
Leptocylindrus spp.		1			1	3			4	1	1	2	2		2	8	1
Stephanopyxis spp.					1												
TOTAL	50	76	67	114	201	66	147	89	210	276	143	375	785	37	97	391	111
SILICOFLAGELLATES																	
Dictyocha fibula																	1
D. speculum		3	2	1	1	4		1	6	4	3	6	4	2	1	2	9
Octactis sp.		2				1			7		1	9	1				7
TOTAL	0	5	2	1	1	5	0	1	13	4	4	15	5	2	1	2	17

APPENDIX H1 (continued)

Sample	S8-35	S8-36	S8-37	S8-38	S8-39	S8-40	S8-41	S8-42	S8-43	S8-44	S8-45	S8-46	S8-47	S8-48	S8-49	S8-50	S8-51
DIATOMS																	
A. brevipes	3											2					
A. groenlandica																	
A. kregeri	3					1		2	2			3	1	1			1
A. lanceolata																	
A. lemmermanii	1	2		2											1		
A. minutissima	3	6	10	21	6	9	6	36	20	12		1	4	4	9	3	21
A. nedosa																	
A. vistulana																	
Achnanthidium biasolettianum	3			1	1				1	2		1			3		
Actinocyclus curvatulus			1	1	1				2	5				1			
A. octonarius			1			2	1		4	2					1		
Actinoptychus senarius	3		1	1	2			1			1						
A. vulgaris			2	8	12	30	11	3			1	2					
Amphora acutiuscula			2				4	4	2	1					1		1
A. coffaeformis			2				1			1	1				1		
A. copulata				2		3	2	1	1	2			1		4		1
A. exigua	1			2					2						1		
Amphora cf. *helensis*	3		2				4	1									2
A. maletractata var. *constricta*				2	2												
A. marina								1									
Amphora sp. (S8-21)																	
Asteromphalus heptacis				1			1		1	1		1			1		1
A. sarcophagus						1				2				1	3		2
Aulacoseira cf. *ambigua*							4										
A. italica var. *subarctica*																	
Azepeitia spp.		1															
Bacillaria paxillifer	1		2		2	1		3	4	1				1	1		1
Bacteriastrum delicatulum	1		1	2	1	1		1	1		2	1		3	4	1	1
Berkeleya rutilans			2			1	3					1			1	1	
Brachysira spp.					1	1								1			1
Caloneis sp. (S8-9)																	
Cocconeis britannica								1									
C. californica																	
C. costata complex	1		1		2	7	4	2	1	2	1			2			1
Cocconeis cf. *dirupta*																	
C. disculus	2	1			2	2	3	4	2	2	1	1	1	2	2		
C. distans							1				1			1			
Cocconeis cf. *molesta*															1		1
C. neothumensis			1		1			1		1		1		1	1		
C. pellucida				1										1			
C. peltoides			1	1		1							1				
C. pinnata					1										1		
C. placentula	1			1	1	4		1				1	1				1
C. scutellum	3		1	3	2	1		1	2	3							
C. stauroneiformis	1				2	2		2	1								
Cocconeis sp. (S8-32)																	
Coscinodiscus diorama						3											
C. radiatus							1				2						
Ctenophora pulchella	1			5	3	3	1				1						
C. choctawhatcheeana	14	6	21	15	26	34	21	29	12	14	3	1	4	7	3		2
C. pseudostelligera																	
Cyclotella rossii																	
C. stelligera				1	1			1		3			1				
C. striata	2		3		1	2	2		2								
C. stylorum	1				1			1			1						
Cyclotella sp. (B04-15/16)	2						2									1	
Cyclotella sp. (S8-6)		3	4	4	2	5	4	2	5	2		1		3	4		2
Cyclotella sp. (S8-19)																	
Cyclotella sp. (S8-25)																	

APPENDIX H1 (continued)

Sample	S8-35	S8-36	S8-37	S8-38	S8-39	S8-40	S8-41	S8-42	S8-43	S8-44	S8-45	S8-46	S8-47	S8-48	S8-49	S8-50	S8-51
Cyclotella sp. (S8-35)	3																
Cymbella cymbiformis		2					1										
C. lanceolata				1													
C. minuta																	
Cymbella sp. (S8-12)																	
Cymbella sp. (S8-32)			1							1							
Delphineis spp.								1									
Denticula spp.																	
Diatoma mesodon					1		1										
Diatoma cf. *tenue*																	
Diatomella minuta							6	4	3	2		2		1			
Dimeragramma sp. (11C-6)				1													
Dimeragramma sp. (S8-5)			1														
Diploneis cf. *bomboides*																1	
D. bombus										1		1			2		
Diploneis cf. *sejuncta*																	
D. smithii									1								
D. smithii var. *recta*																	
Diploneis spp.							1										
Ditylum brightwellii	5	4	5	1	4	4	23	4	2	1					2		11
Eucampia spp.																	
Eunotia spp.	1		1		1			1	1						1	3	2
Fallacia spp.	1			1					1	4							
Fallacia sp. (B04-29)						1									1		
Fallacia sp. (S8-2)																	
Fragilaria capucina complex		2				1			4	4							
F. construens var. *construens*																	
F. investiens	1	1	2		1	1		11	1					2	1	1	3
F. pinnata								7	6				1				
F. sopotensis	1	1	3	7	5	10	2	3	3		1		2	2	2		1
Fragilaria sp. (S8-13)																	
Fragilariopsis atlantica				1	2	21	1							1			
F. cylindriformis	4	7	11	4	6	9	16	3	9	6	4	2	2	5	4	4	6
F. pseudonana	84	24	38	63	47	45	95	66	74	15	10	9	11	12	74	48	52
F. schulzii								1									
Fragilariopsis sp. (3A-7)																	
Fragilariopsis sp. (S8-10)																	
Frustulia rhomboides																	
Gomphonema angustum					1					1							
G. angustatum							2		1								
G. olivaceum					1												
Gomphonema sp.						2		2		2							
Gomphonema sp. (S8-3)																	
Gomphonema sp. (S8-31)																	
Gomphonema sp. (S8-32)																	
Gomphonemensis exigua				2	1			2	5		1						
G. lindae	3		1	1	5	2	3	2		1		1			3	1	
G. obscurum	1			2	6	1	6		5	1				2			
Grammatophora angulosa							2							1			
G. marina				2		2							1				
G. oceanica	1				2		2										
Grammatophora sp. (B04-14)								2						2			3
Grammatophora sp. (S8-43)									1								
Gyrosigma spp.							1		1								
Hannea arcus	1				1			1		1	3	1					
Hyalodiscus scoticus					1	1		1	1		1						1
Licomorpha sp.																	
Luticola mutica							1						1				
Mastogloia exigua			1				3										
Melosira nummuloides			1	4	1	6		3	1	2	1			1	4		1

APPENDIX H1 (continued)

Sample	S8-35	S8-36	S8-37	S8-38	S8-39	S8-40	S8-41	S8-42	S8-43	S8-44	S8-45	S8-46	S8-47	S8-48	S8-49	S8-50	S8-51
Melosira spp.	1			1	4		1		1	1							2
Minidiscus chilensis	1	1	5	3	5	2	5	9	4			4	1	4	5		
Navicula cryptocephala					2												
N. directa					1		1	1									
N. gregaria	3				3	1	3	10	2		2	1	3	1	1		1
N. perminuta	1	2	3	6	4	11	16	10	4	8	4	2	3	2	7	5	4
N. phylleptosoma	1				2		1	1						1		2	
Navicula cf. *ramosissima*					1	1											
Navicula sp. (3C-1)	2			1	6	9	9	6	4	8	4	1		2	7	3	2
Navicula sp. (S8-4)																	
Navicula sp. (S8-8)																	
Navicula sp. (S8-33)																	
Navicula sp. (S8-48)														1			
Nitzschia coarctata						1		2	1	1					1		
N. dissipata														2			
N. fonticola			2	2				2	3	2					2	1	4
N. frustulum	9	15	6	24	11	30	30	25	16	13	7	6	12	21	22	13	26
N. inconspicua			1		2	1	2	1				2				2	2
N. microcephala																	
N. perminuta																	
Nitzschia cf. *sicula* (B04-12)																	
N. valdestriata			1					1		1							
Nitzschia sp. (S8-1)																	
Nitzschia sp. (S8-17)																	
Nitzschia sp. (S8-34)																	
Odontella aurita							2										
O. longicruris		2	2					2	6		1			1			
Opephora horstiana						1			1		1	1			1		
O. marina																	
O. minuta				2													
O. mutabilis				3		4	14	1			2		1	8		2	
O. pacifica					1			1				4				4	
Paralia sulcata	1			4	11	1	9	8	3	5	1	1		1			7
Pinnularia cf. *quadraterea*																	
Plagiogramma staurophorum				1					1		2		1	2	2		
Planothidium delicatulum	7		8	11	10	17	15	20	11	12	5	3	3	4	6	8	8
P. engelbretchtii																	
P. haukiana					3			1	1								1
Pleurosigma spp.	1		1								1						
Protokeelia cholnokyana																	
Pseudonitzschia multiseries	2		3	2		2	2	1	2		2	4	2	9			2
P. seriata		1	8			1	1		2				1	6			
Reimeria spp.						1											
Rhizolenia spp. (spines)																	
Rhoicosphenia curvata		4							4								
Rhopalodia pacifica																	
Seminavis spp.		1					1							2			1
Skeletonema costatum	70	153	127	104	33	11	17	23	37	35	78	35	34	33	45	51	37
S. costatum (weak)	57	195	112	47	44	52	55	49	53	173	217	334	219	293	179	302	210
Stephanodiscus spp.										2							1
Stephanopyxis turris		1														1	
Surirella brebissonii									1	1		1					
Synedra ulna						2											
Tabellaria flocculosa																	
Tabularia fasciculata		2	4	3	2	11	3	5	2	4			1	2	2		
Thalassionema cf. *bacillare*		1							1			1			1	1	
T. nitzschioides	44	39	26	21	78	15	25	20	30	49	56	20	4	4	27	5	32
T. pseudonitzschioides	29	1	6	3	10	5	3	4	15			1			2		2
Thalassiosira aestivalis																	
T. angulata					1				4		4		1		1		

APPENDIX H1 (continued)

Sample	S8-35	S8-36	S8-37	S8-38	S8-39	S8-40	S8-41	S8-42	S8-43	S8-44	S8-45	S8-46	S8-47	S8-48	S8-49	S8-50	S8-51
Thalassiosira binata				2	2			2									
T. bioculata var. *exigua*																	
T. conferta			1			1	2	1	1			1		2			2
T. decipiens	11	9	22	48	30	15	9	15	14	46	30	16	92	9	14	10	8
T. decipiens (large)	4		6	7	7	4	2		3	7	6	2	3		2		1
T. eccentrica	2	1	5	2	2	10	7	11	29	3	4	5	2	4	1	1	1
T. eccentrica (large)										1							
Thalassiosira cf. *eccentrica*	4			5	12	3		5	7								
T. gravida			2	2	11	1				1		1					
T. hendeyi																	
T. hyalina																	
T. kushirensis	2	1		2		1	2			2	4	3			1		
Thalassiosira cf. *leptopus*	5	1	2	7	12	4	6	17	41		1				2		2
T. lundiana						5											
T. minima			1		6						5	1			1		
T. nodulineata																	
T. nordenskioeldii	30	11	26	11	8	15	5	18	2	13	3	3	25	12	7	9	10
T. oceanica														4			
T. oestrupii	3			2		1	5			1					1		1
T. pacifica	20	1	5	15	17	24	3	6	13	12	17	24	58	6	5	11	12
T. poroseriata						1							1		1		
T. punctigera																	
T. rotula	1														1		2
T. tealata								1	1					1			1
T. tenera	39	2		5	1	9	2	5	2	1	3				1	1	
Thalassiosira cf. *tenera*				1		5	1	2									
Thalassiosira sp. (B04-40)																	
Thalassiosira sp. (S8-12)																	
Thalassiosira sp. (S8-27)			1	1											16	1	
Thalassiosira sp. (S8-31)																	
Thalassiosira sp. (S8-35)	10			1	1		1		1		2		1	3		2	
Thalassiothrix longissima						2	1				1			1			
Trachyneis aspera						2		1									
Tryblionella cf. *aerophila*									1		2			1			
Tryblionella sp. (S8-1)																	
Unknown centric 1 (B04-7)																	
Unknown centric (B04-21)					1										1		1
Unknown centric (S8-4)																	
Unknown pennate (S8-7)																	
Unknown pennate 2 (S8-8)																	
Unknown pennate (S8-32)																	
Unknown pennate (S8-36)				1													
Unknown centric (S8-39)					1												
Unknown pennate 1 (S8-41)							1										
Unknown pennate 2 (S8-41)							1										
Unknown pennate (S8-50)																1	
Unknown pennate (S8-52)																	
TOTAL	516	504	509	514	504	502	505	499	509	500	501	510	500	500	502	500	502
CHAETOCEROS																	
Chaetoceros spp.	165	70	108	126	159	156	78	180	217	281	138	56	47	88	136	43	168
Leptocylindrus spp.	11	4	7			4	6	1	2	6	4	4	1	1	3		3
Stephanopyxis spp.																	
TOTAL	176	74	115	126	159	160	84	181	219	287	142	60	48	89	139	43	171
SILICOFLAGELLATES																	
Dictyocha fibula																	
D. speculum	8	1	3	5	14	11	12	5	10	9	3	3	1	4	5	1	1
Octactis sp.	2			4		1							1	1			
TOTAL	10	1	3	9	14	12	12	5	10	9	3	3	2	5	5	1	1

APPENDIX H1 (continued)

Sample	S8-52	S8-53	S8-54	S8-55	S8-56	S8-57	S8-58	S8-59	S8-60	S8-61	S8-62	S8-63	S8-64	S8-65	S8-66	S8-67
DIATOMS																
A. brevipes		2						1								
A. groenlandica																
A. kregeri	1	3											2	2		
A. lanceolata	3															
A. lemnermanii			12		2											
A. minutissima	12	9		5	10	4		4			9	3	1	7	11	5
A. nedosa					1											
A. vistulana																
Achnanthidium biasolettianum	5				2	3				1		1			1	1
Actinocyclus curvatulus	1															
A. octonarius							1							1	1	
Actinoptychus senarius	1	1				1					1		1			
A. vulgaris			1	1		1						1	2		1	
Amphora acutiuscula	1			1		5		3			1			3		
A. coffaeformis				1				1								
A. copulata	1	6	1	3	2		1							1	1	
A. exigua			1													
Amphora cf. *helensis*																
A. maletractata var. *constricta*														3		
A. marina	1															
Amphora sp. (S8-21)																
Asteromphalus heptactis	1	1	1			1		1	1		4		1	2		1
A. sarcophagus	1	1	1		1											
Aulacoseira cf. *ambigua*																
A. italica var. *subarctica*																
Azpeitia spp.	3	1	1				1									
Bacillaria paxillifer	2	1	1										1			
Bacteriastrum delicatulum	4	2	7	4	1	4	1	13	3	2	4	2	1	4	3	2
Berkeleya rutilans	1	3			1									1		
Brachysira spp.																2
Caloneis sp. (S8-9)																
Cocconeis britannica																
C. californica																
C. costata complex	3		2					3	1		1	2		1	1	1
Coccomeis cf. *dirupta*																
C. disculus		1				1		1								
C. distans														1		
Coccomeis cf. *molesta*																1
C. neothumensis	1		1		1				1		1			1	1	4
C. pellucida																
C. peltoides	2												2	1		
C. pinnata						2										
C. placentula	1	1				2										
C. scutellum	2		1	1						2	1				2	
C. stauroneiformis				1					1							
Cocconeis sp. (S8-32)																
Coscinodiscus diorama																
C. radiatus																
Ctenophora pulchella	1															
C. choctawhatcheeana	5		2	6	1	2		1	1		1				5	10
C. pseudostelligera																
Cyclotella rossii																
C. stelligera	1													1		
C. striata			1				1				2				1	1
C. stylorum																
Cyclotella sp. (B04-15/16)			2										1			
Cyclotella sp. (S8-6)													1	4		
Cyclotella sp. (S8-19)																
Cyclotella sp. (S8-25)																

APPENDIX H1 (continued)

Sample	S8-52	S8-53	S8-54	S8-55	S8-56	S8-57	S8-58	S8-59	S8-60	S8-61	S8-62	S8-63	S8-64	S8-65	S8-66	S8-67
Cyclotella sp. (S8-35)																
Cymbella cymbiformis	1												1		1	
C. lanceolata																
C. minuta																
Cymbella sp. (S8-12)																
Cymbella sp. (S8-32)																
Delphineis spp.																
Denticula spp.							2									
Diatoma mesodon						1										
Diatoma cf. *tenue*																
Diatomella minuta	3	1		2												
Dimeragramma sp. (11C-6)								1		1			1			
Dimeragramma sp. (S8-5)																
Diploneis cf. *bomboides*																
D. bombus										1						
Diploneis cf. *sejuncta*																
D. smithii																
D. smithii var. *recta*																
Diploneis spp.																
Ditylum brightwellii	9	1	2	1	1	2	4	8	1		1	5	3	2	1	5
Eucampia spp.																
Eunotia spp.	1					1					3					
Fallacia spp.				2						4				1		
Fallacia sp. (B04-29)			2													
Fallacia sp. (S8-2)																
Fragilaria capucina complex			2													
F. construens var. *construens*																
F. investiens			1	1	1											
F. pinnata			2			1		1								
F. sopotensis	4			5	3			5					1			1
Fragilaria sp. (S8-13)																
Fragilariopsis atlantica											2					
F. cylindriformis	13	139	107	4	6	12	3	2			5	1		2		1
F. pseudonana	33	47	29	38	52	10	3	12	5	3	12	7	10	10	10	13
F. schulzii				3												
Fragilariopsis sp. (3A-7)	3							1								
Fragilariopsis sp. (S8-10)																
Frustulia rhomboides																
Gomphonema angustum	1		2	2									6			1
G. angustatum																
G. olivaceum				1								2				
Gomphonema sp.						2										
Gomphonema sp. (S8-3)																
Gomphonema sp. (S8-31)																
Gomphonema sp. (S8-32)																
Gomphonemensis exigua						1					2					
G. lindae	4			2							6					
G. obscurum	1	3		3	2	4								4	1	2
Grammatophora angulosa																
G. marina																
G. oceanica	2										2					
Grammatophora sp. (B04-14)												2				
Grammatophora sp. (S8-43)																
Gyrosigma spp.		1														
Hannea arcus												1			1	
Hyalodiscus scoticus										1						
Licomorpha sp.										1						
Luticola mutica	1		1					2								
Mastogloia exigua																
Melosira nummuloides	4		2	3		2						1		5	4	2

APPENDIX H1 (continued)

Sample	S8-52	S8-53	S8-54	S8-55	S8-56	S8-57	S8-58	S8-59	S8-60	S8-61	S8-62	S8-63	S8-64	S8-65	S8-66	S8-67
Melosira spp.	4	1	2	1									1			
Minidiscus chilensis	2	1	1	1	1			7			1		2	1		1
Navicula cryptocephala																
N. directa												1				
N. gregaria	5	1	1		3		1		2	1	1	4		2		
N. perminuta	7		4	3	4	2	3	5	3	1		1	4	9	1	6
N. phylleptosoma	1				2	1						1		1		
Navicula cf. *ramosissima*																
Navicula sp. (3C-1)	9		8	7	6			7	1	5	3	3	1	4	1	1
Navicula sp. (S8-4)																
Navicula sp. (S8-8)																
Navicula sp. (S8-33)																
Navicula sp. (S8-48)																
Nitzschia coarctata		1														
N. dissipata																
N. fonticola				2					2			2	2			
N. frustulum	30	6	10	11	8	4	6	16	1	5	6	2	3	13	4	4
N. inconspicua	2	2					1		1		1					1
N. microcephala																
N. perminuta																
Nitzschia cf. *sicula* (B04-12)																
N. valdestriata		1												1	1	
Nitzschia sp. (S8-1)																
Nitzschia sp. (S8-17)																
Nitzschia sp. (S8-34)																
Odontella aurita														1		
O. longicruris	2			1							1			2		1
Opephora horstiana	2							2								
O. marina																
O. minuta																
O. mutabilis	4			2		4		1				2		3	1	
O. pacifica	2						1	5						2		
Paralia sulcata	6				1		8				1			1		2
Pinnularia cf. *quadraterea*																
Plagiogramma staurophorum			2								1			2		
Planothidium delicatulum	23	11	8	4	1	4		10	2	1	2	5	2	7	7	6
P. engelbretchtii						1										
P. haukiana	2				2									1		1
Pleurosigma spp.				1					1						1	
Protokeelia cholnokyana																
Pseudonitzschia multiseries	4	1	16	3		2		14	4		12	9	8	4	2	5
P. seriata	2			1			1	7			2			2	4	5
Reimeria spp.																
Rhizolenia spp. (spines)																
Rhoicosphenia curvata				2												
Rhopalodia pacifica																
Seminavis spp.					2									1		
Skeletonema costatum	43	6	11	113	30	240	37	28	27	19	100	52	64	92	62	60
S. costatum (weak)	67	41	81	175	273	76	384	196	407	410	240	357	346	217	333	295
Stephanodiscus spp.														1		
Stephanopyxis turris																
Surirella brebissonii		1												1		
Synedra ulna																
Tabellaria flocculosa																
Tabularia fasciculata	1	2	2		1			1	1		1	1		1	6	
Thalassionema cf. *bacillare*	1					1	2	1			1	2	1			5
T. nitzschioides	44	8	61	19	10	19	5	5			5	3	9	8	14	4
T. pseudonitzschioides	14	2	15	10	6	7	5	3	11	1	3		2	2	1	5
Thalassiosira aestivalis																
T. angulata	2	2			2	3		4		1	1	1		1	2	1

APPENDIX H1 (continued)

Sample	S8-52	S8-53	S8-54	S8-55	S8-56	S8-57	S8-58	S8-59	S8-60	S8-61	S8-62	S8-63	S8-64	S8-65	S8-66	S8-67
Thalassiosira binata							2			3	1	1				
T. bioculata var. *exigua*				1		1			1							
T. conferta	1	1		1		1			4		1		8	1	2	2
T. decipiens	17	38	41	16	21	19	8	59	5	8	9		1	5	5	2
T. decipiens (large)	3	2	2	3	2			4	3	1	1			2	1	
T. eccentrica	6	1	3	5	2			2	1	3	3	4	2	2		
T. eccentrica (large)				2							1					
Thalassiosira cf. *eccentrica*		2	6													
T. gravida																
T. hendeyi																
T. hyalina																
T. kushirensis	1	1	2			1	1	5		1	2	1	1			4
Thalassiosira cf. *leptopus*	3	1	4								3			1	1	1
T. lundiana																
T. minima	3							1								
T. nodulineata																
T. nordenskioeldii	22	120	22	21	15	5	18	19	10	20	25	18	3	28	12	37
T. oceanica																
T. oestrupii	3				1						2	1		3	2	
T. pacifica	23	27	14	2	18	42	5	36	2	3	10	8	2	24	6	1
T. poroseriata										1	1					
T. punctigera														1		
T. rotula					1	1	6				2	8	1		2	
T. tealata					1									2		
T. tenera				1		1						1			3	1
Thalassiosira cf. *tenera*	2									1						
Thalassiosira sp. (B04-40)																
Thalassiosira sp. (S8-12)																
Thalassiosira sp. (S8-27)	3			1		1							5			1
Thalassiosira sp. (S8-31)																
Thalassiosira sp. (S8-35)				1				2								1
Thalassiothrix longissima																
Trachyneis aspera																
Tryblionella cf. *aerophila*	2					2									2	
Tryblionella sp. (S8-1)																
Unknown centric 1 (B04-7)																
Unknown centric (B04-21)				1		2										
Unknown centric (S8-4)																
Unknown pennate (S8-7)																
Unknown pennate 2 (S8-8)																
Unknown pennate (S8-32)																
Unknown pennate (S8-36)																
Unknown centric (S8-39)																
Unknown pennate 1 (S8-41)																
Unknown pennate 2 (S8-41)																
Unknown pennate (S8-50)																
Unknown pennate (S8-52)	1															
TOTAL	503	504	501	501	500	502	511	500	503	501	501	516	503	506	522	506
CHAETOCEROS																
Chaetoceros spp.	485	51	199	180	438	122	78	159	91	119	173	145	75	111	135	93
Leptocylindrus spp.	7	9	2			1					4	5	9	1	1	3
Stephanopyxis spp.																
TOTAL	492	60	201	180	438	123	78	159	91	119	177	150	84	112	136	96
SILICOFLAGELLATES																
Dictyocha fibula	4								1				1			
D. speculum		8	5		3	3	2	1	1		8		1	8	3	8
Octactis sp.		1									1	2		1	2	
TOTAL	4	9	5	0	3	3	2	1	2	0	9	2	2	9	5	8

APPENDIX H2. Sediment slab microfossil absolute abundance (concentration)

$$C_a = \frac{Nadv_s}{fAwv_p}$$

N = number of valves or skeletons counted
a = area of cover slip (18 × 18 mm = 324000000 μm^2)
d = dilution factor
v_s = initial volume of slurry (mL)
f = number of fields of view examined
A = area of field of view (radius at 1000 × is 105 μm = 34636.14 μm^2)
w = initial sediment mass (g)
v_p = volume of slurry plated onto cover slip (mL)

Sample	Top interval (cm)	Bottom interval (cm)	Initial mass (g)	Initial slurry volume (mL)	Dilution Factor	Volume plated (mL)	Diatom count (valves)	CRS count (valves)	Silico. count (skeletons)	Fields of view examined	Diatom Concentration (× 10^6 valves/g)	CRS Concentration (× 10^6 valves/g)	Silicoflagellate Concentration (× 10^6 skel/g)
			w	v_s	d	v_p	N	N	N	f			
S8-1	870.00	870.20	0.0403	20	5	0.5	503	60	12	85	274.72	32.77	6.55
S8-2	870.20	870.60	0.0406	20	5	0.5	503	120	5	86	269.52	64.30	2.68
S8-3	870.60	870.80	0.0401	20	5	0.5	501	100	5	68	343.74	68.61	3.43
S8-4	870.80	871.05	0.0403	20	5	0.5	513	101	1	49	486.03	95.69	0.95
S8-5	871.05	871.20	0.0401	20	5	0.5	504	94	5	45	522.54	97.46	5.18
S8-6	871.20	871.35	0.0401	20	5	0.5	511	120	3	64	372.51	87.48	2.19
S8-7	871.35	871.60	0.0401	20	5	0.5	510	140	1	76	313.08	85.94	0.61
S8-8	871.60	871.75	0.0401	20	5	0.5	506	399	2	78	302.66	238.66	1.20
S8-9	871.75	871.90	0.0409	20	5	0.5	512	63	1	45	520.45	64.04	1.02
S8-10	871.90	872.05	0.0404	20	5	0.5	504	87	5	69	338.26	58.39	3.36
S8-11	872.05	872.65	0.0409	20	5	0.5	507	155	3	56	414.14	126.61	2.45
S8-12	872.65	872.75	0.0407	20	5	0.5	504	216	3	107	216.52	92.79	1.29
S8-13	872.75	872.90	0.0406	20	5	0.5	507	138	5	81	288.43	78.51	2.84
S8-14	872.90	873.01	0.0403	20	5	0.5	504	219	3	82	285.34	123.99	1.70
S8-15	873.01	873.15	0.0408	20	5	0.5	503	196	7	65	354.85	138.27	4.94
S8-16	873.15	873.30	0.0410	20	5	0.5	508	124	6	95	244.01	59.56	2.88
S8-17	873.30	873.46	0.0406	20	5	0.5	501	142	4	73	316.25	89.64	2.52
S8-18	873.46	873.70	0.0408	20	5	0.5	511	50	0	22	1065.08	104.22	0.00
S8-19	873.70	873.80	0.0402	20	5	0.5	505	75	5	93	252.71	37.53	2.50
S8-20	873.80	873.95	0.0405	20	5	0.5	511	67	2	66	357.66	46.89	1.40
S8-21	873.95	874.05	0.0403	20	5	0.5	503	114	1	78	299.37	67.85	0.60
S8-22	874.05	874.20	0.0405	20	5	0.5	502	199	1	75	309.20	122.57	0.62
S8-23	874.20	874.35	0.0413	20	5	0.5	511	63	5	49	472.41	58.24	4.62
S8-24	874.35	874.50	0.0405	20	5	0.5	509	147	0	32	734.78	212.21	0.00
S8-25	874.50	874.65	0.0410	20	5	0.5	504	89	1	64	359.35	63.46	0.71
S8-26	874.65	874.74	0.0400	20	5	0.5	508	206	13	96	247.50	100.36	6.33
S8-27	874.74	874.90	0.0405	20	5	0.5	511	275	4	52	453.95	244.30	3.55
S8-28	874.90	875.02	0.0400	20	5	0.5	505	142	4	58	407.24	114.51	3.23
S8-29	875.02	875.23	0.0400	20	5	0.5	508	373	15	81	293.34	215.38	8.66
S8-30	875.23	875.35	0.0402	20	5	0.5	500	783	5	103	225.92	353.79	2.26

APPENDIX H2 (continued)

Sample	Top interval (cm)	Bottom interval (cm)	Initial mass (g)	Initial slurry volume (mL)	Dilution Factor	Volume plated (mL)	Diatom count (valves)	CRS count (valves)	Silico. count (skeletons)	Fields of view examined	Diatom Concentration ($\times 10^6$ valves/g)	CRS Concentration ($\times 10^6$ valves/g)	Silicoflagellate Concentration ($\times 10^6$ skel./g)
			w	v_s	d	v_p	N	N	N	f			
S8-31	875.35	875.50	0.0398	20	5	0.5	501	37	2	85	277.06	20.46	1.11
S8-32	875.50	875.65	0.0404	20	5	0.5	503	95	1	103	226.15	42.71	0.45
S8-33	875.65	875.90	0.0401	20	5	0.5	506	383	2	37	638.04	482.95	2.52
S8-34	875.90	876.01	0.0399	20	5	0.5	504	110	17	76	310.95	67.87	10.49
S8-35	876.01	876.27	0.0405	20	5	0.5	516	165	10	52	458.39	146.58	8.88
S8-36	876.27	876.49	0.0401	20	5	0.5	504	70	1	19	1237.59	171.89	2.46
S8-37	876.49	876.65	0.0403	20	5	0.5	509	108	3	50	472.59	100.28	2.79
S8-38	876.65	877.25	0.0408	20	5	0.5	514	126	9	82	287.43	70.46	5.03
S8-39	877.25	877.76	0.0402	20	5	0.5	504	159	14	82	286.05	90.24	7.95
S8-40	877.76	877.97	0.0406	20	5	0.5	502	156	12	91	254.20	79.00	6.08
S8-41	877.97	878.25	0.0402	20	5	0.5	505	78	12	74	317.60	49.05	7.55
S8-42	878.25	878.41	0.0402	20	5	0.5	499	180	5	95	244.45	88.18	2.45
S8-43	878.41	878.50	0.0403	20	5	0.5	509	217	10	75	315.06	134.32	6.19
S8-44	878.50	878.65	0.0406	20	5	0.5	500	281	9	57	404.22	227.17	7.28
S8-45	878.65	878.90	0.0403	20	5	0.5	501	138	3	34	684.07	188.43	4.10
S8-46	878.90	879.10	0.0406	20	5	0.5	510	56	3	32	734.41	80.64	4.32
S8-47	879.10	879.40	0.0399	20	5	0.5	500	47	2	32	732.64	68.87	2.93
S8-48	879.40	879.55	0.0397	20	5	0.5	500	88	5	52	453.13	79.75	4.53
S8-49	879.55	879.75	0.0399	20	5	0.5	502	136	5	59	398.96	108.08	3.97
S8-50	879.75	879.90	0.0403	20	5	0.5	500	43	1	29	800.41	68.84	1.60
S8-51	879.90	880.15	0.0400	20	5	0.5	502	168	1	62	378.70	126.74	0.75
S8-52	880.15	880.30	0.0404	20	5	0.5	503	485	4	90	258.82	249.55	2.06
S8-53	880.30	880.50	0.0412	20	5	0.5	504	51	9	33	693.53	70.18	12.38
S8-54	880.50	880.74	0.0400	20	5	0.5	501	199	5	51	459.47	182.50	4.59
S8-55	880.74	880.95	0.0402	20	5	0.5	501	180	0	54	431.78	155.13	0.00
S8-56	880.95	881.37	0.0402	20	5	0.5	500	438	3	50	465.39	407.68	2.79
S8-57	881.37	881.65	0.0403	20	5	0.5	502	122	3	40	582.62	141.59	3.48
S8-58	881.65	882.00	0.0403	20	1.5	0.5	511	78	2	32	222.40	33.95	0.87
S8-59	882.00	882.20	0.0404	20	1.5	0.5	500	159	1	91	76.33	24.27	0.15
S8-60	882.20	882.56	0.0400	20	1.5	0.5	503	91	2	67	105.34	19.06	0.42
S8-61	882.56	882.95	0.0403	20	5	0.5	501	119	0	20	1162.92	276.22	0.00
S8-62	882.95	883.55	0.0407	20	5	0.5	501	173	9	48	479.79	165.67	8.62
S8-63	883.55	883.81	0.0412	20	5	0.5	516	145	2	27	867.83	243.87	3.36
S8-64	883.81	884.17	0.0402	20	5	0.5	503	75	2	17	1377.01	205.32	5.48
S8-65	884.17	884.30	0.0411	20	5	0.5	506	111	9	48	479.86	105.27	8.54
S8-66	884.30	884.75	0.0404	20	5	0.5	522	135	5	30	805.77	208.39	7.72
S8-67	884.75	885.00	0.0411	20	5	0.5	506	93	8	35	658.09	120.95	10.40
Average			0.0404								453.44	126.06	3.65

APPENDIX H3. Sediment slab major taxa relative abundance (%)*

Sample	S8-1	S8-2	S8-3	S8-4	S8-5	S8-6	S8-7	S8-8	S8-9	S8-10
Achnanthes biasioletta	1.00		0.60			0.39	0.78	0.20		
Achnanthes kregeri		0.60	0.80	0.39	0.20	0.78	0.39	0.79		0.40
Achnanthes lemmermanii			0.00	0.00			0.20			0.60
Achnanthes minutissima	3.21	2.78	2.59	1.17	0.40	1.57	5.69	3.56	3.91	4.96
Actinocyclus curvatulus	0.60					0.20		0.00		
Actinoptychus vulgaris	1.00	0.60				0.78		0.20		0.20
Amphora acutiuscula			0.20							0.20
Amphora copulata		0.40	0.80	0.19	0.40		0.59			1.19
Asteromphalus heptactis			0.40	0.19	0.40	0.20	0.39	0.20	0.20	
Bacteriastrum delicatulum		0.80	0.40	0.19	0.60		0.20	0.40		0.40
Cocconeis costata complex			0.40	0.19	0.40	0.39	0.20	0.40	0.20	
Cocconeis scutellum	1.41	0.40	1.00	0.19	0.40	0.59	0.20	0.79	0.39	0.99
Cyclotella choctawhatcheeana	0.99	0.59	1.57			0.58	0.78	0.78	0.19	0.98
Cyclotella striata		0.40	1.20			0.20	0.59	0.59		
Cyclotella sp. (S8-6)						0.39	1.76			
Diatomella minuta	1.00							0.20	0.39	
Ditylum brightwellii	0.20					0.20		0.99		0.20
Eunotia spp.		0.60	0.20	0.19			0.20	0.40		
Fragilaria investiens	0.20	0.60				0.39	0.39	0.59		0.40
Fragilaria pinnata	0.20							1.58		
Fragilaria sopotensis	1.61	0.20	0.20	0.19		1.17	0.98	0.40	0.39	1.59
Fragilariopsis atlantica	0.20	0.20								0.20
Fragilariopsis cylindriformis	1.41	0.80		0.19	0.60	0.20	0.20	0.59	0.20	0.79
Fragilariopsis pseudonana	3.82	2.58	2.59	2.92	0.99	1.37	1.96	2.37	1.37	4.96
Gomphonema angustum	0.40	0.40	0.40							
Gomphonemensis lindae	0.40	0.20	0.40				0.78	0.40	1.17	
Gomphonemensis obscurum	0.80	0.80	1.20				0.59	0.20		0.40
Grammatophora oceanica	0.20									
Melosira nummuloides	0.60		0.40	0.19	0.40	1.96	0.78	0.40		
Minidiscus chilensis	0.40	0.99	0.60	0.78	2.18	1.57	2.35	1.58	0.98	0.79
Navicula gregaria	0.20		0.20	0.19		0.39		0.00	0.20	0.20
Navicula perminuta	2.41	2.39	2.40	1.17	1.19	0.78	1.57	3.95	0.39	1.59
Nitzschia fonticola		0.20						0.59		0.20
Nitzschia frustulum	6.02	7.16	6.39	1.56	4.56	1.76	4.90	6.13	1.95	6.35
Odontella longicruris		0.20		0.39				0.40		
Opephora horstiana	1.00						0.59	0.20	0.98	0.79
Opephora marina	0.40	0.60	0.20				0.39	0.79		0.20
Opephora minuta		1.19								
Opephora mutabilis	1.20	0.40	0.20		0.79	0.78	0.20	0.79		0.20
Paralia sulcata	0.60	0.99	0.60	1.17	0.20	0.20	1.18	1.19	0.78	0.99
Planothidium delicatulum	4.62	2.58	1.60	1.56	1.79	1.96	3.33	3.36	4.30	6.15
Planothidium haukiana	0.20	0.20	0.40	0.39	0.20		0.39	0.20	0.39	1.39
Pseudonitzschia multiseries	1.41	0.20	0.60	0.78	1.79	0.20	0.98	1.19	0.20	
Pseudonitzschia seriata	0.20	0.40	0.60	0.58	23.21	0.39		0.20		
Skeletonema costatum	12.25	12.72	18.96	54.97	11.11	17.61	3.33	7.11	5.86	14.48
Skeletonema costatum (weak)	8.43	20.28	15.57	5.85	6.55	27.20	8.82	8.10	42.58	17.86
Tabellaria flocculosa	4.42	0.40					0.98		0.98	0.79
Tabularia fasciculata	0.60	0.40	0.20		0.40	0.59	0.59	1.19	0.59	
Thalassionema bacillare	1.20			0.97	0.40				0.20	0.20
Thalassionema nitzschioides	15.06	5.57	6.99	1.56	2.38	0.78	1.76	4.35	2.34	2.18
Thalassionema pseudonitzschioides	1.00	0.60	0.60	0.19	1.39	0.59		0.79	0.39	0.60
Thalassiosira binata	0.20	0.20	0.40		0.20					
Thalassiosira conferta	1.00	0.20	0.40		0.40	0.20	0.39		0.39	0.60
Thalassiosira decipiens	3.82	13.12	10.78	6.24	24.80	9.78	5.49	4.35	3.32	3.97
Thalassiosira eccentrica	2.81	1.79	1.80	0.78	0.79	1.17		1.38	1.76	0.79
Thalassiosira cf. *eccentrica* (S8-23)										
Thalassiosira gravida		0.40					0.20			
Thalassiosira cf. *leptopus*	0.60	0.99	0.40	0.19	0.20	0.78		0.59	0.20	0.79
Thalassiosira minima	0.20			0.00						
Thalassiosira nordenskioeldii	3.61	2.98	3.79	4.29	2.38	11.74	30.59	26.48	10.55	6.55
Thalassiosira pacifica	1.61	0.60	2.00	1.17	5.95	2.94	5.88	0.79	6.25	1.59
Thalassiosira rotula				4.87						
Thalassiosira tenera			0.20			0.20				0.20
Thalassiosira sp. (S8-27)										
Total relative abundance	94.77	90.65	91.19	95.91	97.62	92.95	91.56	91.69	93.94	87.89
Benthics	28.20	26.60	25.70	9.20	11.10	15.10	26.10	30.20	17.60	34.70
CRS	10.66	19.26	16.64	16.45	15.72	19.02	21.54	44.09	10.96	14.72
Silicoflagellates	2.33	0.98	0.99	0.19	0.98	0.58	0.20	0.39	0.19	0.98

*major taxa defined as those which appeared in at least three samples with at least 1% in one sample; no entry for zero values

APPENDIX H3 (continued)

Sample	S8-11	S8-12	S8-13	S8-14	S8-15	S8-16	S8-17	S8-18	S8-19	S8-20
Achnanthes biosioletta	0.59	0.79		0.40		0.39	0.60		0.20	0.78
Achnanthes kregeri	0.39	0.20	1.18	0.60		1.97	0.40			0.39
Achnanthes lemmermanii	0.00	0.20		0.20			0.00	0.39	0.40	0.39
Achnanthes minutissima	2.96	4.17	3.16	4.96	1.99	5.51	3.39	1.17	4.16	3.52
Actinocyclus curvatulus		0.20								
Actinoptychus vulgaris			0.39	0.20						0.20
Amphora acutiuscula		0.20	0.59		0.40		0.20		1.19	0.39
Amphora copulata		0.79	0.79	0.40	0.40	0.39			0.40	0.78
Asteromphalus heptactis	0.39	0.20	0.39	0.40		0.20			3.56	4.70
Bacteriastrum delicatulum		0.60	0.39		0.40	0.79	0.20	0.00		0.20
Cocconeis costata complex		0.20	0.79		0.60				0.59	0.59
Cocconeis scutellum	0.20	0.40		0.60	0.40	0.79		0.78	0.40	0.39
Cyclotella choctawhatcheeana	0.39	1.37	1.55	4.91	0.59					0.20
Cyclotella striata			0.39		0.60	0.20			0.20	
Cyclotella sp. (S8-6)				0.79	0.20				0.20	
Diatomella minuta		0.40			0.40	0.79	0.40		0.79	
Ditylum brightwellii	0.39	0.60	0.20	0.20	0.00	0.39	1.20			
Eunotia spp.	0.20	0.20	0.00		0.60		0.40	0.20	0.20	0.20
Fragilaria investiens	0.20	0.60	0.20	0.99	0.40	0.98			0.40	1.57
Fragilaria pinnata	0.20			0.79		0.39			0.79	
Fragilaria sopotensis		1.59	0.79		0.40	0.59	0.60	0.20	0.59	1.96
Fragilariopsis atlantica			0.00				0.20		0.20	
Fragilariopsis cylindriformis	1.18	1.79	0.59	0.60	1.19	4.72	2.00	0.39	0.59	1.57
Fragilariopsis pseudonana	9.66	10.91	6.51	16.07	11.73	22.64	11.38	1.76	8.12	6.26
Gomphonema angustum			0.39				0.40			0.59
Gomphonemensis lindae		1.19	0.39			0.20	0.20	0.20		0.20
Gomphonemensis obscurum		0.79	0.39	0.40		0.39	0.40	0.98	0.20	0.20
Grammatophora oceanica		1.19								
Melosira nummuloides	0.20	0.20	0.20		0.80	0.98	0.60	0.20	0.40	0.59
Minidiscus chilensis	1.78	0.79	0.59	1.39	2.39	1.57	0.20	0.20	2.18	1.76
Navicula gregaria	0.20	0.20	0.39	0.20	0.20		0.20			0.39
Navicula perminuta	1.58	0.60	2.17	1.98	1.19	4.13	1.80		1.98	1.76
Nitzschia fonticola		0.20		0.20	0.80	0.20	0.20		0.20	
Nitzschia frustulum	5.72	8.93	4.14	4.37	4.97	4.72	6.79	0.78	4.75	7.05
Odontella longicruris	0.39	0.20		0.20		0.39				0.20
Opephora horstiana		1.98	0.20	1.19	0.80					0.39
Opephora marina		0.79		1.39						0.00
Opephora minuta		0.99		0.20	0.40	0.59				0.20
Opephora mutabilis	0.20		1.18	0.40			0.40			
Paralia sulcata	2.56	0.99	0.79	0.20	0.40	0.59	1.00		0.79	
Planothidium delicatulum	3.94	5.95	3.55	4.76	3.78	4.53	2.59	0.78	4.36	2.35
Planothidium haukiana				0.60	0.60	0.98	0.60		0.79	0.39
Pseudonitzschia multiseries	0.20	0.20	0.59	0.99		0.20		0.20		0.98
Pseudonitzschia seriata	0.20	0.60	0.39	0.20	0.20			0.59		
Skeletonema costatum	16.57	11.31	26.82	13.29	6.96	5.71	24.35	14.87	9.90	6.46
Skeletonema costatum (weak)	20.71	10.12	10.26	11.31	7.75	4.72	12.77	66.34	21.98	20.35
Tabellaria flocculosa	2.76	0.20		0.20						
Tabularia fasciculata		1.79	1.38	0.79	0.60	0.98	0.60		0.59	0.39
Thalassionema bacillare		0.40					0.20		0.40	
Thalassionema nitzschioides	3.94	3.37	3.75	0.79	6.96	5.51	2.99	0.20	2.38	9.20
Thalassionema pseudonitzschioides	1.58	0.79	0.20	0.99	1.59	1.38	0.20	0.20	1.39	0.59
Thalassiosira binata	0.20			0.20	0.99	0.39	0.00		0.20	
Thalassiosira conferta	0.59		0.39	0.20	0.80		0.40		1.19	1.17
Thalassiosira decipiens	4.14	2.78	1.38	3.77	18.89	3.74	4.59	3.33	3.17	6.26
Thalassiosira eccentrica	1.38	1.19	0.59		1.19	0.79	4.19	0.20	0.20	0.78
Thalassiosira cf. *eccentrica* (S8-23)										
Thalassiosira gravida					0.20			0.20	0.20	
Thalassiosira cf. *leptopus*	0.59	1.19	0.20		0.80		1.00	0.20	0.20	0.59
Thalassiosira minima		0.40								
Thalassiosira nordenskioeldii	4.93	4.96	11.24	4.96	6.36	2.76	2.40	2.15	1.78	1.76
Thalassiosira pacifica	2.37	1.79	0.59	2.98	4.17	0.98	1.00	1.17	7.52	1.96
Thalassiosira rotula										
Thalassiosira tenera	0.39					0.20	0.40			
Thalassiosira sp. (S8-27)										
Total relative abundance	93.88	91.45	90.11	90.22	94.03	87.40	91.42	97.65	89.70	90.61
Benthics	20.70	37.10	27.80	30.00	21.90	33.70	23.20	6.80	28.70	30.70
CRS	23.41	30.00	21.40	30.29	28.04	19.62	22.08	8.91	12.93	11.59
Silicoflagellates	0.59	0.59	0.98	0.59	1.37	1.17	0.79	0.00	0.98	0.39

APPENDIX H3 (continued)

Sample	S8-21	S8-22	S8-23	S8-24	S8-25	S8-26	S8-27	S8-28	S8-29	S8-30
Achnanthes bioviolella	0.40			0.39				0.20		
Achnanthes kregeri		0.40	0.59	0.39			0.20	0.99	0.39	0.40
Achnanthes lemmermanii	0.20							0.40		
Achnanthes minutissima	4.57	2.19	3.13	0.39	2.58	2.56	2.15	2.97	4.72	7.00
Actinocyclus curvatulus									0.39	0.20
Actinoptychus vulgaris			0.20	0.20	0.40					
Amphora acutiuscula		0.20							0.39	0.60
Amphora copulata	0.40					0.20	0.39			1.20
Asteromphalus heptactis	1.19				0.60		0.20	0.59	0.39	0.20
Bacteriastrum delicatulum	0.20		0.39		0.79	1.57		0.40	1.18	1.00
Cocconeis costata complex	0.20	0.60			0.40			0.20	0.39	0.20
Cocconeis scutellum	0.60	1.20	0.59	0.20		0.39	0.20	0.20	0.39	0.80
Cyclotella choctawhatcheeana		0.40	0.58	0.39	2.14	0.59	0.58	1.17	0.97	0.40
Cyclotella striata	0.20			0.39	0.40	0.79		0.20	0.39	
Cyclotella sp. (S8-6)					0.79	1.18			0.59	
Diatomella minuta						0.20		0.40	1.18	
Ditylum brightwellii		0.60	0.39					0.00	0.20	0.40
Eunotia spp.	1.19	0.40	0.20			0.20		0.20		
Fragilaria investiens	0.60	1.00			0.20		0.39	0.20		
Fragilaria pinnata	0.40		1.17			0.39			0.20	
Fragilaria sopotensis	1.39	1.39	1.76	0.98		2.17		0.20		
Fragilariopsis atlantica										0.20
Fragilariopsis cylindriformis	1.19	2.19	1.37	0.79	0.99	1.77	0.98	4.75	3.94	1.60
Fragilariopsis pseudonana	5.57	10.36	11.15	2.75	5.95	10.83	5.68	31.09	10.04	4.80
Gomphonema angustum			0.78					0.79		
Gomphonemensis lindae	0.99	1.00		0.39	0.20				0.59	
Gomphonemensis obscurum	0.40	0.40		0.79	0.40	0.20			0.20	
Grammatophora oceanica	0.40			0.00	0.40	0.59				
Melosira nummuloides	2.19	0.40	0.39	0.79	1.39	0.98	0.59			0.20
Minidiscus chilensis	0.80	1.79	0.39	0.20	1.19	2.36	1.57	0.40	0.98	3.20
Navicula gregaria		0.20	0.20		0.40	1.18	0.59		0.20	0.40
Navicula perminuta	1.59	1.00	0.59	0.79	1.39	2.17	0.39	1.19	1.77	1.20
Nitzschia fonticola			0.39	0.39		0.59		0.40		1.00
Nitzschia frustulum	7.36	3.98	3.33	1.57	2.38	4.33	3.13	4.55	3.74	7.60
Odontella longicruris	0.20	1.00	0.59		0.40	0.79	0.20	0.20		
Opephora horstiana	0.40	0.80			0.40		0.20	0.20		
Opephora marina										
Opephora minuta	0.40									
Opephora mutabilis	0.80	0.60	0.20				1.96		0.59	
Paralia sulcata	0.80	0.80	0.20	0.20	0.60	0.20	0.78	0.79	0.20	2.00
Planothidium delicatulum	6.36	3.59	1.96	0.59	3.97	4.33	0.59	3.37	3.35	3.00
Planothidium haukiana	0.60	1.20	0.39	0.00	0.79	1.57		0.20	0.20	0.40
Pseudonitzschia multiseries	1.59	0.40	0.39	0.79	0.99	0.20			0.79	0.20
Pseudonitzschia seriata				0.20			0.59		0.20	0.20
Skeletonema costatum	8.95	10.56	16.83	9.43	5.56	8.86	13.50	8.12	5.51	10.60
Skeletonema costatum (weak)	13.12	6.18	18.79	64.64	26.19	15.16	38.94	10.50	7.87	18.00
Tabellaria flocculosa			0.59							0.20
Tabularia fasciculata	1.99	1.79	1.17		0.60	0.59	0.20	0.79	0.59	1.00
Thalassionema bacillare	0.99	1.39			0.20	0.39			0.20	0.40
Thalassionema nitzschioides	5.17	3.39	2.54	1.57	4.76	4.92	0.20	5.94	2.36	3.20
Thalassionema pseudonitzschioides	1.19	1.99	2.74	0.39	1.39	1.38	0.78	2.77	4.13	0.80
Thalassiosira binata	0.20	0.40		0.59	0.20	0.98	9.20	1.78		
Thalassiosira conferta	0.99	1.20		0.79	0.20	0.20	1.57			
Thalassiosira decipiens	1.99	2.79	1.76	1.18	0.79	2.95	1.17	0.99	11.81	6.60
Thalassiosira eccentrica	0.20	2.59	2.54	0.20	0.99	0.39	1.57	0.59	0.39	1.00
Thalassiosira cf. *eccentrica* (S8-23)			4.50	0.39	0.40	0.20				0.60
Thalassiosira gravida		0.20								
Thalassiosira cf. *leptopus*	0.60	2.39	4.50	1.18	8.93	0.79		0.40	0.20	1.40
Thalassiosira minima										
Thalassiosira nordenskioeldii	8.75	16.14	3.91	1.96	15.28	9.45	0.78	1.58	0.98	1.00
Thalassiosira pacifica	0.80	1.39	0.39	2.16	0.20	0.39	0.39	0.99	20.08	3.20
Thalassiosira rotula			0.00		0.20	1.18	0.39			0.20
Thalassiosira tenera		0.20	0.78					0.59		0.60
Thalassiosira sp. (S8-27)							7.44	0.40		
Total relative abundance	88.07	90.64	92.36	98.03	95.99	90.15	97.45	91.67	92.71	87.20
Benthics	36.40	24.10	19.80	8.30	15.90	25.80	11.70	23.20	21.30	31.80
CRS	18.48	28.39	10.98	22.41	15.01	28.85	34.99	21.95	42.34	61.03
Silicoflagellates	0.20	0.20	0.97	0.00	0.20	2.50	0.78	0.79	2.87	0.99

APPENDIX H3 (continued)

Sample	S8-31	S8-32	S8-33	S8-34	S8-35	S8-36	S8-37	S8-38	S8-39	S8-40
Achnanthes biosioletta	0.20	0.80			0.58			0.19	0.20	
Achnanthes kregeri				0.79	0.58					0.20
Achnanthes lenimermanii					0.19	0.40		0.39		
Achnanthes minutissima	4.59	7.95	0.99	3.97	0.58	1.19	1.96	4.09	1.19	1.79
Actinocyclus curvatulus	0.20	0.60	0.20				0.20	0.19	0.20	
Actinoptychus vulgaris		0.20	0.20	0.60			0.39	1.56	2.38	5.98
Amphora acutiuscula				0.20			0.39			
Amphora copulata	0.40	0.40						0.39		0.60
Asteromphalus heptactis		0.20	0.20					0.19		
Bacteriastrum delicatulum		0.60	1.58	0.20	0.19		0.20	0.39	0.20	0.20
Cocconeis costata complex	0.20	0.60	0.20	0.79	0.19		0.20		0.40	1.39
Cocconeis scutellum	0.60	0.60	0.59	0.99	0.58		0.20	0.58	0.40	0.20
Cyclotella choctawhatcheeana	0.60	1.37	0.59	2.14	2.64	1.18	3.96	2.84	4.91	6.34
Cyclotella striata				0.60	0.39		0.59		0.20	0.40
Cyclotella sp. (S8-6)	0.20		0.20	3.17		0.60	0.79	0.78	0.40	1.00
Diatomella minuta	0.40	0.40		0.40						
Ditylum brightwellii		0.20	0.79	3.17	0.97	0.79	0.98	0.19	0.79	0.80
Eunotia spp.	0.40	0.40	0.20	0.20	0.19		0.20		0.20	
Fragilaria investiens	0.40			0.20	0.19	0.20	0.39		0.20	0.20
Fragilaria pinnata		0.40								
Fragilaria sopotensis	0.20	0.80	0.79	0.60	0.19	0.20	0.59	1.36	0.99	1.99
Fragilariopsis atlantica				0.20				0.19	0.40	4.18
Fragilariopsis cylindriformis	0.60	2.98	2.37	2.78	0.78	1.39	2.16	0.78	1.19	1.79
Fragilariopsis pseudonana	8.78	7.55	4.35	9.13	16.28	4.76	7.47	12.26	9.33	8.96
Gomphonema angustum	0.20	0.40	0.20						0.20	
Gomphonemensis lindae				0.60	0.58		0.20	0.19	0.99	0.40
Gomphonemensis obscurum	0.40	0.60	0.40		0.19			0.39	1.19	0.20
Grammatophora oceanica	0.60			0.20	0.19				0.40	
Melosira nummuloides	0.40	0.20	0.79	0.20			0.20	0.78	0.20	1.20
Minidiscus chilensis	0.80	0.60	0.99	0.99	0.19	0.20	0.98	0.58	0.99	0.40
Navicula gregaria	0.80	0.60	0.20	0.20	0.58				0.60	0.20
Navicula perminuta	1.40	1.19	0.79	0.60	0.19	0.40	0.59	1.17	0.79	2.19
Nitzschia fonticola	0.20			0.20			0.39	0.39		
Nitzschia frustulum	3.79	5.17	2.17	2.58	1.74	2.98	1.18	4.67	2.18	5.98
Odontella longicruris		0.99	0.20	0.60		0.40	0.39			
Opephora horstiana			0.20							0.20
Opephora marina				0.20						
Opephora minuta								0.39		
Opephora mutabilis	1.60	1.39	0.40	0.79				0.58		0.80
Paralia sulcata	0.20	1.19	0.20	0.20	0.19			0.78	2.18	0.20
Planothidium delicatulum	1.60	1.39	0.40	1.39	1.36		1.57	2.14	1.98	3.39
Planothidium haukiana		0.20	0.00						0.60	
Pseudonitzschia multiseries	0.80	0.40	0.59		0.39		0.59	0.39		0.40
Pseudonitzschia seriata		0.20	3.36			0.20	1.57			0.20
Skeletonema costatum	18.76	2.78	11.26	10.71	13.57	30.36	24.95	20.23	6.55	2.19
Skeletonema costatum (weak)	17.76	38.97	40.32	18.65	11.05	38.69	22.00	9.14	8.73	10.36
Tabellaria flocculosa			0.59							
Tabularia fasciculata	0.80			0.79		0.40	0.79	0.58	0.40	2.19
Thalassionema bacillare		0.40	0.20	0.20		0.20				
Thalassionema nitzschioides	2.20	0.99	3.95	3.97	8.53	7.74	5.11	4.09	15.48	2.99
Thalassionema pseudonitzschioides	0.60	1.99	0.20	1.98	5.62	0.20	1.18	0.58	1.98	1.00
Thalassiosira binata	0.20	0.80		0.99				0.39	0.40	
Thalassiosira conferta		0.60					0.20			0.20
Thalassiosira decipiens	6.39	0.80	0.79	2.18	2.91	1.79	5.50	10.70	7.34	3.78
Thalassiosira eccentrica	1.20	0.20	0.20	0.79	0.39	0.20	0.98	0.39	0.40	1.99
Thalassiosira cf. *eccentrica* (S8-23)				0.79	0.78			0.97	2.38	0.60
Thalassiosira gravida							0.39	0.39	2.18	0.20
Thalassiosira cf. *leptopus*			0.20	0.60	0.97	0.20	0.39	1.36	2.38	0.80
Thalassiosira minima	0.20					0.00	0.20		1.19	
Thalassiosira nordenskioeldii	5.79	0.99		1.79	5.81	2.18	5.11	2.14	1.59	2.99
Thalassiosira pacifica	3.59	1.59	10.47	1.98	3.88	0.20	0.98	2.92	3.37	4.78
Thalassiosira rotula	0.80	0.20			0.19					
Thalassiosira tenera	1.00	1.79	1.98	6.15	7.56	0.40		0.97	0.20	1.79
Thalassiosira sp. (S8-27)	0.60			0.40			0.20	0.19		
Total relative abundance	90.42	92.63	94.27	90.83	91.40	97.41	96.30	93.89	90.42	87.62
Benthics	22.60	28.20	10.70	19.20	11.20	6.30	10.40	20.80	18.10	26.30
CRS	6.88	15.89	43.08	17.92	24.23	12.20	17.50	19.69	23.98	23.71
Silicoflagellates	0.40	0.20	0.39	3.26	1.90	0.20	0.59	1.72	2.70	2.33

APPENDIX H3 (continued)

Sample	S8-41	S8-42	S8-43	S8-44	S8-45	S8-46	S8-47	S8-48	S8-49	S8-50
Achnanthes biosioletta			0.20	0.40		0.20			0.60	
Achnanthes kregeri		0.40	0.39			0.59	0.20	0.20		
Achnanthes lemmermanii									0.20	
Achnanthes minutissima	1.19	7.21	3.93	2.40		0.20	0.80	0.80	1.79	0.60
Actinocyclus curvatulus		0.00	0.39	1.00				0.20		
Actinoptychus vulgaris	2.18	0.60			0.20	0.39				
Amphora acutiuscula	0.79	0.80	0.39	0.20					0.20	
Amphora copulata	0.40	0.20	0.20	0.40			0.20		0.80	
Asteromphalus heptactis	0.20		0.20	0.20		0.20			0.20	
Bacteriastrum delicatulum		0.20	0.20		0.40	0.20		0.60	0.80	0.20
Cocconeis costata complex	0.79	0.40	0.20	0.40	0.20			0.40		
Cocconeis scutellum		0.20	0.39	0.60						
Cyclotella choctawhatcheeana	3.99	5.49	2.30	2.72	0.60	0.20	0.79	1.38	0.59	
Cyclotella striata	0.40		0.39	0.00						
Cyclotella sp. (S8-6)	0.79	0.40	0.98	0.40		0.20		0.60	0.80	
Diatomella minuta	1.19	0.80	0.59	0.40		0.39		0.20		
Ditylum brightwellii	4.55	0.80	0.39	0.20					0.40	
Eunotia spp.		0.20	0.20						0.20	0.60
Fragilaria investiens		2.20	0.20					0.40	0.20	0.20
Fragilaria pinnata		1.40	1.18				0.20			
Fragilaria sopotensis	0.40	0.60	0.59		0.20		0.40	0.40	0.40	
Fragilariopsis atlantica	0.20							0.20		
Fragilariopsis cylindriformis	3.17	0.60	1.77	1.20	0.80	0.39	0.40	1.00	0.80	0.80
Fragilariopsis pseudonana	18.81	13.23	14.54	3.00	2.00	1.76	2.20	2.40	14.74	9.60
Gomphonema angustum				0.20						
Gomphonemensis lindae	0.59	0.40		0.20		0.20			0.60	0.20
Gomphonemensis obscurum	1.19		0.98	0.20				0.40		
Grammatophora oceanica	0.40									
Melosira nummuloides		0.60	0.20	0.40	0.20			0.20	0.80	
Minidiscus chilensis	0.99	1.80	0.79			0.78	0.20	0.80	1.00	
Navicula gregaria	0.59	2.00	0.39		0.40	0.20	0.60	0.20	0.20	
Navicula perminuta	3.17	2.00	0.79	1.60	0.80	0.39	0.60	0.40	1.39	1.00
Nitzschia fonticola		0.40	0.59	0.40					0.40	0.20
Nitzschia frustulum	5.94	5.01	3.14	2.60	1.40	1.18	2.40	4.20	4.38	2.60
Odontella longicruris		0.40	1.18		0.20			0.20		
Opephora horstiana			0.20		0.20	0.20			0.20	
Opephora marina										
Opephora minuta										
Opephora mutabilis	2.77	0.20			0.40		0.20	1.60		0.40
Paralia sulcata	1.78	1.60	0.59	1.00	0.20	0.20		0.20		
Planothidium delicatulum	2.97	4.01	2.16	2.40	1.00	0.59	0.60	0.80	1.20	1.60
Planothidium haukiana		0.20	0.20							
Pseudonitzschia multiseries	0.40	0.20	0.39		0.40	0.78	0.40	1.80		
Pseudonitzschia seriata	0.20		0.39				0.20	1.20		
Skeletonema costatum	3.37	4.61	7.27	7.00	15.57	6.86	6.80	6.60	8.96	10.20
Skeletonema costatum (weak)	10.89	9.82	10.41	34.60	43.31	65.49	43.80	58.60	35.66	60.40
Tabellaria flocculosa										
Tabularia fasciculata	0.59	1.00	0.39	0.80			0.20	0.40	0.40	
Thalassionema bacillare			0.20			0.20			0.20	0.20
Thalassionema nitzschioides	4.95	4.01	5.89	9.80	11.18	3.92	0.80	0.80	5.38	1.00
Thalassionema pseudonitzschioides	0.59	0.80	2.95			0.20			0.40	
Thalassiosira binata		0.40								
Thalassiosira conferta	0.40	0.20	0.20			0.20		0.40		
Thalassiosira decipiens	2.18	3.01	3.34	10.60	7.19	3.53	19.00	1.80	3.19	2.00
Thalassiosira eccentrica	1.39	2.20	5.70	0.60	0.80	0.98	0.40	0.80	0.20	0.20
Thalassiosira cf. *eccentrica* (S8-23)		1.00	1.38							
Thalassiosira gravida				0.20		0.20				
Thalassiosira cf. *leptopus*	1.19	3.41	8.06		0.20				0.40	
Thalassiosira minima					1.00	0.20			0.20	
Thalassiosira nordenskioeldii	0.99	3.61	0.39	2.60	0.60	0.59	5.00	2.40	1.39	1.80
Thalassiosira pacifica	0.59	1.20	2.55	2.40	3.39	4.71	11.60	1.20	1.00	2.20
Thalassiosira rotula									0.20	
Thalassiosira tenera	0.40	1.00	0.39	0.20	0.60				0.20	0.20
Thalassiosira sp. (S8-27)									3.19	0.20
Total relative abundance	87.56	90.86	90.71	91.32	93.41	96.27	97.99	93.78	93.82	96.40
Benthics	27.50	34.10	21.40	17.40	7.00	6.70	7.00	12.60	16.90	10.20
CRS	13.38	26.51	29.89	35.98	21.60	9.89	8.59	14.97	21.32	7.92
Silicoflagellates	2.32	0.99	1.93	1.77	0.60	0.58	0.40	0.99	0.99	0.20

APPENDIX H3 (continued)

Sample	S8-51	S8-52	S8-53	S8-54	S8-55	S8-56	S8-57	S8-58	S8-59	S8-60
Achnanthes biasioletta		0.99				0.40	0.60			
Achnanthes kregeri	0.20	0.20	0.60							
Achnanthes lemmermanii				2.40		0.40				
Achnanthes minutissima	4.18	2.39	1.79		1.00	2.00	0.80		0.80	
Actinocyclus curvatulus		0.20								
Actinoptychus vulgaris				0.20	0.20		0.20			
Amphora acutiuscula	0.20	0.20			0.20		1.00		0.60	
Amphora copulata	0.20	0.20	1.19	0.20	0.60	0.40		0.20		
Asteromphalus heptactis	0.20	0.20	0.20	0.20			0.20		0.20	0.20
Bacteriastrum delicatulum	0.20	0.80	0.40	1.40	0.80	0.20	0.80	0.20	2.60	0.60
Cocconeis costata complex	0.20	0.60		0.40					0.60	0.20
Cocconeis scutellum		0.40		0.20	0.20					
Cyclotella choctawhatcheeana	0.40	0.98		0.40	1.18	0.20	0.40		0.20	0.20
Cyclotella striata				0.20				0.20		
Cyclotella sp. (S8-6)	0.40									
Diatomella minuta		0.60	0.20		0.40					
Ditylum brightwellii	2.19	1.79	0.20	0.40	0.20	0.20	0.40	0.78	1.60	0.20
Eunotia spp.	0.40	0.20					0.20			
Fragilaria investiens	0.60			0.20	0.20	0.20				
Fragilaria pinnata				0.40			0.20		0.20	
Fragilaria sopotensis	0.20	0.80			1.00	0.60			1.00	
Fragilariopsis atlantica										
Fragilariopsis cylindriformis	1.20	2.58	27.58	21.36	0.80	1.20	2.39	0.59	0.40	
Fragilariopsis pseudonana	10.36	6.56	9.33	5.79	7.58	10.40	1.99	0.59	2.40	0.99
Gomphonema angustum		0.20		0.40	0.40					
Gomphonemensis lindae		0.80			0.40					
Gomphonemensis obscurum		0.20	0.60		0.60	0.40	0.80			
Grammatophora oceanica		0.40								
Melosira nummuloides	0.20	0.80		0.40	0.60		0.40			
Minidiscus chilensis		0.40	0.20	0.20	0.20	0.20			1.40	
Navicula gregaria	0.20	0.99	0.20	0.20		0.60		0.20		0.40
Navicula perminuta	0.80	1.39		0.80	0.60	0.80	0.40	0.59	1.00	0.60
Nitzschia fonticola	0.80				0.40					0.40
Nitzschia frustulum	5.18	5.96	1.19	2.00	2.20	1.60	0.80	1.17	3.20	0.20
Odontella longicruris		0.40			0.20					
Opephora horstiana		0.40							0.40	
Opephora marina										
Opephora minuta										
Opephora mutabilis		0.80			0.40		0.80		0.20	
Paralia sulcata	1.39	1.19				0.20		1.57		
Planothidium delicatulum	1.59	4.57	2.18	1.60	0.80	0.20	0.80		2.00	0.40
Planothidium haukiana	0.20	0.40				0.40				
Pseudonitzschia multiseries	0.40	0.80	0.20	3.19	0.60		0.40		2.80	0.80
Pseudonitzschia seriata		0.40			0.20			0.20	1.40	
Skeletonema costatum	7.37	8.55	1.19	2.20	22.55	6.00	47.81	7.24	5.60	5.37
Skeletonema costatum (weak)	41.83	13.32	8.13	16.17	34.93	54.60	15.14	75.15	39.20	80.91
Tabellaria flocculosa										
Tabularia fasciculata		0.20	0.40	0.40		0.20			0.20	0.20
Thalassionema bacillare		0.20					0.20	0.39	0.20	
Thalassionema nitzschioides	6.37	8.75	1.59	12.18	3.79	2.00	3.78	0.98	1.00	
Thalassionema pseudonitzschioides	0.40	2.78	0.40	2.99	2.00	1.20	1.39	0.98	0.60	2.19
Thalassiosira binata								0.39		
Thalassiosira conferta	0.40	0.20	0.20		0.20		0.20	0.00		0.80
Thalassiosira decipiens	1.79	3.98	7.94	8.58	3.79	4.60	3.78	1.57	12.60	1.59
Thalassiosira eccentrica	0.20	1.19	0.20	0.60	1.00	0.40			0.40	0.20
Thalassiosira cf. *eccentrica* (S8-23)			0.40	1.20						
Thalassiosira gravida										
Thalassiosira cf. *leptopus*	0.40	0.60	0.20	0.80						
Thalassiosira minima		0.60							0.20	
Thalassiosira nordenskioeldii	1.99	4.37	23.81	4.39	4.19	3.00	1.00	3.52	3.80	1.99
Thalassiosira pacifica	2.39	4.57	5.36	2.79	0.40	3.60	8.37	0.98	7.20	0.40
Thalassiosira rotula	0.40				0.00	0.20	0.20	1.17		
Thalassiosira tenera					0.20		0.20			
Thalassiosira sp. (S8-27)		0.60			0.20		0.20			
Total relative abundance	95.42	89.65	95.83	94.81	95.20	96.40	95.82	98.63	94.00	98.81
Benthics	16.70	26.80	10.30	12.00	12.20	10.20	8.40	2.90	13.20	3.20
CRS	25.07	49.09	9.19	28.43	26.43	46.70	19.55	13.24	24.13	15.32
Silicoflagellates	0.20	0.79	1.75	0.99		0.60	0.59	0.39	0.20	0.40

APPENDIX H3 (continued)

Sample	S8-61	S8-62	S8-63	S8-64	S8-65	S8-66	S8-67
Achnanthes biasioletta	0.20		0.19			0.19	0.20
Achnanthes kregeri				0.40	0.40		
Achnanthes lemmermanii							
Achnanthes minutissima		1.80	0.58	0.20	1.38	2.11	0.99
Actinocyclus curvatulus						0.00	
Actinoptychus vulgaris			0.19	0.40		0.19	
Amphora acutiuscula		0.20			0.59	0.00	
Amphora copulata					0.20	0.19	
Asteromphalus heptactis		0.80		0.20	0.40		0.20
Bacteriastrum delicatulum	0.40	0.80	0.39	0.20	0.79	0.57	0.40
Cocconeis costata complex		0.20	0.39		0.20	0.19	0.20
Coccneis scutellum	0.40	0.20				0.38	
Cyclotella choctawhatcheeana		0.20				0.95	1.94
Cyclotella striata		0.40				0.19	0.20
Cyclotella sp. (S8-6)				0.20	0.79		
Diatomella minuta							
Ditylum brightwellii		0.20	0.97	0.60	0.40	0.19	0.99
Eunotia spp.		0.60					
Fragilaria investiens							
Fragilaria pinnata							
Fragilaria sopotensis				0.20			0.20
Fragilariopsis atlantica		0.40					0.00
Fragilariopsis cylindriformis		1.00	0.19		0.40		0.20
Fragilariopsis pseudonana	0.60	2.40	1.36	1.99	1.98	1.92	2.57
Gomphonema angustum				1.19			0.20
Gomphonemensis lindae		1.20					0.00
Gomphonemensis obscurum					0.79	0.19	0.40
Grammatophora oceanica		0.40					
Melosira nummuloides			0.19		0.99	0.77	0.40
Minidiscus chilensis		0.20		0.40	0.20		0.20
Navicula gregaria	0.20	0.20	0.78		0.40		
Navicula perminuta	0.20		0.19	0.80	1.78	0.19	1.19
Nitzschia fonticola			0.39	0.40			
Nitzschia frustulum	1.00	1.20	0.39	0.60	2.57	0.77	0.79
Odontella longicruris		0.20			0.40		0.20
Opephora horstiana							
Opephora marina							
Opephora minuta							
Opephora mutabilis			0.39		0.59	0.19	
Paralia sulcata		0.20			0.20		0.40
Planothidium delicatulum	0.20	0.40	0.97	0.40	1.38	1.34	1.19
Planothidium haukiana					0.20		0.20
Pseudonitzschia multiseries		2.40	1.74	1.59	0.79	0.38	0.99
Pseudonitzschia seriata		0.40			0.40	0.77	0.99
Skeletonema costatum	3.79	19.96	10.08	12.72	18.18	11.88	11.86
Skeletonema costatum (weak)	81.84	47.90	69.19	68.79	42.89	63.79	58.30
Tabellaria flocculosa							
Tabularia fasciculata		0.20	0.19		0.20	1.15	
Thalassionema bacillare		0.20	0.39	0.20			0.99
Thalassionema nitzschioides		1.00	0.58	1.79	1.58	2.68	0.79
Thalassionema pseudonitzschioides	0.20	0.60		0.40	0.40	0.19	0.99
Thalassiosira binata	0.60	0.20	0.19				
Thalassiosira conferta		0.20		1.59	0.20	0.38	0.40
Thalassiosira decipiens	1.80	2.00		0.20	1.38	1.15	0.40
Thalassiosira eccentrica	0.60	0.60	0.78	0.40	0.40		
Thalassiosira cf. *eccentrica* (S8-23)							
Thalassiosira gravida							
Thalassiosira cf. *leptopus*		0.60			0.20	0.19	0.20
Thalassiosira minima							
Thalassiosira nordenskioeldii	3.99	4.99	3.49	0.60	5.53	2.30	7.31
Thalassiosira pacifica	0.60	2.00	1.55	0.40	4.74	1.15	0.20
Thalassiosira rotula		0.40	1.55	0.20		0.38	
Thalassiosira tenera			0.19			0.57	0.20
Thalassiosira sp. (S8-27)				0.99			0.20
Total relative abundance	96.61	96.81	97.48	98.01	93.87	97.50	97.00
Benthics	4.40	7.60	5.60	5.20	14.20	6.70	7.30
CRS	19.19	25.67	21.94	12.98	17.99	20.55	15.53
Silicoflagellates		1.76	0.39	0.40	1.75	0.95	1.56

APPENDIX H4. Sediment slab major taxa absolute abundance ($\times 10^6$ valves/g)*

Sample	S8-1	S8-2	S8-3	S8-4	S8-5	S8-6	S8-7	S8-8	S8-9	S8-10
Achnanthes biosioletta	2.76		2.06			1.46	2.46	0.60		
Achnanthes kregeri		1.61	2.74	1.89	1.04	2.92	1.23	2.39		1.34
Achnanthes lemmermanii							0.61			2.01
Achnanthes minutissima	8.83	7.50	8.92	5.68	2.07	5.83	17.80	10.77	20.33	16.78
Actinocyclus curvatulus	1.65					0.73				
Actinoptychus vulgaris	2.76	1.61				2.92		0.60		0.67
Amphora acutiuscula			0.69							0.67
Amphora copulata		1.07	2.74	0.95	2.07		1.84			4.03
Asteromphalus heptacis			1.37	0.95	2.07	0.73	1.23	0.60	1.02	
Bacteriastrum delicatulum		2.14	1.37	0.95	3.11		0.61	1.20		1.34
Cocconeis costata complex			1.37	0.95	2.07	1.46	0.61	1.20	1.02	
Cocconeis scutellum	3.86	1.07	3.43	0.95	2.07	2.19	0.61	2.39	2.03	3.36
Cyclotella choctawhatcheeana	2.73	1.60	5.40			2.17	2.44	2.37	1.01	3.32
Cyclotella striata		1.07	4.12			0.73	1.84	1.79		
Cyclotella sp. (S8-6)						1.46	5.52			
Diatomella minuta	2.76							0.60	2.03	
Ditylum brightwellii	0.55					0.73		2.99		0.67
Eunotia spp.		1.61	0.69	0.95			0.61	1.20		
Fragilaria investiens	0.55	1.61				1.46	1.23	1.79		1.34
Fragilaria pinnata	0.55							4.79		
Fragilaria sopotensis	4.41	0.54	0.69	0.95		4.37	3.07	1.20	2.03	5.37
Fragilariopsis atlantica	0.55	0.54								0.67
Fragilariopsis cylindriformis	3.86	2.14		0.95	3.11	0.73	0.61	1.79	1.02	2.68
Fragilariopsis pseudonana	10.48	6.97	8.92	14.21	5.18	5.10	6.14	7.18	7.12	16.78
Gomphonema angustum	1.10	1.07	1.37							
Gomphonemensis lindae	1.10	0.54	1.37				2.46	1.20	6.10	
Gomphonemensis obscurum	2.21	2.14	4.12				1.84	0.60		1.34
Grammatophora oceanica	0.55									
Melosira nummuloides	1.65		1.37	0.95	2.07	7.29	2.46	1.20		
Minidiscus chilensis	1.10	2.68	2.06	3.79	11.40	5.83	7.37	4.79	5.08	2.68
Navicula gregaria	0.55		0.69	0.95		1.46			1.02	0.67
Navicula perminuta	6.62	6.43	8.23	5.68	6.22	2.92	4.91	11.96	2.03	5.37
Nitzschia fonticola		0.54						1.79		0.67
Nitzschia frustulum	16.55	19.29	21.96	7.58	23.85	6.56	15.35	18.54	10.17	21.48
Odontella longicruris		0.54		1.89				1.20		
Opephora horstiana	2.76						1.84	0.60	5.08	2.68
Opephora marina	1.10	1.61	0.69				1.23	2.39		0.67
Opephora minuta		3.21								
Opephora mutabilis	3.31	1.07	0.69		4.15	2.92	0.61	2.39		0.67
Paralia sulcata	1.65	2.68	2.06	5.68	1.04	0.73	3.68	3.59	4.07	3.36
Planothidium delicatulum	12.69	6.97	5.49	7.58	9.33	7.29	10.44	10.17	22.36	20.81
Planothidium haukiana	0.55	0.54	1.37	1.89	1.04		1.23	0.60	2.03	4.70
Pseudonitzschia multiseries	3.86	0.54	2.06	3.79	9.33	0.73	3.07	3.59	1.02	
Pseudonitzschia seriata	0.55	1.07	2.06	2.84	121.30	1.46		0.60		
Skeletonema costatum	33.65	34.29	65.18	267.17	58.06	65.61	10.44	21.53	30.50	48.99
Skeletonema costatum (weak)	23.17	54.65	53.52	28.42	34.21	101.33	27.62	24.52	221.60	60.40
Tabellaria flocculosa	12.14	1.07					3.07		5.08	2.68
Tabularia fasciculata	1.65	1.07	0.69		2.07	2.19	1.84	3.59	3.05	
Thalassionema bacillare	3.31			4.74	2.07				1.02	0.67
Thalassionema nitzschioides	41.37	15.00	24.01	7.58	12.44	2.92	5.52	13.16	12.20	7.38
Thalassionema pseudonitzschioides	2.76	1.61	2.06	0.95	7.26	2.19		2.39	2.03	2.01
Thalassiosira binata	0.55	0.54	1.37		1.04					
Thalassiosira conferta	2.76	0.54	1.37		2.07	0.73	1.23		2.03	2.01
Thalassiosira decipiens	10.48	35.36	37.05	30.32	129.60	36.45	17.19	13.16	17.28	13.42
Thalassiosira eccentrica	7.72	4.82	6.17	3.79	4.15	4.37		4.19	9.15	2.68
Thalassiosira cf. *eccentrica* (S8-23)										
Thalassiosira gravida		1.07					0.61			
Thalassiosira cf. *leptopus*	1.65	2.68	1.37	0.95	1.04	2.92		1.79	1.02	2.68
Thalassiosira minima	0.55									
Thalassiosira nordenskioeldii	9.93	8.04	13.04	20.84	12.44	43.74	95.77	80.15	54.89	22.15
Thalassiosira pacifica	4.41	1.61	6.86	5.68	31.10	10.93	18.42	2.39	32.53	5.37
Thalassiosira rotula				23.69						
Thalassiosira tenera			0.69			0.73				0.67
Thalassiosira sp. (S8-27)										

*major taxa defined as those which appeared in at least three samples with at least 1% in one sample; no entry for zero values

APPENDIX H4 (continued)

Sample	S8-11	S8-12	S8-13	S8-14	S8-15	S8-16	S8-17	S8-18	S8-19	S8-20
Achnanthes biosioletta	2.45	1.72		1.13		0.96	1.89		0.50	2.80
Achnanthes kregeri	1.63	0.43	3.41	1.70		4.80	1.26			1.40
Achnanthes lemmermanii		0.43		0.57				4.17	1.00	1.40
Achnanthes minutissima	12.25	9.02	9.10	14.15	7.05	13.45	10.73	12.51	10.51	12.60
Actinocyclus curvatulus		0.43								
Actinoptychus vulgaris			1.14	0.57						0.70
Amphora acutiuscula		0.43	1.71		1.41		0.63	0.00	3.00	1.40
Amphora copulata		1.72	2.28	1.13	1.41	0.96			1.00	2.80
Asteromphalus heptacis	1.63	0.43	1.14	1.13		0.48			9.01	16.80
Bacteriastrum delicatulum		1.29	1.14		1.41	1.92	0.63			0.70
Cocconeis costata complex		0.43	2.28		2.12				1.50	2.10
Cocconeis scutellum	0.82	0.86		1.70	1.41	1.92		8.34	1.00	1.40
Cyclotella choctawhatcheeana	1.63	2.97	4.48	14.00	2.10					0.70
Cyclotella striata			1.14		2.12	0.48			0.50	
Cyclotella sp. (S8-6)				2.26	0.71				0.50	
Diatomella minuta		0.86			1.41	1.92	1.26		2.00	
Ditylum brightwellii	1.63	1.29	0.57	0.57		0.96	3.79			
Eunotia spp.	0.82	0.43			2.12		1.26	2.08	0.50	0.70
Fragilaria investiens	0.82	1.29	0.57	2.83	1.41	2.40			1.00	5.60
Fragilaria pinnata	0.82			2.26		0.96			2.00	
Fragilaria sopotensis		3.44	2.28		1.41	1.44	1.89	2.08	1.50	7.00
Fragilariopsis atlantica							0.63		0.50	
Fragilariopsis cylindriformis	4.90	3.87	1.71	1.70	4.23	11.53	6.31	4.17	1.50	5.60
Fragilariopsis pseudonana	40.02	23.63	18.77	45.86	41.62	55.24	35.98	18.76	20.52	22.40
Gomphonema angustum			1.14				1.26			2.10
Gomphonemensis lindae		2.58	1.14			0.48	0.63	2.08		0.70
Gomphonemensis obscurum		1.72	1.14	1.13		0.96	1.26	10.42	0.50	0.70
Grammatophora oceanica		2.58								0.00
Melosira nummuloides	0.82	0.43	0.57		2.82	2.40	1.89	2.08	1.00	2.10
Minidiscus chilensis	7.35	1.72	1.71	3.96	8.47	3.84	0.63	2.08	5.50	6.30
Navicula gregaria	0.82	0.43	1.14	0.57	0.71	0.00	0.63			1.40
Navicula perminuta	6.53	1.29	6.26	5.66	4.23	10.09	5.68		5.00	6.30
Nitzschia fonticola		0.43		0.57	2.82	0.48	0.63		0.50	
Nitzschia frustulum	23.69	19.33	11.95	12.46	17.64	11.53	21.46	8.34	12.01	25.20
Odontella longicruris	1.63	0.43		0.57		0.96				0.70
Opephora horstiana		4.30	0.57	3.40	2.82					1.40
Opephora marina		1.72		3.96					0.00	
Opephora minuta		2.15		0.57	1.41	1.44				0.70
Opephora mutabilis	0.82		3.41	1.13			1.26			
Paralia sulcata	10.62	2.15	2.28	0.57	1.41	1.44	3.16		2.00	
Planothidium delicatulum	16.34	12.89	10.24	13.59	13.40	11.05	8.21	8.34	11.01	8.40
Planothidium haukiana				1.70	2.12	2.40	1.89		2.00	1.40
Pseudonitzschia multiseries	0.82	0.43	1.71	2.83		0.48		2.08		3.50
Pseudonitzschia seriata	0.82	1.29	1.14	0.57	0.71			6.25		
Skeletonema costatum	68.61	24.49	77.37	37.93	24.69	13.93	77.01	158.41	25.02	23.10
Skeletonema costatum (weak)	85.77	21.91	29.58	32.27	27.51	11.53	40.40	706.58	55.55	72.79
Tabellaria flocculosa	11.44	0.43		0.57						
Tabularia fasciculata		3.87	3.98	2.26	2.12	2.40	1.89		1.50	1.40
Thalassionema bacillare		0.86					0.63		1.00	
Thalassionema nitzschioides	16.34	7.30	10.81	2.26	24.69	13.45	9.47	2.08	6.01	32.90
Thalassionema pseudonitzschioides	6.53	1.72	0.57	2.83	5.64	3.36	0.63	2.08	3.50	2.10
Thalassiosira binata	0.82			0.57	3.53	0.96			0.50	
Thalassiosira conferta	2.45		1.14	0.57	2.82		1.26		3.00	4.20
Thalassiosira decipiens	17.15	6.01	3.98	10.76	67.02	9.13	14.52	35.43	8.01	22.40
Thalassiosira eccentrica	5.72	2.58	1.71		4.23	1.92	13.26	2.08	0.50	2.80
Thalassiosira cf. *eccentrica* (S8-23)										
Thalassiosira gravida					0.71			2.08	0.50	
Thalassiosira cf. *leptopus*	2.45	2.58	0.57		2.82		3.16	2.08	0.50	2.10
Thalassiosira minima		0.86								
Thalassiosira nordenskioeldii	20.42	10.74	32.43	14.15	22.57	6.72	7.57	22.93	4.50	6.30
Thalassiosira pacifica	9.80	3.87	1.71	8.49	14.81	2.40		12.51	19.02	7.00
Thalassiosira rotula										
Thalassiosira tenera	1.63					0.48	1.26			
Thalassiosira sp. (S8-27)										

APPENDIX H4 (continued)

Sample	S8-21	S8-22	S8-23	S8-24	S8-25	S8-26	S8-27	S8-28	S8-29	S8-30
Achnanthes biosioletta	1.19			2.89				0.81		
Achnanthes kregeri		1.23	2.77	2.89			0.89	4.03	1.15	0.90
Achnanthes lemmermanii	0.60	0.00						1.61		
Achnanthes minutissima	13.69	6.78	14.79	2.89	9.27	6.33	9.77	12.10	13.86	15.81
Actinocyclus curvatulus									1.15	0.45
Actinoptychus vulgaris			0.92	1.44	1.43					
Amphora acutiuscula		0.62							1.15	1.36
Amphora copulata	1.19					0.49	1.78			2.71
Asteromphalus heptacis	3.57				2.14		0.89	2.42	1.15	0.45
Bacteriastrum delicatulum	0.60		1.85		2.85	3.90		1.61	3.46	2.26
Cocconeis costata complex	0.60	1.85			1.43			0.81	1.15	0.45
Cocconeis scutellum	1.79	3.70	2.77	1.44		0.97	0.89	0.81	1.15	1.81
Cyclotella choctawhatcheeana		1.23	2.76	2.88	7.68	1.45	2.65	4.78	2.86	0.90
Cyclotella striata	0.60			2.89	1.43	1.95		0.81	1.15	
Cyclotella sp. (S8-6)					2.85	2.92			1.73	
Diatomella minuta						0.49		1.61	3.46	
Ditylum brightwellii		1.85	1.85						0.58	0.90
Eunotia spp.	3.57	1.23	0.92			0.49		0.81		
Fragilaria investiens	1.79	3.08			0.71		1.78	0.81		
Fragilaria pinnata	1.19		5.55			0.97			0.58	
Fragilaria sopotensis	4.17	4.31	8.32	7.22		5.36		0.81		
Fragilariopsis atlantica										0.45
Fragilariopsis cylindriformis	3.57	6.78	6.47	5.77	3.56	4.38	4.44	19.35	11.55	3.61
Fragilariopsis pseudonana	16.66	32.03	52.70	20.21	21.39	26.80	25.76	126.61	29.45	10.84
Gomphonema angustum			3.70					3.23		
Gomphonemensis lindae	2.98	3.08		2.89	0.71				1.73	
Gomphonemensis obscurum	1.19	1.23		5.77	1.43	0.49			0.58	
Grammatophora oceanica	1.19				1.43	1.46				
Melosira nummuloides	6.55	1.23	1.85	5.77	4.99	2.44	2.67			0.45
Minidiscus chilensis	2.38	5.54	1.85	1.44	4.28	5.85	7.11	1.61	2.89	7.23
Navicula gregaria		0.62	0.92		1.43	2.92	2.67		0.58	0.90
Navicula perminuta	4.76	3.08	2.77	5.77	4.99	5.36	1.78	4.84	5.20	2.71
Nitzschia fonticola			1.85	2.89		1.46		1.61		2.26
Nitzschia frustulum	22.02	12.32	15.72	11.55	8.56	10.72	14.21	18.55	10.97	17.17
Odontella longicruris	0.60	3.08	2.77		1.43	1.95	0.89	0.81		
Opephora horstiana	1.19	2.46			1.43		0.89	0.81		
Opephora marina										
Opephora minuta	1.19									
Opephora mutabilis	2.38	1.85	0.92				8.88		1.73	
Paralia sulcata	2.38	2.46	0.92	1.44	2.14	0.49	3.55	3.23	0.58	4.52
Planothidium delicatulum	19.05	11.09	9.24	4.33	14.26	10.72	2.67	13.71	9.82	6.78
Planothidium haukiana	1.79	3.70	1.85		2.85	3.90		0.81	0.58	0.90
Pseudonitzschia multiseries	4.76	1.23	1.85	5.77	3.56	0.49			2.31	0.45
Pseudonitzschia seriata				1.44			2.67		0.58	0.45
Skeletonema costatum	26.78	32.64	79.51	69.29	19.96	21.92	61.30	33.06	16.17	23.95
Skeletonema costatum (weak)	39.28	19.09	88.75	474.94	94.11	37.52	176.78	42.74	23.10	40.67
Tabellaria flocculosa			2.77							0.45
Tabularia fasciculata	5.95	5.54	5.55		2.14	1.46	0.89	3.23	1.73	2.26
Thalassionema bacillare	2.98	4.31			0.71	0.97			0.58	0.90
Thalassionema nitzschioides	15.47	10.47	12.02	11.55	17.11	12.18	0.89	24.19	6.93	7.23
Thalassionema pseudonitzschioides	3.57	6.16	12.94	2.89	4.99	3.41	3.55	11.29	12.13	1.81
Thalassiosira binata	0.60	1.23		4.33	0.71	2.44	41.75	7.26		
Thalassiosira conferta	2.98	3.70		5.77	0.71		7.11			
Thalassiosira decipiens	5.95	8.62	8.32	8.66	2.85	7.31	5.33	4.03	34.65	14.91
Thalassiosira eccentrica	0.60	8.01	12.02	1.44	3.56	0.97	7.11	2.42	1.15	2.26
Thalassiosira cf. *eccentrica* (S8-23)			21.26	2.89	1.43	0.49				1.36
Thalassiosira gravida		0.62								0.00
Thalassiosira cf. *leptopus*	1.79	7.39	21.26	8.66	32.08	1.95		1.61	0.58	3.16
Thalassiosira minima										
Thalassiosira nordenskioeldii	26.19	49.89	18.49	14.44	54.90	23.39	3.55	6.45	2.89	2.26
Thalassiosira pacifica	2.38	4.31	1.85	15.88	0.71	0.97	1.78	4.03	58.90	7.23
Thalassiosira rotula					0.71	2.92	1.78	0.00		0.45
Thalassiosira tenera		0.62	3.70					2.42		1.36
Thalassiosira sp. (S8-27)							33.76	1.61		

APPENDIX H4 (continued)

Sample	S8-31	S8-32	S8-33	S8-34	S8-35	S8-36	S8-37	S8-38	S8-39	S8-40
Achnanthes biosioletta	0.55	1.80			2.67			0.56	0.57	
Achnanthes kregeri				2.47	2.67					0.51
Achnanthes lemmermanii				0.00	0.89	4.91		1.12		
Achnanthes minutissima	12.72	17.98	6.30	12.34	2.67	14.73	9.28	11.74	3.41	4.56
Actinocyclus curvatulus	0.55	1.35	1.26				0.93	0.56	0.57	
Actinoptychus vulgaris		0.45	1.26	1.85			1.86	4.47	6.81	15.19
Amphora acutiuscula				0.62			1.86			
Amphora copulata	1.11	0.90						1.12		1.52
Asteromphalus heptactis		0.45	1.26					0.56		
Bacteriastrum delicatulum		1.35	10.09	0.62	0.89		0.93	1.12	0.57	0.51
Cocconeis costata complex	0.55	1.35	1.26	2.47	0.89		0.93		1.14	3.54
Cocconeis scutellum	1.66	1.35	3.78	3.08	2.67		0.93	1.68	1.14	0.51
Cyclotella choctawhatcheeana	1.65	3.10	3.76	6.64	12.11	14.56	18.73	8.15	14.03	16.12
Cyclotella striata				1.85	1.78		2.79		0.57	1.01
Cyclotella sp. (S8-6)	0.55		1.26	9.87		7.37	3.71	2.24	1.14	2.53
Diatomella minuta	1.11	0.90		1.23						
Ditylum brightwellii		0.45	5.04	9.87	4.44	9.82	4.64	0.56	2.27	2.03
Eunotia spp.	1.11	0.90	1.26	0.62	0.89		0.93		0.57	
Fragilaria investiens	1.11			0.62	0.89	2.46	1.86		0.57	0.51
Fragilaria pinnata		0.90								
Fragilaria sopotensis	0.55	1.80	5.04	1.85	0.89	2.46	2.79	3.91	2.84	5.06
Fragilariopsis atlantica				0.62				0.56	1.14	10.63
Fragilariopsis cylindriformis	1.66	6.74	15.13	8.64	3.55	17.19	10.21	2.24	3.41	4.56
Fragilariopsis pseudonana	24.33	17.08	27.74	28.38	74.62	58.93	35.28	35.23	26.67	22.79
Gomphonema angustum	0.55	0.90	1.26						0.57	
Gomphonemensis lindae				1.85	2.67		0.93	0.56	2.84	1.01
Gomphonemensis obscurum	1.11	1.35	2.52		0.89			1.12	3.41	0.51
Grammatophora oceanica	1.66			0.62	0.89				1.14	
Melosira nummuloides	1.11	0.45	5.04	0.62			0.93	2.24	0.57	3.04
Minidiscus chilensis	2.21	1.35	6.30	3.08	0.89	2.46	4.64	1.68	2.84	1.01
Navicula gregaria	2.21	1.35	1.26	0.62	2.67				1.70	0.51
Navicula perminuta	3.87	2.70	5.04	1.85	0.89	4.91	2.79	3.36	2.27	5.57
Nitzschia fonticola	0.55			0.62			1.86	1.12		
Nitzschia frustulum	10.51	11.69	13.87	8.02	8.00	36.83	5.57	13.42	6.24	15.19
Odontella longicruris		2.25	1.26	1.85		4.91	1.86			
Opephora horstiana			1.26							0.51
Opephora marina				0.62						
Opephora minuta								1.12		
Opephora mutabilis	4.42	3.15	2.52	2.47				1.68		2.03
Paralia sulcata	0.55	2.70	1.26	0.62	0.89			2.24	6.24	0.51
Planothidium delicatulum	4.42	3.15	2.52	4.32	6.22		7.43	6.15	5.68	8.61
Planothidium haukiana		0.45					0.00		1.70	
Pseudonitzschia multiseries	2.21	0.90	3.78		1.78		2.79	1.12		1.01
Pseudonitzschia seriata		0.45	21.44			2.46	7.43			0.51
Skeletonema costatum	51.98	6.29	71.87	33.32	62.18	375.70	117.92	58.16	18.73	5.57
Skeletonema costatum (weak)	49.22	88.12	257.23	57.99	50.64	478.83	103.99	26.28	24.97	26.33
Tabellaria flocculosa			3.78							
Tabularia fasciculata	2.21			2.47		4.91	3.71	1.68	1.14	5.57
Thalassionema bacillare		0.90	1.26	0.62		2.46				
Thalassionema nitzschioides	6.08	2.25	25.22	12.34	39.09	95.77	24.14	11.74	44.27	7.60
Thalassionema pseudonitzschioides	1.66	4.50	1.26	6.17	25.76	2.46	5.57	1.68	5.68	2.53
Thalassiosira binata	0.55	1.80		3.08				1.12	1.14	
Thalassiosira conferta		1.35					0.93			0.51
Thalassiosira decipiens	17.70	1.80	5.04	6.79	13.33	22.10	26.00	30.76	21.00	9.62
Thalassiosira eccentrica	3.32	0.45	1.26	2.47	1.78	2.46	4.64	1.12	1.14	5.06
Thalassiosira cf. *eccentrica* (S8-23)				2.47	3.55			2.80	6.81	1.52
Thalassiosira gravida							1.86	1.12	6.24	0.51
Thalassiosira cf. *leptopus*			1.26	1.85	4.44	2.46	1.86	3.91	6.81	2.03
Thalassiosira minima	0.55						0.93		3.41	
Thalassiosira nordenskioeldii	16.04	2.25		5.55	26.65	27.01	24.14	6.15	4.54	7.60
Thalassiosira pacifica	9.95	3.60	66.83	6.17	17.77	2.46	4.64	8.39	9.65	12.15
Thalassiosira rotula	2.21	0.45			0.89					
Thalassiosira tenera	2.77	4.05	12.61	19.13	34.65	4.91		2.80	0.57	4.56
Thalassiosira sp. (S8-27)	1.66			1.23			0.93	0.56		

APPENDIX H4 (continued)

Sample	S8-41	S8-42	S8-43	S8-44	S8-45	S8-46	S8-47	S8-48	S8-49	S8-50
Achnanthes biosioletta			0.62	1.62		1.44			2.38	
Achnanthes kregeri		0.98	1.24			4.32	1.47	0.91		
Achnanthes lemmermanii									0.79	
Achnanthes minutissima	3.77	17.64	12.38	9.70		1.44	5.86	3.63	7.15	4.80
Actinocyclus curvatulus			1.24	4.04				0.91		
Actinoptychus vulgaris	6.92	1.47			1.37	2.88				
Amphora acutiuscula	2.52	1.96	1.24	0.81					0.79	
Amphora copulata	1.26	0.49	0.62	1.62			1.47		3.18	
Asteromphalus heptacis	0.63		0.62	0.81		1.44			0.79	
Bacteriastrum delicatulum		0.49	0.62		2.73	1.44		2.72	3.18	1.60
Cocconeis costata complex	2.52	0.98	0.62	1.62	1.37			1.81		
Cocconeis scutellum		0.49	1.24	2.43	0.00					
Cyclotella choctawhatcheeana	12.68	13.43	7.26	11.01	4.07	1.44	5.81	6.26	2.37	
Cyclotella striata	1.26		1.24							
Cyclotella sp. (S8-6)	2.52	0.98	3.09	1.62		1.44		2.72	3.18	
Diatomella minuta	3.77	1.96	1.86	1.62		2.88		0.91		
Ditylum brightwellii	14.46	1.96	1.24	0.81					1.59	
Eunotia spp.		0.49	0.62						0.79	4.80
Fragilaria investiens		5.39	0.62					1.81	0.79	1.60
Fragilaria pinnata		3.43	3.71				1.47			
Fragilaria sopotensis	1.26	1.47	1.86		1.37		2.93	1.81	1.59	
Fragilariopsis atlantica	0.63							0.91		
Fragilariopsis cylindriformis	10.06	1.47	5.57	4.85	5.46	2.88	2.93	4.53	3.18	6.40
Fragilariopsis pseudonana	59.75	32.33	45.80	12.13	13.65	12.96	16.12	10.88	58.81	76.84
Gomphonema angustum				0.81						
Gomphonemensis lindae	1.89	0.98		0.81		1.44			2.38	1.60
Gomphonemensis obscurum	3.77		3.09	0.81				1.81		
Grammatophora oceanica	1.26									
Melosira nummuloides		1.47	0.62	1.62	1.37			0.91	3.18	
Minidiscus chilensis	3.14	4.41	2.48			5.76	1.47	3.63	3.97	
Navicula gregaria	1.89	4.90	1.24		2.73	1.44	4.40	0.91	0.79	
Navicula perminuta	10.06	4.90	2.48	6.47	5.46	2.88	4.40	1.81	5.56	8.00
Nitzschia fonticola		0.98	1.86	1.62					1.59	1.60
Nitzschia frustulum	18.87	12.25	9.90	10.51	9.56	8.64	17.58	19.03	17.48	20.81
Odontella longicruris		0.98	3.71		1.37			0.91		
Opephora horstiana			0.62		1.37	1.44		0.00	0.79	
Opephora marina										
Opephora minuta										
Opephora mutabilis	8.80	0.49			2.73		1.47	7.25		3.20
Paralia sulcata	5.66	3.92	1.86	4.04	1.37	1.44		0.91		
Planothidium delicatulum	9.43	9.80	6.81	9.70	6.83	4.32	4.40	3.63	4.77	12.81
Planothidium haukiana		0.49	0.62							
Pseudonitzschia multiseries	1.26	0.49	1.24		2.73	5.76	2.93	8.16		
Pseudonitzschia seriata	0.63		1.24				1.47	5.44		
Skeletonema costatum	10.69	11.27	22.90	28.30	106.50	50.40	49.82	29.91	35.76	81.64
Skeletonema costatum (weak)	34.59	24.00	32.81	139.86	296.29	480.97	320.90	265.53	142.26	483.45
Tabellaria flocculosa										
Tabularia fasciculata	1.89	2.45	1.24	3.23			1.47	1.81	1.59	
Thalassionema bacillare			0.62			1.44			0.79	1.60
Thalassionema nitzschioides	15.72	9.80	18.57	39.61	76.46	28.80	5.86	3.63	21.46	8.00
Thalassionema pseudonitzschioides	1.89	1.96	9.28			1.44			1.59	
Thalassiosira binata		0.98								
Thalassiosira conferta	1.26	0.49	0.62			1.44		1.81		
Thalassiosira decipiens	6.92	7.35	10.52	42.85	49.15	25.92	139.20	8.16	12.72	16.01
Thalassiosira eccentrica	4.40	5.39	17.95	2.43	5.46	7.20	2.93	3.63	0.79	1.60
Thalassiosira cf. *eccentrica* (S8-23)		2.45	4.33							
Thalassiosira gravida				0.81		1.44				
Thalassiosira cf. *leptopus*	3.77	8.33	25.38		1.37				1.59	
Thalassiosira minima					6.83	1.44			0.79	
Thalassiosira nordenskioeldii	3.14	8.82	1.24	10.51	4.10	4.32	36.63	10.88	5.56	14.41
Thalassiosira pacifica	1.89	2.94	8.05	9.70	23.21	34.56	84.99	5.44	3.97	17.61
Thalassiosira rotula									0.79	
Thalassiosira tenera	1.26	2.45	1.24	0.81	4.10				0.79	1.60
Thalassiosira sp. (S8-27)									12.72	1.60

APPENDIX H4 (continued)

Sample	S8-51	S8-52	S8-53	S8-54	S8-55	S8-56	S8-57	S8-58	S8-59	S8-60
Achnanthes biosioletta		2.57				1.86	3.48			
Achnanthes kregeri	0.75	0.51	4.13							
Achnanthes lemmermanii				11.01		1.86				
Achnanthes minutissima	15.84	6.17	12.38		4.31	9.31	4.64		0.61	
Actinocyclus curvatulus		0.51								
Actinoptychus vulgaris				0.92	0.86		1.16			
Amphora acutiuscula	0.75	0.51			0.86		5.80		0.46	
Amphora copulata	0.75	0.51	8.26	0.92	2.59	1.86		0.44		
Asteromphalus heptacis	0.75	0.51	1.38	0.92			1.16		0.15	0.21
Bacteriastrum delicatulum	0.75	2.06	2.75	6.42	3.45	0.93	4.64	0.44	1.98	0.63
Cocconeis costata complex	0.75	1.54		1.83					0.46	0.21
Cocconeis scutellum		1.03		0.92	0.86					
Cyclotella choctawhatcheeana	1.50	2.55		1.83	5.11	0.93	2.31		0.15	0.21
Cyclotella striata				0.92				0.44		
Cyclotella sp. (S8-6)	1.51									
Diatomella minuta		1.54	1.38		1.72					
Ditylum brightwellii	8.30	4.63	1.38	1.83	0.86	0.93	2.32	1.74	1.22	0.21
Eunotia spp.	1.51	0.51					1.16			
Fragilaria investiens	2.26			0.92	0.86	0.93				
Fragilaria pinnata				1.83			1.16		0.15	
Fragilaria sopotensis	0.75	2.06			4.31	2.79			0.76	
Fragilariopsis atlantica										
Fragilariopsis cylindriformis	4.53	6.69	191.27	98.13	3.45	5.58	13.93	1.31	0.31	
Fragilariopsis pseudonana	39.23	16.98	64.67	26.60	32.75	48.40	11.61	1.31	1.83	1.05
Gomphonema angustum		0.51		1.83	1.72					
Gomphonemensis lindae		2.06			1.72					
Gomphonemensis obscurum		0.51	4.13		2.59	1.86	4.64			
Grammatophora oceanica		1.03								
Melosira nummuloides	0.75	2.06		1.83	2.59		2.32			
Minidiscus chilensis		1.03	1.38	0.92	0.86	0.93			1.07	
Navicula gregaria	0.75	2.57	1.38	0.92		2.79		0.44		0.42
Navicula perminuta	3.02	3.60		3.67	2.59	3.72	2.32	1.31	0.76	0.63
Nitzschia fonticola	3.02				1.72					0.42
Nitzschia frustulum	19.61	15.44	8.26	9.17	9.48	7.45	4.64	2.61	2.44	0.21
Odontella longicruris		1.03			0.86					
Opephora horstiana		1.03							0.31	
Opephora marina										
Opephora minuta										
Opephora mutabilis		2.06			1.72		4.64		0.15	
Paralia sulcata	5.28	3.09				0.93		3.48		
Planothidium delicatulum	6.04	11.83	15.14	7.34	3.45	0.93	4.64		1.53	0.42
Planothidium hauckiana	0.75	1.03				1.86				
Pseudonitzschia multiseries	1.51	2.06	1.38	14.67	2.59		2.32		2.14	0.84
Pseudonitzschia seriata		1.03			0.86			0.44	1.07	
Skeletonema costatum	27.91	22.13	8.26	10.09	97.39	27.92	278.54	16.10	4.27	5.65
Skeletonema costatum (weak)	158.42	34.47	56.42	74.28	150.82	254.10	88.21	167.13	29.92	85.24
Tabellaria flocculosa										
Tabularia fasciculata		0.51	2.75	1.83		0.93			0.15	0.21
Thalassionema bacillare		0.51					1.16	0.87	0.15	
Thalassionema nitzschioides	24.14	22.64	11.01	55.94	16.37	9.31	22.05	2.18	0.76	
Thalassionema pseudonitzschioides	1.51	7.20	2.75	13.76	8.62	5.58	8.12	2.18	0.46	2.30
Thalassiosira binata								0.87		
Thalassiosira conferta	1.51	0.51	1.38		0.86		1.16			0.84
Thalassiosira decipiens	6.79	10.29	55.04	39.44	16.37	21.41	22.05	3.48	9.62	1.68
Thalassiosira eccentrica	0.75	3.09	1.38	2.75	4.31	1.86			0.31	0.21
Thalassiosira cf. *eccentrica* (S8-23)			2.75	5.50						
Thalassiosira gravida										
Thalassiosira cf. *leptopus*	1.51	1.54	1.38	3.67						
Thalassiosira minima		1.54							0.15	
Thalassiosira nordenskioeldii	7.54	11.32	165.13	20.18	18.10	13.96	5.80	7.83	2.90	2.09
Thalassiosira pacifica	9.05	11.83	37.15	12.84	1.72	16.75	48.74	2.18	5.50	0.42
Thalassiosira rotula	1.51					0.93	1.16	2.61		
Thalassiosira tenera					0.86		1.16			
Thalassiosira sp. (S8-27)		1.54			0.86		1.16			

APPENDIX H4 (continued)

Sample	S8-61	S8-62	S8-63	S8-64	S8-65	S8-66	S8-67
Achnanthes biosioletta	2.32		1.68			1.54	1.30
Achnanthes kregeri				5.48	1.90		
Achnanthes lemmermanii							
Achnanthes minutissima		8.62	5.05	2.74	6.64	16.98	6.50
Actinocyclus curvatulus							
Actinoptychus vulgaris			1.68	5.48		1.54	
Amphora acutiuscula		0.96			2.85		
Amphora copulata					0.95	1.54	
Asteromphalus heptacis		3.83		2.74	1.90		1.30
Bacteriastrum delicatulum	4.64	3.83	3.36	2.74	3.79	4.63	2.60
Cocconeis costata complex		0.96	3.36		0.95	1.54	1.30
Cocconeis scutellum	4.64	0.96				3.09	
Cyclotella choctawhatcheeana		0.96				7.64	12.75
Cyclotella striata		1.92				1.54	1.30
Cyclotella sp. (S8-6)				2.74	3.79		
Diatomella minuta							
Ditylum brightwellii		0.96	8.41	8.21	1.90	1.54	6.50
Eunotia spp.		2.87					
Fragilaria investiens							
Fragilaria pinnata							
Fragilaria sopotensis				2.74			1.30
Fragilariopsis atlantica		1.92					
Fragilariopsis cylindriformis		4.79	1.68		1.90		1.30
Fragilariopsis pseudonana	6.96	11.49	11.77	27.38	9.48	15.44	16.91
Gomphonema angustum				16.43			1.30
Gomphonemensis lindae		5.75					
Gomphonemensis obscurum					3.79	1.54	2.60
Grammatophora oceanica		1.92					
Melosira nummuloides			1.68		4.74	6.17	2.60
Minidiscus chilensis		0.96		5.48	0.95		1.30
Navicula gregaria	2.32	0.96	6.73		1.90		
Navicula perminuta	2.32		1.68	10.95	8.54	1.54	7.80
Nitzschia fonticola			3.36	5.48			
Nitzschia frustulum	11.61	5.75	3.36	8.21	12.33	6.17	5.20
Odontella longicruris		0.96			1.90		1.30
Opephora horstiana							
Opephora marina							
Opephora minuta							
Opephora mutabilis			3.36		2.85	1.54	
Paralia sulcata		0.96			0.95		2.60
Planothidium delicatulum	2.32	1.92	8.41	5.48	6.64	10.81	7.80
Planothidium hankiana					0.95		1.30
Pseudonitzschia multiseries		11.49	15.14	21.90	3.79	3.09	6.50
Pseudonitzschia seriata		1.92			1.90	6.17	6.50
Skeletonema costatum	44.10	95.77	87.46	175.21	87.25	95.70	78.03
Skeletonema costatum (weak)	951.69	229.84	600.42	947.21	205.79	514.03	383.67
Tabellaria flocculosa							
Tabularia fasciculata		0.96	1.68		0.95	9.26	
Thalassionema bacillare		0.96	3.36	2.74			6.50
Thalassionema nitzschioides		4.79	5.05	24.64	7.59	21.61	5.20
Thalassionema pseudonitzschioides	2.32	2.87		5.48	1.90	1.54	6.50
Thalassiosira binata	6.96	0.96	1.68				
Thalassiosira conferta		0.96		21.90	0.95	3.09	2.60
Thalassiosira decipiens	20.89	9.58		2.74	6.64	9.26	2.60
Thalassiosira eccentrica	6.96	2.87	6.73	5.48	1.90		
Thalassiosira cf. *eccentrica* (S8-23)							
Thalassiosira gravida							
Thalassiosira cf. *leptopus*		2.87			0.95	1.54	1.30
Thalassiosira minima							
Thalassiosira nordenskioeldii	46.42	23.94	30.27	8.21	26.55	18.52	48.12
Thalassiosira pacifica	6.96	9.58	13.45	5.48	22.76	9.26	1.30
Thalassiosira rotula		1.92	13.45	2.74		3.09	0.00
Thalassiosira tenera			1.68			4.63	1.30
Thalassiosira sp. (S8-27)				13.69			1.30

APPENDIX H5. Sediment slab cyclostratigraphy: Depth vs. diatom abundance

Depth (cm)	Diatom Abundance (valves/g)
870.0000	274719528.6
870.1999	274719528.6
870.2000	269518772.3
870.5999	269518772.3
870.6000	343739910.9
870.7999	343739910.9
870.8000	486028524.6
871.0499	486028524.6
871.0500	522539553.1
871.1999	522539553.1
871.2000	372513548.6
871.3499	372513548.6
871.3500	313081734.1
871.5999	313081734.1
871.6000	302661417.0
871.7499	302661417.0
871.7500	520450773.9
871.8999	520450773.9
871.9000	338256071.0
872.0499	338256071.0
872.0500	414135198.3
872.6499	414135198.3
872.6500	216519925.5
872.7499	216519925.5
872.7500	288431325.9
872.8999	288431325.9
872.9000	285336386.7
873.0099	285336386.7
873.0100	354846057.8
873.1499	354846057.8
873.1500	244006710.3
873.2999	244006710.3
873.3000	316252779.9
873.4599	316252779.9
873.4600	1065083301.0
873.6999	1065083301.0
873.7000	252713181.9
873.7999	252713181.9
873.8000	357657602.4
873.9499	357657602.4
873.9500	299373845.3
874.0499	299373845.3
874.0500	309195347.2
874.1999	309195347.2
874.2000	472411311.5
874.3499	472411311.5
874.3500	734781647.1
874.4999	734781647.1
874.5000	359345512.0
874.6499	359345512.0
874.6500	247501598.0
874.7399	247501598.0
874.7400	453950033.8
874.8999	453950033.8
874.9000	407238578.4
875.0199	407238578.4
875.0200	293335227.3
875.2299	293335227.3
875.2300	225918734.2
875.3499	225918734.2
875.3500	277064732.2
875.4999	277064732.2
875.5000	226149126.5
875.6499	226149126.5
875.6500	638042987.2
875.8999	638042987.2
875.9000	310949288.9
876.0099	310949288.9
876.0100	458391814.9
876.2699	458391814.9
876.2700	1237593678.0
876.4899	1237593678.0
876.4900	472594052.0
876.6499	472594052.0
876.6500	287431673.2
877.2499	287431673.2
877.2500	286046178.7
877.7599	286046178.7
877.7600	254203666.7
877.9699	254203666.7
877.9700	317598998.9
878.2499	317598998.9
878.2500	244453582.7
878.4099	244453582.7
878.4100	315062701.3
878.4999	315062701.3
878.5000	404217055.9
878.6499	404217055.9
878.6500	684068011.2
878.8999	684068011.2
878.9000	734411863.4
879.0999	734411863.4
879.1000	732643413.8
879.3999	732643413.8
879.4000	453128807.7
879.5499	453128807.7
879.5500	398955383.0
879.7499	398955383.0
879.7500	800409951.8
879.8999	800409951.8
879.9000	378701962.6
880.1499	378701962.6
880.1500	258815111.5
880.2999	258815111.5
880.3000	693529437.8
880.4999	693529437.8
880.5000	459465680.8
880.7399	459465680.8
880.7400	431780905.2
880.9499	431780905.2
880.9500	465392592.4
881.3699	465392592.4
881.3700	582618403.9
881.6499	582618403.9
881.6500	222398907.7
881.9999	222398907.7
882.0000	76333297.0
882.1999	76333297.0
882.2000	105341613.3
882.5599	105341613.3
882.5600	1162915619.0
882.9499	1162915619.0
882.9500	479786030.4
883.5499	479786030.4
883.5500	867829164.2
883.8099	867829164.2
883.8100	1377014553.0
884.1699	1377014553.0
884.1700	479858262.4
884.2999	479858262.4
884.3000	805774283.5
884.7499	805774283.5
884.7500	658091331.3
884.9999	658091331.3

APPENDIX H6. Sediment slab cyclostratigraphy: Time vs. diatom abundance

Year*	Diatom Abundance (valves/g)	Sample Thickness (cm)
1	274719528.6	0.20
2	269518772.3	0.40
3	343739910.9	0.20
4	486028524.6	0.25
5	522539553.1	0.15
6	372513548.6	0.15
7	313081734.1	0.25
8	302661417.0	0.15
9	520450773.9	0.15
10	338256071.0	0.15
11	414135198.3	0.60
12	216519925.5	0.10
13	288431325.9	0.15
14	285336386.7	0.11
15	354846057.8	0.14
16	244006710.3	0.15
17	316252779.9	0.16
18	1065083301.0	0.24
19	252713181.9	0.10
20	357657602.4	0.15
21	299373845.3	0.10
22	309195347.2	0.15
23	472411311.5	0.15
24	734781647.1	0.15
25	359345512.0	0.15
26	247501598.0	0.09
27	453950033.8	0.16
28	407238578.4	0.12
29	293335227.3	0.21
30	225918734.2	0.12
31	277064732.2	0.15
32	226149126.5	0.15
33	638042987.2	0.25
34	310949288.9	0.11
35	458391814.9	0.26
36	1237593678.0	0.22
37	472594052.0	0.16
38	287431673.2	0.60
39	286046178.7	0.51
40	254203666.7	0.21
41	317598998.9	0.28
42	244453582.7	0.16
43	315062701.3	0.09
44	404217055.9	0.15
45	684068011.2	0.25
46	734411863.4	0.20
47	732643413.8	0.30
48	453128807.7	0.15
49	398955383.0	0.20
50	800409951.8	0.15
51	378701962.6	0.25
52	258815111.5	0.15
53	693529437.8	0.20
54	459465680.8	0.24
55	431780905.2	0.21
56	465392592.4	0.42
57	582618403.9	0.28
58	222398907.7	0.35
59	76333297.0	0.20
60	105341613.3	0.36
61	1162915619.0	0.39
62	479786030.4	0.60
63	867829164.2	0.26
64	1377014553.0	0.36
65	479858262.4	0.13
66	805774283.5	0.45
67	658091331.3	0.25

* synonymous with sample, assuming that each sample represents one year of time

APPENDIX I

Cyclostratigraphy Protocols and Methods

APPENDIX I1

Image and Data Processing Protocol
(after Prokoph and Patterson, in press)

1. Image Acquisition

a. Cleaning core surface

b. Documentation of core completeness, technical defects

2. Image Scanning and Digitizing

a. X-ray imaging:

i. Imaging interval with minimal defects and even sediment slab thickness

ii. For calibration, include mm-distance scale and KODAK gray scale chart (black, white, medium gray) along the entire extent of the scanned slabs

iii. Check for constant x-ray intensity throughout the entire scanned slab and equalize conditions for all slabs

iv. Scan background

v. All images must be scanned at the same resolution, at least 1 pixel = 0.025 mm

3. Image Editing

a. Download digitized x-ray images in image processing software IMAGEJ

b. Correct background colour variation with KODAK gray scale; errors in the sediment colour, for example due to slightly different sediment slab thickness or x-ray intensity fluctuations, can be corrected so that all slabs have the same background colour

4. Line Scan Extraction

a. Rotation of image in position so that laminae are vertical with program IMAGEJ

b. Average values from gray values for 0.3 mm equals a line 3 pixels wide, perpendicular to sedimentary laminae with program IMAGEJ

5. Line Scan Editing (of time series data) in MS EXCEL

- This step can be time-consuming and requires knowledge of sedimentary textures and fabrics

a. Put correct depth values (from top-depth on image description header) to gray scale pixel value for each image by using add-mode of MS EXCEL

b. Interpolate extreme gray values, e.g., due to small fractures or concretions in the sediment, by using adjacent gray values

c. Interpolate lost core or damaged images by mean gray value to sediment slabs on top and bottom

d. Stack time series data of each slab to complete the data set for the complete core

6. Low-frequency Band Wavelet Analysis

a. Wavelet analysis (WA) performed with program CWTNEU5.F that runs under UNIX OS. It is a significantly improved version of CWTA.F (Prokoph and Barthelmes, 1996). The ouput are (a) an ASCII matrix in pgm format that will be transformed in black-and-white or colour 2D graphic with program XVIEW, and (b) a data table that indicates, for example, the cycle length and intensity of maximum wavelet coefficient in each depth interval. WA will detect trends in sedimentation patterns (e.g., thickening upward or thinning upward trends),

sedimentary cycle lengths and abrupt changes in the intensity and duration of sedimentary cycles for an overview n general jumps in cycle patter, major sedimentary cycle lengths for wavelengths longer than 50 years.

7. Sedimentary Cycle Pattern in Depth Domain

- Sedimentary cycle lengths can be translated into duration by using sedimentation rates (sediment accumulation rates) derived from ^{14}C, ^{210}Pb or ^{137}Cs data

8. High-frequency Band Wavelength Analysis

a. This WA transforms thickness data into time-related data, based on the automatic detection of the thickness of the annual cycles. Following results are expected by this method:

b. A set of overlaying cycle durations and lengths will be visualized for each age and core-depth by using wavelet scalograms, respectively. If these cycles are constant over a certain age and depth interval then they can be interpreted as sedimentation-controlling cycles. Such cycles can be sea-level cycles, Milankovitch cycles (e.g., ~400, 100, 40, and 20 kyr), or climatic cycles (~1000 yr Bond cycles, ~11 yr sunspot cycles, El Niño cycles or annual cycles)

9. Depth-to-time Scale Transformation

a. The wavelength with the maximum wavelet intensity ("power") represents the annual cycle thickness. Hence, for each depth interval s_i there will be an annual sedimentation rate sr_i and, consequently a time interval $t_i = s_i / sr_i$. The time intervals will be added and calibrated with ^{14}C, ^{210}Pb or ^{137}Cs data and transformed to the time domain to annual time-scales for the core or slab section,

i.e., each depth interval (pixel location) has an assigned age, and each age has its assigned gray value.

b. Two time series will result: sr(t) and x(t), with x representing the gray value

i. Fluctuation of sedimentation rate in annual resolution

ii. Fluctuation of gray value in annual resolution

c. In addition, any other time-series taken from the core (e.g., diatom abundance, fish populations) can be transformed in the same way from depth to time domain

d. It is necessary to set the resolution of the location axis of the WA high enough (the depth intervals) to guarantee optimal time-resolution

10. WA for sedimentation rate series

- Provides cycles and abrupt changes in sedimentation rate

11. WA for sedimentation rate series

- Provides cycles and abrupt changes in gray value and other series (e.g., diatoms)

12. Time Series Data Editing: for spectral, cross-spectral, correlation and non-linear analysis it is necessary to create surrogate data series (shuffled primary data for significance determination), adjust data to exact annual interval (e.g., non-linear analysis)

13. Spectral (Fourier) Analysis: used for confidence level determination of the detected cycles with software package SPSS. Sedimentary cycles and trends are displayed that are above the red noise, 90%, 95%, and 99% probability of non-randomness

14. Cross-spectral Analysis: performed between time series of sediment gray values, and sedimentation rate. Geochemistry will determine if the image data are valuable

proxies for wavelength-dependent diatom productivity and climate changes. This analysis is carried out in MS EXCEL.

15. **Non-linear Analysis** (in particular correlation dimension analysis): determines whether or not and how many non-linear and cyclic components control the pattern of sedimentation and diatom productivity. This analysis is carried out in the time domain in the programs CORDIM.C and TIMECODM.C.
16. **Correlation and Proxy Parameterization:** while the annual cycle length is constant (365.25 days) through the last million years, other climate cycles (e.g. sunspots are variable and the sedimentary cycles as transformed in time-scale are correlated in MS EXCEL with "real" sunspot cycle length measurements through the last 200 years. The correlation coefficient gives the degree of relation between data and climate change processes.

APPENDIX I2

Wavelet Analysis: Brief Mathematical Theory
(after Prokoph and Patterson, in press)

The continuous wavelet transform (CWT) of a depth-related series *f(t)* is defined as

$$W_\psi(a,b) = \left(\frac{1}{\sqrt{a}}\right)\int f(t)\psi\left(\frac{t-b}{a}\right)dt \ , \qquad (I2.1)$$

where ψ is the base wavelet (which, here, is the Morlet wavelet), the variable a is the scale factor that determines the characteristic frequency or wavelength, $\sqrt{a}$ is replaced by a, the so-called L1-norm, which calculates W and is comparable to the power in spectral analysis (i.e., variance). W stands for the wavelet coefficients, which are given according to a and b in depth-frequency space, and graphically represented by means of a scalogram (Prokoph and Barthelmes, 1996). The Morlet wavelet is formed by a periodic sinusoidal function with a Gaussian envelope and is defined as:

$$\psi^{l}{}_{a,b}(t) = \pi^{-\frac{1}{4}}(al)^{-\frac{1}{2}} e^{-i2\pi\frac{1}{a}(t-b)} e^{-\frac{1}{2}\left(\frac{t-b}{al}\right)^2} \ . \qquad (I2.2)$$

The parameter l represents the relation between periodicity and depth resolution. Parameter $l = 10$ was chosen, which gives sufficiently precise results in resolution of depth and frequency, respectively. The most significant (major) periodicity, $a_{wmax}(b)$ through the succession, can be used to identify variations in accumulation rate and sedimentation directly from the wavelet coefficients, if it represents the same external factor (e.g., annual cycle). The annual cycle thickness represents the sedimentation rate

sr_k as a function of depth and a determination of s_k as a major cycle length in the third column of file CWTDT.DAT. $Ds = k$ was arbitrarily set in the program CWTPC.F by selecting the number of horizons m to be calculated with $k = S/m$ to calculate the time scale by

$$T_l = \sum_{k=1}^{l} \Delta t_k = \frac{\sum_{k=1}^{l} \Delta s_k}{\sum_{k=1}^{l} sr_k} \tag{I2.3}$$

with k =1,2,….n, and l=1 to S. Finally, the non-equidistant time scale was transformed into equidistant annual time intervals Dt =1 year.